UNIVERSITY OF BELGRADE
FACULTY OF PHYSICS

Stefan Đorđević

Page curve in models of 2D dilaton gravity

Doctoral Dissertation

Belgrade, 2026.

UNIVERZITET U BEOGRADU
FIZIČKI FAKULTET

Stefan Đorđević

Pejdžova kriva u modelima 2D dilatonske gravitacije

Doktorska disertacija

Beograd, 2026.

Mentor

prof. dr Voja Radovanović
redovni profesor
Univerzitet u Beogradu – Fizički fakultet

Komisija za odbranu doktorske disertacije

prof. dr Maja Burić
redovni profesor
Univerzitet u Beogradu – Fizički fakultet

dr Branislav Cvetković
naučni savetnik
Univerzitet u Beogradu – Institut za fiziku

prof. dr Marija Dimitrijević Ćirić
redovni profesor
Univerzitet u Beogradu – Fizički fakultet

Datum odbrane doktorske disertacije

Abstract

This dissertation investigates quantum gravity effects and black hole unitarity within the framework of semiclassical two-dimensional dilaton gravity with the aim at resolving the information loss paradox. A central objective is to reproduce the Page curve for the experimentally relevant dimensionally reduced Schwarzschild black hole, in both evaporating and eternal configurations. To this end, we first develop a coherent method for constructing eternal and evaporating black hole geometries based on a symmetric ansatz for two-dimensional spacetimes that admits a Killing vector. With this ansatz in place, we obtain the classical static vacuum solutions to the equations of motion. Next, we describe a classical collapse scenario by smoothly matching two such vacuum regions across an infalling matter shockwave. We then incorporate quantum corrections and solve the quantum-corrected equations of motion in perturbations around the classical vacuum black hole and the classical collapse scenario by specifying the Hartle–Hawking state and the Unruh state, respectively, as the underlying quantum states. The Hartle–Hawking state leads to an eternal black hole solution, whereas the Unruh state describes an evaporating black hole. Finally, by applying the island rule, we successfully derive the Page curve in both of these setups.

The second part of this work investigates how spacetime torsion enters black hole thermodynamics, with the specific aim of preparing the ground for studying its influence on the island formula by identifying viable two-dimensional spacetimes with nonzero torsion. To construct such two-dimensional torsional models, we carry out a dimensional reduction of a five-dimensional Chern–Simons theory. Examining minimal couplings to various matter fields, we uncover distinct cosmological solutions and a charged Riemannian black hole. In particular, coupling gravity to Dirac spinors gives rise to a fermionic soliton-star that undergoes a characteristic phase transition: a fully regular fermionic star configuration collapses into a localized, non-extremal singular horizon once a critical parameter is surpassed. In summary, this work develops a robust computational framework for studying evaporating black holes and supplies two-dimensional spacetime solutions with torsion that can be employed in future analyses of how spacetime torsion alters fine-grained entropy.

Key words: *2D dilaton gravity, black hole thermodynamics, information loss paradox, black hole evaporation, Page curve, island formula, dimensional reduction, Chern-Simons gravity, spacetime torsion*

Research field: **physics**

Research subfield: **high energy physics**

Apstrakt

Ova disertacija istražuje efekte kvantne gravitacije i unitarnost crnih rupa u okviru semiklasične dvodimenzionalne dilatonske gravitacije sa ciljem razrešenja paradoksa gubitka informacija. Glavni cilj disertacije je reprodukcija Pejdžove krive za eksperimentalno relevantnu dimenziono redukovanu Švarcšildovu crnu rupu, kako u isparavajućoj tako i u večnoj konfiguraciji. Najpre razvijamo metod za konstruisanje geometrije večnih i isparavajućih crnih rupa zasnovan na simetričnom ansatzu za dvodimenzionalno prostor-vreme sa Kilingovim vektorom. Koristeći ovaj ansatz, dobijamo klasična statička vakuumska rešenja jednačina kretanja. Zatim opisujemo scenario klasičnog kolapsa glatkim spajanjem dve odgovarajuće vakuumske oblasti preko kolapsirajućeg talasa materije. Potom dodajemo u naš model kvantne korekcije i rešavamo kvantno-korigovane jednačine kretanja korisreći perturbativni razvoj oko klasične vakuumske crne rupe, kao i klasičnog scenarija kolapsa, birajući Hartli-Hokingovo kvatno stanje i Unruhovo kvantno stanje, redom. Na kraju, uspešno izvodimo Pejdžovu krivu u obe konfiguracije.

Drugi deo ove disertacije bavi se uticajem nenulte torzije u prostor-vremenu na termodinamiku crne rupe, sa ciljem izučavanja efekata u formuli sa ostrvom pomoću nalaženja odgovarajućih dvodimenzionalnih prostor-vremena sa nenultom torzijom. Da bismo konstruisali takve dvodimenzionalne modele sa torzijom, primenjujemo dimenzionu redukciju petodimenzionalne Čern–Sajmonsove teorije. Ispitujući minimalna kuplovanja sa različitim poljima materije, otkrivamo razna kosmološka rešenja kao i naelektrisnanu crnu rupu u Rimanovskom sektoru teorije. Posebno, sprezanje gravitacije sa Dirakovim spinorima dovodi do fermionske solitonske zvezde koja doživljava karakterističan fazni prelaz: potpuno regularna konfiguracija fermionske zvezde se kondenzuje u lokalizovani, neekstremalni singularni horizont nakon što se desi fazni prelaz. Ukratko, ovaj rad razvija računarski okvir za proučavanje isparavajućih crnih rupa i pruža rešenja za dvodimenzionalna prostor-vreme sa torzijom.

Ključne reči: *2D dilatonska gravitacija, termodinamika crnih rupa, pardoks gubitka informacija, isparavanje crnih rupa, Pejdžova kriva, pravilo ostrva, dimenziona redukcija, Čern-Sajmons gravitacija*

Naučna oblast: **fizika**

Uža naučna oblast: **fizika visokih energija**

Acknowledgements

First, I would like to express my sincere gratitude to my supervisor, Dr Voja Radovanović, who has been my primary collaborator on the papers forming the core of this thesis. As I am also deeply interested in topological phases of matter, I am grateful to my collaborator Dr Vladimir Juričić, with whom I have recently posted an e-print on arXiv on the topic of non-Hermitian topology in condensed matter physics. I am also thankful to my third collaborator and dear friend, Dr Dušan Đorđević, with whom I am working on the Chern–Simons aspect of the research presented in this thesis. I would further like to acknowledge the continuous and invaluable support I have received from my family and friends. I am particularly grateful to my wife, Ana Đorđević, for the tremendous help she has provided whenever I needed it, both in everyday life and in my scientific work, including many insightful conversations about physics. She is also responsible for producing all the figures in this dissertation. I would also like to express my thanks to Hana Schiff Toman for providing many helpful suggestions on writing in English, which is not my native language, though it is hers. I am likewise deeply grateful to my parents, Jelica and Dragan Đorđević, who have always stood by me in the scientific path I have chosen and encouraged me to embark on this journey in the first place. Finally, I wish to thank everyone who has shared this path with me.

To my lovely wife, Ana
and my dearest parents Jelica and Dragan

Table of Contents

List of Figures

Chapter 1

Introduction

In this dissertation, we study certain thermodynamic aspects of black holes. Black holes arise as some of the earliest known solutions to Einstein's field equations. In 1915, Einstein presented his *General Theory of Relativity* [2], and in that same year Karl Schwarzschild found the first spherically symmetric solution of Einstein's equations [3]. This solution is characterized by the presence of a singularity, that is, a point where the curvature of spacetime ceases to be well defined. In addition, this singularity is concealed behind a surface called the *event horizon*. More precisely, the event horizon is a boundary that separates spacetime into two distinct regions. Inside the region enclosed by the horizon, the future evolution of all particles, including light, is the same: they inevitably end at the singularity. Put differently, once a particle crosses the event horizon, the gravitational field becomes so intense that escaping would demand a speed exceeding that of light, which is physically impossible. As a result, the particle remains confined. Because of these characteristics, this solution is known as a *black hole*.

1.1 Historical overview of the black hole thermodynamics

As research progressed, further black hole solutions were identified, the most general of which is the *Kerr–Newman solution* [4, 5]. This solution provides the most general vacuum configuration of Einstein's equations coupled to electrodynamics, describing a singularity concealed behind an event horizon. Black holes can, in fact, be fully characterized by only a few parameters, i.e., conserved quantities: the mass M, the angular momentum (spin) J, the electric charge Q, and the magnetic charge P. Using Killing vectors, which encode spacetime symmetries, one can determine these conserved quantities. They are connected via the *Smarr relation* [6], which can be derived purely from the spacetime geometry [7]:

$$M = \frac{\kappa A}{4\pi G} + 2\Omega_{\mathrm{H}} J + \Phi_{\mathrm{H}} Q + \Psi_{\mathrm{H}} P, \tag{1.1}$$

where κ denotes the *surface gravity*, A is the area of the event horizon, G is Newton's gravitational constant, Ω_{H} is the angular velocity of the horizon, Φ_{H} is the electric scalar potential at the horizon, and Ψ_{H} is the magnetic scalar potential at the horizon. This formula closely resembles Euler's equation in thermodynamics [8], which prompted many researchers to regard black holes as thermodynamic systems. Taking into account that $M = M(A, J, Q^2, P^2)$ is a homogeneous function of degree $1/2$, together with the Hawking area theorem [9], $\Delta A \geqslant 0$, which is always satisfied, the first law of black hole thermodynamics was established in the mid-20th century in the form [10]:

$$dM = \frac{\kappa}{8\pi G} dA + \Omega_{\mathrm{H}} dJ + \Phi_{\mathrm{H}} dQ + \Psi_{\mathrm{H}} dP. \tag{1.2}$$

From equation (1.2), up to an overall numerical factor, Bekenstein inferred which quantities should be interpreted as the temperature and entropy of a black hole:

$$T = \alpha \frac{\kappa}{8\pi} \quad \wedge \quad S = \frac{A}{\alpha G}. \tag{1.3}$$

Information loss paradox

From a classical standpoint, a black hole that "swallows" everything that comes near it should not exhibit any temperature. Thus, the quantity obtained earlier could not be regarded as a genuine temperature; it was instead understood merely as a mathematical construct highlighting a formal analogy with thermodynamics. This interpretation remained dominant until 1974, when Hawking performed the quantization of fields on the fixed Schwarzschild black hole background. He showed that this semiclassical framework—combining quantum field theory with general relativity—implies that a stationary observer at infinity measures black hole radiation with a thermal spectrum and a well-defined temperature. This result determines the previously undetermined parameter to be $\alpha = 4$ [11, 12, 13]. It was the first clear indication that black holes behave as genuine thermal systems.

Two years before Hawking's discovery, Bekenstein had hypothesized that black holes must carry entropy [14], and the following year he argued that the proportionality constant should be very close to $\alpha = 4$ [15]. Consequently, the expression for black hole entropy is known as the *Bekenstein–Hawking formula* and is written as

$$S_{BH} = \frac{k_B A}{4 l_p^2}, \tag{1.4}$$

where $l_p = \sqrt{\frac{G\hbar}{c^3}}$ denotes the Planck length. Up to this point we have employed natural units with $c = k_B = \hbar = 1$, whereas here the constants have been reinstated to emphasize the physical dimensions.

Thus, the notion that black holes possess entropy was confirmed; however, this led to a new set of problems. The subsequent task was to compute the entropy of the radiation emitted by the black hole, known as *Hawking radiation*. Because this entropy is associated with the subsystem corresponding to the radiation, it is actually the *fine-grained entropy*. In contrast, the Bekenstein–Hawking entropy is a *coarse-grained entropy*, defined as a thermodynamic quantity. Hawking's analysis demonstrated that the fine-grained entropy grows monotonically over time throughout the evaporation process, up until the black hole has completely evaporated. This behavior is incompatible with unitary time evolution in quantum mechanics. Specifically, if the black hole is formed by the collapse of a pure state, as is generally assumed, then after evaporation one is left with a mixed state of radiation. Such an evolution is non-unitary. This inconsistency is referred to as the *Hawking information paradox*. Hawking himself did not consider it a paradox, but instead interpreted it as evidence that black holes act as systems into which information can fall and be permanently lost [16].

In contrast, numerous researchers challenged this conclusion and sought to pinpoint a mistake in Hawking's calculation of the radiation entropy. As a result, in 1992 Page introduced a particular time dependence for the entropy of Hawking radiation so that the overall evolution would remain unitary [17, 18]. This time dependence is now referred to as the *Page curve*.

Throughout the 1990s, a large number of papers on black hole entropy appeared, aiming to address the information paradox, that is, to understand why information seems to be lost. Many authors followed Hawking's argument and assumed that quantum fields propagating on a black hole background do not evolve unitarily. To study this issue, two-dimensional dilaton gravity models were developed as simplified frameworks. The most prominent among these are the CGHS model [19] (named after Callan, Giddings, Harvey, and Strominger) and the JT model [20, 21] (named after Jackiw and Teitelboim). These are not realistic models but rather "toy models," designed to capture only the qualitative features of black hole evaporation; a precise, quantitative treatment still requires numerical computations.

To model black hole evaporation, quantum corrections to the classical theories must be taken into account. When the matter sector consists of massless scalar fields, this leads to the inclusion of the *Polyakov–Liouville term* [22] in the action. However, adding this term alone does not yield analytic solutions, so additional correction terms were introduced to preserve analyticity. For the CGHS model, there are two widely used such extensions: the RST model [23, 24] (named after Russo, Susskind, and Thorlacius) and the BPP model [25] (named after Bose, Parker, and Peleg). In the 1990s, analyses of both of these models pointed to the same outcome: black hole evaporation leads to information loss [26, 25]. These constructions were originally motivated by, and derived from, *string theory*.

Fine-grained entropy in gravitational systems

In parallel with efforts to resolve the information paradox, Gerard 't Hooft introduced the *holographic principle* in 1993 [27]. By revisiting Hawking's original results from the 1970s, he argued that the number of degrees of freedom associated with a black hole scales with the area of its horizon. This notion was then developed further by Susskind in his 1995 work [28], where he treated the entire spacetime as the boundary of a higher-dimensional bulk, effectively portraying the universe as a hologram. The most influential development inspired by the holographic principle came shortly thereafter in Juan Maldacena's 1997 paper, which introduced the AdS/CFT correspondence [29] (Anti-de Sitter/conformal field theory). This work rapidly became the most cited publication in the history of theoretical high-energy physics.

Drawing on ideas from string theory, and AdS/CFT correspondence in particular, Ryu and Takayanagi proposed in 2006 a relation between fine-grained (entanglement) entropy and the conformal field theory defined on the boundary of Anti-de Sitter spacetime. This relation is now known as the *Ryu–Takayanagi formula* [30]. A covariant generalization of this formula was presented in 2007 [31]. The central idea is grounded in the Bekenstein–Hawking expression for black hole entropy:

$$S_I = \min_I \left\{ \operatorname*{ext}_I \left[\frac{A[I]}{4G} \right] \right\}, \tag{1.5}$$

where I denotes a subregion of the boundary of a space-like hypersurface, and $A[I]$ is the area of the corresponding surface I.

Even so, most researchers in this area aimed primarily at reproducing the Page curve, because the principle of unitarity in quantum mechanics is broadly accepted. The Ryu–Takayanagi formula on its own failed to yield the Page curve in any concrete model, but it served as the initial step toward formulating a general expression for the fine-grained entropy of gravitational systems. Substantial advances followed. By carrying out a more sophisticated analysis of the *gravitational path integral*, originally introduced by Gibbons and Hawking [32], Maldacena and Lewkowycz in 2013 derived a formula for the *generalized fine-grained entropy in gravitational systems* [33, 34]:

$$S_{FG} = \min_I \left\{ \operatorname*{\mathbf{ext}}_I \left[\frac{A[I]}{4G} + S_{semi-cl}\left(\Sigma_I \cup \Sigma_{rad}\right) \right] \right\}. \tag{1.6}$$

In this work, they introduced the concept of **islands** Σ_I and their boundary I, which appears in the formula via the Ryu–Takayanagi area term. In addition, they included the semiclassical fine-grained entropy of the combined region made up of the island Σ_I and the Hawking-radiation region Σ_{rad}.

The key insight is that, contrary to the earlier assumption that only a single saddle—the Hawking saddle—contributes, the gravitational path integral actually has two saddle points. Using the replica-wormholes construction, a second saddle point, the replica-wormhole saddle, was identified. The Hawking saddle yields a contribution to the fine-grained entropy that grows indefinitely, whereas the replica-wormhole saddle gives a contribution that decreases monotonically. Taking the minimum of these two competing contributions, the formula (1.6) reproduces the Page curve correctly. Since the replica-wormhole construction arises simply as an implementation of the replica trick in theories with dynamical gravity, it is expected that the island rule should apply to essentially any type of black hole.

In the years that followed, many works appeared that refined this formula into its now-standard form [35, 36, 37]. The main issue was whether it genuinely reproduces the Page curve in explicit models. This was ultimately demonstrated first in JT gravity in 2019 [35, 38, 39], and subsequently in the RST/BPP model in 2021 [40, 41] and the DREH model between 2022 and 2025 [42, 43]. Building on this foundational derivation of the Page curve, it has since been obtained in a broad class of two-dimensional dilaton gravity theories [44, 45, 46, 47, 48, 49, 50, 51, 52, 53, 54, 55, 56, 57, 58, 59], as well as in several higher-dimensional constructions [60, 61, 62, 63, 64]. Additional noteworthy investigations of entanglement entropy in gravitational settings include [65, 66, 67, 68, 69]. At face value, these results may suggest that the information paradox has been resolved. Nonetheless, important issues remain open, such as the detailed quantum state of Hawking radiation, the reconstruction of the relevant causal diamond [70, 71, 72], and related questions.

1.1.1 Chern-Simons theory of gravity

Another major line of research that emerged over the last century is Chern–Simons theory. What started as a purely mathematical construction for analyzing topological invariants of manifolds—especially the Pontryagin characteristic classes—has become a central pillar of contemporary theoretical physics. It is applied not only in gravitational and topological quantum field theory contexts, but also in condensed matter physics to characterize topological phases of matter, such as those appearing in the fractional quantum Hall effect. The theory was first introduced by mathematicians Shiing-Shen Chern and James Simons in their seminal 1974 paper [73]. In this work, they identified a boundary term that cannot be defined globally by a gauge-invariant tensor, yet whose integral over a closed odd-dimensional manifold yields a topological invariant.

The first appearance of Chern-Simons theory in physics occurred when researchers recognized that this mathematical construct exhibits distinctive physical features, largely because its action does not depend on the metric and is therefore topologically invariant. In 1982, Stanley Deser, Roman Jackiw, and Stephen Templeton brought the Chern-Simons term into the realm of physics [74]. They demonstrated that incorporating this term into the Einstein–Hilbert or Maxwell actions in $(2+1)$ dimensions generates a mass for the graviton or photon without violating gauge invariance—a mechanism now known as Topologically Massive Gravity or Topologically Massive Electromagnetism. In 1989, Edward Witten transformed the subject by proving that Chern-Simons theory defines a Topological Quantum Field Theory (TQFT) [75]. He famously employed it to formulate a quantum field theoretic description of the Jones polynomial, a knot invariant in mathematics. This achievement forged a deep link between physics and topology and played a key role in Witten's award of the Fields Medal.

The first concrete application to general relativity appeared in 1988. In $(2+1)$ dimensions, general relativity becomes strikingly simple: it lacks local propagating degrees of freedom and thus realizes a TQFT. Achúcarro and Townsend [76], followed by Witten [77], showed that ordinary three-dimensional general relativity is mathematically equivalent to a pure Chern-Simons gauge theory. This was the first explicit realization of gravity as a pure gauge theory. Building on this, in 1992 Bañados, Teitelboim, and Zanelli found that 3D gravity with a negative cosmological constant admits black hole solutions [78]. Since the bulk theory is purely topological (Chern-Simons), the degrees of freedom accounting for the black hole entropy are entirely localized on the boundary. This represented a major conceptual advance and anticipated the holographic principle.

In the early 1990s, Ali Chamseddine and collaborators formulated Chern-Simons gravity and supergravity in arbitrary odd dimensions [79], exploiting the fact that the CS form exists only in odd-dimensional spacetimes. In contrast to standard Einstein gravity, higher-dimensional Chern-Simons theories for gravity include higher powers of the curvature, yet they uniquely evade the occurrence of pathological "ghosts" (negative-energy modes) that usually plague higher-derivative models. In 1996, Strominger and Vafa demonstrated that string theory can account for the microscopic origin of Bekenstein–Hawking entropy by employing the five-dimensional Chern-Simons term in minimal 5D supergravity and, in this way, successfully counted the microstates of five-dimensional black holes [80].

A key feature of the five-dimensional Chern-Simons theory of gravity is that, although the action has no explicit dependence on torsion, torsion does not vanish on shell, unlike in standard four-dimensional General Relativity. Consequently, one must adopt the Riemann–Cartan geometric framework to correctly analyze solutions with nonzero torsion [81]. More generally, in any spacetime dimension there exists a class of Lagrangians—known as *Lovelock Lagrangians* [82]—that contain higher-order curvature terms while preserving properties analogous to those of ordinary General Relativity. A thorough and foundational exposition of the geometric formulation of Chern-Simons gravity in all odd dimensions is provided by Zanelli in his 2012 work [83], which details the gauge-theoretic construction, the structure of local degrees of freedom, and the way in which one passes from standard General Relativity to these Lovelock-type gravitational theories.

In studying the thermodynamics of any gravitational theory, boundary terms play a crucial rule. The asymptotic symmetries of AdS_3 spacetime were first analyzed by Brown and Henneaux in their 1986 work [84]. A systematic treatment of boundary terms in Chern–Simons theories in odd dimensions was later developed by Mišković and Olea in [85]. Their paper introduces an elegant framework for handling boundary conditions, counterterms, and the regularized evaluation of Noether charges, which is further extended in [86].

The thermodynamics of three-dimensional Chern–Simons gravity with torsion has been explored in [87, 88]. In [87], the authors present a thorough study of three-dimensional black holes in Einstein–Maxwell theory endowed with both gravitational and electromagnetic

Chern–Simons terms. They construct intrinsically rotating, geodesically complete solutions and confirm that their mass, angular momentum, and entropy obey the first law of black hole thermodynamics. In contrast, [88] derives generalized asymptotic configurations for 3D Maxwell Chern–Simons gravity and proposes a new extension that introduces torsion through a deformed Maxwell algebra. They show that, whereas the torsionless sector leads to flat cosmological spacetimes, the torsional sector gives rise to BTZ-like geometries in which the entropy depends not only on the horizon area but also on additional spin-2 fields integrated over the horizon. Finally, in five dimensions, one finds a well-defined BTZ-type black hole with torsion, whose thermodynamics, when coupled to an $SU(2)$ soliton, is analyzed in the recent work [89].

1.2 Motivation

The Einstein–Hilbert action and its black hole predictions form the foundation of contemporary gravitational theory. Over the decades, numerous experiments have been carried out with the aim of testing Einstein's theory of gravity [2], and all have confirmed its validity. The first key success was the explanation of the anomalous precession of Mercury's orbit around the Sun, where the general relativistic correction matches observations with remarkable precision. This was followed by the confirmation of gravitational lensing, in which a single source (typically a galaxy) appears in two distinct directions in the sky as seen from Earth. This effect arises because light is deflected when it passes near a massive body such as a black hole, exactly as predicted by general relativity. The most recent observational breakthroughs provide especially compelling evidence for Einstein's theory: the first ever image of a black hole [90] and the observation of gravitational waves [91].

Another central feature of general relativity is the set of cosmological solutions it admits, many of which describe our universe quite accurately. In this domain, there is an even larger body of experimental data, most notably the observations of the cosmic microwave background (CMB) radiation. Yet general relativity by itself does not account for the small temperature fluctuations observed in the CMB. These are generally viewed as phenomena that require a complete theory of quantum gravity. Consequently, researchers turn to semiclassical methods—where quantum fields are defined on a curved spacetime background—to explain these features, and such approaches have achieved partial success.

The same technique is employed to account for the thermal character of black holes. Consequently, they must emit radiation and lose energy—an effect that cannot be understood without invoking quantum field theory in curved spacetime. Although this phenomenon has not yet been confirmed experimentally, because the predicted temperature of a black hole is on the same order of magnitude as the CMB temperature, it is regarded as an unavoidable aspect of black hole physics. Therefore, it deserves deeper study.

This leads to crucial questions, such as: Do black holes—and by extension, general relativity—respect the principles of quantum mechanics? In particular: Is black hole radiation governed by a unitary time evolution? Furthermore, this issue should be investigated in more intricate settings as well, including cosmological solutions of Einstein's equations.

The island formula (1.6), obtained from the gravitational path integral, offers a framework that reproduces the Page curve and thereby suggests that the underlying evolution is unitary. Nonetheless, this does not yet guarantee that the Hawking radiation itself evolves unitarily, since the Page curve only captures the correct time dependence of the fine-grained entropy. Several questions remain unresolved. For instance: Is it possible, in principle, to reconstruct the full information about the initially infalling matter solely from measurements performed on the Hawking radiation?

At present, the explicit form of the island formula is well understood only in two spatial dimensions. Consequently, the Page curve has been computed primarily in a limited set of "toy models" based on two-dimensional dilaton gravity, and often in the unphysical context of an eternal black hole, which describes a black hole in thermal equilibrium with its surroundings. In this work, we succeed in reproducing the Page curve within a physically relevant DREH model, derived from experimentally tested Einstein's general relativity. Moreover, we achieve this for both the eternal black hole case and the fully evaporating black hole scenario.

The importance of torsion

The second line of research in this dissertation focuses on the dimensionally reduced five-dimensional Chern–Simons theory. Although this is not a physical theory, the first giveaway being that it is define in five spacetime dimensionsit nevertheless admits black hole solutions with non-vanishing torsion. In contrast, general relativity is intrinsically torsion-free, as it is formulated on a Riemannian manifold. However, such manifolds do not exhaust all geometries that can arise from the fundamental postulates of general relativity. In particular, the equivalence principle can be viewed as implying that gravity results from the localization of Poincaré symmetry. When the Poincaré group is localized in this way, the most general resulting manifold is a Riemann–Cartan manifold, which allows for non-zero torsion.

The presence of torsion has not yet been confirmed experimentally, but we still cannot definitively claim that spacetime is torsion-free. In many theoretical frameworks, torsion is intimately connected to the nontrivial interaction between Dirac fermions and gravity, for example in configurations such as fermionic soliton star solutions. The canonical case is the Einstein–Cartan theory, which extends general relativity to a Riemann–Cartan spacetime. In fact, when fermions are absent in this theory, the resulting equations of motion reduce to Einstein's field equations, which enforce vanishing torsion.

The central question to be addressed is: How does non-vanishing torsion affect the fine-grained entropy of gravitational systems such as black holes? Since this problem is too broad, a more precise first step is to ask: How should the island formula (1.6) be modified to incorporate the effects of torsion? At the time of writing this dissertation, this remains unresolved. Even the correct torsion-inclusive generalization of the Ryu–Takayanagi formula is not yet known. In this context, five-dimensional Chern–Simons theory provides an excellent testing ground for exploring torsion, as it admits a BTZ-like black hole solution with torsion. From the viewpoint of the island formula, however, it is natural to dimensionally reduce the full five-dimensional Chern–Simons theory to two dimensions and consequently recast it as a two-dimensional dilaton gravity theory that includes both torsion fields inherited from higher dimensions and torsion intrinsic to two dimensions.

The initial task in pursuing these questions is to obtain solutions with torsion in two-dimensional dilaton gravity. This is the specific goal of this dissertation within this broader research program. Achieving this paves the way for the next step: attempting to modify the Ryu–Takayanagi formula so that torsion is properly taken into account. Ultimately, once the correct torsion-inclusive formula is established, it should be applied to compute the Page curve in the dimensionally reduced, experimentally tested Einstein–Cartan theory of gravity.

1.3 Key results

This dissertation pursues two separate directions within the framework of two-dimensional dilaton gravity. The first focuses on analyzing the fine-grained entropy of gravitational systems, while the second explores a dimensionally-reduced model of five-dimensional Chern-Simons theory, with the ultimate aim of understanding how non-zero torsion influences the fine-grained entropy in such systems. We begin by outlining the central method used to compute the various solutions developed in this thesis.

The first key result is the construction of the symmetric ansatz in Section 3.1, designed to describe 2D spacetimes that admit at least one Killing vector. This ansatz provides a straightforward route to obtain the equations of motion for any static configuration in 2D dilaton gravity, including classical vacuum solutions, asymptotically flat Minkowski-like vacua, and eternal black hole scenarios. Every such solution is characterized by $(\mathrm{F}^+, \mathrm{F}^-, C, f)$, where $\mathrm{F}^\pm$ encode the coordinate transformations from an arbitrary coordinate system to Eddington–Finkelstein coordinates associated with the chosen Killing vector, and C denotes a set of integration constants (or charges) that specify the particular solution. The quantity f represents a collection of arbitrary functions, which typically emerge from residual gauge freedoms in the higher-dimensional parent theory from which the 2D dilaton gravity model is obtained.

The same ansatz can be employed to formulate the classical collapse scenario, as discussed in Section 3.4, where infalling matter propagates along a null hypersurface. In this framework, the spacetime on each side of the null hypersurface must be given by one of the static vacuum solutions. By requiring a continuous matching of these vacuum regions across the infalling matter hypersurface, one relates the parameters of the two solutions. Specifically, the presence of infalling matter induces a discontinuity in F^- and in the charges C, while the other coordinate transformation remains unchanged. In most situations, these junction conditions fully fix the remaining gauge freedom and thereby determine any arbitrary functions that may appear in the general vacuum solutions.

Another important aspect of this matching procedure is that it allows one to obtain a formal expression for the mass of the spacetime in terms of its parameters, providing an alternative route to determine the thermodynamic properties of the theory.

However, in many cases these equations of motion cannot be solved exactly. In such situations, one employs a perturbative expansion in the natural parameter $\hbar$ and determines the equations of motion only up to first order in $\hbar$. This allows the ansatz to be applied to obtain the evaporating black hole solution as well. Because the EMT associated with quantum corrections is of order $\hbar$, one first uses the zeroth-order static solutions to evaluate the EMT, and only then integrates the equations of motion. The solutions in the regions of spacetime separated by the infalling-matter hypersurface are then characterized by $(\mathrm{F}^+, \mathrm{F}^-, C, t_+(\sigma^+), t_-(\sigma^-))$, where the additional functions $t_\pm(\sigma^\pm)$ encode the specific quantum state of the fields. After enforcing continuous matching of the two solutions across the dividing hypersurface the coordinate transformation F^- and constants C receive additional quantum corrections, leading to a quantum-corrected collapse scenario. This procedure is described in full detail in Section 3.4.1.

We have employed this method to obtain both the eternal and evaporating black hole solutions in the DREH model, as presented in Sections 5.2.3 and 5.3, respectively. An analogous procedure is applied in the Riemannian sector of the DR5DCS model, where the corresponding solutions are constructed in Sections 6.2.3 and 6.3, respectively. One might anticipate difficulties near the end-point of evaporation, since the standard non-perturbative solutions in the BPP and RST models exhibit non-analytic behavior in this region of spacetime. Our method, however, captures precisely this non-analyticity and correctly reproduces the energy balance, the thunderpop, and the end-state geometry in each model.

The central findings of this research program are summarized in Chapter 10, where we successfully obtain the Page curve for the DREH model in both the eternal and evaporating black hole scenarios. The perturbative analysis reproduces the expected behavior of the Page curve, determines the Page time, and thereby establishes the unitary time evolution of the fine-grained entropy in the DREH model.

The central outcome of the second line of research is derived in Section 2.3, where the complete 5DCS theory is dimensionally reduced to two dimensions over the 3-sphere, yielding the following action:

$$\begin{aligned} S_{\mathrm{DRCS}_5} =& \frac{k\pi^2}{(\lambda l)^3}\int \mathrm{d}^2x\sqrt{-g}e^{-3\phi}\Bigg\{\left(1+\frac{3}{\mathrm{x}^2}\left(1-\Phi^2-\theta^2\right)\right)\left[\mathrm{R}+2\varepsilon^{\alpha\beta}\partial_\alpha \mathrm{K}_\beta+\frac{2}{l^2}\right] \\ &+\frac{4}{l^2}+\frac{6}{l\mathrm{x}^3}\theta^2\nabla_\alpha\phi^\alpha+\frac{6}{l\mathrm{x}}\left(1+\frac{1}{\mathrm{x}^2}\left(1-\Phi^2-\theta^2\right)\right)\left[\nabla_\alpha\phi^\alpha-\varepsilon^{\alpha\beta}\phi_\alpha \mathrm{K}_\beta\right] \\ &-\frac{6}{\mathrm{x}^2}\left[\nabla_\alpha\phi^\beta\nabla_\beta\phi^\alpha-\nabla_\alpha\phi^\alpha\nabla_\beta\phi^\beta-\varepsilon^{\alpha\beta}\mathrm{K}_\alpha\nabla_\beta\Phi^2\right]\Bigg\}+S_{\mathrm{mat}}, \end{aligned} \tag{1.7}$$

In this manner, a two-dimensional dilaton gravity theory with torsion is obtained. Its properties are examined in detail in Chapter 7. There, it is shown that the general vacuum geometry is inherited from the original 5DCS theory and corresponds to a BTZ black hole with a non-vanishing five-dimensional torsion field, which manifests in the 2D theory as a scalar field θ. This field θ effectively serves as a Lagrange multiplier, imposing a constraint that substantially restricts the phase space of admissible solutions. In Section 7.2.1, we adopt the symmetric ansatz and exploit this constraint to explicitly determine all additional fields originating from the dimensional reduction and the two-dimensional torsion as well, in the presence of two-dimensional matter. We demonstrate that, as long as $\theta \neq 0$, the 2D torsion is necessarily non-vanishing as well.

In Section (7.3) we solve the ensuing equations of motion in the presence of matter that is minimally coupled to gravity. We consider several types of matter fields. The most compelling solutions are found when a Dirac spinor field is minimally-coupled to both gravity and torsion. In that setting, we demonstrate that the system supports a fermionic soliton star configuration with a clearly defined phase transition mechanism. The transition is governed by two parameters, μ and P. For $\left|\frac{\mu}{P}\right| > \frac{\pi}{4}$, the solution corresponds to a completely regular spacetime, free of horizons and singularities. Once this critical threshold is crossed, however, the fermions condense at a particular spacetime location where the fermion density $\bar{\psi}\psi$ diverges. This divergence in the density produces a curvature singularity and a horizon precisely at that location. The associated horizon has non-vanishing surface gravity, so the resulting configuration is non-extremal. We anticipate that including quantum corrections will remove, or "smooth out," this singularity.

Beyond the fermionic star configuration, we uncover a wide variety of additional solutions. In most situations, coupling to scalar fields leads to cosmological solutions. These are typically singular and often describe spacetimes oscillating between a big bang and a big crunch events. In some cases, additional singularities arise in between them, occurring at spacetime locations where the scale factor remains finite. Singularities of this kind are referred to as sudden singularities and have been thoroughly studied in the literature [92, 93].

1.4 Organization

The dissertation is divided into two main parts. The first part, comprising Chapters 2-7, focuses on two-dimensional dilaton gravity. Various models are presented, their equations of motion are solved, and quantum corrections are incorporated, leading to both eternal and evaporating black hole solutions. The second part, consisting of Chapters 8-10, is devoted to the study of fine-grained entropy in the framework of 2D dilaton gravity, where the Page curve is recovered for several different models. The final chapter provides concluding remarks.

In Chapter 2 we present the framework of dimensional reduction. This framework is central to the thesis, since all theories under consideration are obtained from higher-dimensional ones by dimensional reduction. We begin by formulating dimensional reduction on a general Riemannian manifold with a well-defined topology. Using this setup, we then derive the action for a theory reduced over an n-sphere manifold, and subsequently apply it explicitly to reduce the five-dimensional Chern-Simons (5DCS) theory and the four-dimensional Einstein-Hilbert action to two-dimensional dilaton gravity over $\mathbb{S}^3$ and $\mathbb{S}^2$, respectively. In the final section, we carry out the dimensional reduction of the full 5DCS theory to a two-dimensional dilaton gravity with torsion over $\mathbb{S}^3$ by employing the most general spherically symmetric ansatz for both the vielbein and the spin-connection.

Chapter 3 is devoted to the general structure of two-dimensional dilaton gravity. We first introduce the most general symmetric ansatz for a two-dimensional spacetime that admits at least one Killing vector. The ansatz for scalar, spinor, vector, and tensor fields, as well as for the metric and the dilaton is constructed. We then derive the most general covariant conservation laws in 2D dilaton gravity when non-minimal couplings to curvature and torsion are included. Next, we incorporate quantum corrections through the Polyakov–Liouville action and study the transformation properties of the resulting quantum energy-momentum tensor (EMT). The concluding section of this chapter develops the framework for both classical and quantum-corrected gravitational collapse, with particular emphasis on a perturbative expansion in $\hbar$ in the quantum-corrected case.

In Chapter 4 we present an in-depth review of the CGHS model of 2D dilaton gravity, treated as a fundamental toy model for investigating the entropy of Hawking radiation in an asymptotically flat spacetime. We begin by deriving the equations of motion and their general solutions. We then impose a static ansatz setup, solve the resulting static equations of motion, and formulate the classical gravitational collapse scenario. After that, we incorporate Polyakov–Liouville quantum corrections, examine various choices of counterterms that render the quantum-corrected equations exactly solvable, and determine the most general static vacuum solution of these quantum-corrected equations. In the following section, we provide a detailed analysis of the BPP model, which we adopt as our preferred route. We first construct the exact quantum-corrected collapse scenario, and then apply the perturbative method developed in Chapter 3 to demonstrate that it leads to consistent results. The chapter concludes with a discussion of the thermodynamic properties of the CGHS model.

Chapter 5 focuses on the dimensionally reduced four-dimensional Einstein–Hilbert action and is organized into three sections. As before, we start by deriving the classical equations of motion and demonstrate that Birkhoff's theorem is inhered through the dimensional reduction, in the sense that the most general solution of the vacuum equations of motion is the Schwarzschild black hole spacetime. The second section explains how to incorporate Polyakov–Liouville quantum corrections in this setting, derives the most general quantum-corrected static solutions, and discusses both the asymptotically flat static vacuum configuration and the eternal black hole scenario. The final section systematically introduces evaporating black hole solutions. In this part, we explicitly compute the end point of evaporation, determine the final state of black hole radiation, and show that the end-state geometry is the quantum-corrected Minkowski vacuum solution.

In Chapter 6 we study the Riemannian sector of the dimensionally reduced five-dimensional Chern-Simons theory (DR5DCS). The organization closely parallels that of the preceding chapter. In the first section, we derive the classical equations of motion together with their most general vacuum solutions, and then construct the classical collapse scenario and the associated Penrose diagram. The following section introduces quantum corrections into this framework. There we obtain the general static solutions to the quantum-corrected equations of motion and formulate the eternal black hole scenario. The final section is dedicated to the evaporating black hole solution. We explicitly determine the end-point of evaporation, the corresponding final state, and the geometry characterizing this end state.

Chapter 7 is devoted to the full dimensionally reduced 5DCS theory with non-vanishing torsion. Because the equations of motion are, in general, extremely challenging to solve, we immediately adopt the symmetric ansatz of Section 3.1. Within this framework we derive the most general symmetric vacuum solution. The second section addresses the general solution of the gravitational equations of motion. We manage to express all additional fields arising from dimensional reduction, as well as the two-dimensional contorsion, solely in terms of the metric, the dilaton, and their derivatives, and from this we obtain the resulting equations for the dilaton and the metric in terms of the matter EMT and the contorsion current. We then analyze three distinct cases. First, we consider matter with a completely vanishing contorsion current; in this regime the matter EMT is entirely determined by the metric. Next, we investigate how non-vanishing components of the contorsion current modify the equations of motion. The final section examines the coupling of gravity to various matter field theories. We start with a real scalar field, pure electrodynamics, and spinor field theory, then proceed to scalar electrodynamics, and conclude with ideal fluid hydrodynamics.

We now turn to the second part of the dissertation. Chapter 8 is devoted to various notions of entropy in gravitational systems. It is divided into four sections. In the first section, we highlight the distinction between coarse-grained and fine-grained entropy, and clarify what is meant by the fine-grained entropy of quantum fields in a gravitational background. We stress that the crucial ingredient in defining entanglement entropy is the spacetime region in which the degrees of freedom inaccessible to a static observer reside.

The second section focuses on the Von Neumann entropy in gravity. We begin by computing the Von Neumann entropy for a Rindler observer and derive the Unruh effect. In the subsequent subsections, we examine how changing the inaccessible region affects the fine-grained entropy and extend the resulting formulas to curved spacetimes, both with and without reflective boundaries. The next subsection analyzes how the entropy depends on the choice of quantum state of the matter fields. This section concludes with a definition of the Hawking information paradox.

The final section reviews the recent Maldacena–Lewkowycz prescription for evaluating fine-grained entropy in gravitational systems, following [1]. We begin by presenting the central dogma, which states that a black hole can be treated as an ordinary quantum system up to a certain cutoff hypersurface, and then proceed to discuss the reconstruction of the Page curve, the replica wormhole method, and the problem of entanglement wedge reconstruction.

In Chapter 9 we revisit the derivation of the Page curve in the BPP model. We begin by computing the Page curve for an eternal black hole, and subsequently analyze the evaporating black hole case. For both setups, we first examine the no-island configuration, in which one recovers the standard Hawking result, and then demonstrate explicitly how incorporating the island correctly yields the Page curve. At the end of this chapter, we address the reliability of the Page curve calculation and offer a comment on Page time.

Chapter 10 is devoted to the central result of this dissertation, namely the Page curve in the DREH model. It is organized into three sections. In the first section, we derive the Page curve for an eternal black hole, analyze the island and no-island configurations, and comment on their connection to Wald entropy. The second section focuses on the Page curve in a classical collapse setup, where we show that the resulting Page curve exhibits the same asymptotic behavior as in the eternal black hole case, as expected in the absence of quantum back-reaction on the classical geometry. The final section recovers the Page curve for an evaporating black hole, with particular emphasis on distinguishing between the island and no-island configurations.

The main text is supplemented by four appendices. Appendix A introduces the Riemann–Cartan geometry and the spinor conventions employed throughout this dissertation. Appendix B provides further technical details on the polynomials that appear in the evaporating black hole solution of the DREH model discussed in Section 5.3. In Appendix C we present a brief review of the standard four-dimensional Schwarzschild solution. The final Appendix D is devoted to quantum field theory in curved spacetime, with particular focus on the scalar field. We begin by discussing canonical quantization in curved spacetime, Bogoliubov transformations, and the Unruh effect. The fourth section highlights the role of event and Killing horizons within the black hole spacetimes, while the fifth section derives the Kruskal coordinates and the surface gravity by imposing regularity of the metric at the horizon. In the last section, we examine the Hawking effect and Hawking radiation.

Chapter 2

Dimensional reduction

Higher-dimensional gravitational theories are generally difficult to solve. To address this, one often attempts to simplify the problem by reducing the number of dimensions. There exist many consistent methods to carry out such a dimensional reduction. The original historical proposal, due to Kaluza and Klein [94, 95], suggested introducing a fifth coordinate in order to unify Einstein's general relativity with Maxwell's electromagnetism. To account for the fact that we do not observe this fifth coordinate, they assumed it is compactified on a tiny circle with a radius so small that it cannot be detected. Although this framework did not yield the correct value for the electron mass-to-charge ratio, it nonetheless remains a foundational idea in modern string theory, where the compactification is done over small complex Calabi–Yau manifolds, thereby reducing higher-dimensional string theories to an effective four-dimensional theory.

In this section, we present an alternative approach to dimensional reduction. The idea is to impose a symmetric ansatz such that the resulting metric has the required topology, and then integrate out the redundant coordinates. In this way, any solution of the original theory that possesses the specified topology and symmetries automatically becomes a solution of the dimensionally reduced theory. Since it is considerably easier to study the thermodynamic properties in the lower-dimensional framework, this method is particularly valuable, as it ensures that the desired solutions are indeed captured by the reduced theory.

The chapter is divided into three sections. In the first section, we present a general method for performing this type of dimensional reduction on a Riemannian manifold. In the following chapter, we carry out the dimensional reduction over the n-sphere and, as illustrative examples, consider the Einstein–Hilbert action and the Riemannian sector of five-dimensional Chern–Simons theory. In the final part of this chapter, we perform a dimensional reduction of the complete five-dimensional Chern–Simons theory of gravity, which exhibits a black hole solution with torsion, which is of great importance for the study of fine-grained entanglement entropy in gravitational systems with torsion.

2.1 Dimensional reduction of Riemannian manifold

Here we introduce an alternative symmetry-based approach to dimensional reduction of a Riemannian manifold. We begin with an N-dimensional manifold that can be decomposed in $K+1$ disjunctive sub-manifolds $\mathcal{M}_N = \mathcal{M}_n \times \mathcal{M}_{d_1} \times \mathcal{M}_{d_2} \times \cdots \times \mathcal{M}_{d_K}$, each characterized by its own dimension d_a, topology and symmetry properties. The component $\mathcal{M}_n$ represents the final

n-dimensional manifold that remains after the reduction process. The metric on each submanifold is written as $\mathrm{d}s_a^2 = \gamma^{(a)}_{i_a j_a}\mathrm{d}x^{i_a}\mathrm{d}x^{j_a}$. Accordingly, for the metric on the original manifold we adopt the following ansatz:

$$\mathrm{d}s^2 \equiv G_{AB}\mathrm{d}X^A\mathrm{d}X^B = g_{\mu\nu}\mathrm{d}x^\mu\mathrm{d}x^\nu + \sum_{a=1}^{K}\frac{1}{\lambda_a^2}e^{-2\phi_a}\gamma^{(a)}_{i_a j_a}\mathrm{d}x^{i_a}\mathrm{d}x^{j_a}, \tag{2.1}$$

where we have introduced K dilaton fields ϕ_a and dimensional constants λ_a associated with the corresponding submanifolds. We emphasize that the symmetry requirement is that the dilaton fields depend solely on the coordinates of the final manifold, namely $\phi_a = \phi_a(x^\mu)$. We denote the coordinates collectively as $X^A \in \{x^\mu, x^{i_1}, x^{i_2}, ..., x^{i_K}\}$, where Latin indices label the submanifolds and Greek indices are reserved for the final manifold.

The action of the higher-dimensional Riemannian gravity theory may depend only on the curvature invariants, namely:

$$S = \int_{\mathcal{M}_N}\mathrm{d}^N X\sqrt{-G}\mathcal{L}\left(\mathcal{R}, \mathcal{R}_{AB}\mathcal{R}^{AB}, \mathcal{R}_{ABCD}\mathcal{R}^{ABCD}\right). \tag{2.2}$$

Hence, we evaluate these invariants using the ansatz (2.1). In addition to $\Gamma^\rho_{\mu\nu}$ for the resulting manifold and $\Gamma^{k_a}_{i_a j_a}$ for each submanifold over which the dimensional reduction is carried out, the remaining non-vanishing Christoffel symbols are:

$$\begin{aligned}
\Gamma^\mu_{i_a j a} &= \frac{1}{\lambda_a^2}e^{-2\phi_a}\gamma^{(a)}_{i_a j_a}\nabla^\mu\phi_a, \quad &&\forall a \in \{1, 2, ..., K\},\\
\Gamma^{j_a}_{i_a\mu} &= -\delta^{j_a}_{i_a}\nabla_\mu\phi_a, &&\forall a \in \{1, 2, ..., K\}.
\end{aligned} \tag{2.3}$$

The next step is to compute the Riemannian curvature tensor of the initial manifold using Christoffel symbols (2.3) and ansatz (2.1). For non-zero components of the Riemannian tensor, we get:

$$\begin{aligned}
\mathcal{R}^\mu{}_{i_a\nu j_a} &= \frac{1}{\lambda_a^2}e^{-2\phi_a}\gamma^{(a)}_{i_a j_a}\Big(\nabla^\mu\nabla_\nu\phi_a - \nabla^\mu\phi_a\nabla_\nu\phi_a\Big),\\
\mathcal{R}^{i_a}{}_{\mu j_a\nu} &= \delta^{i_a}{}_{j_a}\Big(\nabla_\mu\nabla_\nu\phi_a - \nabla_\mu\phi_a\nabla_\nu\phi_a\Big),\\
\mathcal{R}^{i_a}{}_{j_a k_a l_a} &= R^{(a)i_a}{}_{j_a k_a l_a} + \frac{1}{\lambda_a^2}e^{-2\phi_a}\left(\nabla\phi_a\right)^2\Big(\delta^{i_a}{}_{l_a}\gamma^{(a)}_{j_a k_a} - \delta^{i_a}{}_{k_a}\gamma^{(a)}_{j_a l_a}\Big),\\
\mathcal{R}^{i_a}{}_{i_b j_a j_b} &= -\delta^{i_a}{}_{j_a}\frac{1}{\lambda_b^2}e^{-2\phi_b}\gamma^{(b)}_{i_b j_b}\nabla_\mu\phi_a\nabla^\mu\phi_b,\\
\mathcal{R}^\mu{}_{\nu\rho\sigma} &= R^\mu{}_{\nu\rho\sigma},
\end{aligned} \tag{2.4}$$

where $R^\mu{}_{\nu\rho\sigma}$ and $R^{i_a}{}_{j_a k_a l_a}$ are the Riemannian curvature tensors of the final manifold and the a-th submanifold, respectively. The Ricci tensor is defined by $\mathcal{R}_{AB} = \mathcal{R}^D{}_{ADB}$, and is given by:

$$\begin{aligned}
\mathcal{R}_{\mu\nu} &= R_{\mu\nu} + \sum_{a=1}^{K} d_a\Big(\nabla_\mu\nabla_\nu\phi_a - \nabla_\mu\phi_a\nabla_\nu\phi_a\Big),\\
\mathcal{R}_{i_a j_a} &= R^{(a)}_{i_a j_a} + \frac{1}{\lambda_a^2}e^{-2\phi_a}\gamma^{(a)}_{i_a j_a}\Big(\Box\phi_a - \nabla_\mu\phi_a\nabla^\mu\phi\Big),
\end{aligned} \tag{2.5}$$

where $R_{\mu\nu}$ and $R_{i_a j_a}$ are the Ricci tensors of the final manifold and the a-th submanifold, respectively. In addition, we introduce $\phi \equiv \sum_{a=1}^{K} d_a\phi_a$. The first curvature invariant, the scalar curvature, is directly computed from 2.5:

$$\mathcal{R} = R + (\nabla\phi)^2 - 2e^{\phi}\Box e^{-\phi} + \sum_{a=1}^{K}\left(\lambda_a^2 R^{(a)} e^{2\phi_a} - d_a\,(\nabla\phi_a)^2\right), \tag{2.6}$$

where R and $R^{(a)}$ denote the scalar curvatures associated with their respective manifolds. Finally, we evaluate the quadratic curvature terms. The Ricci squared is as follows:

$$\begin{aligned}\mathcal{R}^{AB}\mathcal{R}_{AB} = R_{\mu\nu}R^{\mu\nu} + + \sum_{a=1}^{K}\lambda_a^4 e^{4\phi_a} R^{(a)}_{i_a j_a} R^{i_a j_a}_{(a)} + \sum_{a,b=1}^{K} d_a d_b e^{\phi_a+\phi_b}\nabla_\mu\nabla_\nu e^{-\phi_a}\nabla^\mu\nabla^\nu e^{-\phi_b} \\ + 2R^{\mu\nu}\sum_{a=1}^{K} d_a\left(\nabla_\mu\nabla_\nu\phi_a - \nabla_\mu\phi_a\nabla_\nu\phi_a\right) + 2\sum_{a=1}^{K}\lambda_a^2 e^{2\phi_a} R^{(a)}\left(\Box\phi_a - \nabla_\mu\phi_a\nabla^\mu\phi\right) \\ + \sum_{a=1}^{K} d_a\left(\Box\phi_a - \nabla_\mu\phi_a\nabla^\mu\phi\right)^2,\end{aligned} \tag{2.7}$$

while the Kreshman scalar is given by:

$$\begin{aligned}\mathcal{R}_{ABCD}\mathcal{R}^{ABCD} = R_{\mu\nu\rho\sigma}R^{\mu\nu\rho\sigma} + 4\sum_{a=1}^{K} d_a e^{2\phi_a}\nabla_\mu\nabla_\nu e^{-\phi_a}\nabla^\mu\nabla^\nu e^{-\phi_a} + 4\sum_{1\leqslant a<b\leqslant K} d_a d_b\left(\nabla_\mu\phi_a\nabla^\mu\phi_b\right)^2 \\ + \sum_{a=1}^{K}\left[\lambda_a^4 e^{4\phi_a} R^{(a)}_{i_a j_a k_a l_a} R^{i_a j_a k_a l_a}_{(a)} - 4\lambda_a^2 e^{2\phi_a} R^{(a)}(\nabla\phi_a)^2 + 2d_a(d_a-1)(\nabla\phi_a)^4\right].\end{aligned} \tag{2.8}$$

We can see that the resulting action is at most fourth order in derivatives of the dilaton fields.

All of these invariants depend on the corresponding invariants of the submanifold on which the reduction is carried out. These are the only terms that explicitly depend on the submanifold coordinates. Substituting (2.6-2.8) into the gravitational action (2.2) and then integrating over the submanifold coordinates yields an action defined on the final manifold. If one or more of the submanifolds is non-compact, divergences can arise when attempting to integrate out the submanifold coordinates. In such cases, an appropriate regularization procedure must be employed to tame those divergences. In most cases the invariants appear in specific combination known as Gauss-Bonnet term [96], firstly introduced in Lovelock gravity [97], and later refined as main ingredient in Gauss-Bonnet gravity:

$$GB = \mathcal{R}^2 - 4\mathcal{R}^{\mu\nu}\mathcal{R}_{\mu\nu} + \mathcal{R}^{\mu\nu\rho\sigma}\mathcal{R}_{\mu\nu\rho\sigma}. \tag{2.9}$$

This term becomes relevant only in theories with more than five dimensions. In two- and three-dimensional theories it is exactly equal to zero; while in four dimensions it appears as a topological term, proportional to the Euler characteristic of the manifold. It arises in topological gravity theories, most notably in five-dimensional Chern–Simons theory.

Finally, we need to substitute the ansatz (2.1) in order to rewrite $\sqrt{-G}$ from (2.2) in terms of the dilaton fields. Because the metric ansatz is block diagonal, its determinant factorizes into a product of $\sqrt{-g}$ contributions, one from each submanifold:

$$\sqrt{-G} \equiv \sqrt{-g}\prod_{a=1}^{K}\sqrt{|\gamma_a|}\left(\frac{1}{\lambda_a}e^{-\phi_a}\right)^{d_a} = \sqrt{-g}e^{-\phi}\prod_{a=1}^{K}\frac{\sqrt{|\gamma_a|}}{\lambda_a^{d_a}}. \tag{2.10}$$

Consequently, the integration decomposes into K separate integrals over submanifolds, each of which can be computed individually. The corresponding action is then defined on the final submanifold. Note that, from the standpoint of this final action, Lagrangian terms of the form $e^{\phi}\nabla_\mu\xi^\mu$ are total derivatives and can therefore be disregarded when deriving the equations of motion.

2.2 Dimensional reduction over n-sphere

In this section we preform the dimensional reduction of manifold $\mathcal{M}\times\mathbb{S}^n$ over the submanifold $\mathbb{S}^n$. Since the n-sphere is a maximally symmetric space, the curvature invariants are given by:

$$R^{(n)} = n(n-1) \quad\wedge\quad R^{(n)}_{ij}R^{ij}_{(n)} = n(n-1)^2 \quad\wedge\quad R^{(n)}_{ijkl}R^{ijkl}_{(n)} = 2n(n-1). \tag{2.11}$$

Placing this into the scalar curvature yields the following:

$$\mathcal{R} = R + n(n-1)\left[(\nabla\phi)^2 + \lambda^2 e^{2\phi}\right] - 2e^{n\phi}\Box e^{-n\phi}. \tag{2.12}$$

The last term in this expression is a surface term. Consequently, it may be omitted from the action, since it does not contribute to the equations of motion. The remaining invariants can likewise be obtained by straightforward substitution. Instead of presenting the full expressions from this procedure, we only provide the resulting form of the Gauss–Bonnet (2.9) term:

$$\begin{aligned} GB =& n(n-1)(n-2)(n-3)\left(\lambda^4e^{4\phi} + 2\lambda^2e^{2\phi}(\nabla\phi)^2 - (\nabla\phi)^4\right) \\ &+ 2n(n-1)\left(\lambda^2e^{2\phi}R + (n-2)(\nabla\phi)^2\left(\Box\phi - (\nabla\phi)^2\right) - 2e^{n\phi}\nabla_\mu\xi^\mu\right), \end{aligned} \tag{2.13}$$

where the last term in the second row $\propto e^{n\phi}\nabla_\mu\xi^\mu$ represents a total derivative in the action and as such can be disregarded.

2.2.1 Dimensional reduction of 4D Einstein-Hilbert action over $\mathbb{S}^2$

In this section, we consider the dimensional reduction of the Einstein–Hilbert action, commonly referred to as the DREH model. The four-dimensional action is given by:

$$S = \frac{1}{16\pi G_N}\int d^4x\sqrt{-G}\mathcal{R}, \tag{2.14}$$

where G_N is the Newton gravitational constant in four dimensions. Since the reduction is preformed over the $\mathbb{S}^2$, the specific four-dimensional metric is given by:

$$G_{AB} = \left(\begin{array}{c|c} g_{\mu\nu} & 0 \\ \hline 0 & \gamma_{ij}\end{array}\right) \quad\wedge\quad \gamma_{ij} = \frac{1}{\lambda^2}\begin{pmatrix} e^{-2\phi} & 0 \\ 0 & e^{-2\phi}\sin^2\theta\end{pmatrix}. \tag{2.15}$$

where the indices correspond to $i,j\in\{2,3\}$, while $\mu,\nu\in\{0,1\}$. Here λ is simply a dimensional parameter. We also assume that $g_{\mu\nu} = g_{\mu\nu}(x^0,x^1)$. In this case, the scalar curvature (2.12) and the Jacobian (2.10) read:

$$\mathcal{R} = R + 2(\nabla\phi)^2 + 2\lambda^2e^{2\phi} - 2e^{2\phi}\Box e^{-2\phi}. \tag{2.16}$$

$$\mathrm{d}^4X\sqrt{-G} = d^2x\mathrm{d}\theta\mathrm{d}\varphi\frac{1}{\lambda^2}\sqrt{-g}e^{-2\phi}\sin\theta. \tag{2.17}$$

After integrating out the angles and neglecting the surface term, we arrive at the following dimensionally reduced action:

$$S_{red} = \frac{1}{4G_N\lambda^2}\int \mathrm{d}^2x\sqrt{-g}e^{-2\phi}\left[R + 2(\nabla\phi)^2 + 2\lambda^2 e^{2\phi}\right]. \tag{2.18}$$

Let us discuss the dimensionality of the constant appearing in front of the action. Its dimension matches that of the gravitational constant in two dimensions. This correspondence enables us to define the two-dimensional gravitational constant as $G = \lambda^2 G_N$. To construct the complete theory, we must also incorporate matter. We introduce matter in the form of a two-dimensional massless scalar field f. The DREH action then takes the following final form:

$$S_{\mathrm{DREH}} = \frac{1}{4G}\int d^2x\sqrt{-g}e^{-2\phi}\left[R + 2(\nabla\phi)^2 + 2\lambda^2 e^{2\phi}\right] - \frac{1}{2}\int d^2x\sqrt{-g}\,(\nabla f)^2. \tag{2.19}$$

Note that, as a consequence of the dimensional reduction, the reduced action exhibits a cosmological constant term as well. In some cases, matter may instead be introduced as a quantity obtained through dimensional reduction by starting from the four-dimensional scalar field action and then performing the reduction. In this formulation, the matter Lagrangian is multiplied by a factor $e^{-2\phi}$ [98].

2.2.2 Dimensional reduction of 5D Chern-Simons theory over $\mathbb{S}^3$

In this subsection, we preform the dimensional reduction of the five-dimensional Chern–Simons (5DCS) action over $\mathbb{S}^3$, obtaining a two-dimensional dilaton gravity theory. Although 5DCS gravity generally allows for non-zero torsion, here we restrict our analysis to the torsion-free Riemannian sector. The action can be written as [99]:

$$S^{(5)}_{\mathrm{CS}} = \frac{k}{2l^3}\int \mathrm{d}^5x\sqrt{-g}\Big[\mathcal{R} + \frac{6}{l^2} + \frac{l^2}{4}\big(\mathcal{R}^2 - 4\mathcal{R}^{AB}\mathcal{R}_{AB} + \mathcal{R}^{ABCD}\mathcal{R}_{CDAB}\big)\Big]. \tag{2.20}$$

In the same way as in the case of Einstein-Hilbert action, we assume that the metric has a block diagonal form:

$$\mathrm{d}s^2 = g_{\mu\nu}\mathrm{d}x^\mu\mathrm{d}x^\nu + \frac{1}{\lambda^2}e^{-2\phi}\mathrm{d}\Omega_3^2, \tag{2.21}$$

where $\phi = \phi(x^0, x^1)$ is a newly introduced dilaton field, $g_{\mu\nu} = g_{\mu\nu}(x^0, x^1)$ is a two-dimensional metric, and $\mathrm{d}\Omega_3^2 = \mathrm{d}\psi^2 + \sin^2\psi(\mathrm{d}\theta^2 + \sin^2\theta\mathrm{d}\varphi^2) \equiv \gamma_{ij}\mathrm{d}x^i\mathrm{d}x^j$ is a $\mathbb{S}^3$ metric. We use Greek indices $\mu,\nu = 0, 1$ for the remaining two-dimensional manifold, and Latin indices $i, j = 2, 3, 4$ for the $\mathbb{S}^3$. For the $\mathbb{S}^3$ reduction, the scalar curvature. For the $\mathbb{S}^3$ reduction, the scalar curvature (2.12), the Gauss-Bonnet term (2.13) and the Jacobian (2.10) read:

$$\mathcal{R} = R + 6\left((\nabla\phi)^2 + \lambda^2 e^{2\phi}\right) - 2e^{3\phi}\Box e^{-3\phi}, \tag{2.22}$$

$$GB = 12\left(\lambda^2 R e^{2\phi} + (\nabla\phi)^2\left(\Box\phi - (\nabla\phi)^2\right) - 2e^{3\phi}\nabla_\mu\xi^\mu\right), \tag{2.23}$$

$$\mathrm{d}^5X\sqrt{-G} = \mathrm{d}^2x\mathrm{d}\psi\mathrm{d}\vartheta\mathrm{d}\varphi\frac{1}{\lambda^3}e^{-3\phi}\sin^2\psi\sin\vartheta. \tag{2.24}$$

Placing expressions (2.22-2.24) into the action (2.20) we get the following final expression for the action of the dimensionally reduced theory:

$$\begin{aligned} S_{\mathrm{DR5DCS-R}} = \frac{k\pi^2}{(\lambda l)^3}\int \mathrm{d}x^2\sqrt{-g}e^{-3\phi}\bigg[&R\left(1 + 3(\lambda l)^2 e^{2\phi}\right) \\ &+ 6\left((\nabla\phi)^2 + \lambda^2 e^{2\phi}\right) + \frac{6}{l^2} + 3l^2(\nabla\phi)^2\left(\Box\phi - (\nabla\phi)^2\right)\bigg] + S_{\mathrm{mat}}, \end{aligned} \tag{2.25}$$

where S_{mat} is a mater action in two dimensions.

2.3 Dimensional reduction of the full 5DCS theory over $\mathbb{S}^3$

Let us first introduce the five-dimensional theory of Chern-Simons gravity, following the introduction in [99]. As a first step, we introduce the $SO(4,2)$ gauge connection:

$$\mathcal{A} = \frac{1}{2}\Omega^{AB}J_{AB} + \frac{1}{l}E^A P_A, \tag{2.26}$$

where J_{AB} and P_A are generators of the $\mathfrak{so}(4,2)$ Lie algebra, satisfying:

$$\begin{aligned}
&[J_{AB}, J_{CD}] = \eta_{AD}J_{BC} + \eta_{BC}J_{AD} - (C \leftrightarrow D),\\
&[J_{AB}, P_C] = \eta_{BC}P_A - \eta_{AC}P_B,\\
&[P_A, P_B] = J_{AB}.
\end{aligned} \tag{2.27}$$

The parameter l denotes the AdS radius. Using this gauge connection, we can then build the Chern–Simons Lagrangian, which in five dimensions takes the form:

$$-\frac{ik}{3}\int \mathrm{Tr}\Big(\mathcal{F}\wedge\mathcal{F}\wedge\mathcal{A} - \frac{1}{2}\mathcal{F}\wedge\mathcal{A}\wedge\mathcal{A}\wedge\mathcal{A} + \frac{1}{5}\mathcal{A}\wedge\mathcal{A}\wedge\mathcal{A}\wedge\mathcal{A}\wedge\mathcal{A}\Big), \tag{2.28}$$

where the trace is taken in a particular representation of the gauge group. After evaluating this trace, the resulting action can be written in the following form:

$$S^{(5)}_{\mathrm{CS}} = \frac{k}{8}\int \varepsilon_{ABCDE}\Big(\frac{1}{l}\mathcal{R}^{AB}\wedge\mathcal{R}^{CD}\wedge E^E + \frac{2}{3l^3}\mathcal{R}^{AB}\wedge E^C\wedge E^D\wedge E^E + \frac{1}{5l^5}E^A\wedge E^B\wedge E^C\wedge E^D\wedge E^E\Big). \tag{2.29}$$

By varying the action (2.29) we arrive at the following set of equations of motion:

$$\begin{aligned}
&\varepsilon_{ABCDE}\big(\mathcal{R}^{AB} + E^A\wedge E^B\big)\big(\mathcal{R}^{CD} + E^C\wedge E^D\big) = 0,\\
&\varepsilon_{ABCDE}\mathcal{T}^A\big(\mathcal{R}^{BC} + E^B\wedge E^C\big) = 0,
\end{aligned} \tag{2.30}$$

These equations do not require the torsion $\mathcal{T}^A = \mathrm{d}E^A + \Omega^A{}_B\wedge E^B$ to vanish. On the other hand, they are satisfied when the torsion is set to zero. Consequently, it is consistent to focus on the torsionless sector of the theory defined by the action (2.20). This is the most common approach in studies of this class of Lovelock gravity, where Riemannian geometry is assumed from the outset, as we did in the previous section.

What is interesting about the 5DCS gravity is that it admits the dimensionally continued BTZ black hole solution [78, 100].

$$\mathrm{d}s^2 = -\left(r^2-\mu\right)\mathrm{d}t^2 + \frac{1}{(r^2-\mu)}\mathrm{d}r^2 + r^2\mathrm{d}\Omega_3^2, \tag{2.31}$$

where $\mathrm{d}\Omega_3^2$ denotes the metric on the 3-sphere. It is straightforward to see that the choice $\mu=-1$ yields AdS space-time. The field equations (2.30) admit solutions not only with spherical symmetry, but also with more general geometries in which $\mathrm{d}\Omega_3^2$ is replaced by an arbitrary $\mathrm{d}\Sigma_3^2$, where Σ_3 is any fixed manifold describing the horizon geometry [101]. A notable characteristic of this BH solution is that it allows for nontrivial axial torsion. Adopting conventions where the indices $\{i,j,k\}\in\{2,3,4\}$ label directions along Σ_3, the nonvanishing torsion components are given by:

$$\mathcal{T}^i = -\frac{\delta}{r}\varepsilon^{ijk}e^j e^k, \tag{2.32}$$

with δ an arbitrary constant, while all remaining torsion components vanish.

The existence of this black hole with torsion makes this theory an interesting testing ground for the effects of torsion on the fine-grained entropy of gravitational systems. Since most of the Page curve reconstructions are carried out within the framework of two-dimensional dilaton gravity, for simplicity, we preform the dimensional reduction of the full 5DCS to two dimensions.

The first step in this procedure is to find ansatz for the spin-connection and the vielbein which exhibits a spherical symmetry of a 3-sphere. We decompose indices as $(A) = (a, i)$, where lower Latin indices from the beginning of the alphabet indicate two-dimensional Lorentz indices, while indices $i, j, k \dots \in \{2, 3, 4\}$. The five-dimensional vielbein is given by:

$$E^a = e^a_0 \mathrm{d}t + e^a_1 \mathrm{d}r \equiv e^a \qquad \wedge \qquad E^i = \frac{e^{-\phi}}{\lambda} e^i, \tag{2.33}$$

where $e^2 = \mathrm{d}\psi$, $e^3 = \sin\psi\, \mathrm{d}\vartheta$, and $e^4 = \sin\psi\, \sin\vartheta\, \mathrm{d}\varphi$; while $\phi = \phi(x^0, x^1)$ is the dilaton field. The most general static, spherically symmetric Riemann–Cartan space-time in five dimensions [102] admits the following ansatz for the spin connection:

$$\begin{aligned}
&\Omega^{01} = A(x^0, x^1)\mathrm{d}x^1 + B(x^0, x^1)\mathrm{d}x^0 \equiv \omega^{01}, \quad \Omega^{0i} = \phi^0 e^i, \\
&\Omega^{1i} = \phi^1(x^0, x^1) e^i, \quad \Omega^{23} = -\cos\psi \mathrm{d}\vartheta + \theta(x^0, x^1) e^4, \\
&\Omega^{24} = -\cos\psi \sin\vartheta \mathrm{d}\varphi - \theta(x^0, x^1) e^3, \quad \Omega^{34} = -\cos\vartheta \mathrm{d}\varphi + \theta(x^0, x^1) e^2,
\end{aligned} \tag{2.34}$$

where A, B, ϕ^0, ϕ^1 and θ are arbitrary functions defined on the final manifold. Then the components of Riemann-Cartan curvature tensor $\mathcal{R}^{AB} = \mathrm{d}\Omega^{AB} + \Omega^A{}_C \wedge \Omega^{CB}$ can be directly computed. To illustrate how one computes components of the form $\mathcal{R}^{ai}$ we explicitly evaluate component $\mathcal{R}^{02}$:

$$\begin{aligned}
\mathcal{R}^{02} &= \mathrm{d}\Omega^{02} + \Omega^0{}_1 \wedge \Omega^{12} + \Omega^0{}_3 \wedge \Omega^{32} + \Omega^0{}_4 \wedge \Omega^{42} \\
&= \mathrm{d}\phi^0 \wedge \mathrm{d}\psi + \omega^0{}_1 \phi^1 \wedge \mathrm{d}\psi - \phi^0\theta \left(e^3 \wedge e^4 - e^4 \wedge e^3\right).
\end{aligned} \tag{2.35}$$

Furthermore, we demonstrate the procedure for calculating the components R^{ij} by explicitly working out $\mathcal{R}^{23}$:

$$\begin{aligned}
\mathcal{R}^{23} &= \mathrm{d}\Omega^{23} + \Omega^2{}_4 \Omega^{43} + \Omega^2{}_0 \Omega^{03} + \Omega^2{}_1 \Omega^{13} \\
&= \sin\psi\, \mathrm{d}\psi \wedge \mathrm{d}\vartheta + \mathrm{d}\theta - \theta^2 \sin\psi\, \mathrm{d}\psi \wedge \mathrm{d}\vartheta - (\phi_0\phi^0 + \phi_1\phi^1) \sin\psi\, \mathrm{d}\psi \wedge \mathrm{d}\vartheta.
\end{aligned}$$

Generalizing this procedure to other components of the Riemannian curvature tensor, we conclude that:

$$\mathcal{R}^{ai} = (\mathrm{d}\phi^a) e^i - \theta\phi^a \varepsilon^{ijk} e^j e^k, \tag{2.36}$$

$$\mathcal{R}^{ij} = (1 - \phi^a\phi_a - \theta^2) e^i e^j + \mathrm{d}\theta\, \varepsilon^{ijk} e^k. \tag{2.37}$$

One must show that ϕ^a indeed forms a two-dimensional Lorentz vector multiplet. Under $SO(4, 2)$ gauge transformations, A transforms according to $\mathcal{A} \mapsto \mathcal{A}_\epsilon = \mathcal{A} - \mathrm{d}\epsilon$, with $\epsilon = \frac{1}{2}\epsilon^{AB} J_{AB} + \epsilon^A P_A$. Two-dimensional Lorentz transformations are produced by choosing $\epsilon = \varepsilon J_{01}$. A straightforward calculation yields:

$$\delta\mathcal{A} = -\mathrm{d}\varepsilon J_{01} - \varepsilon \left(\Omega^{0i} J_{i1} + \Omega^{i1} J_{i0} - \frac{1}{l} E^0 P_1 + \frac{1}{l} E^1 P_0\right), \tag{2.38}$$

from which we conclude:

$$\begin{aligned}\mathcal{A}_\varepsilon =& \left(\omega^{01}-\mathrm{d}\varepsilon\right)J_{01}+\left(\Omega^{0i}+\varepsilon\Omega^{i1}\right)J_{0i}+\left(\Omega^{1i}+\varepsilon\Omega^{0i}\right)J_{1i}\\ &+\frac{1}{2}\Omega^{ij}J_{ij}+\frac{1}{l}\left(e^0-\varepsilon e^1\right)P_0+\frac{1}{l}\left(e^1+\varepsilon e^0\right)P_1.\end{aligned} \tag{2.39}$$

Substituting (2.34), we obtain the following transformation law for ϕ^a:

$$\phi^0 e^i \to \phi^0 e^i - \varepsilon\phi^1 e^i \quad \wedge \quad \phi^1 e^i \to \phi^1 e^1 + \varepsilon\phi^0 e^i, \quad \Longrightarrow \quad \phi^a \mapsto \phi^a + \varepsilon\varepsilon^a{}_b\phi^b. \tag{2.40}$$

Since this quantity indeed transforms as Lorentz vector, we can utilize a vielbein $e_a{}^\mu$ to define a two-dimensional vector ϕ^μ as $\phi^\mu = e_a{}^\mu\phi^a$. Additionally, (2.39) shows that ϕ is a scalar field.

The next step is to evaluate the whole action (2.29) using the ansatz for the spin-connection (2.34) and for the vielbein (2.33). The resulting reduced action is then given by:

$$\begin{aligned}S_{red} = &-\frac{k\pi^2}{(\lambda l)^3}\int_{\mathcal{N}}\varepsilon_{ab}\, e^{-3\phi}\Big[\big(1+3(\lambda l)^2 e^{2\phi}(1-\phi_c\phi^c)\big)\tilde{R}^{ab}+\frac{3}{l^2}\big(1+(\lambda l)^2e^{2\phi}(1-\phi_c\phi^c)\big)e^a\wedge e^b\\ &+6\lambda e^\phi\big(1+(\lambda l)^2 e^{2\phi}(1-\phi_c\phi^c)\big)e^a\wedge \mathrm{d}\phi^b+6(\lambda l)^2e^{2\phi}\mathrm{d}\phi^a\wedge\mathrm{d}\phi^b\Big]\\ &-3(\lambda l)^2\theta^2 e^{-\phi}\left[\tilde{R}^{ab}+\frac{e^a\wedge e^b}{l^2}-2\lambda e^\phi\phi^a T^b\right].\end{aligned}$$

Note that after performing integration by parts in the last term, it becomes clear that θ^2 plays the role of a Lagrange multiplier. When the two-dimensional torsion vanishes, the precise structure of the term containing θ^2 coincides with that of JT gravity [20, 21]. Consequently, assigning a non-zero value to this field greatly simplifies the resulting equations. The action (2.25) reduces to the Riemannian action (2.25) upon setting $\theta = 0$ and imposing $\phi_\mu = \frac{e^{-\phi}}{\lambda}\nabla_\mu\phi$, with $\phi_\mu = e_\mu{}^a\phi_a$. These relations are implied by the torsion-free condition $T^a = 0$.

Now we rewrite the Riemann-Cartan action (2.41) into a more suitable Riemannian form. Using the notation defined in Appendix A, different terms appearing in (2.41) can be expressed in terms of the metric $g_{\mu\nu}$ and the contorsion 1-form K_μ as follows:

$$\varepsilon_{ab}R^{ab} = -\tilde{R} = -\left(\mathrm{R}+2\varepsilon^{\alpha\beta}\partial_\alpha\mathrm{K}_\beta\right), \tag{2.41}$$

$$\varepsilon_{ab}e^a\wedge e^b = -1, \tag{2.42}$$

$$\varepsilon_{ab}\phi^a T^b = -\phi^\mu T^\nu{}_{\mu\nu} = -\varepsilon^{\mu\nu}\phi_\mu\mathrm{K}_\nu, \tag{2.43}$$

$$\varepsilon_{ab}e^a\wedge\mathrm{d}\phi^b = -\tilde{\nabla}_\mu\phi^\mu = -\left(\nabla_\mu\phi^\mu - \varepsilon^{\mu\nu}\phi_\mu\mathrm{K}_\nu\right), \tag{2.44}$$

$$\varepsilon_{ab}\mathrm{d}\phi^a\wedge\mathrm{d}\phi^b = -\left(\tilde{\nabla}_\mu\phi^\mu\tilde{\nabla}_\nu\phi^\nu - \tilde{\nabla}_\mu\phi^\nu\tilde{\nabla}_\nu\phi^\mu\right), \tag{2.45}$$

where R and $\tilde{R}$ are the Riemannian and Riemann-Cartan scalar curvatures, respectively. In addition, expressions (2.42-2.45) should be multiplied by $\mathrm{d}^2x\sqrt{-g}$. To further simplify equations, we define a reduced dilaton filed x by:

$$\mathrm{x} = \frac{1}{\lambda l}e^{-\phi}. \tag{2.46}$$

Putting all terms (2.42-2.45) into action (2.41) and using the reduced field (2.46), the action becomes:

$$\begin{aligned}S_{\mathrm{DRCS}_5} =& \frac{k\pi^2}{(\lambda l)^3}\int \mathrm{d}^2x\sqrt{-g}e^{-3\phi}\Bigg\{\left(1+\frac{3}{\mathrm{x}^2}\left(1-\Phi^2-\theta^2\right)\right)\left[\mathrm{R}+2\varepsilon^{\alpha\beta}\partial_\alpha\mathrm{K}_\beta+\frac{2}{l^2}\right]\\ &+\frac{4}{l^2}+\frac{6}{l\mathrm{x}^3}\theta^2\nabla_\alpha\phi^\alpha+\frac{6}{l\mathrm{x}}\left(1+\frac{1}{\mathrm{x}^2}\left(1-\Phi^2-\theta^2\right)\right)\left[\nabla_\alpha\phi^\alpha-\varepsilon^{\alpha\beta}\phi_\alpha\mathrm{K}_\beta\right]\\ &-\frac{6}{\mathrm{x}^2}\left[\nabla_\alpha\phi^\beta\nabla_\beta\phi^\alpha-\nabla_\alpha\phi^\alpha\nabla_\beta\phi^\beta-\varepsilon^{\alpha\beta}\mathrm{K}_\alpha\nabla_\beta\Phi^2\right]\Bigg\}+S_{\mathrm{mat}},\end{aligned} \tag{2.47}$$

where $\Phi^2 \equiv \phi^\alpha \phi_\alpha$, and S_{mat} denotes the action of the matter fields. The remaining part of the action is attributed to gravity. This action is a functional of the metric $g_{\mu\nu}$, the contorsion K_μ, the vector field ϕ^μ arising from the five-dimensional spin connection, the scalar field θ linked to the five-dimensional torsion, and the dilaton field ϕ, which plays the role of the radial coordinate in five dimensions.

Chapter 3

Dilaton gravity in two dimensions

In the previous chapter, we developed a systematic procedure for performing dimensional reduction of a gravitational theory between arbitrary spacetime dimensions. This process necessarily led to the appearance of new dilaton fields as an integral part of the reduction. Dimensional reduction offers several advantages. First, it yields an effective theory in fewer dimensions, which is significantly more tractable. Second, and more importantly, the reduced theory preserves the solutions of the original higher-dimensional theory that reflect the topology of the manifold used in the reduction. For instance, if one is interested in spherically symmetric vacuum solutions of a higher-dimensional theory, then performing a reduction over a sphere ensures that these configurations remain valid solutions in the lower-dimensional theory. Third, some fine-grained thermodynamic quantities, such as entanglement entropy, are known in closed analytic form only in a smaller number of dimensions. Therefore, applying dimensional reduction is a much need prerequisite for examining these thermodynamic properties.

The dimensionality of the final manifold has not yet been specified. In this chapter, we focus on the general features of two-dimensional dilaton gravity. A two-dimensional spacetime offers an excellent setting for studying entanglement entropy, because in two dimensions there exist well-defined formulas for computing it. As these theories arise from a dimensional reduction of a higher-dimensional theory, their thermodynamic characteristics retain traces of the original higher-dimensional system, thereby providing a window into the thermodynamics of higher dimensional black hole solutions.

In order to study Hawking radiation and its thermodynamic characteristics, one must take into account the back-reaction of quantum fields on the spacetime geometry. This requires computing an effective action, at least up to one-loop order. In the case of a two-dimensional massless scalar field, this effective action is known as the Polyakov–Liouville (PL) action [22]. An additional remarkable feature of the 2D setting is that the PL action is exact at the one-loop level.

As established in the previous chapter, performing a dimensional reduction of a Riemannian spacetime leads to the emergence of several dilaton fields ϕ_a, whose number and structure are determined by the topology of the manifold on which the reduction is carried out. Imposing that the original action contains terms at most quadratic in the curvature, the resulting reduced action has the following form:

$$S[\phi_a, g_{\mu\nu}] \propto \int \mathrm{d}^2x\sqrt{-g}e^{-\sum_a d_a\phi_a}\left(\mathcal{F}_0[\phi_a] + \mathcal{F}_1[\phi_a]R + \mathcal{F}_2[\phi_a]R^2\right), \tag{3.1}$$

where the functionals $\mathcal{F}_i[\phi_a]$ depend on the dilaton fields and involve at most four derivatives. This structure follows directly from (2.6-2.8). Moreover, we have exploited the specific features of the two-dimensional spacetime (A.15) to express both the Riemann curvature tensor and the Ricci tensor solely in terms of the Ricci scalar. Note that for higher-dimensional gravity theories involving the Gauss-Bonnet term (2.9), there is no second-order curvature term in the reduced action as Gauss-Bonnet in 2D vanishes.

For a dimensional reduction of a full Riemann–Cartan theory with non-vanishing torsion, the resulting action involves many additional fields. Besides the dilaton associated with the higher-dimensional vielbeins, there appear both scalar and vector fields arising from the higher-dimensional spin connection. The two-dimensional geometry is then characterized by the metric $g_{\mu\nu}$ and the contorsion K_μ (see Appendix A).

This chapter consists of four main parts. In the first part, we present an ansatz for the metric, 1-form, vector field, spinor field, and more generally for any tensor field in spacetimes that admit at least one non-null Killing vector. To construct this ansatz, we choose one of the dilatons ϕ_a as a radial coordinate, thereby expressing all remaining fields as functions of that single dilaton. The second part addresses how the covariant conservation laws of the energy–momentum tensor are modified in the presence of non-vanishing torsion. Our derivation closely follows [81], but we additionally incorporate non-minimally coupled fields, which leads to an even more intricate structure of the conservation laws. These laws are crucial in deriving several thermodynamical properties of gravitational theories. The penultimate section presents the Polyakov–Liouville action, which serves as the framework for incorporating the quantum corrections. The transformations of the energy-momentum tensor, as well as different vacuum states are discussed in detail. Finally, in the concluding section, we examine how to construct a gravitational collapse scenario within the framework of two-dimensional dilaton gravity. As a by-product of this analysis, we obtain an alternative method for deriving the mass of the spacetime.

3.1 Symmetric ansatz setup for two-dimensional spacetime

We consider an ansatz for symmetric solutions in a two-dimensional spacetime. That implies the presence of at least one Killing vector. We focus on configurations with a single Killing vector, which may be either time-like or space-like. Because these two situations are analogous with respect to the ansatz for the field content of the theory,, we will present the procedure specifically for the case of a time-like Killing vector.

In two dimensions, any stationary spacetime is necessarily static. This indicates that the existence of a time-like Killing vector is the only requirement for the geometry to be static. The ansatz for the metric is taken to have the form:

$$\mathrm{d}s^2 = -e^{2\rho}\mathrm{d}x^+\mathrm{d}x^-, \tag{3.2}$$

so that the conformal gauge is satisfied. This is always possible in two dimensions. Using this ansatz, the Christoffel symbols and scalar curvature are as follows:

$$\Gamma^{\pm}_{\pm\pm} = 2\partial_\pm\rho \qquad \wedge \qquad R = 8e^{-2\rho}\partial_+\partial_-\rho. \tag{3.3}$$

In this gauge, for an arbitrary function f, the scalar quantities are given by:

$$\Box f = -4e^{-2\rho}\partial_+\partial_- f \qquad \wedge \qquad (\nabla f)^2 = -4e^{-2\rho}\partial_+ f\partial_- f. \tag{3.4}$$

Let us assume that there exists a time-like Killing vector:

$$\xi = \partial_t = \mathrm{F}^-(x^-)\partial_- - \mathrm{F}^+(x^+)\partial_+. \tag{3.5}$$

The functions $\mathrm{F}^{\pm}$ are the coordinate transformations from arbitrary coordinates $x^{\pm}$ to the Eddington–Finkelstein–type coordinates $\sigma^{\pm} = t \pm \sigma$, defined by the following relation:

$$\frac{\mathrm{d}\sigma^{\pm}}{\mathrm{d}x^{\pm}} = -\frac{1}{\mathrm{F}^{\pm}}. \tag{3.6}$$

Stating that the spacetime is in the Eddington-Finkelstein gauge amounts to fixing $\mathrm{F}^{+} = -1$ and $\mathrm{F}^{-} = 1$. In this way, we preserve the arbitrary choice of the coordinates within the conformal gauge. Note that we use the same label ξ to denote both the Killing vector and the associated Killing one-form.

The reduced field x can always be introduced by selecting one of the dilatons such that:

$$L\,\mathrm{x} = \frac{1}{\lambda_r} e^{-\phi_r} \equiv r, \tag{3.7}$$

where L is the characteristic length scale of the model (for the AdS spacetime, it is the AdS radius l as in (2.46), while for the Schwarzschild black hole, it equals the Schwarzschild radius a). The quantity r therefore acts as the radial coordinate in the higher-dimensional theory. In two dimensions, we can similarly take $l\mathrm{x}$ to serve as the radial coordinate. This choice is also convenient for comparing the two-dimensional theory with the higher-dimensional one from which it is derived.

For any scalar field f, including the remaining dilaton fields, the presence of a time-like Killing vector implies $\xi^{\mu}\nabla_{\mu} f = 0$, which means that f depends only on the spatial coordinate, $f = f(\mathrm{x})$. The norm of ξ defines the metric function $\Lambda(\mathrm{x})$:

$$\xi^2 = \xi^{\mu}\xi_{\mu} = \mathrm{F}^{+}\mathrm{F}^{-}e^{2\rho} \equiv \Lambda(\mathrm{x}), \tag{3.8}$$

which represents the g_{tt} component of the metric in the (t, r) coordinates. It depends only on the dilaton field (coordinate r) since there is a time-like Killing vector.

In two-dimensional spacetime, a basis in the space of 1-forms can be chosen to be $\{\xi, \star\xi\}$, since these two are orthogonal in a sense $\xi^{\mu}(\star\xi)_{\mu} = 0$. There are also restrictions on the vector fields (1-forms) related to the existence of ξ. Any 1-form A can be expressed as:

$$A = A^{\parallel}(x^{+}, x^{-})\xi - A^{\perp}(x^{+}, x^{-}) \star \xi, \tag{3.9}$$

where $A^{\parallel}$ and $A^{\perp}$ are parallel and perpendicular components of 1-form A with regard to Killing 1-form ξ. Then, the restrictions are given by:

$$\mathcal{L}_{\xi} A = 0 \quad \iff \quad \xi^{\alpha}\nabla_{\alpha} A_{\beta} + A^{\alpha}\nabla_{\beta}\xi_{\alpha} = 0, \tag{3.10}$$

where $\mathcal{L}_{\xi}$ is a Lie derivative along the ξ vector field. Inserting ansatz (3.9) reduces Equation (3.10) to:

$$\left(\xi^{\alpha}\nabla_{\alpha} A^{\parallel}\right)\xi_{\beta} + \left(\xi^{\alpha}\nabla_{\alpha} A^{\perp}\right)\varepsilon_{\beta\delta}\xi^{\delta} = 0. \tag{3.11}$$

The terms in (3.11) are mutually orthogonal, which implies that each one of them is equal to zero. This in turn means that $A^{\parallel} = A^{\parallel}(\mathrm{x})$ and $A^{\perp} = A^{\perp}(\mathrm{x})$. We conclude that any 1-form can be expressed as:

$$A_{\mu} = A^{\parallel}(\mathrm{x})\xi_{\mu} + A^{\perp}(\mathrm{x})\varepsilon_{\mu\nu}\xi^{\nu}. \tag{3.12}$$

The 1-form $\nabla_{\mu}\mathrm{x}$ can also be written in form (3.12), but the condition $\xi^{\mu}\nabla_{\mu}\mathrm{x} = 0$ implies that there is no parallel component:

$$\nabla_{\mu}\mathrm{x} = \frac{1}{L}\mathcal{D}(\mathrm{x})\varepsilon_{\mu\nu}\xi^{\nu}. \tag{3.13}$$

By applying the same reasoning, namely that $\mathcal{L}_\xi T = 0$ for a rank-2 tensor T, we are led to the following ansatz for T:

$$T_{\mu\nu} = T^{\parallel\parallel}(\mathrm{x})\xi_\mu\xi_\nu + T^{\perp\perp}(\mathrm{x})\varepsilon_{\mu\rho}\varepsilon_{\nu\sigma}\xi^\rho\xi^\sigma + \left(T^{\parallel\perp}(\mathrm{x})\xi_\mu\varepsilon_{\nu\rho} + T^{\perp\parallel}(\mathrm{x})\xi_\nu\varepsilon_{\mu\rho}\right)\xi^\rho. \tag{3.14}$$

This procedure can be easily generalized to tensors of any rank. A symmetric ansatz for a spinor field can likewise be formulated. We begin by writing the Kosmann-Lie derivative for a spinor field [103, 104]:

$$\mathcal{L}_\xi\psi = \xi^\mu\nabla_\mu\psi + \frac{1}{4}\nabla_a\xi_b\gamma^a\gamma^b\psi. \tag{3.15}$$

For further information on the spinor notation employed in this work, refer to Appendix A. Imposing that the spinor field satisfies the symmetry condition leads to the following equation:

$$\mathcal{L}_\xi\psi \equiv \begin{pmatrix} -\mathrm{F}^+\partial_+ + \mathrm{F}^-\partial_- + \frac{1}{4}\left(\partial_+\mathrm{F}^+ + \partial_-\mathrm{F}^-\right) \\ -\mathrm{F}^+\partial_+ + \mathrm{F}^-\partial_- - \frac{1}{4}\left(\partial_+\mathrm{F}^+ + \partial_-\mathrm{F}^-\right)\end{pmatrix}\psi = 0. \tag{3.16}$$

Then, the ansatz for the spinor field is given by:

$$\psi = \begin{pmatrix} \left|\frac{\mathrm{F}^+}{\mathrm{F}^-}\right|^{\frac{1}{4}}\varphi(\mathrm{x})e^{i\alpha(\mathrm{x})} \\ \left|\frac{\mathrm{F}^-}{\mathrm{F}^+}\right|^{\frac{1}{4}}\chi(\mathrm{x})e^{i\beta(\mathrm{x})}\end{pmatrix}, \tag{3.17}$$

where φ, χ, α, and β denote unknown functions that depend solely on the dilaton field x.

Now, we can express the tortoise coordinate $\sigma(\mathrm{x}) = \frac{1}{2}(\sigma^+ - \sigma^-) = -\frac{1}{2}\left(\int\frac{\mathrm{d}x^+}{\mathrm{F}^+} + \int\frac{\mathrm{d}x^-}{\mathrm{F}^-}\right)$ and subsequently the metric in the $(t, l\mathrm{x})$ coordinates:

$$\frac{\sigma}{L} = -\int\frac{\mathrm{dx}}{\Lambda\mathcal{D}} = -\frac{1}{2L}\left(\int\frac{\mathrm{d}x^+}{\mathrm{F}^+} + \int\frac{\mathrm{d}x^-}{\mathrm{F}^-}\right), \tag{3.18}$$

$$\mathrm{d}s^2 = \Lambda\mathrm{d}t^2 - \frac{l^2\mathrm{dx}^2}{\Lambda\mathcal{D}^2}. \tag{3.19}$$

Equation (3.18) gives the coordinate dependence of the dilaton field $\mathrm{x} = \mathrm{x}(x^+, x^-)$, while (3.19) implies that another coordinate transformation can be performed to change the metric to a standard form associated with the black hole solutions:

$$\frac{\mathrm{dx}}{\mathrm{d\bar{x}}} = \mathcal{D} \quad\Longrightarrow\quad \mathrm{d}s^2 = \Lambda(\bar{\mathrm{x}})\mathrm{d}t^2 - \frac{l^2\mathrm{d\bar{x}}^2}{\Lambda(\bar{\mathrm{x}})}. \tag{3.20}$$

In some cases, another coordinate transformation may be performed:

$$\frac{\mathrm{dz}}{\mathrm{d\bar{x}}} = -\frac{1}{\sqrt{-\Lambda}} \quad\Longrightarrow\quad \mathrm{d}s^2 = \Lambda(\mathrm{z})\mathrm{d}t^2 + l^2\mathrm{dz}^2, \tag{3.21}$$

when $\Lambda < 0$. In a case when $\Lambda > 0$ a substitution $\mathrm{z} = i\tilde{\mathrm{z}}$ is consistent. New coordinate $\tilde{\mathrm{z}}$ is time-like, implying that the Killing vector ξ is space-like. In this case, we have a cosmological solution.

To summarize, by demanding the existence of a time-like Killing vector field ξ the two-component vector field A^μ is replaced with two scalar functions $A^\parallel(\mathrm{x})$ and $A^\perp(\mathrm{x})$, one orthogonal and the other perpendicular to the Killing field; the two-component spinor field ψ is equivalent to four scalar functions $\varphi(\mathrm{x})$, $\chi(\mathrm{x})$, $\alpha(\mathrm{x})$ and $\beta(\mathrm{x})$; metric is replaced with a function $\Lambda(\mathrm{x})$, while the dilaton field x is regarded as a coordinate and a derivatives of a dilaton field introduce another scalar function $\mathcal{D}(\mathrm{x})$.

Note that the arguments presented here are not applicable when the Killing vector is light-like, because ξ and $\star\xi$ cease to span the entirety of the 1-form space. Since we had to include an auxiliary function $\mathcal{D}$ to play the role of the derivative of the dilaton, an additional integration constant may appear when solving the equations of motion. This constant has no physical significance and therefore must be fixed by imposing suitable conditions. Up to this point, we have not specified the asymptotic behavior of the solution. Requiring the spacetime to be asymptotically flat yields extra conditions on the norm of the time-like Killing vector at infinity and on the behavior of the tortoise coordinate (3.18) at large distances. Interpreting the dilaton x as a radial coordinate, these two constraints read:

$$\lim_{\mathrm{x}\to\infty} \Lambda = -1 \qquad \wedge \qquad \lim_{\mathrm{x}\to\infty} \sigma = +\infty. \tag{3.22}$$

If, instead, the spacetime approaches AdS at infinity, a different set of asymptotic conditions must be enforced:

$$\Lambda \sim -\mathrm{x}^2(\mathrm{x}),\ \mathrm{x}\to\infty \qquad \wedge \qquad \lim_{\mathrm{x}\to\infty} \sigma = +\infty. \tag{3.23}$$

In summary, one must always prescribe the asymptotic form of the norm of the Killing vector, consistent with the spacetime symmetries, and at the same time require that the tortoise coordinate (3.18) diverges to $+\infty$ as the radial coordinate is taken to infinity.

At the end of this subsection, we give a collection of useful expressions involving different vector fields is given here:

$$\nabla_\mu \xi_\nu = \frac{\mathcal{D}}{2L}\frac{\mathrm{d}\Lambda}{\mathrm{dx}}\varepsilon_{\mu\nu}, \tag{3.24}$$

$$\nabla_\mu A^\mu = -\frac{\mathcal{D}}{L}\frac{\mathrm{d}}{\mathrm{dx}}\left(\Lambda A^\perp\right), \tag{3.25}$$

$$\varepsilon^{\mu\nu}\nabla_\mu A_\nu = -\frac{\mathcal{D}}{L}\frac{\mathrm{d}}{\mathrm{dx}}\left(\Lambda A^\parallel\right), \tag{3.26}$$

$$\varepsilon^{\mu\nu}A_\mu B_\nu = \Lambda\left(A^\parallel B^\perp - A^\perp B^\parallel\right), \tag{3.27}$$

$$A^\mu B_\mu = \Lambda\left(A^\parallel B^\parallel - A^\perp B^\perp\right), \tag{3.28}$$

where ξ is the Killing vector field, $\Lambda = \xi^2$, while A and B are two arbitrary vector fields. For the scalars, we have the following set of formulas:

$$R = \frac{\mathcal{D}}{L^2}\frac{\mathrm{d}}{\mathrm{dx}}\left(\mathcal{D}\frac{\mathrm{d}\Lambda}{\mathrm{dx}}\right), \tag{3.29}$$

$$\tilde{R} = \frac{\mathcal{D}}{L^2}\frac{\mathrm{d}}{\mathrm{dx}}\left(\mathcal{D}\frac{\mathrm{d}\Lambda}{\mathrm{dx}} - 2L\Lambda\mathrm{K}^\parallel\right), \tag{3.30}$$

$$\Box\mathrm{x} = -\frac{\mathcal{D}}{L^2}\frac{\mathrm{d}}{\mathrm{dx}}\left(\Lambda\mathcal{D}\right), \tag{3.31}$$

$$\left(\nabla\mathrm{x}\right)^2 = -\frac{\Lambda\mathcal{D}^2}{L^2}, \tag{3.32}$$

where $\mathrm{K}^\parallel$ is a component of contorsion parallel to the Killing field ξ, $\tilde{R}$ is the Riemann-Cartan scalar curvature, while R is the Riemannian scalar curvature. Finally, for the rank-2 tensor field $T_{\mu\nu}$ we have:

$$g^{\mu\nu}T_{\mu\nu} \equiv T = \Lambda\left(T^{\parallel\parallel} - T^{\perp\perp}\right), \tag{3.33}$$

$$\mathrm{F}^{\pm 2}T_{\pm\pm} = \frac{\Lambda^2}{4}\left[T^{\parallel\parallel} + T^{\perp\perp} \mp \left(T^{\parallel\perp} + T^{\perp\parallel}\right)\right]. \tag{3.34}$$

Note that, in the case of a symmetric tensor, we obtain $T^{\parallel\perp} = T^{\perp\parallel}$.

3.2 Covariant conservation laws

In this section, we investigate the modifications to the covariant conservation law for the energy-momentum tensor due to the presence of a non-zero torsion within the two-dimensional theory. In this prescription, the main sources are the energy-momentum tensor $T_{\mu\nu}$ and the contorsion current T^{K}_{μ}, the latter of which is obtained by taking the variational derivative of the matter action with respect to the contorsion. In section 2.3 we show that the fundamental fields of the theory transform as expected with respect to the local Lorentz transformations (2.40) in the case of the dimensional reduction of 5D Chern-Simons theory. Naturally, it is expected that this holds true for any well-defined dimensional reduced theory. We analyze the symmetry properties according to the Poincaré gauge theory (for more details, see [81]). The idea is to localize the Poincaré group. The compensating fields, which are introduced within this process of localization, are interpreted as spin-connection $\omega^{ab}{}_{\mu}$ and vielbeins $e_a{}^{\mu}$, and subsequently the resulting geometry is interpreted as Riemann-Cartan geometry discussed in Appendix A.

The infinitesimal local Poincaré transformations in two dimensions are parametrized by a translation vector $\varepsilon^{\mu}(x)$ and a rotation angle $\theta(x)$, namely:

$$x^{\mu} \mapsto x'^{\mu} = x^{\mu} + \zeta^{\mu}(x) \equiv x^{\mu} + \varepsilon^{\mu}(x) + \theta(x)\varepsilon^{\mu\nu}x_{\nu}, \tag{3.35}$$

where we have used $\theta_{\mu\nu} = \theta\varepsilon_{\mu\nu}$ in two dimensions. The matter fields then transform according to the following law:

$$\phi(x) \mapsto \phi'(x) = e^{\frac{1}{2}\theta_{\mu\nu}(x)M^{\mu\nu}+\varepsilon_{\mu}(x)P^{\mu}}\phi(x), \tag{3.36}$$

where $M_{\mu\nu} = x_{\mu}\partial_{\nu} - x_{\nu}\partial_{\mu} - \Sigma\varepsilon_{\mu\nu}$ and $P_{\mu} = -\partial_{\mu}$ are generators of rotations and translations that belong to the respective representation of the Poincaré group associated with the field ϕ, and $\Sigma_{\mu\nu} = -\Sigma\varepsilon_{\mu\nu}$ is the matrix part of the Lorentz generator. Infinitesimally, the form-variation of the matter fields can be expressed as:

$$\delta_0\phi(x) = \mathcal{P}\phi(x) \equiv \left(\theta\Sigma - \zeta^{\mu}\partial_{\mu}\right)\phi(x). \tag{3.37}$$

When there is a global Poincaré symmetry present, the derivative of a field transforms according to:

$$\delta_0(\partial_{\mu}\phi) = \mathcal{P}\partial_{\mu}\phi - \partial_{\mu}\zeta^{\nu}\partial_{\nu}\phi. \tag{3.38}$$

The localization procedure consists of two steps. First, one introduces a connection (gauge field) so that the transformation law of the newly defined covariant derivative of the field (A.3) has the same form as (3.38), i.e.

$$\delta_0\left(\tilde{\nabla}_{\mu}\phi\right) \equiv \mathcal{P}\tilde{\nabla}_{\mu}\phi - \partial_{\mu}\zeta^{\nu}\tilde{\nabla}_{\nu}\phi. \tag{3.39}$$

Then, one demands that, in the local reference frame, the covariant derivative transforms the same way as in the flat case:

$$\delta_0(\tilde{\nabla}_a\phi) \equiv \mathcal{P}\tilde{\nabla}_a\phi + \theta\varepsilon_a{}^{b}\tilde{\nabla}_b\phi, \tag{3.40}$$

where $\tilde{\nabla}_a\phi \equiv e_a{}^{\mu}\tilde{\nabla}_{\mu}\phi$. Equation (3.40) introduces another set of compensating fields, i.e. vielbeins $e_a{}^{\mu}$. For more details on spinor notations see Appendix A. Using equations (3.39) and (3.40) one derives the form variations of the compensating fields ω_{μ} and $e_a{}^{\mu}$, given by:

$$\delta_0\omega_{\mu} = -\zeta^{\alpha}\partial_{\alpha}\omega_{\mu} - \omega_{\alpha}\partial_{\mu}\zeta^{\alpha} - \partial_{\mu}\theta, \tag{3.41}$$

$$\delta_0 e_a{}^{\mu} = \theta\varepsilon_a{}^{b}e_b{}^{\mu} + e_a{}^{\alpha}\partial_{\alpha}\zeta^{\mu} - \zeta^{\alpha}\partial_{\alpha}e_a{}^{\mu}. \tag{3.42}$$

Next, we define the gauge-invariant quantities, that is, the field-strength tensors for the $\omega^{ab}{}_{\mu}$ connection and the vielbein $e_a{}^{\mu}$, $\tilde{R}^{ab}{}_{\mu\nu}$, and $T^a{}_{\mu\nu}$, respectively, given by equations (A.13) and (A.14). From a geometric standpoint, they represent the curvature and torsion of the underlying Riemann-Cartan manifold. The metric $g_{\mu\nu}$, defined by (A.1), transforms in the following way (using the transformation law for vielbein (3.42)):

$$\delta_0 g^{\mu\nu} = \left(g^{\nu\alpha}\delta^{\mu}{}_{\beta} + g^{\mu\alpha}\delta^{\nu}{}_{\beta}\right)\partial_\alpha\zeta^\beta - \zeta^\alpha\partial_\alpha g^{\mu\nu}. \tag{3.43}$$

Using (3.41-3.42) the separate parts of the spin-connection have the following form variations:

$$\delta_0\Delta_\mu = -\zeta^\alpha\partial_\alpha\Delta_\mu - \Delta_\alpha\partial_\mu\zeta^\alpha - \partial_\mu\theta, \tag{3.44}$$
$$\delta_0\mathrm{K}_\mu = -\zeta^\alpha\partial_\alpha\mathrm{K}_\mu - \mathrm{K}_\alpha\partial_\mu\zeta^\alpha. \tag{3.45}$$

From these equations, it is evident that contorsion K_μ behaves as a 1-form, in contrast to Δ_μ. Finally, we find the transformation laws for the curvature and the torsion. They are given by:

$$\delta_0\tilde{R} = -\zeta^\alpha\partial_\alpha\tilde{R}, \tag{3.46}$$
$$\delta_0 T^\mu = \mathrm{K}^\alpha\partial_\alpha\zeta^\mu - \zeta^\alpha\partial_\alpha\mathrm{K}^\mu. \tag{3.47}$$

It is easy to check that the torsion transforms as a vector under the local Poincaré transformations, that is:

$$\delta T^a = \theta\varepsilon^a{}_b T^b. \tag{3.48}$$

The condition for the invariance of the action results in the following equation for the Lagrangian of the theory:

$$\Delta\tilde{\mathcal{L}} \equiv \delta_0\tilde{\mathcal{L}} + \partial_\alpha\left(\tilde{\mathcal{L}}\zeta^\alpha\right) = 0, \tag{3.49}$$

where $\tilde{\mathcal{L}} \equiv \sqrt{-g}\mathcal{L}$ [81]. For instance, by its very construction, the action (2.47) is invariant under Poincaré transformations. Moreover, it is straightforward to verify that the condition (3.49) holds, making use of the transformation laws (3.42-3.47) and (2.40). This is expected to occur for all properly defined dimensionally reduced theories.

Now, we investigate the conditions which are imposed on the action of the matter fields due to the local Poincaré invariance. To make the matter action manifestly invariant, we demand that its Lagrangian depends only on the quantities that transform covariantly under the Poincaré group, i.e.

$$\mathcal{L}_{\mathrm{M}} = \mathcal{L}_{\mathrm{M}}\left(g^{\mu\nu}, \omega_\mu, \phi, \tilde{\nabla}_\mu\phi, \tilde{R}, T^\mu\right). \tag{3.50}$$

Notice that a non-minimal coupling is allowed since the matter action can directly depend on curvature and torsion. This violates the equivalence principle. Nonetheless, we will continue to examine these scenarios as well. Next, we define the following dynamical currents:

$$\tau_{\mu\nu} \equiv -\frac{2}{\sqrt{-g}}\frac{\partial\tilde{\mathcal{L}}_{\mathrm{M}}}{\partial g^{\mu\nu}}, \quad \sigma^\mu \equiv \frac{\partial\mathcal{L}_{\mathrm{M}}}{\partial\omega_\mu}, \quad \varrho \equiv \frac{\partial\mathcal{L}_{\mathrm{M}}}{\partial\tilde{R}}, \quad \tau_\mu \equiv \frac{\partial\mathcal{L}_{\mathrm{M}}}{\partial T^\mu}. \tag{3.51}$$

Using the form-variations (3.41), (3.43), (3.46-3.47), on-shell condition (3.49) for the matter Lagrangian can be expressed in the following form:

$$\Delta\tilde{\mathcal{L}}_{\mathrm{M}} \equiv \sqrt{-g}\zeta^\beta\mathrm{I}_\beta + \theta\mathrm{I} + \partial_\alpha\left(\sqrt{-g}\Lambda^\alpha\right) = 0, \tag{3.52}$$

where the quantities I, I_β and Λ^α are given by:

$$\Lambda^\alpha = \theta\left[\frac{\partial\mathcal{L}_{\mathrm{M}}}{\partial(\tilde{\nabla}_\alpha\phi)}\Sigma\phi - \sigma^\alpha\right] - \zeta^\beta\left[\frac{\partial\mathcal{L}_{\mathrm{M}}}{\partial(\tilde{\nabla}_\alpha\phi)}\partial_\beta\phi - \mathcal{L}_{\mathrm{M}}\delta^\alpha{}_\beta + \tau^\alpha{}_\beta + \sigma^\alpha\omega_\beta - \tau_\beta\mathrm{K}^\alpha\right], \tag{3.53}$$

$$\mathrm{I} = \partial_\mu\left(\sqrt{-g}\sigma^\mu\right), \tag{3.54}$$

$$\mathrm{I}_\beta = \frac{1}{\sqrt{-g}}\partial_\alpha\left[\sqrt{-g}\left(\tau^\alpha{}_\beta + \sigma^\alpha\omega_\beta - \tau_\beta\mathrm{K}^\alpha\right)\right] + \frac{1}{2}\tau_{\mu\nu}\partial_\beta g^{\mu\nu} - \sigma^\alpha\partial_\beta\omega_\alpha - \tau_\alpha\partial_\beta\mathrm{K}^\alpha - \varrho\partial_\beta\tilde{R}. \tag{3.55}$$

Because the parameters θ and ε^α (or ζ^α) can take any values, nullifying the term $\Delta\tilde{\mathcal{L}}_{\mathrm{M}}$ requires that I, I_β, and Λ^α be equal to zero. With Λ^α being dependent on these parameters as well, each term within the brackets in Equation (3.53) must thus vanish, leading to the following two conditions:

$$\sigma^\alpha = \frac{\partial\mathcal{L}_{\mathrm{M}}}{\partial(\tilde{\nabla}_\alpha\phi)}\Sigma\phi \equiv S^\alpha \tag{3.56}$$

$$-\tau^\alpha{}_\beta + \tau_\beta\mathrm{K}^\alpha = \frac{\partial\mathcal{L}_{\mathrm{M}}}{\partial(\tilde{\nabla}_\alpha\phi)}\tilde{\nabla}_\beta\phi - \delta^\alpha{}_\beta\mathcal{L}_{\mathrm{M}} \equiv T^{(\mathrm{M})\alpha}{}_\beta. \tag{3.57}$$

The first Equation (3.56) demonstrates that the dynamical spin-current σ^α matches the spin tensor of the matter fields S^α. In contrast, the subsequent Equation (3.57) illustrates the relationship between the covariant energy-momentum tensor of the matter fields $T^{(\mathrm{M})\alpha}{}_\beta$ and the dynamical currents specified in (3.51). Note that this quantity is not equal to the energy-momentum tensor derived by varying the matter action with respect to the metric.

By setting $\mathrm{I} = 0$ (3.54) and employing the Riemannian covariant derivative ∇_μ associated with the Levi-Civita connection, we derive the ensuing conservation law for the dynamical spin-current:

$$\nabla_\mu\sigma^\mu = 0. \tag{3.58}$$

Finally, imposing the condition $\mathrm{I}_\beta = 0$ leads to the covariant conservation law associated with the dynamical current $\tau^{\alpha\beta}$, specifically:

$$\nabla_\alpha\tau^{\alpha\beta} = -\frac{1}{2}\tilde{R}\varepsilon^{\beta\alpha}\sigma_\alpha + \nabla_\alpha\left(\mathrm{K}^\alpha\tau^\beta\right) + \tau_\alpha\nabla^\beta\mathrm{K}^\alpha + \varrho\nabla^\beta\tilde{R}, \tag{3.59}$$

where we have once more employed the Riemannian covariant derivative.

Currently, the covariant conservation laws have been identified, but they are related to the dynamical currents specified by Equation (3.51), and not directly to the energy-momentum tensor $T^{\mu\nu}$, which is obtained by varying the matter action in relation to the metric, nor to the contorsion current T^μ_{K}, which results from variation with respect to the contorsion. Since the metric and contorsion are the only independent variables present in the theory, given that torsion, curvature, and the spin connection are intrinsically determined by their derivatives, it inevitably follows that there exist conservation laws that are reliant solely on $T^{\mu\nu}$ and T^μ_{K}. To obtain these, we first express the contorsion current and energy-momentum tensor in terms of dynamical currents. Varying the matter action with respect to contorsion results in:

$$-T^\mu_{\mathrm{K}} = \sigma^\mu + \tau^\mu + 2\varepsilon^{\mu\nu}\partial_\nu\varrho, \tag{3.60}$$

while, the variation with respect to the metric yileds:

$$T^{\mu\nu} = \tau^{\mu\nu} + \frac{1}{2}\left(\varepsilon^{\mu\alpha}g^{\nu\beta} + \varepsilon^{\nu\alpha}g^{\mu\beta}\right)\nabla_\alpha\sigma_\beta + 2\left[\nabla^\mu\nabla^\nu\varrho - g^{\mu\nu}\left(\Box\varrho + \frac{1}{2}\varrho\tilde{R}\right)\right] - \left(\tau^\mu\mathrm{K}^\nu + \tau^\nu\mathrm{K}^\mu\right). \tag{3.61}$$

The next step is to find the covariant derivatives $\nabla_\mu T^\mu_{\mathrm{K}}$ and $\nabla_\mu T^{\mu\nu}$. With the help of covariant conservation laws for σ^μ (3.58) and $\tau^{\mu\nu}$ (3.59) we arrive at the following expressions:

$$\nabla_\mu T^\mu_{\mathrm{K}} = -\nabla_\mu \tau^\mu, \tag{3.62}$$

$$\nabla_\mu T^{\mu\nu} = -\frac{1}{2}\mathrm{R}[\mathrm{K}]\varepsilon^{\nu\rho}\left(\sigma_\rho + \tau_\rho + 2\varepsilon_{\rho\sigma}\nabla^\sigma \varrho\right) - \mathrm{K}^\nu \nabla_\rho \tau^\rho, \tag{3.63}$$

where $\mathrm{R}[\mathrm{K}] = 2\varepsilon^{\mu\nu}\partial_\mu \mathrm{K}_\nu$. In the case of minimal coupling, that is, $\tau^\mu = 0$ and $\varrho = 0$, the covariant conservation laws reduce to the expressions obtained in [81]. As anticipated, dynamical currents, as mentioned in (3.51), can be completely removed from conservation laws and replaced with the contorsion current and energy-momentum tensor. This is achieved by inserting equations (3.60) and (3.62) into Equation (3.63). The resulting expression for the covariant conservation law of the energy-momentum tensor is presented below:

$$\nabla_\mu T^{\mu\nu} = \frac{1}{2}\mathrm{R}[\mathrm{K}]\varepsilon^{\nu\rho}T^{\mathrm{K}}_\rho + \mathrm{K}^\nu \nabla_\rho T^\rho_{\mathrm{K}}. \tag{3.64}$$

Applying the ansatz defined in the section 3.1, Equation (3.64) can be rewritten in the following form:

$$\Lambda \frac{\mathrm{d}T^{\parallel\perp}}{\mathrm{d}\bar{\mathrm{x}}} + 2T^{\parallel\perp}\frac{\mathrm{d}\Lambda}{\mathrm{d}\bar{\mathrm{x}}} = \mathrm{K}^\parallel \frac{\mathrm{d}}{\mathrm{d}\bar{\mathrm{x}}}\left(\Lambda T^\perp_{\mathrm{K}}\right) + T^\perp_{\mathrm{K}}\frac{\mathrm{d}}{\mathrm{d}\bar{\mathrm{x}}}\left(\Lambda \mathrm{K}^\parallel\right), \tag{3.65}$$

$$\Lambda \frac{\mathrm{d}T^{\perp\perp}}{\mathrm{d}\bar{\mathrm{x}}} + \frac{1}{2}\left(3T^{\perp\perp} + T^{\parallel\parallel}\right)\frac{\mathrm{d}\Lambda}{\mathrm{d}\bar{\mathrm{x}}} = \mathrm{K}^\perp \frac{\mathrm{d}}{\mathrm{d}\bar{\mathrm{x}}}\left(\Lambda T^\perp_{\mathrm{K}}\right) + T^\parallel_{\mathrm{K}}\frac{\mathrm{d}}{\mathrm{d}\bar{\mathrm{x}}}\left(\Lambda \mathrm{K}^\parallel\right), \tag{3.66}$$

where we have employed the $\bar{\mathrm{x}}$ coordinate (3.20)The first Equation (3.65) can be integrated, yielding the following:

$$T^{\parallel\perp} = \mathrm{K}^\parallel T^\perp_{\mathrm{K}} + \frac{\mathrm{A}}{\Lambda^2}, \tag{3.67}$$

where A is an arbitrary constant. Placing $T^\parallel_{\mathrm{K}} = T^\perp_{\mathrm{K}} = A = 0$ equations (3.67) gives $T^{\parallel\perp} = 0$, while Equation (3.66) reduces to the standard conversation law of the energy-momentum tensor, i.e.:

$$\nabla_\mu T^{\mu\nu} \equiv -\frac{\mathcal{D}}{2L}\left[\Lambda \frac{\mathrm{d}T^{\perp\perp}}{\mathrm{d}\bar{\mathrm{x}}} + \frac{1}{2}\left(3T^{\perp\perp} + T^{\parallel\parallel}\right)\frac{\mathrm{d}\Lambda}{\mathrm{d}\bar{\mathrm{x}}}\right]\varepsilon^{\nu\rho}\xi_\rho = 0. \tag{3.68}$$

As a final consistency check of our approach, we verify that, upon setting the non-minimally coupled terms τ^μ and ϱ to zero, we reproduce the result of [81]. The spin-current conservation law (3.58) is already identical in form to that given in [81]. Next, from (3.60) we obtain $T^\mu_{\mathrm{K}} = -\sigma^\mu$. Using the spin-current conservation law (3.58), this implies $\nabla_\mu T^\mu_{\mathrm{K}} = 0$. Inserting this into (3.64) yields:

$$\nabla_\mu T^{\mu\nu} = -\frac{1}{2}\mathrm{R}[\mathrm{K}]\varepsilon^{\nu\rho}\sigma_\rho, \tag{3.69}$$

$$\nabla_\mu \sigma^\mu = 0, \tag{3.70}$$

which coincide with the conservation laws for the two-dimensional gravitational theory derived in [81].

3.3 Quantum corrections

In the preceding sections, we have constructed the framework of classical 2D dilaton gravity. To study Hawking radiation, however, it is necessary to account for the back-reaction of quantum fields on the classical geometry. This is achieved by adding the Polyakov–Liouville action [22], which represents the 1-loop effective action of a two-dimensional massless scalar field, namely:

$$e^{\frac{i}{\hbar}S_{\rm PL}} = \int \mathcal{D}\chi e^{\frac{i}{\hbar}\int d^2x\sqrt{-g}\left(-\frac{1}{2}(\nabla\chi)^2\right)}, \tag{3.71}$$

After computing this Gaussian functional integral, we arrive at:

$$S_{\rm PL} = -\frac{\hbar}{96\pi}\int d^2x\int d^2y\sqrt{-g(x)}\sqrt{-g(y)}R(x)G(x-y)R(y). \tag{3.72}$$

Here, $G(x-y)$ denotes the Green's function of the massless Klein–Gordon equation in a curved (1+1)-dimensional spacetime, defined by $\Box G(x-y) = \frac{1}{\sqrt{-g}}\delta^{(2)}(x-y)$. A striking feature of this action is that it is 1-loop exact. In the form given above, the action is manifestly nonlocal. However, one can render it local by introducing an auxiliary scalar field ψ, in terms of which the action becomes:

$$S_{PL} = -\frac{\hbar}{96\pi}\int d^2x\sqrt{-g}\left[2R\psi + (\nabla\psi)^2\right], \tag{3.73}$$

which is on-shell equivalent to (3.72). The field equation of the auxiliary field is as follows:

$$\Box\psi = R. \tag{3.74}$$

By varying the action with respect to the metric we obtain the following energy-momentum tensor of the quantum fields:

$$\langle \Delta T^f_{\mu\nu}\rangle = \frac{\hbar}{48\pi}\left[-2\nabla_\mu\nabla_\nu\psi + \nabla_\mu\psi\nabla_\nu\psi + g_{\mu\nu}\left(2\Box\psi - \frac{1}{2}(\nabla\psi)^2\right)\right]. \tag{3.75}$$

It corresponds to the expectation value of the quantum energy-momentum tensor operator. The limitation of this approach is that it requires the introduction of an additional field. However, Equation (3.74) can be readily solved once we substitute (3.3) into it:

$$\psi = -2\rho + f_+(x^+) + f_-(x^-), \tag{3.76}$$

where $f_\pm$ represent a set of arbitrary functions. Using this result, the energy-momentum tensor is given by:

$$\langle \Delta T^f_{\pm\pm}\rangle = \frac{\hbar}{12\pi}\left[\partial_\pm^2\rho - (\partial_\pm\rho)^2 - t_\pm(x^\pm)\right], \quad \langle \Delta T^f_{+-}\rangle = -\frac{\hbar}{12\pi}\partial_+\partial_-\rho, \tag{3.77}$$

where the functions $t_\pm$ are given in terms of $f_\pm$ by the following relations:

$$t_\pm(x^\pm) = \frac{1}{2}\partial_\pm^2 f_\pm - \frac{1}{4}\left(\partial_\pm f_\pm\right)^2. \tag{3.78}$$

The quantity $\varepsilon = \frac{\hbar}{12\pi}$ serves as a natural expansion parameter in perturbation theory and will be employed in later chapters whenever we deal with a theory that cannot be solved exactly. Finally, we rewrite the EMT of the PL action (3.75) once more, now employing the symmetric ansatz introduced in Section 3.1:

$$\begin{aligned}\langle \Delta T^{(f)}_{\mu\nu}\rangle = -\frac{\hbar}{12\pi}\frac{1}{(2L\Lambda)^2}\Bigg\{&\left[4L^2\big(t_+(\sigma^+)+t_-(\sigma^-)\big) + \frac{1}{2}\Big(\mathcal{D}\frac{\mathrm{d}\Lambda}{\mathrm{dx}}\Big)^2 - 2\Lambda\mathcal{D}\frac{\mathrm{d}}{\mathrm{dx}}\Big(\mathcal{D}\frac{\mathrm{d}\Lambda}{\mathrm{dx}}\Big)\right]\xi_\mu\xi_\nu \\ &+ \left[4L^2\big(t_+(\sigma^+)+t_-(\sigma^-)\big) + \frac{1}{2}\Big(\mathcal{D}\frac{\mathrm{d}\Lambda}{\mathrm{dx}}\Big)^2\right]\varepsilon_{\mu\rho}\varepsilon_{\nu\sigma}\xi^\rho\xi^\sigma \\ &- 4L^2\big(t_+(\sigma^+)-t_-(\sigma^-)\big)\left(\varepsilon_{\mu\rho}\xi_\nu + \varepsilon_{\nu\rho}\xi_\mu\right)\xi^\rho\Bigg\},\end{aligned} \tag{3.79}$$

where we have used the form of the EMT in the arbitrary coordinates $x^{\pm}$, namely expression (3.77), together with the observation that, after inserting the metric ansatz (3.2), the functions $t_{\pm}(x^{\pm})$ transform to the Eddington–Finkelstein coordinates, due to the appearance of the coordinate transformation functions $\mathrm{F}^{\pm}$:

$$(\partial_{\pm}\rho)^2 - \partial_{\pm}^2\rho + t_{\pm}(x^{\pm}) = \frac{1}{4}\left(\partial_{\pm}\ln \mathrm{F}^{\pm}\right)^2 + \frac{1}{2}\partial_{\pm}^2 \ln \mathrm{F}^{\pm} + t_{\pm}(x^{\pm}) + \left(\frac{\lambda}{2\mathrm{F}^{\pm}}\right)^2 \mathcal{F}[\mathrm{x}] \tag{3.80}$$
$$= t_{\pm}(x^{\pm}) - \frac{1}{2}D_{x^{\pm}}\left[\sigma^{\pm}\right] + \left(\frac{\lambda}{2\mathrm{F}^{\pm}}\right)^2 \mathcal{F}[\mathrm{x}] = \frac{1}{\mathrm{F}^{\pm 2}}t_{\pm}(\sigma^{\pm}) + \left(\frac{\lambda}{2\mathrm{F}^{\pm}}\right)^2 \mathcal{F}[\mathrm{x}],$$

where $\mathcal{F}[\mathrm{x}]$ denotes a function which depends only on metric function Λ (3.8) and its derivatives. Note that for (3.79) to be only a function of the dilaton x, functions $t_{\pm}(\sigma^{\pm})$ must be constants.

3.3.1 Transformation properties of the energy–momentum tensor

To proceed with our analysis of these equations, we must first clarify the meaning of the seemingly arbitrary functions $t_{\pm}$ (3.78). To this end, we examine how the energy–momentum tensor behaves under coordinate transformations. To preserve the conformal gauge, we limit our consideration to conformal coordinate transformations, specifically those of the form $y^{\pm} = y^{\pm}(x^{\pm})$. It is enough to focus on the quantum part of the energy–momentum tensor, because the classical contribution is already known to obey the standard tensor transformation law. Under the conformal transformations, the metric function ρ changes in the following way:

$$\rho(y) = \rho(x) + \frac{1}{2}\ln\frac{dy^+}{dx^+} + \frac{1}{2}\ln\frac{dy^-}{dx^-}. \tag{3.81}$$

Since the energy–momentum tensor is required to transform as a tensor, and its classical component already obeys the standard tensor transformation law, the quantum fluctuation of the energy–momentum tensor (3.77) must likewise satisfy this same tensor transformation law, namely:

$$\langle \Delta T^f_{\pm\pm}(y)\rangle = \left(\frac{dx^{\pm}}{dy^{\pm}}\right)^2 \langle \Delta T^f_{\pm\pm}(x)\rangle. \tag{3.82}$$

By enforcing condition 3.82, we arrive at the following expression for the transformation law of the $t_{\pm}$ functions:

$$t_{\pm}(y^{\pm}) = \left(\frac{dx^{\pm}}{dy^{\pm}}\right)^2 \left[t_{\pm}(x^{\pm}) - \frac{1}{2}D_{x^{\pm}}\left[y^{\pm}\right]\right], \quad D_{x^{\pm}}\left[y^{\pm}\right] = \frac{y^{+'''}}{y^{+'}} - \frac{3}{2}\left(\frac{y^{+''}}{y^{+'}}\right)^2. \tag{3.83}$$

The quantity $D_{x^{\pm}}\left[y^{\pm}\right]$ is called the Schwarzian derivative. It represents a functional acting on a function of a single variable. In 3.83 the quantity $y^{+'}$ denotes the first derivative of the function $y^+ = y^+(x^+)$. In order to better understand the nature of the quantity $t_{\pm}$, we perform canonical quantization of the scalar field in curved spacetime (see Appendix D.1). The equation for the scalar field, and its solution, are given by:

$$\Box f = 0 \quad \Longrightarrow \quad \partial_+\partial_- f = 0 \quad \Longrightarrow \quad f(x^+, x^-) = f_+(x^+) + f_-(x^-). \tag{3.84}$$

We define positive-frequency modes as:

$$\partial_0 f^{\omega} = -i\omega f^{\omega} \implies \frac{df^{\omega}_{\pm}(x^{\pm})}{dx^{\pm}} = -i\omega f^{\omega}(x^{\pm}) \implies f^{\omega}_{\pm}(x^{\pm}) = A^{\pm}_{\omega} e^{-i\omega x^{\pm}}. \tag{3.85}$$

The standard scalar product is given by:

$$\left(f_\pm^{\omega_1}, f_\pm^{\omega_2}\right) = -i \int_{x^0=0} dx \sqrt{\gamma} n^\mu \left[f_\pm^{\omega_1}(x^\pm) \nabla_\mu f_\pm^{\omega_2 *}(x^\pm) - f_\pm^{\omega_2 *}(x^\pm) \nabla_\mu f_\pm^{\omega_1}(x^\pm) \right], \tag{3.86}$$

where: $n^\mu = (e^{-\rho}, 0, 0, 0)^T$ i $\sqrt{\gamma} = e^\rho$. By imposing the orthogonality condition of the modes: $(f_\pm^{\omega_1}, f_\pm^{\omega_2}) = \delta(\omega_1 - \omega_2)$, we arrive at the following quantized scalar field:

$$f_\pm(x^\pm) = \int_0^\infty \frac{d\omega}{\sqrt{4\pi\omega}} \left[a_\pm(\omega) e^{-i\omega x^\pm} + a_\pm^\dagger e^{i\omega x^\pm} \right], \tag{3.87}$$

where $a_\pm(\omega)$ and $a_\pm^\dagger(\omega)$ represent the creation and annihilation operators of the modes $f_\pm^\omega$.

We now compute the two–point Green's function. Because the definition of the vacuum state is coordinate–dependent, we label it as $|0, x\rangle$ to underline that it is specified with respect to the $x^\pm$ coordinates. Since the explicit dependence on $\hbar$ is relevant for what follows, we reinstate the factor of $\sqrt{\hbar}$ multiplying the field. The two-point correlation function then takes the form:

$$\begin{aligned} G(x, x') = \langle 0, x| f_\pm(x^\pm) f_\pm(x'^\pm) |0, x\rangle &= \hbar \iint_0^\infty \frac{d\omega d\omega'}{4\pi\sqrt{\omega\omega'}} e^{i\omega' x' - i\omega x^\pm} \langle 0, x| a_\pm(\omega) a_\pm^\dagger(\omega') |0, x\rangle \\ &= \hbar \int_0^\infty \frac{d\omega}{4\pi\omega} e^{i\omega(x'^\pm - x^\pm)} = -\frac{\hbar}{4\pi} \ln\left|x'^\pm - x^\pm\right| + const. \end{aligned} \tag{3.88}$$

Next, we evaluate the expectation value of the energy–momentum tensor by applying $\partial_\pm \partial'_\pm$ to the Green's function and then taking the limit $x' \to x$, which yields:

$$\langle 0, x| \hat{T}^f_{\pm\pm}(x) |0, x\rangle = \lim_{x'^\pm \to x^\pm} \frac{\partial}{\partial x^\pm} \frac{\partial}{\partial x'^\pm} G(x, x') = -\frac{\hbar}{4\pi} \lim_{x'^\pm \to x^\pm} \frac{1}{\left(x'^\pm - x^\pm\right)^2}. \tag{3.89}$$

The energy–momentum tensor operator can be decomposed as $\hat{T}_{\mu\nu} =: \hat{T}_{\mu\nu} : + \langle 0, x| \hat{T}_{\mu\nu} |0, x\rangle$, leading to:

$$\hat{T}^f_{\pm\pm}(x) =: \hat{T}^f_{\pm\pm}(x) : -\frac{\hbar}{4\pi} \lim_{x'^\pm \to x^\pm} \frac{1}{\left(x'^\pm - x^\pm\right)^2}, \tag{3.90}$$

where $: \hat{T}^f_{\mu\nu} :$ denotes the normally ordered part of the energy–momentum tensor expressed in the $x^\pm$ coordinates. This represents the energy–momentum tensor as measured by an observer in the $x^\pm$ frame. The key question is what an observer in the $y^\pm$ frame measures if, for example, the energy–momentum tensor is normally ordered with respect to the $x^\pm$ coordinates (so that an observer in the $x^\pm$ frame detects no excitations of the matter fields). More generally, we may ask how the normally ordered part of the energy–momentum tensor changes under the transformation $x^\pm \mapsto y^\pm$, assuming that the complete energy–momentum tensor satisfies the usual tensor transformation law. We find:

$$\begin{aligned} : \hat{T}^f_{\pm\pm}(y^\pm) : &= \hat{T}^f_{\pm\pm}(y^\pm) + \frac{\hbar}{4\pi} \lim_{y'^\pm \to y^\pm} \frac{1}{\left(y'^\pm - y^\pm\right)^2} \\ &= \lim_{y'^\pm \to y^\pm} \frac{dx^\pm}{dy^\pm} \frac{dx'^\pm}{dy'^\pm} \hat{T}^f_{\pm\pm}(x^\pm) + \frac{\hbar}{4\pi} \lim_{y'^\pm \to y^\pm} \frac{1}{\left(y'^\pm - y^\pm\right)^2} \\ &= \left(\frac{dx^\pm}{dy^\pm}\right)^2 : \hat{T}^f_{\pm\pm}(x) : -\frac{\hbar}{4\pi} \underbrace{\lim_{x'^\pm \to x^\pm} \left[\frac{1}{\left(x'^\pm - x^\pm\right)^2} \frac{dx^\pm}{dy^\pm} \frac{dx'^\pm}{dy'^\pm} - \frac{1}{\left(y'^\pm - y^\pm\right)^2} \right]}_{L}. \end{aligned} \tag{3.91}$$

It remains to evaluate the limit L. We assume that the transformation $y^{\pm} = y^{\pm}(x^{\pm})$ is differentiable, so that whenever $x'^{\pm} \to x^{\pm}$ it follows that $y'^{\pm} \to y^{\pm}$. For convenience, in the calculation of the limit L, we will denote $x^{\pm}$ simply by x and $y^{\pm}$ simply by y. We set $x' - x = \varepsilon \to 0$ and perform an expansion in powers of ε. A representative behavior of such functions is illustrated in Figure 3.1:

$$\begin{aligned} y^{'} &= y + \varepsilon \frac{dy}{dx} + \frac{\varepsilon^2}{2}\frac{d^2y}{dx^2} + \frac{\varepsilon^3}{6}\frac{d^3y}{dx^3}, \\ \frac{dy^{'}}{dx'} &= \frac{dy}{dx} + \varepsilon\frac{d^2y}{dx^2} + \frac{\varepsilon^2}{2}\frac{d^3y}{dx^3}. \end{aligned} \tag{3.92}$$

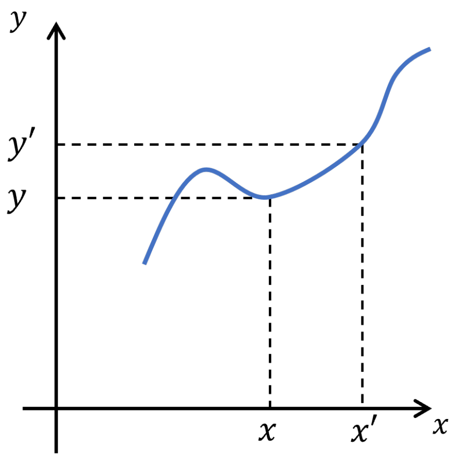

Figure 3.1: Representation of the behavior of the transformation $y(x)$

Furthermore, we use the notation $\frac{dy}{dx} = y'$, $\frac{d^2y}{dx^2} = y''$, and similarly for higher derivatives. We now proceed to evaluate the desired limit of L.:

$$\begin{aligned} L &= \lim_{\varepsilon\to 0}\left[\frac{\frac{dx}{dy}\frac{dx'}{dy'}}{(x'-x)^2} - \frac{1}{(y'-y)^2}\right] = \lim_{\varepsilon\to 0}\frac{(y'-y)^2 - (x'-x)^2\frac{dy}{dx}\frac{dy'}{dx'}}{(x'-x)^2(y'-y)^2\frac{dy}{dx}\frac{dy'}{dx'}} \\ &= \lim_{\varepsilon\to 0}\frac{\left(\varepsilon y' + \frac{\varepsilon^2}{2}y'' + \frac{\varepsilon^3}{6}y'''\right)^2 - \varepsilon^2 y'\left(y' + \varepsilon y'' + \frac{\varepsilon^2}{2}y'''\right) + o(\varepsilon^4)}{\varepsilon^4(y')^4} \\ &= \lim_{\varepsilon\to 0}\frac{(y')^2 + \varepsilon y'y'' + \frac{\varepsilon^2}{3}y'y''' + \frac{\varepsilon^2}{4}(y'')^2 - (y')^4 - \varepsilon y'y'' - \frac{\varepsilon^2}{2}y'y'' + o(\varepsilon^2)}{\varepsilon^2(y')^4} \\ &= \lim_{\varepsilon\to 0}\frac{\frac{1}{4}(y'')^2 - \frac{1}{6}y'y''' + o(1)}{(y')^4} = -\frac{1}{6(y')^2}\left[\frac{y'''}{y'} - \frac{3}{2}\left(\frac{y''}{y'}\right)^2\right] = -\frac{1}{6(y')^2}D_x\left[y\right]. \end{aligned} \tag{3.93}$$

Finally, the transformation law can be written as $:\hat{T}^f_{\pm\pm}(x^{\pm}):$

$$:\hat{T}^f_{\pm\pm}(y^{\pm}) := \left(\frac{dx^{\pm}}{dy^{\pm}}\right)^2\left[:\hat{T}^f_{\pm\pm}(x^{\pm}): + \frac{\hbar}{24\pi}D_{x^{\pm}}\left[y^{\pm}\right]\right]. \tag{3.94}$$

This formula corresponds to a standard transformation law for the energy-momentum tensor in conformal field theory [105]. The coefficient in front of the Schwarzian derivative, when multiplied by $\frac{\hbar}{24\pi}$, defines the central charge, which takes the value $c = 1$ for a free massless boson.

From this we conclude that an energy–momentum tensor that is normally ordered with respect to one coordinate system will, in general, not remain normally ordered after a change of coordinates. This is consistent with the fact that one observer can perceive the vacuum, while another detects a particle spectrum (see Appendix D.1). It is also crucial to note that the Schwarzian derivative enters the transformation, so the transformation law coincides with the one in (3.83) for the quantity $t_{\pm}(x^{\pm})$. Consequently, we obtain

$$\langle\psi| :\hat{T}^f_{\pm\pm}: (x^{\pm})\,|\psi\rangle = -\frac{\hbar}{12\pi}t_{\pm}(x^{\pm}), \tag{3.95}$$

where $|\psi\rangle$ denotes the quantum state of the field. Equation (3.95) gives the expectation value of the normally ordered energy–momentum tensor, and thus indicates whether an observer associated with a particular reference frame measures a particle spectrum or not. On this basis, we characterize the quantum state in which the system is found. The central issue is whether a particle spectrum is present at asymptotic infinity, i.e. at $\mathcal{J}^{\pm}$. Three distinct choices of vacuum state are commonly considered [26, 106]:

- **Boulware state** $|B\rangle$: This is a state that exhibits no energy flux through either of the asymptotic null infinities, $\mathcal{J}^+$ or $\mathcal{J}^-$. In other words, it describes a non-radiating black hole. For this requirement to hold, the energy–momentum tensor must be normally ordered with respect to the Eddington–Finkelstein, asymptotically flat coordinates $\sigma^{\pm}$, specifically:

$$\langle B| : \hat{T}^f_{\pm\pm}(\sigma^{\pm}) : |B\rangle = -\varepsilon t_{\pm}(\sigma^{\pm}) = 0 \quad \Longrightarrow \quad |B\rangle = |0, \sigma\rangle \,. \tag{3.96}$$

- **Hartle–Hawking state** $|HH\rangle$: This is a state in which the energy flux through $\mathcal{J}^+$ and $\mathcal{J}^-$ is equal. In other words, the black hole is in thermal equilibrium with its surroundings [107], evaporating at the same rate at which it absorbs. For this requirement to hold, the energy–momentum tensor must be normally ordered with respect to the Kruskal coordinates $x^{\pm}$, i.e. the coordinates in which the metric remains regular at the horizon, namely:

$$\langle HH| : \hat{T}^f_{\pm\pm}(x^{\pm}) : |HH\rangle = -\varepsilon t_{\pm}(x^{\pm}) = 0 \quad \Longrightarrow \quad |HH\rangle = |0, x\rangle \,. \tag{3.97}$$

- **Unruh state** $|U\rangle$: This state corresponds to a black hole that has no energy flux at $\mathcal{J}^-$ in the distant past, but does exhibit energy flux at $\mathcal{J}^+$ in the far future. In other words, we are dealing with a scenario where, at some point in time, matter collapses and a black hole forms. Prior to the collapse, there is no energy flux, and the energy–momentum tensor is normally ordered with respect to the asymptotically flat coordinates $\sigma^{\pm}$. Once the collapse occurs, the appropriate asymptotically flat coordinates switch to $\hat{\sigma}^{\pm}$. Because the quantum state is defined in terms of the original $\sigma^{\pm}$ coordinates, the energy–momentum tensor is no longer normally ordered in the new asymptotically flat coordinates $\hat{\sigma}^{\pm}$. This mismatch produces an energy flux at $\mathcal{J}^+$, implying that the black hole evaporates.

$$\langle U| : \hat{T}^f_{\pm\pm}(\sigma^{\pm}) : |U\rangle = -\varepsilon t_{\pm}(\sigma^{\pm}) = 0 \quad \Longrightarrow \quad |U\rangle = |0, \sigma\rangle \,. \tag{3.98}$$

In recent years, a new class of quantum states, known as hybrid quantum states, has been explored. This idea was first put forward in [108, 109] within the framework of the RST model [23, 24], where it was shown that the entanglement entropy of quantum fields can exhibit a Page-curve-like behavior even without invoking an island [110]. The core concept is to introduce non-physical, ghost-like fields arranged in a hybrid state. A hybrid state is a mixture of two quantum states (for example, a Hartle–Hawking state for the physical fields together with a Boulware state for the auxiliary non-physical fields, i.e. $|\psi\rangle \equiv |HH\rangle \otimes |B\rangle$). Because of the inclusion of these non-physical fields, the effective central charge of the conformal field theory can become negative. When this occurs, the space-time singularity is removed, which appears to be the primary mechanism driving the Page-curve-like evolution of the entanglement entropy in this setting. In contrast, the resolution of space-time singularities has long been expected to be a hallmark of a fully consistent theory of quantum gravity. Although the island formula (1.6) reproduces a Page curve, it does not, by itself, resolve singularities. This shortcoming can be viewed as a consequence of working within the semiclassical approximation.

3.4 Gravitational collapse scenario

In this section, we explain how to construct a gravitational collapse scenario within the framework of two-dimensional dilaton gravity. For studying the Page curve, one needs an evaporating black hole solution, i.e. a dynamical semi-classical configuration that does not admit a global timelike Killing vector field.

We begin by setting up the classical collapse scenario. The infalling matter is represented as a null shockwave of mass M propagating along the $x^+ = x_0^+$ hypersurface. Once this shockwave reaches the boundary of spacetime, namely the $\mathrm{x} = 0$ hypersurface, a singularity forms together with an event horizon. The energy-momentum tensor for the simplest ingoing shockwave is described using a Dirac δ-function as follows:

$$T_{++} = s\delta\left(x^+ - x_0^+\right), \quad T_{--} = T_{+-} = 0, \tag{3.99}$$

where s is a constant connected to the mass of the shockwave. The mass carried by the energy-momentum tensor is given by [106]:

$$M = \int_\Sigma \mathrm{d}\sigma \sqrt{\gamma} n^\mu \xi^\nu T_{\mu\nu}, \tag{3.100}$$

where Σ is a space-like hypersurface, n is an orthogonal vector to the surface Σ normalized as $n_\mu n^\mu = -1$, ξ is the time-like Killing vector, γ is the induced metric on Σ and $T_{\mu\nu}$ is the energy-momentum tensor. Since ξ is orthogonal to Σ, we can choose n to be proportional to ξ, i.e. $n^\mu = \frac{\xi^\mu}{\sqrt{-\xi\cdot\xi}}$. The induced metric on the hypersurface Σ is then: $\mathrm{d}s^2 = -\Lambda \mathrm{d}\sigma^2$. Substituting all of this into Equation (3.100) gives:

$$M = \int_\Sigma \mathrm{d}\sigma \sqrt{-\Lambda}\xi^\mu \frac{\xi^\nu}{\sqrt{-\Lambda}} T_{\mu\nu} = \int_\Sigma \mathrm{d}\sigma \mathrm{F}^{+2} T_{++} = -\int \frac{\mathrm{d}x^+}{\mathrm{F}^+} s\mathrm{F}^{+2}\delta\left(x^+ - x_0^+\right) = -s\mathrm{F}^+(x_0^+). \tag{3.101}$$

The collapse scenario is illustrated in Figure 3.2. The blue line, representing the matter shockwave, divides the diagram into two parts. Because matter is confined to the shockwave itself, regions I and II are described by vacuum solutions of the form $(\mathrm{F}^+, \mathrm{F}^-, C)$, where $\mathrm{F}^\pm(x^\pm)$ denote conformal transformations from arbitrary coordinates $x^\pm$ to Eddington–Finkelstein coordinates $\sigma^\pm$, and C is a set of constants specifying the solution in Eddington–Finkelstein coordinates (such as the black hole mass or charge). In this way, one encodes the most general static vacuum solution within the formalism developed in 3.1. When crossing the shockwave hypersurface, two of these three parameters can jump, namely C and F^-. To determine these discontinuities, we impose appropriate gluing conditions on the metric and dilaton field.

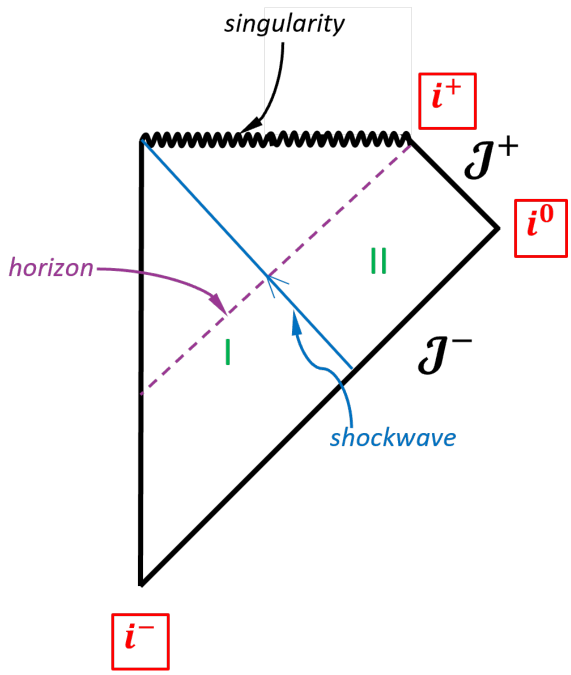

Figure 3.2: Penrose diagram of the gravitational collapse

Both the metric and the dilaton must remain continuous functions of x^+ and x^- across the hypersurface $x^+ = x_0^+$, which implies:

$$e^{2\rho_{\mathrm{I}}}\Big|_{x^+=x_0^+-\epsilon} = e^{2\rho_{\mathrm{II}}}\Big|_{x^+=x_0^++\epsilon}, \qquad e^{-\phi_{\mathrm{I}}}\Big|_{x^+=x_0^+-\epsilon} = e^{-\phi_{\mathrm{II}}}\Big|_{x^+=x_0^++\epsilon}, \tag{3.102}$$

when $\epsilon \to 0$, where the indices I and II refer, respectively, to region I and region II of space-time (see Figure 3.2). In addition to these two continuity conditions, all derivatives of the metric and the dilaton with respect to the coordinate x^- must also be continuous. Finally, we have to examine the $++$ component of the metric equation, since its source term, T_{++}, is proportional to a Dirac δ-function. This function can always be expressed in the following form:

$$\partial_+\mathcal{F} + \mathcal{G}_<\eta(x_0^+ - x^+) + \mathcal{G}_>\eta(x^+ - x_0^+) = \frac{M}{\mathrm{F}^+}\delta\left(x^+ - x_0^+\right), \tag{3.103}$$

where it is repeatedly used that the metric and the dilaton field and their derivatives with respect to x^- must be continuous along the hypersurface $x^+ = x_0^+$. Integrating this equation from $x_0^+ - \epsilon$ to $x_0^+ + \epsilon$ and then taking the limit $\epsilon \to 0$ yields:

$$\mathcal{F}\Big|_<^> = \frac{M}{\mathrm{F}^+(x_0^+)}. \tag{3.104}$$

What we have essentially done here is to split the $++$ equation into a term proportional to the Dirac δ-function, $\partial_+\mathcal{F}$, and a term, $\mathcal{G}_{>/<}$, which is discontinuous at $x^+ = x_0^+$. The latter contribution is integrable at $x^+ = x_0^+$ and therefore its integral vanishes in the limit $\epsilon \to 0$. This constitutes the final condition imposed on the fields. Solving equations (3.102) and (3.104) then determines the parameters of region II of the spacetime in terms of those of region I, or equivalently:

$$\mathrm{F}_{\mathrm{II}}^-(x^-) = \mathrm{F}_{\mathrm{II}}^-\left(\mathrm{F}_{\mathrm{I}}^-(x^-), \phi(x^-, x_0^+), \mathrm{F}_{\mathrm{I}}^+(x_0^+), C_{\mathrm{I}}, M\right), \quad \mathrm{F}_{\mathrm{II}}^+ = \mathrm{F}_{\mathrm{I}}^+, \quad C_{\mathrm{II}} = C_{\mathrm{II}}\left(\mathrm{F}_{\mathrm{I}}^+(x_0^+)), C_{\mathrm{I}}, M\right). \tag{3.105}$$

The net result of this kind of construction is that the static vacuum solutions remain present in both spacetime regions I and II. What does change is the Killing vector, because the component ξ^- becomes discontinuous, rendering the spacetime as a whole non-stationary. As a consequence, the asymptotically flat Eddington–Finkelstein coordinates are modified, going from $\sigma^\pm$ to $\hat{\sigma}^\pm$, since they are defined by:

$$\frac{\mathrm{d}\sigma^\pm}{\mathrm{d}x^\pm} = \mp\frac{1}{\mathrm{F}_{\mathrm{I}}^\pm}, \qquad \frac{\mathrm{d}\hat{\sigma}^\pm}{\mathrm{d}x^\pm} = \mp\frac{1}{\mathrm{F}_{\mathrm{II}}^\pm}, \tag{3.106}$$

specifically the σ^- coordinate. For later convenience, we introduce a new set of coordinates adapted to the shockwave hypersurface:

$$\hat{\mathrm{x}} \equiv \frac{\sigma_0^+ - \sigma^-}{2L}, \qquad \wedge \qquad \delta \equiv e^{-\frac{\sigma^+ - \sigma_0^+}{2L}}, \tag{3.107}$$

where the first coordinate plays the role of a redefined σ^-, and the second encodes a shift in the σ^+ coordinate. Note that $\delta \in (0, 1)$, and it monotonically decreases from 1 to 0 (the latter corresponding to infinity) throughout region II of the spacetime, where the black hole is located. When region I is the flat Minkowski space, we have $\hat{\mathrm{x}} = \mathrm{x}$ at the shockwave hypersurface.

According to the cosmic censorship conjecture [106], any singularity must remain concealed behind some kind of horizon, typically the event horizon. In dynamical spacetimes, however, another type of horizon can arise, known as the apparent horizon, which can lie outside and thus obscure the event horizon. The apparent horizon is defined as the surface behind which all trapped surfaces are located (i.e., all null geodesics converge, preventing light from escaping that region). In dilaton gravity the apparent horizon is determined by the condition $\partial_+ e^{-n\phi} = 0$, because this expression is proportional to the area of the n-sphere in the higher-dimensional theory from which the model is obtained via spherical reduction (see Chapter 2). For considerations involving entropy, the apparent horizon is in fact more relevant than the event horizon itself [26].

3.4.1 Quantum-corrected collapse scenario

Here we assume that quantum corrections are incorporated via the PL action defined in (3.72). The starting point is the same as in the previous section: the infalling matter is modeled as an ingoing null shockwave located on the $x^+ = x_0^+$ hypersurface, which splits the spacetime into two regions. Region I denotes the portion of spacetime prior to the passage of the shockwave, i.e. $x^+ < x_0^+$, and coincides with the corresponding region in the classical setup. The essential new element is that we must now specify the quantum state of the fields, because in the quantum-corrected framework the geometry is characterized by the ordered quintuple $(\mathrm{F}^+, \mathrm{F}^-, t_+, t_-, C)$. Choosing $t_\pm = 0$ then selects the quantum state in which the EMT is normal ordered, as in (3.95).

In region I we introduce the Eddington–Finkelstein coordinates $\sigma^\pm$ and impose that the EMT is normal ordered with respect to these coordinates, i.e. $t_\pm(\sigma^\pm) = 0$. This condition guarantees the absence of Hawking radiation at the $\mathscr{J}^-$ hypersurface, prior to the introduction of the infalling matter. Without the shockwave, this would indicate that the matter fields are prepared in the Boulware state (3.96).

Once the infalling matter is introduced, the asymptotically flat coordinates change from $\sigma^\pm$ to a new set $\hat{\sigma}^\pm$. This is already apparent in the purely classical collapse setup (3.106), and therefore should remain valid when quantum effects are included. Moreover, upon incorporating quantum corrections, these coordinate transformations are expected to receive additional contributions. Since the EMT is no longer normal ordered in the new asymptotically flat coordinates, Hawking radiation is present on the $\mathscr{J}^+$ hypersurface. Consequently, the underlying quantum state is in fact the Unruh state (3.98).

Classically, the model features two stationary geometries with distinct time-like Killing vectors, which are smoothly matched across the $\sigma^+ = \sigma_0^+$ hypersurface. Thus, each region can be regarded as stationary on its own, even though the full spacetime is dynamical. Once quantum corrections are turned on, this picture changes. The geometry in region I may still be treated as stationary with respect to its corresponding Killing vector, but this is no longer true for region II. The key point is that, upon crossing the matching hypersurface, not only the coordinate transformations $\mathrm{F}^\pm$ change, but the functions $t_\pm$ also undergo a change.

In many practical situations, the full vacuum solution $(\mathrm{F}^+, \mathrm{F}^-, t_+, t_-, C)$ cannot be obtained in closed analytic form. When this is the case, one possible approach is to carry out a formal perturbative expansion in the natural small parameter $\varepsilon = \frac{\hbar G}{12\pi}$ (often written without G), which multiplies the EMT components (3.77). At zeroth order in ε one recovers the classical collapse solution. The next step is to expend the fields to first order in ε, namely:

$$\rho \mapsto \rho(\mathrm{x}) + \varepsilon\alpha, \quad \wedge \quad e^{-\phi} \mapsto e^{-\phi(\mathrm{x})} + \varepsilon\theta. \tag{3.108}$$

Since the quantum correction to the EMT already appears at first order in the expansion parameter ε, we insert the fields at zeroth order and evaluate it. The resulting expression is:

$$\langle \Delta T^{(f)}_{\pm\pm} \rangle = -\frac{\varepsilon}{(2L\mathrm{F}^{+})^2}\left[4L^2 t_{\pm}(\sigma^{\pm}) + \frac{1}{4}\left(\mathcal{D}_0 \frac{\mathrm{d}\Lambda_0}{\mathrm{dx}}\right)^2 - \frac{\Lambda_0 \mathcal{D}_0}{2}\frac{\mathrm{d}}{\mathrm{dx}}\left(\mathcal{D}_0 \frac{\mathrm{d}\Lambda_0}{\mathrm{dx}}\right)\right],$$
$$\langle \Delta T^{(f)} \rangle = \frac{\varepsilon}{2L^2}\mathcal{D}_0 \frac{\mathrm{d}}{\mathrm{dx}}\left(\mathcal{D}_0 \frac{\mathrm{d}\Lambda_0}{\mathrm{dx}}\right), \tag{3.109}$$

where Λ_0 and $\mathcal{D}_0$ are given by (3.8) and (3.13), respectively. The explicit dependence on the $x^{\pm}$ coordinates arises from the term $-\frac{\varepsilon}{\mathrm{F}^{\pm}} t_{\pm}(\sigma^{\pm})$. The "$\pm\pm$" equations of motion can always be rewritten as a first-order differential equations for the quantity $e^{-2\rho}\mathcal{D}_0^{-1}\partial_{\pm}\theta - \frac{1}{L}\alpha \mathrm{F}^{\mp}$, that is:

$$\partial_{\pm}\left(\frac{e^{-2\rho}}{\mathcal{D}_0}\partial_{\pm}\theta - \frac{\alpha \mathrm{F}^{\mp}}{L}\right) = \frac{\mathcal{F}\mathrm{F}^{\mp} t_{\pm}(\sigma^{\pm})}{\mathrm{F}^{\pm}} + \frac{\mathrm{F}^{\mp}}{2L}\frac{\mathcal{F}[\mathrm{x}]}{\mathcal{D}_0 \Lambda_0^2}\left[\frac{1}{4}\left(\mathcal{D}_0 \frac{\mathrm{d}\Lambda_0}{\mathrm{dx}}\right)^2 - \frac{\Lambda_0 \mathcal{D}_0}{2}\frac{\mathrm{d}}{\mathrm{dx}}\left(\mathcal{D}_0 \frac{\mathrm{d}\Lambda_0}{\mathrm{dx}}\right)\right]\partial_{\pm}\mathrm{x}. \tag{3.110}$$

The first term on the right-hand side is fixed by the choice of a vacuum state and therefore remains in integral form as a source. The second term depends only on x and is multiplied by a function that is independent of the coordinate associated with the derivative on the left-hand side. Finally, the function $\mathcal{F}[\mathrm{x}]$ depends on the model. Consequently, integration can be carried out. The result is:

$$\partial_{\pm}\theta = \frac{1}{2L}\left[\mathrm{F}^{\mp}(\mathcal{D}_1 + 2\alpha) + \mathrm{G}^{\mp}\right]\mathcal{D}_0 e^{2\rho} + \mathrm{F}^{\mp}\mathcal{D}_0 e^{2\rho}\int \frac{\mathrm{d}x^{+}}{\mathrm{F}^{\pm}} t_{\pm}(\sigma^{\pm})\mathcal{F}[\mathrm{x}], \tag{3.111}$$

where a new set of arbitrary functions $\mathrm{G}^{\pm} = \mathrm{G}^{\pm}(x^{\pm})$ is introduced. They represent the quantum corrections to the coordinate transformations $\mathrm{F}^{\pm}$. The new function $\mathcal{D}_1$ is defined via:

$$\frac{\mathrm{d}\mathcal{D}_1}{\mathrm{dx}} = \frac{\mathcal{F}[\mathrm{x}]}{\mathcal{D}_0 \Lambda_0^2}\left[\frac{1}{4}\left(\mathcal{D}_0 \frac{\mathrm{d}\Lambda_0}{\mathrm{dx}}\right)^2 - \frac{\Lambda_0 \mathcal{D}_0}{2}\frac{\mathrm{d}}{\mathrm{dx}}\left(\mathcal{D}_0 \frac{\mathrm{d}\Lambda_0}{\mathrm{dx}}\right)\right]. \tag{3.112}$$

Employing a combination of the dilaton equation and the trace equation makes it possible to remove the unknown function α and therefore make Equation (3.111) integrable once more. This integration gives a solution for θ in terms of the derivatives of θ, thus making it a first order differential equation for θ. Solving this equation gives a closed form of the θ function in terms of x and the integrals of the sources. These two integrations result in another set of integration constants C_1, which represent quantum corrections to the constants of the classical solution. Combining the zeroth and first order corrections together:

$$\rho(\mathrm{x}) + \varepsilon\alpha \mapsto \rho, \;\; e^{-\phi(\mathrm{x})} + \varepsilon\theta \mapsto e^{-\phi}, \;\; \mathrm{F}^{\pm} + \varepsilon \mathrm{G}^{\pm} \mapsto \mathrm{F}^{\pm}, \;\; C + \varepsilon C_1 \mapsto C, \tag{3.113}$$

we get the quantum-corrected solution that depends on x and the sources $t_{\pm(}\sigma^{\pm})$.

With this, the general vacuum solution to the quantum-corrected equations of motion has been determined to first order in ε. We now turn to the collapse setup. As in the classical analysis, the spacetime is split into two regions, each described by a vacuum solution. In the first part, we select a solution with vanishing energy flux at both future and past null infinity. Consequently, the quantum state is $|0, \sigma\rangle$, which implies $t_{\pm}(\sigma^{\pm}) = 0$. Upon entering the second part of the spacetime, the asymptotically flat coordinates are replaced by $\hat{\sigma}^{\pm}$, but the quantum state itself remains unchanged. In contrast, the solution in part II depends on $t_{\pm}(\hat{\sigma}^{\pm})$. Since this dependence is of order ε, it suffices to evaluate it at zeroth order, so that it is governed solely by the classical coordinate transformations $\mathrm{F}^{\pm}$, namely:

$$t_{\pm}(\hat{\sigma}^{\pm}) = \mathrm{F}^{\pm 2}\left[\frac{1}{4}\left(\partial_{\pm}\ln \mathrm{F}^{\pm}\right)^{2} + \frac{1}{2}\partial_{\pm}^{2}\ln \mathrm{F}^{\pm}\right]. \tag{3.114}$$

Because only the σ^{-} coordinate is transformed non-trivially, we have $t_{-}(\hat{\sigma}^{-}) \neq 0$ as the only non-vanishing component. In this way, the functions $t_{\pm}$ that specify the quantum state are determined in part II of the spacetime. The continuity conditions (3.102) and (3.104) must then be imposed, yielding the quantum-corrected coordinate transformations into part II, as well as the quantum-corrected discontinuity in the constants C, which encode the mass and other charges of the theory. The geometry in part II of the spacetime is thus completely specified.

The quantum-corrected collapse scenario is depicted in Figure 3.3. It closely resembles the classical collapse shown in Figure 3.2. The key distinction is the emergence of region III within the second part of the spacetime. This feature arises from the non-stationary geometry, which gives rise to an evaporating black hole located in region II of the spacetime. In this region, the geometry is such that the apparent horizon, defined by $\partial_{+}e^{-n\phi} = 0$, and the singularity determined by solving $1/R = 0$ meet at a finite point in spacetime, denoted as the end-point of the evaporation $(\sigma_{\mathrm{E}}^{+}, \sigma_{\mathrm{E}}^{-})$. Nevertheless, in many 2D dilaton gravity models [23, 24, 25], the black hole has not radiated away all of its mass by this stage. In accordance with the cosmic censorship conjecture [106], a naked singularity cannot be allowed to form; thus, the remaining mass is discharged as an outgoing shockwave along the hypersurface $\sigma^{-} = \sigma_{\mathrm{E}}^{-}$. This shockwave is commonly referred to in the literature as "the thunderpop."

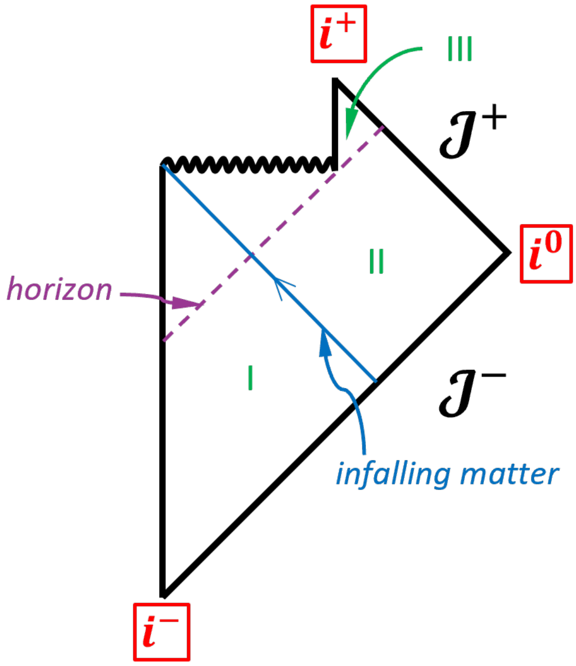

Figure 3.3: Penrose diagram of the quantum-corrected gravitational collapse featuring an evaporating black hole

Next, we need to identify the end-state geometry. The first step is to rewrite the solution using the radial coordinate x and the σ^{-} coordinate, since the hypersurface that separates the evaporating black hole in region II from the end-state geometry of region III is specified by the condition $\sigma^{-} = \sigma_{\mathrm{E}}^{-}$. We then recast the metric and the dilaton field in region II by introducing a running constant $\hat{C} = \hat{C}(\sigma^{-})$, expanded as $\hat{C} = C + \varepsilon\, C_1(\sigma^{-})$. This quantity closely follows the apparent horizon. Because the singularity is typically of ε-order,, the parameter $\hat{C}$ becomes small when the apparent horizon meets the singularity, i.e. near the end point of evaporation. Consequently, in the vicinity of the hypersurface $\sigma^{-} = \sigma_{\mathrm{E}}^{-}$ we can take the limit $\hat{C} \to 0$ within the first-order terms in the solution. In this limit, the solution reduces to one of the static configurations without energy flux at asymptotic infinity. Therefore, the metric and the dilaton field are already smoothly matched across the hypersurface $\sigma^{-} = \sigma_{\mathrm{E}}^{-}$.

Since no further coordinate transformation takes place in this step, the EMT in region III is already normal ordered with respect to the $\hat{\sigma}^{\pm}$ coordinates. We also identify the final vacuum state as $|0, \hat{\sigma}\rangle$. Consequently, the evolution both starts and ends in a pure state, implying that no information is lost during this process. Nevertheless, the final state does not depend on the detailed structure of the initial infalling matter shockwave. To determine whether information is genuinely lost, one must evaluate the entanglement entropy and verify whether it exceeds the coarse-grained limit set by the thermodynamic entropy.

Finally, as already noted, the black hole does not radiate away all of its mass by the time the evaporation reaches its end-point. One should determine how much mass remains by evaluating the emitted energy:

$$E_{rad} = -\varepsilon \int_{-\infty}^{\sigma_{\mathrm{E}}^{-}} \frac{\mathrm{d}\sigma^{-}}{\mathrm{F}^{-}} t_{-}(\hat{\sigma}^{-}) = M + M_{\mathrm{S}_1} - M_{\mathrm{S}_2} - M_0, \tag{3.115}$$

where M is the mass carried by the infalling matter shockwave, M_{S_1} denotes the mass of the initial spacetime of region I, M_{S_2} the mass of the final spacetime of region III, and $M_0 = \mathcal{O}(\varepsilon)$ is the small residual mass of the black hole at the end-point of the evaporation. This remaining mass is expected to be released as an outgoing energy shockwave. Equation (3.115) is referred to as the energy balance equation.

To verify the internal consistency of this treatment, one has to evaluate the EMT at the $\sigma^{-} = \sigma_{\mathrm{E}}^{-}$ hypersurface and demonstrate explicitly that it contains a term proportional to the Dirac-δ function, with mass equal to M_0. This confirms the presence of an outgoing shockwave originating from the evaporation end-point. One way to show this is to use the "$--$" component of the metric equation and integrate it across the $\sigma^{-} = \sigma_{\mathrm{E}}^{-}$ hypersurface. This procedure is analogous to the one previously used when the spacetime was matched across the infalling shockwave hypersurface (3.104).

Chapter 4

Review of the CGHS model

The classical CGHS model [19] is an example of a $2D$ dilaton gravity theory emerging from string theory. We are not be concerned here with the detailed derivation of its action. It can be obtained by dimensionally reducing an extremal magnetically charged black hole. Because the Einstein–Hilbert term in two dimensions is purely topological, gravitational dynamics originates from the interplay between the dilaton, acting as a scalar field, and the spacetime curvature. Furthermore, the model includes matter in the form of N massless scalar fields. The role of these N fields becomes crucial once quantum fluctuations are taken into account. The action of the CGHS model is given by:

$$S_{\mathrm{CGHS}} = \frac{1}{2\pi G}\int \mathrm{d}^2x\sqrt{-g}e^{-2\phi}\left[R + 4\left(\nabla\phi\right)^2 + 4\lambda^2\right] - \frac{1}{2}\sum_{i=1}^{N}\int \mathrm{d}^2x\sqrt{-g}\left(\nabla f_i\right)^2 , \tag{4.1}$$

where ϕ denotes the dilaton field, R the Ricci scalar curvature, λ a constant with dimensions of inverse length, and f_i is the one of the N scalar matter fields in the model. The constant G appearing in the first term is the two-dimensional Newton constant. Although it is often set to one or omitted in the literature, we keep it explicit to maintain dimensional consistency. We refer to the first term as S_g (the gravitational action) and the second as S_m (the matter action).

The chapter is organized into five sections. In the first section, we derive the equations of motion of the model. We then obtain their general solution and impose the static ansatz of Section 3.1. Among the resulting configurations, besides the usual linear dilaton vacuum and the static black hole, we study a particular cosmological solution with charged scalar matter fields. The section concludes with the introduction of a dynamical collapse scenario.

In the second section, we incorporate quantum fluctuations through the Polyakov–Liouville action (3.72), together with an additional correction term in the action designed to render the resulting equations exactly solvable. We examine how this new term modifies the equations of motion and determine the general static solutions using a symmetric ansatz.

The third section is devoted to the BPP model [25], specified by a particular choice of the correction terms. Within the BPP framework, we analyze the linear dilaton vacuum solution, a Minkowski vacuum solution characterized by a vanishing EMT at asymptotic infinity, as well as eternal and evaporating black hole solutions.

The penultimate section focuses on the perturbative treatment of the BPP model introduced in Section 3.4.1, specifically the quantum-corrected gravitational collapse scenario. Whereas the final section discusses the thermodynamical quantities within the classical CGHS model.

4.1 Equations of Motion

By varying the action with respect to the metric $g^{\mu\nu}$ and the dilaton field ϕ, we obtain the corresponding equations of motion:

$$\begin{aligned}
\delta S_g &= \frac{1}{2\pi G}\int \mathrm{d}^2x\sqrt{-g}e^{-2\phi}\Big\{ \left(\delta \ln\left(\sqrt{-g}\right) - 2\delta\phi\right)\left[R + 4\left(\nabla\phi\right)^2 + 4\lambda^2\right] + \delta R + 4\delta\left(\nabla\phi\right)^2 \Big\} \\
&= \frac{1}{2\pi G}\int \mathrm{d}^2x\sqrt{-g}e^{-2\phi}\Big\{ \left(-\frac{1}{2}g_{\mu\nu}\delta g^{\mu\nu} - 2\delta\phi\right)\left[R + 4\left(\nabla\phi\right)^2 + 4\lambda^2\right] \\
&\qquad + R_{\mu\nu}\delta g^{\mu\nu} + g^{\mu\nu}\delta R_{\mu\nu} + 4\nabla_\mu\phi\nabla_\nu\phi\delta g^{\mu\nu} + 8g^{\mu\nu}\nabla_\nu\phi\nabla_\mu\left(\delta\phi\right) \Big\} \\
&= \frac{1}{2\pi G}\int \mathrm{d}^2x\sqrt{-g}e^{-2\phi}\Big\{ \left[-2\left(\left(\nabla\phi\right)^2 + \lambda^2\right)g_{\mu\nu} + 4\nabla_\mu\phi\nabla_\nu\phi + \cancelto{0}{G_{\mu\nu}}\right]\delta g^{\mu\nu} \\
&\qquad + \underbrace{g^{\mu\nu}\delta R_{\mu\nu}}_{A} - 2\left[R + 4\left(\nabla\phi\right)^2 + 4\lambda^2\right]\delta\phi + \underbrace{8g^{\mu\nu}\nabla_\nu\phi\nabla_\mu(\delta\phi)}_{B} \Big\}.
\end{aligned} \tag{4.2}$$

In the second line, we employed the standard relation for the variation of the metric determinant, $\delta\sqrt{-g} = -\frac{1}{2}\sqrt{-g}g_{\mu\nu}\delta g^{\mu\nu}$, along with $\delta(\nabla\phi)^2 = \nabla_\mu\phi\nabla_\nu\phi\delta g^{\mu\nu} + 2g^{\mu\nu}\nabla_\nu\phi\nabla_\mu(\delta\phi)$ [106]. Due to the enhanced symmetry of a $2D$ spacetime, the Ricci tensor is proportional to the metric, which makes the Einstein tensor $G_{\mu\nu} = R_{\mu\nu} - \frac{1}{2}Rg_{\mu\nu}$, appearing in the third line, vanish identically. Thus, we are left with simplifying the terms A and B in (4.2). The term B can be directly simplified via partial integration. Neglecting boundary terms (as they do not influence the equations of motion), we obtain:

$$B = \frac{1}{2\pi G}\int \mathrm{d}^2x\sqrt{-g}e^{-2\phi}\left[-8\Box\phi + 16(\nabla\phi)^2\right]\delta\phi. \tag{4.3}$$

The simplification of term A in (4.2) is more complex. We begin by evaluating the variation $\delta R_{\mu\nu}$. To this end, let us examine the situation in a locally flat reference frame (where $\Gamma^\rho_{\mu\nu} = 0$ but $\partial_\sigma\Gamma^\rho_{\mu\nu} \neq 0$):

$$\delta R_{\mu\nu} = \delta R^\rho{}_{\mu\rho\nu} = \delta\left(\partial_\rho\Gamma^\rho_{\mu\nu} - \partial_\nu\Gamma^\rho_{\rho\mu} - \Gamma^\rho_{\rho\alpha}\Gamma^\alpha_{\mu\nu} - \Gamma^\rho_{\nu\alpha}\Gamma^\alpha_{\mu\rho}\right) = \partial_\rho\left(\delta\Gamma^\rho_{\mu\nu}\right) - \partial_\nu\left(\delta\Gamma^\rho_{\rho\mu}\right). \tag{4.4}$$

It is well established that Christoffel symbols themselves do not transform as tensor components. However, it is also known that the difference between two Christoffel symbols does behave as a tensor component [106]. Since we are dealing with such a quantity, specifically $\delta\Gamma^\rho_{\mu\nu}$, we are allowed to use the principle of minimal substitution. Consequently, we obtain

$$\delta R_{\mu\nu} = \nabla_\rho\left(\delta\Gamma^\rho_{\mu\nu}\right) - \nabla_\nu\left(\delta\Gamma^\rho_{\rho\mu}\right). \tag{4.5}$$

Inserting this relation into the expression for A and carrying out a partial integration (discarding boundary terms) leads to:

$$A = \frac{1}{\pi G}\int \mathrm{d}^2x\sqrt{-g}e^{-2\phi}g^{\mu\nu}\left[\nabla_\rho\phi\,\delta\Gamma^\rho_{\mu\nu} - \nabla_\nu\phi\,\delta\Gamma^\rho_{\mu\rho}\right]. \tag{4.6}$$

Because this quantity is a tensor, it is more convenient to evaluate it in a locally flat reference frame (LFRF). The transformation to such a locally flat reference frame is given by:

$$g_{\mu\nu} \longleftrightarrow \eta_{\mu\nu} \quad\wedge\quad \nabla_\mu \longleftrightarrow \partial_\mu \quad\wedge\quad d^2x\sqrt{-g} \longleftrightarrow d^2x \quad\wedge\quad \partial_\rho g_{\mu\nu} = 0 \quad\wedge\quad \partial_\sigma\partial_\rho g_{\mu\nu} \neq 0. \tag{4.7}$$

Therefore, under this transition, the variations of the Christoffel symbols persist, even though the Christoffel symbols themselves vanish. The term A in the locally flat reference frame then takes the following form:

$$\begin{aligned} A\Big|_{\mathrm{LFRF}} &= \frac{1}{\pi G}\int \mathrm{d}^2x e^{-2\phi}\eta^{\mu\nu}\left[\partial_\rho\phi\,\delta\Gamma^\rho_{\mu\nu} - \partial_\nu\phi\,\delta\Gamma^\rho_{\mu\rho}\right] \\ &= \frac{1}{\pi G}\int \mathrm{d}^2x e^{-2\phi}\partial_\rho\phi\left(\eta^{\lambda\nu}\eta^{\rho\mu} - \eta^{\mu\nu}\eta^{\lambda\rho}\right)\partial_\lambda(\delta g_{\mu\nu}) \\ &= \frac{1}{\pi G}\int \mathrm{d}^2x\left(\eta^{\mu\nu}\eta^{\lambda\rho} - \eta^{\lambda\nu}\eta^{\rho\mu}\right)\partial_\lambda\left(e^{-2\phi}\partial_\rho\phi\right)\delta g_{\mu\nu}. \end{aligned} \tag{4.8}$$

In the first line we applied the transition to the LFRF. In the second line we substituted the expressions for the variation of the metric in the LFRF: $\delta\Gamma^\rho_{\mu\nu} = \frac{1}{2}\eta^{\lambda\rho}\left[\partial_\mu(\delta g_{\nu\lambda}) + \partial_\nu(\delta g_{\mu\lambda}) - \partial_\lambda(\delta g_{\mu\nu})\right]$ and simplified the expression. In the third line we applied partial integration. Following the principle of minimal substitution and returning to a general reference frame, as well as using the relation: $\delta g_{\rho\sigma} = -g_{\rho\mu}g_{\sigma\nu}\delta g^{\mu\nu}$ the term A becomes:

$$A = \frac{1}{2\pi G}\int \mathrm{d}^2x\sqrt{-g}\left[-\nabla_\mu\nabla_\nu e^{-2\phi} + g_{\mu\nu}\Box e^{-2\phi}\right]\delta g^{\mu\nu}. \tag{4.9}$$

By substituting back into the expression 4.2 for the variation of the gravitational action S_g, we obtain:

$$\begin{aligned} \delta S_g = \frac{1}{2\pi G}\int \mathrm{d}^2x\sqrt{-g}e^{-2\phi}\Big\{ &\left[2\nabla_\mu\nabla_\nu\phi + \left(2(\nabla\phi)^2 - 2\Box\phi - 2\lambda^2\right)g_{\mu\nu}\right]\delta g^{\mu\nu} \\ &+ \left[-2R + 8(\nabla\phi)^2 - 8\lambda^2 - 8\Box\phi\right]\delta\phi\Big\}. \end{aligned} \tag{4.10}$$

To derive the complete set of equations of motion, one must also vary the matter action S_m with respect to both the metric $g^{\mu\nu}$ and the matter fields f_i. This procedure mirrors the one applied to the gravitational action S_g. As a consequence, we arrive at the following result:

$$\delta S_m = -\sum_{i=1}^{N}\int \mathrm{d}^2x\sqrt{-g}\Big\{\frac{1}{2}\left[\nabla_\mu f_i\nabla_\nu f_i - \frac{1}{2}g_{\mu\nu}(\nabla f_i)^2\right]\delta g^{\mu\nu} - (\Box f_i)\,\delta f_i\Big\}. \tag{4.11}$$

We observe that the energy–momentum tensor (EMT), given by $T^f_{\mu\nu} \equiv \frac{-2}{\sqrt{-g}}\frac{\delta S_m}{\delta g^{\mu\nu}} = \sum_{i=1}^N T^{(i)}_{\mu\nu}$, coincides with the EMT of massless scalar fields. In this expression, $T^{(i)}_{\mu\nu}$ denotes the EMT corresponding to the i-th particle species, obtained from the action $S^{(i)}_m$ of the associated i-th matter field. Therefore, enforcing Hamilton's principle, $\delta S_{CGHS} = \delta S_g + \delta S_m = 0$, yields the following equations of motion:

$$\begin{aligned} \frac{\delta S}{\delta g^{\mu\nu}} = 0 :&\quad \nabla_\mu\nabla_\nu\phi\, e^{-2\phi} + g_{\mu\nu}\left((\nabla\phi)^2 - \Box\phi - \lambda^2\right)e^{-2\phi} = \frac{\pi G}{2}T^f_{\mu\nu}, \\ \frac{\delta S}{\delta\phi} = 0 :&\quad \Box\phi = (\nabla\phi)^2 - \lambda^2 - \frac{1}{4}R, \\ \frac{\delta S}{\delta f_i} = 0 :&\quad \Box f_i = 0;\ \ \forall i \in \{1,2,...,N\} \\ T^{(i)}_{\mu\nu} \equiv \frac{-2}{\sqrt{-g}}\frac{\delta S^{(i)}_m}{\delta,\, g^{\mu\nu}} :&\quad T^{(i)}_{\mu\nu} = \nabla_\mu f_i\nabla_\nu f_i - \frac{1}{2}g_{\mu\nu}(\nabla f_i)^2\ \ \forall i \in \{1,2,...,N\}. \end{aligned} \tag{4.12}$$

Up to this point, we have treated the first term in the CGHS action as the gravitational action, but it can be interpreted in another way. More precisely, it encodes the coupling between the dilaton and the spacetime curvature and can therefore be viewed as the matter action associated with the dilaton. The truly gravitational contribution is instead given by the Einstein–Hilbert action. Since it appears in the field equations as $0 = G_{\mu\nu} \propto T_{\mu\nu}$, we infer that, in two dimensions, the equations of motion reduce to $T_{\mu\nu} = 0$. With this in mind, we can introduce the dilaton energy–momentum tensor:

$$T^{\phi}_{\mu\nu} = \frac{-2}{\sqrt{-g}}\frac{\delta S_g}{\delta g^{\mu\nu}} = -\frac{2}{\pi G}\left[\nabla_\mu\nabla_\nu\phi + \left((\nabla\phi)^2 - \Box\phi - \lambda^2\right) g_{\mu\nu}\right]e^{-2\phi}. \tag{4.13}$$

We thus find that the equations of motion take the expected form, $T^{\phi}_{\mu\nu} + T^{f}_{\mu\nu} = 0$. This observation will play a crucial role when we later discuss the interpretation of the limit $N \gg 1$ for the matter fields.

4.1.1 General solution of the equations of motion

In this subsection, we proceed to solve the equations of motion (4.12). We adopt light-cone coordinates $x^{\pm} = t \pm x$ and work in the conformal gauge introduced in Chapter 3. Substituting the conformal-gauge metric (3.2) together with the scalar invariants (3.4) into (4.12), we obtain the corresponding equations for ρ and ϕ. Using the identity $\partial_+\partial_- e^{-2\phi} = (-2\partial_+\partial_-\phi + 4\partial_+\phi\,\partial_-\phi)\,e^{-2\phi}$, the equations of motion can be rewritten in the following form:

$$+-: \quad \partial_+\partial_- e^{-2\phi} + \lambda^2 e^{2(\rho-\phi)} = \pi G T^{f}_{+-}, \tag{4.14}$$
$$\pm\pm: \quad -\partial_\pm^2 e^{-2\phi} + 4\partial_\pm\phi\partial_\pm(\phi-\rho)e^{-2\phi} = \pi G T^{f}_{\pm\pm}, \tag{4.15}$$
$$\phi: \quad \partial_+\partial_- e^{-2\phi} - 2\partial_+\partial_-(\phi-\rho)e^{-2\phi} + \lambda^2 e^{2(\rho-\phi)} = 0, \tag{4.16}$$

where the first two equations follow from the metric equation, while the third is derived from the dilaton field equation. Since $T^{(i)}_{+-} = 0$ for massless scalar matter fields and $T^{(i)}_{\pm\pm} = (\nabla_\pm f_i)^2$, equations (4.14) and (4.16) can be combined to yield:

$$\partial_+\partial_-(\phi-\rho) = 0, \tag{4.17}$$

whose general solution takes the form:

$$2(\rho-\phi) = \omega_-(x^-) + \omega_+(x^+) \tag{4.18}$$

where ω_+ and ω_- denote arbitrary functions of a single variable. We can now insert this expression back into Equation (4.14). Doing so gives:

$$e^{-2\phi} = -\lambda^2 \int \mathrm{d}x^- e^{\omega_-} \int \mathrm{d}x^+ e^{\omega_+} + F_+(x^+) + F_-(x^-), \tag{4.19}$$

where $F_\pm(x^\pm)$ constitute another set of arbitrary single-variable functions. We now transition to the $y^\pm$ coordinates, which offer a more suitable description while maintaining the conformal gauge, defined by $\frac{dy^\pm}{dx^\pm} = e^{\omega_\pm}$, leading to the following form of the metric:

$$ds^2 = \frac{dy^+dy^-}{-\lambda^2 y^+y^- + F_+(y^+) + F_-(y^-)}. \tag{4.20}$$

Using (4.19), we can readily determine $e^{-2\phi}$ as follows:

$$e^{-2\phi} = -\lambda^2 y^+ y^- + F_+(y^+) + F_-(y^-). \tag{4.21}$$

In this way, we have demonstrated that one can choose coordinates such that $\rho = \phi$. This particular choice is referred to as the Kruskal gauge condition, as it is directly connected to the Kruskal coordinates appearing in the Schwarzschild solution (see Appendix C.3). From this point onward, we work in the Kruskal gauge. Moreover, instead of denoting the coordinates by $y^\pm$, we use $x^\pm$ to represent the Kruskal coordinates. The remaining task is to solve Equation (4.15), which simplifies to:

$$\frac{d^2 F_\pm}{dx^{\pm 2}} = -\pi G T^f_{\pm\pm}(x^\pm), \tag{4.22}$$

which leads to the following form of the functions $F_\pm$ expressed in terms of the given EMT:

$$F_\pm(x^\pm) = -\pi G \int \mathrm{d}x^\pm \int \mathrm{d}x^\pm T^f_{\pm\pm}(x^\pm) + a_\pm x^\pm + \frac{b}{2}. \tag{4.23}$$

where $a_\pm$ and b are arbitrary constants. From Equation (4.22), it follows that $T^f_{\pm\pm}$ can depend only on $x^\pm$. By inspecting the matter field equations from (4.12), we confirm that this requirement is indeed fulfilled:

$$\Box f_i = 0 \Longrightarrow \partial_+\partial_- f_i = 0 \implies f_i = f_{i+}(x^+) + f_{i-}(x^-) \implies T^{(i)}_{\pm\pm}(x^\pm) = \left(\frac{df_{i\pm}}{dx^\pm}\right)^2. \tag{4.24}$$

Therefore, the general solution of the equations of motion in the Kruskal gauge is given by:

$$e^{-2\phi} = -\lambda^2 x^+ x^- - \pi G \int \mathrm{d}x^+ \int \mathrm{d}x^+ T_{++} - \pi G \int \mathrm{d}x^- \int \mathrm{d}x^- T_{--} + a_+ x^+ + a_- x^- + b. \tag{4.25}$$

In this setup, the geometry is characterized by three constants, $a_\pm$ and b, together with the EMT of the matter fields, $T^f_{\pm\pm}(x^\pm)$. In the absence of matter, the constants $a_\pm$ can be eliminated by an appropriate change of coordinates, $x^\pm \mapsto x^\pm - \frac{a_\mp}{\lambda^2}$. Depending on this choice, we obtain various distinct solutions, i.e. different geometries. It should be remembered that all of this has been formulated in the Kruskal gauge. If required, we can easily switch to other coordinate systems.

4.1.2 Applying the static ansatz setup

In the preceding subsection, we described the standard procedure for solving the CGHS equations of motion in the Kruskal gauge. We now instead employ the symmetric ansatz introduced in Section 3.1, which is obtained by imposing the presence of a time-like Killing vector. In this setup, the natural length scale is determined by λ, implying $L = 1/\lambda$, and the reduced field defined in (3.7) becomes $\mathrm{x} = e^{-\phi}$. By rewriting the metric equation using (3.8) for the metric function Λ, together with (3.13), we obtain:

$$\frac{\mathcal{D}}{4\Lambda}\left[\frac{\mathrm{d}}{\mathrm{dx}}\left(\mathrm{x}^2\mathcal{D}\frac{\mathrm{d}\Lambda}{\mathrm{dx}}\right)\xi_\mu\xi_\nu - \left(\frac{\mathrm{d}}{\mathrm{dx}}\left(\mathrm{x}^2\mathcal{D}\frac{\mathrm{d}\Lambda}{\mathrm{dx}}\right) + 4\mathrm{x}^2\Lambda\frac{\mathrm{d}}{\mathrm{dx}}\left(\frac{\mathcal{D}}{\mathrm{x}}\right)\right)\varepsilon_{\mu\rho}\varepsilon_{\nu\sigma}\xi^\rho\xi^\sigma\right] = \frac{\pi G}{2\lambda^2}T^f_{\mu\nu}, \tag{4.26}$$

where we have employed the auxiliary relations (3.32) and (3.33) for the scalar invariants $\Box\mathrm{x}$ and $(\nabla\mathrm{x})^2$, respectively, as well as (3.24) and (3.29) for the covariant derivative of the Killing vector and the scalar curvature. This equation implies that the only non-zero components of the EMT are the one aligned with the Killing vector, $T^{\|\|}$, and the one orthogonal to it, $T^{\perp\perp}$, while all mixed components vanish. Similarly, for the dilaton equation one gets:

$$\mathcal{D}\frac{\mathrm{d}}{\mathrm{dx}}\left(\Lambda\mathcal{D}\right)+\mathrm{x}+\frac{\mathrm{x}}{4}\mathcal{D}\frac{\mathrm{d}}{\mathrm{dx}}\left(\mathcal{D}\frac{\mathrm{d}\Lambda}{\mathrm{dx}}\right)=0. \tag{4.27}$$

Since the matter field are massless scalar fields, we can use the fact that their EMT is traceless in two dimensions. Thus, taking the trace of the metric Equation (4.26) gives:

$$\frac{\mathrm{d}}{\mathrm{dx}}\left(\mathrm{x}^2\mathcal{D}\frac{\mathrm{d}\Lambda}{\mathrm{dx}}\right)+2\mathrm{x}^2\Lambda\frac{\mathrm{d}}{\mathrm{dx}}\left(\frac{\mathcal{D}}{\mathbf{x}}\right)=0. \tag{4.28}$$

This equation is integrable, resulting into:

$$\frac{1}{2}\mathcal{D}\frac{\mathrm{d}\Lambda}{\mathrm{dx}}+\frac{\Lambda\mathcal{D}}{\mathrm{x}}=C, \tag{4.29}$$

where C is an integration constant. This equation can be regarded as a solution for $\mathcal{D}$. Substituting this solution into the dilaton Equation (4.27) we once again get an integrable equation, the solution being as follows:

$$\Lambda\mathrm{x}^2+C\mathrm{x}\Lambda\mathcal{D}=\mu, \tag{4.30}$$

where μ is another integration constant. Combining equations (4.29) and (4.30) results into a differential equation for Λ whose solution is:

$$\Lambda\mathrm{x}^2-\mu\ln\left|\Lambda\mathrm{x}^2\right|=b-C^2\mathrm{x}^2, \tag{4.31}$$

where yet another integration constant b is introduced. Next, we compute the tortoise coordinate (3.18). Direct calculation, yields

$$\lambda\sigma=-\frac{1}{2C}\ln\left|\Lambda\mathrm{x}^2\right|. \tag{4.32}$$

Finally, one has to enforce the constraints (3.22) for the asymptotical flat solution at infinity. Taking the limit $\mathrm{x}\to\infty$ of Equation (4.31), gives $\Lambda\to -C^2$, implying that $C=\pm 1$. Then, form (4.32) we deduce that $C=-1$, by demanding that $\sigma\to+\infty$ in this limit. Hence, the solution in the asymptotically flat coordinates depends on two constants b and μ and is given by:

$$\Lambda=\begin{cases}-\dfrac{1}{1+(b+2\mu\lambda\sigma)e^{-2\lambda\sigma}}, & \Lambda<0,\\ -\dfrac{1}{1-(b+2\mu\lambda\sigma)e^{-2\lambda\sigma}}, & \Lambda>0,\end{cases}\qquad \mathrm{x}=\begin{cases}\sqrt{b+2\mu\lambda\sigma+e^{2\lambda\sigma}}, & \Lambda<0,\\ \sqrt{b+2\mu\lambda\sigma-e^{2\lambda\sigma}}, & \Lambda>0.\end{cases} \tag{4.33}$$

Next, we compute the components of the EMT by substituting this solution into (4.26). This gives:

$$\Lambda^2T^{\|\|}=\Lambda^2T^{\perp\perp}=\frac{2\mu\lambda^2}{\pi G}. \tag{4.34}$$

In contrast, evaluation of the components of the EMT using the scalar field f and the equation of motion for the i-th field yields the following.

$$T^{\|\|}=T^{\perp\perp}=\frac{\lambda^2}{2}\sum_{i=1}^{N}\left(\mathcal{D}\frac{\mathrm{d}f_i}{\mathrm{dx}}\right)^2,\qquad \frac{\mathrm{d}}{\mathrm{dx}}\left(\Lambda\mathcal{D}\frac{\mathrm{d}f_i}{\mathrm{dx}}\right)=0. \tag{4.35}$$

Hence, the physical interpretation of the constant $\mu>0$ is that it is some type of a charge carried by the matter fields. Since the Equation (4.31) is transcendental when $\mu\neq 0$, we cannot write down the explicit expression for Λ in terms of x.

4.1.3 Static vacuum solutions

In this subsection, we examine the static vacuum solution, defined by the condition $T^f_{\mu\nu} = 0$, which holds when $\mu = 0$, as can be seen from (4.34). From (4.31) it follows that $\mathcal{D} = \mathrm{x}$, and Equation (4.32) provides an expression for Λ solely as a function of x, namely:

$$\Lambda = \frac{b}{\mathrm{x}^2} - 1, \quad \mathcal{D} = \mathrm{x}, \quad 2\lambda\sigma = \ln\left|b - \mathrm{x}^2\right|, \tag{4.36}$$

where the last expression determines the tortoise coordinate (4.32). There are three possible scenarios depending on the sign of the constant b. To see if this solution possesses any singularity, we compute the scalar curvature. Using (3.29) we obtain:

$$R = \frac{4\lambda^2 b}{\mathrm{x}^2}. \tag{4.37}$$

It is now evident that as long as $b \neq 0$ there is a singularity at $\mathrm{x_S} = 0$. When $b = 0$, we have $\Lambda = -1$ throughout the entire spacetime and $R = 0$, so the geometry is simply flat Minkowski spacetime. For $b \neq 0$, in order to determine whether the solution describes a black hole or a naked singularity, we must check for the presence of an event horizon. The event horizon is defined as the hypersurface on which the time-like Killing vector becomes null, i.e., where $\Lambda = 0$. If $b < 0$, then $\Lambda < 0$ everywhere, indicating that no event horizon exists. Conversely, for $b > 0$, imposing $\Lambda = 0$ gives $\mathrm{x_H} = \sqrt{b}$. It is therefore clear that in this case the solution corresponds to a static black hole. Hence, the solutions can be classified according to the sign of the constant b as follows:

- $b = 0$: Flat Minkowski spacetime,
- $b < 0$: Naked singularity,
- $b > 0$: Static black hole.

The cosmic censorship conjecture rules out the formation of naked singularities, which in turn requires that the constant b be nonnegative. Now we examine each of the two allowed cases in detail.

Linear dilaton vacumm

Within the CGHS model, the vacuum configuration is referred to as the linear dilaton vacuum. This terminology stems from the fact that, for $b = 0$, the dilaton field ϕ depends linearly on the spatial coordinate σ. Explicitly, the solution is

$$\mathrm{d}^2 s = -\mathrm{d}t^2 + \mathrm{d}\sigma^2, \quad \phi = -\lambda\sigma, \tag{4.38}$$

and it arises as the limit $b \to 0$ of the general static vacuum solution (4.36). This solution exhibits the full two-dimensional Poincaré symmetry, meaning that, in addition to the Killing vector ∂_t, there are two more Killing vectors: ∂_σ corresponding to spatial translations, and $L = \sigma\partial_t + t\partial_\sigma$ corresponding to Lorentz boosts.

Static black hole

This scenario corresponds to a choice $b > 0$ in the general static solution (4.36). As mentioned before, the event horizon is $\mathrm{x_H} = \sqrt{b}$, while the singularity is $\mathrm{x_S} = 0$. The two extra Killing vectors vanish, leaving only the Killing vector of time translations. Transitioning to the Eddington-Finkelstein coordinates, similarly to the general solution of the CGSH model with matter (4.33), we get:

$$\Lambda = \begin{cases} -\dfrac{1}{1+be^{-2\lambda\sigma}}, & \Lambda < 0, \\ -\dfrac{1}{1-be^{-2\lambda\sigma}}, & \Lambda > 0, \end{cases} \qquad \mathrm{x} = \begin{cases} \sqrt{b+e^{2\lambda\sigma}}, & \Lambda < 0, \\ \sqrt{b-e^{2\lambda\sigma}}, & \Lambda > 0. \end{cases} \tag{4.39}$$

In this coordinate system, the horizon is shifted to infinity, that is, $\sigma_H = -\infty$. Consequently, the two cases in (4.39) represent two coordinate charts that are joined along the event horizon hypersurface located at infinity. The singularity is still determined by $\mathrm{x}_S = 0$, which gives $b = e^{2\lambda\sigma}$ in Eddington-Finkelstein coordinates.

To construct the maximally extended black hole solution, as in the Schwarzschild case, we need to switch to Kruskal coordinates (see Appendix D.5). Our first task is to determine the surface gravity at the horizon:

$$\kappa = \frac{\lambda}{2}\left|\mathcal{D}\frac{\mathrm{d}\Lambda}{\mathrm{dx}}\right|_{\mathrm{H}} = \lambda, \tag{4.40}$$

accordingly, the Kruskal coordinates follow from exponentiating the Eddington–Finkelstein coordinates using the surface gravity, that is:

$$|\lambda x^+| = e^{\lambda\sigma^+} \quad \wedge \quad |\lambda x^-| = e^{-\lambda\sigma^-}, \tag{4.41}$$

where the signs of $x^\pm$ determine four patches connected by the event horizon. In all four patches, the metric and the dilaton exhibit the same form:

$$ds^2 = -\frac{dx^+dx^-}{-\lambda^2x^+x^- + b}, \qquad e^{-2\phi} = -\lambda^2x^+x^- + b. \tag{4.42}$$

As anticipated, in Kruskal coordinates we have $\phi = \rho$. This solution coincides with the general solution (4.33) once the condition of a vanishing EMT is enforced (along with $a_\pm = 0$).

The transformation (4.41) divides the spacetime into four distinct regions, classified according to the signs of the Kruskal coordinates $x^\pm$. As an illustration, region III is characterized by $x^+ < 0$ and $x^- < 0$. Collectively, these four regions serve as coordinate charts that together constitute an atlas for the spacetime manifold. In practical applications, one typically focuses on region I and, in some cases, region II. Region I describes the exterior of the black hole and directly corresponds to the $\Lambda < 0$ case in (4.36), whereas region II describes the black hole interior, where the Killing vector is space-like, i.e. $\Lambda > 0$.

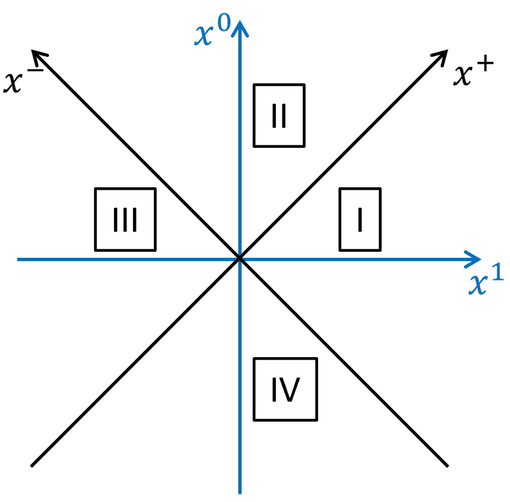

Figure 4.1: Different patches of the spacetime

We now examine the coordinate curves $t =$ const. and $\sigma =$ const. in Kruskal coordinates:

$$t = c : \frac{x^+}{x^-} = e^{2\lambda t} \implies x^+ = c\, x^-,$$
$$\sigma = c : \lambda^2 x^+ x^- = \pm e^{2\lambda\sigma} \implies x^+ x^- = c.$$

In Figure 4.2, the $t =$ const. curves are plotted in red, whereas the $\sigma =$ const. curves appear in blue. The Killing horizons (i.e., the event horizons) lie at $\sigma \to -\infty$ and are drawn in green. Singularities occur in regions I and IV of Figure 4.1, specified by the relation $\lambda^2 x^+ x^- = b$, i.e. $2\lambda\sigma = \ln b$, and are indicated in the figure by a black wavy line.

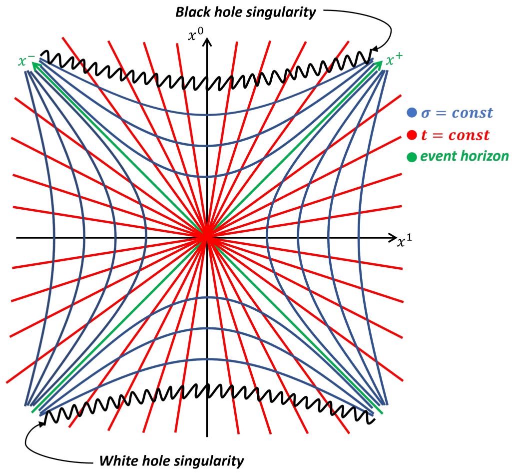

Figure 4.2: Kruskal diagram in CGHS model

We observe that the resulting diagram is completely analogous to the Kruskal diagram of the Schwarzschild solution (see Appendix C.3). Consequently, the corresponding conformal diagrams also match (see Appendix C.4). Even the singularity is described by the same functional relation $x^+ = x^+(x^-)$. We now proceed to identify the standard black-hole (t, r) coordinates, in which the metric assumes the following form:

$$ds^2 = -l(r)dt^2 + \frac{dr^2}{l(r)} \implies \frac{dr}{d\sigma} = \frac{1}{1 \pm be^{-2\lambda\sigma}} \implies e^{2\lambda r} = C\left(e^{2\lambda\sigma} \pm b\right). \tag{4.43}$$

We note that the $\pm$ signs in these expressions determine whether the solution is defined in quadrants I and II or in quadrants III and IV, respectively. Enforcing the condition $r = r_H$ at the horizon leads to $C = \pm\frac{e^{2\lambda r_H}}{b}$. Thus, for $l(r)$ we find:

$$l(r) = 1 - e^{-2\lambda(r-r_H)}, \quad 2\lambda\sigma = \ln\left[\pm b\left(e^{2\lambda(r-r_H)} - 1\right)\right]. \tag{4.44}$$

The singularity is located at:

$$r_S = r_H + \frac{1}{2\lambda}\ln b. \tag{4.45}$$

As in the Schwarzschild case, regions I and II are both represented by the same metric in the (t, r) coordinate system. Spacetime terminates at the value of the radial coordinate r associated with the singularity. The domain $r > r_H$ represents region I in Figure 4.1, while $r < r_H$ denotes region II. Moreover, the dilaton reduces to a linear function of r, namely:

$$\phi = -\frac{1}{2}\ln b - \lambda(r - r_H). \tag{4.46}$$

We still have to clarify the physical interpretation of the constant b, namely how it relates to the black hole mass. Although one could determine this using the ADM formalism, we will not adopt that approach here. Instead, we will deduce the form of this relation from the dynamical setup introduced in the following subsection.

4.1.4 Cosmological solution with charged matter

In this subsection, we examine the general static solution (4.90) in the case where the matter charged with $\mu \neq 0$. The event horizon is defined by the condition $\Lambda = 0$. From Equation

(4.31) we infer that, as long as $\mu \neq 0$, there is no finite value of x that satisfies this condition. Let us first consider the case $\Lambda < 0$. Attempting to determine the apparent horizon from $\partial_+ \mathrm{x}^2 = 0$ leads to the equation $\mu + e^{2\lambda\sigma} = 0$. Since $\mu > 0$, this equation admits no solutions. The curvature scalar is given by

$$R = 4\lambda^2 \left[\left(\frac{e^{2\lambda\sigma} + \mu}{b + 2\mu\lambda\sigma + e^{2\lambda\sigma}} \right)^2 - 1 \right]. \tag{4.47}$$

It is evident that the curvature diverges along the hypersurface $\mathrm{x} = 0$. This equation always admits a solution for a negative value of the coordinate σ. Consequently, this configuration describes a naked singularity and is therefore excluded by the cosmic censorship conjecture.

For $\Lambda > 0$ we are effectively looking for the cosmological solution. The first order of business is to determine under which conditions $\Lambda > 0$ holds. This is the case when:

$$e^{2\lambda\sigma} \leqslant b + 2\mu\lambda\sigma. \tag{4.48}$$

For a fixed value of μ, with $\mu > 0$, there is a critical value of b above which the inequality admits a solution. In Figure 4.3 we plot the functions $f(x) = e^x$ and $g_b(x) = b + \mu x$, where $x = 2\lambda\sigma$. For sufficiently small b, a solution does not always exist. As b increases, one reaches a critical point at which $g_b(x)$ becomes tangent to $f(x)$. Differentiating (4.48), we obtain $2\lambda\sigma_{cr} = \ln\mu$. Substituting this back into (4.48) yields the condition on b:

$$b \geqslant \mu\left(1 - \ln\mu\right). \tag{4.49}$$

For $\mu > e$, this inequality is automatically fulfilled for any positive b.

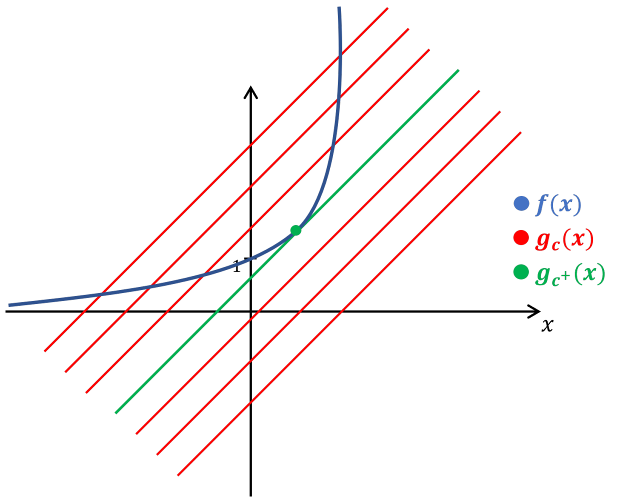

Figure 4.3: Graphical solution to inequality (4.48)

Now assume that condition (4.49) holds. As illustrated in Figure 4.3, inequality (4.48) admits two critical values, denoted by σ_1 and σ_2. Because $\Lambda > 0$, the Killing vector ξ is spacelike, which means that σ plays the role of a time coordinate. We therefore relabel it as $\sigma \mapsto \tau$. The metric then takes the form

$$\mathrm{d}s^2 = \frac{-\mathrm{d}\tau^2 + \mathrm{d}r^2}{(b + 2\mu\lambda\tau)e^{-2\lambda\tau} - 1}, \tag{4.50}$$

which can be cast into the standard cosmological form $\mathrm{d}s^2 = -\mathrm{d}t^2 + a(t)^2\mathrm{d}r^2$, where the new time coordinate t and the derivative of the scale factor $a = \sqrt{\Lambda}$, namely $\dot{a}(t)$, are given by

$$t = \int \frac{\mathrm{d}\tau}{\sqrt{(b + 2\mu\lambda\tau)e^{-2\lambda\tau} - 1}}, \qquad \dot{a}(t) = \lambda \frac{b - \mu + 2\mu\lambda\tau}{\left((b + 2\mu\lambda\tau)e^{-2\lambda\tau} - 1\right)^{3/2}} e^{-2\lambda\tau}. \tag{4.51}$$

From this expression we observe that $\dot{a}(t) < 0$ for $\tau_1 < \tau < \frac{b-\mu}{2\lambda\mu}$, and $\dot{a}(t) > 0$ for $\frac{b-\mu}{2\lambda\mu} < \tau < \tau_2$. Hence, the universe undergoes a contraction phase with $\dot{a}(t) > 0$ until the moment $\tau = \frac{b-\mu}{2\lambda\mu}$, after which it begins to expand to infinity. The curvature becomes singular at both endpoints, so this solution corresponds to a universe that originates as an infinite universe at $\tau = \tau_1$ and terminates in a big rip at $\tau = \tau_2$, once again diverging to infinity.

4.1.5 Dynamical solution and gravitational collapse

In this section, we consider the dynamical solution of the equations of motion (4.14-4.16), closely following the method described in Section 3.4. The overall setup is illustrated in Figure 3.2. The matter content is represented by an infalling shockwave localized on the hypersurface $x^+ = x_0^+$. We begin by re-deriving Equation (3.104) within this framework. Because both ϕ and ρ must remain continuous throughout spacetime, as required by (3.102), the derivatives $\partial_+\phi$ and $\partial_+\rho$ do not contain contributions proportional to the Dirac δ-function. Integrating the equations across the shockwave then yields:

$$\partial_+ e^{-2\phi}\Big|_{>}^{<} = \frac{\pi G M}{\mathrm{F}^+(x_0^+)}. \tag{4.52}$$

Using the ansatz for the derivative of the dilaton (3.13), together with the general static vacuum solution (4.36), we find:

$$2\mathrm{x}\frac{\lambda}{2}\mathrm{F}^-\mathcal{D}e^{2\rho}\Big|_{<}^{>} = \frac{\pi G M}{\mathrm{F}^+(x_0^+)} \quad\Longrightarrow\quad \Lambda \mathrm{x}^2\Big|_{<}^{>} = \frac{\pi G M}{\lambda} \quad\Longleftarrow\quad b_> - b_< = \frac{\pi G M}{\lambda}. \tag{4.53}$$

Imposing continuity of the metric then determines the jump in the function F^-:

$$\frac{\Lambda_{\mathrm{I}}}{\mathrm{F}^-_{\mathrm{I}}} = \frac{\Lambda_{\mathrm{II}}}{\mathrm{F}^-_{\mathrm{II}}} \quad\Longrightarrow\quad \mathrm{F}^-_{\mathrm{II}} = \mathrm{F}^-_{\mathrm{I}}\frac{b_> - \hat{\mathrm{x}}^2}{b_< - \hat{\mathrm{x}}^2} \quad\Longrightarrow\quad \mathrm{F}^-_{\mathrm{II}} = \mathrm{F}^-_{\mathrm{I}}\left(1 + \frac{\frac{\pi G M}{\lambda}}{b_< - \hat{\mathrm{x}}^2}\right), \tag{4.54}$$

where we have introduced the coordinate $\hat{\mathrm{x}}$ defined in (3.107). Hence, the general discontinuity of the solution when crossing the shockwave hypersurface is described by the following relation:

$$\left(\mathrm{F}^+, \mathrm{F}^-, b\right) \mapsto \left(\mathrm{F}^+, \mathrm{F}^-\left(1 + \frac{\frac{\pi G M}{\lambda}}{b - \hat{\mathrm{x}}^2}\right), b + \frac{\pi G M}{\lambda}\right). \tag{4.55}$$

This equation shows how the solution evolves when an additional mass M is added to the total mass of the black hole. The gravitational collapse corresponds to a scenario in which the initial spacetime is the linear dilaton vacuum, specified by $(-1, 1, 0)$, expressed in Eddington–Finkelstein coordinates. The subsequent transition to a black hole solution in region II of the spacetime is then:

$$(-1, 1, 0) \mapsto \left(-1, 1 - \frac{\pi G M}{\lambda}\frac{1}{\hat{\mathrm{x}}^2}, \frac{\pi G M}{\lambda}\right). \tag{4.56}$$

At this stage, the physical relation between the constant b and the black hole mass becomes clear: $b = \frac{\pi G M}{\lambda}$. The final step in the computation is to write down the explicit form of the dilaton field in the $(\delta, \hat{\mathrm{x}})$ coordinate system. In region II of spacetime, the solution takes the form:

$$\Lambda = \frac{\pi G M}{\lambda}\frac{1}{\mathrm{x}^2} - 1, \qquad \mathcal{D} = \mathrm{x}, \qquad \ln\left|b - \mathrm{x}^2\right| = -2\ln\delta + \ln\left|b - \hat{\mathrm{x}}^2\right|. \tag{4.57}$$

From this relation, it is immediately evident that at the shockwave hypersurface $\delta = 1$, we recover the expected identity $\mathrm{x} = \hat{\mathrm{x}}$.

We now rewrite the solution in terms of the Kruskal coordinates (4.41). A straightforward calculation gives:

$$e^{-2\phi} = e^{-2\rho} = -\lambda^2 x^+\left(x^- + \frac{\pi G M}{\lambda^3 x_0^+}\right) + \frac{\pi G M}{\lambda}. \tag{4.58}$$

Conversely, substituting $T_{++} = \frac{M}{\lambda x_0^+}\delta(x^+ - x_0^+)$, together with $\mathrm{F}^+(x_0^+) = -\lambda x_0^+$, into the general CGHS solution (4.81) and then carrying out the integration reproduces the same result, provided that continuity of both the metric and the dilaton field is enforced. For later convenience, we also define the notation $\Delta = \frac{\pi G M}{\lambda^3 x_0^+}$.

Using the coordinate transformations in region II of the spacetime (4.56), we directly calculate the new Eddington-Finkelstein coordinates in region II of the spacetime:

$$\lambda x^+ = e^{\lambda \hat{\sigma}^+} \quad \wedge \quad \lambda(x^- + \Delta) = -e^{-\lambda \hat{\sigma}^-}. \tag{4.59}$$

Inserting these expressions into the solution (4.58), we can immediately confirm that the solution depends solely on the coordinate $\hat{\sigma}$. Therefore, the solution is genuinely static within region II of the spacetime. It should be kept in mind, however, that although the solutions in each of the two spacetime regions are static, the spacetime as a whole does not possess a time-translation symmetry.

To obtain the Penrose diagram, we switch to compactified coordinates. The transformation that produces the required form is:

$$\lambda x^+ = \frac{\pi M G}{\lambda^2 \Delta} \tan y^+ \qquad \wedge \qquad \lambda\left(x^- + \Delta\right) = \lambda \Delta \tan y^-. \tag{4.60}$$

Under this transformation, the point x_0^+ is mapped to $y_0^+ = \frac{\pi}{4}$. In these new coordinates, the metric takes the form:

$$\mathrm{d}s^2 = \begin{cases} \dfrac{\mathrm{d}y^+ \mathrm{d}y^-}{\lambda^2 \cos^2 y^+ \cos^2 y^- \tan y^+ \left(\tan y^- - 1\right)}, & y^+ < \dfrac{\pi}{4} \\ \dfrac{\mathrm{d}y^+ \mathrm{d}y^-}{\lambda^2 \cos^2 y^+ \cos^2 y^- \left(\tan y^+ \tan y^- - 1\right)}, & y^+ > \dfrac{\pi}{4} \end{cases} \tag{4.61}$$

In Figure 4.4, the conformal diagram of the dynamical black hole is displayed. The singularity is specified by $\tan y^+ \tan y^- = 1$, i.e. $y^+ + y^- = \frac{\pi}{2}$, and is depicted as the black wavy line. The infalling matter is shown as the red arrowed curve. The hypersurfaces $i^\pm$ denote future and past timelike infinity (in red), while i^0 represents spatial infinity (in blue). The hypersurfaces $\mathcal{J}^\pm$ correspond to future and past null infinity (in green). The spacetime boundary is drawn as a solid black line. In region II, the event horizon is present, indicated by the solid blue line and given by $x_{\mathrm{H}}^- = -\Delta$. This expression follows from extremizing the two-dimensional area of a sphere, namely by imposing $\partial_+ e^{-2\phi} = 0$ (see Section 3.4). We find that the apparent horizon and the event horizon are identical.

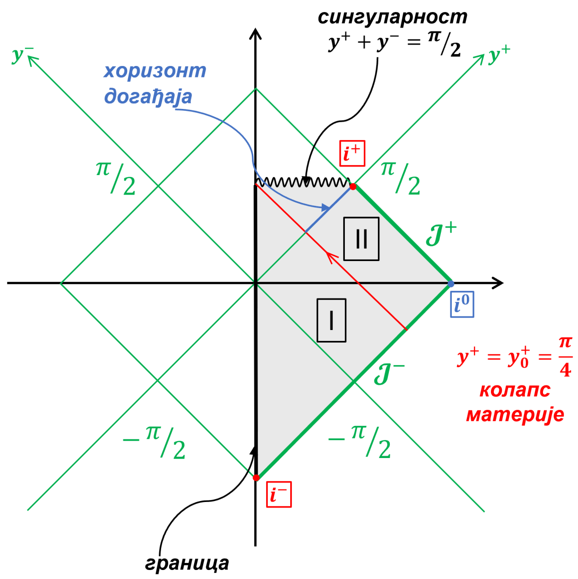

Figure 4.4: Penrose diagram of the dynamical scenario

This configuration does not describe an evaporating black hole. Indeed, the apparent horizon and the singularity meet at future time infinity i^+. Moreover, in region II of the spacetime, the fields are independent of the new time coordinate. To obtain a genuinely evaporating black hole solution, quantum corrections must be taken into account. For more details, see Section 3.4.

4.2 Adding quantum fluctuations

In this section, we incorporate quantum corrections into the classical CGHS model. Gravity is kept classical, while the scalar matter fields are quantized via the Polyakov–Liouville action (3.72). Further details on the quantization procedure for the scalar fields are provided in Section 3.3. Thus, we work within the semiclassical framework of quantum field theory on a fixed classical background geometry [26, 25]:

The central objective of these toy models is to obtain exactly solvable equations of motion that still capture the essential qualitative features of the system. The full CGHS action supplemented only with the PL term is not exactly solvable. For this reason, we introduce an additional correction term in the action, denoted by S_{cor}, which depends exclusively on the dilaton and the geometry. The complete action then takes the form:

$$S_{\text{QC}} = S_g[g, \phi] + S_m[g, f_i] + NS_{\text{PL}}[g, \psi] + S_{\text{cor}}[g, \phi]. \tag{4.62}$$

The first two contributions reproduce the classical CGHS model (4.1). Since S_{PL} is independent of the detailed structure of the matter fields, it is simply multiplied by N when there are N distinct matter fields. In two-dimensional models, the equations of motion reduce to the condition $T_{\mu\nu} = 0$, so we obtain:

$$T^{\phi}_{\mu\nu} + \Delta T^{\phi}_{\mu\nu} + T^{f,cl}_{\mu\nu} + N < \Delta T^{f}_{\mu\nu} >= 0, \tag{4.63}$$

where the various energy–momentum tensors are defined as follows:

$$T^{\phi}_{\mu\nu} = \frac{-2}{\sqrt{-g}}\frac{\delta S_g}{\delta g^{\mu\nu}}, \quad \Delta T^{\phi}_{\mu\nu} = \frac{-2}{\sqrt{-g}}\frac{\delta S_{cor}}{\delta g^{\mu\nu}}, \quad T^{f,cl}_{\mu\nu} = \frac{-2}{\sqrt{-g}}\frac{\delta S_m}{\delta g^{\mu\nu}}, \quad \langle \Delta T^{f}_{\mu\nu} \rangle = \frac{-2}{\sqrt{-g}}\frac{\delta S_{PL}}{\delta g^{\mu\nu}}. \tag{4.64}$$

The correction term S_{corr} can be interpreted as a classical modification of the original CGHS model; consequently, the EMT derived from this part of the action is labeled $\Delta T^{\phi}_{\mu\nu}$. We do not interpret this contribution as a quantum effect. In contrast, the only genuine quantum contributions stem from the Polyakov–Liouville term, so the corresponding EMT is written as $\langle \Delta T^{f}_{\mu\nu} \rangle$. Hence, the total EMT of the matter fields is:

$$T^{f}_{\mu\nu} = T^{f,cl}_{\mu\nu} + \langle \Delta T^{f}_{\mu\nu} \rangle \,. \tag{4.65}$$

Since the correction term must cancel the part of the PL action that renders the equations of motion not exactly solvable, it must scale as $N\hbar$. This creates an apparent tension: the correction term is intended to be classical, yet it is proportional to $\hbar$. To resolve this, let us consider a very large number of matter fields. In that case, the combination $N\hbar$ can be treated as a constant of the same order as $\frac{1}{2\pi G}$. Thus, we need not view it as a small quantum correction, but instead as a finite constant. Since the overall factor in front of the correction term can be chosen as an arbitrary constant that is not intrinsically of order $\hbar$, we are free to set it equal to the constant $N\hbar$.

Due to this correction term, the dilaton field equation of motion is modified as well and takes the following form:

$$\frac{\delta S_g}{\delta \phi} + \frac{\delta S_{corr}}{\delta \phi} = 0. \tag{4.66}$$

4.2.1 The correction term in the action

Here we examine which forms of the correction term in the action can make the equations of motion exactly solvable. While the main body of this work focuses on the BPP model, we introduce here a more general expression for the correction term. It is given by [26, 25]:

$$S_{cor} = \frac{N\hbar}{2\pi}\int \mathrm{d}^2x\sqrt{-g}\left[-C_1\phi R + \frac{C_2}{12}\left(\nabla\phi\right)^2\right], \tag{4.67}$$

where C_1 and C_2 are free parameters whose specific values determine the particular model. In the next section, we demonstrate how to choose these constants so that the resulting model possesses exactly solvable equations of motion. For the moment, we simply note which choices correspond to the most relevant models, namely the RST [23, 24] and BPP [25] models.

- **BPP model**: $C_1 = \frac{1}{12} \quad \wedge \quad C_2 = 1$
- **RST model**: $C_1 = \frac{1}{24} \quad \wedge \quad C_2 = 0$

By explicitly solving the equations of motion in detail, we can see why the constants are fixed in exactly this way. In this section, we keep the constants arbitrary. We now vary the action with respect to the metric and the dilaton field. The same type of term appears repeatedly in this calculation as in (4.2). After performing a large number of simplifications, we arrive at

$$\begin{aligned}\delta S_{cor} = \frac{N\hbar}{2\pi}\int \mathrm{d}^2x\sqrt{-g}\bigg\{&\left[C_1\Big(\nabla_\mu\nabla_\nu\phi - g_{\mu\nu}\Box\phi\Big) + \frac{C_2}{12}\left(\nabla_\mu\phi\nabla_\nu\phi - \frac{1}{2}g_{\mu\nu}\left(\nabla\phi\right)^2\right)\right]\delta g^{\mu\nu}\\ &+\left[-C_1R - \frac{C_2}{6}\Box\phi\right]\delta\phi\bigg\}.\end{aligned} \tag{4.68}$$

After a direct identification with (4.64), we can read off the correction to the energy–momentum tensor and the variation of the correction term with respect to the field ϕ, which are given by:

$$\begin{aligned}\Delta T^{\phi}_{\mu\nu} &= -\frac{N\hbar}{\pi}\left[C_1\Big(\nabla_\mu\nabla_\nu\phi - g_{\mu\nu}\Box\phi\Big) + \frac{C_2}{12}\left(\nabla_\mu\phi\nabla_\nu\phi - \frac{1}{2}g_{\mu\nu}\left(\nabla\phi\right)^2\right)\right],\\ \frac{\delta S_{cor}}{\delta\phi} &= \frac{N\hbar}{2\pi}\left[-C_1R - \frac{C_2}{6}\Box\phi\right].\end{aligned} \tag{4.69}$$

4.2.2 Equations of motion and their general solutions

Now we can write down the full set of equations of motion. On the left–hand side we collect the geometric contributions, i.e. all terms arising from the dilaton energy–momentum tensor, while on the right–hand side we put all matter contributions. Using (3.75) and (4.69), we arrive at the following system:

$$\begin{aligned}&\nabla_\mu\nabla_\nu\phi\, e^{-2\phi} + g_{\mu\nu}\left((\nabla\phi)^2 - \Box\phi - \lambda^2\right)e^{-2\phi}\\ &+\frac{N\hbar G}{2}\left[C_1\Big(\nabla_\mu\nabla_\nu\phi - g_{\mu\nu}\Box\phi\Big) + \frac{C_2}{12}\left(\nabla_\mu\phi\nabla_\nu\phi - \frac{1}{2}g_{\mu\nu}\left(\nabla\phi\right)^2\right)\right] = \frac{\pi G}{2}T^f_{\mu\nu},\\ &\left(-2R + 8\left(\nabla\phi\right)^2 - 8\lambda^2 - 8\Box\phi\right)e^{-2\phi} = N\hbar G\left(C_1R + \frac{C_2}{6}\Box\phi\right),\end{aligned} \tag{4.70}$$

where the only source term entering the equations of motion is the quantum–corrected energy–momentum tensor,

$$T^f_{\mu\nu} = T^{f,cl}_{\mu\nu} + \frac{N\hbar}{48\pi}\Big[-2\nabla_\mu\nabla_\nu\psi + \nabla_\mu\psi\nabla_\nu\psi + g_{\mu\nu}\left(2\Box\psi - \frac{1}{2}(\nabla\psi)^2\right)\Big]. \tag{4.71}$$

The second term in (4.70) precisely coincides with the EMT derived from the PL action in (3.75). Consequently, these equations merely represent a compact rewriting of the relations we have already obtained in the preceding sections. Our next task is to solve this coupled system. Expressing the equations of motion (4.70) in light–cone coordinates $x^\pm$ and choosing the conformal gauge metric (3.2), we find:

$$+-: \partial_+\partial_- e^{-2\phi} + \lambda^2 e^{2(\rho-\phi)} - N\hbar G C_1 \partial_+\partial_-\phi = \pi G T^f_{+-}, \tag{4.72}$$

$$\begin{aligned}\pm\pm: &-\partial_\pm^2 e^{-2\phi} + 4\partial_\pm\phi\partial_\pm(\phi-\rho)e^{-2\phi} + \\ &N\hbar G\left[C_1\left(\partial_\pm^2\phi - 2\partial_\pm\rho\partial_\pm\phi\right) + \frac{C_2}{12}(\partial_\pm\phi)^2\right] = \pi G T^f_{\pm\pm},\end{aligned} \tag{4.73}$$

$$\phi: \partial_+\partial_- e^{-2\phi} - 2\partial_+\partial_-(\phi-\rho)e^{-2\phi} + \lambda^2 e^{2(\rho-\phi)} = N\hbar G\left[-C_1\partial_+\partial_-\rho + \frac{C_2}{12}\partial_+\partial_-\phi\right] \tag{4.74}$$

$$T: T^f_{+-} = -\frac{N\hbar}{12\pi}\partial_+\partial_-\rho \quad \wedge \quad T^f_{\pm\pm} = T^{f,cl}_{\pm\pm} + \frac{N\hbar}{12\pi}\left[\partial_\pm^2\rho - (\partial_\pm\rho)^2 - t_\pm(x^\pm)\right], \tag{4.75}$$

where, in the last line, we have written the components of the quantum–corrected EMT explicitly in terms of the PL EMT components introduced in (3.77).

Next, we choose the constants such that the resulting system of equations admits an exact solution. In the classical CGHS model, the key requirement for obtaining a closed-form analytic solution was the Kruskal gauge condition, which followed from equations (4.14) and (4.16). We now investigate what happens when we combine equations (4.72) and (4.74). This yields

$$N\hbar\left(C_1 - \frac{C_2}{12}\right)\partial_+\partial_-\phi + N\hbar\left(C_1 - \frac{1}{12}\right)\partial_+\partial_-\rho - \frac{2}{G}\partial_+\partial_-(\phi-\rho)e^{-2\phi} = 0. \tag{4.76}$$

In order to obtain the equation $\partial_+\partial_-(\phi-\rho) = 0$, which is required to impose the Kruskal gauge, the constants must satisfy

$$C_1 - \frac{C_2}{12} = -\left(C_1 - \frac{1}{12}\right) \quad \Longrightarrow \quad C_1 = \frac{C_2+1}{24}. \tag{4.77}$$

With this choice, the equation simplifies to

$$\left[N\hbar\left(C_1 - \frac{C_2}{12}\right) - \frac{2}{G}e^{-2\phi}\right]\partial_+\partial_-(\phi-\rho) = 0. \tag{4.78}$$

Consequently, we can also impose the Kruskal gauge condition $\rho = \phi$ in the quantum-corrected case. In both the RST and BPP models, the relation (4.77) between the constants C_1 and C_2 is indeed fulfilled. After enforcing the Kruskal gauge condition, the equations of motion (4.72-4.74) take the form:

$$+-: \quad \partial_+\partial_-\left[e^{-2\phi} + N\hbar G\left(\frac{1}{12} - C_1\right)\phi\right] = -\lambda^2, \tag{4.79}$$

$$\pm\pm: \quad \partial_\pm^2\left[e^{-2\phi} + N\hbar G\left(\frac{1}{12} - C_1\right)\phi\right] = \frac{N\hbar G}{12}t_\pm(x^\pm) - \pi G T^{f,cl}_{\pm\pm}(x^\pm). \tag{4.80}$$

It is clear that this system of equations can be solved exactly by directly integrating the sources, which are now determined by $T^{f,cl}_{\pm\pm}$ together with the function $t_\pm$ defined in (3.78). The particular choice of the functions $t_\pm$ is tied to the specification of the quantum vacuum state (see Section 3.3). The general solution to the quantum-corrected equations of motion is given by:

$$\begin{aligned} e^{-2\phi} + N\hbar G\left(\frac{1}{12} - C_1\right)\phi = -\lambda^2 x^+ x^- - \pi G \int \mathrm{d}x^+ \int \mathrm{d}x^+ \left(T^{f,cl}_{++} - \varepsilon t_+\right) \\ - \pi G \int \mathrm{d}x^- \int \mathrm{d}x^- \left(T^{f,cl}_{--} - \varepsilon t_-\right) + a_+ x^+ + a_- x^- + b. \end{aligned} \tag{4.81}$$

We also introduce the constant $\varepsilon = \frac{N\hbar}{12\pi}$, which multiplies the quantum correction to the matter energy–momentum tensor. Equation (4.81) is transcendental in ϕ, except in the special case $C_1 = \frac{1}{12}$, which corresponds to the BPP model. The quantities $a_\pm$ and b are integration constants, just as in the classical CGHS solution (4.25). Hence, in the BPP case the equations coincide exactly with the classical ones, and for this reason that model will be of particular interest in the following analysis..

4.2.3 General static solution

In this subsection, we solve the system of equations (4.70) by employing the symmetric ansatz introduced in Section 3.1. Once this ansatz is implemented, the equations of motion reduce to:

$$\begin{aligned} &\left[\frac{\mathrm{d}}{\mathrm{dx}}\left(\mathrm{x}^2\mathcal{D}\frac{\mathrm{d}\Lambda}{\mathrm{dx}}\right) + \frac{N\hbar G C_1}{2}\left(\frac{\mathrm{d}}{\mathrm{dx}}\left(\mathcal{D}\frac{\mathrm{d}\Lambda}{\mathrm{dx}}\right) - 4\Lambda\frac{\mathrm{d}}{\mathrm{dx}}\left(\frac{\mathcal{D}}{\mathrm{x}}\right) - \frac{2}{\mathrm{x}}\mathcal{D}\frac{\mathrm{d}\Lambda}{\mathrm{dx}}\right) + \frac{N\hbar G}{12}\frac{C_2}{\mathrm{x}}\frac{\mathrm{d}\left(\Lambda\mathcal{D}\right)}{\mathrm{dx}}\right]\xi_\mu\xi_\nu \\ &- \left[\frac{\mathrm{d}}{\mathrm{dx}}\left(\mathrm{x}^2\mathcal{D}\frac{\mathrm{d}\Lambda}{\mathrm{dx}}\right) + 4\mathrm{x}^2\Lambda\frac{\mathrm{d}}{\mathrm{dx}}\left(\frac{\mathcal{D}}{\mathrm{x}}\right) + \frac{N\hbar G C_1 \mathrm{x}^2}{2}\frac{\mathrm{d}}{\mathrm{dx}}\left(\frac{\mathcal{D}}{\mathrm{x}^2}\frac{\mathrm{d}\Lambda}{\mathrm{dx}}\right) + \frac{N\hbar G C_2 \mathrm{x}}{12}\frac{\mathrm{d}}{\mathrm{dx}}\left(\frac{\Lambda\mathcal{D}}{\mathrm{x}^2}\right)\right]\varepsilon_{\mu\rho}\varepsilon_{\nu\sigma}\xi^\rho\xi^\sigma \\ &= \frac{\pi G}{2\lambda^2}T^f_{\mu\nu} = \frac{\pi G}{2\lambda^2}\left(T^{f,cl}_{\mu\nu} + \langle\Delta T^{(f)}_{\mu\nu}\rangle\right), \end{aligned} \tag{4.82}$$

$$\mathcal{D}\mathrm{x}\frac{\mathrm{d}(\Lambda\mathcal{D})}{\mathrm{dx}} + \frac{\mathrm{x}^2}{4}\mathcal{D}\frac{\mathrm{d}}{\mathrm{dx}}\left(\mathcal{D}\frac{\mathrm{d}\Lambda}{\mathrm{dx}}\right) + \mathrm{x}^2 + \frac{N\hbar G}{8}\mathcal{D}\left[C_1\frac{\mathrm{d}}{\mathrm{dx}}\left(\mathcal{D}\frac{\mathrm{d}\Lambda}{\mathrm{dx}}\right) + \frac{C_2}{6}\frac{\mathrm{d}}{\mathrm{dx}}\left(\frac{\Lambda\mathcal{D}}{\mathrm{x}}\right)\right] = 0, \tag{4.83}$$

where the symmetric-ansatz form of the EMT $\langle\Delta T^{(f)}_{\mu\nu}\rangle$ is provided in Equation (3.79). Because the left-hand side of (4.82) contains no mixed parallel–normal component, the constants associated with the functions $t_\pm$ must coincide. We denote their common value by $t_+(\sigma^+) = t_-(\sigma^-) = \frac{\lambda^2}{4}\Xi$. Subtracting the parallel and orthogonal components of (4.82), we arrive at:

$$\frac{N\hbar G}{2}\left[\frac{1}{2}\left(C_1 - \frac{1}{12}\right)\frac{\mathrm{d}}{\mathrm{dx}}\left(\mathcal{D}\frac{\mathrm{d}\Lambda}{\mathrm{dx}}\right) + \left(\frac{C_2}{12} - C_1\right)\frac{\mathrm{d}}{\mathrm{dx}}\left(\frac{\Lambda\mathcal{D}}{\mathrm{x}}\right)\right] + \mathrm{x}^2\frac{\mathrm{d}}{\mathrm{dx}}\left(\frac{1}{2}\mathcal{D}\frac{\mathrm{d}\Lambda}{\mathrm{dx}} + \frac{\Lambda\mathcal{D}}{\mathrm{x}}\right) = 0. \tag{4.84}$$

This equation is akin to taking the trace of the original system (4.82), together with the property that the EMT of a massless scalar field is traceless. It coincides with Equation (4.76). For this equation to be explicitly integrable, the constants C_1 and C_2 must obey condition (4.77). Imposing that condition and integrating yields

$$\frac{1}{2}\mathcal{D}\frac{\mathrm{d}\Lambda}{\mathrm{dx}} + \frac{\Lambda\mathcal{D}}{\mathrm{x}} = C, \tag{4.85}$$

which is equivalent to (4.29) and encodes the Kruskal gauge condition for a static geometry. Proceeding in complete analogy with the purely classical static solution, we now integrate the dilaton Equation (4.83). The result is

$$\Lambda \mathrm{x}^2 + C\left[\mathrm{x} + \frac{N\hbar G}{2}\left(C_1 - \frac{1}{12}\right)\frac{1}{\mathrm{x}}\right]\Lambda\mathcal{D} = Q, \tag{4.86}$$

where Q denotes an integration constant. Combining (4.85) and (4.86) leads to the following expression for the metric function Λ:

$$\Lambda \mathrm{x}^2 - Q\ln\left|\Lambda \mathrm{x}^2\right| = b - C^2\left(\mathrm{x}^2 + N\hbar G\left(C_1 - \frac{1}{12}\right)\ln \mathrm{x}\right), \tag{4.87}$$

with b introduced as the final integration constant. The tortoise coordinate σ keeps the same form as in (4.32). The last step is to insert all these results back into the original Equation (4.82) and extract the constraints on the classical part of the EMT. We obtain

$$\Lambda^2 T^{\parallel\parallel}_{f,cl} = \Lambda^2 T^{\perp\perp}_{f,cl} = \frac{2\lambda^2}{\pi G}\left(Q + \frac{N\hbar G}{48}\left(\Xi + C^2\right)\right). \tag{4.88}$$

This matches our expectations, as the equation of motion for the matter sector coincides with that of the classical static configuration, thereby introducing an additional charge μ. Consequently, we express Q in terms of the remaining parameters:

$$Q = \mu - \frac{N\hbar G}{48}\left(\Xi + C^2\right). \tag{4.89}$$

As in the purely classical setup, the constant C must be chosen such that the metric satisfies $\Lambda \to -1$ when $\mathrm{x} \to \infty$ and $\sigma \to +\infty$. From (4.87) it follows that $\Lambda \to -C^2$ in this limit, hence the second condition fixes $C = -1$. Finally, we rewrite the solution (4.87) for the metric function in Kruskal coordinates by using $|\Lambda \mathrm{x}^2| = e^{2\lambda\sigma} = -\lambda^2 x^+ x^-$ and reverting to $\mathrm{x} = e^{-\phi}$:

$$e^{-2\phi} + N\hbar G\left(\frac{1}{12} - C_1\right)\phi = -\lambda^2 x^+ x^- - \left(\frac{N\hbar G}{48}(\Xi + 1) - \mu\right)\ln\left|\lambda^2 x^+ x^-\right| + b. \tag{4.90}$$

Note that for $\mu \neq 0$, the geometry remains very similar to the classical case analyzed in Section 4.1.4. The resulting spacetime is a cosmological solution that describes an infinite universe shrinking from an infinite scale factor and subsequently re-expanding back to an infinite scale factor. We now turn to specific vacuum configurations: the linear dilaton vacuum, the static solution, and the static black hole, all specified with $\mu = 0$.

Linear dilaton vacuum

Here we determine which values the constants must take so that the linear dilaton vacuum solves the original field equations. The general solution of this model is given by (4.90). Imposing the condition $e^{-2\phi} = -\lambda^2 x^+ x^-$ leads to:

$$N\hbar G\left(\frac{1}{12} - C_1\right)\phi = \left(\frac{N\hbar G}{24}(\Xi + 1) - 2\mu\right)\phi + b. \tag{4.91}$$

From this relation it follows that the state must be massless, i.e. $b = 0$. Setting $\mu = 0$, the constraint becomes:

$$\frac{1}{24} - C_1 = \Xi. \tag{4.92}$$

For the static configuration with no energy flux at infinity—namely, the Boulware state—the energy-momentum tensor is normal ordered in Eddington–Finkelstein coordinates, which enforces $t_\pm(\sigma^\pm) = \Xi = 0$. Consequently, the linear dilaton vacuum represents a genuine vacuum state, devoid of any particle content, only in the RST model, where one has $C_1 = 1/24$. While in the BPP model, we instead obtain $\Xi = -1$, which corresponds to the Hartle–Hawking state. This connection is demonstrated in the following sections.

Static vacuum solution

A static vacuum solution is defined as one that carries no energy flux through either past or future null infinity. This requirement leads to the choice:

$$\Xi = 0. \tag{4.93}$$

Imposing this together with $\mu = 0$ simplifies the general solution (4.90) to:

$$e^{-2\phi} + N\hbar G\left(\frac{1}{12} - C_1\right)\phi = -\lambda^2 x^+ x^- - \frac{N\hbar G}{48}\ln\left|\lambda^2 x^+ x^-\right| + b. \tag{4.94}$$

In general, this relation is transcendental in ϕ. It becomes algebraically solvable for ϕ only in the BPP model, characterized by $C_1 = 1/12$. This is the main advantage of the BPP model. However, the drawback is that no choice of b can recover the linear dilaton vacuum from this solution. Consequently, the linear dilaton vacuum necessarily carries a nonvanishing energy flux at future null infinity.

Static vacuum black hole solution

Note that for any non-vanishing Q, no event horizon appears at a finite value of x. Since the presence of an event horizon is a prerequisite for a solution to qualify as a black hole [106], we must therefore set $Q = 0$. Moreover, because we are interested in a vacuum configuration, we also impose $\mu = 0$. Under these conditions, we obtain a constraint on the parameter Ξ, namely:

$$\Xi = -1. \tag{4.95}$$

Inserting this relation into the general solution (4.90) yields:

$$e^{-2\phi} + N\hbar G\left(\frac{1}{12} - C_1\right)\phi = -\lambda^2 x^+ x^- + b. \tag{4.96}$$

Here again, we see the benefit of working with the BPP model rather than the RST model. For $C_1 = 1/12$, this solution coincides with the classical expression (4.42).

4.3 BPP model

In this section, we study the various solutions within the BPP model, following the derivation of [25]. Unlike in the previous section, we begin with the most general solution in Kruskal coordinates, and then obtain different geometries by specifying in advance the vacuum state of the quantum fields. We then explicitly compute which of these geometries give rise to a non-vanishing energy flux at infinity. Moreover, we clarify why $\Xi = -1$ (4.95) holds for the static black hole.

As already stated, the BPP model arises when the constants in the correction term of the action 4.67 are fixed to $C_1 = \frac{1}{12}$ and $C_2 = 1$ [25]. With this choice, the general solution to the BPP equations of motion takes the form

$$\begin{aligned} e^{-2\phi} = -\lambda^2 x^+ x^- - \pi G \int \mathrm{d}x^+ \int \mathrm{d}x^+ \left(T^{f,cl}_{++} - \varepsilon t_+ \right) \\ - \pi G \int \mathrm{d}x^- \int \mathrm{d}x^- \left(T^{f,cl}_{--} - \varepsilon t_- \right) + a_+ x^+ + a_- x^- + b, \end{aligned} \tag{4.97}$$

which is obtained by substituting $C_1 = 1/12$ into the general solution of the quantum-corrected CGHS model (4.81).

Equation (4.97) gives the solution for the dilaton (and thus for the metric as well, since $\rho = \phi$ in Kruskal gauge), with $T^{f,cl}_{\pm\pm}$, $t_\pm$, $a_\pm$, and b serving as sources. Relative to the classical CGHS solution (4.25), the only new ingredients are the functions $t_\pm$, which encode the choice of quantum state of the matter fields. Recall that $\varepsilon = \frac{N\hbar}{12\pi}$ is the parameter signaling the presence of quantum corrections in the model; in the limit $\varepsilon \to 0$, the solutions revert to their classical forms.

We now briefly comment on the dimensions of the constants appearing in these expressions. In D spatial dimensions, Newton's law takes the form $F = G\frac{m_1 m_2}{r^{D-1}}$. For $D = 1$, this implies $[G] = \frac{\mathrm{m}}{\mathrm{kg\,s^2}}$. It follows that the combination $\frac{\hbar G}{c^3}$ is dimensionless. Hence, in the product εG the factor $1/c^3$ is effectively absent.

4.3.1 Linear dilaton vacuum

The linear dilaton vacuum corresponds to a solution with flat spacetime, as is already known from the classical CGHS model. For this case, the appropriate choice of sources in Equation (4.97) is:

$$T^{f,cl}_{\pm\pm} = 0 \quad \wedge \quad a_\pm = 0 \quad \wedge \quad b = 0 \quad \wedge \quad t_\pm(x^\pm) = 0. \tag{4.98}$$

The last condition specifies that the quantum state is the Hartle–Hawking vacuum (3.97) (because the energy–momentum tensor is normal ordered in Kruskal coordinates). The metric takes the form:

$$\mathrm{d}s^2 = -\frac{\mathrm{d}x^+ \mathrm{d}x^-}{-\lambda^2 x^+ x^-} \quad \wedge \quad \phi = -\frac{1}{2} \ln \left| \lambda^2 x^+ x^- \right|. \tag{4.99}$$

To verify that we truly have the Hartle–Hawking state, we compute the energy–momentum tensor in the $x^\pm$ coordinates:

$$\langle \Delta T^f_{\pm\pm}(x^\pm) \rangle = \varepsilon \left[\partial^2_\pm \rho - (\partial_\pm \rho)^2 - \cancelto{0}{t_\pm(x^\pm)} \right] = \frac{\varepsilon \lambda^2}{4} \frac{1}{(\lambda x^\pm)^2}. \tag{4.100}$$

Next, we must determine whether there is any energy flux at infinity. To this end, we transform to the asymptotically flat coordinates $\sigma^\pm$ and consider the limit $\sigma \to \infty$:

$$\langle \Delta T^f_{\pm\pm}(\sigma^\pm) \rangle = \left(\frac{\mathrm{d}x^\pm}{\mathrm{d}\sigma^\pm} \right)^2 \langle \Delta T^f_{\pm\pm}(x^\pm) \rangle = \frac{\varepsilon \lambda^2}{4} \Longrightarrow \langle 0, x | \, \Delta \hat{T}^f_{\pm\pm}(\sigma^\pm) \, | 0, x \rangle \Big|_{\mathcal{J}^\pm} = \frac{\varepsilon \lambda^2}{4}. \tag{4.101}$$

We observe that an energy flux is present both at $\mathcal{J}^+$ and $\mathcal{J}^-$, and thus we identify the configuration as a system in thermal equilibrium. Evaluating the temperature of the radiation, we obtain:

$$T = \frac{\kappa}{2\pi\hbar} = \frac{\lambda}{4\pi\hbar}\left|\mathcal{D}\frac{\mathrm{d}\Lambda}{\mathrm{dx}}\right| = \frac{\lambda}{2\pi\hbar}. \tag{4.102}$$

For more details see Appendix D.5. This shows that, even though the geometry is that of Minkowski flat spacetime, there is still a nonvanishing energy flux. This is the same outcome as in the preceding section. Therefore, this solution cannot be identified with the true Minkowski vacuum. The geometry behaves as the geometry in the vicinity of a black hole, although no singularity exists, leading us to classify it as nonphysical.

4.3.2 Eternal black hole solution

Here we present the quantum–corrected static black hole solution, corresponding to the Hartle–Hawking vacuum (3.97) for the matter fields. We require the energy–momentum tensor to be normal ordered in the $x^\pm$ coordinates. Consequently, the setup is specified by the following choice of sources in Equation (4.97):

$$T^{f,cl}_{\pm\pm} = 0 \quad \wedge \quad a_\pm = 0 \quad \wedge \quad b = \frac{\pi GM}{\lambda} \quad \wedge \quad t_\pm(x^\pm) = 0. \tag{4.103}$$

Just as for the linear dilaton vacuum, the metric here also coincides exactly with the classical one (Equation (4.42)):

$$\mathrm{d}s^2 = -\frac{\mathrm{d}x^+\mathrm{d}x^-}{-\lambda^2 x^+x^- + \frac{\pi GM}{\lambda}} \quad \wedge \quad \phi = -\frac{1}{2}\ln\left|-\lambda^2 x^+x^- + \frac{\pi GM}{\lambda}\right|. \tag{4.104}$$

Note that this solution is equivalent to (4.96). We now investigate whether this configuration gives rise to an energy flux at infinity, as is necessary for describing a black hole in thermal equilibrium:

$$\langle \Delta T^f_{\pm\pm}(x^\pm)\rangle = \varepsilon\left[\partial^2_\pm\rho - (\partial_\pm\rho)^2 - \cancelto{0}{t_\pm(x^\pm)}\right] = \frac{\varepsilon\lambda^2}{4}\left[\frac{\lambda x^\mp}{-\lambda^2x^+x^- + \frac{\pi GM}{\lambda}}\right]^2. \tag{4.105}$$

Expressing the energy–momentum tensor in the $\sigma^\pm$ coordinates and then taking the limit $\sigma \to \infty$ yields:

$$\langle \Delta T^f_{\pm\pm}(\sigma^\pm)\rangle = \frac{\varepsilon\lambda^2}{4}\frac{1}{\left(1 + \frac{\pi GM}{\lambda}e^{-2\lambda\sigma}\right)^2} \Longrightarrow \langle 0, x|\, \Delta\hat{T}^f_{\pm\pm}(\sigma^\pm)\, |0, x\rangle\Big|_{\mathcal{J}^\pm} = \frac{\varepsilon\lambda^2}{4}. \tag{4.106}$$

Thus, the energy flux at $\mathcal{J}^\pm$ matches that of the linear dilaton vacuum (4.101). The crucial distinction is that in the present case there is an actual black hole of mass M. In this way we have obtained the eternal black hole configuration, which will serve as the basis for our analysis of the fine-grained entropy of Hawking radiation in Chapter 9.

At the conclusion of this subsection, we determine the value of the Ξ parameter that corresponds to the static black hole configuration. By transforming $t_\pm(x^\pm)$ to Eddington–Finkelstein coordinates using the transformation law (3.83), we obtain:

$$t_\pm(\sigma^\pm) = \left(\frac{\mathrm{d}x^\pm}{\mathrm{d}\sigma^\pm}\right)^2\left[\cancelto{0}{t_\pm(x^\pm)} - \frac{1}{2}D_{x^\pm}[\sigma^\pm]\right] \quad \Longrightarrow \quad t_\pm(\sigma^\pm) = -\frac{\lambda^2}{4}. \tag{4.107}$$

On the other hand, Ξ is defined by $t_\pm(\sigma^\pm) = \frac{\lambda^2}{4}\Xi$, which immediately implies $\Xi = -1$. This coincides with the value previously obtained by requiring the presence of an event horizon in the general static vacuum solution (4.95).

4.3.3 Minkowski vacuum

Since our aim is to study gravitational collapse, we require a vacuum configuration that does not emit radiation at infinity, unlike the situation for the linear dilaton vacuum 4.101. Such a configuration is realized by the Boulware vacuum (3.96), defined by the condition $t_\pm(\sigma^\pm) = 0$. Consequently, the setup is characterized by the following values for the sources in Equation (4.97):

$$T^{f,cl}_{\pm\pm} = 0 \quad \wedge \quad a_\pm = 0 \quad \wedge \quad b = 0 \quad \wedge \quad t_\pm(\sigma^\pm) = 0. \tag{4.108}$$

Let us now examine in more detail the requirement $t_\pm(\sigma^\pm) = 0$. This condition implies that the energy–momentum tensor is normal ordered with respect to the $\sigma^\pm$ coordinates. Equivalently, there is no energy flux through $\mathcal{J}^\pm$. We can verify this explicitly:

$$\langle \Delta T^f_{\pm\pm}(\sigma^\pm)\rangle\Big|_{\mathcal{J}^\pm} = \varepsilon\left[\partial_\pm^2\rho - (\partial_\pm\rho)^2 - t_\pm(\sigma^\pm)\right]\Big|_{\mathcal{J}^\pm} = -\varepsilon t_\pm(\sigma^\pm)\Big|_{\mathcal{J}^\pm}. \tag{4.109}$$

The contributions involving derivatives of the metric must vanish, because ρ must remain finite as $\sigma \to \infty$. A necessary and sufficient condition for this behavior is $t_\pm(\sigma^\pm) = 0$.

To determine the metric, we must now compute $t_\pm(x^\pm)$. This can be achieved by applying the transformation law (3.83) for this quantity, derived in Section 3.3. This yields:

$$t_\pm(x^\pm) = \left(\frac{d\sigma^\pm}{dx^\pm}\right)\left[\cancelto{0}{t_\pm}(\sigma^\pm) - \frac{1}{2}D_{\sigma^\pm}\left[x^\pm\right]\right] = \frac{1}{(\lambda x^\pm)^2}\left(-\frac{1}{2}\right)\left(-\frac{1}{2}\lambda^2\right) = \frac{1}{4(x^\pm)^2}. \tag{4.110}$$

All the required source parameters in Equation (4.97) have now been evaluated. Performing the corresponding integrations yields

$$e^{-2\phi} = e^{-2\rho} = -\lambda^2 x^+ x^- - \frac{\varepsilon\pi G}{4}\ln\left(-\lambda^2 x^+ x^-\right) + C. \tag{4.111}$$

Here C is an arbitrary constant, playing the role of the constant b. We adopt the notation C in order to align with the conventions of [25]. We now determine the metric and dilaton in asymptotically flat coordinates (in quadrant I of Figure 4.1):

$$ds^2 = \frac{-dt^2 + d\sigma^2}{1 - \left(\frac{\varepsilon\pi G}{2}\lambda\sigma - C\right)e^{-2\lambda\sigma}} \;\wedge\; \phi(\sigma) = -\lambda\sigma - \frac{1}{2}\ln\left[1 - \left(\frac{\varepsilon\pi G}{2}\lambda\sigma - C\right)e^{-2\lambda\sigma}\right]. \tag{4.112}$$

It is immediately evident that this configuration is static. Moreover, in the limit $\sigma \to \infty$, we recover the linear dilaton vacuum, precisely as desired. A straightforward computation of the energy–momentum tensor in the $x^\pm$ coordinates, followed by a transformation to the $\sigma^\pm$ coordinates, leads to:

$$\langle \Delta\hat{T}^f_{\pm\pm}(\sigma^\pm)\rangle = \frac{\varepsilon\lambda^2}{4}\left[\left(\frac{1 - \frac{\varepsilon\pi G}{4}e^{-2\lambda\sigma}}{1 - \left(\frac{\varepsilon\pi G}{2}\lambda\sigma - C\right)e^{-2\lambda\sigma}}\right)^2 - \frac{\frac{\varepsilon\pi G}{2}e^{-2\lambda\sigma}}{1 - \left(\frac{\varepsilon\pi G}{2}\lambda\sigma - C\right)e^{-2\lambda\sigma}} - 1\right]$$
$$\Longrightarrow \langle 0,\sigma|\,\Delta\hat{T}^f_{\pm\pm}(\sigma^\pm)\,|0,\sigma\rangle\Big|_{\mathcal{J}^\pm} = 0. \tag{4.113}$$

All these solutions approach the linear dilaton vacuum at $\mathcal{J}^\pm$ because $e^{2\phi}$ vanishes exponentially fast in this region. We now address the interpretation of the constant C [25]. For the spacetime mass (for example, in the ADM formalism) one finds $\frac{\pi G M}{\lambda} = C - C_0$, where C_0 is a reference value corresponding to the massless solution. However, the ADM mass of both the linear dilaton vacuum and the static black hole diverges. This divergence arises from the presence of radiation at $\mathcal{J}^{\pm}$. Since the static solutions have a smaller ADM mass, we are led to expect that the true ground state is given by one of these static configurations.

This also clarifies why the linear dilaton vacuum actually corresponds to the Hartle–Hawking state. It is smoothly connected to the choice $b = 0$ in the general eternal black hole solution (4.104), and not to any particular value of the constant C in the family of static vacuum solutions (4.111). Consequently, it must display the same Hawking radiation as the eternal black hole. We therefore conclude that the genuine vacuum state associated with flat Minkowski spacetime, once quantum corrections are switched off, is represented by one of the static vacuum solutions (4.111).

We now examine the behavior of solution 4.111 in greater detail. From a mathematical standpoint, it closely resembles the cosmological solution discussed in Section (4.1.4). Setting $\mu = -\frac{\varepsilon \pi G}{4}$ renders the two solutions identical. Nonetheless, flipping the sign of μ has significant physical implications. For the cosmological solution, μ is positive, which implies $\Lambda > 0$. By contrast, solution (4.111) is a vacuum solution with $\Lambda < 0$. Consequently, unlike the cosmological case, it should not contain any singularity, as it does not describe a black hole. As in the cosmological case, we begin our analysis with the scalar curvature. A straightforward computation gives:

$$R = 4\lambda^2 \frac{\frac{\varepsilon \pi G}{2} + \frac{(\varepsilon \pi G)^2}{16 \lambda^2 x^+ x^-} - \frac{\varepsilon \pi G}{4} \ln\left(-\lambda^2 x^+ x^-\right) + C}{-\lambda^2 x^+ x^- - \frac{\varepsilon \pi G}{4} \ln\left(-\lambda^2 x^+ x^-\right) + C}. \tag{4.114}$$

Two different kinds of singularities appear in this setting. First, the curvature clearly blows up at $x^{\pm} = 0$. These singularities can be handled in a straightforward way by removing the hypersurfaces $x^+ = 0$ and $x^- = 0$ from the manifold. More interesting, however, is the situation in which the denominator vanishes:

$$-\lambda^2 x^+ x^- - \frac{\varepsilon \pi G}{4} \ln\left(-\lambda^2 x^+ x^-\right) + C = 0 \quad \Longrightarrow \quad e^{2\lambda\sigma} - \frac{\varepsilon \pi G}{2} \lambda \sigma + C = 0. \tag{4.115}$$

We carry out an analysis analogous to that in Section 4.1.4. A graphical representation of the solution to Equation (4.115) is depicted in Figure 4.5. We introduce the functions $f(x) = e^x$ and $g_C(x) = \frac{\varepsilon \pi G}{4} x - C$, and determine their point of intersection. An intersection occurs only when $C < C^*$. The critical value C^* is obtained by identifying the straight line $g_{C^*}(x)$ that is tangent to the curve $f(x)$. The tangency point is located at $x_0 = \ln \frac{\varepsilon \pi G}{4}$. Consequently, for the constant C^* we obtain:

$$C^* = -\frac{\varepsilon \pi G}{4} \left[1 - \ln \frac{\varepsilon \pi G}{4}\right]. \tag{4.116}$$

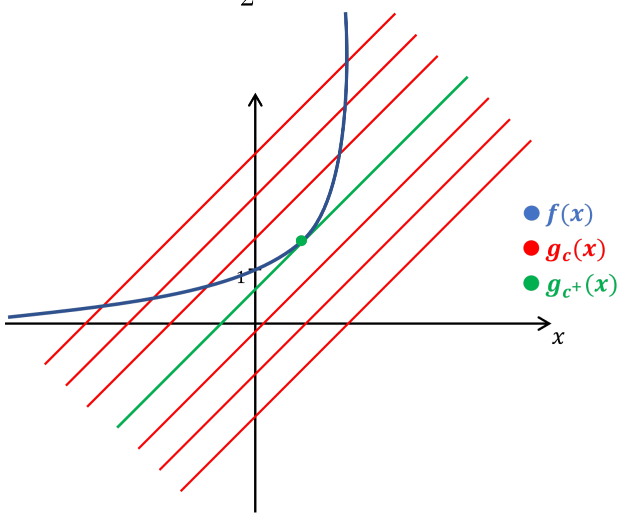

Figure 4.5: The intersection of the functions f and g_C

We conclude that for $C < C^*$ there exist spacelike hypersurfaces given by $\sigma = \sigma_s$, which solve this equation. In this regime, the curves intersect twice, producing two distinct hypersurfaces.

This defines the **strong coupling region**, where strong quantum correlations are expected and the semiclassical approximation breaks down. Consequently, we choose to discard this region.

For $C > C^*$, divergences appear at the hypersurfaces $x^\pm = 0$. In this case, the previously studied equation has no solutions, but we can still identify a strong coupling region. It is located in the neighborhood of the point $2\lambda\sigma_{\min} = \ln \frac{\varepsilon\pi G}{4}$, where the curves are closest to each other.

The terminology "strong coupling region" arises because $e^{2\phi}$ becomes very large there; this factor acts as the coupling strength between the curvature and the dilaton in the action. In our static vacuum configuration, we must avoid both singularities and strong coupling regions. We eliminate them by imposing reflective boundary conditions at the boundary of spacetime. This boundary coincides with one of the hypersurfaces $\sigma = \sigma_b$, so we enforce reflective boundary conditions at $\sigma = \sigma_b$ via:

$$\langle \Delta T^f_{++} \rangle \Big|_{\sigma=\sigma_b} = \langle \Delta T^f_{--} \rangle \Big|_{\sigma=\sigma_b}. \tag{4.117}$$

Hence, a well-defined Minkowski vacuum exists only in the region $\sigma > \sigma_s$ when $C < C^*$, or in the region $\sigma > \sigma_{\min}$ when $C > C^*$, with reflective boundary conditions imposed at $\sigma_b = \sigma_s + \delta$ or $\sigma_b = \sigma_{\min} + \delta$, respectively, where $\delta > 0$.

4.3.4 Evaporating black hole solution

In this subsection, we construct the dynamical scenario for an evaporating black hole. In contrast to Section 4.1.5, the spacetime here is divided not into two, but into three distinct regions. Specifically, evaporation ends at a finite point in the spacetime, and beyond this point the geometry returns to a static vacuum solution. This third region is absent in the purely classical case, where no radiation is present. The solution is fixed by the following choice of source parameters in Equation (4.97):

$$T^{f,cl}_{++} = \frac{M}{\lambda x_0^+}\delta\left(x^+ - x_0^+\right) \quad \wedge \quad T^{f,cl}_{--} = 0 \quad \wedge \quad a_\pm = 0 \quad \wedge \quad t_\pm(\sigma^\pm) = 0. \tag{4.118}$$

For an evaporating black hole, there is no energy flux in the distant past, i.e. at $\mathcal{J}^-$ ($x^+ < x_0^+$), whereas in the far future ($x^+ > x_0^+$) there is an energy flux at $\mathcal{J}^+$. Consequently, the appropriate quantum state is $|\psi\rangle = |0, \sigma\rangle$, namely the Unruh state (3.98). This implies that the metric before the collapse corresponds to one of the Minkowski vacuum states (4.111) with some constant C (region I). After collapse, the metric is determined, as in the classical scenario, by imposing the continuity of both the metric and the dilaton field along the hypersurface $x^+ = x_0^+$. We then obtain:

$$ds^2 = \begin{cases} -\dfrac{dx^+dx^-}{-\lambda^2 x^+x^- - \frac{\varepsilon\pi G}{4}\ln\left(-\lambda^2x^+x^-\right) + C}, & x^+ < x_0^+ \\ -\dfrac{dx^+dx^-}{-\lambda^2 x^+\left(x^- + \Delta\right) - \frac{\varepsilon\pi G}{4}\ln\left(-\lambda^2x^+x^-\right) + \frac{\pi G M}{\lambda} + C}, & x^+ > x_0^+ \end{cases} \tag{4.119}$$

We now focus on region I of the spacetime, i.e. the portion after the shockwave. If the spacetime boundary is fixed by $\sigma = \sigma_b$, then the coordinate x_0^+ coordinate is determined by $-\lambda^2 x_0^+ x_0^- = e^{2\lambda\sigma_b}$. Two distinct possibilities arise. In the first, when the infalling mass satisfies $M < M_{cr}$, it is too small to create a singularity, and the matter shockwave is simply reflected due to the reflective boundary conditions (4.117). Our primary interest, however, lies in the second situation, where the mass exceeds the critical value and a singularity forms, thereby generating region II of the spacetime. By evaluating the curvature, we obtain that the curve along which it diverges, i.e. the singularity, is given by:

$$-\lambda^2 x_{\mathrm{S}}^+ \left(x_{\mathrm{S}}^- + \Delta\right) - \frac{\varepsilon\pi G}{4} \ln\left(-\lambda^2 x_{\mathrm{S}}^+ x_{\mathrm{S}}^-\right) + \frac{\pi G M}{\lambda} + C = 0. \tag{4.120}$$

According to the cosmic censorship hypothesis, an event horizon must exist to conceal this singularity. In addition, there may be an apparent horizon that encloses the event horizon and, therefore, also hides the singularity. The apparent horizon is obtained by solving the equation $\partial_+ e^{-2\phi} = 0$, which yields

$$-\lambda^2 x_{\mathrm{AH}}^+ \left(x_{\mathrm{AH}}^- + \Delta\right) = \frac{\varepsilon\pi G}{4}. \tag{4.121}$$

Once the singularity has formed, the black hole starts to evaporate. To demonstrate this explicitly, one needs to compute the components of the energy–momentum tensor in the asymptotically flat coordinates, which in this case are the $\hat{\sigma}^{\pm}$ coordinates defined in (4.59). The relevant component is $\langle \Delta T^f_{--}(\hat{\sigma}^-)\rangle$ evaluated along the $\mathcal{J}^+$ hypersurface. Since the metric approaches a constant on $\mathcal{J}^+$, the EMT there is given by $\langle \Delta T^f_{--}(\hat{\sigma}^-)\rangle|_{\mathcal{J}^+} = -\varepsilon\, t_-(\hat{\sigma}^-)$. Moreover, from Equation (4.110) we know how the condition $t_-(\sigma^-) = 0$ is modified when we transform to Kruskal gauge coordinates, namely $t_-(x^-) = \frac{1}{4(x^-)^2}$. Thus, using (3.83), we obtain:

$$t_-(\hat{\sigma}^-) = \left(\frac{dx^-}{d\hat{\sigma}^-}\right)^2 \left[t_-(x^-) - \frac{1}{2} D_{x^-}\left[\hat{\sigma}^-\right]\right] = \lambda^2 \left(x^- + \Delta\right)^2 \left[\frac{1}{4\left(x^-\right)^2} - \frac{1}{4\left(x^- + \Delta\right)^2}\right]. \tag{4.122}$$

Expressing this relation in $\hat{\sigma}^-$ coordinate, the EMT along the $\mathcal{J}^+$ hypersurface reads:

$$\langle 0, \sigma | \, \Delta\hat{T}^f_{--}(\hat{\sigma}^-) \, | 0, \sigma\rangle \Big|_{\mathcal{J}^+} = \frac{\varepsilon\lambda^2}{4} \left[1 - \frac{1}{\left(1 + \lambda\Delta e^{\lambda\hat{\sigma}^-}\right)^2}\right]. \tag{4.123}$$

The dynamical nature of this setup manifests itself in the explicit dependence of the EMT on the $\hat{\sigma}^-$ coordinate, in contrast with the static configurations discussed in the previous subsections. As the black hole continues to evaporate, the apparent horizon gradually contracts until it eventually meets the singularity. To locate this event in the spacetime, we have to solve the pair of equations (4.120) and (4.121). Solving for the intersection coordinates x_{E}^+ and x_{E}^-, we find:

$$x_{\mathrm{E}}^+ = \frac{1}{\lambda^2\Delta} \left[e^{1 + \frac{4(\pi G M + \lambda C)}{\varepsilon\pi G\lambda}} - \frac{\varepsilon\pi G}{4}\right] \quad \wedge \quad x_{\mathrm{E}}^- = -\frac{\Delta}{1 - \frac{\varepsilon\pi G}{4} e^{-1 - \frac{4(\pi G M + \lambda C)}{\varepsilon\pi G\lambda}}}. \tag{4.124}$$

Thus, the intersection takes place within a finite time interval. At that moment, the singularity becomes naked. According to the cosmic censorship theorem [106], this is not allowed to occur. This issue is resolved, however, if the entire black hole has evaporated by the time the intersection is reached. For this reason, it is also referred to as the evaporation end-point. We now verify whether the black hole has completely evaporated by calculating the energy emitted via Hawking radiation up to this point. Since the metric at $\mathcal{J}^+$ is flat, namely $\mathrm{d}s^2 = -\mathrm{d}\hat{\sigma}^+\mathrm{d}\hat{\sigma}^-$, the radiated energy is given by:

$$\begin{aligned} E_{rad} &= \int_{-\infty}^{\hat{\sigma}_{\mathrm{E}}^-} d\hat{\sigma}^- \langle \Delta T^f_{--}(\hat{\sigma}^-)\rangle \Big|_{\mathcal{J}^+} = \frac{\varepsilon\lambda^2}{4} \int_{-\infty}^{\hat{\sigma}_{\mathrm{E}}^-} d\hat{\sigma}^- \left[1 - \frac{1}{(1 + \lambda\Delta e^{\lambda\hat{\sigma}^-})^2}\right] \\ &= \frac{\varepsilon\lambda}{4} \int_1^{\xi_{\mathrm{E}}} d\xi \frac{\xi + 1}{\xi^2} = \frac{\varepsilon\lambda}{4} \left[\ln \xi_{\mathrm{E}} + 1 - \frac{1}{\xi_{\mathrm{E}}}\right], \end{aligned} \tag{4.125}$$

where in the second line, we make a change of variables, defining $\xi = 1+\lambda\Delta e^{\lambda\hat{\sigma}^-}$, which implies $\xi_{\mathrm{E}} = \frac{4}{\varepsilon\pi G}e^{1+\frac{4(\pi GM+\lambda C)}{\varepsilon\pi G\lambda}}$ and $1+\frac{1}{\xi_{\mathrm{E}}} = -\frac{\Delta}{x_{\mathrm{E}}^-}$. With these relations, we can then write the radiated energy in an explicit form:

$$\begin{aligned} E_{rad} &= \frac{\varepsilon\lambda}{4}\left[-\ln\frac{\varepsilon\pi G}{4}+1+\frac{4M}{\varepsilon\lambda}+\frac{4C}{\varepsilon\pi G}-\frac{\Delta}{x_{\mathrm{E}}^-}\right] \\ &= M+\frac{\lambda}{\pi G}\left[C+\frac{\varepsilon\pi G}{4}\left(1-\ln\frac{\varepsilon\pi G}{4}\right)\right]-\frac{\varepsilon\lambda\Delta}{4x_{\mathrm{E}}^-} = M+\frac{\lambda}{\pi G}\left(C-C^*\right)-\frac{\varepsilon\lambda\Delta}{4x_{\mathrm{E}}^-}, \end{aligned} \tag{4.126}$$

where the quantity C^*, defined in (4.116), appears in the second line. This shows that the black hole does not fully evaporate by the time the evaporation process reaches its endpoint. We now compute the residual mass. A straightforward calculation gives:

$$\delta M = \left(M+\frac{\lambda}{\pi G}(C-C_0)\right)-E_{rad} = \frac{\lambda}{\pi G}(C^*-C_0)+\frac{\varepsilon\lambda\Delta}{4x_{\mathrm{E}}^-}. \tag{4.127}$$

We observe that, up to the end-point of the evaporation, the black hole emits nearly all of its energy. Yet, the cosmic censorship conjecture requires that the entire initial mass is radiated away at the end-point. We now try to smoothly match the solution along the line $x^- = x_{\mathrm{E}}^-$, so that in region III of the spacetime ($x^- > x_{\mathrm{E}}^-$) we obtain a Minkowski vacuum solution (4.111) characterized by a new constant C' and asymptotically flat coordinates $\hat{\sigma}^{\pm}$, namely:

$$\mathrm{d}s^2 = -\frac{\mathrm{d}\hat{\sigma}^+\mathrm{d}\hat{\sigma}^-}{1-\left(\frac{\varepsilon\pi G}{2}\lambda\hat{\sigma}-C'\right)e^{-2\lambda\hat{\sigma}}} = -\frac{\mathrm{d}x^+\mathrm{d}x^-}{-\lambda^2x^+\left(x^-+\Delta\right)-\frac{\varepsilon\pi G}{4}\ln\left(-\lambda^2x^+\left(x^-+\Delta\right)\right)+C'}. \tag{4.128}$$

To ensure a continuous matching of both the metric and the dilaton field across the hypersurface $x^- = x_{\mathrm{E}}^-$, the following condition must be satisfied:

$$e^{-2\rho}\Big|_{x^-=x_p^{-(+)}} = e^{-2\rho}\Big|_{x^-=x_p^{-(-)}} \quad\Longrightarrow\quad C^{'} = C^*. \tag{4.129}$$

One might then conclude that the difference in the mass of spacetime prior to the beginning of the evaporation and after the evaporation ends $\frac{\lambda}{\pi G}\left(C^*-C_0\right)$ is equal to the mass (4.127), but this is incorrect because (4.127) contains an additional contribution. We must therefore determine the physical origin of this extra term. In regions II and III, the field $e^{-2\phi}$ is given by:

$$\begin{aligned} e^{-2\phi} = -\lambda^2x^+\left(x^-+\Delta\right) &+ \left[-\frac{\varepsilon\pi G}{4}\ln\left(-\lambda^2x^+x^-\right)+\frac{\pi GM}{\lambda}+C\right]\eta(x_{\mathrm{E}}^- - x^-) \\ &+ \left[-\frac{\varepsilon\pi G}{4}\ln\left(-\lambda^2x^+(x^-+\Delta)\right)+C^*\right]\eta(x^- - x_{\mathrm{E}}^-), \end{aligned} \tag{4.130}$$

where η is the Heaviside function. After a careful calculation of the second derivative of $e^{-2\phi}$, we obtain:

$$\begin{aligned} \partial_+^2 e^{-2\phi} &= \frac{\varepsilon\pi G}{4(x^+)^2}, \\ \partial_-^2 e^{-2\phi} &= \frac{\varepsilon\pi G}{4}\left[\frac{1}{(x^-)^2}\eta(x_{\mathrm{E}}^- - x^-)+\frac{1}{(x^-+\Delta)^2}\eta(x^- - x_{\mathrm{E}}^-)\right]+\frac{\varepsilon\pi G\Delta}{4x_{\mathrm{E}}^-\left(x_{\mathrm{E}}^-+\Delta\right)}\delta(x^- - x_{\mathrm{E}}^-), \\ \partial_+\partial_- e^{-2\phi} &= -\lambda^2. \end{aligned} \tag{4.131}$$

These three equations correspond to the original system (4.79-4.80), with the third equation exactly coinciding with (4.79). Because the expression for the asymptotically flat coordinate x^+ is identical in all three spacetime regions, we deduce that $t_+(x^+) = \frac{1}{4(x^+)^2}$ holds everywhere. This is precisely what the first equation states. To interpret the second equation, we must determine $t_-(x^-)$ in the third region. Region III is defined to be the Minkowski vacuum in the $\hat{\sigma}^\pm$ coordinates, so the quantum state there is $|\psi\rangle = |0, \hat{\sigma}\rangle$. This implies $t_-(\hat{\sigma}^-) = 0$, which in turn leads to $t_-(x^-) = \frac{1}{4(x^-+\Delta)^2}$. Therefore, we can now identify the meaning of each term appearing in the second equation:

$$t_-(x^-) = \frac{\eta(x^-_{\mathrm{E}} - x^-)}{4(x^-)^2} + \frac{\eta(x^- - x^-_{\mathrm{E}})}{4\left(x^- + \Delta\right)^2}, \qquad T^{f,cl}_{--}(x^-) = -\frac{\varepsilon\Delta}{4x^-_{\mathrm{E}}\left(x^-_{\mathrm{E}} + \Delta\right)}\delta(x^- - x^-_{\mathrm{E}}). \tag{4.132}$$

Due to the presence of a term proportional to the Dirac δ-function, an additional matter shockwave arises, which exits the black hole and travels to future null infinity at the precise instant when the singularity meets the apparent horizon. To compute the mass transported by this outgoing shockwave, we employ Equation (3.100), taking n^μ to be proportional to the time-like Killing vector in region III, $\xi = \lambda x^+\partial_+ - \lambda\left(x^- + \Delta\right)\partial_-$. The calculation simplifies to:

$$M' = \int_\Sigma \sqrt{\gamma}d\hat{\sigma}\; n^\mu\xi^\nu T_{\mu\nu} = -\frac{\varepsilon\Delta}{4x^-_{\mathrm{E}}\left(x^-_{\mathrm{E}} + \Delta\right)}\mathrm{F}^-(x^-_{\mathrm{E}}) = \frac{\varepsilon\lambda\Delta}{4x^-_{\mathrm{E}}}, \tag{4.133}$$

where we have used $\mathrm{F}^-(x^-_{\mathrm{E}}) = -\lambda(x^-_{\mathrm{E}} + \Delta)$.

Therefore, we find that the mass carried away by this shockwave precisely matches the second term in the expression for δM (4.127). Let us briefly recapitulate the physical picture. At the instant when the singularity reaches the apparent horizon, a small amount of negative energy (since $x^-_{\mathrm{E}} < 0$) is emitted as an outgoing shockwave (the so-called *thunderpop* [23, 24, 25, 26]), which transports the surplus energy to infinity. After this emission, what remains is a static universe with no energy flux at $\mathscr{I}^+$, described by the Minkowski vacuum metric.

What is noteworthy is that the constant C' determining the Minkowski vacuum state in region III of the spacetime is independent of the initial choice of C and in fact coincides with the critical value C^*. As before, we must discard the strong-coupling region, implying that the spacetime boundary in region III is located at $2\lambda\hat{\sigma}_{\mathrm{B}} = \ln\frac{\varepsilon\pi G}{4}$, which, upon rewriting in $x^\pm$ coordinates, becomes:

$$-\lambda^2 x^+_{\mathrm{B}}\left(x^-_{\mathrm{B}} + \Delta\right) = \frac{\varepsilon\pi G}{4}. \tag{4.134}$$

Hence, the boundary in region III is simply the extension of the apparent horizon from region II. It is also evident that the event horizon (in region II) is given by:

$$x^-_{\mathrm{H}} = x^-_{\mathrm{E}}. \tag{4.135}$$

If we expand the metric near the strong-coupling region, i.e., close to the boundary $\hat{\sigma} = \hat{\sigma}_{\mathrm{B}} + \delta$, where $\delta > 0$ is a small parameter, we find:

$$\mathrm{d}s^2 = \frac{-\mathrm{d}t^2 + \mathrm{d}\delta^2}{2\lambda^2\delta^2 + o(\delta^3)}. \tag{4.136}$$

Thus, in the vicinity of $\delta = 0$, the spacetime exhibits the geometry of a semi-infinite throat. The proper distance diverges logarithmically as one approaches the boundary, mirroring the behavior found in higher-dimensional black holes. Furthermore, the curvature remains finite everywhere, so the spacetime is geodesically complete.

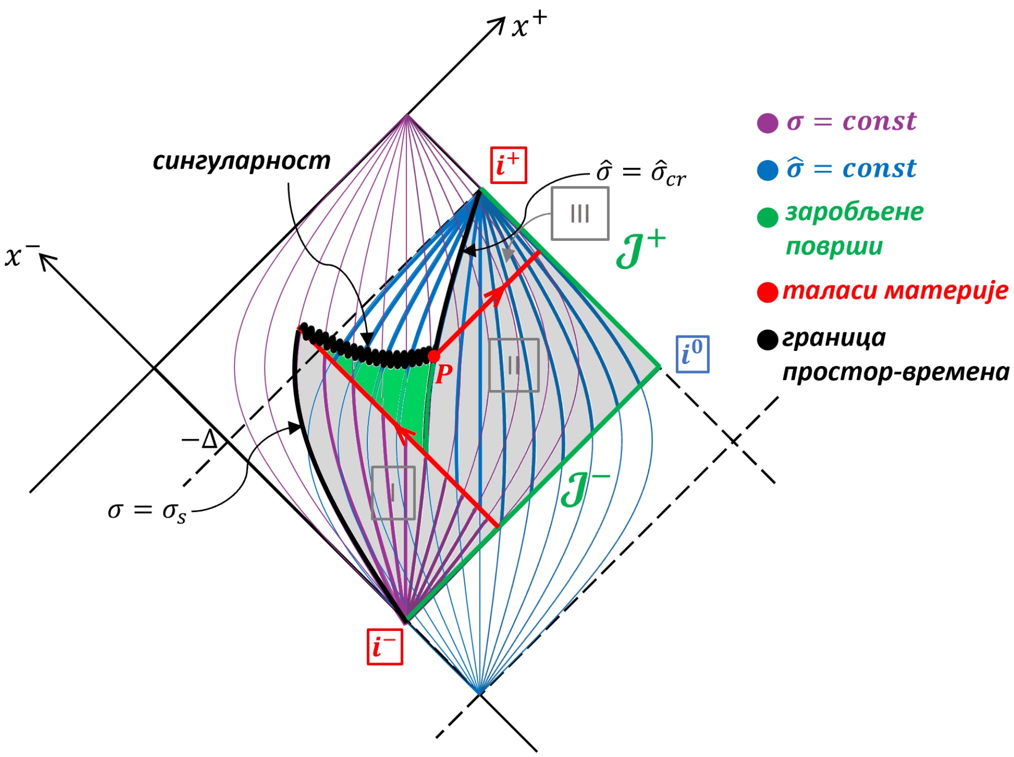

Figure 4.6: Penrose diagram of the evaporating black hole solution in the BPP model

There is still one "degree of freedom" remaining that we have not fixed: the constant C_0, which selects which particular static Minkowski vacuum corresponds to the massless solution. It is natural to demand that the ADM mass of the final spacetime vanish. Under this assumption, the natural assignment is $C_0 = C^*$. However, for this choice, the spacetime in region I acquires a nonzero mass unless $C = C^*$. This consideration motivates us to fix the initial constant C as well. Although such a choice is not strictly required within this model, it provides the most physically meaningful specification of the constants.

The full dynamical picture of the evaporating black hole is presented in Figure 4.6. The axes represent the compactified Kruskal coordinates. One can clearly track the evolution of the spacetime boundary (black line). Initially, it coincides with the boundary of the strongly coupled region of the Minkowski vacuum solution in region I, which is described by Equation (4.115). In this stage, it is a constant-σ hypersurface, $\sigma = \sigma_s$, subject to the reflective boundary conditions (4.117). Entering region II, the boundary turns into a singularity (4.120), indicated by the wavy line in Figure 4.6. In region III, it again becomes a constant-$\hat{\sigma}$ hypersurface, $\hat{\sigma} = \hat{\sigma}_{\mathrm{B}}$ (4.134), representing the continuation of the apparent horizon of region II, defined in (4.121). The trapped surfaces, located between the apparent horizon and the singularity, are shown in green. The initial ingoing shockwave is colored red. The end-point of evaporation (4.124) is explicitly marked, with the outgoing shockwave emerging from it also drawn in red, while in the opposite direction the event horizon (4.135) of the black hole in region II extends.

In region III, the energy–momentum tensor is normal ordered with respect to the $\hat{\sigma}$ coordinates, which implies that the final quantum state is $|\psi\rangle = |0, \hat{\sigma}\rangle$, i.e., a pure state. Since there is no Hawking radiation in this region, the evolution appears to be unitary. Nevertheless, the only parameter describing the initial matter is its mass, and this is also the only piece of information that can be inferred from the final spacetime. Consequently, the model seems to exhibit information loss. However, because there are strong correlations in the vicinity of the boundary, we might expect substantial quantum gravitational effects there, which could provide a mechanism for recovering the apparently lost information. Whether information is actually lost depends on the behavior of the entanglement entropy, more specifically, on whether or not it follows the Page curve. This is discussed in detail in Chapter 9.

Evaporation time

At the end of this section, we determine the total evaporation time. We begin with the relation

$$e^{2\lambda t_{\mathrm{E}}} = -\frac{x_p^+}{x_{\mathrm{E}}^- + \Delta}. \tag{4.137}$$

The evaporation time is evaluated by fixing the integration constant C according to the above choice, i.e. by setting $C = C^*$. With this choice, the intersection point takes the form

$$x_{\mathrm{E}}^+ = \frac{\varepsilon\pi G}{4\lambda^2\Delta}\left[e^{\frac{4M}{\varepsilon\lambda}-1}\right] \quad \wedge \quad x_{\mathrm{E}}^- = -\frac{\Delta}{1-e^{-\frac{4M}{\varepsilon\lambda}}}. \tag{4.138}$$

Substituting these expressions into Equation (4.137) for the evaporation time yields

$$e^{2\lambda t_{\mathrm{E}}} = \frac{\varepsilon\pi G}{4(\lambda\Delta)^2}\left(e^{\frac{4M}{\varepsilon\lambda}}-1\right)^2 \implies 2\lambda t_{\mathrm{E}} = 2\ln\left(e^{\frac{4M}{\varepsilon\lambda}}-1\right) - \ln\frac{4\pi GM^2}{\varepsilon\lambda^2} + 2\ln\left(\lambda x_0^+\right). \tag{4.139}$$

If we now assume that the black hole mass is very large, namely $\frac{4M}{\varepsilon\lambda} \gg 1$, the evaporation time simplifies to

$$\lambda t_p = \frac{4M}{\varepsilon\lambda} - \frac{1}{2}\ln\frac{4\pi GM^2}{\varepsilon\lambda^2} + \ln\left(\lambda x_0^+\right). \tag{4.140}$$

In the large-mass regime, the second term in this expression can also be neglected, since the logarithmic contribution grows much more slowly than the linear one. Let us next consider the behavior of the event horizon (4.135) in this limit: $x^- = x_{\mathrm{E}}^- \approx -\Delta$. Thus, in this regime, the horizon is located slightly below the hypersurface $x^- = -\Delta$. Restoring the physical constants, the evaporation time becomes

$$\Delta t_{\mathrm{E}} = \frac{48\pi M}{N\hbar\lambda^2}, \tag{4.141}$$

where we have discarded the last term in (4.140) as well, since it is constant and therefore negligible compared to the leading term, which scales linearly with the mass.

4.4 Perturbative treatment of the gravitational collapse

In this section, we demonstrate how the perturbative method introduced in Section 3.4.1 can be employed to derive the quantum-corrected collapse scenario discussed in the previous section. We work in Eddington–Finkelstein coordinates. Because the linear dilaton vacuum in the BPP model carries a non-vanishing energy flux at infinity, both spacetime regions I and II (see Fig. 3.3) must be quantum-corrected. When solving the equations, it is not necessary to treat these two regions separately, since the Minkowski vacuum should emerge as the $b \to 0$ limit of the solution in the region $x^+ > x_0^+$, where the black hole exists. We therefore first determine the general solution of the BPP equations of motion.

We begin by expanding the equations of motion (4.72-4.74) for the BPP model to first order in ε, using an expansion analogous to (3.108), namely $\rho \mapsto \rho + \varepsilon\alpha$ and $\phi \mapsto \phi + \varepsilon\theta$. The equations of motion then become:

$$\begin{aligned} \lambda\alpha e^{2\rho} &= \frac{1}{\lambda}\partial_+\partial_-\theta + e^{2\rho}\left(\mathrm{F}^+\partial_+\theta + \mathrm{F}^-\partial_-\theta\right), \\ \partial_\pm\left(e^{-2\rho}\left(\partial_\pm\theta + \lambda\alpha\mathrm{F}^\pm e^{2\rho}\right)\right) &= -\frac{1}{2}e^{\phi-\rho}\partial_\pm^2 e^{\phi-\rho}, \\ \partial_+\partial_-\theta &= \partial_+\partial_-\alpha. \end{aligned} \tag{4.142}$$

Since the right-hand side of Equation (4.73) is already of ε order, a simple substitution of $\phi - \rho$ in zeroth order from (4.36) yields:

$$\partial_\pm\left(e^{-2\rho}\left(\partial_\pm\theta + \lambda\alpha\mathrm{F}^\mp e^{2\rho}\right)\right) = \frac{e^{2(\phi-\rho)}}{\mathrm{F}^{\pm 2}}\left[t_\pm(\hat\sigma^\pm) + \frac{\lambda^2}{4}\right], \tag{4.143}$$

where Equation (4.73) has been recast into the form (3.109). To determine the normal ordered components of the energy-momentum tensor $t_\pm(\hat\sigma^\pm)$ in region II of the spacetime, we make use of (3.114). These components read:

$$t_+(\hat\sigma^+) = 0 \ \wedge \ t_-(\hat\sigma^-) = \frac{\lambda^2}{4}\left(\mathrm{F}^{-2} - 1\right). \tag{4.144}$$

Expressing F^- in terms of ϕ and δ (3.107) with the help of (4.57) and substituting in Equation (4.143), after integration, yields:

$$\begin{aligned} \partial_+\theta &= -\frac{\lambda}{2}\mathrm{F}^- e^{2\rho}\left[2\alpha + \frac{\mathrm{G}^-}{\mathrm{F}^-} + \frac{1}{4}\frac{1}{b - e^{-2\phi}}\right], \\ \partial_-\theta &= -\frac{\lambda}{2}\mathrm{F}^+ e^{2\rho}\left[2\alpha + \frac{\mathrm{G}^+}{\mathrm{F}^+} + \frac{1}{4}\frac{\delta^2}{\delta^2\left(b - e^{-2\phi}\right) - b}\right], \end{aligned} \tag{4.145}$$

where another set of arbitrary fictions $\mathrm{G}^\pm(\sigma^\pm)$ is introduced. These two expressions correspond to (3.111). The function $\mathcal{D}_1$ is determined by direct comparison. Following further the method introduced in Section 3.4.1 we express α from the first equation in (4.142) and substitute it in (4.145). The subsequent integration gives:

$$\begin{aligned} \lambda b\theta e^{2\phi} &= \frac{\lambda}{2}\frac{\mathrm{G}^-}{\mathrm{F}^-} - \mathrm{F}^-\partial_-\theta + \frac{\lambda}{8}e^{2\phi}\left(\ln\left|b - e^{-2\phi}\right| + \mathrm{H}^-\right), \\ \lambda b\theta e^{2\phi} &= \frac{\lambda}{2}\frac{\mathrm{G}^+}{\mathrm{F}^+} - \mathrm{F}^+\partial_+\theta + \frac{\lambda}{8}e^{2\phi}\left(\ln\left|b - \delta^2\left(b - e^{-2\phi}\right)\right| + \mathrm{H}^+\right), \end{aligned}$$

with an additional pair of functions $\mathrm{H}^\pm(x^\pm)$. Requiring these two equations to coincide determines the form of the functions $\mathrm{H}^\pm$ in terms of another constant D, resulting in the following expression:

$$\lambda b\theta e^{2\phi} = \frac{\lambda}{2}\left(be^{2\phi} - 1\right)\left[2\alpha + \frac{\mathrm{G}^+}{\mathrm{F}^+} + \frac{\mathrm{G}^-}{\mathrm{F}^-}\right] + \frac{\lambda}{8}e^{2\phi}\Big[-2\ln\delta - D + 1 + \ln\left|b - \delta^2\left(b - e^{-2\phi}\right)\right|\Big]. \tag{4.146}$$

To obtain the function θ, we follow the same procedure once again. Solving (4.145) for α and substituting the result into (4.146) yields a pair of first-order differential equations for θ (one involving $\partial_+\theta$ and the other involving $\partial_-\theta$). Integrating these two equations introduces a new family of arbitrary functions, which are then fixed by requiring that the two resulting expressions for θ agree. The final form of θ is given by:

$$\theta = \frac{\lambda}{2}\left(be^{2\phi}-1\right)\left(\int \mathrm{d}x^{+}\frac{\mathrm{G}^{+}}{\mathrm{F}^{+2}}+\int \mathrm{d}x^{-}\frac{\mathrm{G}^{-}}{\mathrm{F}^{-2}}\right)+\frac{1}{8}e^{2\phi}\left(1-D-2\ln\delta+\ln\left|b-\delta^{2}\left(b-e^{-2\phi}\right)\right|\right) \tag{4.147}$$

We now switch back to the quantum-corrected fields $\phi+\varepsilon\theta\mapsto\phi$ and $\rho+\varepsilon\alpha\mapsto\rho$, as described in (3.113) by substituting the solutions for α (4.146) and θ (4.147). In this way, we obtain the quantum-corrected counterparts of the expressions in (4.57):

$$\begin{aligned}
&\mathrm{F}^{+}\mathrm{F}^{-}e^{2\rho} = be^{2\phi}-1+\frac{\varepsilon\pi G}{4}e^{2\phi}\left[2\ln\delta+D-1-\ln\left|b-\delta^{2}\left(b-e^{-2\phi}\right)\right|\right],\\
&\ln\left|b-e^{-2\phi}\right|+\frac{\varepsilon\pi G}{4}e^{2\phi}\frac{2\ln\delta+D-1-\ln\left|b-\delta^{2}\left(b-e^{-2\phi}\right)\right|}{be^{2\phi}-1} = -\lambda\left(\int\frac{\mathrm{d}x^{+}}{\mathrm{F}^{+}}+\int\frac{\mathrm{d}x^{-}}{\mathrm{F}^{-}}\right)\equiv 2\lambda\hat{\sigma},
\end{aligned} \tag{4.148}$$

where $\mathrm{F}^{\pm}+\varepsilon\mathrm{G}^{\pm}\mapsto\mathrm{F}^{\pm}$. Taking the limit $b\to 0$ gives the following quantum-corrected Minkowski vacuum solution:

$$\begin{aligned}
\mathrm{F}^{+}\mathrm{F}^{-}e^{2\rho} &= -1+\frac{\varepsilon\pi G}{2}\left(\phi+\phi_0\right)e^{2\phi},\\
\phi+\frac{\varepsilon\pi G}{4}\left(\phi+\phi_0\right)e^{2\phi} &= \frac{\lambda}{2}\left(\int\frac{\mathrm{d}x^{+}}{\mathrm{F}^{+}}+\int\frac{\mathrm{d}x^{-}}{\mathrm{F}^{-}}\right),
\end{aligned} \tag{4.149}$$

where ϕ_0 denotes the integration constant. Choosing Eddington–Finkelstein coordinates as the starting coordinate system is equivalent to fixing $\mathrm{F}^{+}=-1$ and $\mathrm{F}^{-}=1$. If one then performs an additional coordinate transformation to Kruskal coordinates (4.41), it is straightforward to check that, to first order in perturbation theory, the solution (4.149) coincides with the exact Minkowski vacuum solution (4.111). Under this identification, the constant C appearing in (4.111) is related to ϕ_0 via $C=\frac{\varepsilon\pi G}{2}\phi_0$.

In Section 3.4.1, the next step is to smoothly match the solution (4.148) to the initial Minkowski vacuum configuration (4.149). This is done by imposing continuity of $e^{2\rho}$ and ϕ, while allowing their derivatives $\partial_{+}\rho$ and $\partial_{+}\phi$ to exhibit discontinuities across the hypersurface $x^{+}=x_0^{+}$. Under these conditions, the evaporating black hole solution is fixed by specific choices of the constants b, D, and coordinate transformations F^{+} and F^{-} that enter the general solution (4.148):

$$b=\frac{\pi GM}{\lambda},\ D=1+2\phi_0,\ \mathrm{F}^{+}=-1,\ \mathrm{F}^{-}=1-be^{-2\hat{\mathrm{x}}}. \tag{4.150}$$

As we can see, the coordinate transformations do not gain any quantum corrections in this procedure, and the coordinates are the same as in the classical case:

$$2\lambda\hat{\sigma}=-2\ln\delta+\ln\left|b-e^{2\hat{\mathrm{x}}}\right|. \tag{4.151}$$

A direct check shows that solution (4.150) coincides with the exact solution (4.119) expanded to first order in ε.

The end-state of the evaporation

To find the apparent horizon, we solve the equation $\partial_{+}e^{-2\phi}=0$. Employing the solution (4.148), the apparent horizon hypersurface to first order in ε is given by

$$e^{2\hat{\mathrm{x}}}=b+\frac{\varepsilon\pi G}{4}\delta^{2}. \tag{4.152}$$

The scalar curvature, defined as $R = 8e^{-2\rho}\partial_+\partial_-\rho$, is found to be

$$R = \frac{4\lambda^2\tilde{b}\delta^2}{\tilde{b}\delta^2 - b + e^{2\hat{\mathrm{x}}}}, \tag{4.153}$$

where the quantum-corrected constant b is introduced as $\tilde{b} = b - \frac{\varepsilon\pi G}{2}(\hat{\mathrm{x}} - \ln\delta - \phi_0)$. The singularity line is described by

$$e^{2\hat{\mathrm{x}}} = b - \tilde{b}\delta^2, \tag{4.154}$$

since this corresponds to the hypersurface along which the curvature diverges. To obtain the end-point of the evaporation, one must determine where the apparent horizon and singularity hypersurfaces intersect. This intersection can be computed from equations (4.152) and (4.154) to first order in ε, yielding the following result:

$$\delta_{\mathrm{E}}^2 = be^{-\frac{4b}{\varepsilon\pi G}-1-2\phi_0} \quad \wedge \quad e^{2\hat{\mathrm{x}}_{\mathrm{E}}} = b\left[1 + \frac{\varepsilon\pi G}{4}e^{-\frac{4b}{\varepsilon\pi G}-1-2\phi_0}\right]. \tag{4.155}$$

By rewriting the solution in Kruskal coordinates and employing $\delta_{\mathrm{E}}^2 = \frac{x_0^+}{x_{\mathrm{E}}^+}$ together with $e^{2\hat{\mathrm{x}}_{\mathrm{E}}} = -\lambda^2 x_0^+ x_{\mathrm{E}}^-$, we obtain that these expressions reproduce the precise end-point (4.124) to first order in ε.

Next, we show how to extract the end-state geometry. As a first step, we rewrite the solution in terms of the radial coordinate ϕ and the coordinate $\hat{\mathrm{x}}$, since the hypersurface that separates the evaporating black hole from the end-state geometry is defined using this coordinate, specifically by the condition $\hat{\mathrm{x}} = \hat{\mathrm{x}}_{\mathrm{E}}$. For this purpose, we introduce the running b constant:

$$\hat{b} = b + \frac{\varepsilon\pi G}{2}\phi_0 + \frac{\varepsilon\pi G}{4}\ln\left|be^{-2\hat{\mathrm{x}}} - 1\right|. \tag{4.156}$$

Since the deviation from the constant b is of order ε, we can replace every occurrence of b in the first-order perturbation theory with $\hat{b}$. Consequently, equations (4.148) are modified as follows:

$$\begin{aligned} \mathrm{F}^+\mathrm{F}^- e^{2\rho} &= \hat{b}e^{2\phi} - 1 - \frac{\varepsilon\pi G}{4}e^{2\phi}\ln\left|\hat{b} - e^{-2\phi}\right|, \\ \ln\left|\hat{b} - e^{-2\phi}\right| &- \frac{\varepsilon\pi G}{4}\frac{\ln\left|\hat{b} - e^{-2\phi}\right|}{\hat{b} - e^{-2\phi}} = 2\lambda\hat{\sigma}. \end{aligned} \tag{4.157}$$

These two relations are valid for every value of the coordinate $\hat{\mathrm{x}}$. As we move toward the event horizon at $\hat{\mathrm{x}} = \hat{\mathrm{x}}_{\mathrm{E}}$, the quantity $\hat{b}$ decreases smoothly and takes the value:

$$\hat{b}_{\mathrm{E}} = \frac{\varepsilon\pi G}{4}\left(\ln\frac{\varepsilon\pi G}{4} - 1\right), \tag{4.158}$$

at $\hat{\mathrm{x}} = \hat{\mathrm{x}}_{\mathrm{E}}$. Because $\hat{b}_{\mathrm{E}}$ is of order ε at this point, we may set $\hat{b} \to 0$ in the first-order perturbative expansion. After taking this limit, equations (4.157) reduce to the Minkowski vacuum solution (4.149) with constant $\phi_0' = \frac{2}{\varepsilon\pi G}\hat{b}_{\mathrm{E}}$. Comparing with the exact solution (4.128), we find that, upon transforming to Kruskal coordinates, the two solutions coincide to first order.

To determine whether a further outgoing shockwave emerges from the evaporation end-point, we integrate the "$--$" equation in (4.73) from $\sigma_{\mathrm{E}}^- - \epsilon$ to $\sigma_{\mathrm{E}}^- + \epsilon$, and then take the limit $\epsilon \to 0$, which yields:

$$\lim_{\epsilon\to 0} e^{-2\rho}\left[\partial_-\phi + \frac{\varepsilon\pi G}{2}e^{2\phi}\partial_-(\phi - \rho)\right]\Bigg|_{\sigma_{\mathrm{E}}^- - \epsilon}^{\sigma_{\mathrm{E}}^- + \epsilon} = \frac{\lambda b_0}{2\mathrm{F}^-}e^{2(\phi-\rho)}, \tag{4.159}$$

where $b_0 = \frac{\pi G \Delta M}{\lambda}$ and ΔM denotes the mass of the shockwave. By substituting the derivatives directly, we obtain:

$$-\frac{b_0}{\mathrm{F}^-} e^{2(\phi-\rho)} = \frac{\varepsilon\pi G}{4} e^{2\phi} + \frac{\varepsilon\pi G}{2} \frac{1}{b - e^{-2\phi}} + \frac{\varepsilon\pi G}{4} \frac{\delta^2}{b - \delta^2 \left(b - e^{-2\phi}\right)}. \tag{4.160}$$

A careful calculation of this expression yields the following:

$$b_0 = -\frac{\varepsilon\pi G}{4} b e^{-2\hat{\mathrm{x}}_{\mathrm{E}}} - \frac{\varepsilon\pi G}{4} b e^{-2\phi}. \tag{4.161}$$

Since $e^{-2\hat{\mathrm{x}}_{\mathrm{E}}} \propto 1/b$, the first term remains finite in the limit $b \to 0$, whereas the second term vanishes. Consequently, the mass of the thunderpop is:

$$\Delta M = -\frac{\varepsilon\lambda}{4} b e^{-2\mathrm{x}_{\mathrm{E}}} = \frac{\varepsilon\lambda\Delta}{4 x_{\mathrm{E}}^-}, \tag{4.162}$$

which matches the exact expression.

Finally, we turn to verifying the energy balance (3.115) in the BPP model. We begin by evaluating the total energy emitted by the black hole throughout its entire evaporation process:

$$E_{rad} = \varepsilon \int_{-\infty}^{\sigma_{\mathrm{E}}^-} \frac{\mathrm{d}\sigma^-}{\mathrm{F}^-} t_-(\hat{\sigma}^-) = \frac{\varepsilon\lambda}{4}\left[b e^{-2\hat{\mathrm{x}}_{\mathrm{E}}} - \ln\left| b e^{-2\hat{\mathrm{x}}_{\mathrm{E}}} - 1 \right| \right] = M + \frac{\varepsilon\lambda}{4}\left[2\phi_0 - \ln\frac{\varepsilon\pi G}{4} + 1 - \frac{\Delta}{x_{\mathrm{E}}^-} \right], \tag{4.163}$$

where, in the last step, we have made use of the expression (4.144) for $t_-(\hat{\sigma}^-)$. Observe that this result matches exactly the exact formula (4.126). This agreement arises because the coordinate transformation F^-, which enters the computation of the radiated energy, does not acquire quantum corrections in the BPP model. The energy balance can be reformulated in terms of the b-parameters as:

$$b_{rad} = b + \frac{\varepsilon\pi G}{2}\phi_0 - \frac{\varepsilon\pi G}{2}\phi_0' - b_0, \tag{4.164}$$

In this relation, $\frac{\varepsilon\pi G}{2}\phi_0$ represents the mass of the spacetime before the collapse, while $\frac{\varepsilon\pi G}{2}\phi_0'$ corresponds to the mass of the final configuration. The parameter $b = \frac{\pi G M}{\lambda}$ is the b-parameter associated with the incoming shockwave, b_0 denotes the b-parameter of the outgoing shockwave, and $b_{rad} = \frac{\pi G E_{rad}}{\lambda}$ is the b-parameter describing the Hawking radiation.

4.5 Thermodynamical quantities

In this section, we derive the temperature and entropy of the static black hole in the CGHS model. At first glance, discussing black hole entropy might seem meaningless unless one adopts the framework of quantum field theory in curved spacetime. Nonetheless, the temperature can actually be obtained purely from the geometric data (see Appendix D.6). In general, the temperature is given by $T = \frac{\kappa}{2\pi\hbar}$, where κ is the surface gravity calculated in (4.40). For our case, this yields:

$$T = \frac{\lambda}{2\pi} \quad\Longrightarrow\quad T = \frac{\lambda\hbar c}{2\pi k_B}. \tag{4.165}$$

We observe that the temperature is independent of the mass. Applying the thermodynamic relation $\mathrm{d}M = T\,\mathrm{d}S$, we obtain the entropy as $S = \frac{M}{T}$. The integration constant is chosen such that $S = 0$ at $M = 0$. It is customary to express the entropy in terms of the value of the dilaton at the horizon, namely:

$$e^{-2\phi_H} = b = \frac{\pi G M}{\lambda c^2} \qquad \Longrightarrow \qquad M = \frac{\lambda c^2}{\pi G} e^{-2\phi_H} \qquad \Longrightarrow \qquad S = k_B \frac{2c^3}{G\hbar} e^{-2\phi_H}, \tag{4.166}$$

where we have employed the expression for the temperature (4.165) together with the static black hole solution (4.42). Finally, by setting $k_B = \hbar = c = G = 1$, we arrive at the following expressions for the temperature and entropy of a static black hole in the CGHS model:

$$T = \frac{\lambda}{2\pi} \qquad \wedge \qquad S = 2e^{-2\phi_H}. \tag{4.167}$$

Note that these expressions remain valid even after quantum corrections are included, since the surface gravity stays unchanged.

Chapter 5

Dimensionally-reduced Einstein gravity

In this chapter, we set the stage for studying the information loss paradox by computing the Page curve for the theory of dimensionally reduced Einstein–Hilbert gravity (the DREH model). Our primary goal here is to construct the eternal and evaporating black hole scenarios within this theory. In the preceding chapter, we pursued the same objective using the CGHS model of dilaton gravity. That model has the key benefit that its equations of motion remain exactly solvable even after incorporating quantum corrections. This feature is absent in the DREH model. Nonetheless, since Einstein gravity is a thoroughly experimentally tested theory, analyzing entanglement entropy in the DREH model is highly significant. Once quantum corrections are introduced, we employ the perturbative approach described in Section 4.3.4. The reduced action (2.19) was obtained in Chapter 2. For convenience, we rewrite it here:

$$S_{\mathrm{DREH}} = \frac{1}{4G}\int d^2x\sqrt{-g}e^{-2\phi}\left[R + 2(\nabla\phi)^2 + 2\lambda^2 e^{2\phi}\right] - \frac{1}{2}\int d^2x\sqrt{-g}\,(\nabla f)^2\,. \tag{5.1}$$

The first term in (5.1) represents the gravitational action, denoted by S_g, whereas the second term introduces the matter contribution as a single scalar field, labeled S_m. Unlike in the CGHS model, we do not require additional scalar fields, since no correction term can be incorporated into the action that would make the equations of motion exactly solvable.

The chapter is divided into three main sections. In the first section, we solve the classical equations of motion derived from (5.1). We begin by analyzing the vacuum solution, then determine the solution with charged matter, and finally formulate the classical gravitational collapse. In this part we largely follow [111].

In the second section, quantum corrections are included through the Polyakov–Liouville action (3.72). The general static vacuum solution is obtained by employing the static ansatz introduced in Section 3.1. We then examine two specific cases: the vacuum solution associated with the Boulware state of the quantum fields and the eternal black hole solution. Here, our presentation is based on the arguments given in both [42] and [111].

The final section addresses the evaporating black hole scenario. We obtain the solution that satisfies the Unruh vacuum condition, and then demonstrate that the apparent horizon and the singularity meet at a finite point in the spacetime. We also show that the end-state geometry is again described by the static Boulware vacuum solution, and that there is no need to invoke a thunderpop. The entire analysis is carried out to first order in a perturbative expansion in $\hbar$. In this section we mainly follow [111].

5.1 Equations of motion and their solutions

We now proceed to determine the equations of motion obtained by varying the action 5.1.First, we address the gravitational part of the action:

$$\begin{aligned}\delta S_g &= \frac{1}{4G}\int d^2x\Big\{\delta\left(\sqrt{-g}e^{-2\phi}R\right) + 2\delta\sqrt{-g}\left[(\nabla\phi)^2+\lambda^2e^{2\phi}\right]e^{-2\phi} + 2\sqrt{-g}\delta\left(e^{-2\phi}(\nabla\phi)^2\right)\Big\}\\ &= \frac{1}{4G}\int d^2x\sqrt{-g}e^{-2\phi}\Big\{-e^{2\phi}\left[\nabla_\mu\nabla_\nu e^{-2\phi}+g_{\mu\nu}\Box e^{-2\phi}\right]\delta g^{\mu\nu} - 2R\delta\phi\\ &\quad - g_{\mu\nu}\left[(\nabla\phi)^2+\lambda^2e^{2\phi}\right]e^{-2\phi}\delta g^{\mu\nu} + 2\nabla_\mu\phi\nabla_\nu\phi\delta g^{\mu\nu} + 4\left[(\nabla\phi)^2-\Box\phi\right]\delta\phi\Big\}\\ &= \frac{1}{4G}\int d^2x\sqrt{-g}e^{-2\phi}\Big\{\left[2\nabla_\mu\nabla_\nu\phi - 2\nabla_\mu\phi\nabla_\nu\phi + g_{\mu\nu}\left(3(\nabla\phi)^2-2\Box\phi-\lambda^2e^{2\phi}\right)\right]\delta g^{\mu\nu}\\ &\qquad + \left[4(\nabla\phi)^2-4\Box\phi-2R\right]\delta\phi\Big\}.\end{aligned} \tag{5.2}$$

Throughout this computation, the same terms as in the CGHS model appear. In the second line, we employ (4.9) for the variation of the scalar curvature, together with $\delta\ln\left(\sqrt{-g}\right) = -\frac{1}{2}g_{\mu\nu}\delta g^{\mu\nu}$. Moreover, we make use of the enhanced symmetry of the 2D spacetime, which leads to a vanishing Einstein tensor, $G_{\mu\nu} = 0$. The matter contribution is exactly the same as in the CGHS model (4.11), so we simply reproduce it here:

$$\delta S_m = -\int d^2x\sqrt{-g}\Big\{\frac{1}{2}\left[\nabla_\mu f\nabla_\nu f - \frac{1}{2}g_{\mu\nu}(\nabla f)^2\right]\delta g^{\mu\nu} - (\Box f)\,\delta f\Big\}, \tag{5.3}$$

where we have omitted the sum, since the DREH model involves only a single scalar field. Using the same notation for the energy–momentum tensor as in the CGHS model, we arrive at the following equations of motion:

$$\begin{aligned}\frac{\delta S}{\delta g^{\mu\nu}} = 0: &\quad 2\nabla_\mu\nabla_\nu\phi e^{-2\phi} - 2\nabla_\mu\phi\nabla_\nu\phi e^{-2\phi} + g_{\mu\nu}\left(3(\nabla\phi)^2-2\Box\phi-\lambda^2e^{2\phi}\right)e^{-2\phi} = 2GT^f_{\mu\nu},\\ \frac{\delta S}{\delta\phi} = 0: &\quad (\nabla\phi)^2-\Box\phi = \frac{R}{2},\\ \frac{\delta S}{\delta f} = 0: &\quad \Box f = 0,\\ T_{\mu\nu} = \frac{-2}{\sqrt{-g}}\frac{\delta S_m}{\delta g^{\mu\nu}}: &\quad T_{\mu\nu} = \nabla_\mu f\nabla_\nu f - \frac{1}{2}g_{\mu\nu}(\nabla f)^2\end{aligned} \tag{5.4}$$

The metric equation in (5.4) can be simplified. Contracting it with the metric tensor $g^{\mu\nu}$ yields $\Box e^{-2\phi} = 2\lambda^2 + 2GT$, where $T = g^{\mu\nu}T_{\mu\nu}$. Defining a new field $\varphi = e^{-\phi}$ and using the dilaton equation, we arrive, after some algebraic manipulations, at:

$$\nabla_\mu\nabla_\nu\varphi - \frac{1}{2}R_{\mu\nu}\varphi = -G\left(T_{\mu\nu} - \frac{1}{2}g_{\mu\nu}T\right)\varphi^{-1}, \tag{5.5}$$

$$\Box\varphi^2 = 2\lambda^2 + 2GT. \tag{5.6}$$

Note that we have not introduced the reduced field x (2.46) in the same manner as in the CGHS model. Instead, we use φ. The reduced field is defined later, and its definition involves the Schwarzschild radius.

5.1.1 Vacuum solution of classical equations of motion

We now determine the general solution of the classical vacuum equations of motion in the conformal gauge $\mathrm{d}s^2 = -e^{2\rho}\mathrm{d}x^+\mathrm{d}x^-$, introduced in (3.2). In this gauge, the non-zero components of the connection, Ricci tensor, and scalar curvature are listed in (3.3), and the scalar field invariants are specified in (3.4). With these choices, the equations of motion (5.5) and (5.6) take the form:

$$\partial_\pm \left(e^{-2\rho}\partial_\pm\varphi\right) = -GT_{\pm\pm}\varphi^{-1}e^{-2\rho}, \tag{5.7}$$

$$\partial_+\partial_-\varphi + \varphi\partial_+\partial_-\rho = 0, \tag{5.8}$$

$$\partial_+\partial_-\varphi^2 + \frac{\lambda^2}{2}e^{2\rho} = 0. \tag{5.9}$$

In this step, we have made explicit use of the symmetry of the scalar field EMT, the fact that its trace is zero, and that the only non-vanishing components are $T_{\pm\pm}$, which are set to zero when considering the vacuum solution. Integrating Equation (5.7), we obtain:

$$\partial_\pm\varphi = \frac{\lambda}{2}\mathrm{F}^\mp(x^\mp)e^{2\rho}, \tag{5.10}$$

where $\mathrm{F}^\pm(x^\pm)$ denote a set of arbitrary functions. Shortly, it will become evident that they are identified with the Killing vector (3.5) associated with time translations. The functions $\partial_\pm\varphi$ obey the consistency condition $\partial_+\partial_-\varphi = \partial_-\partial_+\varphi$. Making use of this property leads to:

$$\nabla_+\mathrm{F}^+ = \nabla_-\mathrm{F}^-, \tag{5.11}$$

$$\partial_+\partial_-\varphi = \frac{\lambda}{2}\nabla_+\mathrm{F}^+e^{2\rho}. \tag{5.12}$$

Combining this expression with equations (5.9) and (5.10), we can write φ in terms of $\mathrm{F}^\pm$ and ρ as

$$\varphi = -\frac{\lambda}{2}\frac{1+\mathrm{F}^+\mathrm{F}^-e^{2\rho}}{\nabla_+\mathrm{F}^+}. \tag{5.13}$$

We now determine $\partial_+\partial_-\rho$ by inserting equations (5.13) and (5.12) into Equation (5.8):

$$\partial_+\partial_-\rho = \frac{\left(\nabla_+\mathrm{F}^+\right)^2e^{2\rho}}{1+\mathrm{F}^+\mathrm{F}^-e^{2\rho}}. \tag{5.14}$$

One readily verifies that $\partial_-\left(1+\mathrm{F}^+\mathrm{F}^-e^{2\rho}\right) = \mathrm{F}^+\nabla_+\mathrm{F}^+e^{2\rho}$ and that $\partial_+\partial_-\rho = \frac{\partial_-\left(\nabla_+\mathrm{F}^+\right)}{2\mathrm{F}^+}$. Using these relations together with Equation (5.14), we obtain

$$\nabla_+\mathrm{F}^+ = \mathrm{G}^+(x^+)\left(1+\mathrm{F}^+\mathrm{F}^-e^{2\rho}\right)^2, \tag{5.15}$$

where $\mathrm{G}^+(x^+)$ is an arbitrary function. Differentiation with respect to x^+ reproduces the same relation, implying that we also find:

$$\nabla_+\mathrm{F}^+ = \mathrm{G}^-(x^-)\left(1+\mathrm{F}^+\mathrm{F}^-e^{2\rho}\right)^2, \tag{5.16}$$

where $\mathrm{G}^-(x^-)$ is likewise an arbitrary function. Because these two expressions coincide, the functions $G^\pm$ must in fact be equal to the same constant: $\mathrm{G}^+(x^+) = \mathrm{G}^-(x^-) = -\frac{1}{2a}$, where the significance of a will be clarified shortly. Therefore, using Equation (5.13), we arrive at the following result:

$$\nabla_+\mathrm{F}^+ = -\frac{1}{2a}\left(1+\mathrm{F}^+\mathrm{F}^-e^{2\rho}\right)^2 = -\frac{\lambda}{2}\frac{\lambda a}{\varphi^2}. \tag{5.17}$$

We can check that $\nabla_+ \mathrm{F}^+$ likewise obeys $\nabla_+ \mathrm{F}^+ = \mathrm{F}^{\pm}\partial_{\pm} \ln\left(\mathrm{F}^+\mathrm{F}^- e^{2\rho}\right)$. Combined with equations (5.17) and (5.13), this allows the derivatives of φ to be written as:

$$\partial_{\pm}\varphi = -\frac{\lambda}{2\mathrm{F}^{\pm}}\frac{\varphi - \lambda a}{\varphi}. \tag{5.18}$$

By integrating this equation, we obtain the final result, which is expressed by the following two equations:

$$\varphi + \lambda a \ln\left(\frac{\varphi}{\lambda a} - 1\right) = -\frac{\lambda}{2}\left(\int \frac{\mathrm{d}x^+}{\mathrm{F}^+} + \int \frac{\mathrm{d}x^-}{\mathrm{F}^-}\right) \equiv \lambda\sigma, \tag{5.19}$$

$$\mathrm{F}^+\mathrm{F}^- e^{2\rho} = \frac{\lambda a}{\varphi} - 1. \tag{5.20}$$

The general solution of the classical vacuum equations (5.19-5.20) is characterized by one integration constant and two arbitrary functions. We denote it by the ordered triplet $(\mathrm{F}^+, \mathrm{F}^-, a)$. It is clear that this solution is expressed in the form (3.18-3.19). The first line gives the dilaton field and defines the tortoise coordinate, whereas the second line provides the metric functions Λ. The functions $\mathrm{F}^{\pm}$ represent the coordinate transformations from an arbitrary coordinate system to the Eddington–Finkelstein coordinates. Therefore, we conclude that the most general vacuum solution of the DREH equations of motion corresponds to the static Schwarzschild black hole. A natural choice for the dilaton field is $\varphi = e^{-\phi} = \lambda r$, thereby introducing the radial coordinate. Expressing the metric in terms of this radial coordinate yields

$$\mathrm{d}s^2 = -\left(1 - \frac{a}{r}\right)\mathrm{d}t^2 + \frac{\mathrm{d}r^2}{1 - \frac{a}{r}}. \tag{5.21}$$

Thus, the Schwarzschild metric is recovered within the DREH model. By direct comparison with the standard Schwarzschild solution, we identify the constant a as the Schwarzschild radius. The appearance of the Schwarzschild black hole as the most general solution of the vacuum equations of motion in the DREH model is precisely how Birkhoff's theorem [106] manifests itself in this two-dimensional framework. This observation also makes it clear that the model arises from dimensional reduction over $\mathbb{S}^2$. For more details on the standard Schwarzschild solution see Appendix C.

5.1.2 General static solution with charged matter

The key conclusion of the previous subsection is that the most general vacuum solution coincides with a static black hole configuration corresponding to the 4D Schwarzschild geometry. We now turn to determining the most general static solution when the matter fields are permitted to carry a certain type of charge, similarly to the CGHS model in Section 4.1.4. In doing so, we make explicit use of the fact that the classical scalar field EMT is traceless. After imposing the static ansatz of Section 3.1, the equations of motion (5.5-5.6) take the following form:

$$\begin{aligned}
&\frac{2G\Lambda}{\lambda^2\varphi}T_{\mu\nu} = \left[\mathcal{D}^2\frac{\mathrm{d}\Lambda}{\mathrm{d}\varphi} + \frac{\mathcal{D}\varphi}{2}\frac{\mathrm{d}}{\mathrm{d}\varphi}\left(\mathcal{D}\frac{\mathrm{d}\Lambda}{\mathrm{d}\varphi}\right)\right]\xi_\mu\xi_\nu - \left[\frac{\mathrm{d}\left(\Lambda\mathcal{D}^2\right)}{\mathrm{d}\varphi} + \frac{\mathcal{D}\varphi}{2}\frac{\mathrm{d}}{\mathrm{d}\varphi}\left(\mathcal{D}\frac{\mathrm{d}\Lambda}{\mathrm{d}\varphi}\right)\right]\varepsilon_{\mu\rho}\varepsilon_{\nu\sigma}\xi^\rho\xi^\sigma, \\
&\mathcal{D}\frac{\mathrm{d}}{\mathrm{d}\varphi}\left(\Lambda\mathcal{D}\varphi\right) = -1.
\end{aligned} \tag{5.22}$$

The trace of the metric equation gives:

$$\mathcal{D}^2\frac{\mathrm{d}\Lambda}{\mathrm{d}\varphi}+\frac{\mathrm{d}\left(\Lambda\mathcal{D}^2\right)}{\mathrm{d}\varphi}+\mathcal{D}\varphi\frac{\mathrm{d}}{\mathrm{d}\varphi}\left(\mathcal{D}\frac{\mathrm{d}\Lambda}{\mathrm{d}\varphi}\right)=0. \tag{5.23}$$

Substituting the second equation from (5.22) into (5.23) yields an integrable equation. Solving it introduces a positive charge $\mu>0$, associated with the scalar field in the same way as in (4.34) of the CGHS model, namely:

$$\varphi\Lambda^2\mathcal{D}\frac{\mathrm{d}\mathcal{D}}{\mathrm{d}\varphi}=-\mu,\qquad \mathcal{D}^2=\left(\frac{\mu}{\Lambda}-1\right)\left(\frac{\mathrm{d}\left(\Lambda\varphi\right)}{\mathrm{d}\varphi}\right)^{-1},\qquad \Lambda^2T^{\shortparallel\shortparallel}=\Lambda^2T^{\perp\perp}=\frac{\lambda^2\mu}{2G}. \tag{5.24}$$

Inserting this form of $\mathcal{D}_1$ leads to a second-order differential equation for Λ. Integrating once, we obtain:

$$\left(1-\frac{\mu}{\Lambda}\right)\frac{\mathrm{d}\left(\Lambda\varphi\right)}{\mathrm{d}\varphi}=-A-2\mu\ln\left|\Lambda\varphi\right|, \tag{5.25}$$

where A is an additional integration constant. Plugging (5.25) back into the expression for $\mathcal{D}_1$ in (5.24) we see that $A+2\mu\ln|\Lambda\varphi|>0$. Treating (5.25) as a differential equation for φ as a function of $\Lambda\varphi$, we find the solution:

$$\varphi=\frac{\Lambda\varphi}{\mu}+\sqrt{A+2\mu\ln|\Lambda\varphi|}\left[B-\frac{\sqrt{2\pi}\,\mathrm{sgn}(\Lambda)}{2\mu^{3/2}}e^{-\frac{A}{2\mu}}\mathrm{erfi}\left(\sqrt{\ln|\Lambda\varphi|+\frac{A}{2\mu}}\right)\right], \tag{5.26}$$

where B is the final integration constant, and $\mathrm{erfi}(x)$ denotes the imaginary error function, defined by

$$\mathrm{erfi}(x)=\frac{2}{\sqrt{\pi}}\int_0^x e^{t^2}\mathrm{d}t. \tag{5.27}$$

The tortoise coordinate (3.18) can likewise be expressed in terms of $\Lambda\varphi$ and takes the form:

$$\lambda\sigma=\frac{1}{\sqrt{2\mu}}\left[\varphi\sqrt{\ln|\Lambda\varphi|+\frac{A}{2\mu}}+\frac{\sqrt{\pi}\,\mathrm{sgn}(\Lambda)}{2\mu}e^{-\frac{A}{2\mu}}\mathrm{erfi}\left(\sqrt{\ln|\Lambda\varphi|+\frac{A}{2\mu}}\right)\right]. \tag{5.28}$$

The asymptotic behavior of this solution is given by $\varphi=\frac{\Lambda\varphi}{2\mu\ln|\Lambda\varphi|}$. Hence, the geometry is not asymptotically flat, and the solution is therefore completely disconnected from the standard Schwarzschild black hole solution.

5.1.3 Classical gravitational collapse

To describe classical gravitational collapse, we adopt the approach presented in Section 3.4. The energy-momentum tensor is specified as an incoming shockwave with components $T_{++}=-\frac{M}{\mathrm{F}^+(x_0^+)}\delta(x^+-x_0^+)$ and $T_{--}=0$, where M denotes the mass carried by the shockwave. The associated Penrose diagram is depicted in Figure 3.2. The spacetime consists of two regions (I and II in Figure 3.2), which must be joined smoothly. In particular, the metric and the dilaton field are required to match continuously across the hypersurface $x^+=x_0^+$, as imposed by condition (3.102):

$$e^{2\rho_{\mathrm{I}}}\Big|_{x^+=x_0^+-\epsilon}=e^{2\rho_{\mathrm{II}}}\Big|_{x^+=x_0^++\epsilon}, \tag{5.29}$$

$$\varphi_I\Big|_{x^+=x_0^+-\epsilon}=\varphi_{II}\Big|_{x^+=x_0^++\epsilon}, \tag{5.30}$$

when $\epsilon \to 0$, and the indices I and II label parts I and II of the spacetime, respectively, in the same manner as in Section 3.4. In region I, the vacuum solution is specified by $(\mathrm{F}_{\mathrm{I}}^{+}, \mathrm{F}_{\mathrm{I}}^{-}, a_{\mathrm{I}})$, whereas in region II it is characterized by $(\mathrm{F}_{\mathrm{II}}^{+}, \mathrm{F}_{\mathrm{II}}^{-}, a_{\mathrm{II}})$. The final condition (3.104) follows from integrating Equation (5.7). This yields:

$$e^{-2\rho_{\mathrm{II}}}\partial_{+}\varphi_{II}\Big|_{x^{+}=x_{0}^{+}+\epsilon} - e^{-2\rho_{\mathrm{I}}}\partial_{+}\varphi_{I}\Big|_{x^{+}=x_{0}^{+}-\epsilon} = \frac{GM}{\mathrm{F}^{+}}e^{-2\rho}\varphi^{-1}\Big|_{x^{+}=x_{0}^{+}}. \tag{5.31}$$

Equation (5.31), together with (5.10) and (5.29), leads to a discontinuity in the derivatives of the dilaton field and consequently to a discontinuity in the F^{-} coordinate transformation, which is given by:

$$\mathrm{F}_{\mathrm{II}}^{-} = \mathrm{F}_{\mathrm{I}}^{-} + \frac{2MG}{\lambda \mathrm{F}^{+}}e^{-2\rho}\varphi^{-1}\Big|_{x^{+}=x_{0}^{+}}. \tag{5.32}$$

From Equation (5.29) and solution (5.20), together with Equation (5.30), we also find that the constant a undergoes a change at $x^{+} = x_{0}^{+}$.

$$a_{\mathrm{II}} = a_{\mathrm{I}} + \frac{2GM}{\lambda^{2}}. \tag{5.33}$$

Hence, we conclude that the solution in region II of the spacetime takes the following form:

$$\left(\mathrm{F}_{\mathrm{I}}^{+}, \mathrm{F}_{\mathrm{I}}^{-}\left(1 + \frac{2MG/\lambda}{\lambda a_{\mathrm{I}} - \varphi(x_{0}^{+}, x^{-})}\right), a_{\mathrm{I}} + \frac{2MG}{\lambda^{2}}\right). \tag{5.34}$$

Equation (5.34) specifies the structure of the solution in region II, given that region I already contains a black hole solution and that this black hole consumes matter of mass M. Without loss of generality, we may adopt the Eddington–Finkelstein gauge in region I, which corresponds to choosing $\mathrm{F}_{\mathrm{I}}^{+} = -1$ and $\mathrm{F}_{\mathrm{I}}^{-} = 1$. To investigate gravitational collapse, we further set the metric in region I to be that of Minkowski spacetime by taking $a_{\mathrm{I}} = 0$. The associated dilaton field is then $\varphi_{\mathrm{I}} = \frac{\lambda}{2}\left(\sigma^{+} - \sigma^{-}\right)$. With these choices, Equation (5.34) shows that the geometry in region II indeed contains a black hole of mass M:

$$\left(-1, 1 - \frac{4MG/\lambda^{2}}{\sigma_{0}^{+} - \sigma^{-}}, \frac{2MG}{\lambda^{2}}\right). \tag{5.35}$$

Let us now introduce the notation that will be used from this point onward. To begin with, we take the solution in region I of the spacetime to be the Minkowski vacuum, specified by $(-1, 1, 0)$. We then define $\hat{\varphi}(\sigma^{-}) = \frac{\lambda}{2}\left(\sigma_{0}^{+} - \sigma^{-}\right)$. With this function, the coordinate transformations in region II can be written as:

$$\mathrm{F}^{+} = -1, \quad \mathrm{F}^{-} = \frac{\hat{\varphi} - \lambda a}{\hat{\varphi}}. \tag{5.36}$$

Here we omit the index II on the functions $\mathrm{F}_{\mathrm{II}}^{\pm}$ as well as on the constant a_{II}, and simply write $a = \frac{2MG}{\lambda^{2}}$. In region II of the spacetime, relation (5.19) remains valid, so we define new Eddington–Finkelstein coordinates $\hat{\sigma}^{\pm}$ via (3.106). Expressed in terms of $\sigma^{\pm}$, these are:

$$\hat{\sigma}^{+} = \sigma^{+}, \tag{5.37}$$

$$\hat{\sigma}^{-} = \sigma_{0}^{+} - \frac{2}{\lambda}\left[\hat{\varphi} + \lambda a \ln\left(\frac{\hat{\varphi}}{\lambda a} - 1\right)\right]. \tag{5.38}$$

Next, we define the reduced dilaton field (2.46) using the Schwarzschild radius a as:

$$\mathrm{x} = \frac{\varphi}{\lambda a}. \tag{5.39}$$

Moreover, the solutions (5.19) and (5.20) in region II of the spacetime can be recast in terms of the coordinates δ and $\hat{\mathrm{x}}$, defined in (3.107) and the reduced field x:

$$\begin{aligned} &\mathrm{x} + \ln(\mathrm{x}-1) = -\ln\delta + \hat{\mathrm{x}} + \ln(\hat{\mathrm{x}}-1), \\ &\mathrm{F}^+\mathrm{F}^- e^{2\rho} = \frac{1}{\mathrm{x}} - 1. \end{aligned} \tag{5.40}$$

Now we analyze solution (5.40). From the metric equation we infer the presence of a black hole, with a singularity located at $\mathrm{x} = 0$ and an event horizon at $\mathrm{x} = 1$. Recall that $\varphi = \lambda\hat{r}$, where $\hat{r}$ is the radial coordinate in region II of the spacetime. Inspecting solution (5.40) once more, we find that the condition $\varphi = \lambda a$ translates into $\hat{\varphi} = \lambda a$. Consequently, the hypersurfaces corresponding to the horizon and the singularity are given by:

$$\sigma^-_{\mathrm{H}} = \sigma^+_0 - 2a, \tag{5.41}$$
$$\ln\delta_S = \hat{\mathrm{x}}_{\mathrm{S}} + \ln|\hat{\mathrm{x}}_{\mathrm{S}} - 1|, \tag{5.42}$$

respectively. In the limit $t \to \infty$, we obtain $\sigma^+ \to \infty$, which is equivalent to $\delta \to 0$. Applying Equation (5.42), we conclude that the horizon and the singularity meet at future time infinity i^+. This is precisely what one expects, as quantum corrections are absent in this scenario. Both of these lines are depicted in the conformal diagram (see Figure 3.2). In both spacetime regions there exists a timelike Killing vector, but its form changes upon crossing the separating hypersurface. Therefore, the full spacetime is not stationary. This configuration corresponds to the classical CGHS gravitational collapse analyzed in Section 4.1.5.

5.2 Adding quantum corrections

In close analogy with the treatment of the CGHS model in Sections 4.2 and 4.3, we now consider the quantum-corrected DREH model by supplementing the classical DREH action (5.1) with the Polyakov–Liouville term (3.72). Further details on the PL action are provided in Section 3.3. Unlike in the CGHS case, here no additional correction terms can be introduced that render the quantum-corrected equations of motion exactly solvable. Consequently, the dilaton equation of motion in (5.4) remains unchanged. The metric equation, on the other hand, is modified solely through the contribution of the energy–momentum tensor of the quantum fluctuations (3.75), and takes the form:

$$\begin{aligned}\Big[2\nabla_\mu\nabla_\nu\phi - 2\nabla_\mu\phi\nabla_\nu\phi + g_{\mu\nu}\Big(3(\nabla\phi)^2 - 2\Box\phi - \lambda^2 e^{2\phi}\Big)\Big]e^{-2\phi} = 2G_{\mathrm{N}}\Bigg\{\nabla_\mu f\nabla_\nu f - \frac{1}{2}g_{\mu\nu}(\nabla f)^2 \\ + \frac{\hbar}{48\pi}\left[-2\nabla_\mu\nabla_\nu\psi + \nabla_\mu\psi\nabla_\nu\psi + g_{\mu\nu}\left(2\Box\psi - \frac{1}{2}(\nabla\psi)^2\right)\right]\Bigg\},\end{aligned} \tag{5.43}$$

where the EMT of the PL-type quantum fluctuations is explicitly presented in the second line. In this section, we focus exclusively on quantum-corrected vacuum solutions. Therefore, the classical contribution to the EMT is set to zero. In the conformal gauge (3.2), the equations of motion become:

$$\partial_\pm\left(e^{-2\rho}\partial_\pm\varphi\right) = \frac{\hbar G}{12\pi}\left[(\partial_\pm\rho)^2 - \partial_\pm^2\rho + t_\pm(x^\pm)\right]\varphi^{-1}e^{-2\rho}, \tag{5.44}$$

$$\partial_+\partial_-\varphi + \varphi\partial_+\partial_-\rho = 0, \tag{5.45}$$

$$\partial_+\partial_-\varphi^2 + \frac{\lambda^2}{2}e^{2\rho} + \frac{\hbar G}{6\pi}\partial_+\partial_-\rho = 0, \tag{5.46}$$

where the explicit forms of the quantum-corrected EMT components in (3.77) have been employed. From this, we clearly observe that the dilaton Equation (5.45) coincides with (5.8), and therefore remains unchanged. In contrast, the trace Equation (5.9), associated with its quantum-corrected counterpart (5.46), is modified. This modification arises due to the gravitational trace anomaly. Specifically, the trace of the quantum-corrected EMT takes the form $\langle\delta T^{(f)}\rangle = \frac{\hbar}{3}e^{-2\rho}\partial_+\partial_-\rho$, whereas in the classical case the scalar field EMT is traceless.

These quantum-corrected equations are not exactly solvable. Instead, we treat them perturbatively to first order in the expansion parameter $\varepsilon = \frac{\hbar G}{12\pi}$, following the procedure outlined in Section 3.4.1. We apply this method in complete analogy with the BPP model discussed in Section 4.3.4. Concretely, we perform the perturbative expansion by shifting the dilaton as $\varphi \mapsto \varphi + \varepsilon\theta$ and the metric as $\rho \mapsto \rho + \varepsilon\alpha$, as specified in (3.108). The quantum correction to equations (5.44-5.46), expressed in terms of θ and α, is then given by:

$$\partial_\pm\left[e^{-2\rho}\partial_\pm\theta - 2\alpha e^{-2\rho}\partial_\pm\varphi\right] = \left[(\partial_\pm\rho)^2 - \partial_\pm^2\rho + t_\pm(x^\pm)\right]\varphi^{-1}e^{-2\rho}, \tag{5.47}$$

$$\partial_+\partial_-\theta + \varphi\partial_+\partial_-\alpha + \theta\partial_+\partial_-\rho = 0, \tag{5.48}$$

$$\partial_+\partial_-\left(\theta\varphi + \rho\right) + \frac{\lambda^2}{2}\alpha e^{2\rho} = 0. \tag{5.49}$$

The first step in solving these equations is to integrate the first one, Equation (5.47). By expressing ρ from (5.20) and substituting it into $(\partial_\pm\rho)^2 - \partial_\pm^2\rho + t_+(x^\pm)$, this equation can be recast into the form (3.110). After further using the relation (5.18), we obtain:

$$\partial_\pm\left(e^{-2\rho}\partial_\pm\theta - \lambda\alpha\mathrm{F}^\mp\right) = \frac{1}{\mathrm{F}^{\pm 2}}t_\pm(\sigma^\pm)e^{-2\rho}\varphi^{-1} + \frac{\lambda}{2}\mathrm{F}^\mp\lambda a\frac{\varphi - \frac{3}{4}\lambda a}{\varphi^3(\varphi-\lambda a)^2}\partial_\pm\varphi, \tag{5.50}$$

Since $\mathcal{D}_0 = 1$, it follows that $\mathcal{F}[\varphi] = -1/(\varphi - \lambda a)$. We then introduce the function $\mathcal{D}_1(\varphi)$ via its derivative:

$$\frac{\mathrm{d}\mathcal{D}_1}{\mathrm{d}\varphi} = \lambda a\frac{\varphi - \frac{3}{4}\lambda a}{\varphi^3(\varphi-\lambda a)^2}. \tag{5.51}$$

This relation is precisely equivalent to (3.112). Upon integrating (5.50), we arrive at the expressions for the derivatives of θ:

$$\partial_+\theta = \frac{\lambda}{2}\left[\mathrm{F}^-(\mathcal{D}_1 + 2\alpha) + \mathrm{G}^-\right]e^{2\rho} - \mathrm{F}^-e^{2\rho}\int\frac{\mathrm{d}x^+}{\mathrm{F}^+}\frac{t_+(\sigma^+)}{\varphi-\lambda a}, \tag{5.52}$$

$$\partial_-\theta = \frac{\lambda}{2}\left[\mathrm{F}^+(\mathcal{D}_1 + 2\alpha) + \mathrm{G}^+\right]e^{2\rho} - \mathrm{F}^+e^{2\rho}\int\frac{\mathrm{d}x^-}{\mathrm{F}^-}\frac{t_-(\sigma^-)}{\varphi-\lambda a}, \tag{5.53}$$

where $G^\pm(x^\pm)$ are arbitrary functions encoding the quantum corrections to the coordinate transformations. At this stage, the derivatives $\partial_\pm\theta$ are still not known in closed form, because the integrals in (5.52) and (5.53) cannot yet be performed explicitly. The obstacle is the functional dependence $\varphi = \varphi(x^+, x^-)$, which is only implicitly determined by the transcendental

Equation (5.19). For the moment, we therefore keep the solution in this integral representation. In order to integrate (5.52) once more, we must remove the undetermined function α. This can be achieved by using Equation (5.49), together with (5.10) and (5.20), from which we obtain:

$$\theta + \frac{2\mathrm{F}^-}{\lambda}\left(\varphi\partial_-\theta + \theta\partial_-\varphi + \partial_-\rho\right) = \int \mathcal{D}_1 \mathrm{d}\varphi + \frac{\mathrm{G}^-}{\mathrm{F}^-}\varphi - \int \frac{\mathrm{d}x^+}{\mathrm{F}^+}\left(\frac{\lambda a}{\varphi} - 1\right)\int \frac{\mathrm{d}x^+}{\mathrm{F}^+}\frac{t_+(\sigma^+)}{\varphi - \lambda a} + \mathrm{H}^-, \tag{5.54}$$

where we have introduced an additional arbitrary function $\mathrm{H}^-(x^-)$. By eliminating the derivatives $\partial_-\varphi$ and $\partial_-\theta$ using equations (5.18) and (5.53), respectively, and then applying the same procedure once more to Equation (5.53), we obtain:

$$\begin{aligned}\theta =& \frac{\varphi(\varphi-\lambda a)}{\lambda a}\left(\mathcal{D}_1 + 2\alpha + \frac{\mathrm{G}^+}{\mathrm{F}^+}\right) + \frac{\varphi^2}{\lambda a}\frac{\mathrm{G}^-}{\mathrm{F}^-} + \frac{1}{2\varphi} &(5.55)\\ &+ \frac{\varphi}{\lambda a}\left[\int \mathcal{D}_1\mathrm{d}\varphi - \frac{2}{\lambda}(\varphi-\lambda a)\int \frac{\mathrm{d}x^-}{\mathrm{F}^-}\frac{t_-(\sigma^-)}{\varphi-\lambda a} - \int\frac{\mathrm{d}x^+}{\mathrm{F}^+}\left(\frac{\lambda a}{\varphi}-1\right)\int\frac{\mathrm{d}x^+}{\mathrm{F}^+}\frac{t_+(\sigma^+)}{\varphi-\lambda a} - \mathrm{H}^-\right],\\ \theta =& \frac{\varphi(\varphi-\lambda a)}{\lambda a}\left(\mathcal{D}_1 + 2\alpha + \frac{\mathrm{G}^-}{\mathrm{F}^-}\right) + \frac{\varphi^2}{\lambda a}\frac{\mathrm{G}^+}{\mathrm{F}^+} + \frac{1}{2\varphi} &(5.56)\\ &+ \frac{\varphi}{\lambda a}\left[\int \mathcal{D}_1\mathrm{d}\varphi - \frac{2}{\lambda}(\varphi-\lambda a)\int \frac{\mathrm{d}x^+}{\mathrm{F}^+}\frac{t_+(\sigma^+)}{\varphi-\lambda a} - \int\frac{\mathrm{d}x^-}{\mathrm{F}^-}\left(\frac{\lambda a}{\varphi}-1\right)\int\frac{\mathrm{d}x^-}{\mathrm{F}^-}\frac{t_-(\sigma^-)}{\varphi-\lambda a} - \mathrm{H}^+\right].\end{aligned}$$

By equating (5.55) and (5.56) we obtain the following consistency condition:

$$\mathrm{H}^- + \lambda a\frac{\mathrm{G}^-}{\mathrm{F}^-} - \frac{2}{\lambda}\int\frac{\mathrm{d}x^-}{\mathrm{F}^-}t_-(\sigma^-) = \mathrm{H}^+ + \lambda a\frac{\mathrm{G}^+}{\mathrm{F}^+} - \frac{2}{\lambda}\int\frac{\mathrm{d}x^+}{\mathrm{F}^+}t_+.(\sigma^+) = C, \tag{5.57}$$

where C denotes an arbitrary constant. Adding equations (5.55) and (5.56), and making use of (5.57), we express θ in terms of φ and α as:

$$\begin{aligned}\theta =& \frac{\varphi(\varphi-\lambda a)}{\lambda a}\left[\mathcal{D}_1 + 2\alpha + \frac{\mathrm{G}^+}{\mathrm{F}^+} + \frac{\mathrm{G}^-}{\mathrm{F}^-}\right] + \frac{1}{2\varphi} + \frac{\varphi}{\lambda a}\int\mathcal{D}_1\mathrm{d}\varphi &(5.58)\\ &-\frac{\varphi}{\lambda a}\left[\int\frac{\mathrm{d}x^+}{\mathrm{F}^+}\left(\frac{\lambda a}{\varphi}-1\right)\int\frac{\mathrm{d}x^+}{\mathrm{F}^+}\frac{t_+(\sigma^+)}{\varphi-\lambda a} + \int\frac{\mathrm{d}x^-}{\mathrm{F}^-}\left(\frac{\lambda a}{\varphi}-1\right)\int\frac{\mathrm{d}x^-}{\mathrm{F}^-}\frac{t_-(\sigma^-)}{\varphi-\lambda a}\right].\end{aligned}$$

At this stage, a single integration has been performed. As in Section 3.4.1, another integration is required. This is clear from the fact that (5.58) is not yet the final form of the field θ, since it still involves the unknown function α, which must be eliminated. A straightforward way to accomplish this is to use either Equation (5.52) or (5.53), thereby obtaining another first-order differential equation for θ. Note that the constant C defined in (5.57) does not appear explicitly in (5.58); instead, it is absorbed as the integration constant of $\int\mathcal{D}_1\mathrm{d}\varphi$. We later demonstrate that C represents a quantum correction to the constant a. Proceeding with either (5.53) or (5.52) leads to the same outcome: one derives two alternative expressions for θ, each containing its own arbitrary functions, which are then removed by setting these expressions equal to each other. The resulting final expression for θ is:

$$\begin{aligned}\theta = \frac{\varphi-\lambda a}{\varphi}\Bigg[&\frac{\lambda}{2}\left(\int\mathrm{d}x^+\frac{\mathrm{G}^+}{\mathrm{F}^{+2}} + \int\mathrm{d}x^-\frac{\mathrm{G}^-}{\mathrm{F}^{-2}}\right) - \int d\varphi\left(\frac{\lambda a}{2\varphi(\varphi-\lambda a)^2} + \frac{\varphi}{(\varphi-\lambda a)^2}\int\mathcal{D}_1\mathrm{d}\varphi\right)\\ &+\int\frac{\mathrm{d}x^+}{\mathrm{F}^+}\frac{1}{\varphi-\lambda a}\int\frac{\mathrm{d}x^+}{\mathrm{F}^+}t_+(\sigma^+) + \int\frac{\mathrm{d}x^-}{\mathrm{F}^-}\frac{1}{\varphi-\lambda a}\int\frac{\mathrm{d}x^-}{\mathrm{F}^-}t_-(\sigma^-)\Bigg],\end{aligned} \tag{5.59}$$

in terms of x^+, x^-, $t_+(\sigma^+(x^+))$, $t_-(\sigma^-(x^-))$ and $\varphi(x^+,x^-)$. The next step would be to determine α. One possible approach is to use Equation (5.52), from which it is straightforward to derive an expression for α in terms of x^+ and x^-. However, as discussed in Section 3.4.1, this is not required, because we already possess all the information needed to write down the quantum-corrected forms of (5.19-5.20).

Let us first simplify the expressions by using the reduced field $\mathrm{x} = \frac{\varphi}{\lambda a}$ and the coordinate $\hat{\mathrm{x}} = \frac{\hat{\varphi}}{\lambda a}$. In terms of x, the function $\mathcal{D}_1(\mathrm{x})$ and its integral can be written as:

$$\mathcal{D}_1 = \frac{1}{4(\lambda a)^2}\left[\ln\left|1-\frac{1}{\mathrm{x}}\right| - \frac{1}{\mathrm{x}-1} + \frac{3}{2}\frac{1}{\mathrm{x}^2} + \frac{2}{\mathrm{x}}\right], \tag{5.60}$$

$$\int \mathcal{D}_1 \mathrm{d}\varphi = \frac{1}{4\lambda a}\left[(\mathrm{x}-2)\ln\left|1-\frac{1}{\mathrm{x}}\right| - \frac{3}{2}\frac{1}{\mathrm{x}}\right] + C, \tag{5.61}$$

where C is the constant introduced in Equation (5.57). For later convenience, we now define the function:

$$\theta_0(\varphi) = -\int \mathrm{d}\varphi\left(\frac{\lambda a}{2\varphi(\varphi-\lambda a)^2} + \frac{\varphi}{(\varphi-\lambda a)^2}\int \mathcal{D}_1 \mathrm{d}\varphi\right), \tag{5.62}$$

which, upon using Equation (5.61), takes the form:

$$\theta_0(\mathrm{x}) = \frac{-1}{4\lambda a}\frac{1}{\mathrm{x}-1}\left[\frac{1}{2} + (\mathrm{x}^2-3\mathrm{x}+3)\ln|\mathrm{x}-1| - (\mathrm{x}^2-2\mathrm{x}+2)\ln \mathrm{x}\right] + C\left(\frac{1}{\mathrm{x}-1} - \ln|\mathrm{x}-1|\right). \tag{5.63}$$

We furthermore introduce the integrals:

$$\mathrm{I}_\pm = \int \frac{\mathrm{d}x^\pm}{\mathrm{F}^\pm}\frac{1}{\varphi-\lambda a}\int \frac{\mathrm{d}x^\pm}{\mathrm{F}^\pm} t_\pm(\sigma^\pm). \tag{5.64}$$

Using this notation, Equation (5.59) can be recast in a considerably more compact form:

$$\theta = \frac{\mathrm{x}-1}{\mathrm{x}}\left[\frac{\lambda}{2}\left(\int \mathrm{d}x^+\frac{\mathrm{G}^+}{\mathrm{F}^{+2}} + \int \mathrm{d}x^-\frac{\mathrm{G}^-}{\mathrm{F}^{-2}}\right) + \theta_0 + \mathrm{I}\right], \tag{5.65}$$

where $\mathrm{I} = \mathrm{I}_+ + \mathrm{I}_-$. We now proceed to demonstrate that the functions $\mathrm{G}^\pm$ represent the quantum corrections to the coordinate transformations, by examining how Equation (5.19) is modified when these quantum corrections are included. From Equation (5.65) we extract the term involving $\mathrm{G}^\pm$, multiply it by ε, and add it to the right-hand side of Equation (5.19):

$$\varphi + \lambda a \ln\left(\frac{\varphi}{\lambda a} - 1\right) + \varepsilon\frac{\varphi\theta}{\varphi-\lambda a} - \varepsilon\theta_0 - \varepsilon \mathrm{I} = -\frac{\lambda}{2}\left[\int \frac{\mathrm{d}x^+}{\mathrm{F}^+}\left(1-\varepsilon\frac{\mathrm{G}^+}{\mathrm{F}^+}\right) + \int \frac{\mathrm{d}x^-}{\mathrm{F}^-}\left(1-\varepsilon\frac{\mathrm{G}^-}{\mathrm{F}^-}\right)\right]. \tag{5.66}$$

The final step is to revert to the quantum-corrected fields (3.113). If we expand Equation (5.19) to first order in ε, we obtain precisely the term linear in θ that appears in Equation (5.66). On the right-hand side of Equation (5.66), we have the first-order expansion in ε of $(\mathrm{F}^\pm + \varepsilon\mathrm{G}^\pm)^{-1}$, implying that the transformation $\mathrm{F}^\pm + \varepsilon\mathrm{G}^\pm \mapsto \mathrm{F}^\pm$ should be interpreted as the quantum-corrected coordinate transformation. Furthermore, observe that the constant C in Equation (5.63) represents the quantum correction in $\lambda a + \varepsilon C \mapsto \lambda a$. This can be verified straightforwardly by expanding $(\lambda a + \varepsilon C)\ln(\varphi/(\lambda a + \varepsilon C) - 1)$ to first order in ε. We are similarly interested in how quantum corrections modify Equation (5.20). To this end, we now employ the newly defined quantum-corrected coordinate transformations:

$$\mathrm{F}^+\mathrm{F}^- e^{2\rho} \mapsto \mathrm{F}^+\mathrm{F}^- e^{2\rho}\left[1 + \varepsilon\left(2\alpha + \frac{\mathrm{G}^+}{\mathrm{F}^+} + \frac{\mathrm{G}^-}{\mathrm{F}^-}\right)\right]. \tag{5.67}$$

The quantity in brackets of Equation (5.67) also appears in Equation (5.58), which allows us to isolate it from that expression. Before doing so, we introduce another set of integrals:

$$\mathrm{I}'_{\pm} = -\int \frac{\mathrm{d}x^{\pm}}{\mathrm{F}^{\pm}}\left(\frac{\lambda a}{\varphi}-1\right)\int \frac{\mathrm{d}x^{\pm}}{\mathrm{F}^{\pm}}\frac{t_{\pm}(\sigma^{\pm})}{\varphi-\lambda a}. \tag{5.68}$$

We then define $\mathrm{I}' = \mathrm{I}'_{+} + \mathrm{I}'_{-}$, insert this into Equation (5.67), and make use of Equation (5.20) to obtain:

$$\mathrm{F}^{+}\mathrm{F}^{-}e^{2\rho} \mapsto \frac{\lambda a}{\varphi} - 1 - \varepsilon\frac{\lambda a\theta}{\varphi^2} + \varepsilon\left[\frac{\varphi-\lambda a}{\varphi}\mathcal{D}_1 + \frac{\lambda a}{2\varphi^3} + \frac{1}{\varphi}\int \mathcal{D}_1 \mathrm{d}\varphi + \frac{1}{\varphi}\mathrm{I}'\right]. \tag{5.69}$$

The first three terms are precisely the expansion of $\lambda a(\varphi+\varepsilon\theta)^{-1}-1$. Because C is the integration constant of $\int \mathcal{D}_1\mathrm{d}\varphi$, the only term in which it appears is $\varepsilon C/\varphi$, which, once again, demonstrates that C corresponds to the quantum correction to the constant λa. Expressing equations (5.66) and (5.69) in terms of the quantum-corrected reduced field x and the quantum-corrected constant λa, we finally obtain:

$$\begin{aligned}\mathrm{x} + \ln|\mathrm{x}-1| + \frac{\varepsilon}{4(\lambda a)^2}\frac{1}{\mathrm{x}-1}\left[\frac{1}{2} + (\mathrm{x}^2-3\mathrm{x}+3)\ln|\mathrm{x}-1| - (\mathrm{x}^2-2\mathrm{x}+2)\ln\mathrm{x}\right] - \frac{\varepsilon}{\lambda a}\mathrm{I}\\ = -\frac{1}{2a}\left(\int\frac{\mathrm{d}x^{+}}{\mathrm{F}^{+}} + \int\frac{\mathrm{d}x^{-}}{\mathrm{F}^{-}}\right) \equiv \frac{\sigma}{a},\end{aligned} \tag{5.70}$$

$$\mathrm{F}^{+}\mathrm{F}^{-}e^{2\rho} = \frac{1}{\mathrm{x}} - 1 + \frac{\varepsilon}{4(\lambda a)^2}\left[\frac{2\mathrm{x}-3}{\mathrm{x}}\ln\left|1-\frac{1}{\mathrm{x}}\right| + \frac{1}{\mathrm{x}} - \frac{2}{\mathrm{x}^2} + \frac{1}{2}\frac{1}{\mathrm{x}^3}\right] + \frac{\varepsilon}{\lambda a}\frac{\mathrm{I}'}{\mathrm{x}}. \tag{5.71}$$

Equations (5.70) and (5.71) provide the general solution to the vacuum equations (5.47–5.49). They therefore represent the quantum-corrected analogues of equations (5.19) and (5.20) obtained from the classical equations of motion. Consequently, the solution to the quantum-corrected equations of motion is specified by an ordered quintuple $(\mathrm{F}^{+}, \mathrm{F}^{-}, a, t_{+}, t_{-})$. Note that $\mathrm{F}^{\pm}$ and a are now quantum-corrected quantities. An explicit solution can be constructed once the integrals I and I′ have been evaluated. These integrals are not independent, but are linked through equations (5.52) and (5.53), so that it suffices to compute only one of them. Since the condition $t_{\pm}(x^{\pm}) = 0$ specifies the vacuum we adopt (see Section (3.3)), the integrals I and I′ are closely related to the particular choice of vacuum state.

5.2.1 Applying the static ansatz

The general static solution in the classical DREH model is obtained in Section 5.1.2. Once quantum corrections are incorporated, the main distinction is the presence of the gravitational trace anomaly. Consequently, the trace of the EMT on the right-hand side of Equation (5.5) can no longer be neglected. For the quantum-corrected EMT (3.79) it reads:

$$\frac{2G\Lambda}{\lambda^2\varphi}\left(T_{\mu\nu} - \frac{1}{2}g_{\mu\nu}T\right) = \frac{\varepsilon}{\Lambda\mathrm{x}}\left[\frac{\mu}{\varepsilon} - \Xi - \frac{1}{4}\mathcal{D}^2\left(\frac{\mathrm{d}\Lambda}{\mathrm{d}\varphi}\right)^2 + \frac{1}{2}\Lambda\mathcal{D}\frac{\mathrm{d}}{\mathrm{d}\varphi}\left(\mathcal{D}\frac{\mathrm{d}\Lambda}{\mathrm{d}\varphi}\right)\right]\left(\xi_\mu\xi_\nu + \varepsilon_{\mu\rho}\varepsilon_{\nu\sigma}\xi^\rho\xi^\sigma\right), \tag{5.72}$$

where μ and ξ denote the scalar-field charge and the parameter specifying the quantum vacuum state, respectively, defined through:

$$\Lambda^2 T^{\Vert\Vert} = \Lambda^2 T^{\perp\perp} = \frac{\lambda^2\mu}{2G}, \qquad t_{+}(\sigma^{+}) = t_{-}(\sigma^{-}) = \frac{\lambda^2}{4}\Xi. \tag{5.73}$$

Because the action itself does not receive correction terms, the left-hand side of (5.5) remains identical to the classical expression (5.22). Thus, the resulting system of equations takes the form:

$$\mathcal{D}^2\frac{\mathrm{d}\Lambda}{\mathrm{d}\varphi}+\frac{\mathrm{d}\left(\Lambda\mathcal{D}^2\right)}{\mathrm{d}\varphi}+\mathcal{D}\varphi\frac{\mathrm{d}}{\mathrm{d}\varphi}\left(\mathcal{D}\frac{\mathrm{d}\Lambda}{\mathrm{d}\varphi}\right)=0, \tag{5.74}$$

$$\mathcal{D}\frac{\mathrm{d}}{\mathrm{d}\varphi}\left(\Lambda\mathcal{D}\varphi\right)+1+\frac{\varepsilon}{2}\mathcal{D}\frac{\mathrm{d}}{\mathrm{d}\varphi}\left(\mathcal{D}\frac{\mathrm{d}\Lambda}{\mathrm{d}\varphi}\right)=0, \tag{5.75}$$

$$\mathcal{D}^2\frac{\mathrm{d}\Lambda}{\mathrm{d}\varphi}+\frac{\mathcal{D}\varphi}{2}\frac{\mathrm{d}}{\mathrm{d}\varphi}\left(\mathcal{D}\frac{\mathrm{d}\Lambda}{\mathrm{d}\varphi}\right)=\frac{\varepsilon}{\Lambda\mathrm{x}}\left[\frac{\mu}{\varepsilon}-\Xi-\frac{1}{4}\mathcal{D}^2\left(\frac{\mathrm{d}\Lambda}{\mathrm{d}\varphi}\right)^2+\frac{1}{2}\Lambda\mathcal{D}\frac{\mathrm{d}}{\mathrm{d}\varphi}\left(\mathcal{D}\frac{\mathrm{d}\Lambda}{\mathrm{d}\varphi}\right)\right]. \tag{5.76}$$

Since we are not interested in the classical charged matter in this subsection, we set $\mu=0$. By combining the three equations in a particular way, we obtain an expression for $\mathcal{D}$ in terms of Λ and its derivative:

$$\mathcal{D}^2\left[\varphi\frac{\mathrm{d}\Lambda}{\mathrm{d}\varphi}+\Lambda+\frac{\varepsilon}{4\Lambda}\left(\frac{\mathrm{d}\Lambda}{\mathrm{d}\varphi}\right)^2\right]=-1-\frac{\varepsilon\Xi}{\Lambda}. \tag{5.77}$$

Substituting this into (5.74) yields an expression for $\frac{\mathrm{d}\mathcal{D}^2}{\mathrm{d}\varphi}$ in terms of Λ and its derivatives. Consequently, Equation (5.75) reduces to a second-order nonlinear differential equation that determines the metric function Λ:

$$\left(\varphi^2-\varepsilon\right)\frac{\mathrm{d}^2\Lambda}{\mathrm{d}\varphi^2}+2\varphi\frac{\mathrm{d}\Lambda}{\mathrm{d}\varphi}+\frac{3\varepsilon}{2\Lambda}\left(\frac{\mathrm{d}\Lambda}{\mathrm{d}\varphi}\right)^2+\frac{\varepsilon\varphi}{4\Lambda^2}\left(\frac{\mathrm{d}\Lambda}{\mathrm{d}\varphi}\right)^3=\varepsilon\Xi\left[2+\varphi\frac{\mathrm{d}\ln\Lambda}{\mathrm{d}\varphi}-\left(\varphi^2-\varepsilon\right)\frac{\mathrm{d}^2\ln\Lambda}{\mathrm{d}\varphi^2}\right]. \tag{5.78}$$

In general, Equation (5.78) is extremely difficult to solve. In the special case $\Xi=0$, it can be recast as a first-order differential equation for $u=\frac{\mathrm{d}\ln\Lambda}{\mathrm{d}\varphi}$:

$$\left(\varphi^2-\varepsilon\right)\frac{\mathrm{d}u}{\mathrm{d}\varphi}+2\varphi u+\left(\varphi^2+\frac{\varepsilon}{2}\right)u^2+\frac{\varepsilon}{4}\varphi u^3=0 \tag{5.79}$$

This is an Abel differential equation, which is well known to be highly nontrivial to solve; closed-form solutions exist only for a limited set of specific relations among the coefficients multiplying the powers of u. In our situation, these conditions are not met, and an exact analytic solution is not available. Therefore, as anticipated, we resort to a perturbative approach. In the limit $\varepsilon\to 0$, Equation (5.78) simplifies to:

$$\varphi\frac{\mathrm{d}^2\Lambda}{\mathrm{d}\varphi^2}+2\frac{\mathrm{d}\Lambda}{\mathrm{d}\varphi}=0 \quad\Longrightarrow\quad \Lambda=A+\frac{B}{\varphi}, \tag{5.80}$$

where A and B are integration constants. Imposing the asymptotic condition (3.22), i.e. $\Lambda\to -1$ as $\varphi\to\infty$ yields the Schwarzschild solution (5.21) with $B=\lambda a$, as expected. Expanding $\Lambda=\Lambda_0+\varepsilon\Lambda_1$, where Λ_0 denotes the Schwarzschild solution, we obtain the following general solution:

$$\Lambda=\frac{1}{\mathrm{x}}-1+\frac{\varepsilon}{4(\lambda a)^2}\left[\frac{2\mathrm{x}-3}{\mathrm{x}}\ln\left|1-\frac{1}{\mathrm{x}}\right|+\frac{2}{\mathrm{x}}-\frac{2}{\mathrm{x}^2}+\frac{1}{2}\frac{1}{\mathrm{x}^3}\right]+\varepsilon\Xi\left(\frac{2\mathrm{x}-3}{\mathrm{x}}\ln|\mathrm{x}-1|+\frac{1}{2\mathrm{x}}\right), \tag{5.81}$$

where we have employed the reduced field (5.39) and have also dropped the two integration constants in Λ_1. In the most general case, the solution can be written as $\Lambda_1\mapsto\Lambda_1+D_1+\frac{D_2}{\mathrm{x}}$. The constant D_2, however, is absorbed into a as its quantum correction, whereas D_1 represents the quantum-corrected contribution to the constant A in (5.80) and thus merely rescales the entire Killing vector. Consequently, it can be removed by a redefinition of the time coordinate and will be disregarded here. Inserting (5.81) into the expression (5.77) for $\mathcal{D}$, we find:

$$\mathcal{D} = 1 + \frac{\varepsilon}{4(\lambda a)^2}\left[\ln\left|1-\frac{1}{\mathrm{x}}\right| - \frac{1}{\mathrm{x}-1} + \frac{3}{2}\frac{1}{\mathrm{x}^2} + \frac{2}{\mathrm{x}}\right] + \varepsilon\Xi\left[\frac{1}{2} + \ln|\mathrm{x}-1| - \frac{1}{\mathrm{x}-1}\right]. \tag{5.82}$$

Finally, we derive the tortoise coordinate (3.18). A straightforward integration gives:

$$\begin{aligned}\frac{\sigma}{a} = \mathrm{x} + \ln|\mathrm{x}-1| + \frac{\varepsilon}{4(\lambda a)^2}\frac{1}{\mathrm{x}-1}\left[\left(\mathrm{x}^2-2\mathrm{x}+2\right)\ln\left|1-\frac{1}{\mathrm{x}}\right| + \mathrm{x} - \frac{3}{2}\right] \\ + \frac{\varepsilon\Xi}{\mathrm{x}-1}\left[\left(\mathrm{x}^2-\mathrm{x}+1\right)\ln|\mathrm{x}-1| - \frac{1}{2} - \frac{1}{2}(3\mathrm{x}-5)(\mathrm{x}-1)\right].\end{aligned} \tag{5.83}$$

5.2.2 Solution without energy flux at the asymptotic infinity

Here, we focus on the solution for which there is no energy flux in either of the two asymptotic regions of the spacetime. The associated vacuum state is the Boulware vacuum $|0,\sigma\rangle$ (3.96). It is characterized by normal ordering of the EMT with respect to the Eddington–Finkelstein coordinates, that is, by the condition $t_\pm(\sigma^\pm) = 0$. For the general static solution discussed in the previous section, this requirement implies $\Xi = 0$. Consequently, the solution takes the form:

$$\begin{aligned}\Lambda &= \frac{1}{\mathrm{x}} - 1 + \frac{\varepsilon}{4(\lambda a)^2}\left[\frac{2\mathrm{x}-3}{\mathrm{x}}\ln\left|1-\frac{1}{\mathrm{x}}\right| + \frac{2}{\mathrm{x}} - \frac{2}{\mathrm{x}^2} + \frac{1}{2}\frac{1}{\mathrm{x}^3}\right], \\ \mathcal{D} &= 1 + \frac{\varepsilon}{4(\lambda a)^2}\left[\ln\left|1-\frac{1}{\mathrm{x}}\right| - \frac{1}{\mathrm{x}-1} + \frac{3}{2}\frac{1}{\mathrm{x}^2} + \frac{2}{\mathrm{x}}\right], \\ \frac{\sigma}{a} &= \mathrm{x} + \ln|\mathrm{x}-1| + \frac{\varepsilon}{4(\lambda a)^2}\frac{1}{\mathrm{x}-1}\left[\left(\mathrm{x}^2-2\mathrm{x}+2\right)\ln\left|1-\frac{1}{\mathrm{x}}\right| + \mathrm{x} - \frac{3}{2}\right].\end{aligned} \tag{5.84}$$

In contrast to the BPP model (see Section 4.3.3), solution (5.84) admits a well-defined $a \to 0$ limit, which yields Minkowski spacetime, i.e. $\Lambda = -1$, $\mathcal{D} = 1$, and $\sigma = \mathrm{x}a$. This indicates that the Minkowski solution is a regular configuration with no energy flux at null infinities. The solution was first obtained in [111].

One can also derive this solution from the general solution of the quantum-corrected model (5.70-5.71). In that framework, imposing $t_\pm(\sigma^\pm) = 0$ is equivalent to requiring that the integrals $\mathrm{I}_\pm$ (5.64) and $\mathrm{I}'_\pm$ (5.68) vanish. At first glance, the resulting solution appears to diverge in the limit $a \to 0$. However, we must recall that the constant λa is modified as $\lambda a \mapsto \lambda a + \varepsilon C(\lambda a)$. The apparent divergence can be removed by a suitable choice of the constant $C(\lambda a)$, namely $C(\lambda a) = \frac{1}{4\lambda a}$. With this specific choice, the metric function and the tortoise coordinate are exactly transformed into 5.84. Finally, for the function $\mathcal{D}$ in (5.84) we have $\mathcal{D} = 1 + \varepsilon\mathcal{D}_1$, where $\mathcal{D}_1$ is defined in (5.60). Hence, the two derivations are mutually consistent.

Since these configurations correspond to solutions with no energy flux at infinity, they are expected to be horizonless and therefore not to resemble black hole solutions. It has been shown in [112, 113] that the classical horizon disappears once quantum corrections are incorporated. The horizon is defined as the hypersurface on which the Killing vector (3.5) becomes null, i.e. where $\Lambda = 0$. In a perturbative framework, if a horizon is present, its position should be written as $\mathrm{x_H} = \mathrm{x_H^{(0)}} + \varepsilon\mathrm{x_H^{(1)}}$. From (5.84), we immediately deduce that $\mathrm{x_H^{(0)}} = 1$, which represents the classical horizon. The first-order correction is then found by taking the limit $\mathrm{x} \to 1$ of the first-order terms in (5.84). This limit diverges, showing that the perturbative expansion breaks down in the region of spacetime near the classical horizon. Equivalently, one may interpret this divergence as evidence that the quantum corrections actually eliminate the classical horizon. We thus reach the same conclusion as in [112, 113].

Another significant property of solution (5.84) is that it exhibits a curvature singularity whenever the mass parameter is non-vanishing. This can be checked explicitly by evaluating the scalar curvature, which to first order in the perturbative expansion is given by:

$$R = 2\lambda^2 \frac{\lambda a}{(\varphi^2 - \varepsilon)^{3/2}}. \tag{5.85}$$

As expected, this expression vanishes in the massless limit, $a = 0$. This leads to the same conclusion as in the RST and BPP dilaton gravity models [23, 24, 25]. There is, however, a subtle difference between our model and the BPP construction. Furthermore, we find that if the central charge of the conformal matter fields obeys $\varepsilon < 0$, the singularity disappears from this Boulware state at first order in perturbation theory. This phenomenon has been analyzed thoroughly in the context of the RST model [108, 109]. A negative central charge may result from the presence of unphysical, ghost-like fields. Moreover, numerical investigations within the DREH model [114] likewise suggest the appearance of this type of behavior.

5.2.3 Eternal black hole scenario

An eternal black hole solution describes a black hole that is in thermal equilibrium with its environment. Consequently, the quantum fields are in the Hartle–Hawking state (3.97), which is defined by imposing that the normal-ordered EMT vanishes in Kruskal coordinates, $t_\pm(x^\pm) = 0$. By construction, this configuration is static and therefore must belong to the family of solutions (5.81-5.83) for a particular value of the constant Ξ. The defining property of a static black hole is the presence of an event horizon [106]. This horizon is the hypersurface on which the Killing vector becomes null, i.e., where $\Lambda = 0$. However, solving this condition perturbatively in the form $\mathrm{x_H} = 1 + \varepsilon \mathrm{x_H^{(1)}}$ is not feasible as long as the term $\ln|\mathrm{x}-1|$ is present in expression (5.81). Fortunately, there exists a particular choice of Ξ that removes this term. It is given by:

$$\Xi = -\frac{1}{4(\lambda a)^2}. \tag{5.86}$$

The solution can now be written as:

$$\begin{aligned}
\Lambda &= \frac{1}{\mathrm{x}} - 1 + \frac{\varepsilon}{4(\lambda a)^2}\left[-\frac{2\mathrm{x}-3}{\mathrm{x}}\ln\mathrm{x} + \frac{3}{2}\frac{1}{\mathrm{x}} - \frac{2}{\mathrm{x}^2} + \frac{1}{2}\frac{1}{\mathrm{x}^3}\right], \\
\mathcal{D} &= 1 + \frac{\varepsilon}{4(\lambda a)^2}\left[-\ln\mathrm{x} + \frac{3}{2}\frac{1}{\mathrm{x}^2} + \frac{2}{\mathrm{x}} - \frac{1}{2}\right], \\
\frac{\sigma}{a} &= \mathrm{x} + \ln|\mathrm{x}-1| + \frac{\varepsilon}{4(\lambda a)^2}\left[-\ln|\mathrm{x}-1| + \left(1 - \mathrm{x} - \frac{1}{\mathrm{x}-1}\right)\ln\mathrm{x} + \frac{3}{2}(\mathrm{x}-1)\right].
\end{aligned} \tag{5.87}$$

We observe that the integration constants in the Ξ term are fixed such that $\mathrm{x_H} = 1$, because for this value of the dilaton the associated Killing vector becomes null. To locate the singularity, we evaluate the curvature (3.29), which takes the form:

$$R = \frac{2}{a^2\mathrm{x}^3}\left[1 + \frac{\varepsilon}{4(\lambda a)^2}\left(\ln\mathrm{x} + \mathrm{x} - \frac{7}{2} + \frac{1}{\mathrm{x}} + \frac{15}{2}\frac{1}{\mathrm{x}}\right)\right]. \tag{5.88}$$

Consequently, the curvature diverges along the hypersurface approaching the classical singularity at $\mathrm{x_S} \approx 0$. The surface gravity (see Appendix D.5) is given by:

$$\kappa = \frac{1}{2a} \left| \mathcal{D} \frac{\mathrm{d}\Lambda}{\mathrm{dx}} \right|_{\mathrm{H}} = \frac{1}{2a} \left(1 + \frac{\varepsilon}{4(\lambda a)^2} \right). \tag{5.89}$$

We now confirm that the condition (5.86) imposed on the parameter Ξ indeed implements normal ordering of the EMT in Kruskal coordinates. To move to the Kruskal coordinates we use the classical part of the surface gravity. After applying the transformations (see Appendix D.5), we obtain:

$$\frac{\lambda^2}{4}\Xi = t_\pm(\sigma^\pm) = \left(\frac{\mathrm{d}x^\pm}{\mathrm{d}\sigma^\pm} \right)^2 \left[\cancelto{0}{t_\pm}(x^\pm) - \frac{1}{2} D_{x^\pm}[\sigma^\pm] \right] = -\frac{\kappa^2}{4} \quad \Longrightarrow \quad \Xi = -\frac{\kappa^2}{\lambda^2} = -\frac{1}{4(\lambda a)^2}. \tag{5.90}$$

Therefore, the choice (5.86) for Ξ, originally obtained by requiring the presence of an event horizon, is precisely equivalent to selecting the Hartle–Hawking state. Finally, we should examine the nature of the pole of the tortoise coordinate appearing in (5.87). Using the expression for the surface gravity (5.89), we obtain

$$\sigma = \frac{1}{2\kappa} \left[\mathrm{x} + \ln|\mathrm{x}-1| + \frac{\varepsilon}{4(\lambda a)^2} \left(\left(1 - \mathrm{x} - \frac{1}{\mathrm{x}-1} \right) \ln \mathrm{x} + \frac{5}{2}\mathrm{x} - \frac{3}{2} \right) \right]. \tag{5.91}$$

Expressed in this way, the tortoise coordinate exhibits precisely the same near-horizon behavior as in the classical case, namely $\sigma = \frac{1}{2\kappa} \ln|\mathrm{x}-1|$, because the term of order ε vanishes at the horizon $\mathrm{x_H} = 1$. This is made possible by the specific choice of the integration constant of the Ξ term in (5.83).

Next, we demonstrate how to obtain the same result starting from the general solution (5.70-5.71). The sources are the functions $t_\pm(\sigma^\pm)$. For the Hartle–Hawking state, they are specified by Equation (5.90). Hence, we can easily evaluate the integrals I (5.64) and (5.68). Performing the integration, we find:

$$\mathrm{I}' = \Xi \lambda a \left[(2\mathrm{x} - 4) \ln|\mathrm{x}-1| + \big(A_+(x^+) + A_-(x^-) \big) \mathrm{x} + B_+(x^+) + B_-(x^-) \right], \tag{5.92}$$

where $A_\pm(x^\pm)$ and $B_\pm(x^\pm)$ are arbitrary functions. At this point, one has to proceed with caution. If these arbitrary functions are simply discarded, the correct Ξ term in (5.81) cannot be recovered. This issue appears as an artifact of the procedure in which the quantum corrections to the coordinate transformations $\mathrm{G}^\pm$ are eliminated in (5.57) after the first integration. Consequently, choosing $A_\pm$ and $B_\pm$ arbitrarily effectively corresponds to performing an additional coordinate transformation. The appropriate choice of this transformation is fixed by requiring that $\mathrm{F}^\pm$ represent the components of the time-like Killing vector (3.5), i.e. that $\nabla_+ \mathrm{F}^+ = \nabla_- \mathrm{F}^-$. Imposing this condition uniquely determines the arbitrary functions and restores the original solution (5.81).

The solution (5.87) was first derived in [42], albeit in a slightly different form. There, the metric ansatz is taken to be:

$$\mathrm{d}s^2 = -\left(1 - \frac{a}{r} + \frac{\varepsilon m(r)}{r} \right) e^{2\varepsilon\varphi(r)} \mathrm{d}t^2 + \frac{\mathrm{d}r^2}{1 - \frac{a}{r} + \frac{\varepsilon m(r)}{r}}, \tag{5.93}$$

with the functions m and φ specified by:

$$m(r) = \frac{a}{4(\lambda a)^2} \left[-\frac{7}{2} \left(\frac{a}{r} \right)^2 + \frac{a}{r} + \ln\frac{a}{r} - \frac{r}{a} \right] + aC_1, \tag{5.94}$$

$$\varphi(r) = \frac{1}{4(\lambda a)^2} \left[-\frac{3}{2} \left(\frac{a}{r} \right)^2 - 2\frac{a}{r} - \ln\frac{a}{r} \right] + C_2, \tag{5.95}$$

where $r = \mathrm{x}a$. We also use the notation $h = 1 - (a - \varepsilon m)/r$. In this framework, the norm of the Killing vector is as follows:

$$\Lambda = -\left(1 - \frac{a}{r} + \frac{\varepsilon m(r)}{r}\right) e^{2\varepsilon\varphi(r)}. \tag{5.96}$$

Requiring this expression to coincide with the solution (5.81) fixes the constants C_1 and C_2 to

$$C_1 = \frac{7}{8(\lambda a)^2} \quad \wedge \quad C_2 = \frac{1}{8(\lambda a)^2}. \tag{5.97}$$

As an additional consistency check, we note that this particular choice of constants reduces the surface gravity in [42] to (5.89). Moreover, comparing the tortoise coordinate in [42] with (5.91), we find that they coincide up to an integration constant.

5.3 Evaporating black hole scenario

The evaporating black hole scenario describes both the gravitational collapse leading to black hole formation and the subsequent evaporation driven by Hawking radiation. This framework is introduced in Section 3.4. Here we follow [111], where this scenario was first developed within the DREH model.

The purely classical gravitational collapse was analyzed in Section 5.1.3. Since the classical treatment does not include the back-reaction of quantum fields on the geometry, the black hole does not evaporate in that setting. Unlike in the BPP model discussed in Section 4.3, where the Minkowski vacuum carries a non-vanishing energy flux at infinity, in the DREH model the initial spacetime can still be chosen as Minkowski space after quantum corrections are included. This is because the Minkowski metric satisfies the quantum-corrected field equations (5.44)–(5.46) and does not exhibit any energy flux. For the evaporating black hole case, the relevant vacuum state is the Unruh state (3.98), defined by $t_\pm(\sigma^\pm) = 0$. While the initial spacetime has vanishing energy flux at infinity, a non-zero flux appears at future null infinity once the black hole forms, arising from the change in asymptotically flat coordinates (see Section 3.4).

Before the black hole forms (region I of the spacetime in Figure 3.3), we work in the Eddington–Finkelstein gauge, which corresponds to choosing the $\sigma^\pm$ coordinates for the solution (5.70-5.71). In this gauge, the solution takes the form $(-1, 1, a, 0, 0)$. In region II of the spacetime an evaporating black hole is present. There, the Eddington–Finkelstein coordinates are denoted by $\hat{\sigma}^\pm$, and the solution is characterized by $(-1, \mathrm{F}^-, 0, t_-(\hat{\sigma}^-))$. Consequently, we need to determine the functions $t_\pm(\hat{\sigma}^\pm)$ using the transformation law (3.83). Since the coordinate transformation (3.106) is expressed in terms of the functions $\mathrm{F}^\pm$, defined in (5.36), the problem reduces to computing the Schwarzian derivative. The final expression is written in terms of the coordinate $\hat{\mathrm{x}}$:

$$t_+(\hat{\sigma}^+) = 0, \qquad t_-(\hat{\sigma}^-) = -\frac{\lambda^2}{4(\lambda a)^2}\frac{\hat{\mathrm{x}} - \frac{3}{4}}{\hat{\mathrm{x}}^4}. \tag{5.98}$$

Observe that the spacetime depicted in Figure 3.2 differs from that in Figure 3.3 by the presence of a third region (III). This additional region corresponds to the spacetime that remains after the black hole has fully evaporated and is characterized by the end-state geometry. With all necessary ingredients specified, the next task is to determine θ, whose general expression is given in Equation (5.65). This solution, however, is only fixed up to the integral I in (5.64).

The problem therefore reduces to computing these integrals for the particular choice (5.98). Because $t_+ = 0$, the integral I_+ vanishes, leaving us solely with the integral I_-:

$$\mathrm{I} = \int \frac{\mathrm{d}\sigma^-}{\mathrm{F}^-} \frac{1}{\varphi - \lambda a} \int \frac{\mathrm{d}\sigma^-}{\mathrm{F}^-} t_-(\hat{\sigma}^-). \tag{5.99}$$

The inner integral, expressed in terms of the coordinate $\hat{\mathrm{x}}(\sigma^-)$, takes the form

$$\int \frac{\mathrm{d}\sigma^-}{\mathrm{F}^-} t_-(\hat{\sigma}^-) = \frac{1}{8a} \mathrm{F}(\hat{\mathrm{x}}) = \frac{1}{8a} \left[\ln\left(1 - \frac{1}{\hat{\mathrm{x}}}\right) + \frac{1}{\hat{\mathrm{x}}} - \frac{3}{2} \frac{1}{\hat{\mathrm{x}}^2} \right], \tag{5.100}$$

where we have introduced the function $\mathrm{F}(\hat{\mathrm{x}})$. With this, the integral I can be rewritten as

$$\mathrm{I} = -\frac{1}{4\lambda a} \int \frac{\hat{\mathrm{x}}\, \mathrm{d}\hat{\mathrm{x}}}{\hat{\mathrm{x}} - 1} \frac{\mathrm{F}(\hat{\mathrm{x}})}{\mathrm{x} - 1}. \tag{5.101}$$

The key difficulty is that we must integrate with respect to $\hat{\mathrm{x}}$, even though the integrand still involves the field x, and the two variables are related by the transcendental Equation (5.40), which can be cast in the following form:

$$e^{\hat{\mathrm{x}}}(\hat{\mathrm{x}} - 1) = \delta\, e^{\mathrm{x}}(\mathrm{x} - 1). \tag{5.102}$$

To proceed, we must solve Equation (5.102) for $\hat{\mathrm{x}}$, i.e. obtain $\hat{\mathrm{x}} = \hat{\mathrm{x}}(\mathrm{x}, \delta)$. Since in region II of the spacetime we have $\delta < 1$, this equation admits an analytic solution. The full derivation, including a rigorous proof of the uniform convergence of the resulting series, is presented in Appendix B, see Theorems 1 and 3. Here we simply state the final result:

$$\hat{\mathrm{x}} = \begin{cases} 1 - \displaystyle\sum_{n=1}^{\infty} \frac{\delta^n}{n!}\, e^{n(\mathrm{x}-1)} (1 - \mathrm{x})^n\, \mathrm{P}_{n-1}(1), & \mathrm{x} \leqslant 1, \\[2ex] \mathrm{x} - \displaystyle\sum_{n=1}^{\infty} \frac{(1-\delta)^n}{n!} \left(1 - \frac{1}{\mathrm{x}}\right)^n \mathrm{P}_{n-1}\left(\frac{1}{\mathrm{x}}\right), & \mathrm{x} > 1, \end{cases} \tag{5.103}$$

where $\mathrm{P}_n(x)$ are the polynomials introduced in Theorem 1. In the subsequent calculation we also require the function $\ln \hat{\mathrm{x}} = \ln \hat{\mathrm{x}}(\mathrm{x}, \delta)$, which is given by (Theorems 5 and 7)

$$\ln \hat{\mathrm{x}} = \begin{cases} -\displaystyle\sum_{n=1}^{\infty} \frac{\delta^n}{n!}\, e^{n(\mathrm{x}-1)} (1 - \mathrm{x})^n\, \mathrm{Q}_{n-1}(1), & \mathrm{x} \leqslant 1, \\[2ex] \ln \mathrm{x} - \displaystyle\sum_{n=1}^{\infty} \frac{(1-\delta)^n}{n!} \left(1 - \frac{1}{\mathrm{x}}\right)^n \mathrm{Q}_{n-1}\left(\frac{1}{\mathrm{x}}\right), & \mathrm{x} > 1, \end{cases} \tag{5.104}$$

where $\mathrm{Q}_n(x)$ are the polynomials defined in Corollary 1. Making use of the series representations (5.103) and (5.104), together with their uniform convergence (see Appendix B), one readily finds that I can be written as

$$\mathrm{I}(\mathrm{x}, \delta) = \frac{1}{8\lambda a} \begin{cases} \mathrm{I}_0^<(\mathrm{x}) + \mathrm{I}_{-1}^<(\mathrm{x}) \ln \delta - \displaystyle\sum_{n=1}^{\infty} \frac{\delta^n}{n!}\, \mathrm{I}_n^<(\mathrm{x}), & \mathrm{x} < 1, \\[2ex] \mathrm{I}_0^>(\mathrm{x}) + \mathrm{I}_{-1}^>(\mathrm{x}) \ln \delta - \displaystyle\sum_{n=1}^{\infty} \frac{(1-\delta)^n}{n!}\, \mathrm{I}_n^>(\mathrm{x}), & \mathrm{x} > 1, \end{cases} \tag{5.105}$$

where the newly introduced functions I_n are given by

$$\begin{aligned}
\mathrm{I}_0^<(\mathrm{x}) &= \frac{1}{\mathrm{x}-1} - \frac{\mathrm{x}-3}{\mathrm{x}-1}\ln(1-\mathrm{x}) - \ln^2(1-\mathrm{x}) - 2\mathrm{x} + c_0,\\
\mathrm{I}_0^>(\mathrm{x}) &= \frac{1}{\mathrm{x}-1} - \frac{\mathrm{x}-3}{\mathrm{x}-1}\ln\left(1-\frac{1}{\mathrm{x}}\right) - \ln^2(\mathrm{x}-1) - 2\mathrm{L}(\mathrm{x}) + c_0,\\
\mathrm{I}_{-1}^>(\mathrm{x}) &= \mathrm{I}_{-1}^<(\mathrm{x}) = 2\left(\frac{1}{\mathrm{x}-1} - \ln|\mathrm{x}-1| + c_{-1}\right),\\
\mathrm{I}_n^>(\mathrm{x}) &= \int \frac{(2\mathrm{x}-1)\,\mathrm{dx}}{(\mathrm{x}-1)^2}\left(1-\frac{1}{\mathrm{x}}\right)^n \mathrm{P}_{n-1}\left(\frac{1}{\mathrm{x}}\right) + \int \frac{(2\mathrm{x}-3)\,\mathrm{dx}}{(\mathrm{x}-1)^2}\left(1-\frac{1}{\mathrm{x}}\right)^n \mathrm{Q}_{n-1}\left(\frac{1}{\mathrm{x}}\right)\\
&\qquad - \left(1-\frac{1}{\mathrm{x}}\right)^n \frac{\mathrm{P}_{n-1}\left(\frac{1}{\mathrm{x}}\right) + 3\mathrm{Q}_{n-1}\left(\frac{1}{\mathrm{x}}\right)}{\mathrm{x}-1} + c_n,\\
\mathrm{I}_n^<(\mathrm{x}) &= \mathrm{P}_{n-1}(1)\int \frac{(2\mathrm{x}-1)\,\mathrm{dx}}{(\mathrm{x}-1)^2} e^{n(\mathrm{x}-1)}(1-\mathrm{x})^n + \mathrm{Q}_{n-1}(1)\int \frac{(2\mathrm{x}-3)\,\mathrm{dx}}{(\mathrm{x}-1)^2} e^{n(\mathrm{x}-1)}(1-\mathrm{x})^n\\
&\qquad + e^{n(\mathrm{x}-1)}(1-\mathrm{x})^{n-1}\big(\mathrm{P}_{n-1}(1) + 3\mathrm{Q}_{n-1}(1)\big) + \tilde{c}_n,
\end{aligned} \tag{5.106}$$

where $\mathrm{L}(\mathrm{x}) = \frac{\pi^2}{6} - \int_0^{\mathrm{x}} \frac{ds}{s-1}\ln s$, so that $\mathrm{L}(1) = 0$. The constants c_n are free parameters. By comparing (5.106) with (5.70), we can interpret these constants as being associated with a redefinition of the σ^+ coordinate, because the contribution to I that contains them depends solely on $\delta = \delta(\sigma^+)$. On the other hand, the constants $\tilde{c}_n$ are fixed, since the functions I_n must be continuous across the hypersurface at $\mathrm{x} = 1$, which imposes the matching condition $\mathrm{I}_n^>(1) = \mathrm{I}_n^<(1)$.

The integral in (5.101) has been reduced to the simple integrals appearing in (5.106). Consequently, we can express the function $\theta(\mathrm{x}, \delta)$ from Equation (5.65) as

$$\theta(\mathrm{x}, \delta) = \frac{\mathrm{x}-1}{\mathrm{x}}\left[\frac{\lambda}{2}\left(\int d\sigma^+ \frac{\mathrm{G}^+}{\mathrm{F}^{+2}} + \int d\sigma^- \frac{\mathrm{G}^-}{\mathrm{F}^{-2}}\right) + \frac{1}{8\lambda a}\left(\mathrm{S}_0(\mathrm{x}) + \mathrm{S}_{-1}(\mathrm{x})\ln\delta - \sum_{n=1}^{\infty}\frac{\tilde{\delta}^n}{n!}\mathrm{S}_n(\mathrm{x})\right)\right]. \tag{5.107}$$

Here, $\mathrm{S}_0(\mathrm{x}) = \mathrm{I}_0(\mathrm{x}) + (8\lambda a)\theta_0(\mathrm{x})$, $\mathrm{S}_{-1} = \mathrm{I}_{-1}$, and $\mathrm{S}_n = \mathrm{I}_n$. The function $\theta_0(\mathrm{x})$ is defined in (5.63). Note that Equation (5.107) simultaneously covers the cases $\mathrm{x} < 1$ and $\mathrm{x} > 1$, with $\tilde{\delta} = \delta$ for $x < 1$ and $\tilde{\delta} = 1 - \delta$ for $x > 1$. The explicit expression for $\mathrm{S}_0(\mathrm{x})$ is given in (5.109). For $n \geq 1$, the functions $\mathrm{S}_n(\mathrm{x})$ coincide with the corresponding $\mathrm{I}_n(\mathrm{x})$, so we do not rewrite them here. It is straightforward to verify that the set of functions $\mathrm{S}_n(\mathrm{x})$ obeys the recurrence relation

$$n\frac{d\mathrm{S}_n}{d\mathrm{x}} - \frac{1}{\mathrm{x}-1}\frac{d}{d\mathrm{x}}\left(\frac{(\mathrm{x}-1)^2}{\mathrm{x}}\frac{d\mathrm{S}_n}{d\mathrm{x}}\right) = \begin{cases} \dfrac{d\mathrm{S}_{n+1}}{d\mathrm{x}}, & \mathrm{x} > 1,\\ 0, & \mathrm{x} < 1. \end{cases} \tag{5.108}$$

The function S_0 is explicitly given by:

$$\mathrm{S}_0(\mathrm{x}) = \begin{cases} 2\dfrac{\mathrm{x}^2-2\mathrm{x}+2}{\mathrm{x}-1}\ln\mathrm{x} - (2\mathrm{x}-3)\ln(1-\mathrm{x}) - \ln^2(1-\mathrm{x}) - 2\mathrm{x} & \\ \qquad + 8\lambda aC\left(\dfrac{1}{\mathrm{x}-1} - \ln(1-\mathrm{x})\right) + c_0, & \mathrm{x} \leqslant 1,\\ (2\mathrm{x}-1)\ln\mathrm{x} - (2\mathrm{x}-3)\ln(\mathrm{x}-1) - \ln^2(\mathrm{x}-1) - 2\mathrm{L}(\mathrm{x}) & \\ \qquad + 8\lambda aC\left(\dfrac{1}{\mathrm{x}-1} - \ln(\mathrm{x}-1)\right) + c_0, & \mathrm{x} \geqslant 1. \end{cases} \tag{5.109}$$

Using Equation (5.52), we can then compute $\alpha(\mathrm{x},\delta)$ directly. Substituting the obtained expressions for θ and α into the equations of motion (5.47–5.49) confirms that (5.107) indeed provides the required solution.

5.3.1 Evaporating black hole solution

In the preceding subsections, we obtained a solution in region II of the spacetime (see Figure 3.3), where the black hole has already formed. This solution involves several constants: c_0, c_{-1}, c_n, $\tilde{c}_n$, and C. Since the constants c_n and $\tilde{c}_n$ are arbitrary (they encode the choice of the function G^+), we fix them by imposing $\mathrm{S}_n(1)=0$ and setting $c_0=0$. Using Equation (5.52), one can then straightforwardly compute $\alpha(\mathrm{x},\delta)$. Next, by repeating the same procedure as before, namely $\rho+\varepsilon\alpha\mapsto\rho$, $\mathrm{x}+\frac{\varepsilon}{\lambda a}\theta\mapsto\mathrm{x}$, and $\mathrm{F}^\pm+\varepsilon\mathrm{G}^\pm\mapsto\mathrm{F}^\pm$ (see equations (5.66) and (5.67)), we arrive at the following set of equations:

$$\begin{aligned}\mathrm{x}+\ln|\mathrm{x}-1|-\frac{\varepsilon}{8(\lambda a)^2}&\left[\mathrm{S}_0(\mathrm{x})+\mathrm{S}_{-1}(\mathrm{x})\ln\delta-\sum\frac{\tilde{\delta}^n}{n!}\mathrm{S}_n(\mathrm{x})\right]\\ &=-\frac{\lambda}{2}\frac{1}{\lambda a}\left[\int\frac{\mathrm{d}\sigma^+}{\mathrm{F}^+}+\int\frac{\mathrm{d}\sigma^-}{\mathrm{F}^-}\right]\equiv\frac{\hat{\sigma}^+-\hat{\sigma}^-}{2a},\end{aligned}\tag{5.110}$$

$$\mathrm{F}^+\mathrm{F}^-e^{2\rho}=\begin{cases}\left(\frac{1}{\mathrm{x}}-1\right)\Bigg\{1+\frac{\varepsilon}{8(\lambda a)^2}\Bigg[\frac{\mathrm{x}-1}{\mathrm{x}}\frac{\mathrm{dS}_0(\mathrm{x})}{\mathrm{dx}}+\frac{\mathrm{x}-1}{\mathrm{x}}\frac{\mathrm{dS}_{-1}(\mathrm{x})}{\mathrm{dx}}\ln\delta-2c_{-1} & \\ \quad -c_1-\sum_{n=1}^{\infty}\frac{(1-\delta)^n}{n!}\left(\frac{\mathrm{x}-1}{\mathrm{x}}\frac{\mathrm{dS}_n(\mathrm{x})}{\mathrm{dx}}+\mathrm{S}_{n+1}(\mathrm{x})-n\mathrm{S}_n(\mathrm{x})\right)\Bigg]\Bigg\}, & \mathrm{x}\geqslant 1,\\ \left(\frac{1}{\mathrm{x}}-1\right)\Bigg\{1+\frac{\varepsilon}{8(\lambda a)^2}\Bigg[\frac{\mathrm{x}-1}{\mathrm{x}}\frac{\mathrm{dS}_0(\mathrm{x})}{\mathrm{dx}}-\mathrm{S}_{-1}(\mathrm{x})-8(\lambda a)^2\mathcal{D}(\mathrm{x}) & \\ \quad +\frac{\mathrm{x}-1}{\mathrm{x}}\frac{\mathrm{dS}_{-1}(\mathrm{x})}{\mathrm{dx}}\ln\delta-\sum_{n=1}^{\infty}\frac{\delta^n}{n!}\left(\frac{\mathrm{x}-1}{\mathrm{x}}\frac{\mathrm{dS}_n(\mathrm{x})}{\mathrm{dx}}-n\mathrm{S}_n(\mathrm{x})\right)\Bigg]\Bigg\}, & \mathrm{x}\leqslant 1.\end{cases}\tag{5.111}$$

The only remaining free constants are c_{-1} and C. The solution in region II of the spacetime must match continuously with the solution in region I across the hypersurface $\sigma^+=\sigma_0^+$, i.e., at $\delta=1$ (see Figure 3.2). Let us first consider the "++" component of Equation (5.44):

$$\partial_+(e^{-2\rho}\partial_+\varphi)=\frac{\lambda}{2}\frac{\lambda a}{\mathrm{F}^+}\delta(\sigma^+-\sigma_0^+)\varphi^{-1}e^{-2\rho}+\varepsilon\big((\partial_+\rho)^2-\partial_+^2\rho\big)\varphi^{-1}e^{-2\rho}.\tag{5.112}$$

Integrating this relation yields

$$e^{-2\rho}\partial_+\varphi_>-e^{-2\rho}\partial_+\varphi_<=-\frac{\lambda}{2}\lambda a\,\varphi^{-1}e^{-2\rho}-\varepsilon(\partial_+\rho_>-\partial_+\rho_<)\varphi^{-1}e^{-2\rho},\tag{5.113}$$

where the subscript ">" denotes the region $\sigma^+>\sigma_0^+$ and "<" the region $\sigma^+<\sigma_0^+$. The origin of the last term in (5.113) deserves clarification: it is inherited from the final term in (5.112). Since $\partial_+\rho=\frac{\lambda}{4}\frac{\lambda a}{\varphi^2}\eta(\sigma^+-\sigma_0^+)+o(\varepsilon)$, with $\eta(\sigma^+-\sigma_0^+)$ the Heaviside step function, it follows that $\partial_+^2\rho$ contains a contribution proportional to a Dirac δ-function. Using Equation (5.52), one can then establish that

$$\partial_+\varphi_>=\frac{\lambda}{2}\mathrm{F}_>^-e^{2\rho}\left(1+\varepsilon\mathcal{D}(\mathrm{x})\right).\tag{5.114}$$

At $\delta = 1$ we have $\mathrm{x} = \hat{\mathrm{x}}$, $e^{2\rho} = 1$, and $\partial_+ \varphi_< = \lambda/2$. A straightforward computation then leads to the following form for the function $\mathrm{F}^-(\hat{\mathrm{x}})$:

$$\mathrm{F}^- = \left(1 - \frac{1}{\hat{\mathrm{x}}}\right)\left[1 - \varepsilon \mathcal{D}(\hat{\mathrm{x}}) - \frac{\varepsilon}{2(\lambda a)^2}\frac{1}{\hat{\mathrm{x}}^2(\hat{\mathrm{x}}-1)}\right]. \tag{5.115}$$

Now we impose the continuity conditions on ρ and θ. This analysis will be carried out independently in the two separate regions of the spacetime, specifically for $\mathrm{x} > 1$ and for $\mathrm{x} < 1$. We begin with the case $\mathrm{x} > 1$. Substituting $\delta = 1$ into Equation (5.111) and using Equation (5.115), we obtain:

$$\frac{8\lambda a C - 2}{\hat{\mathrm{x}} - 1} + 2c_{-1} + c_1 = 0. \tag{5.116}$$

From Equation (5.116) it follows that $C = \frac{1}{4\lambda a}$ and $c_{-1} = -c_1/2$. Since $c_1 = 7$ was already fixed by the condition $\mathrm{S}_1(1) = 0$, where $S_1(\mathrm{x}) = 2\ln \mathrm{x} - \frac{4}{\mathrm{x}} - \frac{3}{\mathrm{x}^2} + c_1$, we obtain $c_{-1} = -\frac{7}{2}$. The remaining continuity requirement is $\theta(\hat{\mathrm{x}}, 1) = 0$. Using Equation (5.110), this condition becomes:

$$\frac{\lambda}{2}\int \mathrm{d}\sigma^+ \frac{\mathrm{G}^+}{\mathrm{F}^{+2}}\bigg|_{\delta=1} + \frac{\lambda}{2}\int \mathrm{d}\sigma^- \frac{\mathrm{G}^-}{\mathrm{F}^{-2}} = -\frac{\mathrm{S}_0(\hat{\mathrm{x}})}{8\lambda a}. \tag{5.117}$$

To fully specify the solution, we set $\mathrm{G}^+ = 0$, which then yields the following coordinate transformations:

$$\mathrm{F}^- = \left(1 - \frac{1}{\hat{\mathrm{x}}}\right)\left[1 + \frac{\varepsilon}{8(\lambda a)^2}\frac{\hat{\mathrm{x}}-1}{\hat{\mathrm{x}}}\frac{\mathrm{d}\mathrm{S}_0(\hat{\mathrm{x}})}{\mathrm{d}\hat{\mathrm{x}}}\right], \tag{5.118}$$

$$\mathrm{F}^+ = -1, \tag{5.119}$$

$$\hat{\sigma}^- = \sigma_0^+ - 2a\left[\hat{\mathrm{x}} + \ln|\hat{\mathrm{x}} - 1| - \frac{\varepsilon}{8(\lambda a)^2}\mathrm{S}_0(\hat{\mathrm{x}})\right], \tag{5.120}$$

$$\hat{\sigma}^+ = \sigma^+. \tag{5.121}$$

Next, we turn to the region $x < 1$ of the spacetime. Setting $\delta = 1$ in Equation (5.111) yields the following condition:

$$2\ln\hat{\mathrm{x}} - 2\frac{\ln\hat{\mathrm{x}}}{\hat{\mathrm{x}}-1} - \frac{3}{\hat{\mathrm{x}}} - 2 - 2c_{-1} + 2\frac{1 - 4\lambda a C}{\hat{\mathrm{x}} - 1} = \sum_{n=1}^{\infty}\frac{1}{n!}\left[\frac{\hat{\mathrm{x}}-1}{\hat{\mathrm{x}}}\frac{\mathrm{d}\mathrm{S}_n(\hat{\mathrm{x}})}{\mathrm{d}\hat{\mathrm{x}}} - n\mathrm{S}_n(\hat{\mathrm{x}})\right]. \tag{5.122}$$

Inserting $\delta = 1$ into equations (5.103) and (5.104) gives:

$$\hat{\mathrm{x}} = 1 - \sum_{n=1}^{\infty}\frac{\mathrm{P}_{n-1}(1)}{n!}e^{n(\hat{\mathrm{x}}-1)}(1-\hat{\mathrm{x}})^n, \tag{5.123}$$

$$\ln\hat{\mathrm{x}} = -\sum_{n=1}^{\infty}\frac{\mathrm{Q}_{n-1}(1)}{n!}e^{n(\hat{\mathrm{x}}-1)}(1-\hat{\mathrm{x}})^n. \tag{5.124}$$

From Equation (5.106) we obtain the following expression for the derivatives of $\mathrm{S}_n(\mathrm{x})$:

$$\frac{\mathrm{d}\mathrm{S}_n^<(\hat{\mathrm{x}})}{\mathrm{d}\hat{\mathrm{x}}} = \hat{\mathrm{x}}(1-\hat{\mathrm{x}})^{n-2}e^{n(\hat{\mathrm{x}}-1)}\Big[(2-n)\mathrm{P}_{n-1}(1) + (2-3n)\mathrm{Q}_{n-1}(1)\Big]. \tag{5.125}$$

Substituting (5.125) into the first series on the right-hand side of (5.122) and using (5.123) and (5.124), the sum can be evaluated straightforwardly, giving:

$$\frac{\hat{\mathrm{x}}-1}{\hat{\mathrm{x}}}\sum_{n=0}^{\infty}\frac{1}{n!}\frac{\mathrm{d}\mathrm{S}_n^<(\hat{\mathrm{x}})}{\mathrm{d}\hat{\mathrm{x}}} = -2 - 2\frac{\ln\hat{\mathrm{x}}}{\hat{\mathrm{x}}-1} + \frac{1}{\hat{\mathrm{x}}} + \frac{3}{\hat{\mathrm{x}}^2}. \tag{5.126}$$

The second series in (5.122) can be obtained in a similar way: we first differentiate, use the same technique as for the preceding sum, and then integrate, imposing the condition that the sum vanishes at $\hat{\mathrm{x}} = 1$. This procedure leads to:

$$-\sum_{n=1}^{\infty} \frac{\mathrm{S}_n^{<}(\hat{\mathrm{x}})}{(n-1)!} = 2\ln\hat{\mathrm{x}} - \frac{4}{\hat{\mathrm{x}}} - \frac{3}{\hat{\mathrm{x}}^2} + 7 \equiv \mathrm{S}_1^{>}(\hat{\mathrm{x}}). \tag{5.127}$$

By inserting (5.126) and (5.127) into (5.122), one indeed recovers condition (5.116). The remaining requirement is the continuity of the function θ. Using Equation (5.110), this continuity condition can be rewritten as:

$$\mathrm{S}_0^{>}(\hat{\mathrm{x}}) = \mathrm{S}_0^{<}(\hat{\mathrm{x}}) - \sum_{n=1}^{\infty} \frac{\mathrm{S}_n^{<}(\hat{\mathrm{x}})}{n!}. \tag{5.128}$$

Once again, employing equations (5.123) and (5.124), the series in (5.128) can be evaluated, yielding:

$$\sum_{n=1}^{\infty} \frac{\mathrm{S}_n^{<}(\hat{\mathrm{x}})}{n!} = 2\mathrm{L}(\hat{\mathrm{x}}) - 2\hat{\mathrm{x}} - \frac{\hat{\mathrm{x}}-3}{\hat{\mathrm{x}}-1}\ln\hat{\mathrm{x}}. \tag{5.129}$$

Substituting (5.129) into (5.128) one readily verifies that the continuity condition is met.

5.3.2 Asymptotically flat solution

Our final task is to verify whether the solution defined by equations (5.110) and (5.111) is asymptotically flat. For this purpose, it is useful to clarify the behaviour of $\mathrm{S}_n^{>}(\mathrm{x})$ as $\mathrm{x} \to \infty$. We demonstrate that, for $n > 1$, the following relation holds:

$$\mathrm{S}_n^{>}(\mathrm{x}) = (n-1)!\mathrm{S}_1^{>}(\mathrm{x}) + \frac{6}{\mathrm{x}^4}\mathrm{Z}_{2(n-2)}\left(\frac{1}{\mathrm{x}}\right) - 6\mathrm{Z}_{2(n-2)}(1), \tag{5.130}$$

where $\mathrm{Z}_{2(n-2)}(x)$ denotes polynomials of degree $2(n-2)$. Expression (5.130) is written so as to incorporate the condition $\mathrm{S}_n(1) = 0$, given that $\mathrm{S}_1(1) = 0$. We will collectively denote the last two terms in (5.130) by $\mathrm{R}_n(\mathrm{x})$. Using the recurrence relation (5.108), one can derive the following recurrence relation for the functions R_n:

$$\frac{\mathrm{dR}_{n+1}}{\mathrm{dx}} - n\frac{\mathrm{dR}_n}{\mathrm{dx}} = -(n-1)!\frac{24}{\mathrm{x}^5} - \frac{1}{\mathrm{x}-1}\frac{\mathrm{d}}{\mathrm{dx}}\left(\frac{(\mathrm{x}-1)^2}{\mathrm{x}}\frac{\mathrm{dR}_n}{\mathrm{dx}}\right). \tag{5.131}$$

We now substitute $\frac{\mathrm{dR}_n}{\mathrm{dx}} = -\frac{24}{\mathrm{x}^5}\mathrm{M}_n(\mathrm{x})$ into Equation (5.131), which leads to:

$$\mathrm{M}_{n+1} - n\mathrm{M}_n = (n-1)! + 2\left(\frac{2}{\mathrm{x}} - \frac{3}{\mathrm{x}^2}\right)\mathrm{M}_n - \frac{\mathrm{x}-1}{\mathrm{x}}\frac{\mathrm{dM}_n}{\mathrm{dx}}. \tag{5.132}$$

Since $\mathrm{M}_2(\mathrm{x}) = 1$, Equation (5.132) shows that the functions $\mathrm{M}_n(\mathrm{x})$ can be expressed as polynomials in $1/\mathrm{x}$, and that their degree increases by two each time n is incremented by one. Consequently, the degree of the n-th polynomial is $2(n-2)$. After integrating the functions $\mathrm{M}_n/\mathrm{x}^5$, we obtain the representation (5.130) for the functions $\mathrm{S}_n^{>}(\mathrm{x})$. For later convenience, we introduce the shorthand $6\mathrm{Z}_{2(n-2)}(1) = z_n$. To determine whether the spacetime is asymptotically flat, we examine the large–x behavior of the metric, i.e., the limit $\mathrm{x} \to \infty$. We do this term by term using Equation (5.111). The δ-independent term is given by:

$$\left(\frac{\mathrm{x}-1}{\mathrm{x}}\right)^2 \frac{\mathrm{dS}_0^{>}}{\mathrm{dx}} = -2\frac{\mathrm{x}-1}{\mathrm{x}}\ln\left(1-\frac{1}{\mathrm{x}}\right) - \frac{2}{\mathrm{x}} + \frac{1}{\mathrm{x}^2} - \frac{1}{\mathrm{x}^3}, \tag{5.133}$$

from which it follows that this contribution goes to zero as $\mathrm{x} \to \infty$. The term proportional to $\ln\delta/\mathrm{x}$ also vanishes in the limit $\mathrm{x} \to \infty$. Furthermore, since $\frac{\mathrm{dS}_n^>}{\mathrm{dx}} \sim (n-1)!\frac{2}{\mathrm{x}}$ for $\mathrm{x} \to \infty$, this contribution likewise tends to zero. The only remaining term in the sum is

$$\mathrm{S}_{n+1}^> - n\mathrm{S}_n^> = -(z_{n+1} - nz_n) + \mathcal{O}\left(\frac{1}{\mathrm{x}^4}\right). \tag{5.134}$$

Thus, we are finally left with the following expression:

$$\lim_{\mathrm{x}\to\infty} \mathrm{F}^+\mathrm{F}^- e^{2\rho} = -1 - \frac{\varepsilon}{8(\lambda a)^2}\sum_{n=1}^{\infty}\frac{(1-\delta)^n}{n!}(z_{n+1} - nz_n). \tag{5.135}$$

From Equation (5.135) we infer that, in the $\hat{\sigma}^\pm$ coordinates introduced in (5.120) and (5.121), the metric is not asymptotically flat. Since its asymptotic form depends solely on σ^+, we attempt to perform a coordinate transformation that renders the metric flat at infinity:

$$ds^2 = e^{2\rho}\mathrm{d}\sigma^+\mathrm{d}\sigma^- = -\mathrm{F}^+\mathrm{F}^- e^{2\rho}\mathrm{d}\hat{\sigma}^+\mathrm{d}\hat{\sigma}^- = -\mathrm{F}^+\mathrm{F}'^+\mathrm{F}^- e^{2\rho}\mathrm{d}\hat{\sigma}'^+\mathrm{d}\hat{\sigma}^-. \tag{5.136}$$

Requiring that the metric be asymptotically flat in the coordinates $\hat{\sigma}^-$ and $\hat{\sigma}'^+$ is equivalent to choosing

$$\mathrm{F}'^+ = 1 - \frac{\varepsilon}{8(\lambda a)^2}\sum_{n=1}^{\infty}\frac{(1-\delta)^n}{n!}(z_{n+1} - nz_n). \tag{5.137}$$

To determine the new coordinate $\hat{\sigma}'^+$, one must evaluate the integral $\int \frac{\mathrm{d}\hat{\sigma}^+}{\mathrm{F}'^+}$. The resulting expression is

$$\hat{\sigma}'^+ = -2a\ln\delta + \frac{a\varepsilon}{4(\lambda a)^2}\sum_{n=1}^{\infty}\frac{(1-\delta)^n}{n!}z_n + 2aD, \tag{5.138}$$

where D denotes an arbitrary integration constant. We now investigate the behavior of Equation (5.110) for the dilaton field at infinity. Solving Equation (5.138) for $\ln\delta$ and substituting the result into (5.110) leads to:

$$\mathrm{x} + \ln(\mathrm{x}-1) - \frac{\varepsilon}{8(\lambda a)^2}\left[\mathrm{S}_0^>(\mathrm{x}) + \mathrm{S}_{-1}(\mathrm{x})\ln\delta - \sum_{n=1}^{\infty}\frac{(1-\delta)^n}{n!}(\mathrm{S}_n^>(\mathrm{x}) + z_n)\right] = \frac{\hat{\sigma}'^+ - \hat{\sigma}^-}{2a} - D. \tag{5.139}$$

First, we extract the δ-dependent contributions from Equation (5.139). For large x we have

$$\mathrm{S}_n(\mathrm{x}) \sim (n-1)!\big(2\ln\mathrm{x} + 7\big) - z_n, \tag{5.140}$$

which allows us to rewrite the sum appearing in Equation (5.139) as:

$$-\sum_{n=1}^{\infty}\frac{(1-\delta)^n}{n!}\big(\mathrm{S}_n^>(\mathrm{x}) + z_n\big) \sim \ln\delta\big(2\ln\mathrm{x} + 7\big). \tag{5.141}$$

In the limit $\mathrm{x} \to \infty$, the contribution in (5.141) cancels exactly with the term $\mathrm{S}_{-1}(\mathrm{x})\ln\delta$. The $\mathrm{S}_0^>(\mathrm{x})$ contribution in (5.139) behaves as:

$$\lim_{\mathrm{x}\to\infty}\mathrm{S}_0^>(\mathrm{x}) = 2 + \frac{\pi^2}{3}, \tag{5.142}$$

as $\mathrm{x} \to \infty$. The key ingredient in deriving (5.142) is the asymptotic form of $\mathrm{L}(\mathrm{x})$:

$$\mathrm{L}(\mathrm{x}) \sim -\frac{1}{2}\ln^2(\mathrm{x}-1) - \frac{\pi^2}{6}. \tag{5.143}$$

Thus, in the limit $\mathrm{x} \to \infty$, Equation (5.139 simplifies to:

$$\mathrm{x} + \ln(\mathrm{x}-1) - \frac{\varepsilon}{4(\lambda a)^2}\left(\frac{\pi^2}{6}+1\right) = \frac{\hat{\sigma}'^{+} - \hat{\sigma}^{-}}{2a} - D. \tag{5.144}$$

Imposing that the asymptotic behavior of the dilaton field remains unchanged under quantum corrections fixes the constant to be $D = \frac{\varepsilon}{4(\lambda a)^2}\left(\frac{\pi^2}{6}+1\right)$. For simplicity, we can redefine the coordinate transformation for σ^+ by taking $\mathrm{F}^+\mathrm{F}'^+ \mapsto \mathrm{F}^+$ and $\hat{\sigma}'^+ \mapsto \hat{\sigma}^+$. In this new notation, the coordinate transformations become:

$$\mathrm{F}^- = \left(1-\frac{1}{\hat{\mathrm{x}}}\right)\left[1+\frac{\varepsilon}{8(\lambda a)^2}\frac{\hat{\mathrm{x}}-1}{\hat{\mathrm{x}}}\frac{\mathrm{dS}_0(\hat{\mathrm{x}})}{\mathrm{d}\hat{\mathrm{x}}}\right], \tag{5.145}$$

$$\mathrm{F}^+ = -1 + \frac{\varepsilon}{8(\lambda a)^2}\sum_{n=1}^{\infty}\frac{(1-\delta)^n}{n!}(z_{n+1}-nz_n), \tag{5.146}$$

and the corresponding asymptotically flat coordinates read:

$$\hat{\sigma}^- = \sigma_0^+ - 2a\left[\hat{\mathrm{x}} + \ln|\hat{\mathrm{x}}-1| - \frac{\varepsilon}{8(\lambda a)^2}\mathrm{S}_0(\hat{\mathrm{x}})\right], \tag{5.147}$$

$$\hat{\sigma}^+ = \sigma^+ + \frac{2a\varepsilon}{8(\lambda a)^2}\left[\frac{\pi^2}{3} + 2 + \sum_{n=1}^{\infty}\frac{(1-\delta)^n}{n!}z_n\right]. \tag{5.148}$$

We then introduce a new coordinate $\hat{\delta}$ in terms of $\hat{\sigma}^+$:

$$\hat{\delta} = \exp\left\{\left(-\frac{\hat{\sigma}^+ - \sigma_0^+}{2a}\right)\right\}. \tag{5.149}$$

With these definitions, the final forms of the metric and the dilaton field in region II of the spacetime (see Figure 3.2) are as follows,

$$\begin{aligned}\mathrm{F}^+\mathrm{F}^- e^{2\rho} = &\left[1-\frac{\varepsilon}{8(\lambda a)^2}\sum_{n=1}^{\infty}\frac{(1-\delta)^n}{n!}(z_{n+1}-nz_n)\right]\left(\frac{1}{\mathrm{x}}-1\right)\left\{1+\frac{\varepsilon}{8(\lambda a)^2}\left[\frac{\mathrm{x}-1}{\mathrm{x}}\frac{\mathrm{dS}_0^{>}(\mathrm{x})}{\mathrm{dx}}\right.\right.\\ &\left.\left.-\frac{2\ln\delta}{\mathrm{x}-1} - \sum_{n=1}^{\infty}\frac{(1-\delta)^n}{n!}\left(\frac{\mathrm{x}-1}{\mathrm{x}}\frac{\mathrm{dS}_n^{>}(\mathrm{x})}{\mathrm{dx}} + \mathrm{S}_{n+1}^{>}(\mathrm{x}) - n\mathrm{S}_n^{>}(\mathrm{x})\right)\right]\right\}\end{aligned} \tag{5.150}$$

$$\begin{aligned}\mathrm{F}^+\mathrm{F}^- e^{2\rho} = &\left[1-\frac{\varepsilon}{8(\lambda a)^2}\sum_{n=1}^{\infty}\frac{(1-\delta)^n}{n!}(z_{n+1}-nz_n)\right]\left(\frac{1}{\mathrm{x}}-1\right)\left\{1+\frac{\varepsilon}{8(\lambda a)^2}\left[\frac{\mathrm{x}-1}{\mathrm{x}}\frac{\mathrm{dS}_0^{<}(\mathrm{x})}{\mathrm{dx}}\right.\right.\\ &\left.\left.+\mathrm{S}_1^{>}(\mathrm{x}) - \frac{2\ln\delta}{\mathrm{x}-1} - \sum_{n=1}^{\infty}\frac{\delta^n}{n!}\left(\frac{\mathrm{x}-1}{\mathrm{x}}\frac{\mathrm{dS}_n^{<}(\mathrm{x})}{\mathrm{dx}} - n\mathrm{S}_n^{<}(\mathrm{x})\right)\right]\right\}\end{aligned} \tag{5.151}$$

$$\begin{aligned}&\mathrm{x} + \ln(\mathrm{x}-1) - \frac{\varepsilon}{8(\lambda a)^2}\left[\mathrm{S}_0^{>}(\mathrm{x}) - \frac{\pi^2}{3} - 2 + \ln\delta\mathrm{S}_{-1}(\mathrm{x}) - \sum_{n=1}^{\infty}\frac{(1-\delta)^n}{n!}(\mathrm{S}_n^{>}(\mathrm{x}) + z_n)\right]\\ &\qquad = -\ln\hat{\delta} + \hat{\mathrm{x}} + \ln(\hat{\mathrm{x}}-1) - \frac{\varepsilon}{8(\lambda a)^2}\mathrm{S}_0^{>}(\hat{\mathrm{x}}) \equiv \frac{\hat{\sigma}^+ - \hat{\sigma}^-}{2a} \equiv \frac{\hat{\sigma}}{a},\end{aligned} \tag{5.152}$$

$$\begin{aligned}&\mathrm{x} + \ln(1-\mathrm{x}) - \frac{\varepsilon}{8(\lambda a)^2}\left[\mathrm{S}_0^{<}(\mathrm{x}) - \frac{\pi^2}{3} - 2 + \ln\delta\mathrm{S}_{-1}(\mathrm{x}) - \sum_{n=1}^{\infty}\frac{\delta^n}{n!}\mathrm{S}_n^{<}(\mathrm{x}) - \sum_{n=1}^{\infty}\frac{(1-\delta)^n}{n!}z_n\right]\\ &\qquad = -\ln\hat{\delta} + \hat{\mathrm{x}} + \ln(1-\hat{\mathrm{x}}) - \frac{\varepsilon}{8(\lambda a)^2}\mathrm{S}_0^{>}(\hat{\mathrm{x}}) \equiv \frac{\hat{\sigma}^+ - \hat{\sigma}^-}{2a} \equiv \frac{\hat{\sigma}}{a}.\end{aligned} \tag{5.153}$$

Equation (5.150) provides the form of the metric for $\mathrm{x} \geqslant 1$, while Equation (5.151) gives the corresponding expression for $\mathrm{x} \leqslant 1$. The relations (5.152) and (5.153) are the quantum-corrected transcendental equations for the dilaton field $\mathrm{x} = \frac{1}{\lambda a} e^{-\phi}$ in the regimes $\mathrm{x} \geqslant 1$ and $\mathrm{x} \leqslant 1$, respectively, expressed in terms of the coordinates σ^+ (via their dependence on δ) and σ^- (through the dependence on $\hat{\mathrm{x}}$). The functions $\mathrm{S}_0^{>/<}$ and $\mathrm{S}_n^{>/<}(\mathrm{x})$ appearing in (5.150)–(5.153) are defined in Equations (5.109) and (5.106), respectively. Observe that for $\delta = 1$ both (5.150) and (5.151) reduce to Equation (5.145) for the coordinate transformation F^-. Consequently, $e^{2\rho} = 1$ when $\delta = 1$, which enforces continuity of the metric. Moreover, Equations (5.152) and (5.153) show that $\mathrm{x} = \hat{\mathrm{x}}$ when $\delta = 1$, ensuring continuity of the dilaton field. In (5.152) and (5.153) we also identify new asymptotically flat coordinates $\hat{\sigma}^{\pm}$, defined in (5.147) and (5.148). Note that in the following subsections we alternate between the original $\hat{\sigma}^{\pm}$ coordinates and the ones introduced in this subsection.

5.3.3 Evaporation adapted form of the solution

The terms involving $\ln \delta$ appear in the evaporating black hole solution (5.150-5.153). Since $\ln \delta \sim \sigma^+$, these contributions grow without bound at late evaporation times. One might therefore conclude that this behavior leads to a divergent metric at $\mathcal{J}^+$. However, they cancel precisely against the δ terms coming from the sums, so that the metric remains asymptotically flat. Still, their presence in this explicit form is somewhat unexpected. From a physical point of view, the apparent horizon should shrink as the black hole continues to evaporate. Hence, it is natural to expect that the $\ln \delta$ terms are effectively incorporated into the constant λa as part of its quantum corrections. In this subsection, we rewrite the solution (5.150-5.153) guided by this line of reasoning.

As a consequence, the solution is well defined on hypersurfaces specified by $\mathrm{x} = 1 + \mathcal{O}(\tilde{\varepsilon})$ or equivalently $\hat{\mathrm{x}} = 1 + \mathcal{O}(\tilde{\varepsilon})$. We also introduce the notation $\tilde{\varepsilon} = \frac{\varepsilon}{(\lambda a)^2}$. This is relevant because many hypersurfaces of physical interest (apparent horizon, horizon, island, QES, etc.) are described by relations of this form. From the structure of the equations of motion (5.44-5.46) and the method by which they are solved (5.47-5.59), one is naturally led to expect that the formulas for $\partial_{\pm}\mathrm{x}$ (5.52-5.53) remain well defined when $\mathrm{x} = 1 + \mathcal{O}(\tilde{\varepsilon})$, since they follow from straightforward integration of the original equations of motion. This expectation is indeed confirmed:

$$\partial_+ \mathrm{x} = \frac{1}{2a} \Bigg\{ 1 - \frac{1 + \frac{\tilde{\varepsilon}}{4} \ln \delta}{\sqrt{\mathrm{x}^2 - \tilde{\varepsilon}}} \Bigg[1 - \frac{\tilde{\varepsilon}}{8} \Bigg(2(\mathrm{x} - 2) \ln \mathrm{x} - 8 + 5\mathrm{x} + \frac{3}{\mathrm{x}} - (\mathrm{x} - 1) \sum_{n=1}^{\infty} \frac{\delta^n}{n!} \left(\frac{\mathrm{x} - 1}{\mathrm{x}} \frac{d\mathrm{S}_n^<}{d\mathrm{x}} - n \mathrm{S}_n^< \right) \Bigg) \Bigg] \Bigg\}, \tag{5.154}$$

$$\partial_- \mathrm{x} = -\frac{1}{2a\mathrm{F}^-} \Bigg\{ 1 - \frac{1 + \frac{\tilde{\varepsilon}}{4} \ln \delta}{\sqrt{\mathrm{x}^2 - \tilde{\varepsilon}}} \Bigg[1 - \frac{\tilde{\varepsilon}}{8} \Bigg(2(\mathrm{x} - 2) \ln \mathrm{x} - 2(\mathrm{x} - 1) \ln (1 - \mathrm{x}) + 1 - 2\mathrm{x} + \frac{3}{\mathrm{x}} - \frac{(\mathrm{x} - 1)^2}{\mathrm{x}} \sum_{n=1}^{\infty} \frac{\delta^n}{n!} \frac{d\mathrm{S}_n^<}{d\mathrm{x}} \Bigg) \Bigg] \Bigg\}. \tag{5.155}$$

This indicates that the problem emerges in the course of performing the final integration (5.58-5.59). We now introduce a new coordinate:

$$\mathrm{y} = \frac{\mathrm{x}}{1 + \frac{\tilde{\varepsilon}}{4} \ln \delta} \equiv \frac{\mathrm{x}}{\tilde{a}}, \tag{5.156}$$

such that $a\tilde{a}$ can be interpreted as a quantum-corrected version of the constant a. With this substitution, equations (5.154-5.155) take the form:

$$\partial_+ \mathrm{x} = \frac{1}{2a}\left\{1 - \frac{1}{\sqrt{\mathrm{y}^2 - \tilde{\varepsilon}}}\left[1 - \frac{\tilde{\varepsilon}}{8}\left(2(\mathrm{y}-2)\ln\mathrm{y} - 8 + 5\mathrm{y} + \frac{3}{\mathrm{y}}\right.\right.\right.$$
$$\left.\left.\left. -(\mathrm{y}-1)\sum_{n=1}^{\infty}\frac{\delta^n}{n!}\left(\frac{\mathrm{y}-1}{\mathrm{y}}\frac{\mathrm{dS}_n^<}{\mathrm{dy}} - n\mathrm{S}_n^<\right)\right)\right]\right\}, \tag{5.157}$$

$$\partial_- \mathrm{x} = -\frac{1}{2a\mathrm{F}^-}\left\{1 - \frac{1}{\sqrt{\mathrm{y}^2 - \tilde{\varepsilon}}}\left[1 - \frac{\tilde{\varepsilon}}{8}\left(2(\mathrm{y}-2)\ln\mathrm{y} - 2(\mathrm{y}-1)\ln(1-\mathrm{y}) + 1 - 2\mathrm{y} + \frac{3}{\mathrm{y}}\right.\right.\right.$$
$$\left.\left.\left. - \frac{(\mathrm{y}-1)^2}{\mathrm{y}}\sum_{n=1}^{\infty}\frac{\delta^n}{n!}\frac{\mathrm{dS}_n^<}{\mathrm{dy}}\right)\right]\right\}. \tag{5.158}$$

We therefore expect the evaporation dynamics to be determined by the zeroth-order term in $\tilde{\varepsilon}$ in equations (5.157) and (5.158), because the first-order contribution vanishes at $\mathrm{y} = 1$. Hence, we temporarily ignore the $\mathcal{O}(\tilde{\varepsilon})$ term in the square brackets of (5.157), which yields:

$$\partial_+ \mathrm{x}^{(0)} = \frac{1}{2a}\left(1 - \frac{1}{\sqrt{\mathrm{y}^2 - \tilde{\varepsilon}}}\right). \tag{5.159}$$

Next, we introduce a function $\mathcal{J}(\mathrm{x})$ defined implicitly through

$$\tilde{a}\mathcal{J}(\mathrm{y}) = \frac{\sigma^+}{2a}. \tag{5.160}$$

Differentiating (5.160) with respect to σ^+ and substituting (5.159) leads to the following differential equation for $\mathcal{J}$:

$$\frac{\mathrm{d}\mathcal{J}}{\mathrm{dy}} - \frac{\tilde{\varepsilon}}{4}\frac{\sqrt{\mathrm{y}^2 - \tilde{\varepsilon}}}{(1 + \frac{\tilde{\varepsilon}}{4}\mathrm{y})\sqrt{\mathrm{y}^2 - \tilde{\varepsilon}} - 1}\mathcal{J} = \frac{\sqrt{\mathrm{y}^2 - \tilde{\varepsilon}}}{(1 + \frac{\tilde{\varepsilon}}{4}\mathrm{y})\sqrt{\mathrm{y}^2 - \tilde{\varepsilon}} - 1}. \tag{5.161}$$

A solution of (5.161) can then be written as:

$$\mathcal{J}(\mathrm{y}) = -\frac{4}{\tilde{\varepsilon}} + S\exp\left\{\left(\frac{\tilde{\varepsilon}}{4}\tilde{f}(\mathrm{y})\right)\right\}, \tag{5.162}$$

where S is an integration constant to be fixed, and $\tilde{f}(\mathrm{y})$ is defined by:

$$\tilde{f}(\mathrm{y}) = \int \frac{\sqrt{\mathrm{y}^2 - \tilde{\varepsilon}}}{(1 + \frac{\tilde{\varepsilon}}{4}\mathrm{y})\sqrt{\mathrm{y}^2 - \tilde{\varepsilon}} - 1}\mathrm{dy}. \tag{5.163}$$

Upon performing the substitution $\mathrm{z} = \sqrt{\frac{\mathrm{y} - \sqrt{\tilde{\varepsilon}}}{\mathrm{y} + \sqrt{\tilde{\varepsilon}}}}$, the integral (5.163) takes the form

$$\tilde{f} = 8\tilde{\varepsilon}\int \frac{\mathrm{z}^2\mathrm{dz}}{(\mathrm{z}^2 - 1)R(z)}, \tag{5.164}$$

where

$$R(\mathrm{z}) = \mathrm{z}^4 + 2\sqrt{\tilde{\varepsilon}}\left(1 - \frac{\tilde{\varepsilon}^{3/2}}{4}\right)\mathrm{z}^3 - 2\mathrm{z}^2 - 2\sqrt{\tilde{\varepsilon}}\left(1 + \frac{\tilde{\varepsilon}^{3/2}}{4}\right)\mathrm{z} + 1. \tag{5.165}$$

This quartic polynomial can be factorized as

$$R(\mathrm{z}) = (\mathrm{z}^2 + \alpha_1 \mathrm{z} + \beta_1)(\mathrm{z}^2 + \alpha_2 \mathrm{z} + \beta_2). \tag{5.166}$$

The coefficients $\alpha_{1,2}$ and $\beta_{1,2}$ are constrained by

$$\begin{aligned} \alpha_1 + \alpha_2 &= 2\sqrt{\tilde{\varepsilon}}\left(1 - \frac{\tilde{\varepsilon}^{\frac{3}{2}}}{4}\right), \quad \beta_1 + \beta_2 = -2 - \alpha_1\alpha_2, \\ \alpha_1\beta_2 + \alpha_2\beta_1 &= -2\sqrt{\tilde{\varepsilon}}\left(1 + \frac{\tilde{\varepsilon}^{\frac{3}{2}}}{4}\right), \quad \beta_1\beta_2 = 1. \end{aligned} \tag{5.167}$$

Although the system (5.167) can be solved exactly, we instead determine its solution perturbatively up to $\mathcal{O}(\tilde{\varepsilon}^4)$. This yields

$$\begin{aligned} \alpha_1 &= 2\sqrt{\tilde{\varepsilon}}\left(1 - \frac{\tilde{\varepsilon}^{\frac{3}{2}}}{4}\right)\left[1 - \frac{\tilde{\varepsilon}^2}{16}\left(1 + \frac{\tilde{\varepsilon}^{\frac{3}{2}}}{2}\right)\right], \quad \alpha_2 = \frac{\tilde{\varepsilon}^{\frac{5}{2}}}{8}\left(1 + \frac{\tilde{\varepsilon}^{\frac{3}{2}}}{4}\right), \\ \beta_1 &= -1 + \frac{\tilde{\varepsilon}^{\frac{3}{2}}}{2}\left(1 - \frac{\tilde{\varepsilon}^{\frac{3}{2}}}{4} + \frac{\tilde{\varepsilon}^2}{8}\right), \quad \beta_2 = -1 - \frac{\tilde{\varepsilon}^{\frac{3}{2}}}{2}\left(1 + \frac{\tilde{\varepsilon}^{\frac{3}{2}}}{4} + \frac{\tilde{\varepsilon}^2}{8}\right). \end{aligned} \tag{5.168}$$

The corresponding expressions for the roots of the polynomial $R(\mathrm{z})$ are:

$$\mathrm{z}_2^+ = 1 + \frac{\tilde{\varepsilon}^{\frac{3}{2}}}{4} - \frac{\tilde{\varepsilon}^{\frac{5}{2}}}{16} + \frac{\tilde{\varepsilon}^3}{32} + \frac{\tilde{\varepsilon}^{\frac{7}{2}}}{32} - \frac{\tilde{\varepsilon}^4}{64} \tag{5.169}$$

$$\mathrm{z}_2^- = -1 - \frac{\tilde{\varepsilon}^{\frac{3}{2}}}{4} - \frac{\tilde{\varepsilon}^{\frac{5}{2}}}{16} - \frac{\tilde{\varepsilon}^3}{32} - \frac{\tilde{\varepsilon}^{\frac{7}{2}}}{32} - \frac{\tilde{\varepsilon}^4}{64} \tag{5.170}$$

$$\mathrm{z}_1^+ = 1 - \tilde{\varepsilon}^{\frac{1}{2}} + \frac{\tilde{\varepsilon}}{2} - \frac{\tilde{\varepsilon}^{\frac{3}{2}}}{4} + \frac{\tilde{\varepsilon}^2}{8} - \frac{\tilde{\varepsilon}^{\frac{5}{2}}}{16} + \frac{\tilde{\varepsilon}^3}{32} - \frac{\tilde{\varepsilon}^4}{128}, \tag{5.171}$$

$$\mathrm{z}_1^- = -1 - \tilde{\varepsilon}^{\frac{1}{2}} - \frac{\tilde{\varepsilon}}{2} + \frac{\tilde{\varepsilon}^{\frac{3}{2}}}{4} + \frac{3\tilde{\varepsilon}^2}{8} + \frac{3\tilde{\varepsilon}^{\frac{5}{2}}}{16} - \frac{\tilde{\varepsilon}^3}{32} + \frac{5\tilde{\varepsilon}^4}{128}. \tag{5.172}$$

Now the integral (5.164) can be evaluated in a straightforward manner, yielding

$$\begin{aligned} \tilde{f}(\mathrm{z}) =& \frac{4}{\tilde{\varepsilon}} \ln\left|\frac{\mathrm{z}^2 + \alpha_2 \mathrm{z} + \beta_2}{1 - \mathrm{z}^2}\right| + \left(1 - \frac{5}{4}\tilde{\varepsilon}\right)\ln|\mathrm{z} - \mathrm{z}_1^+| - \left(1 - \frac{1}{4}\tilde{\varepsilon}\right)\ln|\mathrm{z} - \mathrm{z}_1^-| \\ &- \left(1 - \frac{3}{4}\tilde{\varepsilon}\right)\ln|\mathrm{z} - \mathrm{z}_2^+| + \left(1 + \frac{3}{4}\tilde{\varepsilon}\right)\ln|\mathrm{z} - \mathrm{z}_2^-| + \frac{\tilde{\varepsilon}}{4}\ln\frac{\tilde{\varepsilon}}{16}. \end{aligned} \tag{5.173}$$

A convenient and consistent choice for the constant S in (5.162) is $S = \frac{4}{\tilde{\varepsilon}} + \frac{9}{2}$, which ensures that the divergent contributions in (5.152) and (5.153) are entirely absorbed into the function $\mathcal{J}(\mathrm{y})$. By expanding $\mathcal{J}$, we obtain

$$\mathcal{J}(\mathrm{y}) = \mathrm{y} + \ln|\mathrm{y}-1| - \frac{\tilde{\varepsilon}}{8}\left[-4\ln \mathrm{y} - (2\mathrm{y}-1)\ln|\mathrm{y}-1| - \ln^2|\mathrm{y}-1| + \frac{2}{\mathrm{y}-1} - 5\mathrm{y}\right] + \frac{9}{2}. \tag{5.174}$$

From (5.174) it follows that the function $\mathcal{J}$ incorporates all divergent terms, including the $\ln\delta$ contribution (after substituting $\mathrm{y} = \frac{\mathrm{x}}{\tilde{a}}$) appearing in (5.152) and (5.153). These equations can therefore be recast in the form:

$$\left(1+\frac{\varepsilon}{4(\lambda a)^2}\ln\delta\right)\mathcal{J}(\mathrm{y})-\frac{\varepsilon}{8(\lambda a)^2}\left[(2\mathrm{y}+3)\ln\mathrm{y}+5\mathrm{y}-2\mathrm{L}(\mathrm{y})-\sum_{n=1}^{\infty}\frac{(1-\delta)^n}{n!}\mathrm{S}_n^{>}(\mathrm{y})\right] \tag{5.175}$$
$$=-\ln\delta+\mathcal{J}(\hat{\mathrm{x}})-\frac{\varepsilon}{8(\lambda a)^2}\left[(2\hat{\mathrm{x}}+3)\ln\hat{\mathrm{x}}+5\hat{\mathrm{x}}-2\mathrm{L}(\hat{\mathrm{x}})\right],\quad \text{when } \mathrm{y}>1$$

$$\left(1+\frac{\varepsilon}{4(\lambda a)^2}\ln\delta\right)\mathcal{J}(\mathrm{y})-\frac{\varepsilon}{8(\lambda a)^2}\left[\frac{2\mathrm{y}^2}{\mathrm{y}-1}\ln\mathrm{y}+3\mathrm{y}-\sum_{n=1}^{\infty}\frac{\delta^n}{n!}\mathrm{S}_{\mathrm{n}}^{<}(\mathrm{y})\right] \tag{5.176}$$
$$=-\ln\delta+\mathcal{J}(\hat{\mathrm{x}})-\frac{\varepsilon}{8(\lambda a)^2}\left[(2\hat{\mathrm{x}}+3)\ln\hat{\mathrm{x}}+5\hat{\mathrm{x}}-2\mathrm{L}(\hat{\mathrm{x}})\right],\quad \text{when } \mathrm{y}<1.$$

Note that both equations are well defined in the vicinity of $\mathrm{y}=1+\mathcal{O}(\tilde{\varepsilon})$, which was the primary objective of this subsection. Next, we determine the general solution under the assumption $\mathrm{y}=1+\frac{\varepsilon}{(\lambda a)^2}\eta$ and $\tilde{a}\gg 0$. This condition yields $\hat{\mathrm{x}}=1+\frac{\varepsilon}{(\lambda a)^2}\mu$. Consequently, both equations (5.175) and (5.176) reduce to:

$$\tilde{a}\mathcal{J}\left(1+\tilde{\varepsilon}\eta\right)=-\ln\delta+\mathcal{J}\left(1+\tilde{\varepsilon}\mu\right). \tag{5.177}$$

Formula (5.177) can be further recast as:

$$\tilde{a}\exp\left\{\left(\frac{\tilde{\varepsilon}}{4}\tilde{f}(1+\tilde{\varepsilon}\eta)\right)\right\}=\exp\left\{\left(\frac{\tilde{\varepsilon}}{4}\tilde{f}(1+\tilde{\varepsilon}\mu)\right)\right\}. \tag{5.178}$$

A detailed analysis of the function $\tilde{f}(\mathrm{z})$ then yields:

$$\tilde{a}^{\frac{4}{\tilde{\varepsilon}}}=\left|\frac{4\mu-1}{4\eta-1}\right|. \tag{5.179}$$

Because the solution is derived only to first order in perturbation theory, we obtain $\tilde{a}^{4/\tilde{\varepsilon}}=\delta$. We expect that this relation will remain valid at higher orders in perturbation theory as well. Under this assumption, Equation (5.179) reduces to:

$$\delta=\left|\frac{4\mu-1}{4\eta-1}\right|. \tag{5.180}$$

Substituting back, yields the following expression:

$$\hat{\mathrm{x}}=1+\frac{\varepsilon}{4(\lambda a)^2}\Big(1+(4\eta-1)\delta\Big). \tag{5.181}$$

Together with (5.157) and (5.158), derivative we give a closed form for the metric derivatives: $\partial_{\pm}\rho$:

$$\partial_+\rho=\frac{1}{4a\tilde{a}}\frac{\mathrm{y}}{(\mathrm{y}^2-\tilde{\varepsilon})^{\frac{3}{2}}}\left\{1+\frac{\tilde{\varepsilon}}{4}\left[(3+2\mathrm{y})\left(1-\frac{1}{\mathrm{y}^2}\right)+2\ln\mathrm{y}\right.\right. \tag{5.182}$$
$$\left.\left.+\frac{1}{2}\sum_{n=1}^{\infty}\frac{\delta^n}{n!}\left(n(1-n\mathrm{y}^2)\mathrm{S}_n^{<}-\frac{\mathrm{y}-1}{\mathrm{y}}(\mathrm{y}^2+\mathrm{y}-1)\frac{\mathrm{dS}_n^{<}}{\mathrm{dy}}\right)\right]\right\},$$

$$\partial_-\rho=-\frac{1}{4a\mathrm{F}^-}\left\{\frac{\hat{\mathrm{x}}^2-1}{\hat{\mathrm{x}}^2}\left(1-\frac{\tilde{\varepsilon}}{4}\mathrm{F}(\hat{\mathrm{x}})\right)-\frac{1}{\tilde{a}}\left(1-\frac{1}{\mathrm{y}^2}\right)\right. \tag{5.183}$$
$$\left.+\frac{\tilde{\varepsilon}}{4\tilde{a}\mathrm{y}^2}\left[(\mathrm{y}^2-1)\left(\ln(1-\mathrm{y})+(2\mathrm{y}-3)\frac{\mathrm{y}^2+2}{2\mathrm{y}^2}\right)+2\ln\mathrm{y}+\frac{(\mathrm{y}^2+1)(\mathrm{y}-1)^2}{2}\sum_{n=1}^{\infty}\frac{\delta^n}{n!}\frac{\mathrm{dS}_n^{<}}{\mathrm{dy}}\right]\right\}.$$

In terms of the function $\mathrm{F}(\hat{\mathrm{x}})$, the coordinate transformation F^{-} can be expressed as:

$$\mathrm{F}^{-}=\frac{\hat{\mathrm{x}}-1}{\hat{\mathrm{x}}}\left[1-\frac{\tilde{\varepsilon}}{4}\left(\mathrm{F}(\hat{\mathrm{x}})+\frac{2\hat{\mathrm{x}}-1}{\hat{\mathrm{x}}^{2}(\hat{\mathrm{x}}-1)}\right)\right]. \tag{5.184}$$

Notice that all these expressions are well defined around the $\mathrm{y}=1$ and $\hat{\mathrm{x}}=1$ hypersurfaces

5.3.4 The end-state of black hole evolution

In the previous subsection, we obtained an evaporating black hole solution generated by collapsing matter. In this subsection, we examine the final state of the black hole's evolution. We adopt the approach described in Section 3.4.1. We first determine the apparent horizon, then analyze the curvature and locate the singularity. Their intersection specifies the end-point of the evaporation. At the conclusion of this subsection, we compute the total energy radiated away from the black hole during its evolution. The apparent horizon is defined by $\partial_{+}e^{-2\phi}=0$, which is equivalent to $\mathrm{x}\partial_{+}\mathrm{x}=0$. Employing formula (5.114), a straightforward calculation gives:

$$\mathrm{x}=1+\frac{\varepsilon}{4(\lambda a)^{2}}\left[\ln\delta+4-(\mathrm{x}-2)\ln\mathrm{x}-\frac{3}{2\mathrm{x}}+\frac{2}{\mathrm{x}^{2}}-\frac{5\mathrm{x}}{2}+\frac{\mathrm{x}-1}{2}\sum_{n=1}^{\infty}\frac{\delta^{n}}{n!}\left(\frac{\mathrm{x}-1}{\mathrm{x}}\frac{\mathrm{dS}_{n}}{\mathrm{dx}}-n\mathrm{S}_{n}\right)\right]. \tag{5.185}$$

Solving Equation (5.185) perturbatively, by choosing ansatz $\mathrm{x}_{AH}=\mathrm{x}_{AH}^{(0)}+\varepsilon\mathrm{x}_{AH}^{(1)}$, we obtain:

$$\mathrm{x}_{AH}=1+\frac{\varepsilon}{4(\lambda a)^{2}}\left(2+\ln\delta\right). \tag{5.186}$$

As time elapses, δ becomes progressively smaller, which correspondingly decreases the apparent horizon. This is precisely the outcome we anticipate. Observe that in computing $\partial_{+}\mathrm{x}$ we have employed expression (5.151). The same expression for the apparent horizon can also be obtained using formula (5.150), given that $\mathrm{x}_{AH}^{(0)}=1$. Adopting the new notation introduced in Section 5.3.3, and setting expression (5.157) equal to zero, the apparent horizon is determined by

$$\mathrm{y}_{AH}=\sqrt{1+\frac{\varepsilon}{(\lambda a)^{2}}}. \tag{5.187}$$

It is straightforward to verify that this relation reproduces the same result as in (5.186). Making use of formula (5.179), the dependence of the apparent horizon on $\hat{\mathrm{x}}(\delta)$ is

$$\hat{\mathrm{x}}_{AH}=1+\frac{\varepsilon}{4(\lambda a)^{2}}\left[1+\left(1+\frac{\varepsilon}{4(\lambda a)^{2}}\ln\delta\right)^{\frac{4(\lambda a)^{2}}{\varepsilon}}\right]. \tag{5.188}$$

Taking the limit $\varepsilon\to 0$ of the expression inside the square brackets, and noting that this term is already of order $\mathcal{O}(\varepsilon)$, we arrive at the following simplified expression for the apparent horizon in the $(\hat{\mathrm{x}},\delta)$ coordinates:

$$\hat{\mathrm{x}}_{AH}(\delta)=1+\frac{\varepsilon}{4(\lambda a)^{2}}(1+\delta). \tag{5.189}$$

The next step is to determine the line of the singularity. To achieve this, we must first compute the scalar curvature (3.3). Employing the equations of motion (5.45-5.46), the curvature can be written in terms of the first derivatives of the dilaton field:

$$R=\frac{2}{a^{2}}\frac{1+4a^{2}e^{-2\rho}\partial_{+}\mathrm{x}\partial_{-}\mathrm{x}}{\mathrm{x}^{2}-\frac{\varepsilon}{(\lambda a)^{2}}}. \tag{5.190}$$

At first glance, Equation (5.190) appears to shift the singularity from $\mathrm{x}_S = 0$ to $\mathrm{x}_S = \frac{\sqrt{\varepsilon}}{\lambda a}$ once quantum corrections are taken into account. If this were indeed the case, it could signal a potential problem for the perturbative treatment. Making use of expression (5.190) together with the recurrence relation (5.108), the scalar curvature can be recast as

$$R = \frac{2}{a^2\mathrm{x}^3}\left\{1 + \frac{\varepsilon}{8(\lambda a)^2}\left[2\ln\mathrm{x} - 3 - \frac{2}{\mathrm{x}} + \frac{15}{\mathrm{x}^2} + 2\mathrm{x} + 2\ln\delta + \frac{(\mathrm{x}-1)^2}{\mathrm{x}}\sum_{n=1}^{\infty}\frac{\delta^n}{n!}\frac{\mathrm{dS}_n(\mathrm{x})}{\mathrm{dx}}\right]\right\}. \tag{5.191}$$

We first examine the beginning of evaporation, $\delta = 1$. Applying the relation (5.126), we obtain

$$R = \frac{2}{a^2\mathrm{x}^3}\left(1 + \frac{3\varepsilon}{2(\lambda a)^2}\frac{1}{\mathrm{x}^2}\right). \tag{5.192}$$

From Equation (5.192), we find that the singularity line admits two distinct solutions:

$$\mathrm{x}_S = 0 \;\text{ and }\; \mathrm{x}_S \approx \sqrt{\frac{3\varepsilon}{2(\lambda a)^2}}. \tag{5.193}$$

Neither of these two solutions matches the expected result $\mathrm{x}_S = \frac{\sqrt{\varepsilon}}{\lambda a}$. This discrepancy may stem from the use of the perturbative approach. Fortunately, one can obtain a non-perturbative expression for the scalar curvature at the beginning of the evaporation. To this end, we solve the equations of motion on the hypersurface $\sigma^+ = \sigma_0^+ + \epsilon,\;\; \epsilon \to 0$. On this hypersurface, the metric is fixed by $e^{2\rho} = 1$, and the dilaton field is given by $\mathrm{x} = \frac{\sigma_0^+ - \sigma^-}{2a}$. This follows from the continuity conditions imposed across the hypersurface. From Equation (5.113) we then find:

$$\mathrm{x}\partial_+\mathrm{x} + \frac{\varepsilon}{(\lambda a)^2}\partial_+\rho = \frac{\mathrm{x}-1}{2a}. \tag{5.194}$$

Using (5.194), one readily verifies that Equation (5.46) holds. Combining (5.45) with (5.194) yields the following differential equation for $\partial_+\rho = f(\mathrm{x}(\sigma^-))$:

$$\frac{\mathrm{d}f}{\mathrm{dx}} = -\frac{1}{2a}\frac{1 + 2a\frac{\varepsilon}{(\lambda a)^2}f}{\mathrm{x}\left(\mathrm{x}^2 - \frac{\varepsilon}{(\lambda a)^2}\right)}. \tag{5.195}$$

The solution of (5.195) is given by:

$$f(\mathrm{x}) = \frac{\lambda^2 a}{2\varepsilon}\left(\frac{Q\mathrm{x}}{\sqrt{\mathrm{x}^2 - \frac{\varepsilon}{(\lambda a)^2}}} - 1\right), \tag{5.196}$$

where Q is an integration constant. By directly comparing (5.196) with the expression for $\partial_+\rho$ obtained from (5.151) in the case $\delta = 1$, we infer that $Q = 1$. Consequently, the solutions for $\partial_\pm\rho$ and $\partial_\pm\mathrm{x}$, together with the condition $\sigma^+ = \sigma_0^+$, take the form:

$$\partial_+\mathrm{x} = \frac{1}{2a}\left(1 - \frac{1}{\sqrt{\mathrm{x}^2 - \frac{\varepsilon}{(\lambda a)^2}}}\right), \qquad \partial_-\mathrm{x} = -\frac{1}{2a}, \tag{5.197}$$

$$\partial_+\rho = \frac{\lambda^2 a}{2\varepsilon}\left(\frac{\mathrm{x}}{\sqrt{\mathrm{x}^2 - \frac{\varepsilon}{(\lambda a)^2}}} - 1\right), \qquad \partial_-\rho = 0. \tag{5.198}$$

The scalar curvature is then given by:

$$R = \frac{2}{a^2}\frac{1}{\left(\mathrm{x}^2 - \frac{\varepsilon}{(\lambda a)^2}\right)^{\frac{3}{2}}}. \tag{5.199}$$

We therefore conclude that, at the beginning of the evaporation, the singularity forms at

$$\mathrm{x}_S = \frac{\sqrt{\varepsilon}}{\lambda a}, \tag{5.200}$$

as anticipated. Restoring all physical constants, this corresponds to $\varphi_S = \sqrt{\frac{\hbar G}{12\pi c^3}}$, which is of the order of the Planck length.

Next, we determine the quantum-corrected expression for the line of singularity given in (5.42). In the y coordinates (defined in Section 5.3.3), the singularity takes the form

$$\mathrm{y}_S = \frac{\sqrt{\varepsilon}}{\lambda a}\frac{1}{1 + \frac{\varepsilon}{4(\lambda a)^2}\ln\delta_S}. \tag{5.201}$$

Substituting (5.201) into Equation (5.176) and expanding the result up to terms of order $\mathcal{O}(\varepsilon)$ yields the following condition for the singularity:

$$\left(1 + \frac{9\varepsilon}{8(\lambda a)^2}\right)\ln\delta_S + \frac{\varepsilon}{8(\lambda a)^2}\sum_{n=1}^{\infty}\frac{\delta_S^n}{n!}\mathrm{S}_n^<(0) = \hat{\mathrm{x}}_S + \ln|\hat{\mathrm{x}}_S - 1| - \frac{\varepsilon}{8(\lambda a)^2}\mathrm{S}_0^>(\hat{\mathrm{x}_S}). \tag{5.202}$$

Thus, Equation (5.202) shows that the singularity (5.42) acquires a quantum correction of order $\mathcal{O}(\varepsilon)$.

The end-point of the evaporation

According to the cosmic censorship conjecture [106], a naked singularity cannot result from gravitational collapse. In contrast, the two hypersurfaces $\mathrm{y}_{AH}(\delta)$ (5.187) and $\mathrm{y}_S(\delta)$ (5.201) intersect at a finite value of the coordinate δ, determined by $\tilde{a}_E = \frac{\sqrt{\varepsilon}}{\lambda a}$. The corresponding point marks the end-point of evaporation, and is given by:

$$\sigma_E^+ = \sigma_0^+ + \frac{8a(\lambda a)^2}{\varepsilon}\left(1 - \frac{\sqrt{\varepsilon}}{\lambda a}\right). \tag{5.203}$$

If we now substitute all constants, expression (5.203) can be rewritten as

$$\sigma_E^+ = \sigma_0^+ + \frac{768\pi M^3 G^2}{\hbar\lambda^4}\left(1 - \frac{\lambda}{4M}\sqrt{\frac{\hbar}{3\pi G}}\right). \tag{5.204}$$

Equation (5.204) shows that the leading contribution to the black hole evaporation time scales as M^3, which agrees with the standard thermodynamic estimate and coincides with the result obtained in [115]. It is convenient to rewrite the evaporation end-point in terms of the δ coordinate:

$$\delta_E = e^{-\frac{4(\lambda a)^2}{\varepsilon}\left(1-\frac{\sqrt{\varepsilon}}{\lambda a}\right)}. \tag{5.205}$$

The quantity (5.205) is extremely small, $\delta_E \ll \frac{\varepsilon}{4(\lambda a)^2}$. Conversely, $\ln\delta_E$ is very large, scaling as $1/\varepsilon$. This indicates that the perturbative expansion ceases to be reliable at this stage.

Nevertheless, by proceeding with care we can still extract meaningful information. To determine the exact location of the evaporation end-point, besides δ_E we must also compute $\hat{\mathrm{x}}_E$. From $\mathrm{y}_E = \mathrm{y}_{AH} = 1 + \frac{\varepsilon}{2(\lambda a)^2}$, we infer that $\hat{\mathrm{x}}_E = 1 + \mathcal{O}(\varepsilon)$. Employing (5.180), the second coordinate of the evaporation end-point is

$$\hat{\mathrm{x}}_E = 1 + \frac{\varepsilon}{4(\lambda a)^2}\left[1 + e^{-\frac{4(\lambda a)^2}{\varepsilon}\left(1-\frac{\sqrt{\varepsilon}}{\lambda a}\right)}\right]. \tag{5.206}$$

Formula (5.206) can equivalently be obtained by using (5.189) and setting $\delta = \delta_E$. Observe that the end-point exhibits the same type of singular behavior as in the BPP model (4.124).

Finally, we discuss the location of the black hole's event horizon, which is determined by $\hat{\mathrm{x}} = \hat{\mathrm{x}}_E$. We expect it to form for $\mathrm{x} < 1$, but initially to lie very close to the $\mathrm{x} = 1$ hypersurface at the beginning of the evaporation. Subsequently, it should gradually move inward until it meets the singularity. To obtain the horizon curve $\mathrm{y}_H(\delta)$, we return to Equation (5.179), which yields

$$\mathrm{y}_H = 1 + \frac{\varepsilon}{4(\lambda a)^2}\left[1 + \left(\frac{\tilde{a}_E}{\tilde{a}_H}\right)^{\frac{4(\lambda a)^2}{\varepsilon}}\right]. \tag{5.207}$$

Observe that in the limit $\tilde{a}_H \to \tilde{a}_E$, expression (5.207) simplifies to $\mathrm{y}_H = \mathrm{y}_{AH}$, as anticipated. It is now straightforward to determine x_H, which is given by

$$\mathrm{x}_H = \left(1 + \frac{\varepsilon}{4(\lambda a)^2}\ln\delta_H\right)\left[1 + \frac{\varepsilon}{4(\lambda a)^2}\left(1 + \frac{\delta_E}{\delta_H}\right)\right]. \tag{5.208}$$

Using Equation (5.190) along the apparent horizon hypersurface, we obtain the non-perturbative expression for the scalar curvature:

$$R_{AH} = \frac{2}{a^2}\frac{1}{\mathrm{x}^2 - \frac{\varepsilon}{(\lambda a)^2}}. \tag{5.209}$$

A perturbative counterpart of this result can also be derived starting from (5.191), which can be recast as

$$R = \frac{2}{a^2}\frac{1}{\mathrm{x}^2 - \frac{\varepsilon}{(\lambda a)^2}}\frac{1}{\sqrt{\mathrm{y}^2 - \frac{\varepsilon}{(\lambda a)^2}}}\left\{1 + \frac{\varepsilon}{4(\lambda a)^2}\left[\ln\mathrm{y} + \frac{(\mathrm{y}^2-1)(2\mathrm{y}-3)}{2\mathrm{y}^2} + \frac{(\mathrm{y}-1)^2}{2\mathrm{y}}\sum_{n=1}^{\infty}\frac{\delta^n}{n!}\frac{\mathrm{dS}_n^<}{\mathrm{dy}}\right]\right\}, \tag{5.210}$$

and, upon inserting (5.187), this expression reduces to (5.209), as required.

The radiated energy

We now evaluate the total energy radiated by the black hole over its entire lifetime. It is given by (3.115):

$$E_{rad} = -\frac{\varepsilon}{G}\int_{-\infty}^{\sigma_E^-}\frac{\mathrm{d}\sigma^-}{\mathrm{F}^-}t_-(\hat{\sigma}^-) = -\frac{\varepsilon}{8aG}\mathrm{F}(\hat{\mathrm{x}}_E). \tag{5.211}$$

Because the Schwarzschild radius λa scales linearly with the mass, it can serve as an energy measure. Accordingly, we can associate the quantity $\lambda a_{rad} = \frac{2E_{rad}G}{\lambda}$ with the radiated energy. Thus, λa_{rad} takes the form:

$$\lambda a_{rad} = -\frac{\varepsilon}{4\lambda a}\mathrm{F}(\hat{\mathrm{x}}_E). \tag{5.212}$$

The function $\mathrm{F}(\hat{\mathrm{x}})$ becomes ill-defined in the limit $\hat{\mathrm{x}} \to 1$. This is precisely the kind of issue discussed in Section 5.3.3. To address it, one needs to compute the first-order correction to $\mathrm{F}(\hat{\mathrm{x}})$:

$$\mathrm{F}(\hat{\mathrm{x}}) = -2\frac{\mathrm{dF}^-}{\mathrm{d}\hat{\mathrm{x}}} + \int \frac{\mathrm{d}\hat{\mathrm{x}}}{\mathrm{F}^-}\left(\frac{\mathrm{dF}^-}{\mathrm{d}\hat{\mathrm{x}}}\right)^2. \tag{5.213}$$

Using Equation (5.176), we find:

$$\frac{1}{\mathrm{F}^-} = \frac{\mathrm{d}\mathcal{J}}{\mathrm{d}\hat{\mathrm{x}}} - \frac{\varepsilon}{8(\lambda a)^2}\left(\frac{2\hat{\mathrm{x}}}{\hat{\mathrm{x}}-1}\ln\hat{\mathrm{x}} + \frac{3}{\hat{\mathrm{x}}} + 7\right), \tag{5.214}$$

$$\frac{\mathrm{dF}^-}{\mathrm{d}\hat{\mathrm{x}}} = -\mathrm{F}^{-2}\left[\frac{\mathrm{d}^2\mathcal{J}}{\mathrm{d}\hat{\mathrm{x}}^2} + \frac{\varepsilon}{8(\lambda a)^2}\left(\frac{3}{\hat{\mathrm{x}}^2} + 2\frac{\ln\hat{\mathrm{x}}-1}{\hat{\mathrm{x}}-1}\right)\right]. \tag{5.215}$$

Since the terms of order $\mathcal{O}(\varepsilon)$ remain regular as $\hat{\mathrm{x}} \to 1$, they can be discarded. After changing variables to z (as defined in (5.164)), the upper integration limit becomes 1, while the lower limit becomes $\mathrm{z}_E = \mathrm{z}_1^+ + \left(\frac{\sqrt{\varepsilon}}{\lambda a}\right)^3 \frac{\delta_E}{4}$, where z_1^+ is given in (5.171). The integral now extends over a narrow interval around $\mathrm{z} = 1$, which allows us to set $\mathrm{z} = 1$ wherever this does not affect the well-definedness of the integrand. The integral then takes the form:

$$\int_\infty^{\hat{\mathrm{x}}_E} \frac{\mathrm{d}\hat{\mathrm{x}}}{\mathrm{F}^-}\left(\frac{\mathrm{dF}^-}{\mathrm{d}\hat{\mathrm{x}}}\right)^2 = -\frac{4(\lambda a)^4}{\varepsilon^2}\int_{\mathrm{z}_E}^1 \frac{(1-\mathrm{z})^4\mathrm{dz}}{(\mathrm{z}-\mathrm{z}_1^+)(\mathrm{z}-\mathrm{z}_2^+)^2}. \tag{5.216}$$

A straightforward evaluation up to order $\mathcal{O}(1)$ yields the following expression for $\mathrm{F}(\hat{\mathrm{x}}_E)$:

$$\mathrm{F}(\hat{\mathrm{x}}_E) = -\frac{4(\lambda a)^2}{\varepsilon} + \frac{8(\lambda a)}{\sqrt{\varepsilon}} + \ln\frac{\varepsilon}{4(\lambda a)^2} + \frac{3}{2}. \tag{5.217}$$

Hence, the radiated energy (5.211) is:

$$E_{rad} = Mc^2\left[1 - \sqrt{\frac{\hbar c}{12\pi M^2 G_N}} - \frac{\hbar c}{192\pi M^2 G_N}\left(\ln\frac{\hbar c}{192\pi M^2 G_N} + \frac{3}{2}\right) + o\left(\frac{\hbar c}{M^2 G_N}\right)\right], \tag{5.218}$$

where we have reinstated all physical constants. Equation (5.218) shows that, during evaporation, nearly the entire initial mass of the black hole is radiated away, leaving only a small remnant of order $\sqrt{\varepsilon}$. This agrees with the results obtained in the RST and BPP dilaton gravity models [23, 24, 25].

5.3.5 The end-state geometry

Having already determined both the evaporation end-point and the total radiated energy in the previous subsection, the final element from Section 3.4.1 that remains to be examined is the geometry of region III of the spacetime (see Figure 3.3). As in the BPP model, analyzing the late-time geometry within the perturbative scheme is difficult because the approximation fails close to the evaporation end-point. Nevertheless, we can still attempt to extract useful information by rewriting the Schwarzschild radius in terms of the $\hat{\mathrm{x}}$ coordinate, rather than the δ coordinate, following the procedure outlined in Section 3.4.1.

We start by evaluating $\mathrm{F}(\hat{\mathrm{x}})$, as defined in formula (5.100), in terms of x and δ. Applying the same procedure as in theorem 1, we obtain

$$\mathrm{F}(\hat{\mathrm{x}}) = \mathrm{F}(\mathrm{x}) + \sum_{n=1}^{\infty}\frac{(\delta-1)^n}{n!}\frac{\partial^n\mathrm{F}(\hat{\mathrm{x}})}{\partial\delta^n}\bigg|_{\delta=1}. \tag{5.219}$$

Following the method used in theorem 5, we derive

$$\left.\frac{\partial^n \mathrm{F}(\hat{\mathrm{x}})}{\partial \delta^n}\right|_{\delta=1} = e^{n\mathrm{x}}(\mathrm{x}-1)^n \left(\frac{e^{-\mathrm{x}}}{\mathrm{x}}\frac{\mathrm{d}}{\mathrm{dx}}\right)^{n-1} \frac{e^{-\mathrm{x}}}{\mathrm{x}}\frac{\mathrm{dF}(\mathrm{x})}{\mathrm{dx}}. \tag{5.220}$$

Independently, one can show by induction that the following identity holds:

$$\left.\frac{\partial^n \mathrm{F}(\hat{\mathrm{x}})}{\partial \delta^n}\right|_{\delta=1} = (-1)^n \left[\frac{1}{2}\frac{(\mathrm{x}-1)^2}{\mathrm{x}}\frac{\mathrm{dS}_n^>(\mathrm{x})}{\mathrm{dx}} - (n-1)!\right]. \tag{5.221}$$

The inductive step reduces to the recurrence relation for the functions $\mathrm{S}_n^>(\mathrm{x})$ given in (5.108). Substituting this form of $\frac{\partial^n \mathrm{F}(\hat{\mathrm{x}})}{\partial \delta^n}|_{\delta=1}$ into the series (5.219), we obtain:

$$\mathrm{F}(\hat{\mathrm{x}}) = \mathrm{F}(\mathrm{x}) + \ln\delta + \frac{(\mathrm{x}-1)^2}{2\mathrm{x}}\sum_{n=1}^{\infty}\frac{(1-\delta)^2}{n!}\frac{\mathrm{dS}_n^>(\mathrm{x})}{\mathrm{dx}}. \tag{5.222}$$

Using Equation (5.222), we remove the $\ln\delta$ contribution from the expressions for the metric (5.150) and for the tortoise coordinate $\hat{\sigma}$ (5.152), which leads to:

$$\begin{aligned}\mathrm{F}^+\mathrm{F}^- e^{2\rho} = \frac{1+\frac{\varepsilon}{4(\lambda a)^2}\mathrm{F}(\hat{\mathrm{x}})}{\mathrm{x}} - 1 + \frac{\varepsilon}{4(\lambda a)^2}\Bigg[&\frac{\mathrm{x}-2}{\mathrm{x}}\ln\frac{\mathrm{x}-1}{\mathrm{x}} + \frac{1}{\mathrm{x}} - \frac{3}{2}\frac{1}{\mathrm{x}^2} + \frac{2}{\mathrm{x}^3}\\ &+\frac{\mathrm{x}-1}{2\mathrm{x}}\sum_{n=1}^{\infty}\frac{(1-\delta)^n}{n!}\left(\mathrm{S}_{n+1}^>(\mathrm{x}) - n\mathrm{S}_n^>(\mathrm{x}) + z_{n+1} - nz_n\right)\Bigg],\end{aligned} \tag{5.223}$$

$$\begin{aligned}\frac{\hat{\sigma}}{a} = \mathrm{x} &+ \left(1+\frac{\varepsilon}{4(\lambda a)^2}\mathrm{F}(\hat{\mathrm{x}})\right)\ln\left(\frac{\mathrm{x}}{1+\frac{\varepsilon}{4(\lambda a)^2}\mathrm{F}(\hat{\mathrm{x}})} - 1\right)\\ &- \frac{\varepsilon}{8(\lambda a)^2}\left[\mathrm{S}_0^>(\mathrm{x}) - \frac{\pi^2}{3} - 2 - 2\left(\frac{\mathrm{x}}{\mathrm{x}-1} - \ln(\mathrm{x}-1)\right)\mathrm{F}(\mathrm{x}) - 9\ln\delta\right]\\ &+ \frac{\varepsilon}{8(\lambda a)^2}\sum_{n=1}^{\infty}\frac{(1-\delta)^n}{n!}\left[\mathrm{S}_n^>(\mathrm{x}) + z_n + \frac{(\mathrm{x}-1)^2}{\mathrm{x}}\left(\frac{\mathrm{x}}{\mathrm{x}-1} - \ln(\mathrm{x}-1)\right)\frac{\mathrm{dS}_n^>(\mathrm{x})}{\mathrm{dx}}\right].\end{aligned} \tag{5.224}$$

In (5.223) and (5.224), the factor $\varphi/\lambda a$ has, to zeroth order in ε, been replaced by $\varphi/\left(\lambda a + \frac{\varepsilon}{4\lambda a}\mathrm{F}(\hat{\mathrm{x}})\right)$. We now introduce a new running Schwarzschild radius, depending on the coordinate σ^-:

$$\lambda\hat{a}(\hat{\mathrm{x}}) = \lambda a + \frac{\varepsilon}{4\lambda a}\mathrm{F}(\hat{\mathrm{x}}). \tag{5.225}$$

To first order in ε, $\lambda\hat{a}$ coincides with λa, which means that in all expressions for the metric and dilaton we may replace λa by $\lambda\hat{a}$.

To analyze the final state of evaporation, we must first determine the behavior along the hypersurface $\hat{\mathrm{x}} = \hat{\mathrm{x}}_E$ for $\delta < \delta_E$. On this hypersurface, $\lambda\hat{a}(\hat{\mathrm{x}}_E)$ is fixed. Since $\mathrm{F}(\hat{\mathrm{x}}_E) \sim \ln\delta_E$, Equation (5.217) leads to $\lambda\hat{a} = \mathcal{O}(\sqrt{\varepsilon})$, which, within first-order perturbation theory, effectively gives $\lambda\hat{a} = 0$. Taking this limit is analogous to the $\mathrm{x}\to\infty$ limit discussed in the previous subsection. From the behavior of $\mathrm{S}_n^>(\mathrm{x})$ given in (5.130), we obtain:

$$\mathrm{S}_n^>(\mathrm{x}) = (n-1)!\mathrm{S}_1^>(\mathrm{x}) - z_n + \mathcal{O}((\lambda\hat{a})^4). \tag{5.226}$$

In the metric Equation (5.223), the first-order correction then vanishes in the limit $\lambda\hat{a}\to 0$, because the sum scales as $\mathcal{O}((\lambda\hat{a})^2)$, while the δ–independent part is of order $\mathcal{O}(\lambda\hat{a})$. We next consider the first-order term in ε in the dilaton Equation (5.224) and again take the $\lambda\hat{a} \to 0$ limit. In this regime, the δ–dependent contribution becomes

$$\frac{\lambda\hat{a}\ln\delta}{(\lambda\hat{a})^2}\left[\mathrm{S}_1^> + \frac{(\mathrm{x}-1)^2}{\mathrm{x}}\left(\frac{\mathrm{x}}{\mathrm{x}-1} - \ln(\mathrm{x}-1)\right)\frac{d\mathrm{S}_1^>}{d\mathrm{x}} - 9\right]. \tag{5.227}$$

This term also disappears in the $\lambda\hat{a} \to 0$ limit, which can be seen by expanding in powers of $\lambda\hat{a}$ and then sending $\lambda\hat{a} \to 0$. A crucial point is that $\ln\delta$ scales as $1/\lambda\hat{a}$, so that the product $\lambda\hat{a}\ln\delta$ remains finite. The δ–independent terms vanish in essentially the same manner as in the $\mathrm{x} \to \infty$ limit. Performing this limit yields the following final results:

$$\mathrm{F}^+\mathrm{F}^- e^{2\rho} = \frac{\lambda\hat{a}_E}{\varphi} - 1, \tag{5.228}$$

$$\varphi + \lambda\hat{a}_E \ln\left(\frac{\varphi}{\lambda\hat{a}_E}\right) = \lambda\hat{\sigma}. \tag{5.229}$$

Since $\lambda\hat{a}_E = \lambda\hat{a}(\hat{\mathrm{x}}_E)$ is of order $\mathcal{O}(\sqrt{\varepsilon})$, equations (5.228) and (5.229) describe a quantum-corrected Minkowski spacetime, as discussed in section 5.2.2. This is encouraging, because we expect the final state to be free of energy fluxes at infinity. The next task is to smoothly match this solution to the vacuum solution along $\hat{\mathrm{x}} = \hat{\mathrm{x}}_E$. This matching has to be performed so that no new coordinate discontinuities are introduced, which implies that the final solution has the form $(\mathrm{F}^+, \mathrm{F}^-, a_f)$, where $\mathrm{F}^\pm$ agree with the coordinate transformations of the evaporating black hole, and a_f is a new constant. Further details are provided in Section 3.4.1.

By analogy with the BPP and RST models of dilaton gravity discussed in Chapter 4, one might anticipate the appearance of a shockwave at the end-point of the evaporation known as a thunderpop. To determine whether such a feature arises in the DREH model, one must smoothly join regions II and III (Figure 3.3) across the $\sigma^- = \sigma_E^-$ hypersurface by integrating the "$--$" component of Equation (5.44):

$$e^{-2\rho}\partial_-\varphi_> - e^{-2\rho}\partial_-\varphi_< = -\frac{\lambda}{2\mathrm{F}^-}\lambda a_0\varphi^{-1}e^{-2\rho} - \varepsilon(\partial_-\rho_> - \partial_-\rho_<)\varphi^{-1}e^{-2\rho}, \tag{5.230}$$

where $\lambda a_0 = \frac{2\Delta MG}{\lambda}$ denotes the mass carried by the shockwave at the end of evaporation, the symbol "$<$" refers to the portion of spacetime with $\sigma^- < \sigma_E^-$, and "$>$" to the portion with $\sigma^- > \sigma_E^-$. The derivatives in (5.230) are readily obtained from equations (5.150) and (5.152) in the region $\sigma^+ < \sigma_0^+$. They are:

$$\partial_-\varphi_< = -\frac{\lambda}{2\mathrm{F}^-}\left\{1 - \frac{\lambda\hat{a}(\hat{\mathrm{x}})}{\sqrt{\varphi^2-\varepsilon}}\left[1 - \frac{\varepsilon}{4(\lambda a)^2}\left((2-\mathrm{x})\mathrm{F}(\mathrm{x}) - \frac{2}{\mathrm{x}} + \frac{3}{\mathrm{x}^2}\right)\right]\right\}, \tag{5.231}$$

$$\partial_-\rho_< = -\frac{1}{2}\partial_-\ln\mathrm{F}^- - \frac{\lambda}{4\mathrm{F}^-}\frac{\lambda\hat{a}(\hat{\mathrm{x}})}{\varphi^2}\left[1 - \frac{\varepsilon}{2(\lambda a)^2}\mathrm{F}(\mathrm{x})\right]. \tag{5.232}$$

Using the expressions (5.70) and (5.71) for the static configuration analyzed in section 5.2.2, we compute the derivatives in the domain $\sigma^- > \sigma_E^-$. These derivatives match (5.231-5.232) upon replacing $\hat{a}$ with a_f. This supports the conclusion that the final state is precisely the static solution presented in section 5.2.2. In direct analogy with equations (5.224-5.223), for $\hat{\mathrm{x}} = \hat{\mathrm{x}}_E$ we take the limit $\lambda\hat{a} \to 0$ to first order in perturbation theory. Under this limit, equations (5.231-5.232) simplify to:

$$\partial_-\varphi_< = -\frac{\lambda}{2\mathrm{F}^-}\left(1 - \frac{\lambda\hat{a}_E}{\varphi}\right), \tag{5.233}$$

$$\partial_-\rho_< = -\frac{1}{2}\partial_-\ln\mathrm{F}^- - \frac{\lambda}{4\mathrm{F}^-}\frac{\lambda\hat{a}_E}{\varphi^2}, \tag{5.234}$$

whereas in the region $\sigma^- > \sigma_E^-$ we find:

$$\partial_- \varphi_> = -\frac{\lambda}{2\mathrm{F}^-}\left(1 - \frac{\lambda a_f}{\varphi}\right), \tag{5.235}$$

$$\partial_- \rho_> = -\frac{1}{2}\partial_- \ln \mathrm{F}^- - \frac{\lambda}{4\mathrm{F}^-}\frac{\lambda a_f}{\varphi^2}. \tag{5.236}$$

Substituting (5.233-5.236) into (5.230) yields the following energy-balance relation:

$$\lambda a_{rad} = \lambda(a - a_f) - \lambda a_0, \tag{5.237}$$

where, using Equation (5.211), we identify $\lambda a_{rad} = \frac{2E_{rad}G}{\lambda} = -\frac{\varepsilon}{4\lambda a}\mathrm{F}(\hat{\mathrm{x}}_E)$. It is thus evident that energy is conserved: the initial mass of the infalling matter, λa, equals the sum of the radiated energy λa_{rad}, the mass of the residual spacetime λa_f, and the energy carried by the thunderpop λa_0.

Since no further coordinate transformation is permitted as the $\hat{\mathrm{x}} = \hat{\mathrm{x}}_E$ hypersurface is crossed, continuity of the metric and the dilaton field, enforced by equations (5.228-5.229), implies that the mass parameter of the final geometry must satisfy $\lambda a_f = \lambda \hat{a}_E$. When this is combined with the energy balance condition (5.237), it follows that there is no thunderpop at the end-point of the evaporation process, i.e. $\lambda a_0 = 0$. This result is valid within a perturbative analysis to first order in ε.

Another important issue to emphasize is that the asymptotically flat solution described in section 5.2.2 develops a curvature singularity already at first order in the perturbative expansion. This behavior is similar to what occurs in the BPP and RST models (Section 4.3.3). As in those cases, one must therefore impose reflective boundary conditions at the hypersurface where the singularity appears.

In conclusion, the final geometry coincides with one of the static, quantum-corrected Minkowski vacuum configurations from section 5.2.2, specified by $t_\pm(\hat{\sigma}^\pm) = 0$. Thus, even though the asymptotically flat coordinates remain continuous across the $\hat{\mathrm{x}} = \hat{\mathrm{x}}_E$ hypersurface and no thunderpop arises at the end of evaporation, the quantum state still undergoes a transition from $|0, \sigma\rangle$ to $|0, \hat{\sigma}\rangle$.

It should be emphasized that we do not know the exact structure of the ε correction to the metric in the $\lambda \hat{a}_E$ term in (5.228), because at this stage perturbation theory ceases to be reliable and higher-order contributions may affect the first-order terms. In particular, there may be an extra contribution beyond $-\frac{\varepsilon}{4\lambda a}\mathrm{F}(\hat{\mathrm{x}}_E)$. The presence of such a term would generate a non-vanishing thunderpop. To clarify this issue, one would require either a non-perturbative solution that captures the end-point of evaporation, or a numerical analysis of the equations of motion (5.44–5.46). However, this uncertainty does not affect the derivation of the energy balance relation (5.237).

Chapter 6

Dimensionally-reduced 5DCS gravity: Riemannian sector

In this chapter, we study the Riemannian sector of the dimensionally-reduced theory of five-dimensional Chern–Simons gravity (DR5DCS). Our analysis follows the same methodological framework as that employed for the CGHS model in Chapter 4 and for the DREH model in Chapter 5. Analogously to the DREH model, we demonstrate that the DR5DCS model does not admit exactly solvable equations of motion once quantum corrections are included. Thus, we resort to the perturbative treatment like in the analysis of the DREH model. The action in the Riemannian sector is obtained in Section 2.2.2 and is explicitly presented in (2.25). For convenience, we rewrite it here:

$$
\begin{aligned}
S_{\mathrm{DR5DCS-R}} =& \frac{k\pi^2}{(\lambda l)^3}\int \mathrm{d}x^2\sqrt{-g}e^{-3\phi}\Big[R\left(1+3(\lambda l)^2 e^{2\phi}\right) \\
&+6\left((\nabla\phi)^2+\lambda^2 e^{2\phi}\right)+\frac{6}{l^2}+3l^2(\nabla\phi)^2\left(\Box\phi-(\nabla\phi)^2\right)\Big]-\frac{1}{2}\int d^2x\sqrt{-g}\,(\nabla f)^2\,,
\end{aligned}
\tag{6.1}
$$

For simplicity, we introduce the constant prefactor of the action as $a=\frac{k\pi^2}{(\lambda l)^3}$. The first term in (5.1) encodes the gravitational action, denoted by S_g, whereas the second term accounts for the matter sector, modeled here as a single scalar field, labeled S_m. The key difference here is the emergence of terms containing four derivatives of the dilaton field, which originate from the Gauss–Bonnet contribution in the full five-dimensional theory.

The chapter is organized into three sections. In the first, we examine the classical theory and demonstrate that the most general vacuum solution of the classical equations of motion corresponds to the dimensionally reduced BTZ black hole. We then analyze the classical gravitational collapse and determine how the spacetime mass depends on the integration constants appearing in the general solution. In the final subsection, we construct in detail the Penrose diagram corresponding to this collapse scenario.

The second section introduces the quantum corrections via the Polyakov-Liouville action. Since the resulting equations of motion cannot be solved exactly, we adopt the perturbative approach outlined in Section 3.4.1, derive the general quantum-corrected solution, and examine the static configurations that mimic the empty AdS spacetime. As in the BPP model, the AdS vacuum ceases to be a fluxless solution once the quantum corrections are included, so we obtain the quantum-corrected AdS spacetime. The final subsection then explores the eternal black hole scenario.

The final section addresses the evaporating black hole scenario. We construct the quantum-corrected collapse model by matching the quantum-corrected AdS spacetime to the evaporating black hole solution. Next, we determine the final state of the evaporation and analyze the geometry of the final spacetime. We demonstrate that it is once again a quantum-correctedagain an AdS spacetime with a particular mass constant. Within first-order perturbation theory the thunderpop does not appear; however, when the solution is computed to higher orders in $\hbar$, one should obtain a non-vanishing mass for the thunderpop.

6.1 Classical equations of motion and their solutions

In this section, we examine the equations of motion, derive and analyze their solutions, and discuss selected thermodynamic properties within the Riemannian sector of the full theory of dimensionally-reduced 5DCS theory. We begin by deriving the general vacuum solution. It is found that the vacuum sector exhibits two distinct branches. We demonstrate that one branch corresponds to the dimensionally-reduced BTZ black hole [78, 116], whereas the other branch yields a family of solutions characterized by an arbitrary function. Consequently, the solution within the first branch is analogous to the Birkhoff-type configuration discussed in Chapter 5, in the sense that the most general solution in this branch is static. At the end of this section, we formulate the classical gravitational collapse scenario.

We begin by varying the the gravitational part of action (6.1) with respect to the metric:

$$\begin{aligned}\delta^{(g)} S_g = a \int \mathrm{d}^2x\sqrt{-g}e^{-3\phi}\Big\{ & 3\left[2 + l^2\left(\Box\phi - 2\left(\nabla\phi\right)^2\right)\right]\nabla_\mu\phi\nabla_\nu\phi\delta g^{\mu\nu} + 3l^2\left(\nabla\phi\right)^2\nabla_\mu\nabla_\nu\phi\delta g^{\mu\nu} \\ & - 3\left[\left((\nabla\phi)^2 + \lambda^2 e^{2\phi}\right) + \frac{1}{l^2} + \frac{l^2}{2}(\nabla\phi)^2\left(\Box\phi - (\nabla\phi)^2\right)\right] g_{\mu\nu}\delta g^{\mu\nu} \\ & + \underbrace{\left(1 + 3(\lambda l)^2 e^{2\phi}\right) g^{\mu\nu}\delta R_{\mu\nu}}_{A} - \underbrace{3l^2\left(\nabla\phi\right)^2 g^{\mu\nu}\partial_\rho\phi\delta\Gamma^\rho_{\mu\nu}}_{B}\Big\}. \end{aligned} \tag{6.2}$$

The only remaining terms to be varied in (6.2) are A and B in the last line. The term A has the same form as in the CGHS case and is therefore obtained from (4.9) by performing the replacement $e^{-2\phi} \mapsto e^{-3\phi} + 3(\lambda l)^2 e^{-\phi}$, namely:

$$A = a\int \mathrm{d}^2x\sqrt{-g}\Big[-\nabla_\mu\nabla_\nu\left(e^{-3\phi} + 3(\lambda l)^2 e^{-\phi}\right) + g_{\mu\nu}\Box\left(e^{-3\phi} + 3(\lambda l)^2 e^{-\phi}\right)\Big]\delta g^{\mu\nu}. \tag{6.3}$$

To compute the term B in (6.2) we move to the locally-flat reference frame (LFRF) defined in (4.7):

$$\begin{aligned} B\Big|_{LFRF} &= -\frac{3al^2}{2}\int \mathrm{d}^2x e^{-3\phi}(\partial\phi)^2\eta^{\mu\nu}\partial_\rho\phi\eta^{\lambda\rho}\Big[\partial_\mu\left(\delta g_{\lambda\nu}\right) + \partial_\nu\left(\delta g_{\lambda\mu}\right) - \partial_\lambda\left(\delta g_{\mu\nu}\right)\Big] \\ &= -\frac{3al^2}{2}\int \mathrm{d}^2x e^{-3\phi}(\partial\phi)^2\partial_\rho\phi\Big[2\eta^{\gamma\alpha}\eta^{\rho\beta} - \eta^{\alpha\beta}\eta^{\rho\gamma}\Big]\partial_\gamma\left(\delta g_{\alpha\beta}\right) \\ &= -3al^2\int \mathrm{d}^2x\Big[\partial_\mu\left(e^{-3\phi}(\partial\phi)^2\partial_\nu\phi\right) - \frac{1}{2}\eta_{\mu\nu}\partial_\rho\left(e^{-3\phi}(\partial\phi)^2\partial^\rho\phi\right)\Big]\delta g^{\mu\nu}. \end{aligned} \tag{6.4}$$

Once more, by applying the identification (4.7), we lift the term B from the locally flat reference frame (6.4) back to a general Riemannian manifold. The resulting expression is:

$$B = -3al^2\int \mathrm{d}^2x\sqrt{-g}\Big[\nabla_\mu\left(e^{-3\phi}(\nabla\phi)^2\nabla_\nu\phi\right) - \frac{1}{2}\eta_{\mu\nu}\nabla_\rho\left(e^{-3\phi}(\nabla\phi)^2\nabla^\rho\phi\right)\Big]\delta g^{\mu\nu}. \tag{6.5}$$

After substituting both terms A and B from (6.3) and (6.5), respectively, and performing algebraic manipulations, we obtain the following equation of motion for the metric field:

$$\begin{aligned}&\left[1+(\lambda l)^2e^{2\phi}-l^2\left(\Box\phi+(\nabla\phi)^2\right)\right]\nabla_\mu\phi\nabla_\nu\phi-\left[1+(\lambda l)^2e^{2\phi}\right]\nabla_\mu\nabla_\nu\phi\\&+\frac{l^2}{2}\left[\nabla_\mu\phi\nabla_\nu\left(\nabla\phi\right)^2+\nabla_\nu\phi\nabla_\mu\left(\nabla\phi\right)^2\right]+\left[\Box\phi-2(\nabla\phi)^2+\lambda^2e^{2\phi}+\frac{1}{l^2}\right]g_{\mu\nu}\\&+l^2\left[(\nabla\phi)^4+\left(\Box\phi-(\nabla\phi)^2\right)\lambda^2e^{2\phi}-\frac{1}{2}\nabla_\rho\phi\nabla^\rho\left(\nabla\phi\right)^2\right]=-\frac{(\lambda l)^3}{6k\pi^2}T_{\mu\nu}e^{3\phi},\end{aligned}\tag{6.6}$$

where $T_{\mu\nu}=\frac{-2}{\sqrt{-g}}\frac{\delta S_{\text{mat}}}{\delta g^{\mu\nu}}$ is the energy-momentum tensor of matter fields. Next, we vary the action (6.1) with respect to the dilaton field:

$$\begin{aligned}\delta^{(\phi)}S_g=-3a\int \mathrm{d}^2x\sqrt{-g}e^{-3\phi}\Bigg\{&\left[R\left(1+(\lambda l)^2e^{2\phi}\right)+6(\nabla\phi)^2+2\lambda^2e^{2\phi}+\frac{6}{l^2}\right]\delta\phi\\&+3l^2(\nabla\phi)^2\left(\Box\phi-(\nabla\phi)^2\right)\delta\phi-l^2(\nabla\phi)^2\Box(\delta\phi)\\&-\left[2+l^2\left(\Box\phi-(\nabla\phi)^2\right)\right]\delta\left((\nabla\phi)^2\right)\Bigg\}.\end{aligned}\tag{6.7}$$

Using $\delta\left((\nabla\phi)^2\right)=2g^{\mu\nu}\nabla_\nu\phi\nabla_\mu(\delta\phi)$ and $\Box(\delta\phi)=g^{\mu\nu}\nabla_\nu\nabla_\mu(\delta\phi)$, and performing an integration by parts, Equation (6.7) can, after some algebraic manipulation, be simplified to:

$$\begin{aligned}3(\nabla\phi)^2-2\Box\phi+l^2&\left[\left(2(\nabla\phi)^2-\Box\phi\right)\Box\phi+\left(\nabla_\mu\nabla_\nu\phi+4\nabla_\mu\phi\nabla_\nu\phi\right)\nabla^\mu\nabla^\nu\phi\right]\\&-3l^2\nabla_\mu\phi\nabla^\mu\left((\nabla\phi)^2\right)=\lambda^2e^{2\phi}+\frac{3}{l^2}+\frac{1}{2}R\left[1+(\lambda l)^2e^{2\phi}-l^2(\nabla\phi)^2\right].\end{aligned}\tag{6.8}$$

After changing to the reduced field x, defined in (2.46) the metric Equation of motion (6.6) becomes:

$$\begin{aligned}&(\mathrm{x}^2+1)\nabla_\mu\nabla_\nu\mathrm{x}+l^2\Box\mathrm{x}\nabla_\mu\mathrm{x}\nabla_\nu\mathrm{x}-\frac{l^2}{2}\left(\nabla_\mu\mathrm{x}\nabla_\nu\left(\nabla\mathrm{x}\right)^2+\nabla_\nu\mathrm{x}\nabla_\mu\left(\nabla\mathrm{x}\right)^2\right)\\&-g_{\mu\nu}\left[(\mathrm{x}^2+1)\Box\mathrm{x}-\frac{\mathrm{x}}{l^2}\left(\mathrm{x}^2+1-l^2\left(\nabla\mathrm{x}\right)^2\right)-\frac{l^2}{2}\nabla^\alpha\mathrm{x}\nabla_\alpha\left(\nabla\mathrm{x}\right)^2\right]=-\frac{1}{6k\pi^2}T_{\mu\nu},\end{aligned}\tag{6.9}$$

It turns out that Equation (6.9) can be simplified even further, using the following identity:

$$\begin{aligned}(\nabla\mathrm{x})^2\nabla_\mu\nabla_\nu\mathrm{x}+\Box\mathrm{x}\nabla_\mu\mathrm{x}\nabla_\nu\mathrm{x}-\frac{1}{2}\left(\nabla_\mu\mathrm{x}\nabla_\nu\left(\nabla\mathrm{x}\right)^2+\nabla_\nu\mathrm{x}\nabla_\mu\left(\nabla\mathrm{x}\right)^2\right)\\=\left[(\nabla\mathrm{x})^2\Box\mathrm{x}-\frac{1}{2}\nabla_\alpha\mathrm{x}\nabla^\alpha\left(\nabla\mathrm{x}\right)^2\right]g_{\mu\nu},\end{aligned}\tag{6.10}$$

where the two identities involving the Levi-Civita tensor (A.16) and (A.17), have been extensively used. The resulting expressions for the equations of motion of both the metric and the dilaton field take the following form:

$$\left(\mathrm{x}^2+1-l^2(\nabla\mathrm{x})^2\right)\left[\nabla_\mu\nabla_\nu\mathrm{x}-g_{\mu\nu}\left(\Box\mathrm{x}-\frac{\mathrm{x}}{l^2}\right)\right]=-\frac{1}{6k\pi^2}T_{\mu\nu},\tag{6.11}$$

$$\left(\mathrm{x}^2+1-l^2\left(\nabla\mathrm{x}\right)^2\right)\left(\mathrm{R}+\frac{2}{l^2}\right)+\frac{4\mathrm{x}^2}{l^2}-4\mathrm{x}\Box\mathrm{x}=2l^2\left(\nabla_\mu\nabla_\nu\mathrm{x}\nabla^\nu\nabla^\mu\mathrm{x}-(\Box\mathrm{x})^2\right),\tag{6.12}$$

where we have used the identity (6.10) to simplify the metric equation.

6.1.1 General vacuum solution

In this section, we address the equations of motion (6.11-6.12) in the absence of matter fields, i.e., in the regime where the energy–momentum tensor $T_{\mu\nu}$ vanishes. The metric equation (6.11) factorizes into the product of two independent terms, thereby giving rise to two distinct branches of solutions. We begin by examining the branch defined by:

$$\nabla_\mu \nabla_\nu \mathrm{x} = g_{\mu\nu}\left(\Box \mathrm{x} - \frac{\mathrm{x}}{l^2}\right). \tag{6.13}$$

Taking the trace of this equation yields $l^2 \Box \mathrm{x} = 2\mathrm{x}$. Combining this result with the dilaton Equation (6.12) leads to the following system of differential equations in the conformal gauge (3.2):

$$\partial_\pm \left(e^{-2\rho}\partial_\pm \mathrm{x}\right) = 0 \quad \Longrightarrow \quad \partial_\pm \mathrm{x} = \frac{1}{2l}\mathrm{F}^\mp e^{2\rho}, \tag{6.14}$$

$$l^2 \Box \mathrm{x} = 2\mathrm{x} \quad \Longrightarrow \quad \partial_\pm \left(\mathrm{F}^+\mathrm{F}^- e^{2\rho} + \mathrm{x}^2\right) = 0, \tag{6.15}$$

$$R + \frac{2}{l^2} = 0. \tag{6.16}$$

From Equation (6.14), it follows directly that the derivatives of the dilaton field take the static ansatz form (3.13) with $\mathcal{D} = 1$. Equation (6.15) implies that the quantity Λ is indeed static $\Lambda = -(\mathrm{x}^2 - \mu)$, where μ denotes an arbitrary integration constant. The final Equation (6.16) is fulfilled automatically. Consequently, the general solution in the first branch can be written as:

$$\begin{aligned}
\mathrm{d}s^2 &= -(\mathrm{x}^2-\mu)\mathrm{d}t^2 + \frac{l^2 \mathrm{d}\mathrm{x}^2}{\mathrm{x}^2-\mu}, \\
\mathrm{x} &= \begin{cases} \sqrt{\mu}\tanh\left[\frac{\sqrt{\mu}}{2l}\left(\int \frac{\mathrm{d}x^+}{\mathrm{F}^+} + \int \frac{\mathrm{d}x^-}{\mathrm{F}^-}\right)\right], & 0 < \mathrm{x} < \sqrt{\mu}, \\ \sqrt{\mu}\coth\left[\frac{\sqrt{\mu}}{2l}\left(\int \frac{\mathrm{d}x^+}{\mathrm{F}^+} + \int \frac{\mathrm{d}x^-}{\mathrm{F}^-}\right)\right], & \mathrm{x} > \sqrt{\mu}, \end{cases}
\end{aligned} \tag{6.17}$$

where the second equation follows directly from the definition of the tortoise coordinate (3.18). There are two coordinate charts that overlap across the $\mathrm{x} = \sqrt{\mu}$ hypersurface. We conclude that the general vacuum solution within the first branch is the two-dimensional BTZ black hole solution [78]. It is defined by two arbitrary function $\mathrm{F}^\pm$ and one constant μ, in other words $\mathrm{RI}(\mathrm{F}^+, \mathrm{F}^-, \mu)$. It represents a static solution and is expressed in the form described in Section 3.1.

The second branch reduces to only one equation, namely:

$$l^2(\nabla \mathrm{x})^2 = \mathrm{x}^2 + 1. \tag{6.18}$$

This equation directly solves the metric equations of motion. However, with some algebraic transformation, one can verify that it also satisfies the dilaton Equation (6.12). Therefore, the general vacuum solution within the second brunch is given by:

$$\mathrm{d}s^2 = 4l^2 \frac{\partial_+ \mathrm{x} \partial_- \mathrm{x}}{\mathrm{x}^2+1} \mathrm{d}x^+ \mathrm{d}x^-, \tag{6.19}$$

where the dilaton field $\mathrm{x} = \mathrm{x}(x^+, x^-)$ is an arbitrary function. This arbitrariness can be attributed to the residual freedom in the five-dimensional gauge transformations. We therefore infer that, in this branch, the solution does not have to be static, and the dilaton field remains an unconstrained function.

Upon applying the static ansatz from Section 3.1, Equation (6.18) reduces to $\mathrm{x}^2+1+\Lambda\mathcal{D}^2 = 0$. Since this is the sole requirement, the most general static vacuum solution in the second branch, expressed in the form (3.18-3.19), is given by:

$$
\begin{aligned}
\mathrm{d}s^2 &= \Lambda(\mathrm{x})\mathrm{d}t^2 + \frac{l^2\mathrm{dx}^2}{\mathrm{x}^2+1}, \\
\int \frac{\mathrm{dx}}{\sqrt{-\Lambda(\mathrm{x})(\mathrm{x}^2+1)}} &= -\frac{1}{2l}\left(\int \frac{\mathrm{d}x^+}{\mathrm{F}^+} + \int \frac{\mathrm{d}x^-}{\mathrm{F}^-}\right),
\end{aligned} \tag{6.20}
$$

Thus, the most general static solution within this sector can be written as $\mathrm{RII}(\mathrm{F}^+, \mathrm{F}^-, \Lambda(\mathrm{x}))$, where the functions $\mathrm{F}^\pm$ are arbitrary and encode the coordinate transformations, and $\Lambda = \Lambda(\mathrm{x})$ is an arbitrary function of the dilaton field.

One can readily verify that both solutions RI (6.17) and RII (6.19) fulfill the five-dimensional Chern-Simons equations of motion (2.30). The first branch represents a dimensionally reduced BTZ black hole [116]. The event horizon is determined by $\mathrm{x}_H = \sqrt{\mu}$. It is linked to the mass of the black hole—on which we will elaborate later—as well as to the surface gravity and, in turn, to the black hole's temperature:

$$
\kappa = \frac{1}{2l}\left|\mathcal{D}\frac{\mathrm{d}\Lambda}{\mathrm{dx}}\right|_H = \frac{\sqrt{\mu}}{l}. \tag{6.21}
$$

6.1.2 General static equations of motion

Let us first examine the metric Equation (6.11). By inserting the ansatz (3.8), (3.13) and employing Equations (3.31) and (3.32), we obtain:

$$
\left(\mathrm{x}^2+1+\Lambda\mathcal{D}^2\right)\Lambda^2\mathcal{D}\frac{\mathrm{d}\mathcal{D}}{\mathrm{dx}} = -\frac{2l^2}{3k\pi^2}\mathrm{F}^{\pm 2}T_{\pm\pm}, \tag{6.22}
$$

$$
\left(\mathrm{x}^2+1+\Lambda\mathcal{D}^2\right)\left(\mathcal{D}\frac{\mathrm{d}}{\mathrm{dx}}(\Lambda\mathcal{D}) + 2\mathrm{x}\right) = -\frac{l^2}{6k\pi^2}T, \tag{6.23}
$$

where T is the trace of the energy-momentum tensor. Recasting these two equations with the rank-two tensor ansatz (3.14) for the EMT, together with the identities (3.33) and (3.34), leads to:

$$
\frac{\mathrm{d}}{\mathrm{dx}}\left(\mathrm{x}^2+1+\Lambda\mathcal{D}^2\right)^2 = -\frac{2l^2}{3k\pi^2}\Lambda T^{\parallel\parallel}, \tag{6.24}
$$

$$
\left(\mathrm{x}^2+1+\Lambda\mathcal{D}^2\right)\left(\mathcal{D}^2\frac{\mathrm{d}\Lambda}{\mathrm{dx}} + 2\mathrm{x}\right) = \frac{l^2}{3k\pi^2}\Lambda T^{\perp\perp}, \tag{6.25}
$$

$$
T^{\perp\parallel} = T^{\parallel\perp} = 0. \tag{6.26}
$$

Next, the dilaton field Equation (6.12) reduces to:

$$
\left(\mathrm{x}^2+1+\Lambda\mathcal{D}^2\right)\left[\mathcal{D}\frac{\mathrm{d}}{\mathrm{dx}}\left(\mathcal{D}\frac{\mathrm{d}\Lambda}{\mathrm{dx}}\right) + 2\right] + 4\mathrm{x}^2 + 4\mathrm{x}\mathcal{D}\frac{\mathrm{d}(\Lambda\mathcal{D})}{\mathrm{dx}} + \mathcal{D}^2\frac{\mathrm{d}\Lambda}{\mathrm{dx}}\frac{\mathrm{d}(\Lambda\mathcal{D}^2)}{\mathrm{dx}} = 0. \tag{6.27}
$$

By subtracting Equations (6.22) and (6.23), then differentiating the resulting expression and employing Equation (6.27), we obtain the following condition for the EMT components:

$$\frac{\mathrm{d}}{\mathrm{dx}}\left(4\mathrm{F}^{\pm 2}T_{\pm\pm}\right)=\Lambda\frac{\mathrm{d}T}{\mathrm{dx}}\quad\Longrightarrow\quad\left(T^{\parallel\parallel}+3T^{\perp\perp}\right)\frac{\mathrm{d}\Lambda}{\mathrm{dx}}+2\Lambda\frac{T^{\perp\perp}}{\mathrm{dx}}=0.\tag{6.28}$$

The final Equation (6.28) expresses the conservation law for the Riemannian EMT of the matter fields, namely $\nabla_\mu T^{\mu\nu}=0$, as previously introduced in Equation (3.68).

It is possible to eliminate $\mathcal{D}$ from Equations (6.24-6.27) and derive one second-order differential equation for the metric function Λ. However, this equation cannot, in general, be solved exactly for arbitrary matter fields, even in the particular case where the EMT is traceless. For this reason, we do not present it here. When the matter is comprised of the massless real scalar fields, the EMT is traceless and satisfies (4.34). In contrast to the Sections 4.1.4 and 5.1.2 where the solution with charged scalar matter is presented in the BPP and DREH models respectively, in case of the DR5DCS model there is no closed form for the charged scalar matter solution.

6.1.3 Classical collapse scenario

Here, we investigate the classical collapse scenario. We strictly follow Section 3.4 where it was first described. The matter fields are incorporated as an ingoing shockwave of massless particles along the $x^+=x_0^+$ hypersurface, with the EMT given in (3.99). This shockwave divides the spacetime into two distinct regions, as illustrated in Figure 3.2. Subsequently, one has to join these regions smoothly by imposing the continuity conditions (3.102) and (3.104).

We start by rewriting the "++" equation of motion (6.11) in the form (3.103). It is given by:

$$\left(\mathrm{x}^2+1-l^2\left(\nabla\mathrm{x}\right)^2\right)\partial_+\left(e^{-2\rho}\partial_+\mathrm{x}\right)=\frac{M}{6k\pi^2\mathrm{F}^+}\delta\left(x^+-x_0^+\right)e^{-2\rho}.\tag{6.29}$$

Next, we integrate Equation (6.29) with respect to the x^+ coordinate over the interval from $x_0^+-\epsilon$ to $x_0^+ +\epsilon$, and then take the limit $\epsilon\to 0$. We assume that x, $\partial_-\mathrm{x}$, ρ and $\partial_-\rho$ are continuous functions, whereas $\partial_+\mathrm{x}$, $\partial_+\rho$, $\partial_+\partial_-\mathrm{x}$, and $\partial_+\partial_-\rho$ are allowed to exhibit discontinuities across the hypersurface $x^+=x_0^+$. Under these conditions, the integration yields:

$$\left(\mathrm{x}^2+1-\frac{1}{2}l^2\left(\nabla\mathrm{x}\right)^2\right)\partial_+\mathrm{x}\Big|_<^>=\frac{M}{6k\pi^2\mathrm{F}^+}\Big|_{x^+=x_0^+},\tag{6.30}$$

where ">" ("<") corresponds to the region of the spacetime where $x^+>x_0^+$ ($x^+<x_0^+$). Using the static ansatz (3.8) and (3.13), Equation (6.30) becomes:

$$\left(\mathrm{x}^2+1+\frac{1}{2}\Lambda\mathcal{D}^2\right)\Lambda\mathcal{D}\Big|_<^>=\frac{Ml}{3k\pi^2},\tag{6.31}$$

which coincides with the form given in (3.104). We now continuously connect two solutions $\mathrm{RI}(\mathrm{F}_\mathrm{I}^+,\mathrm{F}_\mathrm{I}^-,\mu_\mathrm{I})$ and $\mathrm{RI}(\mathrm{F}_\mathrm{II}^+,\mathrm{F}_\mathrm{II}^-,\mu_\mathrm{II})$. Upon inserting the expression (6.17) into Equation (6.31), the latter simplifies to:

$$\mu_\mathrm{II}\left(\mu_\mathrm{II}+2\right)-\mu_\mathrm{I}\left(\mu_\mathrm{I}+2\right)=\frac{2Ml}{3k\pi^2}.\tag{6.32}$$

Requiring the continuity of metric gives the jump in F^- coordinate transformation:

$$\frac{\mathrm{F}^+\mathrm{F}_\mathrm{II}^-e^{2\rho}}{\mathrm{F}^+\mathrm{F}_\mathrm{I}^-e^{2\rho}}=\frac{\mathrm{F}_\mathrm{II}^-}{\mathrm{F}_\mathrm{I}^-}=\frac{\mathrm{x}^2-\mu_\mathrm{II}}{\mathrm{x}^2-\mu_\mathrm{I}}\Big|_{x^+=x_0^+}.\tag{6.33}$$

Finally, one has to verify whether the continuity condition for the dilaton field holds. Since Equation (6.32) requires $\mu_{\rm II} > \mu_{\rm I}$, we must distinguish three separate cases: $0 < {\rm x} < \sqrt{\mu_{\rm I}}$, $\sqrt{\mu_{\rm I}} < {\rm x} < \sqrt{\mu_{\rm II}}$, and ${\rm x} > \sqrt{\mu_{\rm II}}$. These intervals correspond to two coordinate charts that together form the atlas of the BTZ solution (6.17) in both spacetime regions. Thus, we obtain:

$$\sqrt{\frac{\mu_{\rm I}}{\mu_{\rm II}}} = \begin{cases} \dfrac{\tanh\left(\frac{\sqrt{\mu_{\rm II}}}{2l}\left(\sigma_0^+ - \hat{\sigma}^-\right)\right)}{\tanh\left(\frac{\sqrt{\mu_{\rm I}}}{2l}\left(\sigma_0^+ - \sigma^-\right)\right)}, & 0 < {\rm x} < \sqrt{\mu_{\rm I}}, \\ \dfrac{\tanh\left(\frac{\sqrt{\mu_{\rm II}}}{2l}\left(\sigma_0^+ - \hat{\sigma}^-\right)\right)}{\coth\left(\frac{\sqrt{\mu_{\rm I}}}{2l}\left(\sigma_0^+ - \sigma^-\right)\right)}, & \sqrt{\mu_{\rm I}} < {\rm x} < \sqrt{\mu_{\rm II}}, \\ \dfrac{\coth\left(\frac{\sqrt{\mu_{\rm II}}}{2l}\left(\sigma_0^+ - \hat{\sigma}^-\right)\right)}{\coth\left(\frac{\sqrt{\mu_{\rm I}}}{2l}\left(\sigma_0^+ - \sigma^-\right)\right)}, & {\rm x} > \sqrt{\mu_{\rm II}}, \end{cases} \tag{6.34}$$

where $\hat{\sigma}^\pm$ denote Eddington–Finkelstein-like coordinates in region II of the spacetime. One can readily verify that Equations (6.33) and (6.34) are mutually consistent. Moreover, Equation (6.34) serves as the defining relation for the $\hat{\sigma}^-$ coordinate, while the other coordinate remains unchanged, $\hat{\sigma}^+ = \sigma^+$. Therefore, we conclude that the solution in region II takes the form:

$$\begin{cases} {\rm RI}\left({\rm F}_{\rm I}^+, {\rm F}_{\rm I}^- \left[1 + \frac{\mu_{\rm II} - \mu_{\rm I}}{\mu_{\rm I}} \cosh^2\left(\frac{\sqrt{\mu_{\rm I}}}{2l}\left(\sigma_0^+ - \sigma^-\right)\right)\right], \sqrt{\left(\mu_{\rm I}+1\right)^2 + \frac{2Ml}{3k\pi^2}} - 1\right), & {\rm x} < \sqrt{\mu_{\rm I}}, \\ {\rm RI}\left({\rm F}_{\rm I}^+, {\rm F}_{\rm I}^- \left[1 - \frac{\mu_{\rm II} - \mu_{\rm I}}{\mu_{\rm I}} \sinh^2\left(\frac{\sqrt{\mu_{\rm I}}}{2l}\left(\sigma_0^+ - \sigma^-\right)\right)\right], \sqrt{\left(\mu_{\rm I}+1\right)^2 + \frac{2Ml}{3k\pi^2}} - 1\right), & {\rm x} > \sqrt{\mu_{\rm I}}. \end{cases} \tag{6.35}$$

Equation (6.35) describes how the spacetime is modified when an infalling shockwave with mass M is introduced. To obtain a genuine gravitational collapse setup, region I must be described by a massless AdS spacetime. There are two possible values of the parameter μ that yield AdS: $\mu = 0$ and $\mu = -1$. The appropriate choice in this context is $\mu = 0$. This follows from the fact that, for μ in the range between -1 and 0, there are several naked singularities [78, 89], which are forbidden by the cosmic censorship conjecture [106]. Consequently, the classical collapse scenario corresponds to the situation in which the initial spacetime is described by ${\rm RI}(-1, 1, 0)$. Taking the limit $\mu \to 0$ in the solution (6.17) one obtains:

$$ds^2 = -{\rm x}^2 dt^2 + \frac{l^2 d{\rm x}^2}{{\rm x}^2}, \qquad \frac{1}{\rm x} = \frac{1}{2l}\left(\int \frac{dx^+}{{\rm F}^+} + \int \frac{dx^-}{{\rm F}^-}\right), \tag{6.36}$$

where we have used only the second chart, corresponding to ${\rm x} > \sqrt{\mu}$, and set $\mu = 0$. One can readily verify that this metric indeed describes AdS spacetime in Poincaré coordinates. Under the coordinate transformation ${\rm x} = -1/{\rm z}$, the metric is immediately brought into the standard Poincaré patch form, namely

$$ds^2 = \frac{-dt^2 + l^2 d{\rm z}^2}{{\rm z}^2}, \qquad -\frac{1}{\rm x} = {\rm z} = -\frac{1}{2l}\left(\int \frac{dx^+}{{\rm F}^+} + \int \frac{dx^-}{{\rm F}^-}\right). \tag{6.37}$$

Having established that $\mu = 0$ corresponds to empty AdS spacetime, taking this limit in (6.35) yields the following solution in region II of the spacetime:

$${\rm RI}\left(-1, 1 - \mu\left(\frac{\sigma_0^+ - \sigma^-}{2l}\right)^2, \sqrt{1 + \frac{2Ml}{3k\pi^2}} - 1\right). \tag{6.38}$$

The $\hat{\sigma}^{\pm}$ coordinates following the collapse are therefore:

$$\hat{\sigma}^{+} = \sigma^{+}, \tag{6.39}$$

$$\hat{\sigma}^{-} = \sigma_0^{+} - \frac{l}{\sqrt{\mu}} \ln \left| \frac{1 + \frac{\sqrt{\mu}}{2l}\left(\sigma_0^{+} - \sigma^{-}\right)}{1 - \frac{\sqrt{\mu}}{2l}\left(\sigma_0^{+} - \sigma^{-}\right)} \right|. \tag{6.40}$$

Then, the solution in region II of the spacetime is given by:

$$\begin{gathered} \frac{1}{2\sqrt{\mu}} \ln \left| \frac{\mathrm{x} - \sqrt{\mu}}{\mathrm{x} + \sqrt{\mu}} \right| = -\ln \delta + \frac{1}{2\sqrt{\mu}} \ln \left| \frac{1 + \hat{\mathrm{x}}\sqrt{\mu}}{1 - \hat{\mathrm{x}}\sqrt{\mu}} \right|, \\ \mathrm{F}^{+}\mathrm{F}^{-} e^{2\rho} = -\mathrm{x}^2 + \mu, \end{gathered} \tag{6.41}$$

where we have used the collapse-adapted coordinates $(\delta, \hat{\mathrm{x}})$ defined in (3.107). In these coordinates the coordinate transformations take the form:

$$\mathrm{F}^{+} = 1 \quad \wedge \quad \mathrm{F}^{-} = 1 - \mu\hat{\mathrm{x}}^2. \tag{6.42}$$

Note that, on the shockwave hypersurface $\delta = 1$, equations reduce to the solution (6.36). The horizon and the singularity remain $\mathrm{x_H} = \sqrt{\mu}$ and $\mathrm{x_S} = 0$, respectively, or in terms of the $\sigma^{\pm}$ coordinates:

$$\hat{\mathrm{x}}_{\mathrm{H}} = -\frac{1}{\sqrt{\mu}}, \qquad \ln \delta_{\mathrm{S}/i^0} = \frac{1}{2\sqrt{\mu}} \ln \left| \frac{1 + \hat{\mathrm{x}}_{\mathrm{S}/i^0}\sqrt{\mu}}{1 - \hat{\mathrm{x}}_{\mathrm{S}/i^0}\sqrt{\mu}} \right|. \tag{6.43}$$

Observe that these two hypersurfaces intersect at infinity, that is $\sigma_{\mathrm{E}}^{+} = +\infty$, which is consistent with the absence of quantum corrections in the classical setting. Another important point is that the two limits, $\mathrm{x} \to 0$ (corresponding to the singularity) and $\mathrm{x} \to +\infty$ (corresponding to spatial infinity i^0), are described by the same formula in (6.43). The logarithmic term admits two distinct branches. The singularity is characterized by the branch where $\hat{\mathrm{x}}_{\mathrm{S}} < -1/\sqrt{\mu}$, whereas spatial infinity is associated with the interval $-1/\sqrt{\mu} < \hat{\mathrm{x}}_{\mathrm{B}} < 0$.

Figure 6.1 depicts the classical collapse setup in the $(\delta, \hat{\mathrm{x}})$ coordinates (3.107). The ingoing shockwave at $\delta = 1$, shown in red, divides the spacetime into two distinct regions, labeled region I and region II. Through the relation $\mathrm{x} = -1/\mathrm{z}$, spatial infinity is identified with $\mathrm{z} = 0$, while the spacetime boundary at $\mathrm{x} = 0$ is mapped to $\mathrm{z} \to -\infty$. As a result, the ingoing shockwave intersects the spacetime boundary only at infinity, and it is exactly at this location that the singularity forms. In Figure 6.1, this singularity is shown as the wavy black line. The event horizon, dashed purple line, links the singularity to spatial infinity at future time infinity i^{+}, which is located at coordinates $(0, -1/\sqrt{\mu})$. The explicit forms of these hypersurfaces are given in (6.43), and the spacetime metric with the corresponding tortoise coordinate is given in (6.41).

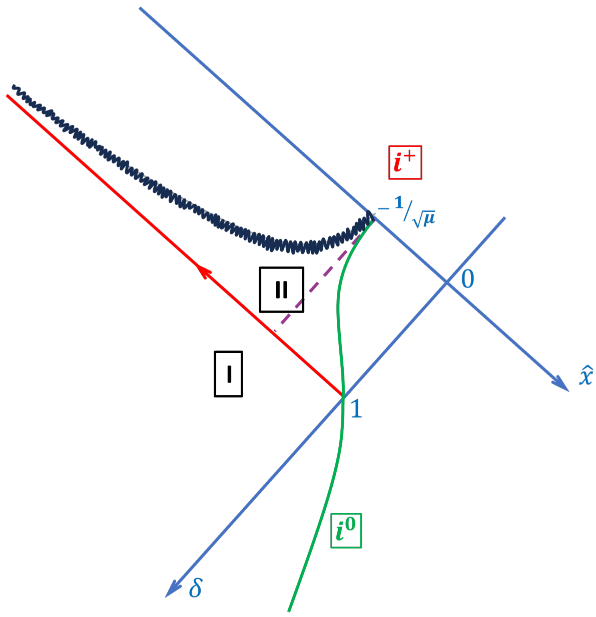

Figure 6.1: Classical gravitational collapse scenario for the BTZ black hole in $(\delta, \hat{\mathrm{x}})$ coordinates.

Next, we turn to the analysis of solutions of type RII. Since $\partial_{-}\mathrm{x}_{<} = \partial_{-}\mathrm{x}_{>}$, the function $\mathcal{D}$ is continuous across the hypersurface $x^+ = x_0^+$, which in turn implies that Λ is also continuous. We therefore conclude that, within this framework of gravitational collapse, solutions of type RII cannot be continuously connected.

Finally, one needs to investigate what happens if the solution in one spacetime region is of type RI, while the solution in the other region is of type RII. As before, the continuity condition for the $\mathcal{D}$ function has to be applied. Because the RI solution satisfies $\mathcal{D} = 1$, the remaining portion of the spacetime corresponds to an AdS patch. Consequently, the problem reduces to that of matching two RI-type solutions, with the caveat that one of them has $\mu = -1$, which, as previously noted, is unphysical.

Observe that Equation (6.38) implies the proper relation between the mass of a BTZ black hole and the parameter μ is:

$$\mu = \sqrt{1 + \frac{2Ml}{3k\pi^2}} - 1. \tag{6.44}$$

This outcome agrees with the result obtained in [117]. It can likewise be reproduced using the ADM formalism [118], or by employing the holographic framework together with the boundary stress-energy tensor [119].

6.1.4 Conformal diagram depicting the classical collapse scenario

In this section, we construct the conformal diagram for the classical gravitational collapse scenario, illustrated in Figure 6.1. Region I represents the massless BTZ black hole, whose metric and tortoise coordinate are given in (6.36). We have seen that, by performing the substitution $\mathrm{x} = -1/\mathrm{z}$, one obtains the Poincaré patch of the two-dimensional AdS spacetime, as defined in (6.37). Because $\mathrm{x} > 0$ implies $\mathrm{z} < 0$, the spacetime of region I corresponds to a part of the left Poincaré patch. We now define the conformal coordinates as:

$$\mathrm{x}^+ = \arctan\left(\frac{\sqrt{\mu}}{2l}\left(\sigma^+ - \sigma_0^+\right)\right), \quad \wedge \quad \mathrm{x}^- = \arctan\left(\frac{\sqrt{\mu}}{2l}\left(\sigma^- - \sigma_0^+\right)\right). \tag{6.45}$$

Then, the spatial infinity i^0, characterized by $\mathrm{x} \to \infty$ prior to the shockwave corresponds to $\mathrm{z} = 0$, or $\sigma_+ = \sigma_-$. In terms of the conformal coordinates (6.45), this condition becomes $\mathrm{x}^+ = \mathrm{x}^-$. Conversely, the spacetime boundary at $\mathrm{x} = 0$ corresponds to the limit $\mathrm{z} \to -\infty$. As a result, it consists of two distinct hypersurfaces:

$$\begin{aligned} \sigma^+ \to -\infty \quad &\Longrightarrow \quad \mathrm{x}^+ = -\frac{\pi}{2}, \\ \sigma^+ \to \infty \quad &\Longrightarrow \quad \mathrm{x}^- = \frac{\pi}{2}, \end{aligned} \tag{6.46}$$

In the absence of the shockwave, we simply recover the left Poincaré patch of AdS spacetime. Once the infalling matter is introduced, the region I terminates at the shockwave hypersurface, which slices through the left Poincaré patch along $\sigma^+ = \sigma_0^+$. In terms of the conformal coordinates, this corresponds to $\mathrm{x}^+ = 0$. Consequently, region II occupies the part of the spacetime characterized by $\mathrm{x}^+ > 0$.

In region II, spatial infinity is again located at $\mathrm{z} = 0$. Due to the change in the asymptotic coordinates, however, this hypersurface becomes curved. Its form is determined by Equation (6.43), which can be written as:

$$\hat{\mathrm{x}}_{i^0}\sqrt{\mu} = \frac{\delta_{i^0}^{2\sqrt{\mu}} - 1}{\delta_{i^0}^{2\sqrt{\mu}} + 1} = \tanh(\sqrt{\mu}\ln\delta_{i^0}) \quad \Longrightarrow \quad \mathrm{x}_{i^0}^- = \arctan\left(\tanh\left(\tan \mathrm{x}_{i^0}^+\right)\right), \tag{6.47}$$

in the conformal coordinates (6.45). The other branch of (6.43) defines the singularity hypersurface generated by the gravitational collapse. The singularity is given by:

$$\hat{\mathrm{x}}_{\mathrm{S}}\sqrt{\mu} = \frac{\delta_{\mathrm{S}}^{2\sqrt{\mu}}+1}{\delta_{\mathrm{S}}^{2\sqrt{\mu}}-1} = \coth(\sqrt{\mu}\ln\delta_{\mathrm{S}}) \quad \Longrightarrow \quad \mathrm{x}_{\mathrm{S}}^{-} = \arctan\left(\coth\left(\tan\mathrm{x}_{\mathrm{S}}^{+}\right)\right), \tag{6.48}$$

in the conformal coordinates (6.45). Finally, the horizon becomes:

$$\hat{\mathrm{x}}_{\mathrm{H}}\sqrt{\mu} = -1 \quad \Longrightarrow \quad \mathrm{x}_{\mathrm{H}}^{-} = \frac{\pi}{4}. \tag{6.49}$$

These three hypersurfaces (6.47), (6.48), and (6.49) intersect at future time infinity i^+. The coordinates of the future time infinity point i^+ and the past time infinity point i^- are:

$$i^+ = \left(\frac{\pi}{4}, \frac{\pi}{2}\right), \quad \wedge \quad i^- = \left(-\frac{\pi}{2}, -\frac{\pi}{2}\right). \tag{6.50}$$

respectively, in the format $(\mathrm{x}^-, \mathrm{x}^+)$. The conformal diagram is shown in Figure 6.2.

Figure 6.2 shows the Penrose diagram for the classical gravitational collapse scenario within the dimensionally-reduced five-dimensional Chern-Simons gravity. Both region I, prior to the collapse, and region II, following the collapse, are clearly displayed. Region I corresponds to the part of the left Poincaré patch of AdS spacetime discussed above. It is separated from the other region by the ingoing shockwave hypersurface, depicted in red. The spacetime boundary at $\mathrm{x} = 0$ is shown as the black line within region I of the diagram. It extends into region II of spacetime, where it represents the black hole singularity (illustrated by the wavy black line), which is concealed behind the event horizon, drawn as the dashed purple line. The spatial infinity i^0 appears as a smooth green line which extends in both regions. The figure also displays both future time infinity i^+ and past time infinity i^-.

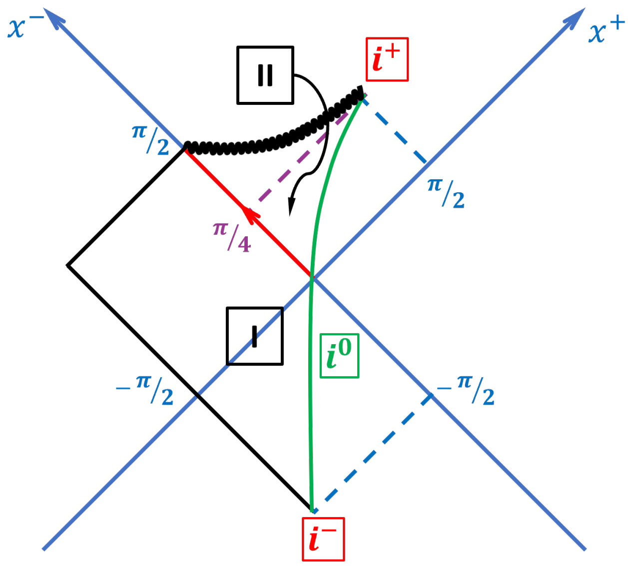

Figure 6.2: Penrose diagram of the classical gravitational collapse for the BTZ black hole.

6.2 Adding quantum corrections

In this section, we incorporate quantum corrections into the classical DR5DCS action (6.1). These corrections are included via the Polyakov–Liouville action (3.72), in the same manner as in the BPP and DREH models. As in the DREH model, equations cannot be solved exactly, so we adopt the perturbative method presented in Section 3.3. Because no counterterms are added, the dilaton Equation of motion (6.12) remains unchanged. In contrast, the metric equation of motion (6.11) is modified by the EMT of the quantum fields (3.77). We now directly express the metric equation in the conformal gauge (3.2):

$$\left(\mathrm{x}^2+1-l^2(\nabla\mathrm{x})^2\right)\partial_\pm\left(e^{-2\rho}\partial_\pm\mathrm{x}\right)=\varepsilon\left[(\partial_\pm\rho)^2-\partial_\pm^2\rho+t_\pm(x^\pm)\right]e^{-2\rho}, \tag{6.51}$$

$$\left(\mathrm{x}^2+1-l^2(\nabla\mathrm{x})^2\right)\left(\frac{2\mathrm{x}}{l^2}-\Box\mathrm{x}\right)=-\frac{\varepsilon}{2}R, \tag{6.52}$$

where, in the second line, we have made use of the trace anomaly of the scalar-field EMT, namely $\langle\Delta T^{(f)}\rangle=\frac{\hbar}{24\pi}R$. Moreover, we introduce a natural perturbative parameter $\varepsilon=\frac{\hbar}{72k\pi^3}$. We then evaluate the quantum-corrected solution corresponding to the first branch (6.17). The derivatives of the dilaton field and of the metric take the form:

$$\partial_\pm\mathrm{x}=-\frac{\mathrm{x}^2-\mu}{2l\mathrm{F}^\pm}\quad\wedge\quad\partial_\pm\rho=-\frac{\mathrm{x}}{2l\mathrm{F}^\pm}-\frac{1}{2}\partial_\pm\ln\mathrm{F}^\pm. \tag{6.53}$$

The first step in the perturbative treatment of these equations is to expand the fields to first order in ε using (3.108), i.e. $\mathrm{x}\mapsto\mathrm{x}+\varepsilon\theta$ and $\rho\mapsto\rho+\varepsilon\alpha$. Since both $\partial_\pm(e^{-2\rho}\partial_\pm\mathrm{x})$ and $\frac{2\mathrm{x}}{l^2}-\Box\mathrm{x}$ are already of first order in ε, quantity $\mathrm{x}^2+1-l^2(\nabla\mathrm{x})^2$ is evaluated at zeroth order. The same reasoning applies to the EMT components. A straightforward calculation based on (6.53) gives:

$$\mathrm{x}^2+1-l^2(\nabla\mathrm{x})^2=\mu+1,\quad R=-\frac{2}{l^2},\quad(\partial_\pm\rho)^2-\partial_\pm^2\rho+t_\pm(x^\pm)=\frac{t_\pm(\sigma^\pm)}{\mathrm{F}^{\pm2}}+\frac{\mu}{4l^2\mathrm{F}^{\pm2}}. \tag{6.54}$$

Upon substituting (6.54), the equations of motion (6.51) and (6.52) take the form (3.109), which reads:

$$\partial_\pm\left(e^{-2\rho}\partial_\pm\theta-\frac{\alpha}{l}\mathrm{F}^\mp\right)=\frac{1}{\mu+1}\left[\frac{t_\pm(\sigma^\pm)}{\mathrm{F}^{\pm2}}+\frac{\mu}{4l^2\mathrm{F}^{\pm2}}\right], \tag{6.55}$$

$$2\theta+4l^2e^{-2\rho}\partial_+\partial_-\theta+4\mathrm{x}\alpha=\frac{1}{\mu+1}. \tag{6.56}$$

The next step is to integrate Equation (6.55) and derive the closed-form expressions for the derivatives of θ, as outlined in (3.110). These expressions are given by:

$$\partial_\pm\theta=\frac{1}{2l}\mathrm{F}^\mp\left[\mathcal{D}_1+2\alpha+\frac{\mathrm{G}^\mp}{\mathrm{F}^\mp}\right]e^{2\rho}-\frac{1}{\mu+1}\mathrm{F}^\mp e^{2\rho}\int\frac{\mathrm{d}x^\pm}{\mathrm{F}^\pm}\frac{t_\pm(\sigma^\pm)}{\mathrm{x}^2-\mu} \tag{6.57}$$

where the function $\mathcal{D}_1$ is defined through:

$$\frac{\mathrm{d}\mathcal{D}_1}{\mathrm{dx}}=\frac{1}{\mu+1}\frac{\mu}{(\mathrm{x}^2-\mu)^2}. \tag{6.58}$$

Next, we need to remove the function α from (6.57). This can be achieved by employing Equation (6.56). As a result, we obtain two first-order differential equations for θ: one involving $\partial_+\theta$ and the other involving $\partial_-\theta$. These equations can be solved, leading to:

$$\begin{aligned}\mathrm{x}\theta=\mathrm{H}^\mp&+\frac{1}{2}\left(\mathrm{x}^2-\mu\right)\left[\frac{\mathrm{G}^-}{\mathrm{F}^-}+\frac{\mathrm{G}^+}{\mathrm{F}^+}+2\alpha+\mathcal{D}_1\right]+\frac{\mathrm{x}}{2(\mu+1)}+\int\mathrm{dx}\mathcal{D}_1\mathrm{x}\\&+\frac{1}{\mu+1}\int\frac{\mathrm{d}x^\pm}{\mathrm{F}^\pm}\mathrm{x}\left(\mathrm{x}^2-\mu\right)\int\frac{\mathrm{d}x^\pm}{\mathrm{F}^\pm}\frac{t_\pm(\sigma^\pm)}{\mathrm{x}^2-\mu}-l\frac{\mathrm{x}^2-\mu}{\mu+1}\int\frac{\mathrm{d}x^\mp}{\mathrm{F}^\mp}\frac{t_\mp(\sigma^-)}{\mathrm{x}^2-\mu},\end{aligned} \tag{6.59}$$

where $\mathrm{H}^{\mp}$ represent another set of arbitrary functions. Furthermore, by using (6.57) we have removed the remaining derivative term $\partial_{\mp}\theta$, which reintroduces the function α. Requiring that the two equations in (6.59) coincide then imposes the following consistency condition on the functions $\mathrm{H}^{\mp}$:

$$\mathrm{H}^- - \frac{l}{\mu+1}\int \frac{\mathrm{d}x^-}{\mathrm{F}^-} t_-(\sigma^-) = \mathrm{H}^+ - \frac{l}{\mu+1}\int \frac{\mathrm{d}x^+}{\mathrm{F}^+} t_+(\sigma^+) = C, \tag{6.60}$$

where we have included an integration constant C. It may be interpreted as the integration constant of $\int \mathrm{d}\mathrm{x}\mathcal{D}\mathrm{x}$. Consequently, by eliminating the $\mathrm{H}^{\mp}$ functions, we obtain:

$$\mathrm{x}\theta = \frac{1}{2}\left(\mathrm{x}^2-\mu\right)\left[\frac{\mathrm{G}^-}{\mathrm{F}^-}+\frac{\mathrm{G}^+}{\mathrm{F}^+}+2\alpha+\mathcal{D}_1\right]+\frac{\mathrm{x}}{2(\mu+1)}+\int \mathrm{d}\mathrm{x}\mathcal{D}_1\mathrm{x}+\frac{\mathrm{I}'_+ + \mathrm{I}'_-}{2(\mu+1)}, \tag{6.61}$$

where the integrals $\mathrm{I}'_{\pm}$ are defined as follows:

$$\mathrm{I}'_{\pm} = 2\int \frac{\mathrm{d}x^{\pm}}{\mathrm{F}^{\pm}}\mathrm{x}\left(\mathrm{x}^2-\mu\right)\int \frac{\mathrm{d}x^{\pm}}{\mathrm{F}^{\pm}}\frac{t_{\pm}(\sigma^{\pm})}{\mathrm{x}^2-\mu}. \tag{6.62}$$

By following the method outlined in Section 3.4.1, a final integration remains to be carried out. Isolating α from (6.57) and substituting it into (6.61) transforms (6.61) into a first-order differential equation for θ. As before, there are two such equations, depending on whether the derivative $\partial_{\pm}\theta$ appears. Solving these equations introduces two additional arbitrary functions, which are then determined by imposing mutual consistency of the two solutions. In this way, one ultimately obtains the following expression for the final solution of θ:

$$\frac{\theta}{\mathrm{x}^2-\mu} = \frac{1}{2l}\left(\int \mathrm{d}x^+\frac{\mathrm{G}^+}{\mathrm{F}^{+2}}+\int \mathrm{d}x^-\frac{\mathrm{G}^-}{\mathrm{F}^{-2}}\right)-\int\frac{\mathrm{d}\mathrm{x}}{\left(\mathrm{x}^2-\mu\right)^2}\left[\frac{\mathrm{x}}{\mu+1}+2\int \mathrm{d}\mathrm{x}\mathcal{D}_1\mathrm{x}\right]+\frac{\mathrm{I}_+ + \mathrm{I}_-}{\mu+1}, \tag{6.63}$$

where we have introduced another set of integrals:

$$\mathrm{I}_{\pm} = \int \frac{\mathrm{d}x^{\pm}}{\mathrm{F}^{\pm}}\frac{1}{\mathrm{x}^2-\mu}\int \frac{\mathrm{d}x^{\pm}}{\mathrm{F}^{\pm}}t_{\pm}(\sigma^{\pm}). \tag{6.64}$$

The final step consists in reverting to the quantum-corrected quantities (3.113). We begin by examining the quantum-corrected metric:

$$\begin{aligned}\mathrm{F}^+\mathrm{F}^-e^{2\rho} &= -(\mathrm{x}^2-\mu)\left[1+\varepsilon\left(\frac{\mathrm{G}^-}{\mathrm{F}^-}+\frac{\mathrm{G}^+}{\mathrm{F}^+}+2\alpha\right)\right]\\ &= -\mathrm{x}^2+\mu-2\varepsilon\mathrm{x}\theta+\varepsilon\left[\frac{\mathrm{x}}{\mu+1}+2\int \mathrm{d}\mathrm{x}\mathcal{D}_1\mathrm{x}+\left(\mathrm{x}^2-\mu\right)\mathcal{D}_1\right]+\frac{\varepsilon}{\mu+1}\left(\mathrm{I}'_+ + \mathrm{I}'_-\right)\\ &= -\left(\mathrm{x}+\varepsilon\theta\right)^2+\mu+\varepsilon\left[\frac{\mathrm{x}}{\mu+1}+2\int \mathrm{d}\mathrm{x}\mathcal{D}_1\mathrm{x}+\left(\mathrm{x}^2-\mu\right)\mathcal{D}_1\right]+\frac{\varepsilon}{\mu+1}\left(\mathrm{I}'_+ + \mathrm{I}'_-\right),\end{aligned} \tag{6.65}$$

where Equation (6.61) has been applied. We now determine the quantum-corrected tortoise coordinate by making use of (6.63):

$$\begin{aligned}\frac{1}{2\sqrt{\mu}}\ln\left|\frac{\mathrm{x}-\sqrt{\mu}}{\mathrm{x}+\sqrt{\mu}}\right|+\frac{\varepsilon\theta}{\mathrm{x}^2-\mu}+\varepsilon\int\frac{\mathrm{d}\mathrm{x}}{\left(\mathrm{x}^2-\mu\right)^2}\left[\frac{\mathrm{x}}{\mu+1}+2\int \mathrm{d}\mathrm{x}\mathcal{D}_1\mathrm{x}\right]-\frac{\varepsilon}{\mu+1}\left(\mathrm{I}_+ + \mathrm{I}_-\right)\\ = -\frac{1}{2l}\left[\int\frac{\mathrm{d}x^+}{\mathrm{F}^+}\left(1-\varepsilon\frac{\mathrm{G}^+}{\mathrm{F}^+}\right)+\int\frac{\mathrm{d}x^-}{\mathrm{F}^-}\left(1-\varepsilon\frac{\mathrm{G}^-}{\mathrm{F}^-}\right)\right].\end{aligned} \tag{6.66}$$

From this equation, it is evident that $\mathrm{G}^{\pm}$ indeed encode the quantum corrections to the coordinate transformations. The only remaining task is to explicitly evaluate all integrals over x that appear in (6.65) and (6.66). These are:

$$\mathcal{D}_1 = -\frac{1}{2(\mu+1)}\left[\frac{1}{2\sqrt{\mu}}\ln\left|\frac{\mathrm{x}-\sqrt{\mu}}{\mathrm{x}+\sqrt{\mu}}\right| + \frac{\mathrm{x}}{\mathrm{x}^2-\mu}\right], \tag{6.67}$$

$$\frac{\mathrm{x}}{\mu+1} + 2\int \mathrm{d}\mathrm{x}\mathcal{D}_1\mathrm{x} + \left(\mathrm{x}^2-\mu\right)\mathcal{D}_1 = -\frac{\mathrm{x}^2}{\mu+1}\frac{1}{2\sqrt{\mu}}\ln\left|\frac{\mathrm{x}-\sqrt{\mu}}{\mathrm{x}+\sqrt{\mu}}\right| + C, \tag{6.68}$$

$$\int\frac{\mathrm{d}\mathrm{x}}{(\mathrm{x}^2-\mu)^2}\left[\frac{\mathrm{x}}{\mu+1} + 2\int \mathrm{d}\mathrm{x}\mathcal{D}_1\mathrm{x}\right] = \frac{1}{\mu+1}\frac{1}{4\sqrt{\mu}}\frac{\mathrm{x}}{\mathrm{x}^2-\mu}\ln\left|\frac{\mathrm{x}-\sqrt{\mu}}{\mathrm{x}+\sqrt{\mu}}\right| + C\frac{\mu+1}{\mu}\mathcal{D}_1. \tag{6.69}$$

Finally, as anticipated, the integration constant C is understood as the quantum correction to the constant μ. In other words, we make the replacement $\mu + \varepsilon C \mapsto \mu$. This removes C from both of the final equations, (6.65) and (6.66). Consequently, the general quantum-corrected solution takes the form:

$$\mathrm{F}^+\mathrm{F}^- e^{2\rho} = -\mathrm{x}^2 + \mu - \frac{\varepsilon}{\mu+1}\left[\frac{\mathrm{x}^2}{2\sqrt{\mu}}\ln\left|\frac{\mathrm{x}-\sqrt{\mu}}{\mathrm{x}+\sqrt{\mu}}\right| - \mathrm{I}'\right], \tag{6.70}$$

$$\frac{1}{2\sqrt{\mu}}\ln\left|\frac{\mathrm{x}-\sqrt{\mu}}{\mathrm{x}+\sqrt{\mu}}\right| + \frac{\varepsilon}{\mu+1}\left[\frac{\mathrm{x}}{\mathrm{x}^2-\mu}\frac{1}{4\sqrt{\mu}}\ln\left|\frac{\mathrm{x}-\sqrt{\mu}}{\mathrm{x}+\sqrt{\mu}}\right| - \mathrm{I}\right] = -\frac{1}{2l}\left(\int\frac{\mathrm{d}x^+}{\mathrm{F}^+} + \int\frac{\mathrm{d}x^-}{\mathrm{F}^-}\right). \tag{6.71}$$

We therefore find that the general quantum-corrected branch-one solution, which is continuously connected to the dimensionally reduced BTZ black hole at the classical level, is defined by $(\mathrm{F}^+, \mathrm{F}^-, \mu, t_+(\sigma^+), t_-(\sigma^-))$. The integrals (6.62) and (6.64) can be evaluated once the quantum state is chosen, because they depend on the functions $t_\pm(\sigma^\pm)$. In particular, the quantum state $|0, x\rangle$ is characterized by $t_\pm(x^\pm) = 0$ (see Section 3.3). We have adopted the shorthand notation $\mathrm{I} = \mathrm{I}_+ + \mathrm{I}_-$ and $\mathrm{I}' = \mathrm{I}'_+ + \mathrm{I}'_-$. Note that these two integrals are not independent; they are related through the equations of motion, so once the quantum state is fixed, only one of them actually needs to be computed. A key property of the solution (6.70-6.71) is that, in contrast to the DREH model (see Section 5.2), Equation (6.71) is not transcendental, and thus x can be written in terms of the coordinates using elementary functions.

Note that we have not addressed the dilaton equation of motion (6.12) explicitly. This equation is automatically fulfilled once the solution (6.70-6.71) is substituted, because it is equivalent to the metric equation combined with the EMT conservation law, which is obeyed by the quantum-corrected EMT (3.75).

For completeness one could also consider the quantum-corrected branch-two solution. Yet this solution is not continuously connected to a well-behaved BTZ black hole and involves an arbitrary function, which likely originates from unfixed five-dimensional gauge transformations. Consequently, it does not constitute a physically meaningful solution. Therefore, we will not examine it further here.

6.2.1 General static quantum-corrected solution

In this subsection, we employ the static ansatz from Section 3.1 for the quantum-corrected equations of motion (6.24-6.26). Upon substituting the explicit expressions for the components of the EMT describing the quantum corrections (3.79), the metric equation of motion simplifies to:

$$T^{\perp\|} = T^{\|\perp} = 0 \qquad \Longrightarrow \qquad t_+(\sigma^+) = t_-(\sigma^-) = \frac{1}{4l^2}\Xi, \tag{6.72}$$

$$\frac{\Lambda}{2}\frac{\mathrm{d}}{\mathrm{dx}}\left(\mathrm{x}^2 + 1 + \Lambda\mathcal{D}^2\right)^2 = \varepsilon\left[\Xi + \frac{1}{4}\left(\mathcal{D}\frac{\mathrm{d}\Lambda}{\mathrm{dx}}\right)^2 - \Lambda\mathcal{D}\frac{\mathrm{d}}{\mathrm{dx}}\left(\mathcal{D}\frac{\mathrm{d}\Lambda}{\mathrm{dx}}\right)\right], \tag{6.73}$$

$$\Lambda\left(\mathrm{x}^2 + 1 + \Lambda\mathcal{D}^2\right)\left(\mathcal{D}^2\frac{\mathrm{d}\Lambda}{\mathrm{dx}} + 2\mathrm{x}\right) = -\varepsilon\left[\Xi + \frac{1}{4}\left(\mathcal{D}\frac{\mathrm{d}\Lambda}{\mathrm{dx}}\right)^2\right], \tag{6.74}$$

where Ξ is a constant related to the state of the quantum fields. To complete this system, we must also include the dilaton equation of motion (6.27). Since both the left-hand side and the right-hand side are of order ε, we can directly insert the classical static solution (6.17). The system of Equations (6.73) and (6.74) then takes the form:

$$\frac{\mathrm{d}\left(\Lambda\mathcal{D}^2\right)}{\mathrm{dx}} = -2\mathrm{x} - \frac{\varepsilon}{\mu+1}\left(\frac{\Xi+\mu}{\mathrm{x}^2-\mu} - 1\right), \tag{6.75}$$

$$\mathcal{D}^2\frac{\mathrm{d}\Lambda}{\mathrm{dx}} = -2\mathrm{x} + \frac{\varepsilon}{\mu+1}\left(\frac{\Xi+\mu}{\mathrm{x}^2-\mu} + 1\right). \tag{6.76}$$

Subtracting Equation (6.76) from Equation (6.75) gives the following solution for the function $\mathcal{D}$:

$$\frac{\mathrm{d}\mathcal{D}^2}{\mathrm{dx}} = \frac{2\varepsilon}{\mu+1}\frac{\Xi+\mu}{\mathrm{x}^2-\mu} = 2\varepsilon\left(\frac{\Xi}{\mu}+1\right)\frac{\mathrm{d}\mathcal{D}_1}{\mathrm{dx}} \qquad \Longrightarrow \qquad \mathcal{D}^2 = 1 + 2\varepsilon\left(\frac{\Xi}{\mu}+1\right)\mathcal{D}_1, \tag{6.77}$$

where we have employed (6.58) to rewrite the solution for $\mathcal{D}$ in terms of the function $\mathcal{D}_1$, presented in (6.67). Upon substituting this expression for $\mathcal{D}$ into (6.76) and performing the integration, the metric function Λ takes the form:

$$\Lambda = -\mathrm{x}^2 + \mu + \varepsilon\left(\frac{\Xi}{\mu}+1\right)\left[\frac{\mathrm{x}}{\mu+1} + 2\int \mathrm{dx}\mathcal{D}_1\mathrm{x} + \left(\mathrm{x}^2-\mu\right)\mathcal{D}_1\right] - \frac{\varepsilon}{\mu+1}\frac{\Xi}{\mu}\left(\mathrm{x}-\sqrt{\mu}\right). \tag{6.78}$$

Finally, we determine the tortoise coordinate using (3.18), which gives:

$$\begin{aligned}\frac{\sigma}{l} = \frac{1}{2\sqrt{\mu}}\ln\left|\frac{\mathrm{x}-\sqrt{\mu}}{\mathrm{x}+\sqrt{\mu}}\right| + \varepsilon\left(\frac{\Xi}{\mu}+1\right)\int\frac{\mathrm{dx}}{\left(\mathrm{x}^2-\mu\right)^2}\left[\frac{\mathrm{x}}{\mu+1} + 2\int\mathrm{dx}\mathcal{D}_1\mathrm{x}\right] \\ - \frac{\varepsilon\Xi}{4\mu^2(\mu+1)}\left(\ln\left|\frac{\mathrm{x}-\sqrt{\mu}}{\mathrm{x}+\sqrt{\mu}}\right| - \frac{\mathrm{x}-\sqrt{\mu}}{\mathrm{x}+\sqrt{\mu}}\right).\end{aligned} \tag{6.79}$$

The solutions (6.77), (6.78), and (6.79) are expressed through the integrals (6.58-6.69). By substituting these expressions, we obtain the following final solution:

$$\begin{aligned}\mathcal{D} &= 1 - \frac{\varepsilon}{2(\mu+1)}\left(\frac{\Xi}{\mu}+1\right)\left[\frac{1}{2\sqrt{\mu}}\ln\left|\frac{\mathrm{x}-\sqrt{\mu}}{\mathrm{x}+\sqrt{\mu}}\right| + \frac{\mathrm{x}}{\mathrm{x}^2-\mu}\right], \\ \Lambda &= -\mathrm{x}^2 + \mu - \frac{\varepsilon}{\mu+1}\left(\frac{\Xi}{\mu}+1\right)\frac{\mathrm{x}^2}{2\sqrt{\mu}}\ln\left|\frac{\mathrm{x}-\sqrt{\mu}}{\mathrm{x}+\sqrt{\mu}}\right| - \frac{\varepsilon}{\mu+1}\frac{\Xi}{\mu}\left(\mathrm{x}-\sqrt{\mu}\right), \\ \frac{\sigma}{l} &= \frac{1}{2\sqrt{\mu}}\ln\left|\frac{\mathrm{x}-\sqrt{\mu}}{\mathrm{x}+\sqrt{\mu}}\right| + \frac{\varepsilon}{\mu+1}\left(\frac{\Xi}{\mu}+1\right)\frac{\mathrm{x}}{\mathrm{x}^2-\mu}\frac{1}{4\sqrt{\mu}}\ln\left|\frac{\mathrm{x}-\sqrt{\mu}}{\mathrm{x}+\sqrt{\mu}}\right| \\ &\quad - \frac{\varepsilon\Xi}{4\mu^2(\mu+1)}\left(\ln\left|\frac{\mathrm{x}-\sqrt{\mu}}{\mathrm{x}+\sqrt{\mu}}\right| - \frac{\mathrm{x}-\sqrt{\mu}}{\mathrm{x}+\sqrt{\mu}}\right).\end{aligned} \tag{6.80}$$

6.2.2 Solution without energy flux at the asymptotic infinity

In this section, we derive the quantum-corrected AdS vacuum solution. By definition, it is a static configuration with no energy flux at asymptotic infinity. The corresponding vacuum state is the Boulware state (3.96), which is implemented by choosing $t_{\pm}(\sigma^{\pm}) = 0$. Equivalently, this means that the EMT of the quantum fields is normal-ordered with respect to the Eddington–Finkelstein coordinates. The general static solution (6.80) depends on the constant Ξ, which is fixed by the choice of vacuum through (6.72). Setting $\Xi = 0$ selects the Boulware state. In this case, the solution simplifies to:

$$\begin{aligned}
\mathcal{D} &= 1 - \frac{\varepsilon}{2(\mu+1)}\left[\frac{1}{2\sqrt{\mu}}\ln\left|\frac{\mathrm{x}-\sqrt{\mu}}{\mathrm{x}+\sqrt{\mu}}\right| + \frac{\mathrm{x}}{\mathrm{x}^2-\mu}\right], \\
\Lambda &= -\mathrm{x}^2 + \mu - \frac{\varepsilon}{\mu+1}\frac{\mathrm{x}^2}{2\sqrt{\mu}}\ln\left|\frac{\mathrm{x}-\sqrt{\mu}}{\mathrm{x}+\sqrt{\mu}}\right|, \\
\frac{\sigma}{l} &= \frac{1}{2\sqrt{\mu}}\ln\left|\frac{\mathrm{x}-\sqrt{\mu}}{\mathrm{x}+\sqrt{\mu}}\right| + \frac{\varepsilon}{\mu+1}\frac{\mathrm{x}}{\mathrm{x}^2-\mu}\frac{1}{4\sqrt{\mu}}\ln\left|\frac{\mathrm{x}-\sqrt{\mu}}{\mathrm{x}+\sqrt{\mu}}\right|.
\end{aligned} \tag{6.81}$$

This solution can be obtained directly from the general solution of the quantum-corrected equations of motion (6.70-6.71). It is specified by $(\mathrm{F}^+, \mathrm{F}^-, \mu, 0, 0)$, which corresponds to the vanishing integrals (6.62) and (6.64). Once these integrals are set to zero, the two solutions coincide.

The important feature of the fluxless solution in the DREH model is that, in the limit of vanishing mass, it remains smoothly connected to the Minkowski vacuum solution (see Section 5.2.2). This feature does not hold in the BPP model. As demonstrated in Section 4.3.1, the linear dilaton vacuum in the BPP framework carries energy flux at both past and future null infinity. Solution (6.81) displays analogous behavior. Although the limit $\mu \to 0$ is well defined, it does not reproduce the AdS vacuum solution. Instead, in this limit the configuration approaches the quantum-corrected AdS spacetime, given by:

$$\mathcal{D} = 1, \qquad \Lambda = -\mathrm{x}^2 + \varepsilon\mathrm{x} + \varepsilon C, \qquad \frac{\sigma}{l} = -\frac{1}{\mathrm{x}} - \frac{\varepsilon}{2\mathrm{x}^2} - \frac{\varepsilon C}{3\mathrm{x}^3}, \tag{6.82}$$

where we have retained the quantum correction C to the μ constant. It is worth emphasizing that, even in the limit $C \to 0$, the solution does not reduce to pure AdS spacetime.

In Sections 4.3.3 and 5.2.2 we show that the fluxless solutions are horizonless in both BPP and DREH models. The same logic follows here as well. Trying to find the horizon reduces to demanding that the norm of the Killing vector vanishes, i.e. $\Lambda = 0$. Solving this equation in a perturbative expansion yields $\mathrm{x_H} = \sqrt{\mu} + \mathcal{O}(\varepsilon)$. At first sight, this suggests the presence of a quantum-corrected horizon. Nevertheless, this solution is not well defined within the perturbative framework, because the quantum correction to Λ vanishes when evaluated on the classical horizon. Consequently, there is actually no horizon within the first-order of the perturbation theory.

Another issue that needs to be addressed is whether the solution (6.81) develops any singularities. In both the BPP and DREH models, the scalar curvature diverges on a certain hypersurface, which must therefore be identified as the boundary of the spacetime. A straightforward calculation of the scalar curvature reveals that it does not receive any quantum corrections within the first order in ε, i.e.:

$$R = -\frac{2}{l^2}. \tag{6.83}$$

From this analysis, we infer that no curvature singularities arise at first order in perturbation theory. Nonetheless, one must keep in mind that $\mathrm{x} > 0$, so within the DR5DCS framework we are still required to impose the reflective boundary conditions (4.117) on the hypersurface at $\mathrm{x} = 0$.

6.2.3 Eternal black hole scenario

In this section, we present the eternal black hole scenario. It describes a black hole in equilibrium with its environment. Consequently, it corresponds to a static configuration and must be specified by choosing a particular value of the constant Ξ within the general static solution (6.80). Because this is a black hole solution, it must possess a well-defined event horizon [106]. The event horizon is specified by the condition $\Lambda = 0$, so the classical location of the horizon is $\mathrm{x_H} = \sqrt{\mu}$. As long as the solution contains a term of the form $\ln|\mathrm{x} - \sqrt{\mu}|$, the quantum correction diverges at the classical horizon, just as in the fluxless solution discussed in the previous section. There is a unique value of Ξ that eliminates the logarithmic contribution in Λ, namely:

$$\Xi = -\mu. \tag{6.84}$$

Substituting this value of Ξ into the general solution (6.80), we obtain the following eternal black hole solution:

$$\begin{aligned}
&\mathcal{D} = 1,\\
&\Lambda = -\mathrm{x}^2 + \mu + \frac{\varepsilon}{\mu+1}\left(\mathrm{x} - \sqrt{\mu}\right),\\
&\frac{\sigma}{l} = \frac{1}{2\sqrt{\mu}}\ln\left|\frac{\mathrm{x}-\sqrt{\mu}}{\mathrm{x}+\sqrt{\mu}}\right| + \frac{\varepsilon}{4\mu(\mu+1)}\left(\ln\left|\frac{\mathrm{x}-\sqrt{\mu}}{\mathrm{x}+\sqrt{\mu}}\right| - \frac{\mathrm{x}-\sqrt{\mu}}{\mathrm{x}+\sqrt{\mu}}\right)
\end{aligned} \tag{6.85}$$

We can now straightforwardly determine the event horizon by solving $\Lambda = 0$. One observes that the integration constant in the Ξ-dependent term of (6.80) is fixed such that the quantum-corrected horizon coincides with the classical one, $\mathrm{x_H} = \sqrt{\mu}$. We then proceed to evaluate the curvature. A direct calculation gives:

$$R = \frac{1}{l^2}\frac{\mathrm{d}^2\Lambda}{\mathrm{dx}^2} = -\frac{2}{l^2} \quad \Longrightarrow \quad \mathrm{x_S} = 0. \tag{6.86}$$

Thus, the singularity does not acquire any quantum corrections as well. The surface gravity is given by:

$$\kappa = \frac{1}{2l}\left|\mathcal{D}\frac{\mathrm{d}\Lambda}{\mathrm{dx}}\right|_{\mathrm{H}} = \frac{\sqrt{\mu}}{l}\left[1 - \frac{\varepsilon}{2(\mu+1)\sqrt{\mu}}\right]. \tag{6.87}$$

To confirm that the solution (6.85) indeed describes an eternal black hole, we must verify that the quantum fields are prepared in the Hartle-Hawking state (3.97). This requirement means that the EMT is normal-ordered in Kruskal coordinates, which are obtained by exponentiating the Eddington-Finkelstein coordinates (see Appendix D.5), using the surface gravity (6.87). Employing the definition of Ξ (6.72) together with the transformation law for the quantum-corrected EMT (3.83), we find:

$$\frac{1}{4l^2}\Xi = t_\pm(\sigma^\pm) = \left(\frac{dx^\pm}{d\sigma^\pm}\right)^2\left[\cancelto{0}{t_\pm}(x^\pm) - \frac{1}{2}D_{x^\pm}[\sigma^\pm]\right] = -\frac{\kappa^2}{4} \quad \Longrightarrow \quad \Xi = -(\kappa l)^2 = -\mu. \tag{6.88}$$

Since this matches (6.84), the solution (6.85) indeed describes an eternal black hole. We now examine the singular behavior of the tortoise coordinate. Using the surface gravity in (6.87) leads to:

$$\sigma = \frac{1}{2\kappa}\left[\ln\left|\frac{\mathrm{x}-\sqrt{\mu}}{\mathrm{x}+\sqrt{\mu}}\right| - \frac{\varepsilon}{2(\mu+1)\sqrt{\mu}}\frac{\mathrm{x}-\sqrt{\mu}}{\mathrm{x}+\sqrt{\mu}}\right]. \tag{6.89}$$

In the general static quantum-corrected solution (6.80), the Ξ-dependent term in the tortoise coordinate is chosen so that there is a single logarithmic pole exactly at the quantum-corrected event horizon $\mathrm{x_H} = \sqrt{\mu}$, where the quantum correction vanishes.

The same solution can be derived from the general quantum-corrected configuration (6.70-6.71) by explicitly evaluating the integrals I and I′. In this setting, the solution is given by $(\mathrm{F}^+, \mathrm{F}^-, \mu, -\frac{\mu}{4l^2}, -\frac{\mu}{4l^2})$. Care is required, since these integrals are defined only up to arbitrary functions, which must be fixed by substituting the solution back into the original equations of motion. An analogous analysis for the DREH model appears in Section 5.2.3.

6.3 Evaporating black hole scenario

The evaporating black hole scenario covers both the gravitational collapse forming the black hole and its later Hawking-radiation-driven evaporation. We use the framework of Section 3.4, adapted to an asymptotically AdS spacetime.

In Section 6.1.3, we studied purely classical gravitational collapse, and in Section 6.1.4 we constructed its conformal diagram. We now extend this to the quantum-corrected case. Including the back-reaction of quantum fields on the classical geometry yields an evaporating black hole. As in the BPP model—and unlike the DREH model—the initial spacetime cannot be the AdS vacuum. We therefore use the quantum-corrected AdS spacetime defined in (6.82). For an evaporating black hole, the relevant vacuum is the Unruh state (3.98), defined by $t_\pm(\sigma^\pm) = 0$. Although the initial spacetime has zero energy flux at infinity, a nonzero flux appears at future null infinity after the black hole forms, due to the change in asymptotic coordinates (see Section 3.4).

The quantum-corrected collapse scenario is shown in Figure 6.3. Before black hole formation, we use the Eddington–Finkelstein gauge, i.e., the $\sigma^\pm$ coordinates of solution (6.82), for which the solution is $(-1, 1, \varepsilon C_0, 0, 0)$. In region II, where an evaporating black hole is present, we use Eddington–Finkelstein coordinates $\hat{\sigma}^\pm$, and the solution is $(-1, \mathrm{F}^-, \mu, 0, t_-(\hat{\sigma}^-))$. We must therefore determine $t_\pm(\hat{\sigma}^\pm)$ via the transformation law (3.83). Since the coordinate transformation (3.6) is written in terms of the functions $\mathrm{F}^\pm$, defined in (6.42), this amounts to computing the Schwarzian derivative. The final result is expressed in terms of the coordinate $\hat{\mathrm{x}}$:

$$t_+(\hat{\sigma}^+) = 0, \quad t_-(\hat{\sigma}^-) = -\frac{\mu}{4l^2}. \tag{6.90}$$

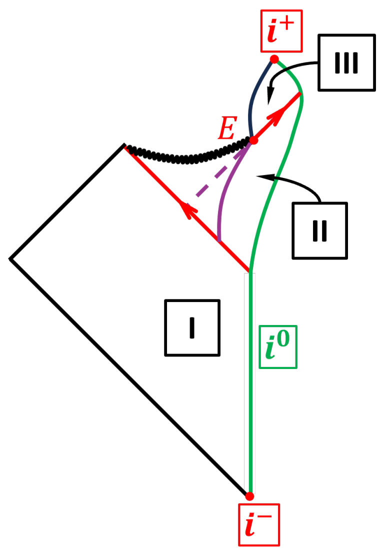

Figure 6.3: Penrose diagram of the quantum-corrected gravitational collapse for the BTZ black hole.

When the back-reaction is included, the classical spacetime depicted in Figure 6.2 acquires a third region as illustrated in Figure 6.3. This additional region represents the static remanent spacetime created as a consequence of the black hole evaporation. It is characterized by the end-state geometry. With all necessary ingredients specified, the next task is to determine θ, whose general expression is given in Equation (6.63). This solution, however, is only fixed up to the integral I in (6.64). The problem therefore reduces to computing these integrals for the particular choice (6.90). Because $t_+ = 0$, the integral I_+ vanishes, leaving us solely with the integral I_-:

$$\mathrm{I} = \int \frac{\mathrm{d}\sigma^-}{\mathrm{F}^-}\frac{1}{\mathrm{x}^2-\mu}\int \frac{\mathrm{d}\sigma^-}{\mathrm{F}^-}t_-(\hat{\sigma}^-). \tag{6.91}$$

We begin by computing the inner integral. Upon applying the substitution in (6.42), the resulting integral evaluates to:

$$\int \frac{\mathrm{d}\sigma^-}{\mathrm{F}^-}t_-(\hat{\sigma}^-) = \frac{\sqrt{\mu}}{4l}\ln\left|\frac{1+\hat{\mathrm{x}}\sqrt{\mu}}{1-\hat{\mathrm{x}}\sqrt{\mu}}\right| \equiv \frac{1}{4l}\mathrm{F}(\hat{\mathrm{x}}), \tag{6.92}$$

where we have defined an additional function $\mathrm{F}(\hat{\mathrm{x}})$. Unlike in the DREH model, $\hat{\mathrm{x}}$ can be expressed in terms of the elementary functions of x and δ. As a result, the integral I simplifies to:

$$\mathrm{I} = \frac{\mathrm{x}}{\mathrm{x}^2-\mu}\frac{1}{4\sqrt{\mu}}\ln\left|\frac{\mathrm{x}-\sqrt{\mu}}{\mathrm{x}+\sqrt{\mu}}\right| + \frac{1}{16\mu}\ln^2\left|\frac{\mathrm{x}-\sqrt{\mu}}{\mathrm{x}+\sqrt{\mu}}\right| + \frac{1}{4}\frac{1}{\mathrm{x}^2-\mu} - (\mu+1)\mathcal{D}_1(\mathrm{x})\ln\delta, \tag{6.93}$$

where the function $\mathcal{D}_1$ is defined in (6.67). Plugging this expression into the solution for θ in (6.63) yields:

$$\begin{aligned}\frac{\theta}{\mathrm{x}^2-\mu} = \frac{1}{2l}\left(\int \mathrm{d}\sigma^+\frac{\mathrm{G}^+}{\mathrm{F}^{+2}} + \int \mathrm{d}\sigma^-\frac{\mathrm{G}^-}{\mathrm{F}^{-2}}\right) + \frac{1}{4(\mu+1)}\left[\frac{1}{4\mu}\ln^2\left|\frac{\mathrm{x}-\sqrt{\mu}}{\mathrm{x}+\sqrt{\mu}}\right| + \frac{1}{\mathrm{x}^2-\mu}\right]\\ - \mathcal{D}_1(\mathrm{x})\left(\ln\delta + C\frac{\mu+1}{\mu}\right).\end{aligned} \tag{6.94}$$

The metric correction α can be obtained directly from the Equation of motion (6.56). The resulting expression is:

$$(\mathrm{x}^2-\mu)\left[2\alpha + \frac{\mathrm{G}^+}{\mathrm{F}^+} + \frac{\mathrm{G}^-}{\mathrm{F}^-}\right] - 2\mathrm{x}\theta = \frac{1}{2(\mu+1)}\left[\frac{\mathrm{x}^2-\mu}{2\sqrt{\mu}}\ln\left|\frac{\mathrm{x}-\sqrt{\mu}}{\mathrm{x}+\sqrt{\mu}}\right| - \mathrm{x}\right] - \frac{\mu}{\mu+1}\ln\delta - C. \tag{6.95}$$

Equations (6.94) and (6.95) describe the quantum modifications of the tortoise coordinate and of the metric solutions, respectively. Hence, the final form of the solution can be written as:

$$\mathrm{F}^+\mathrm{F}^-e^{2\rho} = -\mathrm{x}^2 + \mu - \frac{\varepsilon}{\mu+1}\left[\frac{\mathrm{x}^2-\mu}{4\sqrt{\mu}}\ln\left|\frac{\mathrm{x}-\sqrt{\mu}}{\mathrm{x}+\sqrt{\mu}}\right| - \frac{\mathrm{x}}{2}\right] + \varepsilon\left(\frac{\mu}{\mu+1}\ln\delta + C\right), \tag{6.96}$$

$$\frac{\hat{\sigma}}{l} = \frac{1}{2\sqrt{\mu}}\ln\left|\frac{\mathrm{x}-\sqrt{\mu}}{\mathrm{x}+\sqrt{\mu}}\right| - \frac{\varepsilon}{4(\mu+1)}\left[\frac{1}{4\mu}\ln^2\left|\frac{\mathrm{x}-\sqrt{\mu}}{\mathrm{x}+\sqrt{\mu}}\right| + \frac{1}{\mathrm{x}^2-\mu}\right] + \varepsilon\mathcal{D}_1\left(\ln\delta + C\frac{\mu+1}{\mu}\right). \tag{6.97}$$

Equations (6.96) and (6.97) describe a family of evaporating black hole solutions specified by a constant C and by the coordinate transformation F^-. The transformation F^+ cannot vary across the ingoing shockwave hypersurface. The values of C and F^- are uniquely determined once the continuity conditions (3.102) and (3.104) are enforced.

6.3.1 Evaporating black hole solution

In this subsection, we identify the specific solution among (6.96-6.97) that remains continuously connected to the quantum-corrected AdS vacuum solution across the ingoing shockwave hypersurface. In region I, the solution is provided by (6.82). For clarity, we rewrite it here:

$$e^{2\rho} = \mathrm{x}^2 - \varepsilon \mathrm{x} - \varepsilon C_0, \qquad -\frac{1}{\mathrm{x}} - \frac{\varepsilon}{2\mathrm{x}^2} - \frac{\varepsilon C_0}{3\mathrm{x}^3} = -\ln\delta + \hat{\mathrm{x}}, \tag{6.98}$$

where we have retained the constant C_0, which is linked to the mass of the spacetime in region I. We keep this constant as a diagnostic tool to monitor the energy balance in the model. Nonetheless, from a physical standpoint we must set $C_0 = 0$, because the initial spacetime is required to be massless. Let us now determine the metric and the dilaton field along the ingoing shockwave, that is, on the $\delta = 1$ hypersurface. They are given by:

$$e^{2\rho}\Big|_{\delta=1} = \frac{1}{\hat{\mathrm{x}}^2} - \frac{\varepsilon C_0}{3}, \qquad \mathrm{x}\Big|_{\delta=1} = -\frac{1}{\hat{\mathrm{x}}}\left[1 - \frac{\varepsilon}{2}\hat{\mathrm{x}} + \frac{\varepsilon C_0}{3}\hat{\mathrm{x}}^2\right]. \tag{6.99}$$

The coordinate transformation F^- can now be straightforwardly determined by imposing continuity of the metric across the $\delta = 1$ hypersurface. In this limit, Equation (6.96) reduces to:

$$\mathrm{F}^- e^{2\rho} = \mathrm{x}^2 - \mu - \varepsilon C + \frac{\varepsilon}{\mu+1}\left[\frac{\mathrm{x}^2-\mu}{4\sqrt{\mu}}\ln\left|\frac{\mathrm{x}-\sqrt{\mu}}{\mathrm{x}+\sqrt{\mu}}\right| - \frac{\mathrm{x}}{2}\right]. \tag{6.100}$$

After inserting (6.99), we arrive at the explicit expression for $\mathrm{F}^- = \mathrm{F}^-(\hat{\mathrm{x}})$:

$$\mathrm{F}^- = 1 - (\mu + \varepsilon(C - C_0))\,\hat{\mathrm{x}}^2 - \varepsilon\hat{\mathrm{x}} - \frac{\varepsilon\mu C_0}{3}\hat{\mathrm{x}}^4 + \frac{\varepsilon}{\mu+1}\left[\frac{1-\mu\hat{\mathrm{x}}^2}{4\sqrt{\mu}}\ln\left|\frac{1+\hat{\mathrm{x}}\sqrt{\mu}}{1-\hat{\mathrm{x}}\sqrt{\mu}}\right| + \frac{\hat{\mathrm{x}}}{2}\right]. \tag{6.101}$$

Next, we enforce the "++" equation condition (3.104), which in the DR5DCS model takes the form:

$$\left[\left(\mathrm{x}^2 + 1 - \frac{1}{2}l^2\,(\nabla\mathrm{x})^2\right)\partial_+\mathrm{x} + \varepsilon\partial_+\rho\right]\Big|_{<}^{>} = -\frac{M}{6k\pi^2}\Big|_{x^+=x_0^+}, \tag{6.102}$$

where $>$ and $<$ refer to the sides of region II and region I relative to the $\delta = 1$ hypersurface. Upon substituting solution (6.98) in region I and solutions (6.96-6.97) in region II, Equation (6.102) simplifies to:

$$\mu(\mu+2) + 2\varepsilon\left((\mu+1)C - C_0\right) = \frac{2Ml}{3k\pi^2}. \quad \Longrightarrow \quad C = \frac{C_0}{\mu+1}, \tag{6.103}$$

where we have employed the classical relation (6.44) connecting the mass to the parameter μ. Now that both F^- and C are fixed, we proceed to evaluate the $\hat{\sigma}^-$ coordinate. A straightforward integration gives:

$$\begin{aligned}\frac{\sigma_0^+ - \hat{\sigma}^-}{2l} = \frac{1}{2\sqrt{\mu}}\ln\left|\frac{1+\hat{\mathrm{x}}\sqrt{\mu}}{1-\hat{\mathrm{x}}\sqrt{\mu}}\right| - \frac{\varepsilon}{4(\mu+1)}\left[\frac{1}{4\mu}\ln^2\left|\frac{1+\hat{\mathrm{x}}\sqrt{\mu}}{1-\hat{\mathrm{x}}\sqrt{\mu}}\right| + \frac{\hat{\mathrm{x}}^2}{1-\mu\hat{\mathrm{x}}^2}\right] + \frac{\varepsilon}{2}\frac{\hat{\mathrm{x}}^2}{1-\mu\hat{\mathrm{x}}^2}\\ + \frac{\varepsilon C_0}{3\mu}\left[(1-2\mu)\mathcal{D}_1\left(-\frac{1}{\hat{\mathrm{x}}}\right) - \frac{1}{2\sqrt{\mu}}\ln\left|\frac{1+\hat{\mathrm{x}}\sqrt{\mu}}{1-\hat{\mathrm{x}}\sqrt{\mu}}\right| + \hat{\mathrm{x}}\right].\end{aligned} \tag{6.104}$$

Hence, the solution describing an evaporating black hole can be written as:

$$\mathrm{F}^{+}\mathrm{F}^{-}e^{2\rho} = -\mathrm{x}^2 + \mu + \frac{\varepsilon}{\mu+1}\left[\mu\ln\delta + C_0 - \frac{\mathrm{x}^2-\mu}{4\sqrt{\mu}}\ln\left|\frac{\mathrm{x}-\sqrt{\mu}}{\mathrm{x}+\sqrt{\mu}}\right| + \frac{\mathrm{x}}{2}\right], \tag{6.105}$$

$$\begin{aligned}\frac{1}{2\sqrt{\mu}}\ln\left|\frac{\mathrm{x}-\sqrt{\mu}}{\mathrm{x}+\sqrt{\mu}}\right| - \frac{\varepsilon}{4(\mu+1)}\left[\frac{1}{4\mu}\ln^2\left|\frac{\mathrm{x}-\sqrt{\mu}}{\mathrm{x}+\sqrt{\mu}}\right| + \frac{1}{\mathrm{x}^2-\mu}\right] + \frac{\varepsilon}{\mu}\left(\mu\ln\delta + C_0\right)\mathcal{D}_1(\mathrm{x}) \\ = -\ln\delta + \frac{1}{2\sqrt{\mu}}\ln\left|\frac{1+\hat{\mathrm{x}}\sqrt{\mu}}{1-\hat{\mathrm{x}}\sqrt{\mu}}\right| - \frac{\varepsilon}{4(\mu+1)}\left[\frac{1}{4\mu}\ln^2\left|\frac{1+\hat{\mathrm{x}}\sqrt{\mu}}{1-\hat{\mathrm{x}}\sqrt{\mu}}\right| + \frac{\hat{\mathrm{x}}^2}{1-\mu\hat{\mathrm{x}}^2}\right] + \frac{\varepsilon}{2}\frac{\hat{\mathrm{x}}^2}{1-\mu\hat{\mathrm{x}}^2} \\ + \frac{\varepsilon C_0}{3\mu}\left[(1-2\mu)\mathcal{D}_1\left(-\frac{1}{\hat{\mathrm{x}}}\right) - \frac{1}{2\sqrt{\mu}}\ln\left|\frac{1+\hat{\mathrm{x}}\sqrt{\mu}}{1-\hat{\mathrm{x}}\sqrt{\mu}}\right| + \hat{\mathrm{x}}\right].\end{aligned} \tag{6.106}$$

The solution takes the form $\left(-1, \mathrm{F}^{-}, \sqrt{1+\frac{2Ml}{3k\pi^2}} - 1 + \frac{\varepsilon C_0}{\mu+1}, 0, -\frac{\mu}{4l^2}\right)$, where F^{-} is defined in (6.101). One can readily verify that Equation (6.106) remains valid on the $\delta = 1$ hypersurface. Substituting the expression for x from (6.99) and expanding the left-hand side in powers of ε, we find that it coincides with the right-hand side, viewed as a function of $\hat{\mathrm{x}}$.

6.3.2 Evaporation adapted form of the solution

In this subsection, we follow the approach of Section 5.3.3, where the solution in the DREH model was recast into a form that is manifestly well defined on the classical horizon. The metric in Equation (6.105) is already well defined at the horizon. The tortoise coordinate (6.106), however, does not display the well behavior there. It should exhibit a pole along a well defined hypersurface, but in its current form of the solution, one cannot readily find that hypersurface. Our goal in this section is to resolve this issue. For convenience, we set $C_0 = 0$. We begin by evaluating the derivatives of the dilaton field, which are:

$$\partial_{+}\mathrm{x} = \frac{1}{2l}\left[\mathrm{x}^2 - \tilde{\mu} - \frac{\varepsilon}{\mu+1}\mathrm{x}\right], \tag{6.107}$$

$$\partial_{-}\mathrm{x} = -\frac{1}{2l\mathrm{F}^{-}}\left[\mathrm{x}^2 - \tilde{\mu} + \frac{\varepsilon}{\mu+1}\left(\frac{\mathrm{x}^2-\mu}{4\sqrt{\mu}}\ln\left|\frac{\mathrm{x}-\sqrt{\mu}}{\mathrm{x}+\sqrt{\mu}}\right| - \frac{\mathrm{x}}{2}\right)\right], \tag{6.108}$$

where we have defined the reduced parameter $\tilde{\mu}$ as follows:

$$\tilde{\mu} = \mu + \frac{\varepsilon}{\mu+1}\Big(\mu\ln\delta + C_0\Big). \tag{6.109}$$

Next, we define a new constant $\mathrm{y} = \mathrm{x}/\sqrt{\tilde{\mu}}$. Our goal is to determine a function $\mathcal{J}(\mathrm{y})$ such that $\mathcal{J}(\mathrm{y})/\sqrt{\tilde{\mu}} = \frac{\sigma^{+}}{2l}$. Differentiating this relation with respect to σ^{+} and inserting expression (6.107), we obtain the following first-order differential equation for $\mathcal{J}$:

$$\left[\mathrm{y}^2 - 1 - \frac{\varepsilon}{2(\mu+1)\sqrt{\mu}}\mathrm{y}\right]\frac{\mathrm{d}\mathcal{J}}{\mathrm{dx}} + \frac{\varepsilon}{2(\mu+1)\sqrt{\mu}}\mathcal{J} = 1. \tag{6.110}$$

The general form of the solution to this equation of motion is given by:

$$\mathcal{J}(\mathrm{y}) = \frac{2(\mu+1)\sqrt{\mu}}{\varepsilon}\left(1 - e^{-f(\mathrm{y})}\right) + Se^{-f(\mathrm{y})}, \tag{6.111}$$

where S denotes an arbitrary constant, and the function $f(\mathrm{y})$ is defined as:

$$f(\mathrm{y})=\frac{\varepsilon}{2(\mu+1)\sqrt{\mu}}\int\frac{\mathrm{dy}}{\mathrm{y}^2-1-\frac{\varepsilon}{2(\mu+1)\sqrt{\mu}}\mathrm{y}}=\frac{\varepsilon}{2(\mu+1)\sqrt{\mu}}\frac{1}{\mathrm{y}_+-\mathrm{y}_-}\ln\left|\frac{\mathrm{y}-\mathrm{y}_+}{\mathrm{y}-\mathrm{y}_-}\right|, \tag{6.112}$$

where $\mathrm{y}_\pm$ are solutions of the following quadratic equation:

$$\mathrm{y}^2-1-\frac{\varepsilon}{2(\mu+1)\sqrt{\mu}}\mathrm{y}=0 \quad\Longrightarrow\quad \mathrm{y}_\pm=\pm1+\frac{\varepsilon}{4(\mu+1)\sqrt{\mu}}. \tag{6.113}$$

We have expanded the roots of the given quadratic equation to first order in ε. For the consistency check, we expand the function $\mathcal{J}$ (6.111) to first order in y:

$$\begin{aligned}
f(\mathrm{y})&=\frac{\varepsilon}{4(\mu+1)\sqrt{\mu}}\left[\ln\left|\frac{\mathrm{y}-1}{\mathrm{y}+1}\right|-\frac{\varepsilon}{2(\mu+1)\sqrt{\mu}}\frac{1}{\mathrm{y}^2-1}\right],\\
\mathcal{J}(\mathrm{y})&=\frac{2(\mu+1)\sqrt{\mu}}{\varepsilon}\left(f(\mathrm{y})-\frac{1}{2}f^2(\mathrm{y})\right)+S\left(1-f(\mathrm{y})\right),\\
&=\frac{1}{2}\ln\left|\frac{\mathrm{y}-1}{\mathrm{y}+1}\right|-\frac{\varepsilon}{4(\mu+1)\sqrt{\mu}}\left[\frac{1}{4}\ln^2\left|\frac{\mathrm{y}-1}{\mathrm{y}+1}\right|+\frac{1}{\mathrm{y}^2-1}\right]+S\left[1-\frac{\varepsilon}{4(\mu+1)\sqrt{\mu}}\ln\left|\frac{\mathrm{y}-1}{\mathrm{y}+1}\right|\right],\\
\frac{\mathcal{J}(\mathrm{y})}{\sqrt{\tilde{\mu}}}&=\frac{1}{2\sqrt{\mu}}\ln\left|\frac{\mathrm{x}-\sqrt{\mu}}{\mathrm{x}+\sqrt{\mu}}\right|-\frac{\varepsilon}{4(\mu+1)}\left[\frac{1}{4\mu}\ln^2\left|\frac{\mathrm{x}-\sqrt{\mu}}{\mathrm{x}+\sqrt{\mu}}\right|+\frac{1}{\mathrm{x}^2-\mu}\right]+\frac{\varepsilon}{\mu}\left(\mu\ln\delta+C_0\right)\mathcal{D}_1(\mathrm{x})\\
&\qquad+S\left[1-\frac{\varepsilon}{4\mu(\mu+1)}\ln\left|\frac{\mathrm{x}-\sqrt{\mu}}{\mathrm{x}+\sqrt{\mu}}\right|\right].
\end{aligned} \tag{6.114}$$

We therefore find that the functional $\mathcal{J}$ correctly reproduces the left-hand side of the solution (6.106) for the dilaton field in the case $S=0$. Next, we impose $C_0=0$ and likewise recast the right-hand side of that equation:

$$\frac{1}{\sqrt{\tilde{\mu}}}\mathcal{J}\left(\frac{\mathrm{x}}{\sqrt{\tilde{\mu}}}\right)=-\ln\delta+\frac{1}{\sqrt{\mu}}\mathcal{J}\left(-\frac{1}{\hat{\mathrm{x}}\sqrt{\tilde{\mu}}}\right),\qquad \tilde{\mu}=\mu\left(1+\varepsilon\hat{\mathrm{x}}\right). \tag{6.115}$$

Thus, the appropriate pole in the dilaton solution is determined by the pole of the $\mathcal{J}$ function, namely $\mathrm{y}=\mathrm{y}_+=1+\frac{\varepsilon}{4(\mu+1)\sqrt{\mu}}$, expanded to first order in ε. We now examine the behavior of the solution in the vicinity of the classical horizon, that is, for $\mathrm{y}=1+\frac{\varepsilon}{4(\mu+1)\sqrt{\mu}}\eta$ and $-\frac{1}{\hat{\mathrm{x}}\sqrt{\tilde{\mu}}}=1+\frac{\varepsilon}{4(\mu+1)\sqrt{\mu}}\vartheta$. Equation (6.115) can be recast in the following form:

$$\frac{\mu}{\tilde{\mu}}e^{-2f(\mathrm{y})}=e^{-2f(-1/(\sqrt{\tilde{\mu}}\hat{\mathrm{x}}))}\quad\Longrightarrow\quad\left(\frac{\tilde{\mu}}{\mu}\right)^{\frac{2(\mu+1)\sqrt{\mu}}{\varepsilon}}\left|\frac{\mathrm{y}-\mathrm{y}_+}{\mathrm{y}-\mathrm{y}_-}\right|=\left|\frac{-\frac{1}{\hat{\mathrm{x}}\sqrt{\tilde{\mu}}}-\mathrm{y}_+}{-\frac{1}{\hat{\mathrm{x}}\sqrt{\tilde{\mu}}}-\mathrm{y}_-}\right|, \tag{6.116}$$

where the implication follows after raising the equation to the power $-\frac{2(\mu+1)\sqrt{\mu}}{\varepsilon}$. This relation is valid for all values of y and $\hat{\mathrm{x}}$. We now examine the behavior in the vicinity of the classical horizon. Because both sides of the equation are already of order ε, we can safely take the limit $\varepsilon\to0$ in the remaining parts of the equation. This leads to:

$$\left|\frac{\vartheta-1}{\eta-1}\right|=\left(1+\frac{\varepsilon}{\mu+1}\ln\delta\right)^{\frac{2(\mu+1)\sqrt{\mu}}{\varepsilon}}\quad\Longrightarrow\quad\left|\frac{\vartheta-1}{\eta-1}\right|=\delta^{2\sqrt{\mu}}. \tag{6.117}$$

Here, the final result arises from taking the limit $\varepsilon\to0$ on the left-hand side of the equation.

6.3.3 The end-state of black hole evolution

In the previous subsections evaporating black hole has been found, which resides in region II of the spacetime illustrated in Figure 6.3. The final state of black hole evaporation characterizes both the quantum matter fields in region III and the ultimate geometry of region III. To investigate this end-state, we must first establish that region III indeed exists. As discussed in Section 3.4.1, evaporation terminates when the singularity intersects the apparent horizon. Consequently, we must first identify the hypersurfaces corresponding to the apparent horizon and the singularity. The apparent horizon is specified by the condition $\partial_+ e^{-3\phi} = 0$. Employing (6.107), we obtain:

$$\mathrm{x}^2 - \mu - \frac{\varepsilon}{\mu+1}\left(\mu \ln\delta + C_0\right) - \frac{\varepsilon}{\mu+1}\mathrm{x} = 0 \quad \Longrightarrow \quad \mathrm{x}_{\mathrm{AH}}^2 = \mu\left[1 + \frac{\varepsilon}{\mu+1}\left(\ln\delta + \frac{C_0}{\mu} + \frac{1}{\sqrt{\mu}}\right)\right]. \tag{6.118}$$

For $\delta \approx 1$, the apparent horizon lies close to the classical horizon. As δ decreases, however, $\ln\delta$ becomes more negative, which in turn reduces the radius of the apparent horizon. Consequently, at late times (corresponding to smaller values of δ), it approaches the classical singularity. This is the desired behavior from the standpoint of black hole evaporation, as it indicates that the black hole shrinks over time. Because the apparent horizon initially coincides with the classical horizon at the onset of evaporation, it is more conveniently described in the y coordinate:

$$\mathrm{y}_{\mathrm{AH}} = \sqrt{1 + \frac{\varepsilon}{(\mu+1)\sqrt{\mu}}}. \tag{6.119}$$

We observe that, in this y coordinate, the apparent horizon remains at a fixed value. As demonstrated in the preceding subsection, the y coordinate is well defined throughout the evaporation process, so we may extend our analysis to any time.

Next, we express the apparent horizon in terms of the $\hat{\mathrm{x}}$ coordinate. For this purpose, we employ Equation (6.117), noting that both y and $-1/(\hat{\mathrm{x}}\sqrt{\mu})$ lie close to the classical horizon. After some algebraic manipulation, we obtain:

$$-\frac{1}{\hat{\mathrm{x}}_{\mathrm{AH}}} = \sqrt{\mu} - \frac{\varepsilon}{2} + \frac{\varepsilon}{4(\mu+1)}\left(1 + \delta_{\mathrm{AH}}^{2\sqrt{\mu}}\right), \tag{6.120}$$

where we have used the fact that $\eta = 2$ for y_{AH}.

To identify the singularity line, we first calculate the scalar curvature. A detailed analysis reveals that the scalar curvature receives no quantum corrections, so we have $R = -2/l^2$. Consequently, the singularity remains located at $\mathrm{x_S} = 0$, or, equivalently, at $\mathrm{y_S} = 0$. Inserting $\mathrm{y_S} = 0$ into (6.116) gives:

$$\sqrt{\mu}\hat{\mathrm{x}}_{\mathrm{S}} = \hat{\mathrm{x}}_{\mathrm{S}}\sqrt{\mu} + \frac{\varepsilon}{\sqrt{\mu}}\hat{\mathrm{x}}_{\mathrm{S}}^2 = \frac{\mathrm{y}_+\left(1 + \frac{\varepsilon}{\mu+1}\ln\delta_{\mathrm{S}}\right)^{\frac{2(\mu+1)\sqrt{\mu}}{\varepsilon}} + \mathrm{y}_+^{-1}}{\left(1 + \frac{\varepsilon}{\mu+1}\ln\delta_{\mathrm{S}}\right)^{\frac{2(\mu+1)\sqrt{\mu}}{\varepsilon}} - 1}, \tag{6.121}$$

where y_+ is defined in (6.113). In the limit $\varepsilon \to 0$, the singular line reduces to the classical one given in (6.48). This provides a straightforward consistency test of our perturbative method. An analogous statement holds for the quantum-corrected spatial infinity hypersurface i^0, which is given by:

$$\sqrt{\mu}\hat{\mathrm{x}}_{i^0} = \hat{\mathrm{x}}_{i^0}\sqrt{\mu} + \frac{\varepsilon}{\sqrt{\mu}}\hat{\mathrm{x}}_{i^0}^2 = \frac{\mathrm{y}_+\left(1 + \frac{\varepsilon}{\mu+1}\ln\delta_{i^0}\right)^{\frac{2(\mu+1)\sqrt{\mu}}{\varepsilon}} - \mathrm{y}_+^{-1}}{\left(1 + \frac{\varepsilon}{\mu+1}\ln\delta_{i^0}\right)^{\frac{2(\mu+1)\sqrt{\mu}}{\varepsilon}} + 1}. \tag{6.122}$$

The end-point of the evaporation

The cosmic censorship conjecture [106] rules out the occurrence of naked singularities. In the present context, the singularity becomes naked once it intersects the apparent horizon hypersurface. The intersection point is referred to as the end-point of the evaporation. By setting (6.118) equal to (6.121), we obtain:

$$\ln \delta_{\mathrm{E}} = -\frac{\mu+1}{\varepsilon} - \frac{C_0}{\mu} - \frac{1}{\sqrt{\mu}}. \tag{6.123}$$

Next, we determine the remaining coordinate. Substituting $\ln \delta_{\mathrm{E}}$ directly into (6.120) gives:

$$\delta_{\mathrm{E}} = e^{-\frac{\mu+1}{\varepsilon} - \frac{1}{\sqrt{\mu}}} \qquad \wedge \qquad \hat{\mathrm{x}}_{\mathrm{E}} = -\frac{1}{\sqrt{\mu}}\left[1 + \frac{\varepsilon}{2\sqrt{\mu}} - \frac{\varepsilon}{4(\mu+1)\sqrt{\mu}} e^{-\frac{\mu+1}{\varepsilon} - \frac{1}{\sqrt{\mu}}}\right]. \tag{6.124}$$

Therefore, the evaporation end-point shows the same type of singular behavior in the limit $\varepsilon \to 0$ as in both the BPP model (4.124) and the DREH model (5.205-5.206). The event horizon is determined by the condition $\hat{\mathrm{x}}_{\mathrm{H}} = \hat{\mathrm{x}}_{\mathrm{E}}$. Employing (6.117), we can express the y-coordinate of the event horizon in terms of δ as follows:

$$\mathrm{y}_{\mathrm{H}} = 1 + \frac{\varepsilon}{4(\mu+1)\sqrt{\mu}}\left(1 + \frac{\delta_{\mathrm{E}}}{\delta_{\mathrm{H}}}\right). \tag{6.125}$$

The horizon may also be expressed as a dependence of the dilaton field on the δ coordinate:

$$\mathrm{x}_{\mathrm{H}}^2 = \mu\left[1 + \frac{\varepsilon}{\mu+1}\left(\ln \delta_{\mathrm{H}} + \frac{1}{2\sqrt{\mu}}\left(1 + \frac{\delta_{\mathrm{E}}}{\delta_{\mathrm{H}}}\right)\right)\right]. \tag{6.126}$$

At the beginning of the evaporation the event horizon appears near the classical horizon, because in this regime one has $\delta_{\mathrm{E}} \ll \frac{\varepsilon}{\mu+1} \ll 1$. In this case, it is simply displaced from the classical horizon by $\frac{\varepsilon}{4(\mu+1)}$. As δ evolves towards the end-point of the evaporation, x_{H} tends to zero. We thus deduce that, at the evaporation end-point, all three hypersurfaces—the apparent horizon (6.118), the event horizon (6.126), and the singularity $\mathrm{x}_{\mathrm{S}} = 0$ intersect at the end-point of the evaporation. We now proceed to evaluate the evaporation time, whose leading contribution is:

$$\Delta t_{\mathrm{E}} = \frac{72\pi^3 klc^2}{\hbar}\sqrt{1 + \frac{2ML}{3k\pi^2 c^2}}, \tag{6.127}$$

where we have returned all physical constants. It follows that, in large mass limit, the evaporation time in the DR5DCS model scales as $\sqrt{M}$. Observe that all hypersurfaces were evaluated in the limit $C_0 = 0$, because Equation (6.115) is valid only in this case. We therefore conclude that the behavior of all relevant hypersurfaces coincides with that found in the DREH model. Further discussion can be found in Section 5.3.

The radiated energy

The subsequent step is to evaluate the total energy which has been evaporated from the black hole via Hawking radiation, following the procedure outlined in Section 3.4.1. Nonetheless, expression (3.115) is not applicable for an asymptotically AdS spacetime, since the metric diverges near the asymptotic boundary. Consequently, the conventional definition of energy also becomes divergent. We are therefore required to renormalize the energy expression in light of this behavior. The dilaton field scales as $\mathrm{x} = 1/\epsilon$ with $\epsilon \to 0$. In this limit, the metric assumes the following form:

$$\mathrm{d}s^2 = -e^{2\rho}\mathrm{d}\sigma^+\mathrm{d}\sigma^- \approx \frac{1}{\epsilon^2}\frac{\mathrm{d}\sigma^+}{\mathrm{d}\hat{\mathrm{x}}}\frac{2l}{\mathrm{F}^-}\mathrm{d}\hat{\mathrm{x}}^2 \equiv -\frac{\mathrm{d}\tau^2}{\epsilon^2}, \tag{6.128}$$

where we have defined the parameter τ along the hypersurface at spatial infinity, as specified in (6.122). The total energy is therefore:

$$\begin{aligned}
E_{rad} &= \int_{\tau_0}^{\tau_{\mathrm{E}}} \mathrm{d}\tau \langle \Delta T^{(f)}_{\tau\tau}\rangle \\
&= 2l\int_0^{\hat{\mathrm{x}}_{\mathrm{E}}} \frac{\mathrm{d}\hat{\mathrm{x}}}{\mathrm{F}^-}\left[\left(\frac{\mathrm{d}\sigma^+}{\mathrm{d}\tau}\right)^2 \langle \Delta T^{(f)}_{++}\rangle + \left(\frac{\mathrm{d}\sigma^-}{\mathrm{d}\tau}\right)^2 \cancelto{0}{\langle \Delta T^{(f)}_{--}\rangle} + 2\left(\frac{\mathrm{d}\sigma^+}{\mathrm{d}\tau}\right)\left(\frac{\mathrm{d}\sigma^-}{\mathrm{d}\tau}\right)\cancelto{0}{\langle \Delta T^{(f)}_{+-}\rangle}\right] \\
&= 2l\int_0^{\hat{\mathrm{x}}_{\mathrm{E}}} \frac{\mathrm{d}\hat{\mathrm{x}}}{\mathrm{F}^-}\langle \Delta T^{(f)}_{++}\rangle = -\frac{\hbar\mu}{24\pi l}\int_0^{\hat{\mathrm{x}}_{\mathrm{E}}}\frac{\mathrm{d}\hat{\mathrm{x}}}{\mathrm{F}^-} = -\frac{3k\pi^2}{l}\mu\varepsilon\int_0^{\hat{\mathrm{x}}_{\mathrm{E}}}\frac{\mathrm{d}\hat{\mathrm{x}}}{\mathrm{F}^-} = -\frac{3k\pi^2}{l}\mu\varepsilon\frac{\sigma_0^+ - \hat{\sigma}_{\mathrm{E}}^-}{2l} \\
&= -\frac{3k\pi^2}{2l}\varepsilon\sqrt{\mu}\ln\left|\frac{1+\hat{\mathrm{x}}_{\mathrm{E}}\sqrt{\mu}}{1-\hat{\mathrm{x}}_{\mathrm{E}}\sqrt{\mu}}\right| \quad \Longrightarrow \quad \mu_{rad}(\mu_{rad}+2) = -\varepsilon\sqrt{\mu}\ln\left|\frac{1+\hat{\mathrm{x}}_{\mathrm{E}}\sqrt{\mu}}{1-\hat{\mathrm{x}}_{\mathrm{E}}\sqrt{\mu}}\right|,
\end{aligned} \tag{6.129}$$

where we have introduced a μ-parameter associated with the radiated energy. In the second line, we use the fact that the only nonvanishing component of the quantum-corrected EMT is the "++" component. There, we substitute its explicit expression, $\langle \Delta T^{(f)}_{++}\rangle = -\frac{\mu}{4l^2}$, and observe that the integral simplifies to the definition of the $\hat{\sigma}^-$ coordinate. The third line provides the first-order solution to the integral.

6.3.4 The end-state geometry

As outlined in Section 3.4.1, the final step of formulating the quantum-corrected gravitational collapse scenario is to specify the geometry of region III of the spacetime shown in Figure 6.3. In what follows, we retain the constant C_0, as our goal is to examine how the energy balance is modified throughout the evaporation process. We start by expressing the evaporating black hole solution (6.105-6.106) in terms of the dilaton field and the $\hat{\mathrm{x}}$ coordinate:

$$\mathrm{F}^+\mathrm{F}^-e^{2\rho} = -\mathrm{x}^2 + \hat{\mu} + \frac{\varepsilon C_0}{\mu+1} - \frac{\varepsilon}{\hat{\mu}+1}\left[\frac{\mathrm{x}^2+\hat{\mu}}{4\sqrt{\hat{\mu}}}\ln\left|\frac{\mathrm{x}-\sqrt{\hat{\mu}}}{\mathrm{x}+\sqrt{\hat{\mu}}}\right| - \frac{\mathrm{x}}{2}\right], \tag{6.130}$$

$$\begin{aligned}
\frac{\hat{\sigma}}{l} = \frac{1}{2\sqrt{\hat{\mu}}}\ln\left|\frac{\mathrm{x}-\sqrt{\hat{\mu}}}{\mathrm{x}+\sqrt{\hat{\mu}}}\right| - \frac{\varepsilon}{4(\hat{\mu}+1)}\left[\frac{1}{4\hat{\mu}}\ln^2\left|\frac{\mathrm{x}-\sqrt{\hat{\mu}}}{\mathrm{x}+\sqrt{\hat{\mu}}}\right| + \frac{1}{\mathrm{x}^2-\hat{\mu}}\right] \\
+ \varepsilon\left(\frac{C_0}{\hat{\mu}} - \frac{1}{2\sqrt{\hat{\mu}}}\ln\left|\frac{\mathrm{x}-\sqrt{\hat{\mu}}}{\mathrm{x}+\sqrt{\hat{\mu}}}\right|\right)\mathcal{D}_1(\mathrm{x}),
\end{aligned} \tag{6.131}$$

where we have introduced a running μ-parameter:

$$\hat{\mu} = \mu\left(1 + \frac{\varepsilon}{2(\mu+1)\sqrt{\mu}}\ln\left|\frac{1+\hat{\mathrm{x}}\sqrt{\mu}}{1-\hat{\mathrm{x}}\sqrt{\mu}}\right|\right). \tag{6.132}$$

Next, we evaluate this parameter on the hypersurface $\hat{\mathrm{x}} = \hat{\mathrm{x}}_{\mathrm{E}}$. Observing that the ε-dependent contribution is proportional to the $\hat{\sigma}^-$ coordinate, and employing (6.115), we obtain:

$$\begin{aligned}
\hat{\mu}_{\mathrm{E}} &= \mu\left[1 + \frac{\varepsilon}{\mu+1}\frac{1}{\sqrt{\mu}}\mathcal{J}\left(-\frac{1}{\hat{\mathrm{x}}_{\mathrm{E}}\sqrt{\mu}}\right)\right] = \mu\left[1 + \frac{\varepsilon}{\mu+1}\left(\ln\delta_{\mathrm{E}} + \frac{1}{\sqrt{\tilde{\mu}_{\mathrm{E}}}}\mathcal{J}(0)\right)\right] \\
&= -\frac{\varepsilon}{\mu+1}\left(C_0+\sqrt{\mu}\right),
\end{aligned} \tag{6.133}$$

where we have used $f(0) = \frac{1}{2}\left(\frac{\varepsilon}{2(\mu+1)\sqrt{\mu}}\right)^2$, which implies $\mathcal{J}(0) = \frac{\varepsilon}{4(\mu+1)\sqrt{\mu}} = \mathcal{O}(\varepsilon)$. Consequently, $\mathcal{J}(0)$ can be discarded as it only contributes at order $\mathcal{O}(\varepsilon)$. In the second line we substitute the expression for δ_{E} from (6.123). It follows that $\hat{\mu}_{\mathrm{E}}$ is a first-order quantity in the perturbation theory. Hence, within the first-order contributions of (6.130-6.131) evaluated on the hypersurface $\hat{\mathrm{x}} = \hat{\mathrm{x}}_{\mathrm{E}}$—which separates regions II and III in Figure 6.3—we may safely take the limit $\hat{\mu}_{\mathrm{E}} \to 0$. Implementing this limit gives:

$$\begin{aligned}
\mathrm{F}^{+}\mathrm{F}^{-}e^{2\rho} &= -\mathrm{x}^2 + \varepsilon \mathrm{x} + \hat{\mu}_{\mathrm{E}} + \frac{\varepsilon C_0}{\mu+1}, \\
\frac{\hat{\sigma}}{l} &= -\frac{1}{\mathrm{x}} - \frac{\varepsilon}{2\mathrm{x}^2} - \frac{\hat{\mu}_{\mathrm{E}} + \frac{\varepsilon C_0}{\mu+1}}{3\mathrm{x}^3}.
\end{aligned} \tag{6.134}$$

Since no further coordinate transformation such as the $\hat{\mathrm{x}} = \hat{\mathrm{x}}_{\mathrm{E}}$ hypersurface is traversed, the geometry in region III is described by the solution (6.134). We can directly observe that this corresponds to the quantum-corrected AdS vacuum solution (6.82) for a particular choice of the constant C_f:

$$\varepsilon C_f = \hat{\mu}_{\mathrm{E}} + \frac{\varepsilon C_0}{\mu+1} = -\frac{\varepsilon\sqrt{\mu}}{\mu+1} \quad \Longrightarrow \quad C_f = -\frac{\varepsilon\sqrt{\mu}}{\mu+1}. \tag{6.135}$$

Consequently, in direct analogy with the BPP model (see Section 4.3.4), the resulting geometry is independent of the particular choice of the initial geometry. We emphasize that we have not taken the limit $\mu \to 0$ in the terms containing the constant C_0. This is because C_0 contributes to the constant C in region II (6.103), and therefore must remain fixed.

Finally, we need to determine whether a thunderpop emerging from the end-point of the evaporation. To this end, we consider the "$--$" Equation from (6.51). Integrating it across the dividing hypersurface $\hat{\mathrm{x}} = \hat{\mathrm{x}}_{\mathrm{E}}$ yields:

$$\left[\left(\mathrm{x}^2 + 1 - \frac{1}{2}l^2\left(\nabla \mathrm{x}\right)^2\right)\partial_{-}\mathrm{x} + \varepsilon\partial_{-}\rho\right]\Bigg|_{<}^{>} = \frac{\Delta M}{6k\pi^2 \mathrm{F}^{-}}\bigg|_{\hat{\mathrm{x}}=\hat{\mathrm{x}}_{\mathrm{E}}}, \tag{6.136}$$

where ">" designates region III, while "<" designates region II. The shockwave mass is represented by ΔM. Inserting the solutions (6.105-6.106) and (6.134) gives:

$$\begin{aligned}
-\hat{\mu}_{\mathrm{E}}\left(\hat{\mu}_{\mathrm{E}}+2\right) + 2\varepsilon(C_f - C_0) + \varepsilon\sqrt{\hat{\mu}_{\mathrm{E}}}\ln\left|\frac{\mathrm{x}-\sqrt{\hat{\mu}_{\mathrm{E}}}}{\mathrm{x}+\sqrt{\hat{\mu}_{\mathrm{E}}}}\right| \\
+ \frac{\varepsilon}{\hat{\mu}_{\mathrm{E}}+1}(\mathrm{x}^2 + \hat{\mu}_{\mathrm{E}} + 2)\left[\frac{\mathrm{x}^2 - \hat{\mu}_{\mathrm{E}}}{4\sqrt{\hat{\mu}_{\mathrm{E}}}}\ln\left|\frac{\mathrm{x}-\sqrt{\hat{\mu}_{\mathrm{E}}}}{\mathrm{x}+\sqrt{\hat{\mu}_{\mathrm{E}}}}\right| + \frac{\mathrm{x}}{2}\right] = \frac{2\Delta M l}{3k\pi^2}.
\end{aligned} \tag{6.137}$$

By taking the limit $\hat{\mu}_{\mathrm{E}} \to 0$ in the x-dependent terms, this equation simplifies to:

$$-\hat{\mu}_{\mathrm{E}}\left(\hat{\mu}_{\mathrm{E}}+2\right) + 2\varepsilon(C_f - C_0) = \frac{2\Delta M l}{3k\pi^2}. \tag{6.138}$$

A direct calculation, carried out strictly to first order in the perturbative parameter, yields the following result:

$$\hat{\mu}_{\mathrm{E}}\left(\hat{\mu}_{\mathrm{E}}+2\right) = \mu(\mu+2) + \varepsilon\sqrt{\mu}\ln\left|\frac{1+\hat{\mathrm{x}}_{\mathrm{E}}\sqrt{\mu}}{1-\hat{\mathrm{x}}_{\mathrm{E}}\sqrt{\mu}}\right| = \mu(\mu+2) - \mu_{rad}(\mu_{rad}+2), \tag{6.139}$$

where we have employed the expression (6.129) for the radiated energy. Consequently, we verify that the black hole has lost nearly all of its mass by the time the evaporation process reaches its end-point. Substituting this relation into (6.138) yields the following energy balance equation:

$$\mu(\mu+2) = \mu_{rad}(\mu_{rad}+2) + 2\varepsilon(C_f - C_0) - \frac{2\Delta M l}{3k\pi^2}. \tag{6.140}$$

The mass of the initial shockwave, $M \sim \mu(\mu+2)$, together with the mass constant of the pre-collapse geometry, $2\varepsilon C_0$, is equal to the sum of the radiated energy, $E_{\text{rad}} \sim \mu_{\text{rad}}(\mu_{\text{rad}}+2)$, the mass constant of the final geometry, $2\varepsilon C_f$, and the small amount of negative energy, ΔM, carried away by the outgoing shockwave (thunderpop) that appears at the end-point of the evaporation. Therefore, we infer that energy is conserved in the dimensionally reduced model of 5D Chern–Simons gravity.

Substituting the expression for C_f from (6.135) into the energy balance Equation (6.140) yields the following formula for the energy of the thunderpop:

$$\Delta M = -\frac{3k\pi^2}{2l}\left(\frac{2\varepsilon\mu C_0}{\mu+1} + \hat{\mu}_{\text{E}}^2\right). \tag{6.141}$$

The first term is proportional to the mass constant of the initial spacetime, which we set to be $C_0 = 0$ for physical reasons. Since $\hat{\mu}_{\text{E}}$ is a quantity of $\mathcal{O}(\varepsilon)$ order, the second term in (6.141) is not reliable within the first-order perturbative expansion. This implies that there is no thunderpop within the first order, the same result as in the DREH model (5.237). However, we expect that Equation (6.138) should be of non-perturbative origin, Since Equations (6.103) and (6.135) imply that the mass constant of the spacetime is inherited after each discontinuity is crossed, it should also be of non-perturbative origin. This two together give a non-vanishing thunderpop energy but only in higher orders of the perturbation theory.

In summary, the resulting geometry matches one of the static, quantum-corrected AdS vacuum solutions (6.82), characterized by $t_\pm(\hat{\sigma}^\pm) = 0$. Therefore, although there is no discontinuity in the coordinate transformations across $\hat{\mathrm{x}} = \hat{\mathrm{x}}_E$, the quantum state nonetheless transitions from $|0,\sigma\rangle$ to $|0,\hat{\sigma}\rangle$.

Chapter 7

Full dimensionally reduced theory of 5DCS gravity

In this chapter, we study the full dimensionally-reduced theory of five-dimensional Chern–Simons gravity (DR5DCS). The action is obtained in Section 2.3 and written explicitly in (2.47). For convenience, we rewrite it here:

$$
\begin{aligned}
S_{\mathrm{DRCS}_5} =&\frac{k\pi^2}{(\lambda l)^3}\int \mathrm{d}^2x\sqrt{-g}e^{-3\phi}\Bigg\{\left(1+\frac{3}{\mathrm{x}^2}\left(1-\Phi^2-\theta^2\right)\right)\left[\mathrm{R}+2\varepsilon^{\alpha\beta}\partial_\alpha \mathrm{K}_\beta+\frac{2}{l^2}\right]\\
&+\frac{4}{l^2}+\frac{6}{l\mathrm{x}^3}\theta^2\nabla_\alpha\phi^\alpha+\frac{6}{l\mathrm{x}}\left(1+\frac{1}{\mathrm{x}^2}\left(1-\Phi^2-\theta^2\right)\right)\left[\nabla_\alpha\phi^\alpha-\varepsilon^{\alpha\beta}\phi_\alpha \mathrm{K}_\beta\right]\\
&-\frac{6}{\mathrm{x}^2}\left[\nabla_\alpha\phi^\beta\nabla_\beta\phi^\alpha-\nabla_\alpha\phi^\alpha\nabla_\beta\phi^\beta-\varepsilon^{\alpha\beta}\mathrm{K}_\alpha\nabla_\beta\Phi^2\right]\Bigg\}+S_{\mathrm{mat}},
\end{aligned}
\tag{7.1}
$$

where ϕ^μ and θ denote fields originating from the five-dimensional spin-connection, $\mathrm{x} = e^{-\phi}$ is the reduced dilaton field, $\varepsilon^{\alpha\beta}$ is the Levi–Civita tensor, $g_{\mu\nu}$ is the metric, and K_μ is the two-dimensional contorsion. Furthermore, $\Phi^2 = \phi_\mu\phi^\mu$. It is immediately apparent that the field θ plays the role of a Lagrange multiplier, thereby imposing a constraint on the system of equations. Consequently, when $\theta \neq 0$, an additional equation arises, which substantially restricts the phase space of admissible solutions. This property is particularly advantageous when attempting to solve the equations of motion.

The chapter is divided into three sections. In the first, we derive the equations of motion and impose the symmetric ansatz introduced in Section 3.1. We then solve the vacuum equations and demonstrate that their most general solution is the BTZ black hole with non-zero θ torsion. Consequently, this solution is directly inherited from the parent 5DCS theory.

The second section focuses on general solutions in the presence of non-vanishing matter fields. The matter sector is strictly two-dimensional, meaning that the only sources in the theory are the matter energy-momentum tensor and the contorsion current, obtained by varying the matter action with respect to the metric and the contorsion, respectively. In this part, the θ-field constraint is heavily used to solve equations of motion for the additional fields, including the two-dimensional contorsion, and to derive the resulting source equations in terms of the metric function Λ, the dilaton field, and their derivatives. A variety of distinct cases arise in the course of solving the equations, and these are summarized in Table 7.1.

The final section explores explicit solutions once the form of matter minimally coupled to gravity is specified in the $\theta \neq 0$ sector of the theory; for $\theta = 0$ the model reduces to its Riemannian sector, which was analyzed in the preceding chapter. Several types of field theories are considered. We first introduce matter as a real scalar field and obtain cosmological solutions. Next, we examine the general solutions of the equations of motion coupled to pure electrodynamics. In this setting, we show that no solutions with $\theta \neq 0$ exist; however, there is a well-defined charged black hole solution when the theory is restricted to the Riemannian sector. The subsequent subsection studies the coupling to a spinor field, where we identify a fermionic star soliton solution together with a well-defined phase transition mechanism. We then analyze gravity coupled to scalar electrodynamics, for which the general solution is again of cosmological type. The section concludes with the case where the matter content is given by an ideal fluid.

7.1 Equation of motion and the symmetric ansatz

In this section we derive the equations of motion for the complete dimensionally-reduced 5DCS theory defined by the action (7.1). Since we do not impose vanishing torsion from the outset, the full set of independent fields is $\{g_{\mu\nu}, \mathrm{K}^\mu, \phi, \phi^\mu, \theta\}$. We start by varying the action with respect to the metric. The corresponding field equation is:

$$\begin{aligned}
&(\mathrm{x}^2+1)\nabla_\mu\nabla_\nu \mathrm{x} - \frac{1}{l}\nabla_\alpha\phi^\alpha\phi_\mu\phi_\nu + \frac{1}{2l}\left(\phi_\mu\nabla_\nu\Phi^2 + \phi_\nu\nabla_\mu\Phi^2\right) - \nabla_\mu\nabla_\nu\left(\mathrm{x}\theta^2\right)\\
&\quad - 2\varepsilon^{\alpha\beta}\left(\nabla_\alpha \mathrm{x} + \frac{1}{l}\phi_\alpha\right)\mathrm{K}_\beta\phi_\mu\phi_\nu - \left[\left(\nabla_\mu \mathrm{x} + \frac{1}{l}\phi_\mu\right)\nabla_\nu\Phi^2 + \left(\nabla_\nu \mathrm{x} + \frac{1}{l}\phi_\nu\right)\nabla_\mu\Phi^2\right]\\
&\quad + \left(\nabla^\alpha \mathrm{x} + \frac{1}{l}\phi^\alpha\right)A^\sigma\varepsilon^{\rho\delta}\nabla_\delta\phi^\lambda\left[\varepsilon_{\lambda\alpha}\left(g_{\mu\sigma}g_{\nu\rho} + g_{\nu\sigma}g_{\mu\rho}\right) + \varepsilon_{\sigma\rho}\left(\varepsilon_{\mu\alpha}\varepsilon_{\nu\lambda} + \varepsilon_{\nu\alpha}\varepsilon_{\mu\lambda}\right)\right]\\
&\quad + 2\mathrm{x}\left(\nabla_\mu \mathrm{x} + \frac{1}{l}\phi_\mu\right)\left(\nabla_\nu \mathrm{x} + \frac{1}{l}\phi_\nu\right) + \frac{1}{2l}\varepsilon^{\rho\sigma}\nabla_\rho\phi_\sigma\left(\phi_\mu\varepsilon_{\nu\alpha} + \phi_\nu\varepsilon_{\mu\alpha}\right)\phi^\alpha\\
&\quad - \frac{1}{2}\Phi^2\left[\nabla_\mu\left(\nabla_\nu \mathrm{x} + \frac{1}{l}\phi_\nu\right) + \nabla_\nu\left(\nabla_\mu \mathrm{x} + \frac{1}{l}\phi_\mu\right)\right] + g_{\mu\nu}\left(\Box\left(\mathrm{x}\theta^2\right) - \frac{\mathrm{x}\theta^2}{l^2}\right)\\
&\quad + g_{\mu\nu}\left[2\left(\nabla^\alpha \mathrm{x} + \frac{1}{l}\phi^\alpha\right)\nabla_\alpha\left(\Phi^2 - \frac{1}{2}\mathrm{x}^2\right) + \Phi^2\nabla_\alpha\left(\nabla^\alpha \mathrm{x} + \frac{1}{l}\phi^\alpha\right)\right]\\
&\quad - g_{\mu\nu}\left[(\mathrm{x}^2+1)\Box \mathrm{x} - \frac{\mathrm{x}}{l^2}\left(\mathrm{x}^2 + 1 - \Phi^2\right) + \frac{1}{2l}\phi^\alpha\nabla_\alpha\Phi^2\right] = -\frac{1}{6k\pi^2}T_{\mu\nu},
\end{aligned} \tag{7.2}$$

where we have already eliminated the original dilaton ϕ in favor of the reduced dilaton field x defined in (2.46). Notice that only a single term involves the two-dimensional contorsion. Varying the action with respect to the contorsion then gives:

$$\left(\mathrm{x}^2 + 1 - \theta^2 - \Phi^2\right)\left(\nabla_\mu \mathrm{x} + \frac{1}{l}\phi_\mu\right) - \mathrm{x}\nabla_\mu\theta^2 = \frac{1}{6k\pi^2}\varepsilon_{\mu\nu}T^\nu_{\mathrm{K}}, \tag{7.3}$$

where we have introduced the contorsion current $T^\mu_{\mathrm{K}} = -\frac{1}{\sqrt{-g}}\frac{\delta S_{\mathrm{mat}}}{\delta \mathrm{K}_\mu}$. In an analogous manner, variation with respect to the scalar field associated with the five-dimensional torsion function, θ, yields:

$$\mathrm{x}\theta\left[\mathrm{R} + 2\varepsilon^{\alpha\beta}\partial_\alpha\mathrm{K}_\beta + \frac{2}{l^2} - \frac{2}{l\mathrm{x}}\varepsilon^{\alpha\beta}\phi_\alpha\mathrm{K}_\beta\right] = -\frac{1}{6k\pi^2}T_{(\theta)}, \tag{7.4}$$

with $T_{(\theta)} = -\frac{1}{\sqrt{-g}}\frac{\delta S_{\mathrm{mat}}}{\delta\theta}$. It is worth emphasizing that in the limit of vanishing contorsion this equation turns into a constraint which, for $\theta \neq 0$, fixes the scalar curvature to the constant

AdS value. This is why we interpret the field θ as playing the role of a Lagrange multiplier in the action. Finally, varying the action (7.1) with respect to the vector field ϕ^μ and the dilaton field ϕ gives:

$$\varepsilon_\sigma{}^\nu\left[\varepsilon_{\rho\mu}\nabla^\sigma\phi^\rho-\phi_\mu\mathrm{K}^\sigma-\frac{\mathrm{x}}{l}\varepsilon_\mu{}^\sigma\right]\left(\nabla_\nu\mathrm{x}+\frac{1}{l}\phi_\nu\right)-\frac{1}{2l}\left(\mathrm{x}^2+1-\theta^2-\Phi^2\right)\varepsilon_{\mu\nu}\mathrm{K}^\nu=\frac{1}{12k\pi^2\lambda l}T^{(\phi)}_\mu, \tag{7.5}$$

$$\begin{aligned}\left(\mathrm{x}^2+1-\theta^2-\Phi^2\right)\left[\mathrm{R}+2\varepsilon^{\alpha\beta}\partial_\alpha\mathrm{K}_\beta+\frac{2}{l^2}\right]+\frac{4\mathrm{x}^2}{l^2}+\frac{4\mathrm{x}}{l}\left(\nabla_\alpha\phi^\alpha-\varepsilon^{\alpha\beta}\phi_\alpha\mathrm{K}_\beta\right)\\ -2\left(\nabla_\mu\phi_\nu\nabla^\nu\phi^\mu-\nabla_\mu\phi^\mu\nabla_\nu\phi^\nu-\varepsilon^{\alpha\beta}\mathrm{K}_\alpha\nabla_\beta\Phi^2\right)=-\frac{1}{3k\pi^2}\frac{1}{\mathrm{x}}T^{(\phi)},\end{aligned} \tag{7.6}$$

where the matter sources for ϕ^μ and ϕ are defined as $T^{(\phi)}_\mu=-\frac{1}{\sqrt{-g}}\frac{\delta S_{\mathrm{mat}}}{\delta\phi^\mu}$ and $T^{(\phi)}=-\frac{1}{\sqrt{-g}}\frac{\delta S_{\mathrm{mat}}}{\delta\phi}$, respectively.

All equations of motion (7.2-7.6) are explicitly written so that, upon imposing $\phi_\mu=-l\nabla_\mu\phi$, $\mathrm{K}_\mu=0$ and $\theta=0$, they reduce to the Riemannian sector of the theory (6.11-6.12). Using equations (7.3-7.6), the metric equation (7.2) can be further recast in the following form:

$$\begin{aligned}\left(\mathrm{x}^2+1-\theta^2-\Phi^2\right)\Bigg\{\nabla_\mu\phi_\nu+\nabla_\nu\phi_\mu-\frac{1}{\mathrm{x}}\left(\phi_\mu\nabla_\nu\mathrm{x}+\phi_\nu\nabla_\mu\mathrm{x}\right)-\frac{2}{l\mathrm{x}}\phi_\mu\phi_\nu+(\phi_\mu\varepsilon_{\nu\sigma}+\phi_\nu\varepsilon_{\mu\sigma})\mathrm{K}^\sigma\\ -2g_{\mu\nu}\left[\nabla_\alpha\phi^\alpha-\frac{1}{\mathrm{x}}\phi^\alpha\nabla_\alpha\mathrm{x}-\frac{1}{l\mathrm{x}}\Phi^2+\frac{\mathrm{x}}{l}\right]\Bigg\}=\frac{l}{3k\pi^2}\bar{T}_{\mu\nu},\end{aligned} \tag{7.7}$$

where we have introduced a reduced EMT, which incorporates contributions from additional sources beyond the standard EMT, and is defined as

$$\begin{aligned}\bar{T}_{\mu\nu}=T_{\mu\nu}-\frac{1}{2l\mathrm{x}}\left(\phi_\mu\varepsilon_{\nu\sigma}+\phi_\nu\varepsilon_{\mu\sigma}\right)T^\sigma_{\mathrm{K}}+\frac{1}{2}\left(g_{\mu\sigma}\varepsilon_{\nu\rho}+g_{\nu\sigma}\varepsilon_{\mu\rho}\right)\nabla^\sigma T^\rho_{\mathrm{K}}-g_{\mu\nu}\varepsilon^{\alpha\beta}\left(\nabla_\alpha T^{\mathrm{K}}_\beta-\frac{1}{l\mathrm{x}}\phi_\alpha T^{\mathrm{K}}_\beta\right)\\ -\frac{1}{2\lambda l}\left(\phi_\mu T^{(\phi)}_\nu+\phi_\nu T^{(\phi)}_\mu\right).\end{aligned} \tag{7.8}$$

In this representation, the equation makes it manifest that, even in the presence of non-zero torsion, the enhanced symmetry of the 5DCS theory ensures the appearance of the simple prefactor $\mathrm{x}^2+1-\theta^2-\Phi^2$, in complete analogy with the Riemannian sector (6.11).

Because the full theory's equations of motion are extremely complicated, we restrict our analysis to solutions that admit at least one Killing vector. When this vector is time-like, we focus on static, black-hole-type configurations. Conversely, if it is space-like, the resulting solutions describe cosmological spacetimes. Consequently, we proceed directly to implementing the symmetric ansatz introduced in Section 3.1. Employing equations (3.12), (3.13), and (3.19), we obtain the following ansatz for ϕ_μ, K_μ, $\nabla_\mu\mathrm{x}$, and the metric:

$$\phi_\mu=\phi^{\parallel}(\mathrm{x})\xi_\mu+\phi^\perp(\mathrm{x})\varepsilon_{\mu\nu}\xi^\nu,\ \ \mathrm{K}_\mu=\mathrm{K}^{\parallel}(\mathrm{x})\xi_\mu+\mathrm{K}^\perp(\mathrm{x})\varepsilon_{\mu\nu}\xi^\nu,\ \ \nabla_\mu\mathrm{x}=\frac{1}{l}\mathcal{D}(\mathrm{x})\varepsilon_{\mu\nu}\xi^\nu,\ \ \xi^2=\Lambda(\mathrm{x}). \tag{7.9}$$

Using (7.9) equations of motion (7.3-7.7) can be rewritten in the following form:

$$\Lambda^2\left(\mathrm{x}^2+1-\theta^2-\Phi^2\right)\left\{\mathcal{D}\frac{\mathrm{d}\phi^\perp}{\mathrm{dx}}-\frac{1}{\mathrm{x}}\left(\phi^{\parallel 2}+\phi^\perp\left(\phi^\perp+\mathcal{D}\right)\right)+l\left(\phi^\parallel\mathrm{K}^\perp+\phi^\perp\mathrm{K}^\parallel\right)\right.$$
$$\left.\mp\left[\mathcal{D}\frac{\mathrm{d}\phi^\parallel}{\mathrm{dx}}-\frac{1}{\mathrm{x}}\phi^\parallel\left(2\phi^\perp+\mathcal{D}\right)+l\left(\phi^\parallel\mathrm{K}^\parallel+\phi^\perp\mathrm{K}^\perp\right)\right]\right\}=\frac{2l^2}{3k\pi^2}\mathrm{F}^{\pm 2}\bar{T}_{\pm\pm},\quad(7.10)$$

$$\left(\mathrm{x}^2+1-\theta^2-\Phi^2\right)\left[\mathcal{D}\frac{\mathrm{d}}{\mathrm{dx}}\left(\Lambda\phi^\perp\right)+\frac{1}{\mathrm{x}}\Lambda\left(\phi^{\parallel 2}-\phi^\perp\left(\phi^\perp+\mathcal{D}\right)\right)-2\mathrm{x}\right.$$
$$\left.+l\Lambda\left(\phi^\parallel\mathrm{K}^\perp-\phi^\perp\mathrm{K}^\parallel\right)\right]=\frac{l^2}{6k\pi^2}\bar{T},\quad(7.11)$$

$$\Lambda\left(\mathrm{x}^2+1-\theta^2-\Phi^2\right)\phi^\parallel=\frac{l}{6k\pi^2}\varepsilon^{\mu\nu}\xi_\mu T^{\mathrm{K}}_\nu,\quad(7.12)$$

$$\Lambda\left[\left(\mathrm{x}^2+1-\theta^2-\Phi^2\right)\left(\phi^\perp+\mathcal{D}\right)-\mathrm{x}\mathcal{D}\frac{\mathrm{d}\theta^2}{\mathrm{dx}}\right]=\frac{l}{6k\pi^2}\xi^\mu T^{\mathrm{K}}_\mu,\quad(7.13)$$

$$\mathrm{x}\theta\left[\mathcal{D}\frac{\mathrm{d}}{\mathrm{dx}}\left(\mathcal{D}\frac{\mathrm{d}\Lambda}{\mathrm{dx}}-2l\Lambda\mathrm{K}^\parallel\right)+2+\frac{2}{\mathrm{x}}l\Lambda\left(\phi^\perp\mathrm{K}^\parallel-\phi^\parallel\mathrm{K}^\perp\right)\right]=-\frac{l^2}{6k\pi^2}T^{(\theta)},\quad(7.14)$$

$$\phi^\parallel\left[\mathcal{D}\left(2\Lambda\frac{\mathrm{d}\phi^\perp}{\mathrm{dx}}+\left(2\phi^\perp+\mathcal{D}\right)\frac{\mathrm{d}\Lambda}{\mathrm{dx}}\right)-2\mathrm{x}+2l\Lambda\left(\phi^\parallel\mathrm{K}^\perp-\left(\phi^\perp+\mathcal{D}\right)\mathrm{K}^\parallel\right)\right]$$
$$-l\left(\mathrm{x}^2+1-\theta^2-\Phi^2\right)\mathrm{K}^\perp=\frac{l}{6k\pi^2\lambda}\frac{\xi^\mu T^{(\phi)}_\mu}{\Lambda},\quad(7.15)$$

$$\mathcal{D}\left[2\Lambda\phi^\parallel\frac{\mathrm{d}\phi^\parallel}{\mathrm{dx}}+\left(\phi^{\parallel 2}+\phi^\perp\left(\phi^\perp+\mathcal{D}\right)\right)\frac{\mathrm{d}\Lambda}{\mathrm{dx}}\right]-2\mathrm{x}\left(\phi^\perp+\mathcal{D}\right)+2l\Lambda\phi^\perp\left(\phi^\parallel\mathrm{K}^\perp-\left(\phi^\perp+\mathcal{D}\right)\mathrm{K}^\parallel\right)$$
$$-l\left(\mathrm{x}^2+1-\theta^2-\Phi^2\right)\mathrm{K}^\parallel=\frac{l}{6k\pi^2\lambda}\frac{\varepsilon^{\mu\nu}\xi_\mu T^{(\phi)}_\nu}{\Lambda},\quad(7.16)$$

$$\left(\mathrm{x}^2+1-\theta^2-\Phi^2\right)\left[\mathcal{D}\frac{\mathrm{d}}{\mathrm{dx}}\left(\mathcal{D}\frac{\mathrm{d}\Lambda}{\mathrm{dx}}-2l\Lambda\mathrm{K}^\parallel\right)+2\right]+4\mathrm{x}^2-4\mathrm{x}\mathcal{D}\frac{\mathrm{d}\left(\Lambda\phi^\perp\right)}{\mathrm{dx}}$$
$$-\mathcal{D}\frac{\mathrm{d}\Phi^2}{\mathrm{dx}}\left(\mathcal{D}\frac{\mathrm{d}\Lambda}{\mathrm{dx}}-2l\Lambda\mathrm{K}^\parallel\right)-4l\mathrm{x}\Lambda(\phi^\parallel\mathrm{K}^\perp-\phi^\perp\mathrm{K}^\parallel)=-\frac{l^2}{3k\pi^2}\frac{1}{\mathrm{x}}T^{(\phi)}.\quad(7.17)$$

The first pair of equations (7.10-7.11) describe, respectively, the "$\pm\pm$" component and the trace of the metric equation of motion (7.7). The following two equations (7.12-7.13) give the parallel and normal components of the contorsion equation (7.3). The equation of motion for the θ field (7.4) simplifies to (7.14) once the symmetric ansatz is imposed. Equations (7.15-7.16) represent the normal and parallel components of the equation (7.5) for the vector field ϕ^μ. Finally, the last equation (7.17) is equivalent to (7.6) for the dilaton field.

Within this chapter, we restrict ourselves to theories whose matter content is strictly two-dimensional, which implies

$$T^{(\phi)}=T^{(\phi)}_\mu=T^{(\theta)}=0.\quad(7.18)$$

Thus, the only non-vanishing sources are the EMT, $T_{\mu\nu}\neq 0$, and the contorsion current, $T^{\mathrm{K}}_\mu\neq 0$. Since equations (7.14-7.17) contain no sources, they act as constraints inherited from the five-dimensional theory and, as such, are analyzed later. We first turn to the equations (7.10-7.11), rewriting them in terms of the symmetric ansatz components of the EMT. Employing (3.33) and (3.34), they take the form:

$$\left(\mathrm{x}^2+1-\theta^2-\Phi^2\right)\left[\mathcal{D}\frac{\mathrm{d}\phi^{\perp}}{\mathrm{dx}}-\frac{1}{\mathrm{x}}\left(\phi^{\shortparallel 2}+\phi^{\perp}\left(\phi^{\perp}+\mathcal{D}\right)\right)+l\left(\phi^{\shortparallel}\mathrm{K}^{\perp}+\phi^{\perp}\mathrm{K}^{\shortparallel}\right)\right]$$
$$=\frac{l^2}{6k\pi^2}\left(T^{\shortparallel\shortparallel}+T^{\perp\perp}\right)+\frac{l}{6k\pi^2}\left[\mathcal{D}\frac{\mathrm{d}T_{\mathrm{K}}^{\shortparallel}}{\mathrm{dx}}-\frac{1}{\mathrm{x}}\left(\phi^{\shortparallel}T_{\mathrm{K}}^{\perp}+\phi^{\perp}T_{\mathrm{K}}^{\shortparallel}\right)\right], \tag{7.19}$$

$$\left(\mathrm{x}^2+1-\theta^2-\Phi^2\right)\left[\mathcal{D}\frac{\mathrm{d}\phi^{\shortparallel}}{\mathrm{dx}}-\frac{1}{\mathrm{x}}\phi^{\shortparallel}\left(2\phi^{\perp}+\mathcal{D}\right)+l\left(\phi^{\shortparallel}\mathrm{K}^{\shortparallel}+\phi^{\perp}\mathrm{K}^{\perp}\right)\right]$$
$$=\frac{l^2}{3k\pi^2}T^{\shortparallel\perp}+\frac{l}{6k\pi^2}\left[\mathcal{D}\frac{\mathrm{d}T_{\mathrm{K}}^{\perp}}{\mathrm{dx}}-\frac{1}{\mathrm{X}}\left(\phi^{\shortparallel}T_{\mathrm{K}}^{\shortparallel}+\phi^{\perp}T_{\mathrm{K}}^{\perp}\right)\right], \tag{7.20}$$

$$\left(\mathrm{x}^2+1-\theta^2-\Phi^2\right)\left[\mathcal{D}\frac{\mathrm{d}}{\mathrm{dx}}\left(\Lambda\phi^{\perp}\right)+\frac{\Lambda}{\mathrm{x}}\left(\phi^{\shortparallel 2}-\phi^{\perp}\left(\phi^{\perp}+\mathcal{D}\right)\right)-2\mathrm{x}+l\Lambda\left(\phi^{\shortparallel}\mathrm{K}^{\perp}-\phi^{\perp}\mathrm{K}^{\shortparallel}\right)\right]$$
$$=\frac{l^2\Lambda}{6k\pi^2}\left(T^{\shortparallel\shortparallel}-T^{\perp\perp}\right)+\frac{l}{6k\pi^2}\left[\mathcal{D}\frac{\mathrm{d}\left(\Lambda T_{\mathrm{K}}^{\shortparallel}\right)}{\mathrm{dx}}+\frac{\Lambda}{\mathrm{x}}\left(\phi^{\shortparallel}T_{\mathrm{K}}^{\perp}-\phi^{\perp}T_{\mathrm{K}}^{\shortparallel}\right)\right]. \tag{7.21}$$

Using equations (7.13-7.12) together with (7.15-7.16), equation (7.19) reduces to

$$\left(\mathrm{x}^2+1-\theta^2-\Phi^2\right)\phi^{\shortparallel}2l\Lambda\mathrm{K}^{\shortparallel}=\frac{l^2}{3k\pi^2}T^{\shortparallel\perp}. \tag{7.22}$$

If one multiplies equation (7.19) by Λ and subtracts it from (7.21), one finds:

$$\left(\mathrm{x}^2+1-\theta^2-\Phi^2\right)\left[\mathcal{D}\phi^{\perp}\frac{\mathrm{d}\Lambda}{\mathrm{dx}}-2\mathrm{x}-2l\Lambda\phi^{\perp}\mathrm{K}^{\shortparallel}\right]=-\frac{l^2}{3k\pi^2}\Lambda T^{\perp\perp}+\frac{l}{6k\pi^2}\mathcal{D}\frac{\mathrm{d}\Lambda}{\mathrm{dx}}T_{\mathrm{K}}^{\shortparallel}. \tag{7.23}$$

Conversely, adding instead of subtracting yields:

$$\left(\mathrm{x}^2+1-\theta^2-\Phi^2\right)\left[2\Lambda\left(\mathcal{D}\frac{\mathrm{d}\phi^{\perp}}{\mathrm{dx}}-\frac{1}{\mathrm{x}}\phi^{\perp}\left(\phi^{\perp}+\mathcal{D}\right)\right)+\mathcal{D}\phi^{\perp}\frac{\mathrm{d}\Lambda}{\mathrm{dx}}-2\mathrm{x}+2l\Lambda\phi^{\shortparallel}\mathrm{K}^{\perp}\right]$$
$$=\frac{l}{6k\pi^2}\left[2l\Lambda T^{\shortparallel\shortparallel}+\mathcal{D}\left(\frac{\mathrm{d}\Lambda}{\mathrm{dx}}T_{\mathrm{K}}^{\shortparallel}+2\Lambda\frac{\mathrm{d}T_{\mathrm{K}}^{\shortparallel}}{\mathrm{dx}}\right)-\frac{2}{\mathrm{x}}\Lambda\phi^{\perp}T_{\mathrm{K}}^{\shortparallel}\right]. \tag{7.24}$$

The relations (7.13-7.12) admit no substantial further simplification and read:

$$\left(\mathrm{x}^2+1-\theta^2-\Phi^2\right)\phi^{\shortparallel}=\frac{l}{6k\pi^2}T_{\mathrm{K}}^{\perp}, \tag{7.25}$$

$$\left(\mathrm{x}^2+1-\theta^2-\Phi^2\right)\left(\phi^{\perp}+\mathcal{D}\right)-\mathrm{x}\mathcal{D}\frac{\mathrm{d}\theta^2}{\mathrm{dx}}=\frac{l}{6k\pi^2}T_{\mathrm{K}}^{\shortparallel}. \tag{7.26}$$

For later convenience, we now define the following auxiliary source-dependent functions:

$$\begin{aligned}\tilde{T}^{\perp\perp}&=\frac{l}{6k\pi^2}\left(2l\Lambda T^{\perp\perp}-T_{\mathrm{K}}^{\shortparallel}\frac{\mathrm{d}\Lambda}{\mathrm{d\bar{x}}}\right),\\ \tilde{T}^{\shortparallel\shortparallel}&=\frac{l}{6k\pi^2}\left(2l\Lambda T^{\shortparallel\shortparallel}+T_{\mathrm{K}}^{\shortparallel}\frac{\mathrm{d}\Lambda}{\mathrm{d\bar{x}}}+2\Lambda\frac{\mathrm{d}T_{\mathrm{K}}^{\shortparallel}}{\mathrm{d\bar{x}}}\right),\\ \tilde{T}^{\shortparallel\perp}&=\frac{l}{6k\pi^2}2l\Lambda T^{\shortparallel\perp},\ \ \tilde{T}^{\shortparallel/\perp}=\frac{l}{6k\pi^2}T^{\shortparallel/\perp},\end{aligned} \tag{7.27}$$

and, analogously, we introduce auxiliary functions for the fields:

$$\mathcal{Z} = \mathrm{x}^2 + 1 - \theta^2 - \Phi^2, \tag{7.28}$$

$$\mathcal{S} = \frac{\mathrm{d}\Lambda}{\mathrm{d}\bar{\mathrm{x}}} - 2l\Lambda \mathrm{K}^{\parallel}. \tag{7.29}$$

The complete symmetric system of equations of motion is represented by the equations containing the sources: the EMT (7.22-7.24) and the contorsion current (7.25-7.26). In addition to this set, four constraints (7.14-7.17) must be imposed. These constraints originate from the dimensional reduction procedure. Further details can be found in Section 2.3.

7.1.1 General symmetric vacuum solutions

In this section we derive the most general solution of the vacuum equations of motion (7.10–7.17) that admits at least one Killing vector. In the vacuum case, all source terms vanish, i.e. $T_{\mu\nu} = T^{\mu}_{\mathrm{K}} = T^{\mu}_{(\phi)} = T^{(\theta)} = T^{(\phi)} = 0$. As in the Riemannian sector discussed in Section 6.1.1, the complete theory again splits into two distinct branches of solutions. We first analyze the branch characterized by $\mathrm{x}^2 + 1 - \theta^2 - \Phi^2 \neq 0$.

From equation (7.12), we infer $\phi^{\parallel} = 0$. Then, using (7.15) we obtain $\mathrm{K}^{\perp} = 0$. Next, combining (7.10) with (7.11) and inserting the resulting expression into (7.16) leads to $\mathrm{K}^{\parallel} = 0$. Thus, the remaining nontrivial equations reduce to

$$\mathcal{D}\frac{\mathrm{d}\phi^{\perp}}{\mathrm{dx}} = \frac{1}{\mathrm{x}}\phi^{\perp}\left(\phi^{\perp} + \mathcal{D}\right), \tag{7.30}$$

$$\mathcal{D}\phi^{\perp}\frac{\mathrm{d}\Lambda}{\mathrm{dx}} = 2\mathrm{x}, \tag{7.31}$$

$$\mathrm{x}\mathcal{D}\frac{\mathrm{d}\theta^2}{\mathrm{dx}} = \left(\mathrm{x}^2 + 1 - \theta^2 + \Lambda\phi^{\perp 2}\right)\left(\phi^{\perp} + \mathcal{D}\right), \tag{7.32}$$

$$\theta\left[\mathcal{D}\frac{\mathrm{d}}{\mathrm{dx}}\left(\mathcal{D}\frac{\mathrm{d}\Lambda}{\mathrm{dx}}\right) + 2\right] = 0. \tag{7.33}$$

We now change to the coordinate $\bar{\mathrm{x}}$ as introduced in (3.20). Equation (7.30) can be integrated directly, yielding $\bar{\mathrm{x}} = -\frac{\mathrm{x}}{\phi^{\perp}}$. Substituting this relation into (7.31) and integrating gives the metric function $\Lambda = -(\bar{\mathrm{x}}^2 - \mu)$, where μ is an integration constant. With this form of Λ, equation (7.33) is automatically fulfilled. The remaining equation (7.32) can then be integrated to obtain the θ field:

$$\theta^2 = 1 + \frac{1}{3}\phi^{\perp 2} + \frac{\eta}{\phi^{\perp}}, \tag{7.34}$$

where η is another integration constant. A straightforward check confirms that (7.5) is satisfied as well.

Hence, the solution is specified by two arbitrary coordinate transformations $\mathrm{F}^{\pm}$, an arbitrary function of the dilaton $\phi^{\perp}(\mathrm{x})$, and the constants μ and η, which we collectively denote by

$\mathrm{RCI}(\mathrm{F}^+, \mathrm{F}^-, \phi^\perp(\bar{\mathrm{x}}), \mu, \eta)$:

$$
\begin{aligned}
&\mathrm{d}s^2 = -(\bar{\mathrm{x}}^2-\mu)\mathrm{d}t^2 + \frac{l^2\mathrm{d}\bar{\mathrm{x}}^2}{\bar{\mathrm{x}}^2-\mu},\\
&\bar{\mathrm{x}} = \begin{cases} \sqrt{\mu}\tanh\left[\frac{\sqrt{\mu}}{2l}\left(\int\frac{\mathrm{d}x^+}{\mathrm{F}^+}+\int\frac{\mathrm{d}x^-}{\mathrm{F}^-}\right)\right], & 0<\bar{\mathrm{x}}<\sqrt{\mu},\\ \sqrt{\mu}\coth\left[\frac{\sqrt{\mu}}{2l}\left(\int\frac{\mathrm{d}x^+}{\mathrm{F}^+}+\int\frac{\mathrm{d}x^-}{\mathrm{F}^-}\right)\right], & \bar{\mathrm{x}}>\sqrt{\mu},\end{cases}\\
&\phi^{\shortparallel}=0,\ \mathrm{K}^{\shortparallel}=0,\ \mathrm{K}^\perp=0,\ \mathrm{x}=-\bar{\mathrm{x}}\phi^\perp(\bar{\mathrm{x}}),\\
&\theta^2 = 1+\frac{1}{3}\mu\phi^{\perp 2}(\bar{\mathrm{x}})+\frac{\eta}{\phi^\perp(\bar{\mathrm{x}})}.
\end{aligned}
\tag{7.35}
$$

Choosing $\phi^\perp=-1$ and $\theta=0$, which corresponds to fixing $\eta=1+\mu/3$, brings this solution back to the generic branch-one solution in the Riemannian sector of the theory (6.17), as anticipated.

The other branch is defined by $\mathrm{x}^2+1-\theta^2-\Phi^2=0$. Consequently, equations (7.10-7.12) are satisfied identically. From equation (7.13) it follows that $\theta^2=\theta_0^2=\text{const}$. After some straightforward algebra, one finds that equations (7.15-7.16) reduce to the dilaton equation (7.17). Therefore, the system effectively boils down to the following two equations:

$$
\theta_0\left[\mathcal{D}\frac{\mathrm{d}}{\mathrm{dx}}\left(\mathcal{D}\frac{\mathrm{d}\Lambda}{\mathrm{dx}}-2l\Lambda\mathrm{K}^{\shortparallel}\right)+2+\frac{2}{\mathrm{x}}l\Lambda\left(\phi^\perp\mathrm{K}^{\shortparallel}-\phi^{\shortparallel}\mathrm{K}^\perp\right)\right]=0,
\tag{7.36}
$$

$$
\mathcal{D}\left[2\Lambda\frac{\mathrm{d}\phi^\perp}{\mathrm{dx}}+\left(2\phi^\perp+\mathcal{D}\right)\frac{\mathrm{d}\Lambda}{\mathrm{dx}}\right]-2\mathrm{x}+2l\Lambda\left(\phi^{\shortparallel}\mathrm{K}^\perp-\left(\phi^\perp+\mathcal{D}\right)\mathrm{K}^{\shortparallel}\right)=0.
\tag{7.37}
$$

Inspection of (7.36-7.37) shows that the case $\theta_0=0$ is somewhat special, because only a single differential equation, namely (7.37), remains. In this situation, the solution is specified by two coordinate transformations $\mathrm{F}^\pm$ and four arbitrary functions of the coordinate $\bar{\mathrm{x}}$. The field $\mathrm{K}^\perp$ is then determined from equation (7.37), whereas $\phi^{\shortparallel}$ is obtained from the constraint $\mathrm{x}^2+1=\Lambda\left(\phi^{\shortparallel 2}-\phi^{\perp 2}\right)$. The coordinate $\bar{\mathrm{x}}$ is fixed by evaluating the integral (3.18). We denote this family of solutions by $\mathrm{RCIIB}(\mathrm{F}^+,\mathrm{F}^-\Lambda(\bar{\mathrm{x}}),\phi^\perp(\bar{\mathrm{x}}),\mathrm{K}^{\shortparallel}(\bar{\mathrm{x}}),\mathrm{x}(\bar{\mathrm{x}}))$.

By imposing $\phi^{\shortparallel}=\mathrm{K}^\perp=\mathrm{K}^{\shortparallel}=0$ and $\phi^\perp=-\mathcal{D}$, the single equation (7.37) is automatically fulfilled, provided that the condition $\mathrm{x}^2+1+\Lambda\mathcal{D}^2=0$ holds. Consequently, only one arbitrary function, $\Lambda(\mathrm{x})$, remains undetermined. Hence, this solution effectively coincides with the general branch-two solution of the Riemannian sector equations of motion (6.20).

The case with $\theta_0\neq 0$ is genuinely Riemann–Cartan. Both differential equations are still present, so the solution now depends on one fewer arbitrary function and on two additional constants, θ_0 and C. We denote this solution by $\mathrm{RCIIA}(\mathrm{F}^+,\mathrm{F}^-\Lambda(\bar{\mathrm{x}}),\phi^\perp(\bar{\mathrm{x}}),\mathrm{x}(\bar{\mathrm{x}}),\theta_0,C)$. It is explicitly given by

$$
\begin{aligned}
\mathrm{x}^2+1-\theta_0^2&=\Lambda\left(\phi^{\shortparallel 2}-\phi^{\perp 2}\right),\ \theta=\theta_0,\\
l\Lambda\mathrm{K}^{\shortparallel}&=\frac{1}{2}\frac{\mathrm{d}\Lambda}{\mathrm{d}\bar{\mathrm{x}}}-\frac{C-\Lambda\phi^\perp}{\mathrm{x}},\\
l\Lambda\phi^{\shortparallel}\mathrm{K}^\perp&=\mathrm{x}+\phi^\perp\left[\frac{1}{2}\frac{\mathrm{d}\Lambda}{\mathrm{d}\bar{\mathrm{x}}}-\frac{C-\Lambda\phi^\perp}{\mathrm{x}}\right]+\mathrm{x}\frac{\mathrm{d}}{\mathrm{d}\bar{\mathrm{x}}}\left(\frac{C-\Lambda\phi^\perp}{\mathrm{x}}\right).
\end{aligned}
\tag{7.38}
$$

In this regime, the contorsion is completely determined by the metric, the dilaton field, and the vector field ϕ^μ. These fields themselves, however, remain arbitrary, subject only to the brunch condition.

A straightforward substitution confirms that all three solution families, RCI (7.35), RCIIA (7.38), and RCIIB, also satisfy the five-dimensional equations of motion (2.30). In addition, the five-dimensional BTZ black hole with torsion (2.31–2.32) remains a valid solution of this dimensionally-reduced 5DCS theory, within the first branch. The presence of some of the arbitrary functions in the branch-two solutions is an artifact of the unfixed five-dimensional gauge symmetries. To verify if this solutions are stable, one should see how they change when small perturbations of the sources are introduces. A further comment on this issue is given in Section 7.2.4.

7.2 General solutions with non-vanishing matter fields

In this section, we analyze the gravity equations of motion in the presence of matter. As our focus excludes the vacuum solutions, at least one component of the EMT and/or the contorsion current must be non-vanishing. The main aim is to find solutions for the additional field content, i.e. the contorsion K^{μ}, vector field ϕ^{μ} and θ in terms of the dilaton field x and the metric function Λ, and subsequently express the remaining equations in terms of the sources and Λ.

One of the equations of motion (7.14) is inherently satisfied when $\theta = 0$, significantly altering both the form of the equations of motion and their corresponding solutions. Moreover, since the function $\mathcal{Z}$ appears as a prefactor in most equations, whether it vanishes or not gives rise to additional distinct cases. Further special instances require individual consideration. Therefore, we provide Table 7.1, which summarizes all these cases. The initial column of the table indicates the non-zero source, whereas the subsequent three columns outline the conditions that specify the solution. The axillary function $\mathcal{J}$ appearing in Table 7.1 varies from case to case, and for that reason it is defined for each particular case, while P is an integration constant relevant to some cases. Using the axillary functions of the sources (7.27), the conservation laws for the EMT (3.66) and (3.67) can be rewritten in the following form:

$$\begin{aligned}
&2\Lambda\frac{\mathrm{d}\tilde{T}^{\perp\perp}}{\mathrm{d}\bar{\mathrm{x}}}+\frac{\mathrm{d}\Lambda}{\mathrm{d}\bar{\mathrm{x}}}\left(\tilde{T}^{\shortparallel\shortparallel}+\tilde{T}^{\perp\perp}\right)=4l\Lambda\mathrm{K}^{\perp}\frac{\mathrm{d}}{\mathrm{d}\bar{\mathrm{x}}}\left(\Lambda\tilde{T}^{\perp}_{\mathrm{K}}\right)-2\Lambda\tilde{T}^{\shortparallel}_{\mathrm{K}}\frac{\mathrm{d}\mathcal{S}}{\mathrm{d}\bar{\mathrm{x}}},\\
&\tilde{T}^{\shortparallel\perp}=2l\Lambda\mathrm{K}^{\shortparallel}\tilde{T}^{\perp}_{\mathrm{K}}+\frac{const.}{\Lambda},
\end{aligned}\tag{7.39}$$

where within our model the constant in the second equation vanishes. The second condition is automatically satisfied on equations (7.22) and (7.25). It is straight-forward to check that the first conservation law is satisfied in each case separately.

It turns out that any free, minimally-coupled matter field theory possesses an identically vanishing contorsion current. For scalar and vector fields this is straightforward. The subtlety arises for spinor fields, where the contorsion appears explicitly in the action. Even so, when one varies the action with respect to the contorsion, the ensuing contorsion current manifestly vanishes. A non-zero value for this current occurs only once non-minimal couplings are introduced. Consequently, we focus in particular on setups where the energy-momentum tensor is the only non-vanishing source. In such a situation we automatically obtain $\phi^{\shortparallel} = \mathrm{K}^{\perp} = 0$, as well as $T^{\shortparallel\perp} = 0$. There are for configurations with non-vanishing θ field. In all these configurations the solution is determined by three integration constants η, P, and D, and is most conveniently expressed in the z coordinate (3.21). On the other hand, if one allows the θ field to vanish, the theory collapses to the purely Riemannian sector analyzed in the preceding chapter.

The case when the parallel component of the contorsion current together with the EMT does not vanish is of great importance when there is non-minimal coupling of the matter fields only to the curvature of the spacetime. In the two-dimensional case, terms linear in curvature have the following form:

$$S_{int} \propto \int \varepsilon_{ab} R^{ab} F = -\int \mathrm{d}^2 x \sqrt{-g} \left(\mathrm{R} + 2\varepsilon^{\alpha\beta} \nabla_\alpha \mathrm{K}_\beta \right) F, \tag{7.40}$$

where F denotes a scalar function related to the field content within the theory. The second equality comes from expression (2.42). The second term in expression (7.40) is significant for the purpose of our argument. Varying with respect to K_μ leads to the following expression for the source of contorsion:

$$T^\mu_{\mathrm{K}} \propto \varepsilon^{\mu\nu} \nabla_\nu F = \frac{\mathcal{D}}{l} \frac{\mathrm{d}F}{\mathrm{dx}} \xi^\mu, \tag{7.41}$$

implying that only a parallel component of the contorsion current exists. Even adding a quadratic term in the Riemann-Cartan curvature, or any function of R, leads to an identical outcome. Since $T^\perp_{\mathrm{K}} = 0$, once again $\phi^\parallel = 0$ and $\mathrm{K}^\perp = 0$, as well as $T^{\parallel\perp} = 0$.

In this situation, the solutions reduce to those of the previous case when one takes the limit in which the contorsion current vanishes. However, for $\theta \neq 0$ there are five distinct solutions, in contrast to the earlier case. The presence of a non-zero parallel component of the contorsion current yields a BTZ-like solution with non-vanishing EMT, together with an arbitrary $\phi^\perp$ function and constants P and η. In contrast with the preceding case, when $\theta = 0$ the non-vanishing $T^\parallel_{\mathrm{K}}$ leads to a much richer spectrum of solutions, which can display a non-zero two-dimensional torsion, as shown in Table 7.1. Finally, only in this scenario can a vanishing $\mathcal{Z}$ function be imposed. This provides an additional perspective on the stability of the vacuum solutions RCIIA (7.38) and RCIIB.

Finally, the most general case arises when the normal component of the contorsion current does not vanish. This situation occurs only in the presence of a non-minimal coupling of the matter action to the two-dimensional torsion. The solutions in the $\theta \neq 0$ sector are then characterized by two constants, η and P, whereas the $\theta = 0$ sector resembles the previous case and reduces to it in the limit where the normal component of the contorsion current goes to zero.

In what follows, we do not organize this section according to which component of the contorsion current vanishes. Instead, we directly solve the equations and thereby explain why the various cases appear. The discussion is structured around three main scenarios: two scenarios with $\mathcal{Z} \neq 0$, distinguished by whether θ is present or absent, and a third scenario with $\mathcal{Z} = 0$. Moreover, when $\mathcal{Z} \neq 0$, we further distinguish three cases according to which components of the contorsion current are non-vanishing. Throughout all of these cases, we assume that both the dilaton field and the metric are non-zero, i.e., $\mathrm{x} \neq 0$ and $\Lambda \neq 0$.

7.2.1 Solutions when $\mathcal{Z} \neq 0$ and $\theta \neq 0$

We begin by analyzing the constraint equations. Since $\theta \neq 0$, condition (7.14) is satisfied, and consequently the dilaton field equation (7.17) becomes considerably simpler, as the scalar curvature term drops out. After additionally substituting (7.15) and (7.16) into (7.17), we

Source	Condition 1	Condition 2	Condition 3	Condition 4
$T_\mu^{\mathrm{K}} = 0$	$\theta \neq 0 \ \wedge \ \mathcal{Z} \neq 0$	$\Lambda > 0$	$\mathrm{x}^2 + \Lambda\phi^{\perp 2} > 0$	/
		$\Lambda < 0$	$\mathrm{x}^2 + \Lambda\phi^{\perp 2} > 0$	/
			$\mathrm{x}^2 + \Lambda\phi^{\perp 2} < 0$	/
			$\mathrm{x}^2 + \Lambda\phi^{\perp 2} = 0$	/
	$\theta = 0 \ \wedge \ \mathcal{Z} \neq 0$	$\phi^\perp \neq 0$	$\mathcal{S}^2 + 4\Lambda \neq 0 \ \wedge \ \mathcal{J} \neq 0$	$\mathcal{S}' + 2 = 0$
				$\mathcal{S}' + 2 \neq 0$
			$\mathcal{S}^2 + 4\Lambda \neq 0 \ \wedge \ \mathcal{J} = 0$	/
			$\mathcal{S}^2 + 4\Lambda = 0$	/
		$\phi^\perp = 0$	/	/
$T_{\mathrm{K}}^\perp = 0$	$\theta \neq 0 \ \wedge \ \mathcal{Z} \neq 0$	$\mathcal{S}\phi^\perp \neq 2\mathrm{x}$	$\Lambda > 0$	$\mathrm{x}^2 + \Lambda\phi^{\perp 2} > 0$
			$\Lambda < 0$	$\mathrm{x}^2 + \Lambda\phi^{\perp 2} > 0$
				$\mathrm{x}^2 + \Lambda\phi^{\perp 2} < 0$
				$\mathrm{x}^2 + \Lambda\phi^{\perp 2} = 0$
		$\mathcal{S}\phi^\perp = 2\mathrm{x}$	/	/
	$\theta = 0 \ \wedge \ \mathcal{Z} \neq 0$	$\phi^\perp \neq 0 \ \wedge \ \mathcal{D} \neq 0$	$\mathcal{S}^2 + 4\Lambda \neq 0 \ \wedge \ \mathcal{J} \neq 0$	$\tilde{T}^{\perp\perp} \neq 0$
				$\tilde{T}^{\perp\perp} = 0$
			$\mathcal{S}^2 + 4\Lambda \neq 0 \ \wedge \ \mathcal{J} = 0$	$\mathcal{Z} \neq 2/3$
				$\mathcal{Z} = 2/3$
			$\mathcal{S}^2 + 4\Lambda = 0$	$\tilde{T}^{\perp\perp} \neq 0$
				$\tilde{T}^{\perp\perp} = 0$
		$\mathcal{D} = 0$	/	/
		$\phi^\perp = 0$	/	/
	$\mathcal{Z} = 0$	/	/	/
$T_{\mathrm{K}}^\perp \neq 0$	$\theta \neq 0 \ \wedge \ \mathcal{Z} \neq 0$	$\Phi^2 \neq \mathrm{x}^2 \ \wedge \ \phi^\perp \neq 0$	$P \neq 0$	$\mathcal{S}^2 + 4\Lambda \notin \{0, P^2\}$
				$\mathcal{S}^2 + 4\Lambda = P^2$
				$\mathcal{S}^2 + 4\Lambda = 0$
			$P = 0$	$\mathcal{S}^2 + 4\Lambda \neq 0$
				$\mathcal{S}^2 + 4\Lambda = 0$
		$\Phi^2 = \mathrm{x}^2 \ \wedge \ \phi^\perp \neq 0$	$\mathcal{S}^2 + 4\Lambda \neq 0$	/
			$\mathcal{S}^2 + 4\Lambda = 0$	/
		$\phi^\perp = 0$	/	/
	$\theta = 0 \ \wedge \ \mathcal{Z} \neq 0$	$\phi^\perp \neq 0 \ \wedge \ \mathcal{D} \neq 0$	$\mathcal{S}^2 + 4\Lambda \neq 0 \ \wedge \ \mathcal{J} \neq 0$	$\tilde{T}^{\perp\perp} \neq 0$
				$\tilde{T}^{\perp\perp} = 0$
			$\mathcal{S}^2 + 4\Lambda \neq 0 \ \wedge \ \mathcal{J} = 0$	$\mathcal{Z} \neq 2/3$
				$\mathcal{Z} = 2/3$
			$\mathcal{S}^2 + 4\Lambda = 0$	$\tilde{T}^{\perp\perp} \neq 0$
				$\tilde{T}^{\perp\perp} = 0$
		$\mathcal{D} = 0$	/	/
		$\phi^\perp = 0$	/	/

Table 7.1: Classification of the solutions to the equations of motion

obtain:

$$\frac{4}{\mathrm{x}} l \left(\mathrm{x}^2 - \Phi^2\right) \varepsilon^{\alpha\beta} \phi_\alpha \mathrm{K}_\beta = \frac{2}{\mathrm{x}} \Lambda \phi^\perp \mathcal{D} \frac{\mathrm{d}}{\mathrm{dx}} \left(\mathrm{x}^2 - \Phi^2\right) + \frac{4}{\mathrm{x}} \left(\mathrm{x}^2 - \Phi^2\right) \left(\mathrm{x} - \mathcal{D} \frac{\mathrm{d}\left(\Lambda \phi^\perp\right)}{\mathrm{dx}}\right) - \mathcal{D} \left(\frac{\mathrm{d}\Phi^2}{\mathrm{dx}} - \frac{2}{\mathrm{x}} \Phi^2\right) \left(\mathcal{D} \frac{\mathrm{d}\Lambda}{\mathrm{dx}} - 2l\Lambda \mathrm{K}^{\parallel}\right). \tag{7.42}$$

Observe that (7.42) is identically fulfilled when $\Phi^2 = \mathrm{x}^2$, indicating that this special case must be treated independently. Accordingly, the subsection is split into five parts, distinguished by which components of the contorsion current vanish and by whether the condition $\Phi^2 = \mathrm{x}^2$ holds.

Completely vanishing contorsion current

Here we solve the equations of motion in the case where $T_{\mathrm{K}}^{\parallel} = T_{\mathrm{K}}^{\perp} = 0$. Because $\mathcal{Z} \neq 0$, equation (7.25) enforces $\phi^{\parallel} = 0$, which in turn simplifies equation (7.15) to $\mathrm{K}^\perp = 0$. From equation (7.22) we further obtain $T^{\parallel\perp} = 0$. Consequently, the system of equations simplifies to:

$$\mathcal{Z} \left[\phi^\perp \frac{\mathrm{d}\Lambda}{\mathrm{d}\bar{\mathrm{x}}} - 2\mathrm{x} - 2l\Lambda\phi^\perp \mathrm{K}^{\parallel}\right] = -\tilde{T}^{\perp\perp}, \tag{7.43}$$

$$\mathcal{Z} \left[2\Lambda \left(\frac{\mathrm{d}\phi^\perp}{\mathrm{d}\bar{\mathrm{x}}} - \frac{1}{\mathrm{x}} \phi^\perp \left(\phi^\perp + \mathcal{D}\right)\right) + \phi^\perp \frac{\mathrm{d}\Lambda}{\mathrm{d}\bar{\mathrm{x}}} - 2\mathrm{x}\right] = \tilde{T}^{\parallel\parallel}, \tag{7.44}$$

$$\mathcal{Z} \left(\phi^\perp + \mathcal{D}\right) = \mathrm{x} \frac{\mathrm{d}\theta^2}{\mathrm{d}\bar{\mathrm{x}}}, \tag{7.45}$$

$$\left(\phi^\perp + \mathcal{D}\right) \left[\phi^\perp \frac{\mathrm{d}\Lambda}{\mathrm{d}\bar{\mathrm{x}}} - 2\mathrm{x} - 2l\Lambda\phi^\perp \mathrm{K}^{\parallel}\right] = l\mathcal{Z}\mathrm{K}^{\parallel}, \tag{7.46}$$

$$\frac{\mathrm{d}}{\mathrm{d}\bar{\mathrm{x}}} \left(\frac{\mathrm{d}\Lambda}{\mathrm{d}\bar{\mathrm{x}}} - 2l\Lambda \mathrm{K}^{\parallel}\right) + 2 + \frac{2}{\mathrm{x}} l\Lambda\phi^\perp \mathrm{K}^{\parallel} = 0, \tag{7.47}$$

$$\left[2\Lambda \left(\frac{\mathrm{d}\phi^\perp}{\mathrm{d}\bar{\mathrm{x}}} - \frac{1}{\mathrm{x}} \phi^\perp \left(\phi^\perp + \mathcal{D}\right)\right) + \phi^\perp \frac{\mathrm{d}\Lambda}{\mathrm{d}\bar{\mathrm{x}}} - 2\mathrm{x}\right] \left[\phi^\perp \frac{\mathrm{d}\Lambda}{\mathrm{d}\bar{\mathrm{x}}} - 2\mathrm{x} - 2l\Lambda\phi^\perp \mathrm{K}^{\parallel}\right] = 0. \tag{7.48}$$

By imposing that the second bracket in (7.48) vanishes, the EMT is set to zero, implying $T^{\parallel\parallel} = T^{\perp\perp} = 0$, and the resulting solution coincides exactly with (7.35). This case is not of particular interest, since we are focusing on configurations where at least one EMT component is non-zero. Consequently, the first bracket in (7.48) must vanish, which leads to

$$\frac{\mathrm{d}}{\mathrm{d}\bar{\mathrm{x}}} \left(\Lambda \phi^{\perp 2} + \mathrm{x}^2\right) = \frac{2}{\mathrm{x}} \left(\Lambda \phi^{\perp 2} + \mathrm{x}^2\right) \left(\phi^\perp + \mathcal{D}\right). \tag{7.49}$$

Taken together with equation (7.44), this condition also eliminates the parallel component of the EMT, i.e. $T^{\parallel\parallel} = 0$, while the normal component remains non-zero. Depending on the signs of Λ and $\Lambda\phi^{\perp 2} + \mathrm{x}^2$, four distinct cases must be considered. In all of these cases, the coordinate z, defined by equation (3.21), is employed.

- $\underline{\Lambda > 0}$: Integrating equation (7.49) results into the following solution for $\phi^\perp$:

$$\phi^\perp = \frac{\mathrm{x}}{\sqrt{\Lambda}} \tan \mathrm{z}. \tag{7.50}$$

Using this solution as well as the definition of the z coordinate (3.21), equation (7.45) can be integrated resulting in a solution for the θ field:

$$\theta^2 = 1 + \frac{1}{3}\left(\frac{\mathrm{x}}{\cos \mathrm{z}}\right)^2 + \eta \frac{\cos \mathrm{z}}{\mathrm{x}}, \tag{7.51}$$

where η is an integration constant. Next, direct integration of equation (7.47) results into:

$$2l\Lambda \mathrm{K}^{\parallel} = \frac{\mathrm{d}\Lambda}{\mathrm{d}\bar{\mathrm{x}}} + 2\sqrt{\Lambda}\tan \mathrm{z} - \frac{P}{\cos \mathrm{z}}, \tag{7.52}$$

where P is another integration constant. Using the solutions (7.50-7.52) makes equation (7.46) integrable, giving the following solution for the dilaton field:

$$\frac{2}{3}\left(\frac{\mathrm{x}}{\cos \mathrm{z}}\right)^3 = \frac{D\cos \mathrm{z}}{\sqrt{-\Lambda} - \frac{P}{2}\sin \mathrm{z}} + \eta, \tag{7.53}$$

where D is the final integration constant. Placing solutions (7.50-7.53) in the last remaining equation (7.43) gives a condition for the EMT:

$$T^{\perp\perp} = \frac{6k\pi^2 D}{l^2}\frac{1}{\Lambda^{3/2}}. \tag{7.54}$$

- $\underline{\Lambda < 0 \wedge \mathrm{x}^2 + \Lambda\phi^{\perp 2} > 0}$: In this case, the solution to the equation (7.49) is given by the following expression:

$$\phi^{\perp} = \frac{\mathrm{x}}{\sqrt{-\Lambda}}\tanh \mathrm{z}. \tag{7.55}$$

Integrating equations (7.45) and (7.47) yields:

$$\theta^2 = 1 + \frac{1}{3}\left(\frac{\mathrm{x}}{\cosh \mathrm{z}}\right)^2 + \eta \frac{\cosh \mathrm{z}}{\mathrm{x}}, \tag{7.56}$$

$$2l\Lambda \mathrm{K}^{\parallel} = \frac{\mathrm{d}\Lambda}{\mathrm{d}\bar{\mathrm{x}}} - 2\sqrt{-\Lambda}\tanh \mathrm{z} - \frac{P}{\cosh \mathrm{z}}, \tag{7.57}$$

respectively. The solution to equation (7.46) and the constraint on the perpendicular component of the EMT are given by:

$$\frac{2}{3}\left(\frac{\mathrm{x}}{\cosh \mathrm{z}}\right)^3 = \frac{D\cosh \mathrm{z}}{\sqrt{-\Lambda} - \frac{P}{2}\sinh \mathrm{z}} + \eta, \tag{7.58}$$

$$T^{\perp\perp} = -\frac{6k\pi^2 D}{l^2}\frac{1}{(-\Lambda)^{3/2}}. \tag{7.59}$$

Similarly to the previous case, the solution depends on three constants η, P and D.

- $\underline{\Lambda < 0 \wedge \mathrm{x}^2 + \Lambda\phi^{\perp 2} < 0}$: Equation (7.49) gives the following solution:

$$\phi^{\perp} = \frac{\mathrm{x}}{\sqrt{-\Lambda}}\coth \mathrm{z}. \tag{7.60}$$

Equations (7.45) and (7.47) reduce to:

$$\theta^2 = 1 - \frac{1}{3}\left(\frac{\mathrm{x}}{\sinh \mathrm{z}}\right)^2 + \eta \frac{\sinh \mathrm{z}}{\mathrm{x}}, \tag{7.61}$$

$$2l\Lambda \mathrm{K}^{\parallel} = \frac{\mathrm{d}\Lambda}{\mathrm{d}\bar{\mathrm{x}}} - 2\sqrt{-\Lambda}\coth \mathrm{z} - \frac{P}{\sinh \mathrm{z}}, \tag{7.62}$$

respectively. The answer to equation (7.46) along with the condition on the perpendicular component of the EMT is expressed as:

$$\frac{2}{3}\left(\frac{\mathrm{x}}{\sinh \mathrm{z}}\right)^3 = \frac{D\sinh \mathrm{z}}{\sqrt{-\Lambda}+\frac{P}{2}\cosh \mathrm{z}} - \eta, \tag{7.63}$$

$$T^{\perp\perp} = -\frac{6k\pi^2 D}{l^2}\frac{1}{(-\Lambda)^{3/2}}. \tag{7.64}$$

In a manner akin to the earlier situations, the solution relies on three constants: η, P, and D.

- $\underline{\Lambda < 0 \,\wedge\, \mathrm{x}^2 + \Lambda\phi^{\perp 2} = 0}$: The specific condition in this case automatically satisfies equation (7.49) and implies:

$$\phi^{\perp} = \pm\frac{\mathrm{x}}{\sqrt{-\Lambda}} \tag{7.65}$$

It is straight-forward to integrate both equations (7.45) and (7.47). The solution is given by:

$$\theta^2 = 1 + \frac{\eta}{\mathrm{x}}e^{\pm \mathrm{z}}. \tag{7.66}$$

$$2l\Lambda \mathrm{K}^{\parallel} = \frac{\mathrm{d}\Lambda}{\mathrm{d}\bar{\mathrm{x}}} \mp 2\sqrt{-\Lambda} + 2Pe^{\mp \mathrm{z}}. \tag{7.67}$$

In this instance, solving the integral of equation (7.46) results in:

$$\frac{2}{3}\left(\mathrm{x}e^{\mp \mathrm{z}}\right)^3 = \frac{\eta}{P}\left[\left(\pm\sqrt{-\Lambda} - \frac{P}{2}e^{\mp \mathrm{z}}\right)e^{\mp \mathrm{z}} + D\right], \tag{7.68}$$

while the constraint imposed on the EMT is given by:

$$T^{\perp\perp} = \pm\frac{6k\pi^2\eta P}{l^2}\frac{1}{(-\Lambda)^{3/2}}. \tag{7.69}$$

We conclude that, in this final case, the solution once again depend on three constants η, P and D.

Non-vanishing parallel component of contorsion current

In this section, we assume that $T_{\mathrm{K}}^{\parallel} \neq 0$ while $T_{\mathrm{K}}^{\perp} = 0$. Due to analogous reasons presented in the preceding section, it holds that $\phi^{\parallel} = \mathrm{K}^{\perp} = T^{\parallel\perp} = 0$. Consequently, we have the following system of equations remaining:

$$\mathcal{Z}\left[\phi^{\perp}\frac{\mathrm{d}\Lambda}{\mathrm{d}\bar{\mathrm{x}}} - 2\mathrm{x} - 2l\Lambda\phi^{\perp}\mathrm{K}^{\shortparallel}\right] = -\tilde{T}^{\perp\perp}, \tag{7.70}$$

$$\mathcal{Z}\left[2\Lambda\left(\frac{\mathrm{d}\phi^{\perp}}{\mathrm{d}\bar{\mathrm{x}}} - \frac{1}{\mathrm{x}}\phi^{\perp}\left(\phi^{\perp}+\mathcal{D}\right)\right) + \phi^{\perp}\frac{\mathrm{d}\Lambda}{\mathrm{d}\bar{\mathrm{x}}} - 2\mathrm{x}\right] = \tilde{T}^{\shortparallel\shortparallel} - \frac{2}{\mathrm{x}}\Lambda\phi^{\perp}\tilde{T}^{\shortparallel}_{\mathrm{K}}, \tag{7.71}$$

$$\mathcal{Z}\left(\phi^{\perp}+\mathcal{D}\right) - \mathrm{x}\frac{\mathrm{d}\theta^2}{\mathrm{d}\bar{\mathrm{x}}} = \tilde{T}^{\shortparallel}_{\mathrm{K}}, \tag{7.72}$$

$$\left(\phi^{\perp}+\mathcal{D}\right)\left[\phi^{\perp}\frac{\mathrm{d}\Lambda}{\mathrm{d}\bar{\mathrm{x}}} - 2\mathrm{x} - 2l\Lambda\phi^{\perp}\mathrm{K}^{\shortparallel}\right] = l\mathcal{Z}\mathrm{K}^{\shortparallel}, \tag{7.73}$$

$$\frac{\mathrm{d}}{\mathrm{d}\bar{\mathrm{x}}}\left(\frac{\mathrm{d}\Lambda}{\mathrm{d}\bar{\mathrm{x}}} - 2l\Lambda\mathrm{K}^{\shortparallel}\right) + 2 + \frac{2}{\mathrm{x}}l\Lambda\phi^{\perp}\mathrm{K}^{\shortparallel} = 0, \tag{7.74}$$

$$\left[2\Lambda\left(\frac{\mathrm{d}\phi^{\perp}}{\mathrm{d}\bar{\mathrm{x}}} - \frac{1}{\mathrm{x}}\phi^{\perp}\left(\phi^{\perp}+\mathcal{D}\right)\right) + \phi^{\perp}\frac{\mathrm{d}\Lambda}{\mathrm{d}\bar{\mathrm{x}}} - 2\mathrm{x}\right]\left[\phi^{\perp}\frac{\mathrm{d}\Lambda}{\mathrm{d}\bar{\mathrm{x}}} - 2\mathrm{x} - 2l\Lambda\phi^{\perp}\mathrm{K}^{\shortparallel}\right] = 0. \tag{7.75}$$

In contrast to the previous section, setting the second bracket in equation (7.75) to zero does not lead to the EMT disappearing, as $T^{\shortparallel}_{\mathrm{K}}$ remains non-zero. Then equations (7.73) and (7.70) reduce to $\mathrm{K}^{\shortparallel} = 0$ and $\tilde{T}^{\perp\perp} = 0$, respectively. The metric function Λ is completely determined from (7.74), that is:

$$\Lambda = -\left(\bar{\mathrm{x}}^2 - \mu\right), \tag{7.76}$$

where μ is an integration constant. Using this solution (7.76) together with equation (7.75) results in the following:

$$\mathrm{x} = -\bar{\mathrm{x}}\phi^{\perp}(\bar{\mathrm{x}}). \tag{7.77}$$

Putting (7.76) and (7.77) into equation (7.71) results into a condition for the EMT, given by:

$$\tilde{T}^{\shortparallel\shortparallel} + \frac{2}{\bar{\mathrm{x}}}\Lambda\tilde{T}^{\shortparallel}_{\mathrm{K}} = 0. \tag{7.78}$$

The last equation (7.72) can be directly integrated giving a solution for the θ filed:

$$\theta^2 = 1 + \frac{1}{3}\mu\phi^{\perp 2} + \frac{1}{\phi^{\perp}}\left(\eta + \int\frac{\mathrm{d}\bar{\mathrm{x}}}{\bar{\mathrm{x}}}\tilde{T}^{\shortparallel}_{\mathrm{K}}\right), \tag{7.79}$$

where η is the integration constant.

Choosing the first bracket in (7.75) to vanish we arrive at the same equation (7.49) as in the case when the entire contorsion current vanishes, namely:

$$\frac{\mathrm{d}}{\mathrm{d}\bar{\mathrm{x}}}\left(\Lambda\phi^{\perp 2} + \mathrm{x}^2\right) = \frac{2}{\mathrm{x}}\left(\Lambda\phi^{\perp 2} + \mathrm{x}^2\right)\left(\phi^{\perp}+\mathcal{D}\right). \tag{7.80}$$

To proceed further, we must examine four separate cases due to the varying options for the signs of Λ and $\mathrm{x}^2 + \Lambda\phi^{\perp 2}$.

- $\underline{\Lambda > 0}$: Similarly to the previous section, equations (7.80), (7.71) and (7.74) reduce to the following:

$$\phi^{\perp} = \frac{\mathrm{x}}{\sqrt{\Lambda}}\tan\mathrm{z}, \tag{7.81}$$

$$\tilde{T}^{\shortparallel\shortparallel} = 2\sqrt{\Lambda}\tilde{T}^{\shortparallel}_{\mathrm{K}}\tan\mathrm{z}, \tag{7.82}$$

$$2l\Lambda\mathrm{K}^{\shortparallel} = \frac{\mathrm{d}\Lambda}{\mathrm{d}\bar{\mathrm{x}}} + 2\sqrt{\Lambda}\tan\mathrm{z} - \frac{P}{\cos\mathrm{z}}, \tag{7.83}$$

where P is the standard integration constant related to the parallel component of the contorsion. Equation (7.72) can be directly integrated using (7.81) resulting in:

$$\theta^2 = 1 + \frac{1}{3}\left(\frac{\mathrm{x}}{\cos \mathrm{z}}\right)^2 + \frac{\cos \mathrm{z}}{\mathrm{x}}\left(\eta + I\right), \tag{7.84}$$

where η is another constant and $I = -\int \frac{\mathrm{dz}\sqrt{\Lambda}}{\cos \mathrm{z}} \tilde{T}^{\shortparallel}_{\mathrm{K}}$. Equation (7.70) gives the solution for x in the following form:

$$\frac{2}{3}\left(\frac{\mathrm{x}}{\cos \mathrm{z}}\right)^3 = \frac{\tilde{T}^{\perp\perp}\sqrt{\Lambda}}{2}\frac{\cos \mathrm{z}}{\sqrt{\Lambda} - \frac{P}{2}\sin \mathrm{z}} + \eta + I, \tag{7.85}$$

The final equation (7.73) gives another condition for the EMT:

$$\frac{\mathrm{d}}{\mathrm{dz}}\left(\sqrt{\Lambda}\tilde{T}^{\perp\perp}\right) + \frac{2\sqrt{\Lambda}\tilde{T}^{\shortparallel}_{\mathrm{K}}}{\cos \mathrm{z}}\frac{\sqrt{\Lambda} - \frac{P}{2}\sin \mathrm{z}}{\cos \mathrm{z}} = 0. \tag{7.86}$$

- $\underline{\Lambda < 0 \ \wedge \ \mathrm{x}^2 + \Lambda\phi^{\perp 2} > 0}$: Analogues to the previous case, integration of equations (7.80), (7.71) and (7.74) results into:

$$\phi^{\perp} = \frac{\mathrm{x}}{\sqrt{-\Lambda}}\tanh \mathrm{z}, \tag{7.87}$$

$$\tilde{T}^{\shortparallel\shortparallel} = -2\sqrt{-\Lambda}\tilde{T}^{\shortparallel}_{\mathrm{K}}\tanh \mathrm{z}, \tag{7.88}$$

$$2l\Lambda\mathrm{K}^{\shortparallel} = \frac{\mathrm{d}\Lambda}{\mathrm{d}\bar{\mathrm{x}}} - 2\sqrt{-\Lambda}\tanh \mathrm{z} - \frac{P}{\cosh \mathrm{z}}. \tag{7.89}$$

The other three equations provide solutions for the θ and x fields, along with an additional constraint for the EMT:

$$\theta^2 = 1 + \frac{1}{3}\left(\frac{\mathrm{x}}{\cosh \mathrm{z}}\right)^2 + \frac{\cosh \mathrm{z}}{\mathrm{x}}\left(\eta + I\right), \tag{7.90}$$

$$\frac{2}{3}\left(\frac{\mathrm{x}}{\cosh \mathrm{z}}\right)^3 = \frac{\tilde{T}^{\perp\perp}\sqrt{-\Lambda}}{2}\frac{\cosh \mathrm{z}}{\sqrt{-\Lambda} - \frac{P}{2}\sinh \mathrm{z}} + \eta + I, \tag{7.91}$$

$$\frac{\mathrm{d}}{\mathrm{dz}}\left(\sqrt{-\Lambda}\tilde{T}^{\perp\perp}\right) + \frac{2\sqrt{-\Lambda}\tilde{T}^{\shortparallel}_{\mathrm{K}}}{\cosh \mathrm{z}}\frac{\sqrt{-\Lambda} - \frac{P}{2}\sinh \mathrm{z}}{\cosh \mathrm{z}} = 0, \tag{7.92}$$

where the integral I is given by:

$$I = \int \frac{\mathrm{dz}\sqrt{-\Lambda}}{\cosh \mathrm{z}}\tilde{T}^{\shortparallel}_{\mathrm{K}}. \tag{7.93}$$

- $\underline{\Lambda < 0 \ \wedge \ \mathrm{x}^2 + \Lambda\phi^{\perp 2} < 0}$: Solving equations (7.80), (7.71) and (7.74) yileds:

$$\phi^{\perp} = \frac{\mathrm{x}}{\sqrt{-\Lambda}}\coth \mathrm{z}, \tag{7.94}$$

$$\tilde{T}^{\shortparallel\shortparallel} = -2\sqrt{-\Lambda}\tilde{T}^{\shortparallel}_{\mathrm{K}}\coth \mathrm{z}, \tag{7.95}$$

$$2l\Lambda\mathrm{K}^{\shortparallel} = \frac{\mathrm{d}\Lambda}{\mathrm{d}\bar{\mathrm{x}}} - 2\sqrt{-\Lambda}\coth \mathrm{z} - \frac{P}{\sinh \mathrm{z}}. \tag{7.96}$$

Once again, the remaining equations reduce to the expected solutions:

$$\theta^2 = 1 - \frac{1}{3}\left(\frac{\mathrm{x}}{\sinh \mathrm{z}}\right)^2 + \frac{\sinh \mathrm{z}}{\mathrm{x}}\left(\eta + I\right), \tag{7.97}$$

$$\frac{2}{3}\left(\frac{\mathrm{x}}{\sinh \mathrm{z}}\right)^3 = \frac{\tilde{T}^{\perp\perp}\sqrt{-\Lambda}}{2}\frac{\sinh \mathrm{z}}{\sqrt{-\Lambda} + \frac{P}{2}\cosh \mathrm{z}} - (\eta + I), \tag{7.98}$$

$$\frac{\mathrm{d}}{\mathrm{dz}}\left(\sqrt{-\Lambda}\tilde{T}^{\perp\perp}\right) - \frac{2\sqrt{-\Lambda}\tilde{T}^{\shortparallel}_{\mathrm{K}}}{\sinh \mathrm{z}}\frac{\sqrt{-\Lambda} + \frac{P}{2}\cosh \mathrm{z}}{\sinh \mathrm{z}} = 0, \tag{7.99}$$

where the integral I is given by:

$$I = \int \frac{\mathrm{dz}\sqrt{-\Lambda}}{\sinh \mathrm{z}} \tilde{T}^{\parallel}_{\mathrm{K}}. \tag{7.100}$$

- $\underline{\Lambda < 0 \,\wedge\, \mathrm{x}^2 + \Lambda \phi^{\perp 2} = 0}$: According to the condition defining this case, equation (7.80) is solved, resulting in:

$$\phi^{\perp} = \pm \frac{\mathrm{x}}{\sqrt{-\Lambda}}. \tag{7.101}$$

The solutions to equations (7.71) and (7.74) have the standard form:

$$\tilde{T}^{\parallel\parallel} = \mp 2\sqrt{-\Lambda}\tilde{T}^{\parallel}_{\mathrm{K}}, \tag{7.102}$$

$$2l\Lambda \mathrm{K}^{\parallel} = \frac{\mathrm{d}\Lambda}{\mathrm{d}\bar{\mathrm{x}}} \mp 2\sqrt{-\Lambda} + 2Pe^{\mp \mathrm{z}}. \tag{7.103}$$

Integrating equation (7.72) yields:

$$\theta^2 = 1 + \frac{e^{\pm \mathrm{z}}}{\mathrm{x}} \left(\eta + I\right), \tag{7.104}$$

where $I = \int \mathrm{dz}\sqrt{-\Lambda}\tilde{T}^{\parallel}_{\mathrm{K}} e^{\mp \mathrm{z}}$. Equation (7.70) reduces to a constraint for the $T^{\perp\perp}$, that is:

$$\frac{1}{2}\sqrt{-\Lambda}\tilde{T}^{\perp\perp} \pm P(\eta + I) = 0, \tag{7.105}$$

while the final equation (7.73) gives the following solution for x:

$$\frac{2}{3}P\left(\mathrm{x}e^{\mp \mathrm{z}}\right)^3 = (\eta + I)\left(\pm\sqrt{-\Lambda} - \frac{P}{2}e^{\mp \mathrm{z}}\right)e^{\mp \mathrm{z}} + \eta D - \int \mathrm{dz}\sqrt{-\Lambda}\tilde{T}^{\parallel}_{\mathrm{K}}\left(\pm\sqrt{-\Lambda} - \frac{P}{2}e^{\mp \mathrm{z}}\right)e^{\mp 2\mathrm{z}}. \tag{7.106}$$

We conclude that if a non-zero parallel component of the contorsion current is present, the solutions depend on three integration constants η, P, and D similar to those in the prior section. Moreover, by taking the limit $T^{\parallel}_{\mathrm{K}} \to 0$, these solutions align with those derived earlier.

Non-vanishing normal component of contorsion current when $\Phi^2 \neq \mathrm{x}^2$ and $\phi^{\perp} \neq 0$

Here, we derive the most general solution to the equations of motion (7.10-7.17). In the previous two sections, the condition $\phi^{\perp} \neq 0$ was assumed, which does not automatically hold when $T^{\perp}_{\mathrm{K}} \neq 0$. This particular situation is analyzed independently in the following sections.

After multiplying equation (7.14) by $\mathrm{x}^2 - \Phi^2$ and substituting equation (7.42) into this modified equation, we reach an integrable form. Upon integration, the resulting expression is as follows:

$$\frac{\mathrm{d}\Lambda}{\mathrm{d}\bar{\mathrm{x}}} + \frac{2}{\mathrm{x}}\Lambda\phi^{\perp} - 2l\Lambda\mathrm{K}^{\parallel} = \frac{P}{\mathrm{x}}\sqrt{|\mathrm{x}^2 - \Phi^2|}, \tag{7.107}$$

where P is an arbitrary integration constant. We use a following convention:

$$\mathrm{x}^2 - \Phi^2 = \pm\left|\mathrm{x}^2 - \Phi^2\right|. \tag{7.108}$$

Placing (7.107) in equation (7.42) we arrive at the following expression for $\mathrm{K}^{\perp}$:

$$\begin{aligned} 2l\Lambda\phi^{\shortparallel}\mathrm{K}^{\perp} = P\left[\frac{\mathrm{d}}{\mathrm{d}\bar{\mathrm{x}}}\sqrt{|\mathrm{x}^2-\Phi^2|} - \frac{1}{\mathrm{x}}\left(\phi^{\perp}+\mathcal{D}\right)\sqrt{|\mathrm{x}^2-\Phi^2|}\right] \\ -\left[2\Lambda\left(\frac{\mathrm{d}\phi^{\perp}}{\mathrm{d}\bar{\mathrm{x}}} - \frac{1}{\mathrm{x}}\phi^{\perp}\left(\phi^{\perp}+\mathcal{D}\right)\right) + \phi^{\perp}\frac{\mathrm{d}\Lambda}{\mathrm{d}\bar{\mathrm{x}}} - 2\mathrm{x}\right]. \end{aligned} \tag{7.109}$$

Substituting solutions for $\mathrm{K}^{\shortparallel}$ (7.107) and $\mathrm{K}^{\perp}$ (7.109) in equations (7.15) and (7.16) gives:

$$l\mathcal{Z}\mathrm{K}^{\shortparallel} = P\phi^{\perp}\frac{\mathrm{d}}{\mathrm{d}\bar{\mathrm{x}}}\sqrt{|\mathrm{x}^2-\Phi^2|} - \frac{\mathrm{d}}{\mathrm{d}\bar{\mathrm{x}}}\left(\mathrm{x}^2-\Phi^2\right), \tag{7.110}$$

$$l\mathcal{Z}\mathrm{K}^{\perp} = P\phi^{\shortparallel}\frac{\mathrm{d}}{\mathrm{d}\bar{\mathrm{x}}}\sqrt{|\mathrm{x}^2-\Phi^2|}. \tag{7.111}$$

Equation (7.22), together with (7.25), implies that the parallel component of the contorsion, as well as the variable $\mathcal{S}$, as defined in (7.29), are fully specified by the sources and the metric function Λ, leading to:

$$\mathrm{K}^{\shortparallel} = \frac{T^{\shortparallel\perp}}{T^{\perp}_{\mathrm{K}}}, \qquad \mathcal{S} = \frac{\mathrm{d}\Lambda}{\mathrm{d}\bar{\mathrm{x}}} - 2l\Lambda\frac{T^{\shortparallel\perp}}{T^{\perp}_{\mathrm{K}}} \tag{7.112}$$

Equations (7.107) and (7.109) can be regarded as solutions for $\mathrm{K}^{\shortparallel}$ and $\mathrm{K}^{\perp}$, respectively, in terms of the metric and ϕ^{μ} vector field. Using these, contorsion is removed from the equations of motion, leading to the following set of equations:

$$\mathcal{Z}\left(\mathcal{S}\phi^{\perp}-2\mathrm{x}\right) = -\tilde{T}^{\perp\perp}, \tag{7.113}$$

$$\mathcal{Z}P\left[\frac{\mathrm{d}}{\mathrm{d}\bar{\mathrm{x}}} - \frac{1}{\mathrm{x}}\left(\phi^{\perp}+\mathcal{D}\right)\right]\sqrt{|\mathrm{x}^2-\Phi^2|} = \tilde{T}^{\shortparallel\shortparallel} - \frac{2}{\mathrm{x}}\Lambda\phi^{\perp}\tilde{T}^{\shortparallel}_{\mathrm{K}}, \tag{7.114}$$

$$\mathcal{Z}\phi^{\shortparallel} = \tilde{T}^{\perp}_{\mathrm{K}}, \tag{7.115}$$

$$\mathcal{Z}\left(\phi^{\perp}+\mathcal{D}\right) - \mathrm{x}\frac{\mathrm{d}\theta^2}{\mathrm{d}\bar{\mathrm{x}}} = \tilde{T}^{\shortparallel}_{\mathrm{K}}, \tag{7.116}$$

$$\frac{\mathcal{Z}}{2\Lambda}\left(\frac{\mathrm{d}\Lambda}{\mathrm{d}\bar{\mathrm{x}}} - \mathcal{S}\right) = P\phi^{\perp}\frac{\mathrm{d}}{\mathrm{d}\bar{\mathrm{x}}}\sqrt{|\mathrm{x}^2-\Phi^2|} - \frac{\mathrm{d}}{\mathrm{d}\bar{\mathrm{x}}}\left(\mathrm{x}^2-\Phi^2\right), \tag{7.117}$$

$$\mathcal{Z}\left(\frac{\mathrm{d}\mathcal{S}}{\mathrm{d}\bar{\mathrm{x}}}+2\right) = 2P\mathrm{x}\frac{\mathrm{d}}{\mathrm{d}\bar{\mathrm{x}}}\sqrt{|\mathrm{x}^2-\Phi^2|} - \mathcal{S}\frac{\mathrm{d}}{\mathrm{d}\bar{\mathrm{x}}}\left(\mathrm{x}^2-\Phi^2\right), \tag{7.118}$$

$$\mathcal{S}\mathrm{x} + 2\Lambda\phi^{\perp} = P\sqrt{|\mathrm{x}^2-\Phi^2|}. \tag{7.119}$$

The equations (7.113-7.116) are analogous to the initial equations (7.23-7.26); equation (7.119) is a reformulation of expression (7.107). Moreover, equation (7.117) corresponds to (7.110), whereas (7.118) is obtained by subtracting (7.110), multiplied by $\phi^{\perp}$, from equation (7.111).

All fields can be expressed in terms of $\sqrt{|\mathrm{x}^2-\Phi^2|}$, $\mathcal{Z}$ and sources. By concurrently solving equations (7.113) and (7.119) with respect to x and $\phi^{\perp}$, we obtain:

$$\left(\mathcal{S}^2+4\Lambda\right)\phi^{\perp} = \sqrt{|\mathrm{x}^2-\Phi^2|}\left[2P - \frac{\mathcal{S}\tilde{T}^{\perp\perp}}{\mathcal{Z}\sqrt{|\mathrm{x}^2-\Phi^2|}}\right], \tag{7.120}$$

$$\left(\mathcal{S}^2+4\Lambda\right)\mathrm{x} = \sqrt{|\mathrm{x}^2-\Phi^2|}\left[P\mathcal{S} + \frac{2\Lambda\tilde{T}^{\perp\perp}}{\mathcal{Z}\sqrt{|\mathrm{x}^2-\Phi^2|}}\right], \tag{7.121}$$

while $\phi^{\shortparallel}$ is determined from (7.115):

$$\phi^{\shortparallel} = \frac{\tilde{T}^{\perp}_{\mathrm{K}}}{\mathcal{Z}}. \tag{7.122}$$

Next, we examine expression (7.119) by taking its square. After multiplication by $\mathcal{Z}^2$ and substitution of (7.113) and (7.115) we arrive at:

$$\left(\mathcal{S}^2+4\Lambda\mp P^2\right)\mathcal{Z}^2\left(\mathrm{x}^2-\Phi^2\right)=\Lambda\left(\tilde{T}^{\perp\perp 2}-\left(\mathcal{S}^2+4\Lambda\right)\tilde{T}_{\mathrm{K}}^{\perp 2}\right), \tag{7.123}$$

where we have used the convention defined in (7.108). Equations (7.117) and (7.118) are transformed into the following equivalent set of equations:

$$\frac{\mathcal{Z}}{2}\frac{\mathrm{d}}{\mathrm{d}\bar{\mathrm{x}}}\left(\mathcal{S}^2+4\Lambda\right)=-\left(\mathcal{S}^2+4\Lambda\mp P^2\right)\frac{\mathrm{d}}{\mathrm{d}\bar{\mathrm{x}}}\left(\mathrm{x}^2-\Phi^2\right), \tag{7.124}$$

$$\frac{\mathcal{Z}^2}{2\Lambda}\left[\mathcal{S}^2+4\Lambda+2\Lambda\frac{\mathrm{d}\mathcal{S}}{\mathrm{d}\bar{\mathrm{x}}}-\mathcal{S}\frac{\mathrm{d}\Lambda}{\mathrm{d}\bar{\mathrm{x}}}\right]=P\tilde{T}^{\perp\perp}\frac{\mathrm{d}}{\mathrm{d}\bar{\mathrm{x}}}\sqrt{\left|\mathrm{x}^2-\Phi^2\right|}. \tag{7.125}$$

with the help of expression (7.119). Observe that these two equations are identical when $\mathcal{S}^2+4\Lambda=0$, which indicates that we need to revisit the original set of equations in this scenario. Observing this new set of equations (7.120-7.125), together with equations (7.114) and (7.116), we conclude that the solving procedure branches depending on whether $\mathcal{S}^2+4\Lambda\in\{0,\pm P^2\}$ and whether constant P vanishes. Let us first examine the cases where $P\neq 0$.

- $\underline{P\neq 0}$: Combining equations (7.114) and (7.116) leads to an integrable equation, the solution of which is given by:

$$\theta^2=1+\frac{1}{3}\left(\mathrm{x}^2-\Phi^2\right)+\frac{1}{P}\frac{\eta+I}{\sqrt{\left|\mathrm{x}^2-\Phi^2\right|}}, \tag{7.126}$$

  where η is an integration constant, while integral I is defined as:

$$I=-\int\mathrm{d}\bar{\mathrm{x}}\left(\tilde{T}^{\parallel\parallel}+\mathcal{S}\tilde{T}_{\mathrm{K}}^{\parallel}\right). \tag{7.127}$$

  Now, we have also expressed $\mathcal{Z}$ solely in terms of $\left|\mathrm{x}^2-\Phi^2\right|$ and the sources. Here, we have another branching of the solution depending on whether the quantity $\mathcal{S}^2+4\Lambda\mp P^2$ and/or $\mathcal{S}^2+4\Lambda$ is non-zero.

  ⋆ $\underline{\mathcal{S}^2+4\Lambda\mp P^2\neq 0\ \wedge\ \mathcal{S}^2+4\Lambda\neq 0}$: From (7.123) we get a solution for $\left|\mathrm{x}^2-\Phi^2\right|$:

$$\pm\frac{2}{3}\left|\mathrm{x}^2-\Phi^2\right|^{\frac{3}{2}}=\mathcal{J}+\frac{\eta+I}{P}, \tag{7.128}$$

  where we have introduced a function $\mathcal{J}$ of the source fields, that is:

$$\mathcal{J}=\pm'\sqrt{\frac{\pm\Lambda\left(\tilde{T}^{\perp\perp 2}-\left(\mathcal{S}^2+4\Lambda\right)\tilde{T}_{\mathrm{K}}^{\perp 2}\right)}{\mathcal{S}^2+4\Lambda\mp P^2}}, \tag{7.129}$$

  with additional sign choice denoted by $\pm'$. The remaining three equations (7.124), (7.125) and (7.116) reduce to the constraints placed upon the sources, given by:

$$\tilde{T}^{\parallel\parallel}+\mathcal{S}\tilde{T}_{\mathrm{K}}^{\parallel}=\frac{P}{2}\mathcal{J}\frac{\mathrm{d}}{\mathrm{d}\bar{\mathrm{x}}}\ln\left|\Lambda\left(\tilde{T}^{\perp\perp 2}-\left(\mathcal{S}^2+4\Lambda\right)\tilde{T}_{\mathrm{K}}^{\perp 2}\right)\right|, \tag{7.130}$$

$$\mathcal{S}^2+4\Lambda+2\Lambda\frac{\mathrm{d}\mathcal{S}}{\mathrm{d}\bar{\mathrm{x}}}-\mathcal{S}\frac{\mathrm{d}\Lambda}{\mathrm{d}\bar{\mathrm{x}}}=\mp\frac{P\Lambda\tilde{T}^{\perp\perp}}{2\mathcal{J}}\frac{\mathrm{d}}{\mathrm{d}\bar{\mathrm{x}}}\ln\left|\mathcal{S}^2+4\Lambda\mp P^2\right|, \tag{7.131}$$

$$\tilde{T}_{\mathrm{K}}^{\parallel}\pm\frac{P\mathcal{S}}{2\mathcal{J}}\frac{\frac{\mathrm{d}}{\mathrm{d}\bar{\mathrm{x}}}\left(\Lambda\tilde{T}_{\mathrm{K}}^{\perp 2}\right)}{\mathcal{S}^2+4\Lambda\mp P^2}=\frac{2\Lambda\frac{\mathrm{d}\tilde{T}^{\perp\perp}}{\mathrm{d}\bar{\mathrm{x}}}+\tilde{T}^{\perp\perp}\frac{\mathrm{d}\Lambda}{\mathrm{d}\bar{\mathrm{x}}}}{\mathcal{S}^2+4\Lambda}\left[1\pm\frac{P\mathcal{S}}{2\mathcal{J}}\frac{\tilde{T}^{\perp\perp}}{\mathcal{S}^2+4\Lambda\mp P^2}\right]. \tag{7.132}$$

Lastly, the perpendicular component of contorsion is expressed as follows:

$$l\mathrm{K}^{\perp} = \mp\frac{P\tilde{T}_{\mathrm{K}}^{\perp}}{4\mathcal{J}}\frac{\mathrm{d}}{\mathrm{d}\bar{\mathrm{x}}}\ln\left|\mathcal{S}^2 + 4\Lambda \mp P^2\right|. \tag{7.133}$$

⋆ $\underline{\mathcal{S}^2 + 4\Lambda = \pm P^2}$: From (7.123) we have a condition for the sources:

$$\tilde{T}^{\perp\perp 2} = \pm P^2 \tilde{T}_{\mathrm{K}}^{\perp 2}, \tag{7.134}$$

which implies that $\mathrm{x}^2 > \Phi^2$, meaning the plus sign is applicable in this case. Equation (7.124) is automatically solved. Equation (7.116) gives fourth, and final, condition for the sources, i.e.

$$4\Lambda\tilde{T}_{\mathrm{K}}^{\shortparallel} = 2\frac{\mathrm{d}}{\mathrm{d}\bar{\mathrm{x}}}\left(\Lambda\tilde{T}^{\perp\perp}\right) - \mathcal{S}\tilde{T}^{\perp\perp} + \mathcal{S}\tilde{T}^{\shortparallel\shortparallel}. \tag{7.135}$$

Unfortunately, within this scenario, equation for $\mathcal{J} = \mathcal{Z}\sqrt{|\mathrm{x}^2 - \Phi^2|}$ cannot be solved in general. It is given by:

$$\frac{\mathrm{d}\mathcal{J}}{\mathrm{d}\bar{\mathrm{x}}} = \frac{P}{2\Lambda\tilde{T}^{\perp\perp}}\left(\frac{\mathrm{d}\mathcal{S}}{\mathrm{d}\bar{\mathrm{x}}} + 2\right)\mathcal{J}^2 + \frac{1}{P}\left(\tilde{T}^{\shortparallel\shortparallel} + S\tilde{T}_{\mathrm{K}}^{\shortparallel}\right). \tag{7.136}$$

⋆ $\underline{\mathcal{S}^2 + 4\Lambda = 0}$: In this scenario, equation (7.125) still holds, implying that:

$$\sqrt{|\mathrm{x}^2 - \Phi^2|} = Q = const. \tag{7.137}$$

This outcome annuls the right-hand side of both equations (7.117) and (7.118), leading to:

$$\mathcal{S} = -2\bar{\mathrm{x}}, \quad \Lambda = -\bar{\mathrm{x}}^2. \tag{7.138}$$

Simultaneously solving equations (7.113), (7.115) and (7.119) yields a solution for the fields x and ϕ^{μ} in terms of the sources, as well as one condition for the EMT:

$$\mathrm{x} = \frac{Q\bar{\mathrm{x}}}{P}\left(\frac{P^2\tilde{T}_{\mathrm{K}}^{\perp 2}}{\tilde{T}^{\perp\perp 2}} \mp 1\right) - \frac{PQ}{4\bar{\mathrm{x}}}, \tag{7.139}$$

$$\phi^{\perp} = -\frac{Q}{P}\left(\frac{P^2\tilde{T}_{\mathrm{K}}^{\perp 2}}{\tilde{T}^{\perp\perp 2}} \mp 1\right) - \frac{PQ}{4\bar{\mathrm{x}}^2}, \tag{7.140}$$

$$\phi^{\shortparallel} = -\frac{PQ}{\bar{\mathrm{x}}}\frac{\tilde{T}_{\mathrm{K}}^{\perp}}{\tilde{T}^{\perp\perp}}, \tag{7.141}$$

$$\pm\frac{2}{3}Q^3 = -\frac{\bar{\mathrm{x}}}{P}\tilde{T}^{\perp\perp} + \frac{\eta + I}{P}. \tag{7.142}$$

Since $\mathcal{S}$ and Λ have a form given by (7.137), the contorsion vanishes entirely, i.e.

$$\mathrm{K}^{\shortparallel} = \mathrm{K}^{\perp} = T^{\shortparallel\perp} = 0. \tag{7.143}$$

The last remaining equation (7.116) reduces to another condition for the sources:

$$\tilde{T}_{\mathrm{K}}^{\shortparallel} = \left[\frac{\bar{\mathrm{x}}}{P^2}\left(\frac{P^2\tilde{T}_{\mathrm{K}}^{\perp 2}}{\tilde{T}^{\perp\perp 2}} \pm 1\right) + \frac{1}{4\bar{\mathrm{x}}}\right]\frac{\mathrm{d}}{\mathrm{d}\bar{\mathrm{x}}}\left(\bar{\mathrm{x}}\tilde{T}^{\perp\perp}\right) - \frac{1}{\tilde{T}^{\perp\perp}}\frac{\mathrm{d}}{\mathrm{d}\bar{\mathrm{x}}}\left(\bar{\mathrm{x}}^2\tilde{T}_{\mathrm{K}}^{\perp 2}\right). \tag{7.144}$$

- $\underline{P=0}$: Now, equation (7.114) gives a condition for the parallel component of the EMT:

$$\tilde{T}^{\shortparallel\shortparallel} = \frac{2}{\mathrm{x}}\Lambda\phi^{\perp}\tilde{T}^{\shortparallel}_{\mathrm{K}}. \tag{7.145}$$

In addition, from (7.109) we conclude that:

$$\mathrm{K}^{\perp} = 0. \tag{7.146}$$

The investigation analyzes two distinct scenarios, based on whether $\mathcal{S}^2 + 4\Lambda$ is non-zero.

  - ⋆ $\underline{\mathcal{S}^2 + 4\Lambda \neq 0}$: Under the condition $P \to 0$, the equations (7.120-7.122) remain valid, providing corresponding solutions for ϕ^{μ} and x. Meanwhile, equations (7.114), (7.116) and (7.125) simplify to the same constraints on sources as given by (7.130-7.132) in the limit $P \to 0$. Consequently, equation (7.123) yields the solution for θ:

$$\theta^2 = 1 + \mathrm{x}^2 - \Phi^2 + \frac{\mathcal{J}}{\sqrt{|\mathrm{x}^2 - \Phi^2|}}, \tag{7.147}$$

where $\mathcal{J}$ is given by:

$$\mathcal{J} = \pm' \sqrt{\pm\left(\frac{\Lambda\tilde{T}^{\perp\perp 2}}{\mathcal{S}^2 + 4\Lambda} - \Lambda\tilde{T}^{\perp 2}_{\mathrm{K}}\right)}. \tag{7.148}$$

Using the function $\mathcal{J}$, the integration of the final equation (7.124) becomes straightforward, resulting in:

$$\pm\frac{2}{3}\left|\mathrm{x}^2 - \Phi^2\right|^{\frac{3}{2}} = D - \frac{1}{2}\int \mathrm{d}\bar{\mathrm{x}}\mathcal{J}\frac{\mathrm{d}}{\mathrm{d}\bar{\mathrm{x}}}\ln\left|\mathcal{S}^2 + 4\Lambda\right|, \tag{7.149}$$

where D is an integration constant. Furthermore, condition (7.131) allows us to determine $\mathcal{S}$ purely as a function of the metric. The solution is expressed as follows:

$$\mathcal{S} = \begin{cases} -2\sqrt{\Lambda}\tan\mathrm{z}; & \Lambda > 0 \\ 2\sqrt{-\Lambda}\coth\mathrm{z}; & \Lambda < 0,\ \mathcal{S}^2 + 4\Lambda > 0 \\ 2\sqrt{-\Lambda}\tanh\mathrm{z}; & \Lambda < 0,\ \mathcal{S}^2 + 4\Lambda < 0 \end{cases}, \tag{7.150}$$

where we have used the z coordinate defined in (3.21).

  - ⋆ $\underline{\mathcal{S}^2 + 4\Lambda = 0}$: The condition defining this case, can be rewritten in the following form:

$$\mathcal{S} = \pm 2\sqrt{-\Lambda}. \tag{7.151}$$

From (7.145) we have:

$$\tilde{T}^{\shortparallel\shortparallel} + \mathcal{S}\tilde{T}^{\shortparallel}_{\mathrm{K}} = 0. \tag{7.152}$$

Equations (7.113) together with equation (7.119) gives the fourth condition for the sources:

$$\tilde{T}^{\perp\perp} = 0. \tag{7.153}$$

Equations (7.117) and (7.118) are equivalent in this case. With the help of (7.118), equation (7.116) becomes integrable, giving the following expression for x (and $\phi^{\perp}$ through (7.113)):

$$\mathcal{Z}\mathrm{x} = \frac{S\mathcal{Z}\phi^{\perp}}{2} = \frac{e^{\pm 2\mathrm{z}}}{\sqrt{-\Lambda}}\left(\eta + \int \mathrm{d}\mathrm{z}\Lambda\tilde{T}^{\shortparallel}_{\mathrm{K}}e^{\mp 2\mathrm{z}}\right), \tag{7.154}$$

where the $\pm$ notation is defined by (7.151). Direct calculation yields:

$$\theta^2 = 1 + \mathrm{x}^2 - \Phi^2 \pm' \frac{\sqrt{-\Lambda}\tilde{T}^{\perp}_{\mathrm{K}}}{\sqrt{\mathrm{x}^2 - \Phi^2}}, \tag{7.155}$$

where another sign convection $\pm'$ is defined. The last equation (7.117) can be directly integrated, resulting into:

$$\frac{2}{3}\left(\mathrm{x}^2 - \Phi^2\right)^{\frac{3}{2}} = D \pm' \frac{1}{4}\int \mathrm{d}z\mathcal{S}\tilde{T}^{\parallel}_{\mathrm{K}}\left(\frac{\mathrm{d}\mathcal{S}}{\mathrm{d}\bar{\mathrm{x}}} + 2\right). \tag{7.156}$$

Non-vanishing normal component of contorsion current when $\Phi^2 = \mathrm{x}^2$ and $\phi^{\perp} \neq 0$

The defining condition gives a solution for $\phi^{\parallel}$ in terms of $\phi^{\perp}$ and x:

$$\phi^{\parallel} = \pm\sqrt{\frac{\mathrm{x}^2 + \Lambda\phi^{\perp 2}}{\Lambda}} \tag{7.157}$$

In this case, equation (7.42) is solved. It is easy to see that the components of the contorsion satisfy the following condition:

$$\phi^{\parallel}\mathrm{K}^{\parallel} = \phi^{\perp}\mathrm{K}^{\perp}. \tag{7.158}$$

This equation, together with equation (7.14) gives the following solution for the K^{μ} in terms of ϕ^{μ} and x:

$$l\mathrm{K}^{\parallel} = \frac{\phi^{\perp}}{2\mathrm{x}}\left(\frac{\mathrm{d}\mathcal{S}}{\mathrm{d}\bar{\mathrm{x}}} + 2\right), \quad l\mathrm{K}^{\perp} = \frac{\phi^{\parallel}}{2\mathrm{x}}\left(\frac{\mathrm{d}\mathcal{S}}{\mathrm{d}\bar{\mathrm{x}}} + 2\right), \tag{7.159}$$

where $\mathcal{S}$ is given by:

$$\mathcal{S} = \frac{\mathrm{d}\Lambda}{\mathrm{d}\bar{\mathrm{x}}} - 2l\Lambda\frac{T^{\parallel\perp}}{T^{\perp}_{\mathrm{K}}}. \tag{7.160}$$

The full system of equations now simplifies to:

$$\left(1 - \theta^2\right)\left(\mathcal{S}\phi^{\perp} - 2\mathrm{x}\right) = -\tilde{T}^{\perp\perp}, \tag{7.161}$$

$$\left(1 - \theta^2\right)\left[\frac{\mathrm{d}}{\mathrm{d}\bar{\mathrm{x}}} - \frac{1}{\mathrm{x}}\left(\phi^{\perp} + \mathcal{D}\right)\right]\left(2\Lambda\phi^{\perp} + \mathcal{S}\mathrm{x}\right) = \tilde{T}^{\parallel\parallel} - \frac{2}{\mathrm{x}}\Lambda\phi^{\perp}\tilde{T}^{\parallel}_{\mathrm{K}}, \tag{7.162}$$

$$\left(1 - \theta^2\right)\sqrt{\frac{\mathrm{x}^2 + \Lambda\phi^{\perp 2}}{\Lambda}} = \pm\tilde{T}^{\perp}_{\mathrm{K}}, \tag{7.163}$$

$$\left(1 - \theta^2\right)\left(\phi^{\perp} + \mathcal{D}\right) - \mathrm{x}\frac{\mathrm{d}\theta^2}{\mathrm{d}\bar{\mathrm{x}}} = \tilde{T}^{\parallel}_{\mathrm{K}}, \tag{7.164}$$

$$\left(1 - \theta^2\right)\left(\frac{\mathrm{d}\mathcal{S}}{\mathrm{d}\bar{\mathrm{x}}} + 2\right) = 2\mathrm{x}\frac{\mathrm{d}}{\mathrm{d}\bar{\mathrm{x}}}\left(2\Lambda\phi^{\perp} + \mathcal{S}\mathrm{x}\right), \tag{7.165}$$

$$\left(\frac{\mathrm{d}\Lambda}{\mathrm{d}\bar{\mathrm{x}}} - \mathcal{S}\right) = \frac{1}{\mathrm{x}}\Lambda\phi^{\perp}\left(\frac{\mathrm{d}\mathcal{S}}{\mathrm{d}\bar{\mathrm{x}}} + 2\right), \tag{7.166}$$

where $\phi^{\parallel}$ and K^{μ} have been entirely removed from the original equations by employing (7.157) and (7.159), respectively. Expressing $\mathcal{D}$ from equation (7.164) and substituting it into the equation (7.162), followed by integration, yields:

$$\left(1 - \theta^2\right)\left(2\Lambda\phi^{\perp} + \mathcal{S}\mathrm{x}\right) = \eta + I, \tag{7.167}$$

where η is an integration constant, and integral I is defined by:

$$I = \int \mathrm{d}\bar{\mathrm{x}} \left(\tilde{T}^{\shortparallel\shortparallel} + \mathcal{S}\tilde{T}^{\shortparallel}_{\mathrm{K}} \right). \tag{7.168}$$

Solving equations (7.161) and (7.167) in terms of $\phi^{\perp}$ and x gives the following:

$$(\mathcal{S} + 4\Lambda)\, \mathcal{Z}\phi^{\perp} = 2(\eta + I) - \mathcal{S}\tilde{T}^{\perp\perp}, \tag{7.169}$$

$$(\mathcal{S} + 4\Lambda)\, \mathcal{Z}\mathrm{x} = \mathcal{S}(\eta + I) + 2\Lambda\tilde{T}^{\perp\perp}. \tag{7.170}$$

Once again, a special case emerges when $\mathcal{S}^2 + 4\Lambda = 0$, which is analyzed separately.

- $\underline{\mathcal{S}^2 + 4\Lambda \neq 0}$: Equations (7.169) and (7.170) well define a solution for $\mathcal{Z}\phi^{\perp}$ and $\mathcal{Z}\mathrm{x}$. Next, substituting this solution into equations (7.163) and (7.166) we arrive at two conditions for the sources, given by:

$$(\eta + I)^2 = \left(\mathcal{S}^2 + 4\Lambda\right) \Lambda\tilde{T}^{\perp 2}_{\mathrm{K}} - \Lambda\tilde{T}^{\perp\perp 2}, \tag{7.171}$$

$$(\eta + I) \left[\mathcal{S}^2 + 4\Lambda + 2\Lambda\frac{\mathrm{d}\mathcal{S}}{\mathrm{d}\bar{\mathrm{x}}} - \mathcal{S}\frac{\mathrm{d}\Lambda}{\mathrm{d}\bar{\mathrm{x}}} \right] = \frac{1}{2}\Lambda\tilde{T}^{\perp\perp}\frac{\mathrm{d}}{\mathrm{d}\bar{\mathrm{x}}}\left(\mathcal{S}^2 + 4\Lambda\right). \tag{7.172}$$

Using equations (7.169), (7.170) as well as condition (7.172), equation (7.164) becomes the following constraint for the sources:

$$4\Lambda\tilde{T}^{\shortparallel}_{\mathrm{K}} = 2\Lambda\frac{\mathrm{d}\tilde{T}^{\perp\perp}}{\mathrm{d}\bar{\mathrm{x}}} + \left(\frac{\mathrm{d}\Lambda}{\mathrm{d}\bar{\mathrm{x}}} - \mathcal{S}\right)\tilde{T}^{\perp\perp} + \mathcal{S}\tilde{T}^{\shortparallel\shortparallel} - \left(\frac{\mathrm{d}\mathcal{S}}{\mathrm{d}\bar{\mathrm{x}}} + 2\right)(\eta + I). \tag{7.173}$$

The last remaining unknown function $\mathcal{Z}$ is determined by solving equation (7.165). The solution is given by:

$$\frac{2}{3}\left(\frac{\eta + I}{\mathcal{Z}}\right)^3 = D + \int \frac{\mathrm{d}\bar{\mathrm{x}}\,(\eta + I)^2}{\mathcal{S}\,(\eta + I) + 2\Lambda\tilde{T}^{\perp\perp}}\left(\frac{\mathrm{d}\mathcal{S}}{\mathrm{d}\bar{\mathrm{x}}} + 2\right). \tag{7.174}$$

Note that $\theta^2 = 1 - \mathcal{Z}$.

- $\underline{\mathcal{S}^2 + 4\Lambda = 0}$: This scenario resembles the related situation where $\mathrm{x}^2 \neq \Phi^2$ and $P \neq 0$. We begin by examining equation (7.166), which can be rewritten in the following way:

$$\left(2\Lambda\phi^{\perp} + \mathcal{S}\mathrm{x}\right)\left(\frac{\mathrm{d}\mathcal{S}}{\mathrm{d}\bar{\mathrm{x}}} + 2\right) = 0. \tag{7.175}$$

The first bracket in (7.175) cannot be zero because this would lead to $\tilde{T}^{\perp}_{\mathrm{K}} = 0$, contradicting the primary assumption. Then, equations (7.175) gives the following solution for the metric:

$$\Lambda = -\bar{\mathrm{x}}^2, \;\; \mathcal{S} = -2\bar{\mathrm{x}}. \tag{7.176}$$

Consequentially, equation (7.165) implies:

$$2\Lambda\phi^{\perp} + \mathcal{S}\mathrm{x} = Q, \tag{7.177}$$

where $Q \neq 0$ is a constant. Then, simultaneously solving equations (7.163) and (7.177) yields:

$$\mathrm{x} = Q\left[\frac{\bar{\mathrm{x}}\tilde{T}^{\perp 2}_{\mathrm{K}}}{\tilde{T}^{\perp\perp 2}} - \frac{1}{4\bar{\mathrm{x}}}\right], \tag{7.178}$$

$$\phi^{\perp} = -Q\left[\frac{\bar{\mathrm{x}}\tilde{T}^{\perp 2}_{\mathrm{K}}}{\tilde{T}^{\perp\perp 2}} + \frac{1}{4\bar{\mathrm{x}}}\right]. \tag{7.179}$$

From equation (7.161)we have the following solution for the θ-field:

$$\theta^2 = 1 + \frac{\bar{\mathrm{x}}}{Q}\tilde{T}^{\perp\perp}. \tag{7.180}$$

Equations (7.167) and (7.164) reduce to two constraints placed upon the EMT and contorsion current, given by:

$$\bar{\mathrm{x}}\tilde{T}^{\perp\perp} = \eta + I, \tag{7.181}$$

$$\tilde{T}^{\parallel}_{\mathrm{K}} = \left[\frac{\bar{\mathrm{x}}\tilde{T}^{\perp 2}_{\mathrm{K}}}{\tilde{T}^{\perp\perp 2}} + \frac{1}{4\bar{\mathrm{x}}}\right]\frac{\mathrm{d}}{\mathrm{d}\bar{\mathrm{x}}}\left(\bar{\mathrm{x}}\tilde{T}^{\perp\perp}\right) - \frac{1}{\tilde{T}^{\perp\perp}}\frac{\mathrm{d}}{\mathrm{d}\bar{\mathrm{x}}}\left(\bar{\mathrm{x}}^2\tilde{T}^{\perp 2}_{\mathrm{K}}\right). \tag{7.182}$$

Non-vanishing normal component of contorsion current when $\phi^{\perp} = 0$

If the normal component of the contorsion current is zero, the equations of motion necessitate a non-zero $\phi^{\perp}$. Conversely, the presence of a non-vanishing $T^{\perp}_{\mathrm{K}}$ alters this condition. In the last two sections, we considered $\phi^{\perp}$ to be non-zero, hence the scenario where $\phi^{\perp}$ equals zero requires a separate analysis. It is easy to express all fields in terms of $\mathcal{Z}$, the EMT, and the contorsion current.

$$\mathrm{x} = \frac{\tilde{T}^{\perp\perp}}{2\mathcal{Z}},\ \phi^{\parallel} = \frac{\tilde{T}^{\perp}_{\mathrm{K}}}{\mathcal{Z}},\ \phi^{\perp} = 0, \tag{7.183}$$

$$2l\Lambda\mathrm{K}^{\parallel} = \frac{\tilde{T}^{\parallel\perp}}{\tilde{T}^{\perp}_{\mathrm{K}}},\ 2l\Lambda\mathrm{K}^{\perp} = \frac{\tilde{T}^{\parallel\parallel} + \tilde{T}^{\perp\perp}}{\tilde{T}^{\perp}_{\mathrm{K}}}, \tag{7.184}$$

$$\theta^2 = \left(\frac{\tilde{T}^{\perp\perp}}{2\mathcal{Z}}\right)^2 + 1 - \frac{\Lambda\tilde{T}^{\perp 2}_{\mathrm{K}}}{\mathcal{Z}^2} - \mathcal{Z}. \tag{7.185}$$

These expressions directly solve equations (7.22-7.25). Equations (7.16) and (7.14) become conditions for the sources given by:

$$2\tilde{T}^{\parallel}_{\mathrm{K}} = \frac{\mathrm{d}\tilde{T}^{\perp\perp}}{\mathrm{d}\bar{\mathrm{x}}} + \frac{\tilde{T}^{\perp\perp}}{2\Lambda}\left(\frac{\mathrm{d}\Lambda}{\mathrm{d}\bar{\mathrm{x}}} - \mathcal{S}\right), \tag{7.186}$$

$$\tilde{T}^{\parallel\parallel} = \frac{1}{2}\tilde{T}^{\perp\perp}\frac{\mathrm{d}\mathcal{S}}{\mathrm{d}\bar{\mathrm{x}}}, \tag{7.187}$$

where $\mathcal{S}$ defined by (7.29) is expressed in terms of the sources as well:

$$\mathcal{S} = \frac{\mathrm{d}\Lambda}{\mathrm{d}\bar{\mathrm{x}}} - 2l\Lambda\frac{T^{\parallel\perp}}{T^{\perp}_{\mathrm{K}}}, \tag{7.188}$$

the same as in the previous two sections. The remaining three equations read:

$$\mathcal{Z}^3\frac{\tilde{T}^{\parallel\parallel} + \tilde{T}^{\perp\perp}}{2\Lambda\tilde{T}^{\perp 2}_{\mathrm{K}}} = \frac{1}{2}\mathcal{S}\tilde{T}^{\perp\perp}\frac{\mathrm{d}}{\mathrm{d}\bar{\mathrm{x}}}\ln\left(\frac{\tilde{T}^{\perp\perp}}{\mathcal{Z}}\right) + \tilde{T}^{\parallel\parallel}, \tag{7.189}$$

$$\mathcal{Z}\left(\frac{\mathrm{d}\mathcal{S}}{\mathrm{d}\bar{\mathrm{x}}} + 2\right) = \frac{\tilde{T}^{\parallel\parallel}\tilde{T}^{\perp\perp}}{\mathcal{Z}^2} + \mathcal{S}\frac{\mathrm{d}}{\mathrm{d}\bar{\mathrm{x}}}\left(\frac{\Lambda\tilde{T}^{\perp 2}_{\mathrm{K}}}{\mathcal{Z}^2}\right), \tag{7.190}$$

$$2\tilde{T}^{\parallel}_{\mathrm{K}} = \frac{\mathrm{d}\tilde{T}^{\perp\perp}}{\mathrm{d}\bar{\mathrm{x}}} - \frac{1}{6}\frac{\mathrm{d}}{\mathrm{d}\bar{\mathrm{x}}}\left(\frac{\tilde{T}^{\perp\perp}}{\mathcal{Z}}\right)^3 + \frac{\tilde{T}^{\perp\perp}}{\mathcal{Z}}\frac{\mathrm{d}}{\mathrm{d}\bar{\mathrm{x}}}\left(\frac{\Lambda\tilde{T}^{\perp 2}_{\mathrm{K}}}{\mathcal{Z}^2}\right). \tag{7.191}$$

Combining all three equations (7.189-7.191) we obtain an integrable equation, the solution of which is given by the following expression:

$$\Lambda\tilde{T}_{\mathrm{K}}^{\perp 2} = \frac{1}{4}\tilde{T}^{\perp\perp 2}\left(1 - \frac{\mathcal{S}^2}{P^2}\right), \tag{7.192}$$

where $P \in \mathbb{R} \cup \{\infty\}$ represents a constant of integration. Note that when P takes on an infinite value, it corresponds to the scenario previously encountered where $\mathrm{x}^2 = \Phi^2$. Substituting (7.192) into equation (7.191) eliminates $\mathcal{Z}$ form the equation, giving another constraint on the sources:

$$2\tilde{T}_{\mathrm{K}}^{\shortparallel} = \frac{\mathrm{d}\tilde{T}^{\perp\perp}}{\mathrm{d}\bar{\mathrm{x}}} - \frac{\mathcal{S}}{2P^2}\frac{\mathrm{d}\mathcal{S}}{\mathrm{d}\bar{\mathrm{x}}}. \tag{7.193}$$

In conclusion, the integration of equation (7.190) allows us to directly determine the unknown variable $\mathcal{Z}$, which is represented by the subsequent expression:

$$\frac{1}{6}\left(\frac{\mathcal{S}\tilde{T}^{\perp\perp}}{\mathcal{Z}}\right)^3 = D + \int \mathrm{d}\bar{\mathrm{x}}\frac{P^2\mathcal{S}^2}{P^2 - \mathcal{S}^2}\left(\frac{\mathrm{d}\mathcal{S}}{\mathrm{d}\bar{\mathrm{x}}} + 2\right)\tilde{T}^{\perp\perp}. \tag{7.194}$$

Note that the case corresponding to $P \to \infty$ results in the vanishing parallel component of contorsion. This can be easily seen by comparing equations (7.186) and (7.193).

7.2.2 Solutions when $\mathcal{Z} \neq 0$, $\theta = 0$ and $\phi^{\perp} \neq 0$

In this section, we investigate the solutions to the equations of motion when $\theta = 0$. This is a rather special case, since equation (7.14) is trivially solved. We solve equations by expressing all fields in terms of $\mathcal{Z}$ and the sources, and then we solve the equation for $\mathcal{Z}$, defined in (7.28). The multiplication of equation (7.15) by $\phi^{\perp}$ followed by subtraction of equation (7.16) results in the following expression:

$$l\phi^{\perp}\mathrm{K}^{\perp} = \phi^{\shortparallel}\left[l\mathrm{K}^{\shortparallel} + \frac{\mathrm{d}}{\mathrm{d}\bar{\mathrm{x}}}\ln\mathcal{Z}\right]. \tag{7.195}$$

Expression (7.195) represents a way to remove the orthogonal component of the contorsion from other equations. The $\phi^{\shortparallel}$ is easily obtained form (7.25):

$$\phi^{\shortparallel} = \frac{\tilde{T}_{\mathrm{K}}^{\perp}}{\mathcal{Z}}. \tag{7.196}$$

Equation (7.22), as in previous sections, represents a constraint for the sources, that is:

$$\left(\frac{\mathrm{d}\Lambda}{\mathrm{d}\bar{\mathrm{x}}} - \mathcal{S}\right)\tilde{T}_{\mathrm{K}}^{\perp} = \tilde{T}^{\shortparallel\perp}. \tag{7.197}$$

where we have used the definition for $\mathcal{S}$ (7.29) to eliminate $\mathrm{K}^{\shortparallel}$ in the last step. Multiplying equation (7.16) by $\mathcal{Z}^2$ and employing original equations (7.22) and (7.26), as well as (7.195) and (7.196) we arrive at:

$$-\tilde{T}^{\perp\perp}\tilde{T}_{\mathrm{K}}^{\shortparallel} + \frac{\mathrm{d}}{\mathrm{d}\bar{\mathrm{x}}}\left(\Lambda\tilde{T}_{\mathrm{K}}^{\perp 2}\right) = \frac{\mathcal{Z}^3 - 2\Lambda\tilde{T}_{\mathrm{K}}^{\perp 2}}{2\Lambda}\left(\frac{\mathrm{d}\Lambda}{\mathrm{d}\bar{\mathrm{x}}} - \mathcal{S}\right). \tag{7.198}$$

Equation (7.24) is transformed into the following form:

$$\mathcal{Z}^2\frac{\mathrm{d}\mathcal{Z}}{\mathrm{d}\bar{\mathrm{x}}} + \tilde{T}^{\perp\perp}\tilde{T}_{\mathrm{K}}^{\shortparallel} + \frac{\mathcal{Z}^3}{2\Lambda}\left(\frac{\mathrm{d}\Lambda}{\mathrm{d}\bar{\mathrm{x}}} - \mathcal{S}\right) = 2\tilde{T}_{\mathrm{K}}^{\shortparallel}\mathcal{Z}\mathrm{x} + \tilde{T}^{\shortparallel\shortparallel}\mathcal{Z}\phi^{\perp}. \tag{7.199}$$

upon utilizing equations (7.26), (7.195), and (7.198). We rewrite equations (7.23) and (7.26) in full:

$$\mathcal{Z}\left(\mathcal{S}\phi^{\perp}-2\mathrm{x}\right)=-\tilde{T}^{\perp\perp}, \tag{7.200}$$

$$\mathcal{Z}\left(\phi^{\perp}+\mathcal{D}\right)=\tilde{T}^{\parallel}_{\mathrm{K}}. \tag{7.201}$$

Employing the quartet of equations obtained earlier (7.198-7.201), we reformulate the final equation (7.17) as:

$$2\Lambda\frac{\mathrm{d}\tilde{T}^{\perp\perp}}{\mathrm{d}\bar{\mathrm{x}}}+\frac{\mathrm{d}\Lambda}{\mathrm{d}\bar{\mathrm{x}}}\left(\tilde{T}^{\perp\perp}+\tilde{T}^{\parallel\parallel}\right)+2\Lambda\tilde{T}^{\parallel}_{\mathrm{K}}\frac{\mathrm{d}\mathcal{S}}{\mathrm{d}\bar{\mathrm{x}}}=2\frac{\frac{1}{2\Lambda}\left(\frac{\mathrm{d}\Lambda}{\mathrm{d}\bar{\mathrm{x}}}-\mathcal{S}\right)+\frac{\mathrm{d}}{\mathrm{d}\bar{\mathrm{x}}}\ln\mathcal{Z}}{\mathcal{Z}\phi^{\perp}}\frac{\mathrm{d}}{\mathrm{d}\bar{\mathrm{x}}}\left(\Lambda\tilde{T}^{\perp}_{\mathrm{K}}\right)^{2}. \tag{7.202}$$

Note that this equation is the conservation law for the EMT given by (3.66) rewritten using redefined EMT components $\tilde{T}_{\mu\nu}$. These five equations (7.198-7.202), together with the definition of $\mathcal{Z}=\mathrm{x}^2+1-\Phi^2$, form a complete set of equations that are analyzed in this section. Substituting x from (7.200) into the definition for $\mathcal{Z}$, we derive a quadratic equation for $\mathcal{Z}\phi^{\perp}$:

$$\left(\mathcal{S}^2+4\Lambda\right)\left(\mathcal{Z}\phi^{\perp}\right)^2+2\mathcal{S}\tilde{T}^{\perp\perp}\left(\mathcal{Z}\phi^{\perp}\right)+\tilde{T}^{\perp\perp2}-4\Lambda\tilde{T}^{\perp2}_{\mathrm{K}}-4\mathcal{Z}^2\left(\mathcal{Z}-1\right)=0. \tag{7.203}$$

Upon examining equation (7.203), it becomes clear that the scenario where $\mathcal{S}^2+4\Lambda=0$ requires independent examination. The solution for x and $\phi^{\perp}$ is given by:

$$\mathcal{Z}\mathrm{x}=\begin{cases}\mathcal{M}\tilde{T}^{\perp\perp}\pm\sqrt{\mathcal{J}}, & \mathcal{S}^2+2\Lambda\neq0\\ \frac{1}{4}\tilde{T}^{\perp\perp}+\frac{\Lambda\tilde{T}^{\perp}_{\mathrm{K}}+\mathcal{Z}^2\left(\mathcal{Z}-1\right)}{\tilde{T}^{\perp\perp}}, & \mathcal{S}^2+4\Lambda=0\end{cases} \tag{7.204}$$

$$\mathcal{S}\mathcal{Z}\phi^{\perp}=\begin{cases}\left(2\mathcal{M}-1\right)\tilde{T}^{\perp\perp}\pm2\sqrt{\mathcal{J}}, & \mathcal{S}^2+2\Lambda\neq0\\ -2\tilde{T}^{\perp\perp}\left[\frac{1}{4}-\frac{\Lambda\tilde{T}^{\perp}_{\mathrm{K}}+\mathcal{Z}^2\left(\mathcal{Z}-1\right)}{\tilde{T}^{\perp\perp2}}\right], & \mathcal{S}^2+2\Lambda=0\end{cases} \tag{7.205}$$

here, we have defined two more axillary quantities:

$$\mathcal{J}=\left(2\mathcal{M}-1\right)\left[\frac{1}{2}\mathcal{M}\tilde{T}^{\perp\perp2}-\Lambda\tilde{T}^{\perp2}_{\mathrm{K}}-\mathcal{Z}^2\left(\mathcal{Z}-1\right)\right], \tag{7.206}$$

$$\mathcal{M}=\frac{2\Lambda}{\mathcal{S}^2+4\Lambda}. \tag{7.207}$$

This section is divided into three parts, akin to the previous section, contingent on which components of the contorsion current are non-zero. Each part has three distinctive cases depending on whether $\mathcal{S}^2+4\Lambda$ or $\mathcal{J}$ vanish.

Completely vanishing contorsion current

From Equation (7.196), we deduce that $\phi^{\parallel}=0$ because $\tilde{T}^{\perp}_{\mathrm{K}}=0$. Subsequently, utilizing (7.195) and (7.197), it follows that $\mathrm{K}^{\perp}=0$ and $T^{\parallel\perp}=0$, respectively. Additionally, since $\tilde{T}^{\parallel}_{\mathrm{K}}$ is zero, according to (7.198), we have:

$$\frac{\mathrm{d}\Lambda}{\mathrm{d}\bar{\mathrm{x}}}=\mathcal{S},\ \mathrm{K}^{\parallel}=0. \tag{7.208}$$

We are now facing the subsequent set of equations:

$$\mathcal{Z}^2\frac{\mathrm{d}\mathcal{Z}}{\mathrm{d}\bar{\mathrm{x}}} = \tilde{T}^{\shortparallel\shortparallel}\mathcal{Z}\phi^{\perp}, \tag{7.209}$$
$$\phi^{\perp} + \mathcal{D} = 0, \tag{7.210}$$
$$2\Lambda\frac{\mathrm{d}\tilde{T}^{\perp\perp}}{\mathrm{d}\bar{\mathrm{x}}} + \frac{\mathrm{d}\Lambda}{\mathrm{d}\bar{\mathrm{x}}}\left(\tilde{T}^{\perp\perp} + \tilde{T}^{\shortparallel\shortparallel}\right) = 0, \tag{7.211}$$

In this case $\tilde{T}^{\perp\perp} \neq 0$, since otherwise it follows from (7.211) that $\tilde{T}^{\shortparallel\shortparallel} = 0$, and the whole EMT vanishes.

- $\underline{\mathcal{S}^2 + 4\Lambda \neq 0 \ \wedge \ \mathcal{J} \neq 0}$: Upon utilizing all the equations, equation (7.210) is re-expressed as follows:

$$\mathcal{Z}^3\left(\frac{\mathrm{d}\mathcal{S}}{\mathrm{d}\bar{\mathrm{x}}} + 2\right) = \tilde{T}^{\perp\perp}\tilde{T}^{\shortparallel\shortparallel} \tag{7.212}$$

two separate cases must be addressed at this point.

  - ⋆ $\underline{\mathcal{S}' + 2 = 0}$: Given that $\mathcal{S} = \frac{\mathrm{d}\Lambda}{\mathrm{d}\bar{\mathrm{x}}}$, it follows that the metric corresponds entirely to that of the BTZ black hole:

$$\Lambda = -\left(\bar{\mathrm{x}}^2 - \mu\right), \tag{7.213}$$

    where μ is a constant. From equation (7.212) we get;

$$\tilde{T}^{\shortparallel\shortparallel} = 0, \tag{7.214}$$

    as a condition for the EMT. The other two equations are easily solved giving:

$$\mathcal{Z} = const. \quad \tilde{T}^{\perp\perp} = \frac{D}{\bar{\mathrm{x}}}, \tag{7.215}$$

    where D is another constant.
  - ⋆ $\underline{\mathcal{S}' + 2 \neq 0}$: Now, $\mathcal{Z}$ is given by equation (7.212), that is:

$$\mathcal{Z}^3 = \frac{\tilde{T}^{\perp\perp}\tilde{T}^{\shortparallel\shortparallel}}{\frac{\mathrm{d}\mathcal{S}}{\mathrm{d}\bar{\mathrm{x}}} + 2}. \tag{7.216}$$

    Substituting this result into equation (7.209) we arrive at the following constraint for the EMT:

$$\frac{1}{3}\frac{\mathrm{d}}{\mathrm{d}\bar{\mathrm{x}}}\left(\frac{\tilde{T}^{\perp\perp}\tilde{T}^{\shortparallel\shortparallel}}{\frac{\mathrm{d}\mathcal{S}}{\mathrm{d}\bar{\mathrm{x}}} + 2}\right)^3 = \tilde{T}^{\shortparallel\shortparallel}\left[\left(2\mathcal{M} - 1\right)\tilde{T}^{\perp\perp} \pm 2\sqrt{\mathcal{J}}\right], \tag{7.217}$$

    where $\mathcal{J}$ is expressed only in terms of the EMT, by substituting (7.216). The last equation (7.211) is already a covariant conservation law for the EMT.

- $\underline{\mathcal{S}^2 + 4\Lambda \neq 0 \ \wedge \ \mathcal{J} = 0}$: The condition $\mathcal{J} = 0$, and reduces to:

$$\Lambda\tilde{T}^{\perp\perp 2} = \mathcal{Z}^2\left(\mathcal{Z} - 1\right)\left(\mathcal{S}^2 + 4\Lambda\right). \tag{7.218}$$

  Using (7.218) equation (7.211) becomes:

$$\mathcal{Z}^3\left(\frac{\mathrm{d}\mathcal{S}}{\mathrm{d}\bar{\mathrm{x}}} + 2\right) = \tilde{T}^{\perp\perp}\tilde{T}^{\shortparallel\shortparallel} \tag{7.219}$$

Equation (7.210) can now be recast as:

$$(3\mathcal{Z}-2)\,\tilde{T}^{\shortparallel\shortparallel}=0. \tag{7.220}$$

Together with (7.209) and (7.219), equation (7.220) implies that the metric and the EMT are fully determined:

$$\Lambda=-\left(\bar{\mathrm{x}}^2-\mu\right),\ \tilde{T}^{\shortparallel\shortparallel}=0,\ \Lambda\tilde{T}^{\perp\perp 2}=4\mu\mathcal{Z}^2\left(\mathcal{Z}-1\right), \tag{7.221}$$

where μ and $\mathcal{Z}$ are constants.

- $\underline{\mathcal{S}^2+4\Lambda=0}$: This condition, together with $\frac{\mathrm{d}\Lambda}{\mathrm{d}\bar{\mathrm{x}}}=\mathcal{S}$ directly implies:

$$\Lambda=-\bar{\mathrm{x}}^2,\ \ \mathcal{S}=-2\bar{\mathrm{x}}. \tag{7.222}$$

Equation (7.210) reduces to the following condition:

$$\tilde{T}^{\shortparallel\shortparallel}=0, \tag{7.223}$$

while the two remaining equations (7.209) and (7.211) yield:

$$\tilde{T}^{\perp\perp}=\frac{D}{\bar{\mathrm{x}}},\ \ \mathcal{Z}=const, \tag{7.224}$$

where D is another constant.

Non-vanishing parallel component of contorsion current

Given that $\tilde{T}^{\perp}_{\mathrm{K}}=0$, it follows that $\phi^{\shortparallel}=\mathrm{K}^{\perp}=T^{\shortparallel\perp}=0$. The system of equation now transforms into:

$$\mathcal{Z}^2\frac{\mathrm{d}\mathcal{Z}}{\mathrm{d}\bar{\mathrm{x}}}=\tilde{T}^{\shortparallel}_{\mathrm{K}}\tilde{T}^{\perp\perp}+\mathcal{Z}\phi^{\perp}\left(\tilde{T}^{\shortparallel\shortparallel}+\mathcal{S}\tilde{T}^{\shortparallel}_{\mathrm{K}}\right), \tag{7.225}$$

$$\mathcal{Z}\left(\phi^{\perp}+\mathcal{D}\right)=\tilde{T}^{\shortparallel}_{\mathrm{K}}, \tag{7.226}$$

$$\frac{\mathcal{Z}^3}{2\Lambda}\left(\frac{\mathrm{d}\Lambda}{\mathrm{d}\bar{\mathrm{x}}}-\mathcal{S}\right)=-\tilde{T}^{\perp\perp}\tilde{T}^{\shortparallel}_{\mathrm{K}}, \tag{7.227}$$

$$2\Lambda\frac{\mathrm{d}\tilde{T}^{\perp\perp}}{\mathrm{d}\bar{\mathrm{x}}}+\frac{\mathrm{d}\Lambda}{\mathrm{d}\bar{\mathrm{x}}}\left(\tilde{T}^{\perp\perp}+\tilde{T}^{\shortparallel\shortparallel}\right)+2\Lambda\tilde{T}^{\shortparallel}_{\mathrm{K}}\frac{\mathrm{d}\mathcal{S}}{\mathrm{d}\bar{\mathrm{x}}}=0. \tag{7.228}$$

- $\underline{\mathcal{S}^2+4\Lambda\neq 0\ \wedge\ \mathcal{J}\neq 0}$:With the assistance of the complete system of equations, Equation (7.226) can be reformulated as follows:

$$\begin{aligned}0=&\left[\left(2\mathcal{M}-1\right)\tilde{T}^{\perp\perp}\pm 2\sqrt{\mathcal{J}}\right]\times\\&\left[\mathcal{S}\tilde{T}^{\shortparallel}_{\mathrm{K}}-\left(\left(2\mathcal{M}-1\right)\tilde{T}^{\perp\perp}\pm 2\sqrt{\mathcal{J}}\right)\right]\times\\&\left[\frac{\Lambda\tilde{T}^{\shortparallel}_{\mathrm{K}}}{\mathcal{M}}\left(2+\frac{\mathcal{S}\frac{\mathrm{d}\mathcal{M}}{\mathrm{d}\bar{\mathrm{x}}}}{2\mathcal{M}-1}\right)+\left(\frac{\mathrm{d}\Lambda}{\mathrm{d}\bar{\mathrm{x}}}-\mathcal{S}\right)\left(\tilde{T}^{\shortparallel\shortparallel}+\mathcal{S}\tilde{T}^{\shortparallel}_{\mathrm{K}}\right)\right].\end{aligned} \tag{7.229}$$

The first bracket in (7.229) cannot be equal to zero, since it is proportional to $\phi^{\perp}\neq 0$. Solution diverges into two potential outcomes based on the selection of the disappearing bracket.

- $\underline{\mathrm{x} = const}$: This scenario occurs when the middle bracket is set to zero. This indicates that $\tilde{T}^{\shortparallel}_{\mathrm{K}} = \mathcal{Z}\phi^{\perp}$, which consequently leads to $\mathcal{D} = 0$, or $\mathrm{x} = const$. Expressing $\tilde{T}^{\shortparallel\shortparallel}$ from (7.228) and using equation (7.227) together with the defining condition of this case, equation (7.225) is satisfied. Now, in terms of x and $\mathcal{Z}$ all fields can be expressed:

$$\phi^{\perp} = \pm\sqrt{\frac{\mathcal{Z} - (\mathrm{x}^2+1)}{\Lambda}}, \tag{7.230}$$

$$\tilde{T}^{\perp\perp} = \mathcal{Z}\left[2\mathrm{x} \mp \mathcal{S}\sqrt{\frac{\mathcal{Z} - (\mathrm{x}^2+1)}{\Lambda}}\right], \tag{7.231}$$

$$\tilde{T}^{\shortparallel}_{\mathrm{K}} = \pm\mathcal{Z}\sqrt{\frac{\mathcal{Z} - (\mathrm{x}^2+1)}{\Lambda}}, \tag{7.232}$$

where we have introduced a new sign convention. Equation (7.228) holds as a condition for the sources, whereas the final equation (7.227) transforms into an algebraic expression that determines $\mathcal{Z}$:

$$\begin{aligned}&\left(\frac{\mathrm{d}\Lambda}{\mathrm{d}\bar{\mathrm{x}}} - 3\mathcal{S}\right)^2\mathcal{Z}^2 + 4\left(\mathrm{x}^2+1\right)\left[\left(\mathrm{x}^2+1\right)\mathcal{S}^2 + 4\mathrm{x}^2\Lambda\right]\\&+4\left[\mathcal{S}\left(\mathrm{x}^2+1\right)\left(\frac{\mathrm{d}\Lambda}{\mathrm{d}\bar{\mathrm{x}}} - 3\mathcal{S}\right) - 4\mathrm{x}^2\Lambda\right]\mathcal{Z} = 0.\end{aligned} \tag{7.233}$$

- $\underline{\mathrm{x} \neq const. \wedge \tilde{T}^{\perp\perp} \neq 0}$: Here, the third bracket in (7.229) must vanish, leading to the following reduced set of equations:

$$\left(\frac{\mathrm{d}\Lambda}{\mathrm{d}\bar{\mathrm{x}}} - \mathcal{S}\right)\left(\tilde{T}^{\shortparallel\shortparallel} + \mathcal{S}\tilde{T}^{\shortparallel}_{\mathrm{K}}\right) = -\frac{\Lambda\tilde{T}^{\shortparallel}_{\mathrm{K}}}{\mathcal{M}}\left(2 + \frac{\mathcal{S}\frac{\mathrm{d}\mathcal{M}}{\mathrm{d}\bar{\mathrm{x}}}}{2\mathcal{M}-1}\right), \tag{7.234}$$

$$\Lambda\tilde{T}^{\shortparallel}_{\mathrm{K}}\tilde{T}^{\perp\perp}\frac{\mathrm{d}}{\mathrm{d}\bar{\mathrm{x}}}\left(\mathcal{S}^2+4\Lambda\right) = \left(\frac{\mathrm{d}\Lambda}{\mathrm{d}\bar{\mathrm{x}}} - \mathcal{S}\right)\frac{\mathrm{d}}{\mathrm{d}\bar{\mathrm{x}}}\left(\Lambda\tilde{T}^{\perp\perp 2}\right), \tag{7.235}$$

$$\mathcal{Z}^3\frac{\mathrm{d}}{\mathrm{d}\bar{\mathrm{x}}}\left(\mathcal{S}^2+4\Lambda\right) = -2\frac{\mathrm{d}}{\mathrm{d}\bar{\mathrm{x}}}\left(\Lambda\tilde{T}^{\perp\perp 2}\right), \tag{7.236}$$

$$\frac{\mathrm{d}}{\mathrm{d}\bar{\mathrm{x}}}\ln\left[\mathcal{Z}^2\left(\mathcal{S}^2+4\Lambda\right)\right] = \pm\frac{4\sqrt{\mathcal{J}}}{\mathcal{S}\mathcal{M}\tilde{T}^{\perp\perp}}\left[1 + \frac{\mathcal{S}\frac{\mathrm{d}\mathcal{M}}{\mathrm{d}\bar{\mathrm{x}}}}{2\left(2\mathcal{M}-1\right)}\right]. \tag{7.237}$$

Note that $\tilde{T}^{\perp\perp} \neq 0$ implies that $\frac{\mathrm{d}\Lambda}{\mathrm{d}\bar{\mathrm{x}}} \neq \mathcal{S}$. Equation (7.236) is a solution for $\mathcal{Z}$, while the remaining three equations can be regarded as conditions for the sources.

- $\underline{\mathrm{x} \neq const. \wedge \tilde{T}^{\perp\perp} = 0}$: Here, the final bracket in equation (7.229) results in zero. Referring to equation (7.72), we find $\frac{\mathrm{d}\Lambda}{\mathrm{d}\bar{\mathrm{x}}} = \mathcal{S}$. Substituting this expression into (7.229), we derive $\frac{\mathrm{d}\mathcal{S}}{\mathrm{d}\bar{\mathrm{x}}} + 2 = 0$. These conditions together provide the subsequent metric solution:

$$\Lambda = -\left(\bar{\mathrm{x}}^2 - \mu\right),\ \mathcal{S} = -2\bar{\mathrm{x}}, \tag{7.238}$$

where μ is a constant. After the integration of equation (7.225) we arrive at:

$$\phi^{\perp} + \frac{1}{3}\mu\phi^{\perp 3} = \eta - \int\frac{\mathrm{d}\bar{\mathrm{x}}}{\bar{\mathrm{x}}}\tilde{T}^{\shortparallel}_{\mathrm{K}}, \tag{7.239}$$

where η is another integration constant. The dilaton is then derived directly form (7.200):

$$\mathrm{x} = -\bar{\mathrm{x}}\phi^{\perp}. \tag{7.240}$$

The last equation (7.228) becomes the following condition for the sources:

$$\tilde{T}^{\shortparallel\shortparallel} = -\frac{2\Lambda}{\bar{\mathrm{x}}}\tilde{T}^{\shortparallel}_{\mathrm{K}}. \tag{7.241}$$

- $\underline{\mathcal{S}^2 + 4\Lambda \neq 0 \;\wedge\; \mathcal{J} = 0}$: Inserting equation (7.225) into (7.228) modifies equation (7.228) as follows:

$$\left[\mathcal{S}\left(3\mathcal{Z} - 2\right) - \mathcal{Z}\frac{\mathrm{d}\Lambda}{\mathrm{d}\bar{\mathrm{x}}}\right]\frac{\mathrm{d}}{\mathrm{d}\bar{\mathrm{x}}}\left[\mathcal{Z}^2\left(\mathcal{S}^2 + 4\Lambda\right)\right] = 0. \tag{7.242}$$

Choosing that the derivative in (7.242) vanishes and employing equation (7.226) leads to:

$$\left(3\mathcal{Z} - 2\right)\left[\frac{2}{\mathcal{S}}\left(2\mathcal{M} - 1\right) + \frac{\mathrm{d}\mathcal{M}}{\mathrm{d}\bar{\mathrm{x}}}\right] = 0. \tag{7.243}$$

In this case there is another branching of the solution.

 ⋆ $\underline{\mathcal{Z}\sqrt{\mathcal{S}^2 + 4\Lambda} = \pm\sqrt{Q} \;\wedge\; \mathcal{Z} \neq 2/3}$: We have fully determined $\mathcal{Z}$ in this case, which implies that both (7.205) and (7.204) are the final solutions for $\phi^{\perp}$ and x. Equations (7.242) is satisfied. The remaining equations (7.225) and (7.227), together with the condition $\mathcal{J} = 0$, reduce to the following set of the conditions for the sources:

$$\tilde{T}^{\shortparallel\shortparallel\shortparallel} + \mathcal{S}\tilde{T}^{\shortparallel}_{\mathrm{K}} = 0, \tag{7.244}$$

$$\tilde{T}^{\shortparallel}_{\mathrm{K}} = \frac{1}{2}\frac{\tilde{T}^{\perp\perp}}{\mathcal{S}^2 + 4\Lambda}\frac{\frac{\mathrm{d}\Lambda}{\mathrm{d}\bar{\mathrm{x}}} - \mathcal{S}}{\pm\sqrt{\frac{\mathcal{S}^2 + 4\Lambda}{Q}} - 1}, \tag{7.245}$$

$$\Lambda\tilde{T}^{\perp\perp 2} = Q\left(\pm\sqrt{\frac{Q}{\mathcal{S}^2 + 4\Lambda}} - 1\right), \tag{7.246}$$

respectively. Finally, equation (7.243) gives the following solution for $\mathcal{S}$ in terms of the metric:

$$\mathcal{S} = \begin{cases} -2\sqrt{\Lambda}\tan\mathrm{z}; & \Lambda > 0 \\ 2\sqrt{-\Lambda}\coth\mathrm{z}; & \Lambda < 0,\ \mathcal{S}^2 + 4\Lambda > 0 \\ 2\sqrt{-\Lambda}\tanh\mathrm{z}; & \Lambda < 0,\ \mathcal{S}^2 + 4\Lambda < 0 \end{cases}. \tag{7.247}$$

 ⋆ $\underline{\mathcal{Z}\sqrt{\mathcal{S}^2 + 4\Lambda} = \sqrt{Q} \;\wedge\; \mathcal{Z} = 2/3}$: The equations (7.242) and (7.243) are automatically solved once more, thereby completely determining $\mathcal{Z}$, and in turn x and $\phi^{\perp}$. Taking these two conditions into account, $\mathcal{S}$ can be completely described by Λ, i.e.

$$\mathcal{S}^2 = \frac{9Q}{4} - 4\Lambda. \tag{7.248}$$

The remaining equations (7.225) and (7.227) as well as the condition $\mathcal{J} = 0$ give:

$$\mathcal{S}\tilde{T}^{\shortparallel\shortparallel\shortparallel} = 4\Lambda\tilde{T}^{\shortparallel}_{\mathrm{K}}, \tag{7.249}$$

$$\tilde{T}^{\shortparallel}_{\mathrm{K}} = \frac{4\tilde{T}^{\perp\perp}}{9Q}\left(\frac{\mathrm{d}\Lambda}{\mathrm{d}\bar{\mathrm{x}}} - \mathcal{S}\right), \tag{7.250}$$

$$\Lambda\tilde{T}^{\perp\perp 2} = -\frac{Q}{3}, \tag{7.251}$$

respectively.

⋆ $\underline{\mathcal{S}\left(3\mathcal{Z}-2\right)=\mathcal{Z}\frac{\mathrm{d}\Lambda}{\mathrm{d}\bar{\mathrm{x}}}}$: Substituting this condition into equation (7.72) and using $\mathcal{J}=0$, we arrive at:

$$\tilde{T}^{\shortparallel}_{\mathrm{K}}=-\frac{\mathcal{S}\tilde{T}^{\perp\perp}}{\mathcal{S}^2+4\Lambda}. \tag{7.252}$$

Looking at (7.205) we conclude that $\tilde{T}^{\shortparallel}_{\mathrm{K}}=\mathcal{Z}\phi^{\perp}$, meaning $\mathcal{D}=0$, or $\mathrm{x}=const$. Combining the condition $\mathcal{J}=0$ with equation (7.204), $\mathcal{Z}$ is given by:

$$\mathcal{Z}=1+\frac{\mathrm{x}^2}{2\mathcal{M}}. \tag{7.253}$$

The remaining equations, give the following conditions placed upon the EMT and contorsion current:

$$\tilde{T}^{\perp\perp}=\frac{\mathrm{x}}{\mathcal{M}}\left(1+\frac{\mathrm{x}^2}{2\mathcal{M}}\right), \tag{7.254}$$

$$2\Lambda\tilde{T}^{\shortparallel}_{\mathrm{K}}=-\mathrm{x}\mathcal{S}\left(1+\frac{\mathrm{x}^2}{2\mathcal{M}}\right), \tag{7.255}$$

$$\tilde{T}^{\shortparallel\shortparallel}=\frac{\mathrm{x}\Lambda}{\mathcal{S}\mathcal{M}^2}\left(1+\frac{\mathrm{x}^2}{2\mathcal{M}}\right)\left[\frac{\mathrm{d}\mathcal{M}}{\mathrm{d}\bar{\mathrm{x}}}-\frac{2\mathcal{S}\mathcal{M}^2}{\Lambda}\right], \tag{7.256}$$

$$\frac{\mathrm{d}\Lambda}{\mathrm{d}\bar{\mathrm{x}}}=\mathcal{S}\frac{2\mathcal{M}+3\mathrm{x}^2}{2\mathcal{M}+\mathrm{x}^2}. \tag{7.257}$$

- $\underline{\mathcal{S}^2+4\Lambda=0}$: This is the final scenario when $\tilde{T}^{\perp}_{\mathrm{K}}=0$. Let us start by analyzing equation (7.226). It can be transformed in the following form:

$$\left(\frac{1}{4}-\frac{\mathcal{Z}^2\left(\mathcal{Z}-1\right)}{\tilde{T}^{\perp\perp2}}\right)\left[2\Lambda\tilde{T}^{\shortparallel}_{\mathrm{K}}-\mathcal{S}\tilde{T}^{\perp\perp}\left(\frac{1}{4}-\frac{\mathcal{Z}^2\left(\mathcal{Z}-1\right)}{\tilde{T}^{\perp\perp2}}\right)\right]\left(\tilde{T}^{\shortparallel\shortparallel}+\mathcal{S}\tilde{T}^{\shortparallel}_{\mathrm{K}}\right)=0. \tag{7.258}$$

The first bracket in (7.258) cannot be equal to zero, since it is proportional to $\phi^{\perp}$, leading to the two possible scenarios.

⋆ $\underline{\mathrm{x}=const}$: This case corresponds to choosing the middle bracket in equation (7.258) to be zero. Comparing with equation (7.205), it follows that $\tilde{T}^{\shortparallel}_{\mathrm{K}}=\mathcal{Z}\phi^{\perp}$, which indicates that $\mathcal{D}=0$, leading to the conclusion that x is constant. Equation (7.228) remains as a conservation law for the EMT, while (7.225) is automatically satisfied for the case of constant dilaton. All fields are expressed in terms of $\mathcal{Z}$. The solution in this case then reduces to the solution in the case where $\mathcal{S}^2+4\Lambda\neq 0\ \wedge\ \mathcal{J}\neq 0$ with the condition $\mathcal{S}^2+4\Lambda=0$.

⋆ $\underline{\mathrm{x}\neq const\ \wedge\ \tilde{T}^{\perp\perp}\neq 0}$: Here equation (7.258) gives:

$$\tilde{T}^{\shortparallel\shortparallel}+\mathcal{S}\tilde{T}^{\shortparallel}_{\mathrm{K}}=0, \tag{7.259}$$

which together with (7.228) results into a solution for EMT in terms of the metric:

$$\tilde{T}^{\perp\perp}=\frac{D}{\sqrt{-\Lambda}}, \tag{7.260}$$

while together with (7.225) a solution for $\mathcal{Z}$ is reached:

$$\mathcal{Z}=\frac{\eta}{\sqrt{-\Lambda}}e^{\pm\mathrm{z}}, \tag{7.261}$$

where we have used z-coordinate defined via (3.21). The final condition is given by equation (7.227):

$$\tilde{T}^{\shortparallel}_{\mathrm{K}} = -\frac{\eta^3}{3D}\frac{\mathrm{d}}{\mathrm{dz}}\left(\frac{e^{\mp 3\mathrm{z}}}{(-\Lambda)^{\frac{3}{2}}}\right). \tag{7.262}$$

This solution is parametrized by two constants η and D.

⋆ $\underline{\mathrm{x} \neq const \ \wedge \ \tilde{T}^{\perp\perp} = 0}$: From (7.227) we have a formula for the metric:

$$\Lambda = -\bar{\mathrm{x}}^2, \ \mathcal{S} = -2\bar{\mathrm{x}}. \tag{7.263}$$

Then, the other equations reduce to:

$$\tilde{T}^{\shortparallel\shortparallel} = 2\bar{\mathrm{x}}\tilde{T}^{\shortparallel}_{\mathrm{K}}, \tag{7.264}$$

$$\phi^{\perp} = \eta - \int \frac{\mathrm{d}\bar{\mathrm{x}}}{\bar{\mathrm{x}}}\tilde{T}^{\shortparallel}_{\mathrm{K}}, \tag{7.265}$$

$$\mathrm{x} = -\bar{\mathrm{x}}\left[\eta - \int \frac{\mathrm{d}\bar{\mathrm{x}}}{\bar{\mathrm{x}}}\tilde{T}^{\shortparallel}_{\mathrm{K}}\right]. \tag{7.266}$$

Non-vanishing normal component of contorsion current

The system of equations defining this case is given by:

$$\mathcal{Z}^2\frac{\mathrm{d}\mathcal{Z}}{\mathrm{d}\bar{\mathrm{x}}} = -\frac{\mathcal{Z}^3}{2\Lambda}\left(\frac{\mathrm{d}\Lambda}{\mathrm{d}\bar{\mathrm{x}}} - \mathcal{S}\right) + \mathcal{Z}\phi^{\perp}\left(\tilde{T}^{\shortparallel\shortparallel} + \mathcal{S}\tilde{T}^{\shortparallel}_{\mathrm{K}}\right), \tag{7.267}$$

$$\mathcal{Z}\left(\phi^{\perp} + \mathcal{D}\right) = \tilde{T}^{\shortparallel}_{\mathrm{K}}, \tag{7.268}$$

$$-\tilde{T}^{\perp\perp}\tilde{T}^{\shortparallel}_{\mathrm{K}} + \frac{\mathrm{d}}{\mathrm{d}\bar{\mathrm{x}}}\left(\Lambda\tilde{T}^{\perp 2}_{\mathrm{K}}\right) = \frac{\mathcal{Z}^3 - 2\Lambda\tilde{T}^{\perp 2}_{\mathrm{K}}}{2\Lambda}\left(\frac{\mathrm{d}\Lambda}{\mathrm{d}\bar{\mathrm{x}}} - \mathcal{S}\right), \tag{7.269}$$

$$\begin{aligned} &2\Lambda\frac{\mathrm{d}\tilde{T}^{\perp\perp}}{\mathrm{d}\bar{\mathrm{x}}} + \frac{\mathrm{d}\Lambda}{\mathrm{d}\bar{\mathrm{x}}}\left(\tilde{T}^{\perp\perp} + \tilde{T}^{\shortparallel\shortparallel}\right) + 2\Lambda\tilde{T}^{\shortparallel}_{\mathrm{K}}\frac{\mathrm{d}\mathcal{S}}{\mathrm{d}\bar{\mathrm{x}}} \\ &\qquad = 2\frac{\frac{1}{2\Lambda}\left(\frac{\mathrm{d}\Lambda}{\mathrm{d}\bar{\mathrm{x}}} - \mathcal{S}\right) + \frac{\mathrm{d}}{\mathrm{d}\bar{\mathrm{x}}}\ln\mathcal{Z}}{\mathcal{Z}\phi^{\perp}}\frac{\mathrm{d}}{\mathrm{d}\bar{\mathrm{x}}}\left(\Lambda\tilde{T}^{\perp}_{\mathrm{K}}\right)^2, \end{aligned} \tag{7.270}$$

together with the solutions for $\phi^{\perp}$ and x, given by (7.205) and (7.204) respectively. As the method of solving of these equations mirrors that of the earlier section, with identical scenarios arising, we do not examine it here.

7.2.3 Solutions when $\mathcal{Z} \neq 0$, $\theta = 0$ and $\phi^{\perp} = 0$

The same way as in section 7.2.1 all fields can be expressed in terms of the sources, that is:

$$\mathrm{x} = \frac{\tilde{T}^{\perp\perp}}{2\mathcal{Z}}, \ \phi^{\shortparallel} = \frac{\tilde{T}^{\perp}_{\mathrm{K}}}{\mathcal{Z}}, \ \phi^{\perp} = 0, \tag{7.271}$$

$$2l\Lambda\mathrm{K}^{\shortparallel} = \frac{\tilde{T}^{\shortparallel\perp}}{\tilde{T}^{\perp}_{\mathrm{K}}}, \ 2l\Lambda\mathrm{K}^{\perp} = \frac{\tilde{T}^{\shortparallel\shortparallel} + \tilde{T}^{\perp\perp}}{\tilde{T}^{\perp}_{\mathrm{K}}}, \tag{7.272}$$

while the solution for θ (7.185) becomes a condition given by:

$$\frac{1}{4}\tilde{T}^{\perp\perp 2} = \Lambda\tilde{T}^{\perp 2}_{\mathrm{K}} + \mathcal{Z}^2\left(\mathcal{Z} - 1\right). \tag{7.273}$$

The remaining equations have the same form as in 7.2.1, given by:

$$2\tilde{T}_{\mathrm{K}}^{\shortparallel} = \frac{\mathrm{d}\tilde{T}^{\perp\perp}}{\mathrm{d}\bar{\mathrm{x}}} + \frac{\tilde{T}^{\perp\perp}}{2\Lambda}\left(\frac{\mathrm{d}\Lambda}{\mathrm{d}\bar{\mathrm{x}}} - \mathcal{S}\right) \tag{7.274}$$

$$\mathcal{Z}^3\frac{\tilde{T}^{\shortparallel\shortparallel} + \tilde{T}^{\perp\perp}}{2\Lambda\tilde{T}_{\mathrm{K}}^{\perp 2}} = \frac{1}{2}\mathcal{S}\tilde{T}^{\perp\perp}\frac{\mathrm{d}}{\mathrm{d}\bar{\mathrm{x}}}\ln\left(\frac{\tilde{T}^{\perp\perp}}{\mathcal{Z}}\right) + \tilde{T}^{\shortparallel\shortparallel}, \tag{7.275}$$

$$\mathcal{Z}\left(\frac{\mathrm{d}\mathcal{S}}{\mathrm{d}\bar{\mathrm{x}}} + 2\right) = \frac{\tilde{T}^{\shortparallel\shortparallel}\tilde{T}^{\perp\perp}}{\mathcal{Z}^2} + \mathcal{S}\frac{\mathrm{d}}{\mathrm{d}\bar{\mathrm{x}}}\left(\frac{\Lambda\tilde{T}_{\mathrm{K}}^{\perp 2}}{\mathcal{Z}^2}\right), \tag{7.276}$$

$$2\tilde{T}_{\mathrm{K}}^{\shortparallel} = \frac{\mathrm{d}\tilde{T}^{\perp\perp}}{\mathrm{d}\bar{\mathrm{x}}} - \frac{1}{6}\frac{\mathrm{d}}{\mathrm{d}\bar{\mathrm{x}}}\left(\frac{\tilde{T}^{\perp\perp}}{\mathcal{Z}}\right)^3 + \frac{\tilde{T}^{\perp\perp}}{\mathcal{Z}}\frac{\mathrm{d}}{\mathrm{d}\bar{\mathrm{x}}}\left(\frac{\Lambda\tilde{T}_{\mathrm{K}}^{\perp 2}}{\mathcal{Z}^2}\right). \tag{7.277}$$

As in previous sections, we investigate three distinct scenarios, depending on which components of contorsion current vanish.

- $\underline{T_{\mathrm{K}}^{\mu} = 0}$: In this case, as always, we have $\phi^{\shortparallel} = \mathrm{K}^{\perp} = T^{\shortparallel\perp} = 0$. From equation (7.26) we get $\mathcal{D} = 0$, which indicates $\mathrm{x} = const$. Since $\mathcal{Z} = \mathrm{x}^2 + 1$, from (7.23) we conclude that $\tilde{T}^{\perp\perp}$ is also constant:
$$\tilde{T}^{\perp\perp} = -\tilde{T}^{\shortparallel\shortparallel} = 2\mathrm{x}\left(\mathrm{x}^2 + 1\right), \tag{7.278}$$
where we have also used equation (7.24). The remaining equations are then solved by the following metric:
$$\Lambda = -\left[\frac{3\mathrm{x}^2 + 1}{\mathrm{x}^2 + 1}\bar{\mathrm{x}}^2 - \mu\right], \tag{7.279}$$
where μ is a constant. Finally, this metric implies a vanishing parallel component of the contorsion.

- $\underline{T_{\mathrm{K}}^{\perp} = 0}$: In this scenario, $\tilde{T}_{\mathrm{K}}^{\shortparallel}$ is not equal to zero, but the condition of vanishing normal component of the contorsion current still implies $\phi^{\shortparallel} = \mathrm{K}^{\perp} = T^{\shortparallel\perp} = 0$. It resembles the earlier case, with the sole difference being that the dilaton, and subsequently the EMT, is not required to remain constant. The dilaton is found as a solution of $2\mathrm{x}\left(\mathrm{x}^2 + 1\right) = \tilde{T}^{\perp\perp}$ as a function $\mathrm{x} = f(\tilde{T}^{\perp\perp})$. Then, all other fields can be expressed in terms of f, that is:
$$l\mathrm{K}^{\shortparallel} = -\frac{2ff'}{1 + f^2}\frac{\mathrm{d}\tilde{T}^{\perp\perp}}{\mathrm{d}\bar{\mathrm{x}}}, \tag{7.280}$$
$$\tilde{T}_{\mathrm{K}}^{\shortparallel} = \left(f^2 + 1\right)f'\frac{\mathrm{d}\tilde{T}^{\perp\perp}}{\mathrm{d}\bar{\mathrm{x}}}, \tag{7.281}$$
$$\frac{\mathrm{d}\mathcal{S}}{\mathrm{d}\bar{\mathrm{x}}} = -2\frac{3f^2 + 1}{f^2 + 1}, \tag{7.282}$$
$$\tilde{T}^{\shortparallel\shortparallel} = -\tilde{T}^{\perp\perp}. \tag{7.283}$$

- $\underline{T_{\mathrm{K}}^{\perp} \neq 0}$: This is the most general case. Using equation (7.273), normal component of contorsion current is removed from the system of equations. Also, $\tilde{T}^{\shortparallel\shortparallel}$ is eliminated using (7.276). After this, we are left with three equations which cannot be further simplified at this point.

7.2.4 Solutions when $\mathcal{Z} = 0$

This is the final special scenario, corresponding to a vacuum solutions of type RCIIA (7.38) and RCIIB. Equations (7.22-7.26) reduce to a following set of conditions:

$$\tilde{T}^{\perp\perp} = \tilde{T}^{\shortparallel\perp} = \tilde{T}^{\perp}_{\mathrm{K}} = \tilde{T}^{\shortparallel\shortparallel} - \frac{2}{\mathrm{x}}\Lambda\phi^{\perp}\tilde{T}^{\shortparallel}_{\mathrm{K}} = 0, \tag{7.284}$$

$$\tilde{T}^{\shortparallel}_{\mathrm{K}} = -\mathrm{x}\frac{\mathrm{d}\theta^2}{\mathrm{d}\bar{\mathrm{x}}}. \tag{7.285}$$

These equations imply that $\theta^2 \neq const.$ since otherwise all sources vanish. Using the condition $\mathcal{Z} = 0$, the remaining four equations (7.14-7.17) are rewritten in the following form:

$$\frac{\mathrm{d}}{\mathrm{d}\bar{\mathrm{x}}}\left(\frac{\mathrm{d}\Lambda}{\mathrm{d}\bar{\mathrm{x}}} - 2l\Lambda\mathrm{K}^{\shortparallel}\right) + 2 + \frac{2}{\mathrm{x}}l\Lambda\left(\phi^{\perp}\mathrm{K}^{\shortparallel} - \phi^{\shortparallel}\mathrm{K}^{\perp}\right) = 0, \tag{7.286}$$

$$\phi^{\shortparallel}\mathcal{A} = 0, \tag{7.287}$$

$$\phi^{\perp}\mathcal{A} = \frac{\mathrm{d}\theta^2}{\mathrm{d}\bar{\mathrm{x}}}, \tag{7.288}$$

$$2\mathrm{x}\mathcal{A} = \frac{\mathrm{d}\theta^2}{\mathrm{d}\bar{\mathrm{x}}}\left(\frac{\mathrm{d}\Lambda}{\mathrm{d}\bar{\mathrm{x}}} - 2l\Lambda\mathrm{K}^{\shortparallel}\right), \tag{7.289}$$

where $\mathcal{A}$ is a function of the fields and their derivatives given by:

$$\begin{aligned}\mathcal{A} = \left(\phi^{\perp} + \mathcal{D}\right)\left(\frac{\mathrm{d}\Lambda}{\mathrm{d}\bar{\mathrm{x}}} - 2l\Lambda\mathrm{K}^{\shortparallel}\right) + 2\Lambda\frac{\mathrm{d}\phi^{\perp}}{\mathrm{d}\bar{\mathrm{x}}} + \phi^{\perp}\frac{\mathrm{d}\Lambda}{\mathrm{d}\bar{\mathrm{x}}}\\ - 2\mathrm{x} + 2l\Lambda\phi^{\shortparallel}\mathrm{K}^{\perp}.\end{aligned} \tag{7.290}$$

Given that θ is not a constant, equation (7.288) indicates $\mathcal{A} \neq 0$, consequently leading to $\phi^{\shortparallel} = 0$. The nullification of $\phi^{\shortparallel}$ removes $\mathrm{K}^{\perp}$ from the equations entirely, thus making it an arbitrary function. By applying equations (7.289) and (7.288) and substituting the resultant form into equation (7.286), we derive an integrable equation, presented with the subsequent solution:

$$\Lambda = -\left(\frac{\mathrm{x}^2}{\phi^{\perp 2}} - \mu\right), \tag{7.291}$$

where μ is the integration constant. The parallel component of contorsion is then given by:

$$2l\Lambda\mathrm{K}^{\shortparallel} = \frac{\mathrm{d}\Lambda}{\mathrm{d}\bar{\mathrm{x}}} \mp 2\sqrt{\mu - \Lambda}. \tag{7.292}$$

The last remaining equation of the four is automatically satisfied by the condition $\mathcal{Z} = 0$. The solutions for x and θ are as follows:

$$\theta^2 = 1 + \mu\phi^{\perp 2}, \tag{7.293}$$

$$\mathrm{x} = \pm\phi^{\perp}\sqrt{\Lambda - \mu}. \tag{7.294}$$

Finally, integrating (7.285) results in the solution for $\phi^{\perp}$:

$$\phi^{\perp 3} = \eta \mp \frac{3}{2\mu}\int\frac{\mathrm{d}\bar{\mathrm{x}}}{\sqrt{\mu - \Lambda}}\tilde{T}^{\shortparallel}_{\mathrm{K}}. \tag{7.295}$$

We conclude that this special case is dependent on two constants μ and η, and an arbitrary function $\mathrm{K}^{\perp}$ and can only manifest itself when $T^{\shortparallel}_{\mathrm{K}} \neq 0$ and $T^{\perp}_{\mathrm{K}} = 0$. Thus, we can see that the corresponding vacuum solutions are stable only when there is a non-vanishing parallel component of the contorsion current.

7.3 Adding matter minimally coupled to gravity

In this section, we examine how various matter fields couple to gravity. The fields are assumed to be minimally coupled, which means that the quantities $\tau_\mu = 0$ and $\varrho = 0$ introduced in (3.51), and therefore the matter Lagrangian takes the form $\mathcal{L}_{\mathrm{M}} = \mathcal{L}_{\mathrm{M}}\left(g^{\mu\nu}, \omega_\mu, \phi_r, \tilde{\nabla}_\mu \phi_r\right)$. The set ϕ_r denotes the complete matter sector of the theory. The notation used for each type of matter field follows the conventions summarized in Table 7.2.

Field	Label	Additional fields
R-scalars	F	/
C-scalars	f	$f \equiv Fe^{i\gamma}$
U(1) gauge	$\mathcal{A}$	$\mathcal{F}_{\mu\nu} \equiv \partial_\mu \mathcal{A}_\nu - \partial_\nu \mathcal{A}_\mu$
Spinors	ψ	$\psi = \left(\varphi e^{i\alpha} \quad \chi e^{i\beta}\right)^T$
Fluids	u^μ	ρ, p, μ

Table 7.2: Field content

We begin by examining configurations in which a single field is present. Next, we consider the localization of the $U(1)$ symmetry, which leads to scalar and spinor electrodynamics. We then turn to ideal fluid hydrodynamics. In all of these cases, the contorsion current T^μ_{K} vanishes, so the energy-momentum tensor (EMT) is the only remaining source. When θ is set to zero, the theory reduces to its purely Riemannian sector, as described in the previous section. Since Riemannian solutions were the focus of the preceding chapter, we do not study them here and instead confine our analyzes to configurations with a non-vanishing θ field. Consequently, the relevant solutions of the gravitational equations of motion are characterized by $T^\mu_{\mathrm{K}} = 0$, $\theta \neq 0$, and $\mathcal{Z} \neq 0$ (corresponding to the first four entries in Table 7.1). After eliminating the additional gravity-related fields, the full set of gravitational equations of motion simplifies to:

$$\begin{cases} T^{\perp\perp} = \dfrac{6k\pi^2 D}{l^2}\dfrac{1}{\Lambda^{3/2}}, \quad T^{\shortparallel\shortparallel} = T^{\shortparallel\perp} = 0, \quad \Lambda > 0, \\ T^{\perp\perp} = -\dfrac{6k\pi^2 D}{l^2}\dfrac{1}{(-\Lambda)^{3/2}}, \quad T^{\shortparallel\shortparallel} = T^{\shortparallel\perp} = 0, \quad \Lambda < 0. \end{cases} \tag{7.296}$$

Hence, the EMT is entirely determined in terms of the single metric function Λ. To obtain a complete description, these equations must be supplemented by the equations of motion for the matter fields. Another key point to emphasize is that $\mathrm{K}^{\shortparallel} \neq 0$, because if it were zero, then D would also be zero and the EMT would vanish.

7.3.1 Real scalar field theory

It turns out that the massless scalars directly imply the vanishing θ field. For that reason we investigate a more general theory with an arbitrary scalar potential. In other words, we investigate the interacting scalar field theories within this subsection. Therefore, the action for the real scalar field, minimally-coupled to gravity, is given by:

$$S_{\mathrm{RSF}} = -\int \mathrm{d}^2x\sqrt{-g}\left[\frac{1}{2}(\nabla F)^2 + V[F]\right], \tag{7.297}$$

where $V[F]$ is the scalar potential. The variation with respect to the metric gives the following energy-momentum tensor:

$$T_{\mu\nu} = \partial_\mu F \partial_\nu F - \left[\frac{1}{2}(\nabla F)^2 + V[F]\right] g_{\mu\nu}, \tag{7.298}$$

which, after applying the Symmetric ansatz of Section 3.1, more precisely equation (3.14), reduces to:

$$l^2 T^{\perp\perp} = \frac{1}{2}\left(\frac{\mathrm{d}F}{\mathrm{d}\bar{\mathrm{x}}}\right)^2 + \frac{l^2}{\Lambda}V[F], \tag{7.299}$$

$$l^2 T^{\parallel\parallel} = \frac{1}{2}\left(\frac{\mathrm{d}F}{\mathrm{d}\bar{\mathrm{x}}}\right)^2 - \frac{l^2}{\Lambda}V[F], \tag{7.300}$$

where we have employed the $\bar{\mathrm{x}}$ coordinate defined in (3.20). The equation of motion for the scalar field is:

$$\Box F = \frac{\mathrm{d}V}{\mathrm{d}F} \equiv V'[F] \quad \Longrightarrow \quad \frac{\mathrm{d}}{\mathrm{d}\bar{\mathrm{x}}}\left(\Lambda\frac{\mathrm{d}F}{\mathrm{d}\bar{\mathrm{x}}}\right) + l^2 V'[F] = 0. \tag{7.301}$$

Using the conditions for sources (7.296) together with the expressions (7.299) and (7.300) we arrive at the following two equations:

$$V[F] = \frac{3k\pi^2 D}{l^2}\frac{1}{\sqrt{|\Lambda|}}, \quad \left(\frac{\mathrm{d}F}{\mathrm{d}\bar{\mathrm{x}}}\right)^2 = \frac{6k\pi^2 D}{\Lambda}\frac{1}{\sqrt{|\Lambda|}}. \tag{7.302}$$

It is obvious that $V = 0$ implies $D = 0$, in other words, the complete vanishing of the EMT. For that reason we must have a non-vanishing scalar potential. Using (7.302) equation (7.301) is automatically satisfied. With the help of these equations, all relevant physical quantities are expressed in terms of F as follows:

$$\begin{aligned} &\mathrm{d}s^2 = \frac{1}{V}\left[\left(\frac{3k\pi^2 D}{l^2}\right)^2\frac{\mathrm{d}t^2}{|V|} - \frac{1}{2}\mathrm{d}F^2\right], \quad \mathrm{z} = \pm\int\frac{\mathrm{d}F}{\sqrt{2l^2 V}}, \\ &R = 8V\sqrt{|V|}\frac{\mathrm{d}^2}{\mathrm{d}F^2}\left(\frac{1}{\sqrt{|V|}}\right), \quad \kappa = \sqrt{2}\frac{6k\pi^2|D|}{l^2}\left|\frac{\mathrm{d}}{\mathrm{d}F}\left(\frac{1}{\sqrt{|V|}}\right)\right|_H. \end{aligned} \tag{7.303}$$

The last equation in (7.303) represents an expression for surface gravity if the horizon exists. From the first expression, we conclude that, if the horizon exists, it is given by $V[F_H] = 0$. Now, we look into some specific choices of the scalar potential. Firstly, the free real scalar field theory is analyzed, i.e. $V[F] = \frac{1}{2}m^2F^2$. Since $\Lambda > 0$, we redefine coordinates in (3.21) by taking $\tau = l\mathrm{z}$ as the new time coordinate, and defining the spatial coordinate as $r = 2mlt$. The solution is a de Sitter space-time:

$$\Lambda = (2ml)^2 e^{4m\tau}, \quad F = \pm\sqrt{\frac{3k\pi^2 D}{(ml)^3}}e^{-m\tau}. \tag{7.304}$$

The curvature is $R = 8m^2$, meaning that the de Sitter radius is $1/(2m)$. After placing (7.304) into (7.296) we arrive at the following final solution for the free scalar field theory:

$$\begin{aligned} &\mathrm{d}s^2 = -\mathrm{d}\tau^2 + e^{4m\tau}\mathrm{d}r^2, \quad \mathrm{x} = \cos\frac{\tau}{l}\left[\frac{3}{2}\left(\frac{D\cos\frac{\tau}{l}}{2mle^{2m\tau} - \frac{P}{2}\sin\frac{\tau}{l}} + \eta\right)\right]^{\frac{1}{3}}, \\ &\theta^2 = 1 + \frac{1}{3}\left(\frac{\mathrm{x}}{\cos\frac{\tau}{l}}\right)^2 + \eta\frac{\cos\frac{\tau}{l}}{\mathrm{x}}, \quad l\mathrm{K}^{\parallel} = \left[1 + \frac{1}{2ml}\tan\frac{\tau}{l} - \frac{P}{8(ml)^2}\frac{e^{-2m\tau}}{\cos\frac{\tau}{l}}\right]e^{-2m\tau}, \\ &\phi^{\parallel} = \mathrm{K}^{\perp} = 0, \quad \phi^{\perp} = \frac{\mathrm{x}}{2ml}\tan\frac{\tau}{l}e^{-2m\tau}, \quad F = \pm\sqrt{\frac{3k\pi^2 D}{(ml)^3}}e^{-m\tau}. \end{aligned} \tag{7.305}$$

Note that the parallel component of contorsion exhibits many poles in time, in particular whenever $\tau_n = (2n+1)\frac{\pi}{2}l$ the $\cos\frac{\tau}{l}$ vanishes leading to a divergence. All other functions exhibit a well defined behavior at all finite values of τ. This situation can be interpreted as a sequence of sudden singularities, in which the scale factor stays fixed while certain fields may blow up. Specifically, in this setup the parallel component of the contorsion becomes divergent. Solutions of this kind are well known and have been extensively analyzed in various gravitational theories [92, 93].

7.3.2 Pure electrodynamics

The action for pure electrodynamics is formulated in terms of the $U(1)$ gauge potential $\mathcal{A} = \mathcal{A}_\mu \mathrm{d}x^\mu$ and depends solely on the field strength tensor $\mathcal{F} = \mathrm{d}\mathcal{A}$. Because the exterior derivative is insensitive to torsion, the action keeps exactly the same form as in the Riemannian sector, namely:

$$S_{\mathrm{ED}} = -\frac{1}{4}\int \mathrm{d}x^2 \sqrt{-g}\, \mathcal{F}_{\mu\nu}\mathcal{F}^{\mu\nu}. \tag{7.306}$$

Varying this action with respect to the metric and the gauge field leads to the following EMT and Maxwell equation:

$$T_{\mu\nu} = \mathcal{F}_{\mu\rho}\mathcal{F}_{\nu}{}^{\rho} - \frac{1}{4} g_{\mu\nu}\mathcal{F}_{\alpha\beta}\mathcal{F}^{\alpha\beta} \qquad \wedge \qquad \nabla_\mu \mathcal{F}^{\mu\nu} = 0. \tag{7.307}$$

In two spacetime dimensions, any rank-2 antisymmetric tensor must be proportional to the Levi-Civita tensor. Consequently, equation (7.307) simplifies to

$$\mathcal{F}_{\mu\nu} = \mathcal{F}\varepsilon_{\mu\nu} \qquad \Longrightarrow \qquad T_{\mu\nu} = -\frac{1}{2}\mathcal{F}^2 g_{\mu\nu}, \quad \wedge \quad \partial_\mu \mathcal{F} = 0. \tag{7.308}$$

Hence, the scalar function $\mathcal{F}$ must be constant. Interpreting this constant as the electric charge, we denote it by $\mathcal{F} = Q$. Implementing the symmetric ansatz of Section 3.1 yields

$$T_{\mu\nu} = -\frac{Q^2}{2\Lambda}\left(\xi_\mu\xi_\nu - \varepsilon_{\mu\rho}\varepsilon_{\nu\sigma}\xi^\rho\xi^\sigma\right) \qquad \Longrightarrow \qquad \Lambda T^{\perp\perp} = -\Lambda T^{\shortparallel\shortparallel} = \frac{Q^2}{2}, \tag{7.309}$$

$$\mathcal{F}_{\mu\nu} = \frac{1}{l}\frac{\mathrm{d}}{\mathrm{d}\bar{\mathrm{x}}}\left(\Lambda \mathcal{A}^{\shortparallel}\right)\varepsilon_{\mu\nu}, \tag{7.310}$$

where we have used expression (3.26) in the second line. On the other hand, the constraints (7.296) enforce $T^{\shortparallel\shortparallel} = 0$, which immediately leads to $T^{\perp\perp} = 0$. We thus infer that no solution exists for $\theta \neq 0$, and the theory collapses to its purely Riemannian branch. This mirrors the situation for a scalar field: the massless case admits no solution, whereas introducing a non-vanishing scalar potential allows one to recover a solution. By analogy, a massive vector field might also support solutions; however, since a mass term explicitly breaks the $U(1)$ gauge symmetry, we do not pursue that possibility here.

Note that the field strength tensor in (7.310) is independent of the perpendicular component of the electromagnetic field. Consequently, this component merely specifies a gauge choice and therefore does not carry any physical degrees of freedom.

Charged black hole in the Riemannian sector

When the theory is restricted to its Riemannian sector, one obtains a charged black hole solution. Inserting the EMT components from (7.309) into the general static field equations (6.24-6.25) of the Riemannian theory yields

$$\frac{\mathrm{d}}{\mathrm{dx}}\left(\mathrm{x}^2+1+\Lambda\mathcal{D}^2\right)^2=\frac{l^2Q^2}{3k\pi^2}, \tag{7.311}$$

$$\left(\mathrm{x}^2+1+\Lambda\mathcal{D}^2\right)\left(\mathcal{D}^2\frac{\mathrm{d}\Lambda}{\mathrm{dx}}+2\mathrm{x}\right)=\frac{l^2Q^2}{6k\pi^2}. \tag{7.312}$$

If we multiply the second equation by 2 and subtract it from the first, we obtain $\mathcal{D}=1$. The metric function Λ is then determined by integrating the first equation, giving

$$\Lambda=-\left(\mathrm{x}^2+1-\sqrt{(\mu+1)^2+\frac{Q^2l^2}{3k\pi^2}\mathrm{x}}\right). \tag{7.313}$$

This form is chosen so that, in the limit $Q\to0$, the solution reduces to the vacuum configuration (6.17). To evaluate the tortoise coordinate (3.18), one should compute the integral $-\int\frac{\mathrm{dx}}{\Lambda}$. However, this integral cannot be represented in terms of elementary functions in a convenient form, and we therefore do not determine the tortoise coordinate here.

To check whether the singularity shifts away from the hypersurface $\mathrm{x}=0$, we calculate the scalar curvature:

$$l^2R=\frac{\mathrm{d}^2\Lambda}{\mathrm{dx}^2}=-2-\left(\frac{Q^2l^2}{6k\pi^2}\right)^2\left((\mu+1)^2+\frac{Q^2l^2}{3k\pi^2}\mathrm{x}\right)^{-\frac{3}{2}}<0. \tag{7.314}$$

Hence, the geometry is not a patch of AdS spacetime, but the curvature remains strictly negative, indicating that the singularity stays at $\mathrm{x_S}=0$ once the black hole is charged.

To locate the horizon, we solve $\Lambda=0$. This equation admits two real roots, one negative and one positive. Because we restrict to $\mathrm{x}>0$, only the positive root is physically relevant, so there is a single horizon. This is in contrast to the Reissner–Nordström charged black hole, which possesses two horizons—an inner and an outer one [106]. Finally, we evaluate the surface gravity:

$$\kappa=\frac{1}{2l}\left|\frac{\mathrm{d}\Lambda}{\mathrm{dx}}\right|_{\mathrm{H}}=\frac{1}{l}\left[\mathrm{x_H}-\frac{Q^2l^2}{12k\pi^2}\left((\mu+1)^2+\frac{Q^2l^2}{3k\pi^2}\mathrm{x_H}\right)^{-\frac{1}{2}}\right]. \tag{7.315}$$

As equation $\Lambda=0$ is a quartic equation for $\mathrm{x_H}$, a closed-form expression for the horizon location does exist, but we do not present it here because it is an extremely cumbersome combination of nested radicals.

7.3.3 Spinor field theory

In this subsection, we investigate how matter composed of Dirac spinor fields influences the gravitational equations of motion. We employ the symmetric Dirac action presented in Appendix A and defined in (A.24). For convenience we rewrite it here:

$$S_D=-\int\mathrm{d}^2x\sqrt{-g}\left[\frac{1}{2}\bar{\psi}\gamma^\mu\tilde{\nabla}_\mu\psi-\frac{1}{2}\tilde{\nabla}_\mu\bar{\psi}\gamma^\mu\psi-V\left[\sigma\right]\right], \tag{7.316}$$

where $V\left[\sigma\right]$ denotes the spinor potential, and we denote the bilinear invariant by $\sigma = \bar{\psi}\psi$. For a free massive spinor field one has $V[\bar{\psi}\psi] = m\bar{\psi}\psi$, while the Lorentz-covariant derivatives take the form:

$$\tilde{\nabla}_\mu \psi = \left(\partial_\mu + \omega_\mu \frac{\sigma_3}{2}\right)\psi, \quad \tilde{\nabla}_\mu \bar{\psi} = \partial_\mu \bar{\psi} - \bar{\psi}\frac{\sigma_3}{2}\omega_\mu. \tag{7.317}$$

Further details regarding the spinor conventions are provided in Appendix A. Since $\omega_\mu = \Delta_\mu + \mathrm{K}_\mu$, the action depends explicitly on the contorsion. Varying the action with respect to the contorsion yields:

$$T^\mu_{\mathrm{K}} = \frac{1}{2}\bar{\psi}\left\{\frac{\sigma_3}{2}, \gamma^\mu\right\}\psi \quad \Longrightarrow \quad T^\mu_{\mathrm{K}} = 0, \tag{7.318}$$

where the anticommutator manifestly vanishes because $\gamma^\mu \in \{\sigma_1, \sigma_2\}$. Consequently, the contorsion current is zero even in the presence of minimally coupled Dirac spinors, in agreement with the statement made at the beginning of this section. Variation with respect to the metric and the Dirac field then produces the following EMT of the Dirac field and the usual Dirac equation of motion:

$$\begin{aligned} T_{\mu\nu} =& \frac{1}{4}\left[\bar{\psi}\gamma_\mu\tilde{\nabla}_\nu\psi + \bar{\psi}\gamma_\nu\tilde{\nabla}_\mu\psi - \left(\tilde{\nabla}_\mu\bar{\psi}\right)\gamma_\nu\psi - \left(\tilde{\nabla}_\nu\bar{\psi}\right)\gamma_\mu\psi\right], \\ &\left(\gamma^\mu\tilde{\nabla}_\mu - V'\left[\sigma\right]\right)\psi = 0. \end{aligned} \tag{7.319}$$

Note that the EMT displays the same qualitative behavior as the contorsion current (7.318). In particular, all spin-connection contributions collect into anticommutator terms that identically vanish. Consequently, it depends only on ordinary partial derivatives. We now implement the symmetric spinor ansatz from (3.17). As a first step, we recast the energy-momentum tensor:

$$T_{\mu\nu} = \frac{1}{l\sqrt{-\Lambda}}\left(\varphi^2\frac{\mathrm{d}\alpha}{\mathrm{d}\bar{\mathrm{x}}} - \chi^2\frac{\mathrm{d}\beta}{\mathrm{d}\bar{\mathrm{x}}}\right)\varepsilon_{\mu\rho}\varepsilon_{\nu\sigma}\xi^\rho\xi^\sigma + \frac{1}{2l\sqrt{-\Lambda}}\left(\varphi^2\frac{\mathrm{d}\alpha}{\mathrm{d}\bar{\mathrm{x}}} + \chi^2\frac{\mathrm{d}\beta}{\mathrm{d}\bar{\mathrm{x}}}\right)\left(\varepsilon_{\mu\rho}\xi_\nu + \varepsilon_{\nu\rho}\xi_\mu\right)\xi^\rho. \tag{7.320}$$

Next, the Dirac equation in (7.319) simplifies, upon separating its real and imaginary parts, to the following four equations:

$$\frac{\mathrm{d}}{\mathrm{d}\bar{x}}\ln\left(\varphi(-\Lambda)^{\frac{1}{4}}\right) - \frac{l}{2}\mathrm{K}^{\shortparallel} = \frac{lV'\left[\sigma\right]}{\sqrt{-\Lambda}}\frac{\chi}{\varphi}\sin(\beta-\alpha), \tag{7.321}$$

$$\frac{\mathrm{d}}{\mathrm{d}\bar{x}}\ln\left(\chi(-\Lambda)^{\frac{1}{4}}\right) - \frac{l}{2}\mathrm{K}^{\shortparallel} = \frac{lV'\left[\sigma\right]}{\sqrt{-\Lambda}}\frac{\varphi}{\chi}\sin(\beta-\alpha), \tag{7.322}$$

$$\frac{\mathrm{d}\alpha}{\mathrm{d}\bar{\mathrm{x}}} = -\frac{lV'\left[\sigma\right]}{\sqrt{-\Lambda}}\frac{\chi}{\varphi}\cos(\beta-\alpha), \tag{7.323}$$

$$\frac{\mathrm{d}\beta}{\mathrm{d}\bar{\mathrm{x}}} = \frac{lV'\left[\sigma\right]}{\sqrt{-\Lambda}}\frac{\varphi}{\chi}\cos(\beta-\alpha). \tag{7.324}$$

It is immediately evident that, in the massless case $V=0$, the derivatives of both phases α and β vanish. As a consequence, the entire EMT in (7.320) is zero. Hence, no solution with $\theta \neq 0$ exists, and the theory collapses to its purely Riemannian sector. We therefore reach the same conclusion as in the real scalar field case: a non-vanishing spinor potential is required in order to obtain a solution with $\theta \neq 0$. Expressing this system in terms of the coordinate z from

(3.21), we obtain:

$$\frac{\mathrm{d}\alpha}{\mathrm{dz}} = lV'[\sigma]\frac{\chi}{\varphi}\cos(\beta-\alpha), \tag{7.325}$$

$$\frac{\mathrm{d}\beta}{\mathrm{dz}} = -lV'[\sigma]\frac{\varphi}{\chi}\cos(\beta-\alpha), \tag{7.326}$$

$$\frac{\mathrm{d}}{\mathrm{dz}}\left(\frac{\varphi}{\chi}\right) = lV'[\sigma]\left[\left(\frac{\varphi}{\chi}\right)^2 - 1\right]\sin(\beta-\alpha), \tag{7.327}$$

$$\frac{\mathrm{d}}{\mathrm{dz}}\ln\left(\varphi\chi\sqrt{-\Lambda}\right) + l\sqrt{-\Lambda}\mathrm{K}^{\parallel} = -lV'[\sigma]\left(\frac{\varphi}{\chi}+\frac{\chi}{\varphi}\right)\sin(\beta-\alpha), \tag{7.328}$$

where the last two relations follow from subtracting and adding (7.321) and (7.322), respectively. The first three equations constitute a closed subsystem for α, β, and the ratio $\frac{\varphi}{\chi}$, with $V'[\sigma]$ left arbitrary. Nonetheless, this subsystem can be integrated to express the phases in terms of $\frac{\varphi}{\chi}$, yielding:

$$\begin{aligned} \cos(\beta-\alpha) &= \frac{\omega}{2}\left(\frac{\varphi}{\chi}-\frac{\chi}{\varphi}\right), \\ \alpha+\beta &= -\arcsin\left[\frac{1}{2}\frac{\omega}{\sqrt{1+\omega^2}}\left(\frac{\varphi}{\chi}+\frac{\chi}{\varphi}\right)\right] + \gamma_0, \end{aligned} \tag{7.329}$$

where ω and γ_0 are integration constants. Substituting this solution into (7.328) and eliminating the phase dependence via (7.327), we arrive at:

$$\frac{\mathrm{d}}{\mathrm{dz}}\ln\left[\varphi\chi\sqrt{-\Lambda}\left(\frac{\varphi}{\chi}-\frac{\chi}{\varphi}\right)\right] + l\sqrt{-\Lambda}\mathrm{K}^{\parallel} = 0 \quad \Longrightarrow \quad \frac{\mathrm{d}}{\mathrm{dz}}\ln\left(\sigma\sqrt{-\Lambda}\right) + l\sqrt{-\Lambda}\mathrm{K}^{\parallel} = 0, \tag{7.330}$$

where we used $\sigma = \bar{\psi}\psi = -2\varphi\chi\cos(\beta-\alpha)$ together with the solution (7.329).

We now proceed to impose the conditions (7.296). The constraint $T^{\parallel\parallel} = 0$ is trivially fulfilled, because the EMT (7.320) does not have a parallel component. Imposing $T^{\parallel\perp} = 0$ is equivalent to simultaneously enforcing equations (7.323) and (7.324). The remaining condition, associated with the perpendicular component of the EMT, simplifies to

$$\frac{3k\pi^2 D}{l\Lambda} = -\frac{lV'[\sigma]}{\sqrt{-\Lambda}}\varphi\chi\cos(\beta-\alpha) \quad \Longrightarrow \quad \sigma V'[\sigma] = -\frac{6k\pi^2 D}{l^2\sqrt{-\Lambda}}, \tag{7.331}$$

where we have once again employed the definition of σ. Equation (7.331) is interpreted as an equation determining the function σ in terms of the metric function Λ once the spinor potential is specified. Thus, expressing σ as a function of Λ via (7.331) and substituting this relation into equation (7.330) yields a first-order differential equation for Λ. Solving this equation fixes both Λ and σ. Subsequently, the remaining equation (7.327) becomes explicitly integrable. Its solution can be written as

$$\varphi = \chi\sqrt{\frac{e^{2s}+\frac{1}{4}(\omega^2+1)e^{-2s}+1}{e^{2s}+\frac{1}{4}(\omega^2+1)e^{-2s}-1}}, \qquad s = l\int V'[\sigma]\mathrm{dz}. \tag{7.332}$$

The overall problem therefore reduces to solving equation (7.330), once the algebraic equation for σ in (7.331) has been resolved.

All of these equations hold for both $\Lambda > 0$ and $\Lambda < 0$ by analytic continuation. For a black hole solution to exist, there must be an event horizon. Since it is defined by $\Lambda = 0$, such a horizon can arise only if the function $\sigma V'[\sigma]$ has a pole in $\mathbb{R} \cup \{\pm\infty\}$. In that case, one can analytically match the two coordinate patches corresponding to opposite signs of the metric function Λ, thereby constructing a black hole geometry: the interior region is described on a chart with $\Lambda > 0$, and the exterior region on a chart with $\Lambda < 0$, as usual. We now turn to a discussion of particular choices for the spinor potential $V[\sigma]$.

- $\underline{V[\sigma] = 0}$: This choice corresponds to a theory of massless spinors. As discussed above, this condition leads to a vanishing EMT, so within this framework there is no nontrivial solution.

- $\underline{V[\sigma] = m\sigma}$: For massless spinors, we have $V'[\sigma] = m$, a constant. Therefore, equation (7.331) implies $\sigma\sqrt{-\Lambda} = \text{const.}$, and equation (7.330) reduces to $\mathrm{K}^{\shortparallel} = 0$. Consequently, even the massive Dirac field admits no solution, since $\mathrm{K}^{\shortparallel} = 0$ again causes the EMT to vanish on the gravitational side of the field equations.

- $\underline{V[\sigma] = -b \ln|\sigma|}$: For this potential we obtain $V'[\sigma] = -b/\sigma$. Substituting into equation (7.331) yields a flat spacetime:
$$\Lambda_0 = -\left(\frac{6k\pi^2 D}{bl^2}\right)^2. \tag{7.333}$$
When $\Lambda < 0$, three distinct cases arise. Without loss of generality, we present only the case in which $\mathrm{K}^{\shortparallel}$ is given by (7.57). Integrating equation (7.330) then gives:
$$\sigma = \frac{\sigma_0}{\sinh \mathrm{z}} \exp\left(-\frac{P}{2\sqrt{-\Lambda_0}} \arctan(\sinh \mathrm{z})\right), \tag{7.334}$$
while s, defined in (7.332), can be written in terms of the hypergeometric function as follows:
$$s = \frac{4ilb}{\sigma_0(2-ia)} \left(\frac{1+i\sinh(\mathrm{z})}{2}\right)^{1-\frac{ia}{2}} {}_2F_1\left(1-\frac{ia}{2}, -\frac{ia}{2}; 2-\frac{ia}{2}; \frac{1+i\sinh(\mathrm{z})}{2}\right) + s_0, \tag{7.335}$$
where $a = \frac{P}{2\sqrt{-\Lambda_0}}$.

- $\underline{V[\sigma] = m\sigma - \frac{g}{2}\sigma^2}$: Taking the derivative yields $V'[\sigma] = m - g\sigma$. For convenience, we now restrict to the massless case. Solving (7.331) for σ then gives
$$\sigma = Q(-\Lambda)^{-\frac{1}{4}}, \qquad D = \frac{gl^2Q^2}{6k\pi^2}. \tag{7.336}$$
The metric follows by directly integrating (7.330). We evaluate it in each of the four distinct cases introduced in the previous section:
$$\sqrt{|\Lambda|} = \begin{cases} \dfrac{P}{2}\sin\bar{\mathrm{z}} + \left(\dfrac{P}{2}\ln|\sec\bar{\mathrm{z}} + \tan\bar{\mathrm{z}}| + \mu\right)\cos^2\bar{\mathrm{z}}, & \Lambda > 0, \\ \dfrac{P}{2}\sinh\mathrm{z} + \left(\dfrac{P}{2}\arctan(\sinh\mathrm{z}) + \mu\right)\cosh^2\mathrm{z}, & \Lambda < 0,\ \mathrm{x}^2 + \Lambda\phi^{\perp 2} > 0, \\ -\dfrac{P}{2}\cosh\mathrm{z} + \left(\mu - \dfrac{P}{2}\ln\left|\tanh\dfrac{\mathrm{z}}{2}\right|\right)\sinh^2\mathrm{z}, & \Lambda < 0,\ \mathrm{x}^2 + \Lambda\phi^{\perp 2} < 0, \\ \pm\dfrac{2}{3}Pe^{\mp\mathrm{z}} + \mu e^{\pm 2\mathrm{z}}, & \Lambda < 0,\ \mathrm{x}^2 + \Lambda\phi^{\perp 2} = 0, \end{cases} \tag{7.337}$$

where μ denotes an integration constant. We now determine the scalar curvature in each of these regimes to examine whether the resulting spacetimes develop curvature singularities:

$$R = -\frac{4}{l^2}\begin{cases} 1 - \tan^2 \bar{\mathrm{z}} + \dfrac{P \sin \bar{\mathrm{z}}}{2\sqrt{\Lambda}\cos^2 \bar{\mathrm{z}}}, & \Lambda > 0, \\ 1 + \tanh^2 \mathrm{z} + \dfrac{P \sinh \mathrm{z}}{2\sqrt{-\Lambda}\cosh^2 \mathrm{z}}, & \Lambda < 0,\ \mathrm{x}^2 + \Lambda\phi^{\perp 2} > 0, \\ 1 + \coth^2 \mathrm{z} + \dfrac{P \cosh \mathrm{z}}{2\sqrt{-\Lambda}\sinh^2 \mathrm{z}}, & \Lambda < 0,\ \mathrm{x}^2 + \Lambda\phi^{\perp 2} < 0, \\ 2 \mp \dfrac{P}{\sqrt{-\Lambda}} e^{\mp \mathrm{z}}, & \Lambda < 0,\ \mathrm{x}^2 + \Lambda\phi^{\perp 2} = 0. \end{cases} \tag{7.338}$$

Finally, we obtain the surface gravity for these geometries whenever a horizon is present. It takes the form

$$\kappa = \frac{1}{l}\begin{cases} \dfrac{P}{\cosh \mathrm{z_H}}, & \Lambda < 0,\ \mathrm{x}^2 + \Lambda\phi^{\perp 2} > 0, \\ \dfrac{P}{\sinh \mathrm{z_H}}, & \Lambda < 0,\ \mathrm{x}^2 + \Lambda\phi^{\perp 2} < 0, \\ -2P e^{\mp \mathrm{z_H}}, & \Lambda < 0,\ \mathrm{x}^2 + \Lambda\phi^{\perp 2} = 0. \end{cases} \tag{7.339}$$

We observe that the parameter P is directly tied to the surface gravity: once P is set to zero, κ vanishes as well.

We first consider the case $\Lambda > 0$. Setting $P = 0$, the solution simplifies to $\sqrt{\Lambda} = \mu \cos^2 \bar{\mathrm{z}}$, and the metric takes the form

$$\mathrm{d}s^2 = -\mathrm{d}\tau^2 + \mu l^2 \cos^4 \frac{\tau}{l} \mathrm{dr}^2, \tag{7.340}$$

where we have introduced the rescaled time coordinate $\tau = l\bar{\mathrm{z}}$. The corresponding curvature becomes divergent at $\tau = (2n+1)\frac{\pi}{2}l$, with $n \in \mathbb{Z}$. This describes a cosmological spacetime oscillating through a succession of big bang and big crunch events.

For $P \neq 0$, this basic pattern persists: curvature singularities still occur at $\tau = \pm(2n+1)\frac{\pi}{2}l$. However, in this case the scale factor remains finite at those points, so these singularities correspond to a sequence of sudden singularities [92, 93]. In addition, there now appears another series of curvature singularities at the zeros of the scale factor, where $\Lambda = 0$, located at $\tau = \tau_{\mathrm{S}} + 2n\pi l$, with $\tau_{\mathrm{S}} \in \left(-\frac{\pi}{2}, \frac{\pi}{2}\right) l$. Consequently, the $P \neq 0$ solution can be understood as an oscillatory universe evolving between the big bang and the big crunch events with two additional sudden curvature singularities occurring between each such pair of events.

We now turn to the cases with $\Lambda < 0$. The first question to address, when considering a spacetime that possesses a time-like Killing vector, is whether a Killing horizon exists [106], characterized by $\Lambda = 0$. Let us determine under which conditions this equation admits a solution. We begin with the case $\mathrm{x}^2 + \Lambda\phi^{\perp 2} > 0$ and introduce the variable $u = \sinh \mathrm{z}$. With this substitution, the equation becomes:

$$f(u) = \frac{u}{1+u^2} + \arctan(u) = -\frac{2\mu}{P} \quad \Longrightarrow \quad f'(u) = \frac{2}{(u^2+1)^2} > 0. \tag{7.341}$$

Hence, $f(u)$ is a monotonically increasing and its range is confined to the interval $(-\frac{\pi}{2}, \frac{\pi}{2})$. Consequently, there is always a unique solution precisely when:

$$\left|\frac{\mu}{P}\right| < \frac{\pi}{4}. \tag{7.342}$$

If no horizon is present, i.e. when $\left|\frac{\mu}{P}\right| > \frac{\pi}{4}$, then there is likewise no curvature singularity. In this regime, the solution describes the ground state of a stable fermionic soliton star spacetime that is globally regular. The gravitational attraction, mediated by the dilaton/metric, is exactly counterbalanced by the repulsive spin–torsion coupling. As the system tends to contract (which would drive Λ to zero), the spin–torsion interaction energy increases more rapidly than the gravitational potential energy, thereby preventing the emergence of an event horizon. The value $\left|\frac{\mu}{P}\right| = \frac{\pi}{4}$ marks a critical mass and signals a phase transition. For $\left|\frac{\mu}{P}\right| < \frac{\pi}{4}$, the gravitational attraction dominates over the spin–torsion repulsion, and a horizon is formed. This horizon simultaneously generates a curvature singularity at the same spacetime location, rendering it a singular horizon.

If P does not vanish, then the surface gravity (7.339) is finite and non-zero, implying that the horizon is non-extremal. Consequently, this stationary, naked, finite-temperature singular horizon is viewed as an idealized but unstable classical background. In practice, the horizon acts like a usual bifurcate Killing horizon, except that the curvature singularity lies precisely on it. In analogy with the Reissner–Nordström solution, this horizon plays the role of the inner Cauchy horizon, which is subject to blueshift instability and gives rise to classical mass inflation.

Next, we analyze the solution corresponding to $\mathrm{x}^2 + \Lambda\phi^{\perp 2} < 0$. In the limit $P \to 0$, this reduces to a configuration that still possesses a horizon at $\mathrm{z_H} = 0$. Yet, for $P = 0$ the surface gravity is zero, so the solution represents a completely stable extremal ground state. We then study how the horizon position changes when $P \neq 0$. Defining $u = \tanh\frac{\mathrm{z}}{2}$, the condition $\Lambda = 0$ becomes

$$f(u) = \frac{1}{4}\left(u^2 - \frac{1}{u^2}\right) + \ln|u| = \frac{2\mu}{P}. \tag{7.343}$$

Since $|u| < 1$, it follows that $f(u) > 0$, implying the existence of a two symmetric horizons at $\pm\mathrm{z_H}$, whenever $\mu P > 0$. As before, these horizons are singular, just as in the previous case, and the same line of reasoning applies. However, inspecting the curvature (7.338) now reveals an additional singularity between the two singular horizons at $\mathrm{z_S} = 0$, which cannot be removed by any means. The remaining case, $\mathrm{x}^2 + \Lambda\phi^{\perp 2} = 0$, displays qualitatively the same behavior as the one just discussed. The difference is that the limit $P \to 0$ now yields AdS spacetime, because the scalar curvature is a negative constant.

We argue that these configurations are still viable solutions of the coupled Dirac–Chern–Simons theory. The origin of the singular horizon in all these examples is directly tied to a blow up in the fermionic density function σ at the horizon, since σ is inversely proportional to the metric function Λ. Consequently, the phase transition—most clearly visible in the first case—can be understood as a condensation process of the fermion mass at the singular horizon. In this sense, the mechanism behind the formation of the singular horizon is understood, and it should no longer be regarded as a naked singularity. Instead, it signifies a spacetime locus at which the fermionic star soliton solution condenses. Because an infinite amount of fermion mass accumulates at this horizon, the geometry must react with a curvature singularity. One may anticipate that incorporating quantum corrections would smooth out this singularity, while preserving a maximum of the fermionic density function in the lower phase at the same spacetime position. Another open question is whether taking into account the fermion mass m in the spinor potential can in any way remove or regularizes this singular horizon.

To further clarify the nature of this fermionic star solution, we may fix the boundary of the star and smoothly match it to the general vacuum solution of Section 7.1.1. In doing so, the fermionic star soliton is interpreted as a compact object embedded in a larger spacetime. The open question is where exactly to place the star's boundary: right at the singular horizon where the fermions condense, or outside of it?

In contrast, the hard singularity that appears in the last two families of solutions is a direct consequence of the coupling to torsion, as the torsion itself diverges at $\mathrm{z_S} = 0$, independently of the choice of matter fields. We expect that, once the Polyakov–Liouville-type quantum corrections (3.72) are taken into account, the singular behavior of the horizon will be resolved, yet a maximum of the fermionic density function will remain there. In this interpretation, the singular horizon acts as a massive barrier that prevents anything from reaching the genuine singularity at $\mathrm{z_S} = 0$. Alternatively, one can regard this singularity as a strong-coupling region between the torsion and the metric, where quantum gravity effects become essential, in close analogy with the CGHS model discussed in Chapter 4. In that case, this region should be removed from the classical spacetime description by imposing reflective boundary conditions on the singular horizon hypersurface, thereby effectively turning it into a reflective spacetime boundary.

7.3.4 Scalar electrodynamics

Here we study how a $U(1)$-localized complex scalar field theory modifies the gravitational equations of motion. Accordingly, the matter action is

$$S_{\mathrm{mat}} = -\int \mathrm{d}^2x\sqrt{-g}\Big[(D_\mu f)^* D^\mu f + V\left[|f|\right] + \frac{1}{4}\mathcal{F}_{\mu\nu}\mathcal{F}^{\mu\nu}\Big], \tag{7.344}$$

where $V\left[|f|\right]$ denotes the potential of the scalar field, and the $U(1)$-covariant derivative is defined in the usual way as $D_\mu f = \nabla_\mu f + iq\mathcal{A}_\mu f$, with q the electric charge carried by the complex scalar field particles. We begin by examining the electromagnetic sector. Varying the action with respect to the gauge field leads to

$$\nabla_\nu \mathcal{F}^{\mu\nu} = iq\Big(f^* D^\mu f - f\left(D^\mu f\right)^* \Big) \equiv J^\mu, \tag{7.345}$$

from which we recover the standard $U(1)$ current associated with the scalar field. Implementing the symmetric ansatz of Section 3.1, this equation becomes

$$\left[\frac{\mathrm{d}^2}{\mathrm{d}\bar{\mathrm{x}}^2}\left(\Lambda\mathcal{A}^{\shortparallel}\right) + 2(ql)^2F^2\mathcal{A}^{\shortparallel}\right]\xi_\mu + 2qlF^2\left[\frac{\mathrm{d}\gamma}{\mathrm{d}\bar{\mathrm{x}}} + ql\mathcal{A}^{\perp}\right]\varepsilon_{\mu\nu}\xi^\nu = 0, \tag{7.346}$$

where we use the notation introduced in Table 7.2 for the complex scalar field. As in Section 7.3.2, the component of (7.346) normal to ξ_μ shows that $\mathcal{A}^\perp$ serves as a gauge choice, since the phase γ of the complex scalar field remains arbitrary until the gauge is fixed. Consequently, only the parallel component of this equation provides a nontrivial equation of motion. We now vary the action with respect to the scalar field and obtain:

$$D_\mu D^\mu F = V'\left[F\right] \quad \Longrightarrow \quad \frac{\mathrm{d}}{\mathrm{d}\bar{\mathrm{x}}}\left(\Lambda\frac{\mathrm{d}F}{\mathrm{d}\bar{\mathrm{x}}}\right) + (ql)^2\Lambda\mathcal{A}^{\shortparallel 2}F + \frac{l^2}{2}V'\left[F\right] = 0. \tag{7.347}$$

We now turn to the gravitational sector of the theory. The EMT of the matter fields is

$$T_{\mu\nu} = (D_\mu f)^* D_\nu f + (D_\nu f)^* D_\mu f - g_{\mu\nu}\Big((D_\alpha f)^* D^\alpha f + V[F] + \frac{1}{2}\mathcal{F}^2\Big), \tag{7.348}$$

where we have employed the reduced form of the electromagnetic EMT obtained in (7.308). Implementing the symmetric ansatz yields

$$\begin{aligned} l^2\Lambda T_{\mu\nu} = &\left[\Lambda\left(\left(\frac{\mathrm{d}F}{\mathrm{d}\bar{\mathrm{x}}}\right)^2 + (ql)^2F^2\mathcal{A}^{\shortparallel 2}\right) - l^2V[F] - \frac{1}{2}\left(\frac{\mathrm{d}\left(\Lambda\mathcal{A}^{\shortparallel}\right)}{\mathrm{d}\bar{\mathrm{x}}}\right)^2\right]\xi_\mu\xi_\nu \\ &+ \left[\Lambda\left(\left(\frac{\mathrm{d}F}{\mathrm{d}\bar{\mathrm{x}}}\right)^2 + (ql)^2F^2\mathcal{A}^{\shortparallel 2}\right) + l^2V[F] + \frac{1}{2}\left(\frac{\mathrm{d}\left(\Lambda\mathcal{A}^{\shortparallel}\right)}{\mathrm{d}\bar{\mathrm{x}}}\right)^2\right]\varepsilon_{\mu\rho}\varepsilon_{\nu\sigma}\xi^\rho\xi^\sigma \end{aligned} \tag{7.349}$$

Imposing the constraints (7.296) on the energy–momentum tensor (7.349) leads to the following pair of equations:

$$\Lambda\left(\left(\frac{\mathrm{d}F}{\mathrm{d}\bar{\mathrm{x}}}\right)^2 + (ql)^2F^2\mathcal{A}^{\shortparallel 2}\right) = l^2V[F] + \frac{1}{2}\left(\frac{\mathrm{d}\left(\Lambda\mathcal{A}^{\shortparallel}\right)}{\mathrm{d}\bar{\mathrm{x}}}\right)^2, \tag{7.350}$$

$$\frac{6k\pi^2D}{\sqrt{|\Lambda|}} = \Lambda\left(\left(\frac{\mathrm{d}F}{\mathrm{d}\bar{\mathrm{x}}}\right)^2 + (ql)^2F^2\mathcal{A}^{\shortparallel 2}\right) + l^2V[F] + \frac{1}{2}\left(\frac{\mathrm{d}\left(\Lambda\mathcal{A}^{\shortparallel}\right)}{\mathrm{d}\bar{\mathrm{x}}}\right)^2. \tag{7.351}$$

Combining (7.350) and (7.351), one finds that the remaining two equations (7.346) and (7.347) become identical. Consequently, the system of equations simplifies to:

$$\left(\frac{\mathrm{d}F}{\mathrm{d}\bar{\mathrm{x}}}\right)^2 = \frac{3k\pi^2D}{\Lambda}\frac{1}{\sqrt{|\Lambda|}} - (ql)^2F^2\mathcal{A}^{\shortparallel 2}, \tag{7.352}$$

$$\left(\frac{\mathrm{d}\left(\Lambda\mathcal{A}^{\shortparallel}\right)}{\mathrm{d}\bar{\mathrm{x}}}\right)^2 = \frac{6k\pi^2D}{\sqrt{|\Lambda|}} - 2l^2V[F], \tag{7.353}$$

$$\frac{3k\pi^2D}{|\Lambda|^{3/2}}\frac{\mathrm{d}|\Lambda|}{\mathrm{d}\bar{\mathrm{x}}} = 4(ql)^2F^2\mathcal{A}^{\shortparallel}\frac{\mathrm{d}\left(\Lambda\mathcal{A}^{\shortparallel}\right)}{\mathrm{d}\bar{\mathrm{x}}} - l^2V'[F]\frac{\mathrm{d}F}{\mathrm{d}\bar{\mathrm{x}}}. \tag{7.354}$$

This system of equations can in principle be solved numerically. Nonetheless, we confine our subsequent analysis to the simplest, massless case with $V[F] = 0$. From equation (7.350) it follows that $\Lambda > 0$, and equation (7.351) further requires $D > 0$. Consequently, we are looking for cosmological solutions. Expressing the system in terms of the z coordinate (3.21) and introducing a new constant Q via $6k\pi^2D = Q^2$, we obtain:

$$\frac{\mathrm{d}\left(\Lambda\mathcal{A}^{\shortparallel}\right)}{\mathrm{d}\tau} = Q\Lambda^{1/4}, \quad \frac{\mathrm{d}\Lambda}{\mathrm{d}\tau} = \frac{8(ql)^2}{Q}F^2\Lambda\mathcal{A}^{\shortparallel}\Lambda^{3/4}, \quad \Lambda\left(\frac{\mathrm{d}F}{\mathrm{d}\tau}\right)^2 + (ql)^2F^2\left(\Lambda\mathcal{A}^{\shortparallel}\right)^2 = \frac{Q^2}{2}\sqrt{\Lambda}. \tag{7.355}$$

This system is invariant under scale transformations, which implies that all relevant fields can be expressed as power laws. A straightforward calculation leads to the solution:

$$\Lambda = \left(\frac{Qql}{3\sqrt{2}}\right)^4\mathrm{z}^8, \quad \Lambda\mathcal{A}^{\shortparallel} = \frac{Q^2ql}{9\sqrt{2}}\mathrm{z}^3, \quad F = \frac{\sqrt{3}}{ql}\mathrm{z}^{-1}. \tag{7.356}$$

Since the gauge potential itself is not directly physical, we instead determine the electric field. The resulting physical configuration of fields is

$$\mathrm{d}s^2 = -\mathrm{d}\tau^2 + \left(\frac{Qq}{3l\sqrt{2}}\right)^4\tau^8l^2\mathrm{d}r^2, \quad \mathcal{F} = \frac{3\sqrt{2}}{q}\tau^{-2}, \quad F = \frac{\sqrt{3}}{q}\tau^{-1}, \tag{7.357}$$

where we have introduced the time coordinate $\tau = lz$. The remaining fields are specified in (7.50-7.53) and are the same as in the case of the real scalar field (7.305). The cosmological singularity occurs at $\tau = 0$, where the spatial section collapses to a point, and both the electric field and the scalar field become divergent. Analogously to the case of a real scalar field, the parallel component of the contorsion displays a sequence of sudden singularities [92, 93].

Note that this does not represent the general solution of system (7.355). The system can be recast as a single first-order, second-kind Abel differential equation, which does not admit an exact closed-form solution. The solution provided here corresponds to an exact singular fixed point within the parameter space of solutions. Any other choice of initial conditions leads to phase-space trajectories that spiral around or away from this exact analytical solution, their behavior being fully determined by the aforementioned Abel differential equation.

7.3.5 Ideal fluid dynamics

In this subsection, we examine how the geometry responds to the matter content described by the energy–momentum tensor of an ideal fluid, namely:

$$T_{\mu\nu} = (p+\rho)u_\mu u_\nu + p g_{\mu\nu}. \tag{7.358}$$

Expressing this using the symmetric ansatz introduced in Section 3.1, we obtain:

$$T_{\mu\nu} = \left[(p+\rho)u^{\shortparallel 2} + \frac{p}{\Lambda}\right]\xi_\mu\xi_\nu + (p+\rho)u^{\shortparallel}u^{\perp}\left(\varepsilon_{\mu\rho}\xi_\nu + \varepsilon_{\nu\rho}\xi_\mu\right)\xi^\rho + \left[(p+\rho)u^{\perp 2} - \frac{p}{\Lambda}\right]\varepsilon_{\mu\rho}\varepsilon_{\nu\sigma}\xi^\rho\xi^\sigma. \tag{7.359}$$

To the equations (7.296), we must supplement a condition on the four–velocity, namely:

$$u_\mu u^\mu = -1 \quad \Longrightarrow \quad \Lambda\left(u^{\shortparallel 2} - u^{\perp 2}\right) = -1. \tag{7.360}$$

We first impose the condition $T^{\shortparallel\perp} = 0$. This leads to the conclusion that either $u^{\shortparallel} = 0$ or $u^{\perp} = 0$, since the choice $p + \rho = 0$ would cause the entire EMT to vanish identically.

- $\underline{u^{\shortparallel} = 0}$: In this case, the condition $T^{\shortparallel\perp} = 0$ is automatically fulfilled. From equation (7.360) we obtain the normal component of the four-velocity:

$$u^{\perp} = \pm\frac{1}{\sqrt{\Lambda}}, \tag{7.361}$$

which requires $\Lambda > 0$. Thus, we are dealing with the cosmological solution. The vanishing of the parallel component of the EMT imposes $p = 0$, while its normal component yields the density as a function of the metric function Λ:

$$p = 0 \quad \wedge \quad \rho = \frac{6k\pi^2 D}{l^2\sqrt{\Lambda}}. \tag{7.362}$$

- $\underline{u^{\perp} = 0}$: In an analogous way, the condition $T^{\shortparallel\perp} = 0$ is again satisfied, and equation (7.360) now provides the parallel component of the four-velocity:

$$u^{\shortparallel} = \pm\frac{1}{\sqrt{-\Lambda}}, \tag{7.363}$$

which enforces $\Lambda < 0$. Consequently, we are considering the static star solution, once the stellar boundary is specified and the metric is matched across this boundary to one of the general vacuum solutions of Section 7.1.1. Unlike the previous case, the constraint $T^{\parallel\parallel} = 0$ implies $\rho = 0$, and from the normal component of the EMT we obtain the pressure as a function of Λ:

$$p = -\frac{6k\pi^2 D}{l^2\sqrt{-\Lambda}}, \quad \wedge \quad \rho = 0. \tag{7.364}$$

Note that in both branches the metric function Λ remains arbitrary. This reflects the gauge freedom inherited from the underlying five-dimensional Chern–Simons theory. Consequently, any choice of metric solves the full set of equations of motion. One might say that an additional thermodynamic relation $p = p(\rho)$ is missing. However, the equations of motion already enforce that either the pressure or the density must vanish, so there is no room to introduce an extra independent equation into the system.

Conversely, one would typically prefer a setup where the spacetime metric is dynamically determined. This is only possible once an additional field is incorporated into the matter sector. For instance, including an electromagnetic field merely shifts the EMT by $T^{ED}_{\mu\nu} = -\frac{Q^2}{2} g_{\mu\nu}$ (see Section 7.3.2). In this case, the equations reduce to:

$$\begin{cases} p = \dfrac{Q^2}{2} \quad \wedge \quad \rho = \dfrac{6k\pi^2 D}{l^2\sqrt{\Lambda}} - \dfrac{Q^2}{2}, \qquad u^{\parallel} = 0, \\ p = -\dfrac{6k\pi^2 D}{l^2\sqrt{-\Lambda}} + \dfrac{Q^2}{2}, \quad \wedge \quad \rho = -\dfrac{Q^2}{2}, \quad u^{\perp} = 0. \end{cases} \tag{7.365}$$

At this stage it becomes consistent to impose an additional thermodynamic relation $p = p(\rho)$. Yet p and ρ are already fully determined in terms of the metric, so enforcing this relation restricts the solution to flat Minkowski spacetime, where both the pressure and the density of the ideal fluid turn out to be constant. If we then continuously match the $u^{\perp} = 0$ solution to a generic vacuum configuration from Section 7.1.1, the result is a perfectly homogeneous torsion star, with both the two-dimensional torsion and the θ-component of the five-dimensional torsion remaining non-zero in a BTZ background endowed with θ torsion.

Including a massless real scalar field leads to the same outcome: the equations of motion still only admit flat Minkowski spacetime with torsion. However, once a non-trivial scalar potential is introduced, the equations of motion become genuinely dynamical, and one obtains a non-constant pressure, density, and metric.

Finally, it would be worthwhile to explore the role of the Polyakov–Liouville quantum corrections (3.72) in this ideal-fluid thermodynamic framework. We anticipate that the quantum-corrected solution will select a definite metric function Λ once the condition $p = p(\rho)$ is imposed, because the Polyakov–Liouville EMT (3.79) depends explicitly on derivatives of Λ.

Chapter 8

Entanglement entropy in gravitational systems

In this chapter, we derive explicit expressions for several notions of entropy that occur in gravitational systems. As a preliminary step, we emphasize the distinction between fine–grained and coarse–grained entropy [8, 26]. These are general notions in statistical physics and information theory and are not intrinsically tied to gravitational phenomena. We clarify their role and relevance in gravitational settings in the first section of this chapter.

In the subsequent second section, we compute the fine–grained entropy in several particular setups introduced in the preceding section. We begin by analyzing the situation of a uniformly accelerated observer in the Minkowski vacuum. Such an observer perceives a thermal particle spectrum characterized by a temperature proportional to the observer's proper acceleration, a phenomenon known as the Unruh effect [120, 121, 122]. We then extend this analysis to a broader class of observers, considering both flat and curved spacetime backgrounds [26].

In the following section, we investigate matter in a coherent state, together with the quantum–corrected entropy of the black hole [26]. Our discussion is carried out within the framework of the BPP model. The characterization of the collapsing matter as a coherent state is physically motivated by the fact that, in a wide class of systems in condensed matter physics, the ground state is accurately described by a coherent state. Consequently, it is natural to assume that the matter that creates the singularity resides in its ground state. In this section, we also provide a precise formulation of what we refer to as the Hawking information paradox.

In the final section of this chapter, beginning from the main hypothesis—referred to as the central dogma—which posits that a black hole can be regarded as an ordinary quantum system up to a certain boundary surface, we derive the central result of this work, namely the formula for the fine–grained entropy in gravitational systems [1]. We then conclude with several remarks on open issues related to the black hole information paradox, including in particular the outstanding challenges associated with the reconstruction of the causal diamond (entanglement wedge reconstruction) [1].

8.1 Coarse–grained and fine–grained entropy

As previously indicated, this section has no direct connection with gravitational phenomena, since these are general concepts in physics. Broadly speaking, a fine-grained description of a system provides a detailed microscopic characterization of all its degrees of freedom. By contrast, a coarse-grained description is obtained by averaging or integrating over these microscopic details, thereby retaining only a reduced set of macroscopic or effective variables. In the following, we illustrate this distinction using a concrete example based on the notion of entropy.

The fundamental quantity used in thermodynamics is the von Neumann (Gibbs) entropy. In classical mechanics it is defined as a functional of the probability distribution of occupied states over phase space, $\rho(\vec{p}, \vec{q})$,

$$S_{FG}[\rho] = -k_B \int \left(\prod_{i=1}^{n} dp_i dq_i \right) \rho \ln \rho, \tag{8.1}$$

where k_B denotes the Boltzmann constant, and n represents the dimensionality of the configuration space. This is an example of a fine–grained quantity, as it is constructed directly from the microscopic distribution function ρ. Consequently, it encodes the complete set of microscopic details pertaining to the system under consideration and is, by definition, fine–grained. In particular, it is well defined at every point in phase space. Moreover, by Liouville's theorem, which implies $\frac{d\rho}{dt} = 0$ along Hamiltonian trajectories, the associated entropy remains exactly conserved in time. Therefore, this entropy—often identified with the von Neumann (or Gibbs) entropy in the classical limit—cannot be regarded as thermodynamic entropy, since it does not increase with time.

Gibbs introduced a systematic procedure for constructing a coarse–grained quantity from the fine–grained quantity ρ. Specifically, one partitions the phase space into a collection of cells and, within each cell, performs a local averaging of ρ. This averaging procedure yields the coarse–grained quantity $\bar{\rho}$. This clarifies the distinction between "coarse–grained" and "fine–grained" descriptions: the former corresponds to a smoothed, cell-averaged representation of the latter. On this basis, one can now define the coarse–grained entropy in analogy with the von Neumann entropy, but formulated in terms of the coarse–grained distribution $\bar{\rho}$:

$$S_{CG}[\bar{\rho}] = -k_B \int \left(\prod_{i=1}^{n} dp_i dq_i \right) \bar{\rho} \ln \bar{\rho}, \tag{8.2}$$

$$\bar{\rho}(x) = \sum_{C} p_\rho(C) \rho_C(x), \quad p_\rho(C) = \int_C \rho(x) \left(\prod_{i=1}^{n} dp_i dq_i \right). \tag{8.3}$$

Here, we have extracted the macroscopic properties from the quantity ρ, as they are completely encoded in the coarse-grained quantity $\bar{\rho}$. This coarse-graining procedure is precisely what the entropy is intended to capture. With this definition, the entropy constructed from $\bar{\rho}$ is consistent with, and indeed satisfies, the second law of thermodynamics. There is, however, an alternative way to elucidate the distinction between these types of entropy. In the case of quantum mechanical systems, the fine-grained (von Neumann) entropy is given by:

$$S_{FG} = -k_B \operatorname{Tr}\{\hat{\rho} \ln \hat{\rho}\} \quad \text{and} \quad \langle \hat{A} \rangle_\rho = \operatorname{Tr}\left\{ \hat{\rho} \hat{A} \right\}, \ \forall \hat{A}, \tag{8.4}$$

where $\hat{\rho}$ denotes the density matrix of the system under consideration. For a system prepared in a pure state, this quantity becomes equal to zero. It therefore quantifies the deviation of the system from a pure state, that is, the degree of statistical uncertainty (or lack of information) of the state of the system. The key property of the density matrix — which encodes the maximal microscopic information accessible about the system— is expressed in the second equation given above. This relation indicates that, using the density matrix, one can compute the expectation value of any observable of the system.

In practice, one typically does not measure the complete set of observables of a system, but rather restricts attention to those that are of macroscopic relevance, hereafter referred to as coarse–grained quantities. We denote this selected set of observables by $\left\{\hat{A}_i\right\}$. Consider now the set of all density operators $\tilde{\rho}$ that satisfy the following condition:

$$\mathrm{Tr}\left\{\tilde{\rho}\hat{A}_i\right\} = \mathrm{Tr}\left\{\hat{\rho}\hat{A}_i\right\}, \ \forall \hat{A}_i, \tag{8.5}$$

and compute the von Neumann entropy for each of these density matrices, subsequently maximizing this functional. The density matrix $\tilde{\rho}$ that maximizes the von Neumann entropy is identified as the coarse–grained density matrix $\bar{\rho}$. The corresponding value of the entropy is then interpreted as the thermodynamic entropy. This construction is equivalent to the standard coarse–graining procedure employed in classical statistical mechanics.

From the very definitions of these entropies, it directly follows that the fine–grained entropy is always less than or equal to the coarse–grained entropy, i.e., $S_{\mathrm{FG}} \leq S_{\mathrm{CG}}$. This inequality is evident because we can always choose $\tilde{\rho} = \hat{\rho}$, which in general does not maximize the entropy, whereas $\bar{\rho}$ does. Equivalently, one may interpret S_{CG} as a measure of the effective total number of degrees of freedom accessible to the system, thus providing an upper bound on the amount of entanglement that the system can share with another system.

8.1.1 Fine-grained entropy in gravitation

Thus far, we have analyzed entropy in a general context. We now turn to its specific implications for gravitational systems. In particular, we aim to clarify the physical meaning of the von Neumann entropy in a gravitational setting—most notably for quantum fields in curved spacetime, such as Hawking radiation—and to identify and characterize the coarse–grained entropy associated with a black hole.

When we seek the entropy of the radiation outside the black hole, we are necessarily dealing with a fine–grained entropy, since it represents a subsystem of the full quantum gravitational system: in effect, the degrees of freedom associated with the black hole itself have been traced out. To understand this more concretely, consider a stationary observer located asymptotically far from the black hole. For such an observer, there exists a finite spacetime region that is causally inaccessible. This inaccessible region is bounded by the apparent horizon of the black hole, since light cannot escape from it. This implies the existence of degrees of freedom localized behind the event horizon, to which the external observer has no access. Assuming that the black hole forms from the gravitational collapse of matter initially prepared in a pure quantum state, the state of the entire system, consisting of the black hole and its Hawking radiation—remains pure, denoted by $|\psi\rangle$, at all times. Nevertheless, based on the considerations in the preceding paragraph, the stationary observer cannot access all of the degrees of freedom associated with this global state. The density operator corresponding to the full system is given by $\hat{\rho} = |\psi\rangle\langle\psi|$. Hawking radiation accessible to the observer is quantum-mechanically entangled with the degrees of freedom residing inside the black hole, the reduced density matrix actually measured by the observer is obtained by taking the partial trace over the degrees of freedom beneath the apparent horizon:

$$\hat{\rho}_{out} = \mathrm{Tr}_{in}\{|\psi\rangle\langle\psi|\}. \tag{8.6}$$

The total information related to the Hawking radiation observed by the observer at infinity is contained in this density matrix. From it we obtain both the temperature of the radiation and all correlations that may arise within it. The next step is to determine the entropy of the radiation. We define it as the von Neumann entropy given in terms of the density matrix $\hat{\rho}_{out}$:

$$S_{FG} = -k_B\,\mathrm{Tr}\{\hat{\rho}_{out}\ln\hat{\rho}_{out}\}. \tag{8.7}$$

In this trace, it is explicitly assumed that the relevant region of spacetime lies within the domain containing Hawking radiation. This means that when evaluating this quantity, it is first necessary to specify a spacelike hypersurface Σ (that is, a hypersurface of constant coordinate time, $t=$ const.). This hypersurface determines the instant at which the entropy is measured. In this manner, an explicit time dependence is introduced directly into the expression for S_{FG}. We then define the spatial region A' in which live the degrees of freedom accessible to the observer, as the causal diamond over some part of the hypersurface Σ. The remainder of the hypersurface Σ defines one or more causal diamonds, where the degrees of freedom are inaccessible to the observer. We denote this region by A. When computing S_{FG}, we trace the degrees of freedom living in region A. What holds is that the quantity S_{FN} associated with region A is equal to the corresponding quantity S_{FN} associated with region A', because along the region A the quantum state is pure on the combined region $(A \cup A')$ [8, 26].

In the case of a black hole A, this region is defined as the causal diamond over the part of the hypersurface Σ lying beneath the apparent horizon. This was considered to be the correct way to determine the fine–grained entropy in gravitational systems. However, this method is not consistent with the unitarity of quantum mechanics, and thus we encounter a problem. The resolution comes with the introduction of islands [1]. We discuss them in more detail in the fourth section of this chapter. Therefore, the entropy obtained in this way is referred to as the von Neumann entropy rather than the fine–grained entropy in gravitational systems. It remains important, since it constitutes a part of the formula for fine–grained entropy in gravitational systems.

In the next section we calculate the von Neumann entropy $S_{FN}(\Sigma)$ for different regions A. First, we analyze the Unruh effect. This is the case when the region A is the entire left quadrant of Minkowski spacetime. Then, we generalize the obtained result to an arbitrary region in Minkowski spacetime. The next step is to generalize these results to curved spacetime. Finally, we determine what happens when we are in a spacetime that has a boundary, with reflective boundary conditions defined on it, as in the dynamical scenario in the BPP model.

In Figure 8.1, an arbitrary region $A = [x_1^+, x_2^+] \times [x_1^-, x_2^-]$ is shown. The spacelike hypersurface Σ is depicted by the green line. It passes through the points (x_1^+, x_2^-) and (x_2^+, x_1^-). However, whichever hypersurface we choose, as long as it passes through these two points, the value of the von Neumann entropy is the same. This is a consequence of the fact that the entropy depends only on the spacetime interval between these points, i.e., on the area of this causal diamond [1]. Therefore, we say that the entropy is associated with the causal diamond, and not with the hypersurface.

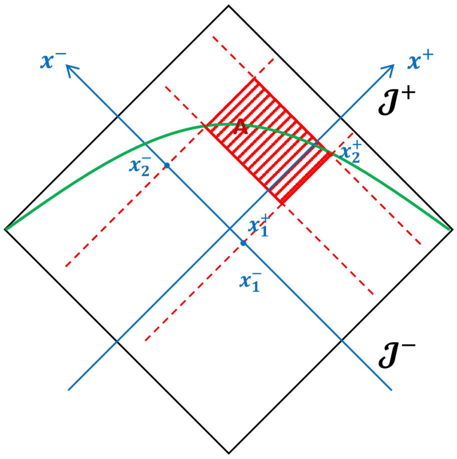

Figure 8.1: Arbitrary region A that contains the inaccessible degrees of freedom.

In the previous chapter we dealt with various gravitational models, but the matter was always represented by massless scalar fields. Now we see why this was important, i.e., how much it simplifies the calculation of entropy. Namely, the Klein–Gordon equation $\Box\phi = 0$ reduces to $\partial_+\partial_-\phi = 0$, as we saw in Section 2.2.4 when discussing the transformation properties of the energy–momentum tensor. The solution of this equation is $\phi(x^+, x^-) = \phi_+(x^+) + \phi_-(x^-)$. Consequently, the left–propagating modes are completely independent of the right–propagating modes. This also allows us to compute the entropy independently, i.e., first determine the entropy arising from the right–propagating modes, then from the left–propagating modes, and finally add them together to obtain the total entropy. However, this is no longer true when we have collapse, because in that case there is a boundary with reflective boundary conditions. In such a situation the modes are no longer independent, and it is necessary to separately analyze what happens in this case.

8.2 Von Neumann entropy in gravity

As already mentioned in the previous section, in this section we determine the von Neumann entropy in different cases of the region A that is inaccessible to a given observer. First, we deal with the Unruh effect, the phenomenon in which a uniformly accelerated observer detects a thermal spectrum of particles. The specific coordinates used to describe this reference system are called Rindler coordinates. The derivation of these coordinates and their relation to the uniformly accelerated observer is presented in Appendix B (Section B.3). In the present context, we restrict ourselves to their utilization.

Throughout, we initially restrict our analysis to the right–propagating modes. The contribution from the left–propagating modes is subsequently incorporated by analogy, as their respective contributions to the entropy are mutually independent. Furthermore, we denote the coordinates in which the quantum vacuum is defined by $x^{\pm}$, and those corresponding to the observer by $\sigma^{\pm}$. In this section we consistently use the facts from Appendix B, related to quantum field theory in curved spacetime.

8.2.1 Minkowski vacuum and region type: $A = (-\infty, 0] \times [0, +\infty)$

This choice of region A corresponds to a uniformly accelerated observer. Here we apply Unruh's method for determining the Bogoliubov coefficients (see Appendix D.3 as well as [122]). The main idea we use lies in the fact that entropy does not depend on the basis of functions we choose. Therefore, we can select modes in convenient coordinates. Since the case corresponds to a Rindler observer, we choose Rindler coordinates.

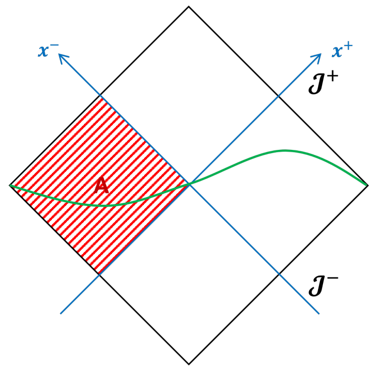

Figure 8.2: Region A that contains the inaccessible degrees of freedom in a case of the Rindler observer.

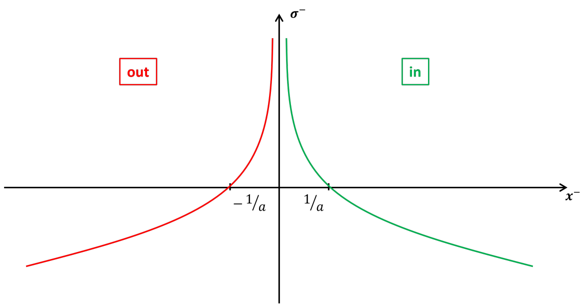

Figure 8.3: Function $\sigma^- = \sigma^-(x^-)$ for the case of Rindler observer.

The Rindler coordinates are given by the following relation (see Appendix D.3): $\sigma^-_{out} = -\frac{1}{a}\ln(-ax^-) \ \wedge \ \sigma^-_{in} = -\frac{1}{a}\ln(ax^-)$. The constant a represents the acceleration of the Rindler observer. We notice that they can be combined using the absolute value:

$$\sigma^- = -\frac{1}{a}\ln\left|ax^-\right|. \tag{8.8}$$

In Figure 8.3, the graph of the dependence of this function is shown.

The first thing we need to do is determine the positive–frequency modes. For the right–propagating waves in the region A', we have:

$$\partial_t\phi^\omega = -i\omega\phi^\omega \implies \frac{d\phi^\omega_{out}}{d\sigma^-_{out}} = -i\omega\phi^\omega_{out} \implies \phi^\omega_{out} = \frac{1}{\sqrt{4\pi\omega}}\theta(-x^-)e^{-i\omega\sigma^-_{out}}. \tag{8.9}$$

In the left quadrant (i.e., region A) the timelike Killing vector, which we use here to define the modes, changes direction, and for this reason there is no "$-$" on the right–hand side of the defining equation for the modes:

$$\partial_{-t}\phi^\omega = -i\omega\phi^\omega \implies \frac{d\phi^\omega_{in}}{d\sigma^-_{in}} = i\omega\phi^\omega_{in} \implies \phi^\omega_{in} = \frac{1}{\sqrt{4\pi\omega}}\theta(x^-)e^{i\omega\sigma^-_{in}}. \tag{8.10}$$

From Section 2.2.4 3.3 we know that the normalization constant is given by: $\frac{1}{\sqrt{4\pi\omega}}$ (Equation (3.86)). These are the modes defined in their respective regions A' and A. Therefore, the field can be expanded in terms of them in the following way:

$$\phi_- = \int_0^\infty d\omega \left[a_{out}(\omega)\phi^\omega_{out} + a_{in}(\omega)\phi^\omega_{in} + a^\dagger_{out}(\omega)\phi^{\omega*}_{out} + a^\dagger_{in}(\omega)\phi^{\omega*}_{in}\right]. \tag{8.11}$$

The correct method would now be to use the Minkowski modes and determine the Bogoliubov coefficients (see Appendix D.2). However, this is a very demanding problem, so here we apply Unruh's trick [122]. We want to express the Rindler modes in terms of the Minkowski coordinates $x^{\pm}$ and analytically continue them to the entire spacetime. If we succeed, we obtain a set of mutually orthogonal modes defined over the whole Minkowski spacetime and expressed in Minkowski coordinates. This means that we have obtained a basis in Minkowski coordinates. This basis must also correspond to the Minkowski vacuum, so in fact we have obtained the Minkowski modes. We begin with the ϕ^{ω}_{out} mode and attempt to analytically continue it to the entire spacetime:

$$\begin{aligned}
\phi^{\omega}_{out} &= \frac{1}{\sqrt{4\pi\omega}}\theta(-x^-)e^{-i\omega\sigma^-_{out}} = \frac{1}{\sqrt{4\pi\omega}}\theta(-x^-)\left(-ax^-\right)^{\frac{i\omega}{a}} \\
\phi^{\omega}_{in} &= \frac{1}{\sqrt{4\pi\omega}}\theta(x^-)e^{i\omega\sigma^-_{in}} = \frac{1}{\sqrt{4\pi\omega}}\theta(x^-)\left(ax^-\right)^{-\frac{i\omega}{a}} \\
\phi^{\omega*}_{in} &= \frac{1}{\sqrt{4\pi\omega}}\theta(x^-)\left(ax^-\right)^{\frac{i\omega}{a}} = \frac{1}{\sqrt{4\pi\omega}}\theta(x^-)\left(-e^{-i\pi}ax^-\right)^{\frac{i\omega}{a}} = \frac{1}{\sqrt{4\pi\omega}}e^{\frac{\pi\omega}{a}}\theta(x^-)\left(-ax^-\right)^{\frac{i\omega}{a}} \\
\phi^{\omega*}_{out} &= \frac{1}{\sqrt{4\pi\omega}}\theta(-x^-)\left(-ax^-\right)^{-\frac{i\omega}{a}} = \frac{1}{\sqrt{4\pi\omega}}\theta(-x^-)\left(e^{i\pi}ax^-\right)^{-\frac{i\omega}{a}} = \frac{1}{\sqrt{4\pi\omega}}e^{\frac{\pi\omega}{a}}\theta(-x^-)\left(ax^-\right)^{-\frac{i\omega}{a}} \\
&\implies \phi^{\omega}_{out} + e^{-\frac{\pi\omega}{a}}\phi^{\omega*}_{in} = \frac{1}{\sqrt{4\pi\omega}}\left[\theta(-x^-)+\theta(x^-)\right]\left(-ax^-\right)^{\frac{i\omega}{a}} = \frac{1}{\sqrt{4\pi\omega}}\left(-ax^-\right)^{\frac{i\omega}{a}} \propto \phi^{\omega}_1
\end{aligned} \tag{8.12}$$

$$\implies \phi^{\omega}_{in} + e^{-\frac{\pi\omega}{a}}\phi^{\omega*}_{out} = \frac{1}{\sqrt{4\pi\omega}}\left[\theta(-x^-)+\theta(x^-)\right]\left(ax^-\right)^{-\frac{i\omega}{a}} = \frac{1}{\sqrt{4\pi\omega}}\left(ax^-\right)^{-\frac{i\omega}{a}} \propto \phi^{\omega}_2. \tag{8.13}$$

We observe that, by adding the term proportional to $\phi^{\omega*}_{\text{in}}$, we obtain a mode that is well defined everywhere in Minkowski spacetime. It is now necessary to clarify why, in the third line, we used the representation $-1 = e^{-i\pi}$, whereas in the fourth line we wrote $-1 = e^{i\pi}$. The underlying reason is that we require the Minkowski modes to be well defined throughout the whole spacetime under analytic continuation of x^- into the complex plane. To this end, let us examine the analyticity condition for the mode $f^{\omega}_{-} \propto e^{-i\omega x^-}$ in the limit $x^- \to \infty$. We see that $f^{\omega}_{-} \propto e^{i\omega\,\mathrm{Re}\{x^-\}+\omega\,\mathrm{Im}\{x^-\}}$, and thus conclude that $\mathrm{Im}\{x^-\} < 0$. In the third line, we attempt to move from the point x^- to the point $-x^-$ in the complex plane. From $\mathrm{Im}\{x^-\} < 0$, we know that they must be connected through the lower half–plane, so we perform a rotation by $-\pi$, thereby acquiring the phase $e^{-i\pi}$, since this corresponds to the negative mathematical direction. In the fourth line we move from the point $-x^-$ back to the point x^-, again through the lower half–plane, thereby acquiring the phase $e^{i\pi}$, since this corresponds to the positive mathematical direction. The foregoing analysis is equivalent to imposing the condition that for the Minkowski modes to be analytic in the whole complex plane, the branch cut of the power function needs be placed in the upper half–plane. The next step is the normalization of the modes $\phi^{\omega}_{1,2}$:

$$\begin{aligned}
(\phi^{\omega}_{1,2}, \phi^{\omega'}_{1,2}) &= C^{\omega}_{1,2}C^{\omega'*}_{1,2}\left[(\phi^{\omega}_{out,in}, \phi^{\omega'}_{out,in}) + e^{-\frac{2\pi\omega}{a}}(\phi^{\omega*}_{in,out}, \phi^{\omega'*}_{in,out})\right] \\
&= \left|C^{\omega}_{1,2}\right|\left(1+e^{-\frac{2\pi\omega}{a}}\right)\delta(\omega-\omega').
\end{aligned} \tag{8.14}$$

Thus, the Minkowski modes (operators) are expressed in terms of the Rindler modes (operators) in the following way:

$$\begin{aligned}
\phi_1^\omega &= \frac{1}{\sqrt{2\sinh\frac{\pi\omega}{a}}}\left[\phi_{out}^\omega e^{\frac{\pi\omega}{2a}} + \phi_{in}^{\omega *} e^{-\frac{\pi\omega}{2a}}\right]; a_1(\omega) &= \frac{1}{\sqrt{2\sinh\frac{\pi\omega}{a}}}\left[a_{out}(\omega)e^{\frac{\pi\omega}{2a}} - a_{in}^\dagger(\omega)e^{-\frac{\pi\omega}{2a}}\right] \\
\phi_2^\omega &= \frac{1}{\sqrt{2\sinh\frac{\pi\omega}{a}}}\left[\phi_{in}^\omega e^{\frac{\pi\omega}{2a}} + \phi_{out}^{\omega *} e^{-\frac{\pi\omega}{2a}}\right]; a_2(\omega) &= \frac{1}{\sqrt{2\sinh\frac{\pi\omega}{a}}}\left[a_{in}(\omega)e^{\frac{\pi\omega}{2a}} - a_{out}^\dagger(\omega)e^{-\frac{\pi\omega}{2a}}\right]
\end{aligned} \tag{8.15}$$

We immediately observe that the Bogoliubov coefficients have been obtained. The set of modes $\{\phi_1^\omega, \phi_2^\omega \,|\, \omega \in \mathbb{R}_0^+\}$ constitutes a complete basis in the Hilbert space associated with fields on Minkowski spacetime, and consequently the annihilation operators defined above must annihilate the Minkowski vacuum. This procedure is commonly referred to as Unruh's trick. Its primary purpose is to express the Minkowski vacuum state $|0_M\rangle$ as a superposition of Fock states supported in the left and right Rindler wedges.In the general case, this expansion can be written in the following way:

$$|0_M\rangle = \sum_{n_1,\ldots,n_s=0}^{\infty} \sum_{m_1,\ldots,m_s=0}^{\infty} A_{n_1 n_2 \ldots n_s}^{m_1 m_2 \ldots m_s} |n_1, n_2, \ldots, n_s, out\rangle \otimes |m_1, m_2, \ldots, m_s, in\rangle\,, \tag{8.16}$$

where $\{|n\rangle \,|\, n \in \{1, 2, \ldots, s\}\}$ denotes a basis of the single–particle state space in the *in/out* sector, and $A_{n_1 n_2 \ldots n_s}^{m_1 m_2 \ldots m_s}$ are expansion coefficients to be determined. We fix the dimension of this single–particle state space to be s, without, however, restricting ourselves to the case in which s is finite. The corresponding basis of the Fock space, constructed from Slater permanents, is then given by:

$$|n_1, n_2, \ldots, n_s, in/out\rangle = \frac{\left(a_{in/out}^\dagger(\omega_1)\right)^{n_1} \ldots \left(a_{in/out}^\dagger(\omega_s)\right)^{n_s}}{\sqrt{n_1! n_2! \ldots n_s!}} \left|0_{in/out}\right\rangle, \tag{8.17}$$

where $\{\omega_n \,|\, n \in \{1, 2, \ldots, s\}\}$ are the single–particle eigenenergies corresponding to the eigenstates of $\{|n\rangle \,|\, n \in \{1, 2, \ldots, s\}\}$. We see that everything has been discretized, since this makes the notation simpler for calculations. The analogous statement holds in the continuous case as well. The Minkowski vacuum is defined as the vacuum annihilated by the Minkowski annihilation operators, i.e.:

$$(\forall k \in \{1, 2, .., s\}) \;\; a_1(\omega_k)\,|0_M\rangle = 0, \tag{8.18}$$

$$a_2(\omega_k)\,|0_M\rangle = 0. \tag{8.19}$$

By solving the system of equations obtained from these two conditions and by directly applying the defining actions of annihilation and creation operators on the basis in Fock space, we obtain the following relations for the coefficients in the expansion:

$$(\forall k \in \{1, 2, \ldots, s\}) \;\; A_{n_1 n_2 \ldots n_s}^{m_1 m_2 \ldots m_s} = \sqrt{\frac{m_k}{n_k}}\, e^{-\frac{\pi\omega_k}{a}} A_{n_1 \ldots n_k - 1 \ldots n_s}^{m_1 \ldots m_k - 1 \ldots m_s} \tag{8.20}$$

$$A_{n_1 n_2 \ldots n_s}^{m_1 m_2 \ldots m_s} = \sqrt{\frac{n_k}{m_k}}\, e^{-\frac{\pi\omega_k}{a}} A_{n_1 \ldots n_k - 1 \ldots n_s}^{m_1 \ldots m_k - 1 \ldots m_s}. \tag{8.21}$$

The relation (8.20) is obtained by solving the Equation (8.18), whereas the relation (8.21) is derived from the Equation (8.19). We immediately observe that $n_k = m_k$, $\forall k$, so we can write:

$$A_{n_1 n_2 \ldots n_s}^{m_1 m_2 \ldots m_s} = \alpha_{n_1 n_2 \ldots n_s} \delta_{n_1 m_1} \delta_{n_2 m_2} \ldots \delta_{n_s m_s} \tag{8.22}$$

$$\alpha_{n_1 n_2 \ldots n_s} = e^{-\frac{\pi\omega_k}{a}} \alpha_{n_1 \ldots n_k - 1 \ldots n_s}, \;\; \forall k. \tag{8.23}$$

At this stage, the determination of all coefficients in the expansion becomes straightforward. By successively lowering the coefficient k from n_k to 0, we generate n_k factors of the exponential term $e^{-\frac{\pi\omega_k}{a}}$. If we reduce all the coefficients to zero and denote $\alpha_{00\ldots0} = C$, we obtain:

$$|0_M\rangle = C \sum_{n_1,n_2,\ldots,n_s=0}^{\infty} e^{-\frac{\pi}{a}\sum_{k=1}^{s} n_k\omega_k} |n_1, n_2, ..., n_s, out\rangle \otimes |n_1, n_2, ..., n_s, in\rangle . \tag{8.24}$$

In this context, it is evident that C represents the normalization constant. What remains is to determine it:

$$1 = \langle 0_M|0_M|0_M|0_M\rangle = |C|^2 \left(\sum_{n_1=0}^{\infty} e^{-\frac{2\pi n_1\omega_1}{a}}\right)\left(\sum_{n_2=0}^{\infty} e^{-\frac{2\pi n_2\omega_2}{a}}\right) \ldots \left(\sum_{n_s=0}^{\infty} e^{-\frac{2\pi n_s\omega_s}{a}}\right). \tag{8.25}$$

Therefore, the Minkowski vacuum is given by:

$$|0_M\rangle = \sqrt{\prod_{k=1}^{s}\left(1 - e^{-\frac{2\pi\omega_k}{a}}\right)} \sum_{n_1,\ldots,n_s=0}^{\infty} e^{-\frac{\pi}{a}\sum_{k=1}^{s} n_k\omega_k} |n_1, ..., n_s, out\rangle \otimes |n_1, ..., n_s, out\rangle . \tag{8.26}$$

This formula can be written in a more compact form by explicitly expanding the state in the Fock basis. After a straightforward calculation, we obtain:

$$|0_M\rangle = \sqrt{\prod_{k=1}^{s}\left(1 - e^{-\frac{2\pi\omega_k}{a}}\right)} \exp\left\{\sum_{k=1}^{s} e^{-\frac{\pi\omega_k}{a}} a^\dagger_{out}(\omega_k) \otimes a^\dagger_{in}(\omega_k)\right\} |0_{out}\rangle \otimes |0_{in}\rangle . \tag{8.27}$$

The subsequent step is to determine the density matrix as perceived by a uniformly accelerated observer, under the assumption that an inertial observer in Minkowski spacetime detects no particle flux, i.e., that the quantum state is the Minkowski vacuum. This density matrix is obtained by performing a partial trace over the degrees of freedom associated with region A:

$$\begin{aligned}\hat{\rho}_{out} &= \mathrm{Tr}_{in}\{|0_M\rangle\langle 0_M|\} \qquad (8.28)\\ &= \sum_{n_1,n_2,\ldots,n_s=0}^{\infty} \langle n_1, ..., n_s, in|0_M|n_1, ..., n_s, in|0_M\rangle \langle 0_M|n_1, ..., n_s, in|0_M|n_1, ..., n_s, in\rangle\end{aligned}$$

$$\hat{\rho}_{out} = \left[\prod_{k=1}^{s}\left(1 - e^{-\frac{2\pi\omega_k}{a}}\right)\right] \sum_{n_1,\ldots,n_s=0}^{\infty} e^{-\frac{2\pi}{a}\sum_{k=1}^{s} n_k\omega_k} |n_1, ..., n_s, out\rangle \langle n_1, ..., n_s, out| . \tag{8.29}$$

The first observation is that the resulting density matrix is diagonal. Moreover, using the fact that the energy of the state $|n_1, n_2, \ldots, n_s, out\rangle$ is equal to $\sum_{k=1}^{s} n_k\omega_k$, we conclude that the emitted radiation is described by a thermal state. The prefactor in front of expression (8.29) can be identified with the inverse partition function, while the corresponding temperature is easily determined as follows:

$$\hat{\rho}_{out} = \frac{1}{\mathcal{Z}} e^{-\beta H} \quad \Longrightarrow \quad \mathcal{Z} = \prod_{k=1}^{s} \frac{1}{1 - e^{-\frac{2\pi\omega_k}{a}}} \quad \wedge \quad T = \frac{a}{2\pi}. \tag{8.30}$$

It is now evident that we have rigorously recovered the Bose–Einstein distribution for a one–dimensional gas [8]. Consequently, we have established that a uniformly accelerated observer (the Rindler observer) detects a thermal flux of particles characterized by a temperature proportional to the magnitude of the observer's proper acceleration, Equation (8.30). The final goal of this section is to determine the von Neumann entropy associated with the radiation as measured by the Rindler observer (throughout, we adopt units in which $k_B = 1$):

$$
\begin{aligned}
S_{FN} &= -\operatorname{Tr}\{\hat{\rho}_{out} \ln \hat{\rho}_{out}\} = -C^2 \sum_{n_1, n_2, \ldots n_s = 0}^{\infty} e^{-\frac{2\pi}{a}\sum_{k=1}^{s} n_k \omega_k} \ln\left(C^2 e^{-\frac{2\pi}{a}\sum_{k=1}^{s} n_k \omega_k}\right) \\
&= -\ln C^2 + \frac{2\pi}{a} C^2 \sum_{n_1, n_2, \ldots, n_s = 0}^{\infty} e^{-\frac{2\pi}{a}\sum_{k=1}^{s} n_k \omega_k} (n_1\omega_1 + n_2\omega_2 + \ldots + n_s\omega_s) \\
&= -\ln C^2 + \frac{2\pi}{a} C^2 \left[\left(\sum_{n_1=0}^{\infty} e^{-\frac{2\pi n_1 \omega_1}{a}} n_1\omega_1\right)\left(\sum_{n_2=0}^{\infty} e^{-\frac{2\pi n_2 \omega_2}{a}}\right) \ldots \left(\sum_{n_s=0}^{\infty} e^{-\frac{2\pi n_s \omega_s}{a}}\right) + \ldots\right] \\
&= -\ln C^2 + \frac{2\pi}{a} \sum_{k=1}^{s} \frac{\sum_{n=0}^{\infty} e^{-\frac{2\pi n \omega_k}{a}} n\omega_k}{\sum_{n=0}^{\infty} e^{-\frac{2\pi n \omega_k}{a}}} = -\sum_{k=1}^{s} \ln\left(1 - e^{-\frac{2\pi\omega_k}{a}}\right) + \frac{2\pi}{a} \sum_{k=1}^{s} \frac{\omega_k}{e^{\frac{2\pi\omega_k}{a}} - 1} \\
&= -\frac{L}{2\pi} \int_0^{\infty} d\omega \ln\left(1 - e^{-\frac{2\pi\omega}{a}}\right) + \frac{L}{a} \int_0^{\infty} \frac{\omega d\omega}{e^{\frac{2\pi\omega}{a}} - 1} \qquad (8.31) \\
&= \frac{L}{2\pi}\left[-\omega \ln\left(1 - e^{-\frac{2\pi\omega}{a}}\right)\Big|_0^{\infty} + \int_0^{\infty} \frac{\omega d\omega}{1 - e^{-\frac{2\pi\omega}{a}}} \left(-e^{-\frac{2\pi\omega}{a}}\right)\left(-\frac{2\pi}{a}\right)\right] + \frac{L}{a} \int_0^{\infty} \frac{\omega d\omega}{e^{\frac{2\pi\omega}{a}} - 1}
\end{aligned}
$$

In the fifth line we have replaced the discrete sum by a continuous integral. The quantity L denotes the dimension of spacetime expressed in the σ^- coordinates, which are naturally adapted to the Rindler observer. In the final line we have carried out an integration by parts. The boundary contribution vanishes, while the remaining two terms coincide. Continuing the computation yields:

$$
S_{FN} = \frac{2L}{a} \int_0^{\infty} \frac{\omega d\omega}{e^{\frac{2\pi\omega}{a}} - 1} = \frac{2L}{a}\left(\frac{a}{2\pi}\right)^2 \int_0^{\infty} \frac{\xi d\xi}{e^{\xi} - 1} = \frac{aL}{2\pi^2}\frac{\pi^2}{6} = \frac{aL}{12} \Longrightarrow S_{FN} = \frac{\pi LT}{6}. \qquad (8.32)
$$

We have obtained the entropy of a one–dimensional gas [8]. This is in agreement with the expected result. The only remaining task is to determine the length L. It represents the length of the interval in the σ^-_{out} coordinates. However, this length is infinite, since $\sigma^-_{out} \in (-\infty, \infty)$. This means that we must introduce certain ultraviolet $X^-_{\min}$ (UV) and infrared $X^-_{\max}$ (IR) cut–offs [26]. We define them in globally flat coordinates, i.e. in the x^- coordinates. Therefore:

$$
S_{FN} = \frac{aL}{12} = \frac{a}{12}\left[\max\{\sigma^-_{in}\} - \min\{\sigma^-_{in}\}\right] = \frac{\cancel{a}}{12}\frac{1}{\cancel{a}} \ln\frac{X^-_{\max}}{X^-_{\min}} = \frac{1}{12} \ln\frac{X^-_{\max}}{X^-_{\min}}. \qquad (8.33)
$$

In addition to representing the acceleration of the Rindler observer, parameter a also defines the trajectory of that observer (see Appendix D.3). We observe that the result is independent of the trajectory, that is, on the hypersurface passing through the endpoints of the region A, just as expected. In our setup, the ultraviolet (UV) parameter characterizes infinitesimal length scales in the neighborhood of the point $x^- = 0$. Therefore, it is sometimes called the short–distance parameter and is denoted by δ^-. In order to compute the total entropy of the radiation perceived by a Rindler observer, it is necessary to incorporate both the right–propagating and left–propagating modes. The inclusion of the left–propagating modes introduces only the additional parameters $X^+_{\max/\min}$, and thus the total entropy can be expressed as [26]:

$$
S_{FN} = \frac{1}{12} \ln\frac{X^+_{max} X^-_{max}}{\delta^2}. \qquad (8.34)
$$

Here we have introduced the short–distance parameter $\delta = \sqrt{\delta^+\delta^-}$, which constitutes a Lorentz-invariant quantity, in contrast to the individual components $\delta^\pm$, which do not possess Lorentz invariance. The divergent behavior observed in the vicinity of $x^- = 0$ arises from the entanglement between the field modes localized infinitesimally to the left of this point and those localized infinitesimally to its right. This implies that the parameter δ is always present, even when the region A is finite. This does not constitute an issue, since it is a quantity invariant under all spacetime symmetries and therefore does not affect any physical observable or intermediate step in the computation, behaving as an integration constant. One can also perform a renormalization of entropy to resolve this issue. We may further note that the logarithmic behavior of the entropy is expected due to the invariance of entropy under scaling of vacuum fluctuations of a massless scalar field.

Finally, it is important to examine certain properties of the transformation $\sigma^- = \sigma^-(x^-)$, in order to facilitate its generalization to more complex problems:

- The mappings $\sigma^-_{out}(x^-)$ and $\sigma^-_{in}(x^-)$ are bijective on their respective domains; consequently, each admits a well-defined inverse function.
- The coordinate σ^- takes values over the entire real line, $(-\infty, +\infty)$, in both regions.
- The time coordinate associated with σ^- evolves in opposite directions in the regions A and A'. This behavior is linked to the differing monotonic properties of the functions σ_{in} and σ_{out}.
- At the boundary between the regions A and A', both functions converge to the same limiting value (in this case $+\infty$). Consequently, it is possible to define an analytic continuation across this boundary.

In the remainder of this section, we follow the derivations presented in [26].

8.2.2 Minkowski vacuum and region type: $A = [x_1^+, x_2^+] \times [x_1^-, x_2^-]$

We now extend the results derived in the preceding section to an arbitrary finite region A. As previously demonstrated, the central idea consists in selecting an appropriate coordinate system satisfying the conditions formulated at the end of the previous section, thereby achieving a clear and unambiguous separation between the regions A and A'. In Figure 8.4, an arbitrary region A is depicted. The constant a appearing here has no interpretation as acceleration; rather, it is included solely to ensure dimensional consistency. This parameter specifies the exact form of the trajectory within region A [123].

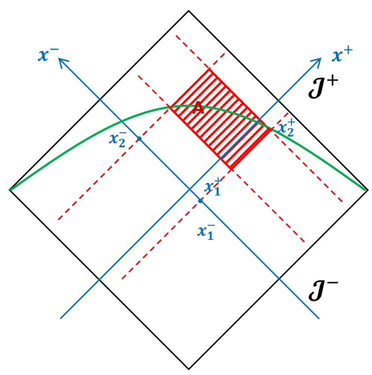

Figure 8.4: Arbitrary region A that contains the inaccessible degrees of freedom.

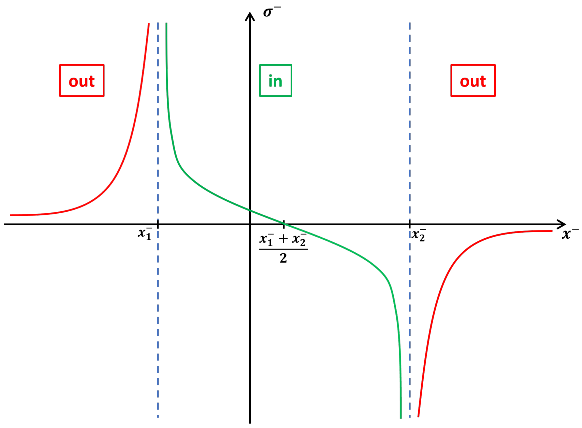

Figure 8.5: Function $\sigma^- = \sigma^-(x^-)$ for the case of an arbitrary region A.

A suitable transformation is given by:

$$\sigma_{in}^- = -\frac{1}{a}\ln\frac{x^- - x_1^-}{x_2^- - x^-}, \tag{8.35}$$

$$\sigma_{out}^- = -\frac{1}{a}\ln\frac{x_1^- - x^-}{x_2^- - x^-}. \tag{8.36}$$

We immediately notice that Equations (8.35) and (8.36) can be combined using the absolute value:

$$\sigma^- = -\frac{1}{a}\ln\left|\frac{x^- - x_1^-}{x_2^- - x^-}\right|. \tag{8.37}$$

It follows directly from the above construction that the functions σ_{in}^- and σ_{out}^-, defined in this manner, are monotone on their respective domains, though they exhibit distinct types of monotonicity. Moreover, each function attains the entire range $(-\infty, +\infty)$ over its domain. Consequently, both σ_{in}^- and σ_{out}^- are bijective. We observe that all four conditions formulated in the preceding chapter are satisfied. In particular, these functions exhibit behavior that is analogous to the coordinate transformation leading to Rindler coordinates.

Let us analyze what these newly introduced coordinates mean. By defining $\sigma^\pm = \tau \pm \sigma$ and rewriting the metric in terms of these variables, we obtain:

$$ds^2 = a^2(x_2^- - x_1^-)(x_2^+ - x_1^+)\frac{-d\tau^2 + d\sigma^2}{4\left(\cosh\left(a\tau\right) + \cosh\left(a\sigma\right)\right)^2}. \tag{8.38}$$

If we now wish to determine what the $\sigma =$ const. curves represent, we introduce the constant $c = e^{2a\sigma}$ that specifies which trajectory is under consideration, and determine the form of this trajectory in the (t, x) coordinates. We obtain:

$$\left(x - \frac{c(x_2^+ - x_1^-) + x_2^- - x_1^+}{2(c-1)}\right)^2 - \left(t - \frac{c(x_2^+ + x_1^-) - x_2^- - x_1^+}{2(c-1)}\right)^2 = \frac{c(x_2^- - x_1^-)(x_2^+ - x_1^+)}{(c-1)^2}. \tag{8.39}$$

It is evident that this is a hyperbola, just as in the case of Rindler coordinates (see Appendix D.3). This is the curve passing through the boundary points of region A, and at the same time it represents a segment of a trajectory of a Rindler observer with proper acceleration proportional to the inverse of the surface of region A. Therefore, we see that we have indeed carried out a direct generalization of Rindler coordinates to a region A of finite dimensions.

We now apply an analogous procedure as in the case of the Rindler observer. First, we define the *in* and *out* modes in a completely analogous manner:

$$\begin{aligned}\phi_{in}^\omega &= \frac{1}{\sqrt{4\pi\omega}}\left[\theta(x^- - x_1^-) - \theta(x_2^- - x^-)\right] e^{i\omega\sigma_{in}^-},\\ \phi_{out}^\omega &= \frac{1}{\sqrt{4\pi\omega}}\left[\theta(x^- - x_2^-) + \theta(x_1^- - x^-)\right] e^{-i\omega\sigma_{out}^-}.\end{aligned} \tag{8.40}$$

The further procedure for calculating the entropy is equivalent, and thus reduces to:

$$S_{FN} = \frac{a}{12}\left[\sigma_{in}^-(x_1^- + \delta_1^-)) - \sigma_{in}^-(x_2^- - \delta_2^-)\right] = \frac{1}{12}\left[\ln\frac{x_2^- - x_1^-}{\delta_2^-} - \ln\frac{\delta_1^-}{x_2^- - x_1^-}\right]. \tag{8.41}$$

We subtract in the opposite order, since $\sigma_{in}^-(x^-)$ is a decreasing function. Also, note that we have once again introduced the short–distance cut–off. Now, we explain what these $\delta^\pm$ represent. As expected, we again encounter UV divergences at the boundaries of region A, since there the fluctuations of short–wavelength modes become entangled. In order to regularize this UV divergence, we introduce the short–distance cut–off δ. It can be understood in the following way: we draw all possible spacelike hypersurfaces and assign to each a thickness δ at the boundary of our region A. This means that δ defines a foliation of spacetime.

In order to obtain the total expression for the entropy, it is necessary to add the contribution of the left–propagating modes, and thus we obtain:

$$S_{FN} = \frac{1}{12} \ln \frac{(x_2^+ - x_1^+)^2 (x_2^- - x_1^-)^2}{\delta_1^+ \delta_1^- \delta_2^+ \delta_2^-}. \tag{8.42}$$

This expression can alternatively be interpreted as follows: it can be decomposed into the sum of two contributions corresponding to the Rindler case, each term being associated with one of the boundaries of the region A. In this formulation, the squared spacetime interval plays the role of the cutoff parameter IC.

However, the expression derived above does not represent the full entropy. In particular, an additional contribution must be taken into account, arising from the omission of the $\omega = 0$ (constant) mode in the preceding analysis. Its contribution cannot be neglected because it contains an infinite number of quantum states within itself. Within region A it remains constant; however, outside this region it can decay in infinitely many distinct ways. Let us first identify which modes were included in the derivation of the formula above. We have accounted for those modes that are narrow compared to the width of the interval $[x_1^-, x_2^-]$, i.e. modes with short wavelengths. Accordingly, these modes extend either through the boundary at $x^- = x_1^-$ or through the boundary at $x^- = x_2^-$. We interpret the above expression as representing the sum of the respective contributions arising from the entanglement of states localized at one boundary of the interval and at its opposite boundary. The modes that have been omitted from the analysis are those that extend across the entire interval, i.e., modes characterized by long wavelengths. It can be shown that these long-wavelength modes are perfectly correlated with the spatially constant mode within the interval, such that the vacuum state can be expressed in the following form:

$$|0_M\rangle = |\text{short}\rangle \otimes |\text{long}\rangle \otimes |\text{uncorrelated}\rangle \,. \tag{8.43}$$

In this expression, $|\text{short}\rangle$ denotes the modes with short wavelengths, whose contribution has already included in our expression for the von Neumann entropy; $|\text{uncorrelated}\rangle$ denotes the modes that are well localized, either entirely within the interval or entirely outside it; and $|\text{long}\rangle$ denotes the modes whose wavelengths exceed the width of the interval, and whose contribution has not been included. For $|\text{long}\rangle$ we expect the following form:

$$|\text{long}\rangle \propto \prod_{k=0}^{\max} \sum_{n_k=0}^{\infty} |n_k, R\rangle \otimes |n_k, L\rangle \otimes |n_k, in\rangle \,. \tag{8.44}$$

Since all these modes have wavelengths larger than the width of the interval, we may consider that the k-th mode has width $2^k(x_2^- - x_1^-)$, i.e. it is 2^k times wider than the interval; n_k denotes the number of excitations of this mode. The states $|n_k, R\rangle$ represent the part of the k-th mode localized to the right of the interval, in the sense $x^- > x_2^-$, while the states $|n_k, L\rangle$ correspond to the part of the k-th mode localized to the left of the interval, in the sense $x^- < x_1^-$. The remaining states $|n_k, in\rangle$ represent the part of the k-th mode localized inside the interval. This is the part corresponding to the $\omega = 0$ mode. Since this part is maximally correlated both with $|n_k, R\rangle$ and with $|n_k, L\rangle$ (as we see from the assumed form of $|\text{long}\rangle$), taking the trace over $|n_k, in\rangle$ gives the same result as taking the trace over $|n_k, L\rangle \otimes |n_k, in\rangle$ (or $|n_k, R\rangle \otimes |n_k, in\rangle$). This leads us to the conclusion that obtaining the density matrix for the $\omega = 0$ mode is equivalent to tracing either over the part to the left of the interval or over the part to the right of the interval. We conclude that here too we may use the entropy formula from the Rindler case.

In Figure 8.6 one long–wavelength mode is shown. The reasoning may also be the following: since the mode is constant within the interval $[x_1^-, x_2^-]$, compressing the interval does not qualitatively change the result. If we compress the length of the interval to zero, it is evident that we obtain the Rindler case. This means that the width of the interval can be regarded as the width of the hypersurface at $x^- = 0$, which is equivalent to introducing our short–distance parameter, and we conclude that $\delta = x_2^- - x_1^-$.

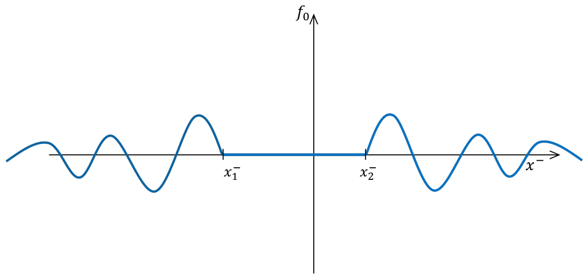

Figure 8.6: Representation of the long–wavelength modes.

It is now evident that the length of the interval serves as the UV parameter. Of course, we also need to have an IC parameter, as in the Rindler case. This means that the contribution of the long–wavelength modes to the entropy is given by:

$$S_{FN,\text{long}} = \frac{1}{12} \ln \frac{X_{\text{max}}^-}{x_2^- - x_1^-}. \tag{8.45}$$

By incorporating the left–propagating modes and sum them with the previously determined short–wavelength modes, we obtain the following final result in this section:

$$S_{FN} = \frac{1}{6} \ln \frac{(x_2^+ - x_1^+)(x_2^- - x_1^-)}{\delta_1 \delta_2} + \frac{1}{12} \ln \frac{X_{\text{max}}^+ X_{\text{max}}^-}{(x_2^+ - x_1^+)(x_2^- - x_1^-)}. \tag{8.46}$$

Here, we used the notation $\delta_1 = \sqrt{\delta_1^+ \delta_1^-}$ and $\delta_2 = \sqrt{\delta_2^+ \delta_2^-}$. We have once again written them in Lorentz–invariant form. Moreover, the event interval $(x_2^+ - x_1^+)(x_2^- - x_1^-)$ is a Lorentz–invariant quantity, so the entire expression for the von Neumann entropy is a Lorentz–invariant quantity. It is also important that δ does not depend on the location in spacetime, because we want the foliation to be the same in every part of spacetime. We see that this is an important condition in the generalization to curved spacetime. It is furthermore important to note that the contribution of the $\omega = 0$ mode is not relevant for the applications to black hole physics.

8.2.3 Generalization to curved spacetime

In this section we generalize the results from the previous section to curved spacetime. Before proceeding, we first extend the discussion to a general quantum state defined on Minkowski spacetime. This need no longer be the Minkowski vacuum, but may instead be the vacuum in some other coordinates. The only essential requirement is that there exists a globally flat coordinate system, i.e. that the spacetime is Minkowski.

Let us assume that an observer living in the coordinates $y^{\pm} = y^{\pm}(x^{\pm})$ perceives no particle flux, i.e. sees the vacuum. This means that the quantum state is no longer the Minkowski vacuum $|0, x\rangle$, but rather $|\psi\rangle = |0, y\rangle$. We can now repeat exactly the same procedure as in the case of Unruh, only in the $y^{\pm}$ coordinates. The subsequent reasoning is entirely the same, so we may immediately write that the entropy (arising from the right–propagating modes) is given by:

$$S_{FN} = \frac{1}{12} \ln \frac{(y_2^- - y_1^-)^2}{\hat{\delta}_1^- \hat{\delta}_2^-}. \tag{8.47}$$

We immediately notice that we have neglected the contribution of the constant mode. It must be considered separately, but since it is not of interest for our analysis of black holes, we do not address it. However, we now see that the short–distance cut–off depends on the position in spacetime. At the end of the previous section we stated that this is not desirable, so it is necessary to transform it into Minkowski coordinates. Since it indeed behaves like a vector corresponding to a length, the following holds:

$$\hat{\delta}^{\mu} = \frac{\partial y^{\mu}}{\partial x^{\nu}} \delta^{\nu} \quad \Longrightarrow \quad \hat{\delta}^- = \frac{dy^-}{dx^-} \delta^- \;\wedge\; \hat{\delta}^+ = \frac{dy^+}{dx^+} \delta^+, \tag{8.48}$$

where $\delta^{\pm}$ are indeed constants throughout the entire spacetime. Therefore, the direct generalization gives us:

$$S_{FN} = \frac{1}{12} \ln \frac{(y_2^+ - y_1^+)^2 (y_2^- - y_1^-)^2}{y_1^{+'} y_1^{-'} y_2^{+'} y_2^{-'} \delta_1^+ \delta_1^- \delta_2^+ \delta_2^-}. \tag{8.49}$$

Since $\delta_{1,2}^{\pm}$ are now defined in globally inertial coordinates, the above expression is indeed Lorentz invariant. This is the direct generalization of the expression for the von Neumann entropy in curved spacetime. In two dimensions we can always choose the conformal gauge. The relation between the $y^{\pm}$ and $x^{\pm}$ coordinates is likewise given by a conformal transformation, so we have:

$$ds^2 = -dx^+ dx^- = -\frac{dx^+}{dy^+} \frac{dx^-}{dy^-} dy^+ dy^- = -e^{2\rho} dy^+ dy^- \quad \Longrightarrow \quad y^{+'} y^{-'} = e^{-2\rho}. \tag{8.50}$$

By applying this relation, we obtain the principal formula derived in this section:

$$S_{FN} = \frac{1}{12} \ln \frac{(y_2^+ - y_1^+)^2 (y_2^- - y_1^-)^2}{\delta^4 e^{-2\rho_1} e^{-2\rho_2}} \quad \wedge \quad ds^2 = -e^{2\rho} dy^+ dy^-. \tag{8.51}$$

This formula is important because it can be applied in curved spacetime. As we know, in this case we may also define the vacuum in some coordinates $y^{\pm}$. The only difference in the reasoning so far is: whether δ is a constant, and what that even means in curved spacetime. We do not have globally inertial coordinates in curved spacetime, but we do have locally inertial coordinates. Everything is consistent as long as we define δ in locally flat coordinates at the corresponding points in spacetime, which, of course, we can do. This means that the von Neumann entropy remains invariant under the action of local Lorentz transformations. Furthermore, let us note that it is permissible to perform yet another arbitrary $SL(2, \mathrm{C})$ transformation on the $y^{\pm}$ coordinates due to the symmetries of the quantum vacuum. This implies that the $SL(2, \mathrm{C})$ group should not alter the von Neumann entropy. This condition is, obviously, satisfied.

It is further necessary to impose a constraint on ρ such that the conformal factor $e^{2\rho}$ does not vary significantly within the layer of thickness δ. This condition is required to ensure that the spacetime foliation is well defined and physically meaningful within that region. Let us now generalize the formula from the Rindler case to curved spacetime. This generalization is also direct:

$$S_{FN} = \frac{1}{12}\ln\frac{Y^+_{\max}Y^-_{\max}}{\hat{\delta}^+_P\hat{\delta}^-_P} = \frac{1}{12}\ln\frac{Y^+_{\max}Y^-_{\max}}{y^{+'}_P y^{-'}_P\delta^+_P\delta^-_P} \quad\Longrightarrow\quad S_{FN} = \frac{1}{12}\ln\frac{Y^+_{\max}Y^-_{\max}}{\delta^2 e^{-2\rho_P}}. \tag{8.52}$$

Here, P is an arbitrary point that divides spacetime into the left and right quadrants. In the initial derivation this was the point $x^- = 0$.

8.2.4 Spacetime with reflective boundary conditions

Up to this point, the left–propagating and right–propagating modes have been treated as independent. However, when the spacetime boundary is located at a finite position rather than at asymptotic infinity, then reflective boundary conditions are imposed at that boundary. Due to these conditions, the left– and right–propagating modes are no longer independent. This means that correlations exist between them. We must take this into account when determining the entropy.

The spacetime manifold is enclosed by an idealized, perfectly reflecting mirror, specified at the boundary by the condition $y^+ = y^-$ (see Figure 8.7). As a first step, we introduce the coordinate y^+, which parametrizes the left–propagating modes on $\mathcal{J}^-$. Then, we introduce the coordinate y^-, such that the defining relation is satisfied on the mirror itself. In Figure 8.7 it is clearly shown what happens with the right–propagating modes. We observe that they exhibit the same behavior as the left–propagating modes in the interval $y^+ \in [y_2^-, y_1^-]$ on $\mathcal{J}^-$. Conclusion: Evaluating the partial trace over the left– and right–propagating modes that live in the region A is equivalent to determining the trace over the region $A = [y_2^-, y_1^-] \cup [y_1^+, y_2^+]$ on $\mathcal{J}^-$, restricted exclusively to the left–propagating modes.

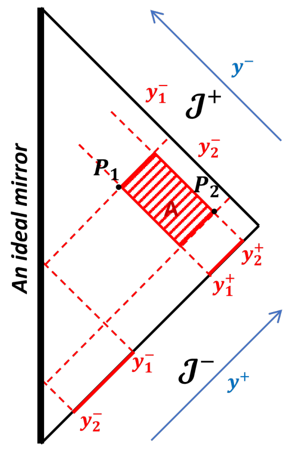

Figure 8.7: Region A that contains the inaccessible degrees of freedom in spacetime with a boundary represented by an ideal mirror.

In this case, it is necessary to evaluate the trace over a region consisting of two disjoint intervals. The corresponding computation is considerably more involved, and its detailed treatment is deferred to the subsequent section. Let us consider a spacelike hypersurface Σ and a point P on it (see Figure 8.8). The causal diamond above the portion of the hypersurface from point P to the mirror represents our region A. Through this process the previously two intervals merge into one: $y^+ \in [y_P^-, y_P^+]$. This is already a well–known problem, so we may immediately write:

$$S_{FN} = \frac{1}{12} \ln \frac{(y_P^+ - y_P^-)^2}{\delta^2 e^{-2\rho_P}}. \tag{8.53}$$

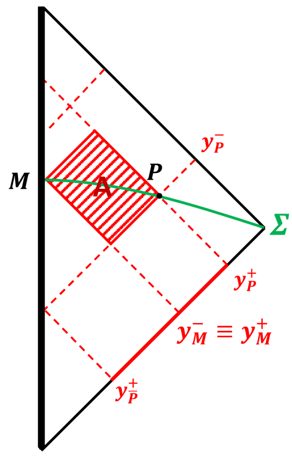

Figure 8.8: Region A that contains the inaccessible degrees of freedom in the spacetime with a boundary.

In the collapse models, we address here, the boundary was not defined by such a relation, but rather by one of the type $y^+ - y^- = \text{const}$. This does not present a problem, since we can repeat the same mapping process of point P. We then state that it is mapped to the point $\bar{P}$. The interval on $\mathcal{J}^-$ is then given by $y^+ \in [y_{\bar{P}}^+, y_P^+]$. Let us also note that $\hat{\delta}_{\bar{P}}^+ = \hat{\delta}_P^-$, so it necessarily holds that $\hat{\delta}_{\bar{P}}^+ \hat{\delta}_P^+ = \delta^2 e^{-2\rho_P}$. Therefore, the generalized formula in the case of spacetime with reflective boundary conditions and a boundary defined by the above equation is given by:

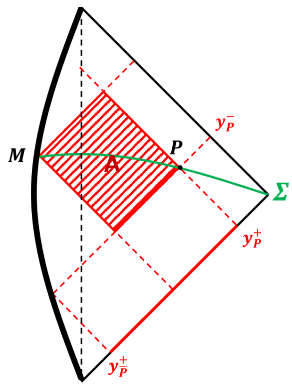

Figure 8.9: Region A that contains the inaccessible degrees of freedom in spacetime with a curved boundary.

$$S_{FN} = \frac{1}{12} \ln \frac{(y_P^+ - y_{\bar{P}}^+)^2}{\delta^2 e^{-2\rho_P}}. \tag{8.54}$$

It turns out that a minor error was made in the course of this calculation. Consider two wave packets localized in the interval $y^+ \in [y_{\bar{P}}^+, y_P^+]$ and entangled with modes outside this interval. What may happen is that interference of these wave packets occurs on the hypersurface Σ. This interference can be destructive. We assume that this is precisely the case. Although both wave packets are entangled with modes outside the interval, their coherent sum is not entangled with the modes in the A' region on the hypersurface Σ due to destructive interference.

This implies that we are accounting for a higher degree of correlation than what actually exists. In Figure 8.10 one such situation is illustrated. For modes with wavelengths small compared to the width of the interval, the error we make is very small. However, as the wavelength of the mode increases, the associated error correspondingly becomes larger. From the dimensional standpoint, it turns out that this error enters the expression as a dimensionless constant of order $O(1)$. Consequently, it does not depend on the UV and IC cut–offs, and we may absorb it into the short–distance cut–off δ.

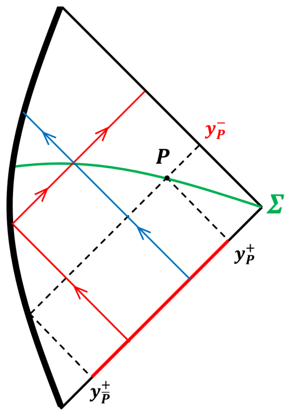

Figure 8.10: Penrose diagram which illustrate the interference of the wave packets.

8.2.5 Case of two disjunct intervals

In this section we determine the von Neumann entropy in the case with two disjoint intervals, namely $A = \left([x_1^+, x_2^+] \times [x_1^-, x_2^-]\right) \cup \left([x_3^+, x_4^+] \times [x_3^-, x_4^-]\right)$. This result will play a pivotal role in the subsequent analysis of the island rule and in the derivation of the expression for fine–grained entropy in gravitational systems. In Figure 8.11 the conformal diagram corresponding to this situation is shown, with the region A marked.

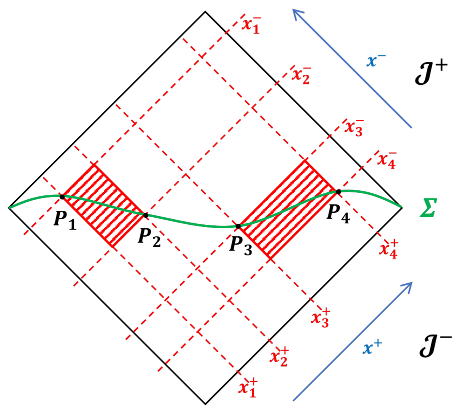

Figure 8.11: Region A, which contains the inaccessible degrees of freedom, in the case where it consists of two disconnected intervals.

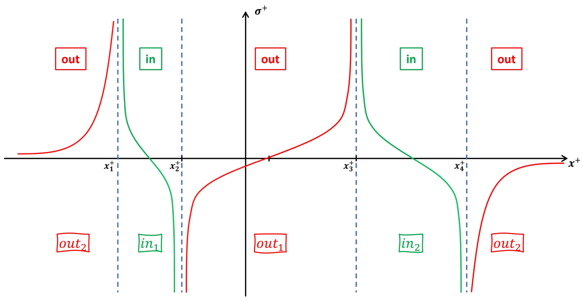

Figure 8.12: Function $\sigma^- = \sigma^-(x^-)$ for a case of a disconnected region A.

The most direct approach one can try is to introduce new coordinates by summing the contributions corresponding to the individual single-interval cases, and subsequently examine whether these coordinates exhibit the required properties.: $\sigma^- = -\frac{1}{a} \ln \left| \frac{x^- - x_1^-}{x_2^- - x^-} \cdot \frac{x^- - x_3^-}{x_4^- - x^-} \right|$. We immediately observe that nearly all of the required conditions are fulfilled. The difficulty arises from the fact that the maps $\sigma^-_{\text{in/out}}$ are not bijective.

Since there exist two disjoint regions in_1 and in_2 (see Figure 8.11), the mapping $\sigma^-_{in}(x^-)$ is actually a mapping $1-2$, and not bijective. We can resolve this problem by introducing the functions: $\sigma^-_{in,1}$, $\sigma^-_{in,2}$, $\sigma^-_{out,1}$, $\sigma^-_{out,2}$. Each is defined on the corresponding domain shown in Figure 8.12. In this manner, a bijective mapping is obtained, ensuring a one-to-one correspondence between elements of the involved sets. Consequently, now we have four different types of positive–frequency modes:

$$\begin{aligned}
\phi^{\omega}_{in,1} &= \frac{1}{\sqrt{4\pi\omega}}\left[\theta(x^- - x_1^-) - \theta(x_2^- - x^-)\right] e^{i\omega\sigma^-_{in,1}}, \\
\phi^{\omega}_{in,2} &= \frac{1}{\sqrt{4\pi\omega}}\left[\theta(x^- - x_3^-) - \theta(x_4^- - x^-)\right] e^{i\omega\sigma^-_{in,2}}, \\
\phi^{\omega}_{out,1} &= \frac{1}{\sqrt{4\pi\omega}}\left[\theta(x^- - x_2^-) - \theta(x_3^- - x^-)\right] e^{-i\omega\sigma^-_{out,1}}, \\
\phi^{\omega}_{out,2} &= \frac{1}{\sqrt{4\pi\omega}}\left[\theta(x^- - x_4^-) + \theta(x_1^- - x^-)\right] e^{-i\omega\sigma^-_{out,2}}.
\end{aligned} \tag{8.55}$$

Upon performing the analytic continuation, the argument of the logarithm is positive in both of the *in* regions and negative in both of the *out* regions. Consequently, the same Bogoliubov coefficient is obtained as the prefactor of both *in* modes.

We conclude that the *in*-modes are maximally entangled with each other; therefore, we can form a linear combination of these solutions and interpret the result as the new “in"-mode, which is consistently defined across both regions. An analogous construction can be performed for the *out*-modes:

$$\phi^{\omega}_{in} = \phi^{\omega}_{in,1} + \phi^{\omega}_{in,2} \tag{8.56}$$

$$\phi^{\omega}_{out} = \phi^{\omega}_{out,1} + \phi^{\omega}_{out,2}. \tag{8.57}$$

Effectively, the problem is reduced to that of two regions, *in* and *out*. This means that, as in every case so far, we are allowed to apply the result from the Rindler case:

$$\begin{aligned}
S_{FN} &= -\frac{a}{12}\left[\sigma^-_{in}(x_2^- - \delta_2^-) - \sigma^-_{in}(x_1^- + \delta_1^-) + \sigma^-_{in}(x_4^- - \delta_4^-) - \sigma^-_{in}(x_3^- + \delta_3^-)\right] \\
&= \frac{1}{12}\ln\left|\frac{x_2^- - x_1^-}{\delta_2^-}\frac{x_2^- - x_3^-}{x_4^- - x_2^-}\frac{x_2^- - x_1^-}{\delta_1^-}\frac{x_4^- - x_1^-}{x_1^- - x_3^-}\frac{x_4^- - x_1^-}{x_2^- - x_4^-}\frac{x_4^- - x_3^-}{\delta_4^-}\frac{x_2^- - x_3^-}{x_3^- - x_1^-}\frac{x_4^- - x_3^-}{\delta_3^-}\right| \\
&= \frac{1}{12}\ln\frac{(x_2^- - x_1^-)^2(x_3^- - x_2^-)^2(x_4^- - x_1^-)^2(x_4^- - x_3^-)^2}{(x_4^- - x_2^-)^2(x_3^- - x_1^-)^2\delta_1^-\delta_2^-\delta_3^-\delta_4^-}.
\end{aligned} \tag{8.58}$$

The subsequent stage of the analysis consists in incorporating the left–propagating modes, followed by the generalization to curved spacetime. By analogy with the preceding sections, the development of this part follows straightforwardly. The final result is given by:

$$S_{FN} = \frac{1}{6}\ln\frac{d_{12}^2 d_{23}^2 d_{14}^2 d_{34}^2}{\delta^4 d_{24}^2 d_{13}^2 e^{-\rho_1}e^{-\rho_2}e^{-\rho_3}e^{-\rho_4}}, \text{ with } d_{ij}^2 = (x_i^+ - x_j^+)(x_i^- - x_j^-). \tag{8.59}$$

As in the preceding analysis, the contribution from the $\omega = 0$ mode should be treated separately. This aspect is not addressed in the present work, as it is not directly connected to the analysis of Hawking radiation in black holes. If one of the points were at infinity, we would simply replace some of the d_{ij} terms using the IC cut–offs. Thus, the formula remains valid in those cases as well.

It remains to analyze the situation in which the spacetime manifold possesses a spacetime boundary with reflective boundary conditions, while the other end of the region A is not the spacetime boundary itself. We have previously demonstrated that this case corresponds to the configuration involving two disjoint intervals on $\mathcal{J}^-$, namely $A = [y_2^+, y_1^+] \cup [y_1^+, y_2^+]$. In Figure 8.13 this case is illustrated. It should also be noted that a residual error arising from the destructive interference of the wave packets persists; however, this contribution can once again be effectively absorbed into the UV cut–off.

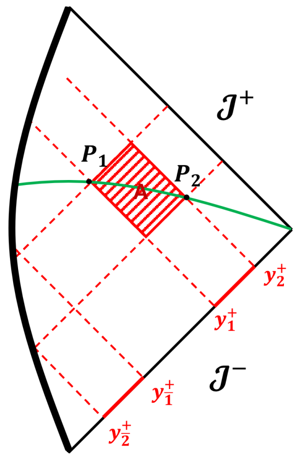

Figure 8.13: Region A that contains the inaccessible degrees of freedom in the case of the spacetime with reflective boundary conditions.

The formula follows directly from equation (8.58):

$$S_{FN} = \frac{1}{12} \ln \frac{(x_1^+ - x_2^+)^2 (x_1^+ - x_2^+)^2 (x_1^+ - x_1^+)^2 (x_2^+ - x_2^+)^2}{\delta^4 (x_2^+ - x_1^+)^2 (x_1^+ - x_2^+)^2 e^{-2\rho_1} e^{-2\rho_2}}. \tag{8.60}$$

Equations (8.59) and (8.60) constitute the most significant results in this section. The reason lies in the fact that they are necessary for determining the fine–grained entropy in gravitational systems, and thereby for reproducing the Page curve.

8.3 Quantum states and black hole entropy

This section is organized into three subsections. In the first subsection, we address the concept of coherent states. This analysis is particularly significant, as the coherent state constitutes a fundamental reference state for a wide class of physical systems encountered in nature. Next, we address the coarse–grained entropy of the black hole, with the aim of finding the quantum correction to the Bekenstein–Hawking entropy formula. In these two subsections, we continue to follow the approach of [26]. Finally, we analyze the entropy associated with Hawking radiation and formulate the Hawking information paradox (in the sense of [1]), which represents the central focus of the present study.

8.3.1 Matter in coherent state

Thus far, the quantum state of the scalar field has always been the vacuum in some coordinates. The only thing we have done was to change the coordinates in which this vacuum state was defined. However, for the quantum state of matter it is expected to be a coherent state. The goal of this section is to show that the von Neumann entropy carried by a coherent state built upon some vacuum is the same as the von Neumann entropy carried by that vacuum. We use a simple model that adequately describes the situation. Our system consists of two uncoupled linear harmonic oscillators. Let their annihilation operators be given by a_1 and a_2. This is equivalent to considering a bosonic system with two levels. We perform the most general possible Bogoliubov transformation and define new annihilation operators:

$$a_1(\gamma) = \frac{1}{\sqrt{1-\gamma^2}}\left(a_1 - \gamma a_2^\dagger\right) \quad \wedge \quad a_2(\gamma) = \frac{1}{\sqrt{1-\gamma^2}}\left(a_2 - \gamma a_1^\dagger\right), \tag{8.61}$$

where $\gamma \in \mathbb{R}$ and $\gamma^2 < 1$. By an analogous procedure to the one used for constructing the vacuum in Minkowski space, we can construct it in this case as well and express it in terms of the vacuum for the individual decoupled oscillators:

$$|0_\gamma\rangle = \sqrt{1-\gamma^2}e^{\gamma a_1^\dagger \otimes a_2^\dagger}|0_1\rangle \otimes |0_2\rangle = \sqrt{1-\gamma^2}\sum_{n=0}^{\infty}\gamma^n |n,1\rangle \otimes |n,2\rangle. \tag{8.62}$$

As in the case of the Minkowski vacuum, here too we can determine the density matrix associated with the first subspace, by taking the trace over the second subspace:

$$\rho_1^\gamma = \mathrm{Tr}_2\{|0_\gamma\rangle\langle 0_\gamma|\} = (1-\gamma^2)\sum_{n=0}^{\infty}\gamma^{2n}|n,1\rangle\langle n,1|. \tag{8.63}$$

We see that we have obtained a thermal density matrix with the temperature defined through $e^{-\beta\omega} = \gamma^2$, where ω is the frequency of the first oscillator. We now proceed to determine the coherent state. This is the state that is an eigenstate of the annihilation operators, i.e. it is defined by:

$$a_1(\gamma)|\gamma,\alpha_1,\alpha_2\rangle = \alpha_1|\gamma,\alpha_1,\alpha_2\rangle \quad \wedge \quad a_2(\gamma)|\gamma,\alpha_1,\alpha_2\rangle = \alpha_2|\gamma,\alpha_1,\alpha_2\rangle \tag{8.64}$$

The general quantum state in this basis is given by the following expression:

$$|\gamma,\alpha_1,\alpha_2\rangle = \sum_{n_1,n_2=0}^{\infty} A_{n_1n_2}|n_1,n_2\rangle, \tag{8.65}$$

where $A_{n_1n_2}$ are unknown constants. By substituting this form into the eigenvalue problem stated above and using the defining relations for the action of annihilation operators on the states in Fock space, we obtain the following recurrence relations for the coefficients $A_{n_1n_2}$:

$$A_{n_1n_2} = \frac{\alpha_1}{\sqrt{n_1}}A_{n_1-1,n_2} \;\wedge\; A_{n_1n_2} = \frac{\alpha_2}{\sqrt{n_2}}A_{n_1,n_2-1} \quad \Longrightarrow \quad A_{n_1n_2} = \frac{\alpha_1^{n_1}\alpha_2^{n_2}}{\sqrt{n_1!n_2!}}C, \tag{8.66}$$

where C is the normalization constant. Let us now determine the constant C:

$$1 = \langle\gamma,\alpha_1,\alpha_2|\gamma,\alpha_1,\alpha_2\rangle = |C|^2\sum_{n_1,n_2=0}^{\infty}\frac{|\alpha_1|^{2n_1}|\alpha_2|^{n_2}}{n_1!n_2!} = |C|^2 e^{|\alpha_1|^2+|\alpha_2|^2}. \tag{8.67}$$

Therefore, the coherent state is given by:

$$|\gamma,\alpha_1,\alpha_2\rangle = e^{-\frac{1}{2}\left(|\alpha_1|^2+|\alpha_2|^2\right)}e^{\alpha_1 a_1^\dagger(\gamma)+\alpha_2 a_2^\dagger(\gamma)}|0_\gamma\rangle. \tag{8.68}$$

Now that we have the coherent state, it would be useful to determine the entropy carried by this state. For this purpose, we begin by introducing new shifted annihilation operators:

$$\hat{a}_1(\gamma) = a_1(\gamma) - \alpha_1 \wedge \hat{a}_2(\gamma) = a_2(\gamma) - \alpha_2 \Longrightarrow \hat{a}_1(\gamma)|\gamma,\alpha_1,\alpha_2\rangle = \hat{a}_2(\gamma)|\gamma,\alpha_1,\alpha_2\rangle = 0. \tag{8.69}$$

In this way we have introduced the operators $\hat{a}_{1,2}(\gamma)$ which annihilate the coherent state. For them, the coherent state is the vacuum. We now ask whether we can also shift the original operators $a_{1,2}$ so that we obtain the operators $\hat{a}_{1,2} = a_{1,2} - b_{1,2}$, which are related to the operators $a_{1,2}(\gamma)$ via the same Bogoliubov transformation, namely:

$$a_1(\gamma) = \frac{1}{\sqrt{1-\gamma^2}} \left(\hat{a}_1 - \gamma \hat{a}_2^\dagger \right) + \frac{b_1 - \gamma b_2^*}{\sqrt{1-\gamma^2}} = \hat{a}_1(\gamma) + \alpha_1 \quad \Longrightarrow \quad \alpha_1 = \frac{b_1 - \gamma b_2^*}{\sqrt{1-\gamma^2}}. \tag{8.70}$$

Using an analogous procedure, we obtain the second relation as well. Thus, we have two equations with two unknowns. Solving this system of linear equations, we get:

$$b_1 = \frac{\alpha_1 + \gamma \alpha_2^*}{\sqrt{1-\gamma^2}} \quad \wedge \quad b_2 = \frac{\alpha_2 + \gamma \alpha_1^*}{\sqrt{1-\gamma^2}}. \tag{8.71}$$

We have succeeded in imposing that the same Bogoliubov transformations hold between $\hat{a}_{1,2}$ and $\hat{a}_{1,2}(\gamma)$ as those that hold between $a_{1,2}$ and $a_{1,2}(\gamma)$. Therefore, we can now write:

$$|\gamma, \alpha_1, \alpha_2\rangle = \sqrt{1-\gamma^2} e^{\gamma \hat{a}_1^\dagger \otimes \hat{a}_2^\dagger} \left|\hat{0}_1\right\rangle \otimes \left|\hat{0}_2\right\rangle \quad \wedge \quad \rho_1^{\gamma'} = (1-\gamma^2) \sum_{n=0}^{\infty} \gamma^{2n} \left|\hat{n}, 1\right\rangle \left\langle \hat{n}, 1\right| . \tag{8.72}$$

We observe that the forms of the density matrices ρ_1^{γ} and $\rho_1^{\gamma'}$ are completely identical, sole distinction arises from their representations in different bases. This certainly does not affect the eigenvalues of the matrices themselves, nor the entropy obtained from them. This means that the entropy associated with a coherent state is identical to that of the underlying vacuum state on which the coherent state is constructed.

We observe that, for each mode considered individually, the Bogoliubov transformation coincides with that obtained in the case of the Minkowski vacuum the only point to keep in mind being that $\gamma = e^{-\pi\omega}$. The general Minkowski coherent state is given by:

$$|\vec{\alpha}, 0_M\rangle \propto \prod_j \left(e^{\alpha_{1j} a_1^\dagger(\omega_j) + \alpha_{2j} a_{\omega_j}^\dagger} |0_M, j\rangle \right), \tag{8.73}$$

where $|0_M, j\rangle$ denotes the vacuum state that is annihilated by the operators $a_1(\omega_j)$ and $a_2(\omega_j)$. We see that this expression can, in fact, be written as the following tensor product:

$$|\vec{\alpha}, 0_M\rangle \propto \bigotimes_j \left|\gamma_j = e^{-\pi\omega_j}, \alpha_{out,j}, \alpha_{in,j}\right\rangle . \tag{8.74}$$

It is now evident that the previously derived result can be easily generalized to encompass both the Minkowski vacuum and Minkowski coherent states. If we consider a vacuum state defined with respect to a set of coordinates $y^\pm = y^\pm(x^\pm)$, obtained via a conformal transformation of the Minkowski coordinates, it follows that the preceding results remain valid without modification. The further generalization to curved spacetime is direct. On this basis, we have demonstrated that the following statement holds:

The formula for the fine-grained entropy in the case when the quantum state of matter is a vacuum state (whether in flat or in curved spacetime) and in the case when it is a coherent state built upon that vacuum is the same.

8.3.2 Black hole entropy

In this section we determine the formula for the coarse-grained entropy of the black hole. The main goal is to obtain the quantum correction to the Bekenstein–Hawking formula derived in Section 4.5 in the case of the classical CGHS model. There, we obtained that the following holds:

$$M = \frac{\lambda}{\pi G} e^{-2\phi_H} \quad \wedge \quad S = \frac{2}{G} e^{-2\phi_H} \quad \wedge \quad T = \frac{\lambda}{2\pi}. \tag{8.75}$$

Our objective is to compute the quantum-corrected entropy for the BPP model and to express this quantity, once again, in terms of the value of the dilaton at the horizon, namely ϕ_H.The only modification arises in the functional dependence $M = M(\phi_H)$, since it is known that the temperature remains invariant under the inclusion of quantum fluctuations.

Consider a black hole surrounded by radiation in a cavity of finite dimensions. Consider adiabatically introducing a small quantity of left-propagating matter with mass ΔM. This procedure corresponds to an evolution through a sequence of equilibrium configurations, implying that the relevant quantum state is the Hartle–Hawking vacuum. At some point, this matter crosses below the apparent horizon. At that moment, the apparent horizon expands outward due to the increase in the mass of black hole, and consequently the entropy of the black hole changes by ΔS_{BH}. On the other hand, as the horizon expands, a portion of the radiation becomes captured by the horizon, leading to a change in the entropy of the matter outside the horizon, ΔS_{mat}. Therefore, the total change in entropy is given by:

$$\Delta S_{BH} + \Delta S_{mat} = \frac{\Delta M}{T}. \tag{8.76}$$

In the case of a black hole in thermal equilibrium we have the Hartle–Hawking state, and the components of the metric are given by:

$$e^{-2\rho} = e^{-2\phi} = -\lambda^2 x^+ (x^- + \Delta) + \frac{\pi G M}{\lambda}. \tag{8.77}$$

The apparent horizon is given by $\partial_+ e^{-2\phi} = 0$, i.e. $x_H^- = -\Delta$. This means that on the horizon we have $\Delta e^{-2\phi_H} = \frac{\pi G \Delta M}{\lambda}$. Furthermore, it should be emphasized that the collapse of the additional mass ΔM entails a modification of the parameter Δ, with the consequence that x_H^- attains more negative values. We therefore obtain the anticipated result that the horizon undergoes a shift, specifically manifesting as an expansion. Thus, we have:

$$\frac{\Delta M}{T} = \frac{2}{G} \Delta e^{-2\phi_H}. \tag{8.78}$$

It is now necessary to evaluate the change in the entropy of the matter located outside the horizon. One possible approach is to introduce this quantity by employing the expression for the entropy S_{FN} of quantum fields defined in the exterior region of the horizon. At first glance this may seem somewhat strange, since we expect the coarse-grained entropy, while for the entropy of the fields outside the horizon, we use the expression for the fine-grained entropy. We justify this by assuming that the matter fields outside the horizon are strongly entangled with the matter fields inside the horizon, so that the coarse-grained entropy of these fields is approximately equal to their fine-grained entropy.

In Figure 8.14, the region A in this case is shown. We see that this corresponds to the generalization of the Rindler result in curved spacetime, and therefore we use the formula from Section 3.2.3:

$$S_{FN} = \frac{N}{6}\left[\rho_H + \frac{1}{2}\ln\frac{-X^+_{\max}X^-_{\max}}{\delta^2}\right]. \quad (8.79)$$

We multiply by N since we have N matter fields. Now we consider the IC divergent part of this expression, since that is the dominant term:

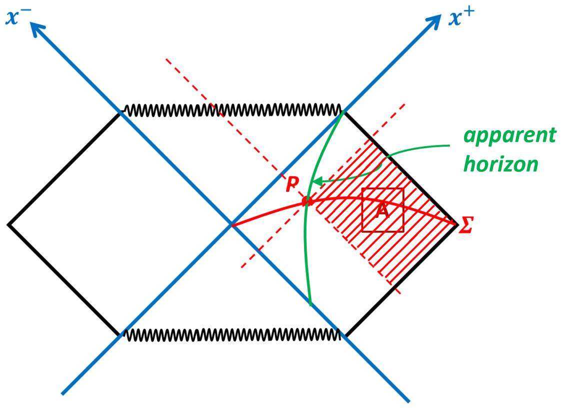

Figure 8.14: Region A that contains the inaccessible degrees of freedom in the eternal black hole setting.

$$S_{FN} \approx \frac{N}{12}\ln\left(-X^+_{\max}X^-_{\max}\right) = \frac{N}{12}2\lambda\sigma_{\max} = 2N\frac{\pi}{6}TL, \quad (8.80)$$

where L is the linear dimension of the cavity, i.e. $L = \sigma_{\max}$. We have obtained $2N$ times the expression for the thermodynamic entropy of a one-dimensional gas. The factor of two appears because of the left- and right-propagating waves, and N because we have N different types of waves. This serves as our justification for stating that we have made a good choice for ΔS_{mat}. The only quantity that changes in this expression is ρ_H, so we have:

$$\Delta S_{mat} = \frac{N}{6}\Delta\rho_H = \frac{N}{6}\Delta\phi_H. \quad (8.81)$$

By combining these expressions, we obtain:

$$\Delta S_{BH} = \frac{\Delta M}{T} - \Delta S_{mat} = \Delta\left(\frac{2}{G}e^{-2\phi_H} - \frac{N}{6}\phi_H\right) \implies S_{BH} = \frac{2}{G}e^{-2\phi_H} - \frac{N}{6}\phi_H. \quad (8.82)$$

This is the quantum-corrected Bekenstein–Hawking formula, determined up to an integration constant, which is not of great importance. This expression may be interpreted as $\frac{A}{4G}$, where we have incorporated the quantum correction to the area A. We now proceed to determine the precise ratio between this quantum correction and the classical value appearing in the Bekenstein–Hawking entropy formula:

$$\frac{\Delta S_{BH}}{S^{(0)}_{BH}} = -\frac{N\hbar G}{12c^3}\phi_H e^{2\phi_H} = \frac{N\hbar\lambda}{24\pi cM}\ln\frac{\pi GM}{\lambda c^2}. \quad (8.83)$$

Consequently, this quantity is of order $\hbar$ and can thus be consistently interpreted as a genuine quantum correction.

8.3.3 Hawking information paradox

In this section, we present a precise formulation of the Hawking information paradox [16]. This paradox constitutes the central focus of the present study and was initially introduced and qualitatively discussed in the introductory section. Namely, in the 1970s Stephen Hawking made one of the most important discoveries in the theory of gravitation. He demonstrated that black holes are indeed thermal objects. Consequently, they must be characterized by a well-defined temperature and are predicted to emit radiation. Furthermore, he demonstrated that this radiation is purely thermal radiation without any correlations. The entirety of this result is obtained within the framework of quantum field theory in curved spacetime, employing a methodology that is almost identical to the one used to derive the Unruh effect in Section 8.2.1.

If we assume that the black hole was formed by the collapse of matter that was in a pure state, specifically in a coherent state, it is a strange conclusion that after the evaporation process we obtain a final state which is a thermal ensemble, representing a mixed state. The thermal aspects arise because we divide the vacuum, or the coherent state (see Section 4.3.1), into two parts: the one located inside the black hole and the one outside it. As we know, the vacuum represents an entangled state in quantum field theory. This means that the entire vacuum is a pure state, but certain degrees of freedom are entangled at short distances. For these reasons, when we observe only half of spacetime, we obtain a mixed state. We have already seen all of this in Section 8.2 when we derived the formulas for the von Neumann entropy in gravity. What physically happens can be explained in the following way:

At all times, the vacuum creates and annihilates particle/antiparticle pairs. The particle and antiparticle from one pair are mutually entangled. What can happen is that one particle from the pair is created just below the horizon and goes into the singularity, while the other is created just above the horizon and escapes to asymptotic infinity. The latter particle represents Hawking radiation.

In Figure 8.15 one such process is illustrated. In this process, the two particles form a pure (entangled) state. However, if we observe only one particle, say a, we find that it is in a mixed state, which behaves as a thermal state at the Hawking temperature. We have already encountered this in the case of the Rindler observer. The procedure is entirely analogous: one first determines the Bogoliubov coefficients and subsequently performs a partial trace over the degrees of freedom localized inside the black hole, thereby obtaining the reduced density matrix describing the degrees of freedom accessible to an observer located outside the black hole.

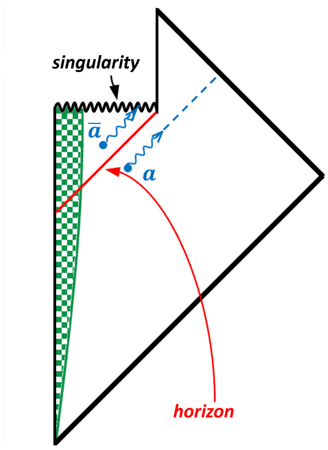

Figure 8.15: Penrose diagram depicting an entangled pair of particles.

This observation implies that, at early times, the entropy associated with the radiation exhibits a monotonic increase, a behavior that is fully consistent with general expectations for the dynamical evolution of entropy in any quantum system. The problem arises when the entropy of the radiation becomes larger than the Bekenstein–Hawking entropy, which represents the coarse-grained entropy of the black hole. From that moment onward, the radiation can no longer be entangled with the degrees of freedom of the black hole, because the black hole has a smaller thermodynamic entropy, and therefore a smaller number of degrees of freedom than the radiation. This is also clear since we know that the fine-grained entropy is always less than the coarse-grained entropy. The conclusion is the following:

If we assume that the black hole is formed from a pure state, then we expect that the total state of the system consisting of the black hole and Hawking radiation is a pure state at every moment in time. Consequently, the entropy of the radiation must be equal to the fine-grained entropy of the black hole, which must be smaller than the coarse-grained entropy of the black hole, i.e. the Bekenstein–Hawking entropy.

However, it appears that the entropy of the radiation reaches the value of the Bekenstein–Hawking entropy and, after that moment, continues to increase. This means that our system state can no longer be a pure state, but instead becomes a mixed state. This leads to two problems:

1. **Unitarity is violated:** We started from a pure state and ended up in a mixed state. Hawking believed this to be a property of quantum gravity, and therefore argued that a black hole cannot be regarded as an ordinary quantum system, since evolution in quantum mechanics must necessarily be unitary.
2. No matter how complex the state whose collapse formed the black hole, at the end of the evaporation process only a thermal ensemble remains, without any correlations. In such a state there certainly cannot be as much information as there was in the initial pure state from which the black hole was formed.

We may conclude that the black hole destroys information. This phenomenon is called the Hawking information paradox. As we have already mentioned, Hawking did not consider this to be a paradox, but rather a property of quantum gravity[16]. On the other hand, if we wished to regard the black hole as an ordinary quantum system, then at the moment when the entropy of the radiation and the Bekenstein–Hawking entropy become equal, the entropy of the radiation must begin to decrease, eventually dropping to zero at the end of the evolution, since only the radiation remains, which must be in a pure state.

The moment when the condition $S_{rad} = S_{BH}$ holds is called the Page time and is denoted by t_P, after the physicist Don Page who proposed the curve that the radiation entropy should follow in order for the evolution to be unitary[17, 18]. In Figure 8.16 both Hawking's curve (red) and Page's curve (green) are shown.

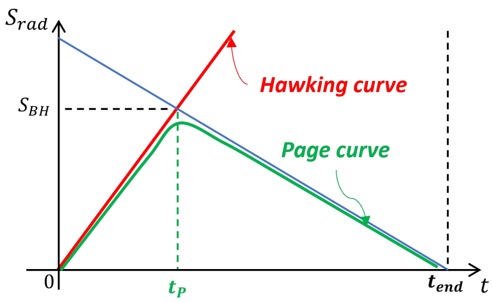

Figure 8.16: Page curve visualization.

We give few more comments:

- As the black hole evaporates, its mass decreases. This is called the backreaction of Hawking radiation on the black hole, and we have already taken it into account. It does not solve the problem.

- When the black hole approaches the end of its life, its size becomes of the order of Planck length. At that point we expect strong quantum gravity effects to manifest, and the semiclassical approximation in which we are working ceases to be valid. This also does not solve the problem, since at the Page time the black hole is still very large.
- Since the problem depends on the very definition of fine-grained entropy, which is a macroscopic quantity, small corrections to the Hamiltonian and/or quantum states near the horizon cannot resolve the problem. This means that the paradox is valid at all orders of perturbation theory, and its resolution must be non-perturbative in the gravitational constant G.
- It would be expected that a quantity such as fine-grained entropy is not exactly given by the semiclassical approximation, and it was previously thought that this was the case—that there would be corrections to the semiclassical formula once a theory of quantum gravity was found. However, today it is no longer believed to be so; rather, it is considered that this formula gives the entropy of the exact quantum state of the radiation.
- To resolve the problem, it is clear that we must change the very definition of fine-grained entropy. We deal with this extensively in the next section.

8.4 Fine-grained entropy formula in gravitational systems

In this section, we address the central formula of the present work, namely the formula for fine-grained entropy in gravitational systems [29, 34, 33]. It is of considerable significance, as it enables the successful reproduction of the Page curve, which is the primary objective of the present study. This section is organized into four subsections. First, we address the primary working hypothesis, hereafter referred to as the central dogma[1]. Then we analyze the formula for fine-grained entropy. We describe how we reconstruct the Page curve for the fine-grained entropy of the black hole, and subsequently for the fine-grained entropy of the radiation. In the third part we provide a sketch of the derivation of the formula itself. Finally, in the fourth part we discuss the still unresolved questions related to the information paradox. Throughout this section we follow the analysis presented in [1].

8.4.1 Central dogma

In the previous section we introduced the idea of the information paradox. We now attempt to resolve it. The main hypothesis is given by:

From the outside, the black hole represents an ordinary quantum system with $\frac{A}{4G}$ degrees of freedom that evolve unitarily.

We now examine the consequences of this assumption and how they lead to a modification of the formula for fine-grained entropy in gravitational systems.

The black hole, together with the entire spacetime region enclosed by a given hypersurface, can be effectively modeled by the quantum system posited in the central dogma. The precise location of this hypersurface remains undetermined. We refer to it as the cut-off surface. In Figure 8.17 it is shown in blue.

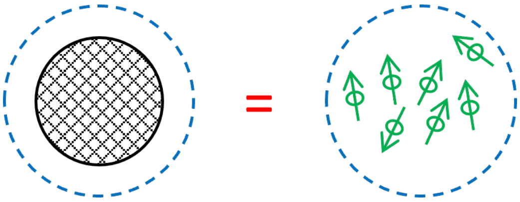

Figure 8.17: Visualization of the black hole as an ordinary quantum system.

It is well known that the entropy can be expressed by the following formula: $S = \ln W$, where W is the number of possible microstates. In quantum mechanics this corresponds to the dimension of the Hilbert space of states. We notice first that the Hilbert space is associated with a system that has finite dimension. The problem arises from the fact that these microscopic degrees of freedom do not manifest in the gravitational description, in which a black hole is characterized by only a small set of macroscopic parameters (such as mass, spin, charge, etc.). Moreover, an additional issue arises that warrants consideration. Under the assumption of unitary time evolution, there must exist a corresponding Hamiltonian operator that generates this unitary evolution. This Hamiltonian likewise does not appear manifestly in the gravitational description. What is known to exist within the gravitational formulation is the Hamiltonian constraint; however, this constitutes a global condition that applies to the entirety of spacetime. According to the central dogma, it is necessary to isolate only the part corresponding to the exterior, and standardized methodology for achieving this remains undetermined.

We provide additional remarks regarding the cut-off surface. It represents a reflective wall that bounds the system we call the black hole, which evolves unitarily. However, when we have an asymptotically flat geometry, we do not know where this hypersurface should be located. We draw an imaginary surface far from the event horizon (we expect it to be at least several Schwarzschild radii away from the black hole), and everything inside it we call the black hole. This quantum system is now coupled to the degrees of freedom that reside outside this region. The region outside this boundary surface is regarded as a quantum system with fixed spacetime, i.e. semiclassical. There we ignore large metric fluctuations, but we can still account for weakly interacting gravitons. The evolution of the entire system should be unitary. We now arrive at the following conclusion:

The gravitational response is compared with that of a quantum system coupled to degrees of freedom localized far from the black hole, defined on an imaginary cut-off surface.

We now proceed to analyze the formulation of entropy in the context of gravitational systems. As a first step, we investigate the underlying physical significance of the coarse-grained entropy associated with the composite system comprising the black hole and radiation. Hawking has already demonstrated that it is determined by the expression for the generalized entropy, which can be written as:

$$S_{gen} = \frac{A}{4G} + S_{outside}, \tag{8.84}$$

where the first term represents the Bekenstein–Hawking entropy, and the second term denotes the contribution of quantum fields outside the black hole horizon. It satisfies the second law of thermodynamics, namely: $\Delta S_{gen} \geqslant 0$, and thus it is indeed the coarse-grained entropy.

Hawking derived this formula using the Euclidean gravitational path integral [32]:

$$
\begin{aligned}
\mathcal{Z} &= \int \mathcal{D}g_{\mu\nu}\mathcal{D}\phi e^{-\frac{1}{\hbar}S_E[g_{\mu\nu},\phi]} \\
&= \int \mathcal{D}g_{\mu\nu}\mathcal{D}\phi \exp\left\{-\frac{1}{\hbar}\left[S_E[g^{(0)}_{\mu\nu},\phi^{(0)}] + \cancelto{0}{\left.\frac{\delta S_E}{\delta\phi}\right|_{(0)}}\delta\phi + \frac{1}{2}\left.\frac{\delta^2 S_E}{\delta\phi^2}\right|_{(0)}(\delta\phi)^2 + \ldots\right]\right\} \\
&= e^{-\frac{1}{\hbar}S_E[g^{(0)}_{\mu\nu},\phi^{(0)}]}\int \mathcal{D}g_{\mu\nu}\mathcal{D}\phi \exp\left\{-\frac{1}{2\hbar}\left.\frac{\delta^2 S_E}{\delta\phi^2}\right|_{(0)}(\delta\phi)^2 + \ldots\right\} = e^{-\frac{1}{\hbar}S_E[g^{(0)}_{\mu\nu},\phi^{(0)}]}\mathcal{Z}_{quantum}. \qquad (8.85)
\end{aligned}
$$

In the preceding expression, we have implemented an expansion about the saddle point, which is determined by the classical equations of motion (indicated by the superscript (0)). Consequently, the contribution that is linear in the variation vanishes, and only the quadratic contribution remains. This partition function receives contributions from both geometry and quantum fields. The gravitational part is obtained by evaluating the action on the classical equations of motion, while the quantum part is obtained with fixed geometry (the semiclassical approximation). The geometry is inquired to be smooth on the horizon. This observation is associated with the fact that an observer in free fall does not register any locally discernible physical effect upon crossing the event horizon (see Appendix D.5). To obtain the entropy from these expressions, we can use the standard thermodynamic formulas:

$$S = (1 - \beta\partial_\beta)\ln\mathcal{Z} \quad \wedge \quad E = -\partial_\beta \ln\mathcal{Z}. \qquad (8.86)$$

Utilizing these mathematical expressions, Hawking derived his generalized formula for entropy. The first term corresponds to the surface term in S_{gen}, while the second term corresponds to the quantum part of the partition function. This formula represents the coarse-grained entropy of the system consisting of black hole and Hawking radiation. In this case, $S_{outside}$ plays the role of the fine-grained entropy of the radiation. This leads to a non-unitary evolution. Our goal is to ensure that the evolution remains unitary; consequently, it is necessary to modify this formula accordingly. It can be shown that this formula is equivalently obtained from the expression for the generalized entropy. The sole distinction is that we now select a different boundary surface. In place of the event horizon, we consider the surface that extremizes the generalized entropy functional, i.e., the surface on which the generalized entropy attains its minimum value. We now proceed to clarify more precisely the intended meaning of this statement. Consider a surface I that is genuinely two-dimensional within the spacetime, i.e., it is not a hypersurface but rather an embedded spatial surface. This means that it is localized in one spatial dimension as well as in time. We define it as the surface that minimizes the generalized entropy functional, and consequently refer to it as the quantum extremal surface (QES). In fact, it minimizes the entropy in the spatial direction, while maximizing it in the temporal direction. If there are several such surfaces, it is necessary to select the one that gives the global minimum.The procedure for its determination is as follows:

We begin by selecting a spacelike hypersurface specified by a constant-time slice ($t = const.$). On this hypersurface, we then determine the surface that minimizes the generalized entropy functional. Subsequently, we consider the family of all such spacelike hypersurfaces and identify the one whose corresponding minimizing surface yields the maximal value of the generalized entropy.

Therefore, the formula for fine-grained entropy in gravitational systems is given by:

$$S_{FG} = \min_{X} \left\{ \operatorname*{ext}_{X} \left[\frac{A[X]}{4G} + S_{\text{semi-cl}}\left(\Sigma_X\right) \right] \right\}. \tag{8.87}$$

Here, X represents the surface of interest, while Σ_X denotes the portion of the spacelike hypersurface that lies between X on one side and the cut-off surface on the other, the latter specifying the quantum system being studied. This construction determines the causal diamond that contains the region in which the degrees of freedom of the quantum system under consideration are localized. The von Neumann entropy of the quantum fields on Σ_X is written as $S_{\text{semi-cl}}(\Sigma_X)$. We adopt this notation to stress that all computations are carried out within the semiclassical approximation. This is the key relation of our analysis, originally derived by Maldacena and Lewkowycz [33]. In most situations, the point X is located inside the black hole, that is, behind the event horizon. The core idea can be expressed as follows:

We initiate the analysis by identifying a trial surface I located outside the event horizon of the black hole. We then continuously deform and extend this surface across the horizon to the interior region in order to determine the configuration that realizes the desired minimal value.

Since the surface X lies in the interior of the black hole, this implies that the entropy depends on the properties of the black hole's interior. What is unexpected is that it does not depend on the entire interior of the black hole, but only on a restricted subset of that interior region. The entire procedure is derived from the Euclidean gravitational path integral, using a method similar to the one Hawking employed to obtain the expression for generalized entropy. A sketch of this derivation is presented in Section 8.4.3. It is necessary to provide a more precise definition of the notion of a "quantum extremal surface" as it pertains to the surface X. It is an ordinary geometric surface. We call it quantum because it bounds the region in which the quantum fields reside.

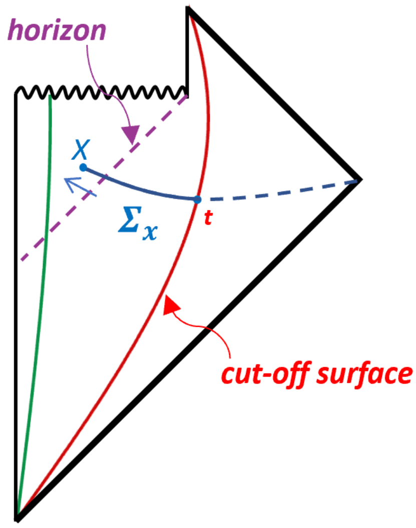

Figure 8.18: Penrose diagram showing the quantum extremal surface.

8.4.2 Page curve reproduction for the black hole subsystem

We now apply the fine-grained entropy formula for gravitational systems to a black hole treated as a quantum subsystem. At the moment of black hole formation, no Hawking quanta have escaped. Thus, for a point X inside the event horizon, no QES is encountered, and the construction extends to the asymptotic boundary of spacetime. In this regime, the surface term vanishes, leaving only $S_{\text{semi-cl}}(\Sigma_X)$, which evaluates to zero.

As time passes, the first quanta escape the region of the black hole, resulting in an increase of the fine-grained entropy S_{FG} due to the growth of the second term in the corresponding expression. At the moment t_1, the entropy remains smaller than the Bekenstein–Hawking value S_{BH}. However, by time t_2 the fine-grained entropy exceeds S_{BH}. This behavior coincides precisely with the original semiclassical prediction obtained by Hawking. We have entropy that keeps increasing as time goes on, rising higher and higher until the entire black hole evaporates. This case is referred to as the case with zero QES.

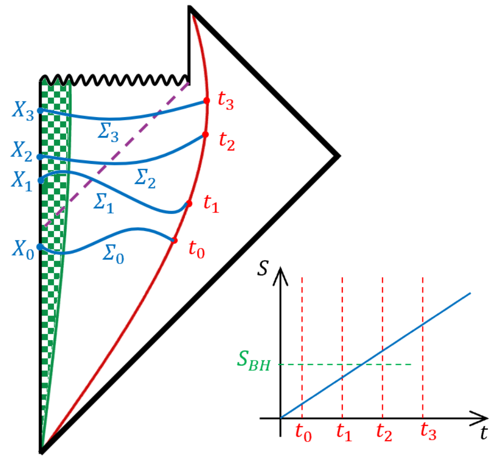

Figure 8.19: Penrose diagram depicting to the zero QES phase.

However, what happens is the emergence of an additional QES shortly after the Hawking radiation leaves the region of the black hole. The location of this surface depends on the amount of radiation that has escaped from the black hole and is therefore an explicit function of time. The expression for generalized entropy now includes a surface term. Moreover, this surface term is dominant compared to the semiclassical term, since only a very small amount of radiation has escaped the black hole up to this moment. It turns out that this QES lies very close to the horizon, so in the initial moments the contribution of the surface term is very large. This means that the contribution of this QES is far greater than the contribution in the case with zero QES. This case is referred to as the case with a nonzero QES.

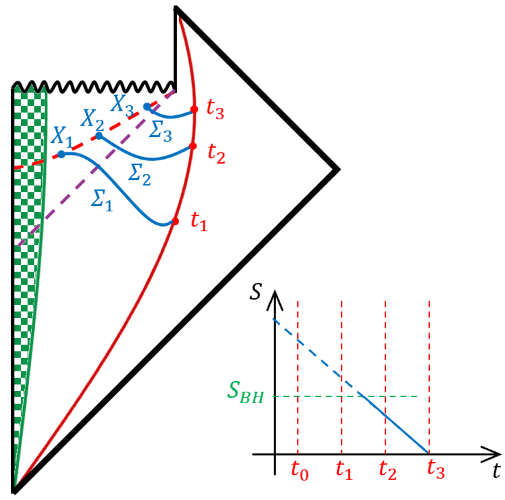

Figure 8.20: Penrose diagram depicting to the non-zero QES phase.

Based on the previous conclusion, We observe that, in the early stages of the evaporation process, the global minimum is governed by the trivial (zero) quantum extremal surface (QES). However, as time progresses, due to the evaporation of the black hole the horizon area decreases, and thus the contribution of the nonzero QES also decreases. At some point between the moments t_1 and t_2, this decreasing contribution becomes smaller than the increasing one given by the zero QES. Since, in calculating S_{FG}, we use the QES that provides the minimal contribution, at this moment the QES used to compute the entropy changes, and the entropy begins to decrease. We say that in that moment, a phase transition has occurred.

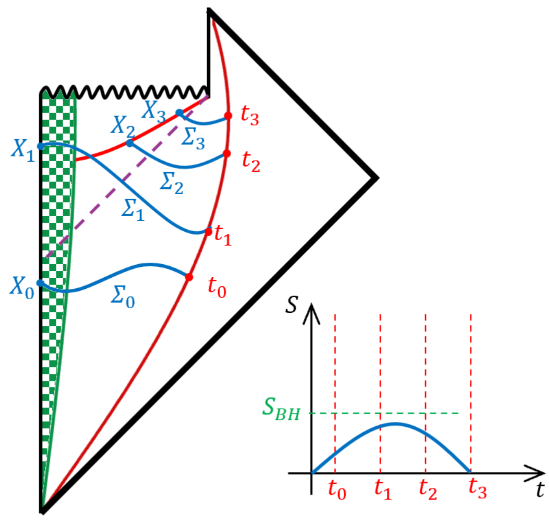

Figure 8.21: Penrose diagram depicting the phase transition.

At the phase transition point, the previously dominant contribution associated with the trivial (zero) QES remains smaller than the Bekenstein–Hawking entropy S_{BH}. Consequently, the resulting entanglement entropy exhibits the characteristic behavior associated with the Page curve. This follows from the observation that the entropy computed from the nonvanishing quantum extremal surface (QES) tracks the thermodynamic entropy of the black hole. The underlying reason is that the QES is located in close proximity to the event horizon, which is used in the calculation of thermodynamic entropy. As it does not exceed S_{BH}, since QES is still below the horizon, the intersection point cannot be above the value S_{BH}. This moment corresponds to the Page time that we define in Section 8.3.3 when discussing Hawking's information paradox.

We thus observe that the Page curve is successfully reproduced, provided that a nonvanishing quantum extremal surface (QES) is indeed present inside the black hole horizon.It is required to demonstrate the existence of a surface exhibiting saddle-point behavior, that is, a surface for which displacements in the spatial direction from a given point result in an increase in entropy, whereas displacements in the temporal direction from the same point result in a decrease in entropy. We do not provide that proof here, but we give an intuitive analysis showing that such a surface should exist by considering what happens in the direction of left-propagating waves.

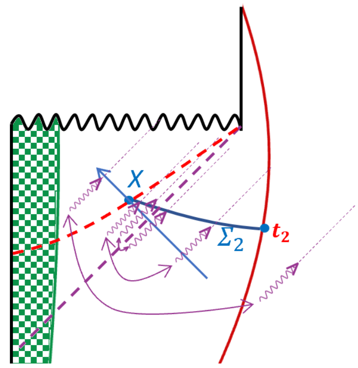

Figure 8.22: Penrose diagram which demonstrates of the existence of a non-zero QES.

What is firmly established is that the surface term decreases as we approach the point $r = 0$. The remaining question is how the quantity $S_{\text{semi-cl}}(\Sigma_X)$ behaves in this limit. Consider the process in which the hypersurface X is initially precisely positioned at the event horizon and subsequently adiabatically translated to radii inside the horizon, following the direction of left-propagating waves. The new quanta that we collect on the hypersurface Σ_X as X is lowered beneath the horizon are entangled with the quanta that resided on Σ_X in the region between the horizon and the cut-off surface. This implies that by this process we purify the quantum state along Σ_X, since we include both members of the pairs. This continues until we have collected all the quanta entangled with those living on the part of Σ_X to the right of the horizon. At that point we have maximally purified the state along Σ_X. During this process, the entropy $S_{\text{semi}-\text{cl}}(\Sigma_X)$ decreases, reflecting the progressive purification of the system's state. However, if we further decrease X, we begin to register quanta that are entangled with quanta which have already propagated beyond the black hole region, i.e., which lie outside the cut-off surface. This means that the entropy $S_{\text{semi}-\text{cl}}(\Sigma_X)$ starts to increase again. We conclude that along this direction there indeed exists a local minimum for $S_{\text{semi}-\text{cl}}(\Sigma_X)$, and therefore also for S_{FG}, given that the surface contribution exhibits a monotonically decreasing behavior.
We conclude:

During the evaporation of a black hole, two distinct quantum extremal surfaces (QESs) emerge. One corresponds to the original Hawking saddle: it is located at the asymptotic boundary of spacetime (the so-called zero quantum extremal surface) and yields a contribution to the entropy that increases monotonically with time. The other QES is situated just inside the event horizon and yields a contribution to the entropy that decreases monotonically with time. At any given time, the fine-grained entropy of the radiation is given by the minimum of these two QES contributions, thereby reproducing the characteristic Page curve.

8.4.3 Page curve reproduction for the Hawking radiation subsystem

In the preceding section, we derived the fine-grained entropy of the black hole subsystem and demonstrated that our results reproduce the expected Page curve. However, this did not pose an issue. The difficulty manifests in the context of the entropy associated with Hawking radiation. In earlier analyses, this entropy was computed solely in terms of the von Neumann entropy of the radiation subsystem. Within that framework, the entropy appears to increase monotonically throughout the black hole evaporation process and, at a certain stage, surpasses the Bekenstein–Hawking entropy of the black hole itself—an outcome that is regarded as inconsistent. This inconsistency indicates that the standard formula for the entropy of Hawking radiation must be modified or supplemented by additional contributions. Once again, we use the formula for fine-grained entropy in gravitational systems. Nevertheless, this needs to be justified since the radiation under consideration is localized in a region where the gravitational field is extremely weak. Under such circumstances, one would ordinarily not expect a formula for gravitational systems to be applicable. The rationale for employing this expression is that the quantum state of the radiation itself has been determined through the application of gravitational theory.

At this point, one may inquire how this formula is to be applied in precise terms. Thus far, we have consistently considered a specific gravitational system within the spatial domain in which the formula was intended to be utilized. That system was a black hole. Conversely, in the present setting there is no black hole in the region occupied by the radiation. Furthermore, up to this point the hypersurface Σ_I has been assumed to be connected. We now relax this assumption and allow for the possibility that it is not connected. If Σ_I is a disconnected region, then the area of its boundary surface increases, which in turn leads to an enhancement of the corresponding boundary (or "area") contribution in the expression for the fine-grained entropy. Consequently, to maintain consistency, the expression for the generalized entropy must be adjusted downward (i.e., reduced) to compensate for this increase. The only way to achieve this is to reduce the value of $S_{\text{semi-cl}}(\Sigma_X)$. This objective can be realized by incorporating a part of the black hole interior in such a way as to purify the quantum state, thereby providing pairs for those particles localized in the region exterior to the cut-off surface. The region we add is called the island region, and the surface that bounds it is the island or the island boundary. This means that the island is the quantum extremal surface in this case. Based on this analysis, we conclude that the fine-grained entropy is now calculated according to the formula for entropy via the island rule, given by the following expression:

$$S_{FG} = \min_{I} \left\{ \operatorname*{ext}_{I} \left[\frac{A[I]}{4G} + S_{\text{semi-cl}} \left(\Sigma_I \cup \Sigma_{rad} \right) \right] \right\}. \tag{8.88}$$

It should be emphasized that this quantity corresponds to the von Neumann entropy of the precise quantum state of the radiation. Nonetheless, the exact quantum state itself is not known; only its entropy is accessible. This situation is schematically represented in Figure 8.23. The island I is situated behind the black hole horizon in the interior region, as is theoretically anticipated. We now examine its evolution as a function of time. An analogous mechanism to that governing the fine-grained entropy of the black hole is found to operate in this context, and, as a consequence, the resulting entropy profile reproduces the Page curve at late times.

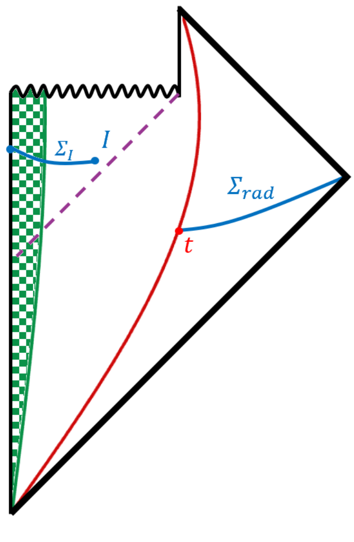

Figure 8.23: Penrose diagram depicting the island and the radiation hypersurfaces.

As in the case of the black hole, at the beginning of the evaporation process no QES is formed and therefore there is no island. Consequently, the expression is determined solely by its semiclassical contribution, which vanishes because no quantum of radiation has yet escaped from the vicinity of the black hole. As time progresses, radiation begins to leave the black hole region, and consequently the expression for $S_{\text{semi-cl}}(\Sigma_{rad})$ begins to increase. As before, this expression extremizes the generalized entropy at each moment of the evaporation process, but it does not need to be the global minimum at every moment. This part of the analysis corresponds to Hawking's result, where the fine-grained entropy of the radiation monotonically increases during evaporation.

As before, the island (nonzero QES) that extremizes the generalized entropy appears shortly after the beginning of the evaporation process and is located near the horizon, so the entropy calculated using this QES has a very large value at the start of evaporation and is therefore not the global minimum. However, as time progresses, the horizon shrinks, and so does the entropy contribution in the case when we have an island, until it eventually becomes the global minimum and a phase transition occurs.

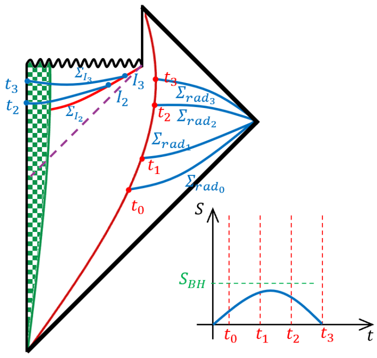

Figure 8.24: Penrose diagram depicting the phase transition for the radiation entropy.

In the subsequent evolution, we calculate S_{FG} using the configuration with the island, which leads to a monotonically decreasing entropy until the end of the evaporation process, when it vanishes. We therefore conclude that we have once again reproduced the Page curve, this time in the case of Hawking radiation. If the black hole was formed from a pure state, we expect that the fine-grained entropy of the black hole subsystem and the Hawking radiation subsystem are equal at every moment. Indeed, this is the case. The reason lies in the fact that the position of the quantum extremal surface in the case of the black hole subsystem coincides with the position of the island. We conclude that the surface terms in the expressions for fine-grained entropy are the same in both cases. Since here we have the Cauchy surface given by $\Sigma_I \cup \Sigma_X \cup \Sigma_{rad}$, the von Neumann entropy associated with Σ_X must be equal to the von Neumann entropy associated with $\Sigma_I \cup \Sigma_{rad}$, because the quantum state is pure along the entire Cauchy surface. This implies that $S_{\text{semi-cl}}(\Sigma_X) = S_{\text{semi-cl}}(\Sigma_I \cup \Sigma_{rad})$. Since in both cases we extremize the same function, the entropies must be equal. We conclude:

The fine-grained entropy of the black hole subsystem is equal to that of the Hawking radiation subsystem at each moment throughout the evaporation process. Consequently, this construction reproduces the characteristic Page curve for the entropy of Hawking radiation.

The sole reason of success in reproducing the Page curve for the Hawking radiation subsystem lies in the fact that we included the interior of the black hole when calculating the fine-grained entropy of Hawking radiation. Moreover, it is entirely expected that we would reproduce the Page curve once we include the black hole interior, since this process purifies the quantum state of the outgoing radiation. At first glance, it may seem as though we inserted the interior by hand and that there is no physical justification for doing so. However, as we stated at the beginning of this section, the formula for fine-grained entropy in gravitational systems can be derived using the Euclidean gravitational path integral. The method used is called the replica wormhole method, and we discuss it in the next section.

8.4.4 Replica wormhole method

In this section, we present an outline of the derivation of the expression for fine-grained entropy in gravitational systems[33, 34, 38, 124, 125, 126]. We consider the case where the black hole has completely evaporated. We neglect the details of the immediate vicinity of the completion of the evaporation process, since in this regime strong quantum-gravitational effects become relevant and the semiclassical approximation ceases to be valid.

From the standpoint of entropy evaluation, the relevant geometric configuration is depicted topologically in Figure 8.25. We consider as our starting point the unnormalized pure state $|\psi\rangle$ describing the matter content that undergoes gravitational collapse and gives rise to the singularity. The goal is to evolve it into some final radiation state $|j\rangle$ using the gravitational path integral. In this way we obtain the transition amplitude from the initial state $|\psi\rangle$ to the final state $|j\rangle$, i.e. $\langle j|\psi|j|\psi\rangle$. In Figure 8.25, a representation of this transition amplitude is shown. The ocher line represents the evolution from the $|\psi\rangle$ state (interior) to the $|j\rangle$ state (exterior) of the matter.

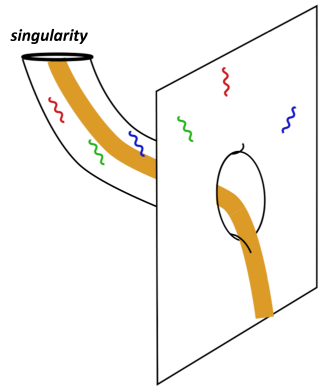

Figure 8.25: The diagram representing the transition amplitude: $\langle j|\psi\rangle$, taken from [1].

Based on the state $|\psi\rangle$ we can form the density matrix: $\hat{\rho} = |\psi\rangle\langle\psi|$. In Figure 8.25, a diagram is shown representing the matrix element of this density matrix in the basis of the Hilbert space of the final radiation: $\rho_{ij} = \langle i|\psi\rangle\langle\psi|j\rangle$. Here we have two interiors corresponding to $|\psi\rangle$, so they are identified, and two exteriors where the final radiation states $|i\rangle$ and $|j\rangle$ reside.

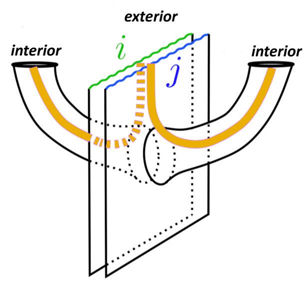

Figure 8.26: The diagram representing the matrix element: ρ_{ij}, taken from [1].

The objective is to determine whether the post-evaporation state $\hat{\rho}$ corresponds to a pure state or a mixed state. To this end, we employ the standard criterion for assessing the purity of a quantum state:

$$\mathrm{Tr}\left\{\hat{\rho}^2\right\} = \left(\mathrm{Tr}\{\hat{\rho}\}\right)^2 . \tag{8.89}$$

If this relation is satisfied, the state is pure, otherwise, the state is mixed. In order to verify this using the diagram, we must first represent the diagram for:

$$\mathrm{Tr}\{\hat{\rho}\} = \sum_i \langle i|\psi|i|\psi\rangle\langle\psi|i|\psi|i\rangle . \tag{8.90}$$

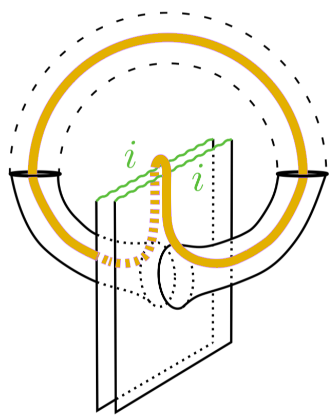

Figure 8.27: The diagram representing: $\mathrm{Tr}\{\hat{\rho}\}$, taken from [1].

Here the exterior regions are also identified, therefore, we obtain a closed loop. This implies that we need to sum over the final states $|i\rangle$. To verify the equality stated above, it is necessary to additionally express:

$$\mathrm{Tr}\{\hat{\rho}^2\} = \sum_{i,j} \langle i|\psi|i|\psi\rangle \langle \psi|j|\psi|j\rangle \langle j|\psi|j|\psi\rangle \langle \psi|i|\psi|i\rangle\,. \tag{8.91}$$

It is clear how we identify the final states (the exteriors) due to the summation; however, it is also necessary to identify the interiors, in order to have summation over both i and j. There are two ways to connect the interiors and form a closed loop. The first way is to connect the interior of the matrix element $\langle i|\psi|i|\psi\rangle$ with the interior of the matrix element $\langle j|\psi|j|\psi\rangle$, and then repeat the same for the second pair. In this way we obtain one large loop (Figure 8.28). The second way is to connect the interiors of the matrix elements $\langle i|\psi|i|\psi\rangle$ and $\langle i|\psi|i|\psi\rangle$ with each other, as well as the interiors of the matrix elements $\langle j|\psi|j|\psi\rangle$ and $\langle j|\psi|j|\psi\rangle$. It is clear that this case decomposes into two loops (Figure 8.29).

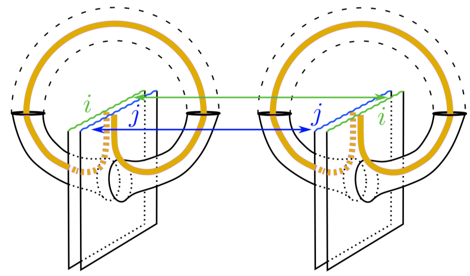

Figure 8.28: The diagram representing: $\mathrm{Tr}\{\hat{\rho}^2\}$ - Hawking saddle point, taken from [1].

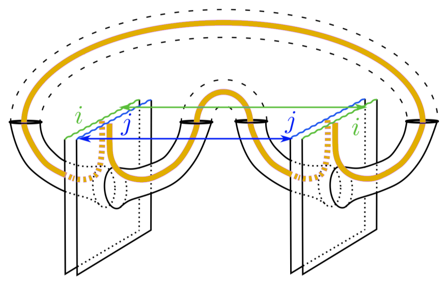

Figure 8.29: The diagram representing: $\mathrm{Tr}\{\hat{\rho}^2\}$ - replica wormhole saddle point, taken from [1].

In quantum mechanics—and in the present context as well—it is a fundamental requirement that one performs a sum over all possible configurations. In this case, this entails summing over all admissible geometric topologies, that is, over all distinct ways of connecting the interior regions. The first contribution we obtain cannot be factorized into two separate loops and corresponds to Hawking's saddle-point configuration. In contrast, the second diagram clearly factorizes into two loops, indicating that it represents the product of two diagrams associated with $\mathrm{Tr}\{\hat{\rho}\}$. This contribution is associated with the saddle-point configuration of the replica wormhole, implying that the final state $\hat{\rho}$ at the end of the evaporation process is pure. Since the entropy of a pure state is equal to zero, the second diagram represents the dominant term in the saddle-point approximation of the Euclidean gravitational path integral, namely:

$$\mathcal{Z} = \int \mathcal{D}g_{\mu\nu}\mathcal{D}\phi e^{-S_E[g_{\mu\nu},\phi]} \approx e^{-S_{E,RW}} + e^{-S_{E,H}} = 1 + e^{-S_{E,H}} \approx 1. \tag{8.92}$$

We conclude that the main contribution enforces unitarity. What may still pose an issue is that Hawking's saddle point remains present. It yields an exponentially suppressed contribution, and we therefore anticipate that it will not pose a significant issue once the complete quantum theory of gravity is taken into consideration. With this, we have shown that the state at the end of the black hole evaporation process is a pure state. However, it is necessary to determine the entropy of either of the two subsystems at every moment during the evaporation process. To derive the formula for fine-grained entropy in gravitational systems at each moment in time, we employ the replica trick:

$$S_{FG} = (1 - n\partial_n)\,\mathrm{Tr}\{\hat{\rho}^n\}\Big|_{n=1}. \tag{8.93}$$

here $\hat{\rho}$ denotes the density matrix of either of the two subsystems. In determining $\mathrm{Tr}\{\hat{\rho}^n\}$, the interiors can be connected in many different ways, which makes the calculation considerably more complicated. Once we compute $\mathrm{Tr}\{\hat{\rho}^n\}$ for arbitrary $n \in \mathbb{N}$, we perform an analytic continuation to $n \in \mathbb{R}$, and then take the limit $\lim_{n\to 1}$. Among all possibilities, we must select the one that gives the minimal contribution. It turns out that, under this analytic continuation to continuous n, this precisely corresponds to the process of finding the quantum extremal surface, which we described in Section 8.4.1. A detailed proof of this statement is omitted here; however, its validity should be evident on intuitive grounds.

Finally, several additional observations warrant consideration:

1. To reconstruct the exact quantum state of the emitted radiation, it is, in principle, necessary to perform a path integral over the complete space of geometries, incorporating all nonperturbative contributions. At present, this procedure cannot be carried out in any existing formulation of quantum gravity. What is established in this framework is that we use the semiclassical state. On the basis of this state, we compute the fine-grained entropy of the radiation. Moreover, we know that the fine-grained entropy obtained from the semiclassical state is equal to the one we would obtain using the exact quantum state. If we wished to measure some simple observables, the semiclassical state would be sufficient. However, in the case of complex observables this is not enough. We need to know the exact quantum state of the system.

2. Since the quantum state of the radiation contains information about the interior of the black hole, very complex measurements performed on the degrees of freedom of the radiation can alter spacetime by creating wormholes that would lead us into the interior of the black hole [125, 127, 128]. We discuss this further in the following subsection.

3. We obtain the quantity S_{FG} by evaluating the Euclidean gravitational path integral. This is not a well-defined quantity. It remains unclear which saddle points ought to be taken into account and which ought to be excluded. It may happen that there exist theories which do not use the replica wormhole saddle point, but rather Hawking's. We expect such theories not to be fully consistent. Another relevant issue is the choice of integration contour in the computation of the gravitational path integral.

4. Another conceptual difficulty concerns the specification of the cut-off hypersurface that defines the boundary of the quantum subsystem associated with the black hole. We are not certain whether the formula for fine-grained entropy in gravitational systems is valid at all if the boundary surface is not at infinity.

8.4.5 Entanglement wedge reconstruction

At first sight, the reconstruction of the Page curve appears to provide a resolution of the black hole information paradox. However, this conclusion is not fully justified and important issues remain unresolved. Several of these issues are examined in detail in the following section. In the central dogma we mentioned the degrees of freedom by which we describe the black hole from the perspective of an observer located outside the black hole. The question is: Which part of the black hole interior do they describe? To answer this question, let us consider the formula for fine-grained entropy in gravitational systems. It depends on the interior of the black hole, but only up to the quantum extremal surface. We then arrive at the following conclusion:

The degrees of freedom from the central dogma describe the geometry only up to the quantum extremal surface. Given that the entropy is associated with the entire causal diamond, we may regard it as providing a characterization of that causal diamond.

This causal diamond is referred to as the entanglement wedge of the black hole [70, 71, 72], because it contains the degrees of freedom that describe the black hole. There are three relevant regimes that alternate over time. The first regime corresponds to times $t < t_p$ and describes the period before the phase transition has occurred. In this case, no QES is present, and consequently the entire interior is described by the degrees of freedom of the black hole. The second regime corresponds to the period $t_p < t < t_{end}$, where t_{end} denotes the moment at which the evaporation process is completed. In this period, the phase transition has already taken place, and therefore a QES is present. Then the degrees of freedom of the black hole reside only in the portion of the interior up to the QES, while the remainder of the interior belongs to the island, which is part of the radiation. This means that after the Page time, the degrees of freedom of the radiation partly reside in the interior of the black hole. The third situation corresponds to the period after the evaporation process has finished, i.e. $t > t_{end}$. The region inside the cut-off surface is now just a flat space, while the entire region beneath the event horizon belongs to the island, i.e. to the degrees of freedom of the radiation. These three regimes are illustrated in Figures 8.30, 8.31, and 8.32.

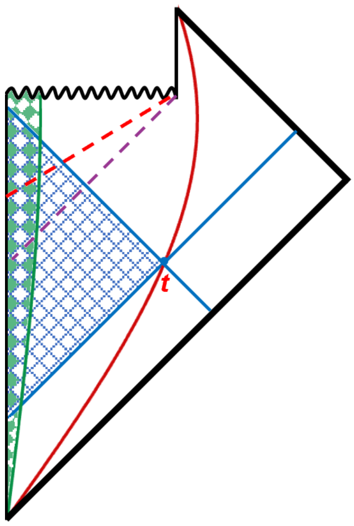

Figure 8.30: Penrose diagram corresponding to the spacetime before the critical point, i.e. $t < t_p$.

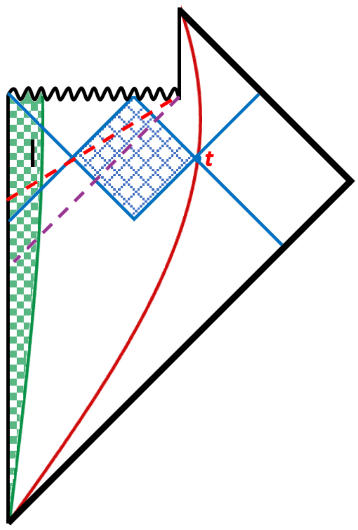

Figure 8.31: Penrose diagram corresponding to the spacetime at the critical point, i.e. $t_p < t < t_{end}$.

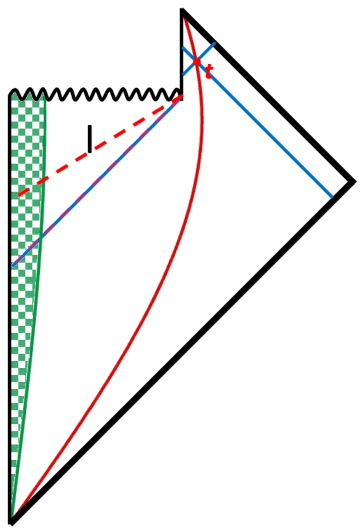

Figure 8.32: Penrose diagram corresponding to the spacetime after the critical point, i.e. $t > t_{end}$.

We conclude:

After the Page time has been reached, the majority of the microscopic degrees of freedom originally localized inside the event horizon are encoded in the emitted Hawking radiation rather than in the remaining black hole. Upon completion of the evaporation process, all degrees of freedom that were previously contained within the horizon become fully transferred to, and are entirely represented by, the radiation.

Let us now consider another scenario in which the majority of the degrees of freedom located inside the black hole horizon are associated with radiation. This implies that the action of semiclassical operators localized in the region behind the horizon modifies the entropy of the emitted radiation, in accordance with the standard expression for fine-grained entropy in gravitational systems. Throughout, we assume that this entropy represents the entropy of the exact quantum state of the radiation. Consequently, semiclassical operators from the region beneath the horizon of the black hole alter the exact quantum state of the radiation. [129, 130, 131] Then, from general theorems of quantum information theory it follows that there exists a mapping known as the Petz map, which enables us to recover information related to that exact quantum state [132, 133]. In the case of simple gravitational theories, this mapping can be easily constructed using the gravitational path integral, via the replica wormhole method. It is important to emphasize that the quantum measurements that would need to be performed on the degrees of freedom of the radiation are extremely complex, with a complexity that is exponential in the Bekenstein–Hawking entropy of the black hole [134, 135]. A generalization of this idea to the most general cases and theories has not yet been achieved.

When we speak of the degrees of freedom of the black hole, we usually mean the quantum fields that reside in the region beneath the event horizon. It is evident that these degrees of freedom differ from those mentioned in the central dogma. There, the relevant degrees of freedom are those of the black hole from the perspective of an observer far away from it. We know that the degrees of freedom counted via quantum fields beneath the horizon may lie either on one side or the other of the quantum extremal surface. The degrees of freedom that we refer to as the black hole degrees of freedom are those that reside to the right of the quantum extremal surface. This means that they represent only a portion of all the degrees of freedom that exist beneath the horizon. It is important to understand precisely which degrees of freedom under consideration in this context.

In light of this observation, we have thereby resolved an additional paradox originally formulated by Wheeler in 1964 [136]. Namely, he pointed out that there exist classical geometries which outwardly appear as black holes, but beneath the horizon can possess arbitrarily large entropy—much greater than one quarter of the horizon area. He called them bags of gold. The resolution of this paradox is analogous:

When the entropy of the interior exceeds the area of the throat (the horizon), the causal diamond corresponding to the degrees of freedom of the black hole describes only the portion of the interior that does not include this arbitrarily large entropy.

In Figure 8.33, one such bag-of-gold geometry is shown. We observe that the spacetime geometry of the evaporating black hole discussed in the preceding section (and in the present one) assumes, after the Page time, a configuration that is effectively analogous to a bag-of-gold geometry. This lies in the fact that the degrees of freedom of the black hole correspond to only a very small portion of the degrees of freedom residing beneath the horizon of the black hole.

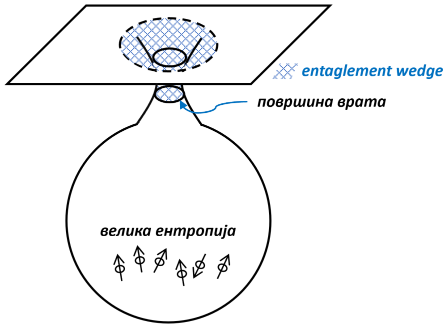

Figure 8.33: Visualization of the Bag-of-gold geometry.

With this section we conclude our analysis of entropy in gravitational systems. In the subsequent chapter, we undertake a detailed and explicit reconstruction of the Page curve within specific, well-defined models of two-dimensional dilaton gravity. This goal will be accomplished by utilizing the formula for fine-grained entropy in gravitational systems, the derivation and detailed analysis of which constituted the primary focus of the present chapter.

Chapter 9

Page curve in the BPP model

In this chapter, we illustrate how the Page curve is reproduced within the BPP model of two-dimensional dilaton gravity introduced in Section 4.3. As already shown in Chapter 4.3, the BPP model is exactly solvable. This allows for an exact semi-classical evaluation of the Page curve up to the end-point of the evaporation process, beyond which the corrections from the full theory of quantum gravity will become relevant [1]. We now demonstrate how equation (1.6) is applied to compute the Page curve for both eternal and evaporating black hole scenarios in the BPP model. The chapter is organized into two sections.

In the first section, we reproduce the Page curve for the eternal black hole studied in Section (4.3.2). Our analysis follows the derivations in [41] and [57]. We begin with the no–island configuration, in which we recover the standard Hawking result: the Page curve increases monotonically with time [16]. We then apply the fine–grained entropy formula for gravitational systems (1.6), which allows us to obtain the Page curve for this setup.

A crucial point is that, for an eternal black hole, we do not expect the entropy of radiation to decrease at late times. Instead, it should asymptotically approach and then remain at the value $2S_{BH}$. This behavior is due to the fact that the black hole is in thermal equilibrium, so the flux of Hawking radiation it emits is balanced by the flux it absorbs. Consequently, the entropy grows monotonically until it reaches its maximum value, namely $2S_{BH}$, defined in (1.4). The factor of two arises because an eternal black hole has two asymptotically flat regions. Moreover, since S_{BH} is the coarse–grained black hole entropy, the fine–grained entropy of the radiation cannot exceed this bound (see Section 8.1).

In the second part, we then reconstruct the Page curve for an evaporating black hole in the BPP model introduced in Section 4.3.4, again following the derivation of [41]. As before, we start by analyzing the setup without including an island, which reproduces the standard Hawking result [16]. We then demonstrate how the inclusion of an island at late times in the evaporation process (i.e., after the Page time) resolves the paradox. The Page curve is computed in two coordinate systems: we first locate the island in asymptotically flat coordinates, and subsequently repeat the analysis in Kruskal coordinates, obtaining, of course, identical results. Unlike the eternal black hole case, the Page curve here decreases and eventually goes to zero at the end-point of the evaporation.

9.1 Page curve in the eternal black hole scenario

In this section, we compute the fine-grained entropy of Hawking radiation for the eternal black hole in the BPP model introduced in Section 4.3.2. The discussion is divided into two parts. First, we study the configuration without an island and reproduce Hawking's original result. Next, we perform the full entropy calculation using the fine-grained entropy formula for gravitational systems (1.6). In the late stages of evaporation, we demonstrate the emergence of an island region outside the horizon that contributes to the constant term in the entanglement entropy. This contribution causes the Page curve to saturate at $2S_{BH}$, thereby recovering the purity of the initial quantum state at the end of evaporation. Throughout this section, we follow the derivation presented in [57].

9.1.1 No-island configuration

In the absence of an island in the spacetime, the formula (1.6) simplifies to just the second term, namely $S_{semi-cl}(\Sigma_{rad})$. Because the region containing the degrees of freedom that are inaccessible to the asymptotic observer is simply connected, and there is no spacetime boundary on which reflective boundary conditions are imposed, the appropriate expression for the entanglement entropy of quantum fields in curved spacetime is given by (8.51). For convenience, we rewrite it here:

$$S_{FG} = \frac{N}{12} \ln \frac{(x_R^+ - x_L^+)^2 (x_R^- - x_L^-)^2}{\delta^4 e^{-2\rho_R} e^{-2\rho_L}}, \tag{9.1}$$

where we have included an overall factor of N in (8.51) because the BPP model contains N distinct scalar field species. In addition, the expression is written in Kruskal coordinates (4.41), as we are focusing on the eternal black hole setup.

Figure 9.1 depicts the region A that is inaccessible to an asymptotic observer (as defined in Figure 8.1) for the case of an eternal black hole. The two asymptotically flat regions are denoted by R and L in both Figure 9.1 and equation (9.1). In each of these regions, we introduce a cut-off surface at $\sigma = b$. Since we are interested in evaluating the entropy at a fixed time t, we consider the hypersurface $t =$ const. in the right wedge. The segment of this hypersurface that supports the radiation degrees of freedom, Σ_{rad}, extends from spatial infinity i^0 to the cut-off surface.

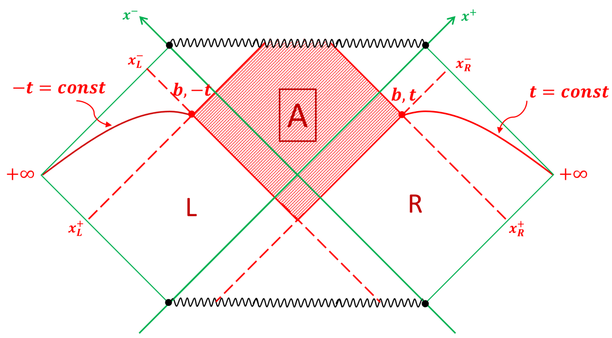

Figure 9.1: Penrose diagram illustrating the no-island setup for an eternal black hole in the BPP model

In the left asymptotically flat region, radiation exits the black hole region along the x^-–axis. At the same time, the Killing vector reverses its direction, implying that the time coordinate t in the right asymptotically flat region corresponds to the time coordinate $-t$ in the left asymptotically flat region. Because of these two effects, the boundary point of region A in the left asymptotically flat region appears as the mirror reflection of the corresponding boundary point in the right asymptotically flat region, as illustrated in Figure 9.1.

Since Killing time is defined in Eddington–Finkelstein coordinates, we first need to rewrite the Kruskal coordinates $x^{\pm}_{L/R}$ in terms of the asymptotically flat coordinates $\sigma^{\pm}$, and therefore in terms of t and b, using the transformation law (4.41). Doing so gives:

$$\lambda x_R^+ = e^{\lambda(t+b)}, \quad \lambda x_R^- = -e^{-\lambda(t-b)}, \quad \lambda x_L^+ = -e^{\lambda(-t+b)}, \quad \lambda x_L^- = e^{-\lambda(-t-b)}. \tag{9.2}$$

We now proceed to evaluate the fine–grained entropy (9.1). As a first step, we compute the differences $(x_R^\pm - x_L^\pm)$ by substituting (9.2):

$$\begin{aligned} \lambda\left(x_R^+ - x_L^+\right) &= e^{\lambda(t+b)} + e^{\lambda(b-t)} = e^{\lambda b}\left(e^{\lambda t} + e^{-\lambda t}\right) = 2e^{\lambda b}\cosh(\lambda t), \\ \lambda\left(x_R^- - x_L^-\right) &= -e^{\lambda(b-t)} - e^{\lambda(t+b)} = -e^{\lambda b}\left(e^{-\lambda t} + e^{\lambda t}\right) = -2e^{\lambda b}\cosh(\lambda t). \end{aligned} \tag{9.3}$$

The left-right symmetry requires $\rho_L = \rho_R$. Consequently, for the metric (4.104) evaluated at the boundaries of the region A (see Figure 9.1) we find:

$$e^{-2\rho_R} = e^{-2\rho_L} = -\lambda^2 x_R^+ x_R^- + \frac{\pi GM}{\lambda} = e^{2\lambda b} + \frac{\pi GM}{\lambda} = -\lambda^2 x_L^+ x_L^- + \frac{\pi GM}{\lambda}. \tag{9.4}$$

Inserting (9.3) and (9.4) into the original expression for the entanglement entropy (9.1) leads to:

$$S_{FG} = \frac{N}{6}\ln\frac{4\cosh^2(\lambda t)}{(\lambda\delta)^2\left(1 + \frac{\pi GM}{\lambda}e^{-2\lambda b}\right)}. \tag{9.5}$$

Let us now analyze the behavior of this function at the beginning of the evaporation process. Recall that S_{FG} is defined only up to a renormalization constant (because of the divergence $\ln\delta$ as $\delta \to 0$). We can therefore choose this constant so that $S_{FG} = 0$ at $t = 0$. For $t = 0$ we have $\cosh(\lambda t) = 1$, and the expression simplifies to:

$$S_{FG} = \frac{N}{6}\ln\frac{4}{(\lambda\delta)^2\left(1 + \frac{\pi GM}{\lambda}e^{-2\lambda b}\right)} = 0 \quad \Longrightarrow \quad S_{FG} = \frac{N}{3}\ln\Big[\cosh(\lambda t)\Big]. \tag{9.6}$$

Expanding this expression around $t = 0$, we obtain:

$$S_{FG} = \frac{N}{6}(\lambda t)^2. \tag{9.7}$$

Thus, near $t = 0$ the entropy grows quadratically in time. We now turn to the late–time behavior of (9.5):

$$\cosh(\lambda t) = \frac{1}{2}\left(e^{\lambda t} + \cancelto{0}{e^{-\lambda t}}\right) \approx \frac{1}{2}e^{\lambda t} \quad \Longrightarrow \quad S_{FG} \approx \frac{N}{3}\lambda t - \frac{N}{3}\ln 2. \tag{9.8}$$

We thus arrive at the main conclusion of this section: in the setup without an island, the Page curve is not recovered. Instead, we reproduce the standard Hawking result [16], where the entropy increases monotonically with time. This monotonic growth is incompatible with unitarity, since beyond a certain time S_{FG} exceeds the bound set by the coarse–grained entropy $2S_{BH}$. The time at which this happens is the Page time, determined by:

$$S_{FG} = 2S_{BH} \quad \Longrightarrow \quad \frac{N}{3}\lambda c t_p = 2\frac{2c^3}{G\hbar}\frac{\pi GM}{\lambda c^2} \quad \Longrightarrow \quad t_p = \frac{12\pi M}{N\hbar\lambda^2}. \tag{9.9}$$

9.1.2 Island configuration

When the island is present, both the area contribution and the semi-classical entanglement entropy term in expression (1.6) for the fine-grained entropy are non-zero. Furthermore, the presence of the island implies that the region A in Figure 9.2, which is inaccessible to the observer, is composed of two disconnected components. Consequently, the semi-classical part of the fine-grained entropy is given by equation (8.59), namely:

$$S_{semi-cl} = \frac{N}{6} \ln \frac{d_{12}^2 d_{23}^2 d_{14}^2 d_{34}^2}{\delta^4 d_{24}^2 d_{13}^2 e^{-\rho_1} e^{-\rho_2} e^{-\rho_3} e^{-\rho_4}}, \tag{9.10}$$

where $d_{ij}^2 = (x_i^+ - x_j^+)(x_i^- - x_j^-)$ represents the Minkowski distance between the corresponding points depicted in Figure 9.2 in Kruskal coordinates. As before, we multiply expression (9.10) by N because the BPP model contains N species of scalar fields. We assign the indices i and j such that the identification $(1,2,3,4) \longleftrightarrow (Ra, Rb, La, Lb)$ holds. As in the preceding section, R labels the right wedge and L the left wedge of the spacetime. Meanwhile, a designates the boundary of the island region, and b labels the cut-off hypersurface. All these hypersurfaces are explicitly marked in Figure 9.2.

Figure 9.2 shows the region A that an asymptotic observer cannot access (as defined in Figure 8.1) for an eternal black hole in the presence of an island. The island, labeled by I, is highlighted in blue. For an eternal black hole, the non-zero QES is expected to appear very close to the quantum-corrected horizon, but still outside it. In the right asymptotically flat region, the island's coordinates are $(t', -a)$. We denote the spatial coordinate by $-a$ because the island should be located near the horizon, which is given by $\sigma_{\rm H} \to -\infty$ (4.39).

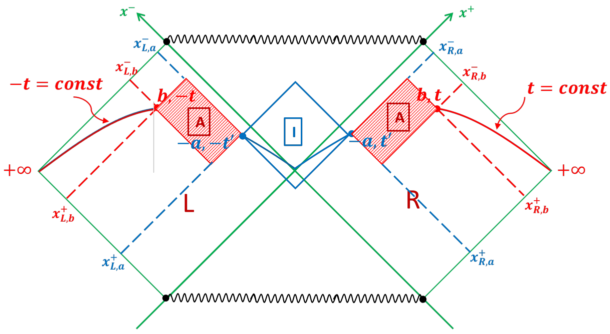

Figure 9.2: Penrose diagram illustrating the island setup for an eternal black hole in the BPP model

In direct analogy with the case without an island, we send the island's boundary point to the left asymptotically flat region by reflecting it across the time axis. In this way, its coordinates become $(-t', -a)$, which encodes the fact that the time-like Killing vector in the left wedge is oriented in the opposite direction. Note that we have not identified the island's time coordinate with the time coordinate on the cut-off surface. This choice is motivated by the requirement that the generalized entropy must be extremized with respect to both space and time: the entropy must be maximized along the temporal direction and minimized along the spatial direction.

The first step in evaluating the fine-grained entropy (9.10) is to express the Minkowski distances in the Kruskal coordinates in terms of the Eddington–Finkelstein coordinates, using (4.41). This yields

$$\begin{aligned} &\lambda x_{Rb}^+ = e^{\lambda(t+b)}, \quad \lambda x_{Rb}^- = -e^{-\lambda(t-b)}, \quad \lambda x_{Lb}^+ = -e^{\lambda(-t+b)}, \quad \lambda x_{Lb}^- = e^{-\lambda(-t-b)}, \\ &\lambda x_{Ra}^+ = e^{\lambda(t'-a)}, \quad \lambda x_{Ra}^- = -e^{-\lambda(t'+a)}, \quad \lambda x_{La}^+ = -e^{\lambda(-t'-a)}, \quad \lambda x_{La}^- = e^{-\lambda(-t'+a)}. \end{aligned} \tag{9.11}$$

Substituting (9.11), the Minkowski distances d_{ij}^2 can then be written in terms of t, t', a, and b as

$$\begin{aligned}
\lambda^2 d_{12}^2 &= (x_{Rb}^+ - x_{Ra}^+)(x_{Rb}^- - x_{Ra}^-) = \left(e^{\lambda(t+b)} - e^{\lambda(t'-a)}\right)\left(-e^{\lambda(b-t)} + e^{-\lambda(t'+a)}\right), \\
\lambda^2 d_{34}^2 &= (x_{Lb}^+ - x_{La}^+)(x_{Lb}^- - x_{La}^-) = \left(-e^{\lambda(b-t)} + e^{-\lambda(t'+a)}\right)\left(e^{\lambda(t+b)} - e^{\lambda(t'-a)}\right), \\
\lambda^2 d_{14}^2 &= (x_{Rb}^+ - x_{Lb}^+)(x_{Rb}^- - x_{Lb}^-) = \left(e^{\lambda(t+b)} + e^{-\lambda(t-b)}\right)\left(-e^{-\lambda(t-b)} - e^{\lambda(t+b)}\right), \\
\lambda^2 d_{23}^2 &= (x_{Ra}^+ - x_{La}^+)(x_{Ra}^- - x_{La}^-) = \left(e^{\lambda(t'-a)} + e^{-\lambda(t'+a)}\right)\left(-e^{-\lambda(t'+a)} - e^{\lambda(t'-a)}\right), \\
\lambda^2 d_{24}^2 &= (x_{Ra}^+ - x_{Lb}^+)(x_{Ra}^- - x_{Lb}^-) = \left(e^{\lambda(t'-a)} + e^{\lambda(b-t)}\right)\left(-e^{-\lambda(t'+a)} - e^{\lambda(t+b)}\right), \\
\lambda^2 d_{13}^2 &= (x_{Rb}^+ - x_{La}^+)(x_{Rb}^- - x_{La}^-) = \left(e^{\lambda(t+b)} + e^{-\lambda(t'+a)}\right)\left(-e^{\lambda(b-t)} - e^{\lambda(t'-a)}\right).
\end{aligned} \tag{9.12}$$

From these expressions we see that $d_{12}^2 = d_{34}^2$ and $d_{24}^2 = d_{13}^2$. Moreover,

$$\lambda^2 d_{14}^2 = -4e^{2\lambda b}\cosh^2(\lambda t), \qquad \lambda^2 d_{23}^2 = -4e^{-2\lambda a}\cosh^2(\lambda t'). \tag{9.13}$$

In the early phase of evaporation, the configuration without an island gives the minimal value of the fine-grained entropy (1.6), so we focus instead on the late-time regime, where the dominant configuration is expected to include an island. Consider, in the late-time limit $\lambda t \gg 1$ and $\lambda t' \gg 1$, the following ratio:

$$\frac{d_{23}^2 d_{14}^2}{d_{24}^2 d_{13}^2} = 16e^{2\lambda(b-a)}\frac{\cosh^2(\lambda t)\cosh^2(\lambda t')}{\left(e^{\lambda(t+b)} + e^{-\lambda(t'+a)}\right)^2\left(e^{\lambda(b-t)} + e^{\lambda(t'-a)}\right)^2} \sim 1, \qquad t, t' \to \infty. \tag{9.14}$$

Since the logarithm of the quantity in (9.14) appears in the semi-classical entropy (9.10), this behavior implies that it can be ignored in the late-time limit. The other necessary ingredient is the eternal black hole metric (4.104), which, using left–right symmetry, takes the form

$$\begin{aligned}
e^{-2\rho_1} &= e^{-2\rho_4} = e^{2\lambda b} + \frac{\pi G M}{\lambda} \equiv e^{-2\rho_b}, \\
e^{-2\rho_2} &= e^{-2\rho_3} = e^{-2\lambda a} + \frac{\pi G M}{\lambda} \equiv e^{-2\rho_a}.
\end{aligned} \tag{9.15}$$

After substituting (9.12) and (9.15), and using the late-time behavior of (9.14), the semi-classical entropy of the quantum fields becomes

$$S_{semi-cl} = \frac{N}{6}\ln\left(\frac{d_{12}^4}{\delta^4}e^{2\rho_a}e^{2\rho_b}\right) = \frac{N}{6}\ln\frac{\left(e^{\lambda(t+b)} - e^{\lambda(t'-a)}\right)^2\left(-e^{\lambda(b-t)} + e^{-\lambda(t'+a)}\right)^2}{(\lambda\delta)^2\left(e^{2\lambda b} + \frac{\pi G M}{\lambda}\right)\left(e^{-2\lambda a} + \frac{\pi G M}{\lambda}\right)}. \tag{9.16}$$

Now we extremize (9.16) with respect to the temporal coordinate. This can be done without including the surface contribution in (1.6), since that term depends only on the static black hole metric and is therefore time independent. Extremizing (9.16) gives the relation between the time at the island boundary and the time at the cut-off surface:

$$\partial_{t'} S_{gen} = \partial_{t'} S_{semi-cl} = \frac{N}{3}\frac{\partial_{t'} d_{12}^2}{d_{12}^2} = \frac{2N\lambda}{3d_{12}^2}e^{\lambda(b-a)}\sinh\left(\lambda(t-t')\right) = 0 \implies t' = t. \tag{9.17}$$

It is important to note that this relation between t and t' is valid only in the asymptotic late-time regime, $\lambda t \gg 1$ and $\lambda t' \gg 1$. This justifies imposing the condition $\lambda t' \gg 1$ simultaneously with $\lambda t \gg 1$. We can therefore rewrite (9.16) in the following static form:

$$S_{semi-cl} = \frac{N}{3}\rho_a + \frac{N}{3}\ln\frac{\left(e^{\lambda b} - e^{-\lambda a}\right)^2}{(\lambda\delta)^2\sqrt{e^{2\lambda b} + \frac{\pi GM}{\lambda}}}. \tag{9.18}$$

We choose the regularization of the UV cut-off so that the semi-classical entropy (9.18) is given by:

$$S_{semi-cl} = \frac{N}{3}\left(\rho_a - \rho_b\right) + \frac{2N}{3}\ln\left(e^{\lambda b} - e^{-\lambda a}\right) - \frac{2N}{3}\ln 2 - \frac{2N}{3}\lambda b. \tag{9.19}$$

Next, we examine the surface term in (1.6). It is not a priori obvious whether this contribution should be identified solely with the classical Bekenstein–Hawking entropy (1.4), or instead with its quantum-corrected counterpart (8.82) evaluated at the island boundary. Following [57], we adopt the quantum-corrected expression. An additional factor of 2 is required, as the geometry contains two asymptotically flat regions. The area term is therefore:

$$\frac{A[I]}{4G} = 2\left[\frac{2}{G\hbar}e^{-2\phi_a} - \frac{N}{6}\phi_a\right] + C = \frac{4}{G\hbar}\left[e^{-2\lambda a} + \frac{\pi GM}{\lambda}\right] + \frac{N}{6}\ln\left(e^{-2\lambda a} + \frac{\pi GM}{\lambda}\right) + C. \tag{9.20}$$

In Section 8.3.2 we pointed out that the quantum-corrected area term (8.82) is fixed only up to an additive constant C. This contribution is absent when the island is moved all the way down to the boundary of spacetime. However, this situation is not equivalent to imposing $\frac{A[I]}{4G} = 0$ in the limit $a \to \infty$, because in that case one recovers the Bekenstein–Hawking entropy (8.82), as $a \to \infty$ corresponds to the event horizon. A natural prescription for choosing the constant C is to require that at the moment of the black hole formation, i.e. in the combined limit $a \to \infty$ and $M \to 0$, the expression (9.20) goes to zero. It is important to emphasize that the order in which these limits are taken matters. With this prescription, the constant C is given by

$$C = -\frac{N}{6}\ln\frac{\pi GM}{\lambda}. \tag{9.21}$$

With this choice, the full expression for the generalized entropy, obtained by adding (9.19) and (9.20), takes the form:

$$S_{gen} = \frac{4}{G\hbar}\left[e^{-2\lambda a} + \frac{\pi GM}{\lambda}\right] - \frac{N}{3}\rho_b + \frac{2N}{3}\ln\left(1 - e^{-\lambda(a+b)}\right) - \frac{2N}{3}\ln 2 - \frac{2N}{3}\lambda b + C, \tag{9.22}$$

where we have adopted the Kruskal gauge $\rho_a = \phi_a$ and inserted the metric solution (4.104). We now extremize this expression along the spatial direction, that is, with respect to the parameter a:

$$\partial_a S_{gen} = -\frac{8\lambda}{G\hbar}e^{-2\lambda a} + \frac{2N\lambda}{3}\frac{1}{e^{\lambda(a+b)} - 1} = 0 \iff e^{2\lambda a} - \frac{12}{NG\hbar}e^{\lambda b}e^{\lambda a} + \frac{12}{NG\hbar} = 0. \tag{9.23}$$

Thus, we arrive at a quadratic equation in $e^{\lambda a}$. Its solutions are:

$$e^{\lambda a_\pm} = \frac{6}{NG\hbar}e^{\lambda b}\left[1 \pm \sqrt{1 - \frac{NG\hbar}{3}e^{-2\lambda b}}\right]. \tag{9.24}$$

Equation (9.24) yields two quantum extremal surfaces. To identify which of these corresponds to the correct island boundary, we must determine which root gives the global minimum of (9.22). We begin by examining the expression under the square root in (9.24):

$$1-\frac{NG\hbar}{3}e^{-2\lambda b}>0 \quad\implies\quad e^{2\lambda b}>\frac{NG\hbar}{3}. \tag{9.25}$$

Since both b and the black hole mass M are expected to be large, we consider the two limiting regimes $e^{2\lambda b}\gg\frac{NG\hbar}{3}$ and $\frac{\pi GM}{\lambda}\gg e^{2\lambda b}$. Implementing these approximations in (9.24) gives

$$e^{\lambda a_+}\approx\frac{12}{NG\hbar}e^{\lambda b} \quad\wedge\quad e^{\lambda a_-}\approx e^{-\lambda b}. \tag{9.26}$$

We first analyze the effect of substituting the a_- root into the generalized entropy (9.22). In this case we find

$$\frac{1}{G\hbar}e^{-2\lambda a}\to\frac{1}{G\hbar}e^{2\lambda b}\to\infty,\qquad \ln\left(1-e^{-\lambda(a+b)}\right)\to\ln\left(\frac{NG\hbar}{12}e^{-2\lambda b}\right)\to-\infty, \tag{9.27}$$

so that the generalized entropy diverges, $S_{gen}\to\infty$, in the limits under consideration. In contrast, using the a_+ root we obtain

$$e^{-2\lambda a}\to\left(\frac{NG\hbar}{12}\right)^2e^{-2\lambda b}\to0,\quad \ln\left(1-e^{-\lambda(a+b)}\right)\to\ln\left(1-\frac{NG\hbar}{12}e^{-2\lambda b}\right)\to-\frac{NG\hbar}{12}e^{-2\lambda b}\to0. \tag{9.28}$$

Thus, the a_+ root leads to a finite, well-defined limit of the generalized entropy (9.22), and therefore corresponds to the global minimum. Consequently, the fine-grained entropy is obtained by inserting a_+ from (9.24) into (9.22), which yields

$$\begin{aligned}S_{FG}&=\frac{4}{G\hbar}\left[\left(\frac{NG\hbar}{12}\right)^2e^{-2\lambda b}+\frac{\pi GM}{\lambda}\right]-\frac{N}{3}\rho_b-\frac{2N}{3}\frac{NG\hbar}{12}e^{-2\lambda b}-\frac{2N}{3}\ln 2-\frac{2N}{3}\lambda b+C\\&=\frac{4\pi M}{\lambda\hbar}+\frac{N}{6}\ln\left(e^{2\lambda b}+\frac{\pi GM}{\lambda}\right)-\frac{N^2G\hbar}{18}e^{-2\lambda b}-\frac{2N}{3}\ln 2-\frac{2N}{3}\lambda b+C\\&\approx\frac{4\pi M}{\lambda\hbar}+\frac{N}{6}\ln\frac{\pi GM}{\lambda}+C=2S_{BH}.\end{aligned}\tag{9.29}$$

It is evident that the global minimum corresponds to the a_+ root in (9.24). In the first line of (9.29) we employed the approximation $\frac{NG\hbar}{12}e^{-2\lambda b}\ll1$. Next, in the second line we simplified the resulting expression. In the third line we assumed a very large mass, namely $\frac{\pi GM}{\lambda}\gg e^{2\lambda b}$, and inserted the expression (9.21) for the constant C. As a result, we find that the entropy we obtain is approximately equal to $2S_{BH}$, as expected. We therefore conclude that, within this model, we have successfully reproduced the Page curve, which is given by:

$$S_{FG}=\mathbf{min}\left\{\frac{N}{3}\lambda t,2S_{BH}\right\}. \tag{9.30}$$

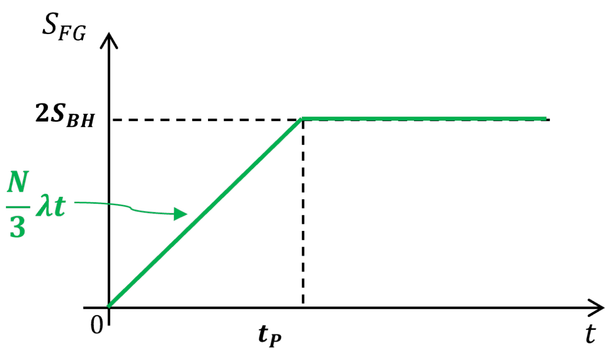

Figure 9.3: Page curve for an eternal black hole in the BPP model

9.2 Page curve in the evaporating black hole scenario

Here we study the entanglement entropy of the evaporating black hole solution in the BPP model introduced in Section 4.3.4. The discussion is organized into four subsections. In the first, we investigate the no-island configuration, which reproduces Hawking's original result and leads to information loss. We then consider the entanglement entropy in the presence of an island. In this case we demonstrate that the island forms behind the horizon, as expected, and that the Page curve is correctly obtained using the formula for the fine-grained entropy in gravitational systems (1.6). The third subsection is devoted to analyzing the Page time. The full computation is performed in asymptotically flat Eddington–Finkelstein coordinates, since these provide the time measured by an asymptotic stationary observer. In the final subsection, we repeat the calculation of the island location, now working in Kruskal coordinates (4.2). For most of this chapter we closely follow the derivation presented in [41].

9.2.1 No-island configuration

Unlike an eternal black hole, an evaporating black hole possesses a well-defined spacetime boundary on which reflective boundary conditions are imposed. Consequently, we must employ the expression (8.54) for the entanglement entropy of the quantum fields, which explicitly incorporates these reflective boundary conditions. In the no-island setup, the fine-grained entropy (1.6) therefore simplifies to the semiclassical contribution given by (8.54), namely:

$$S_{FG} = \frac{N}{12} \ln \frac{(\sigma^+_S - \sigma^+_{\bar{S}})^2}{\delta^2 e^{-2\rho_S(\sigma)}}. \tag{9.31}$$

Because we are considering an evaporating black hole, the relevant quantum state is the Unruh vacuum (3.98). The EMT is normal ordered with respect to the asymptotically flat coordinates defined before the collapse, namely the Eddington–Finkelstein coordinates $\sigma^\pm$. Thus entropy (9.31) is expressed in terms of these coordinates.

Figure 9.4 depicts the evaporating black hole scenario. The constant-time slice supporting the radiation degrees of freedom is indicated in red. It stretches from spatial infinity i^0 and intersects the cut-off surface (dashed blue line) at a point with coordinates (t, b). The point S represents the projection of this intersection onto past null infinity $\mathcal{J}^-$, while the point $\bar{S}$ is obtained by reflecting (t, b) across the spacetime boundary and then projecting onto the $\mathcal{J}^-$ hypersurface. This explains the labels S and $\bar{S}$ used in (9.31). The region inaccessible to an asymptotic observer is shaded in red. The spacetime boundary is given by equation (4.115), namely $2\lambda\sigma_{cr} = \ln \frac{\varepsilon\pi G}{4}$. Hence, the reflective boundary conditions imply:

$$\sigma^+_{\bar{S}} = \sigma^-_{\bar{S}} + 2\sigma_{cr} = \sigma^-_S + 2\sigma_{cr}. \tag{9.32}$$

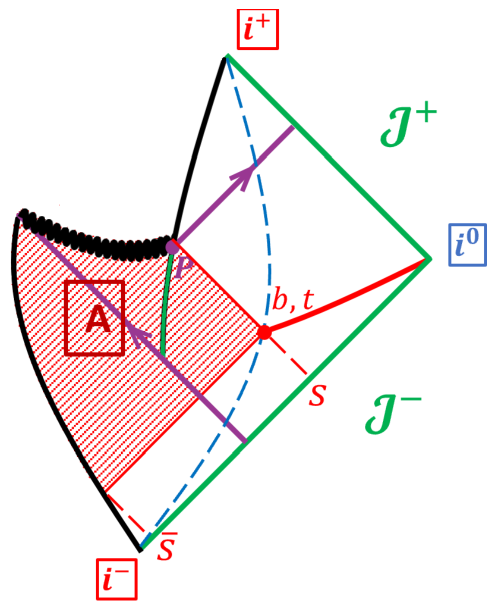

Figure 9.4: Penrose diagram illustrating the no-island setup for an evaporating black hole in the BPP model

The notion of time is specified using the asymptotically flat coordinates of region II (Figure 4.6), namely the $\hat{\sigma}^{\pm}$ coordinates introduced in equation (4.59). Consequently, in order to examine the time dependence of (9.31), we must rewrite it in terms of the $\hat{\sigma}^{\pm}$ coordinates. Implementing (9.32), the coordinate difference in (9.31) becomes

$$\sigma_S^+ - \sigma_{\bar{S}}^+ = \sigma_S^+ - \sigma_S^- - \frac{1}{\lambda}\ln\frac{\varepsilon\pi G}{4} = 2\sigma_S - \frac{1}{\lambda}\ln\frac{\varepsilon\pi G}{4}, \tag{9.33}$$

while the metric (4.119) can be written as

$$\begin{aligned} e^{2\lambda b} &= -\lambda^2 x_S^+(x_S^- + \Delta) = e^{2\lambda\sigma_S} - \lambda\Delta e^{\lambda(t+b)} \implies \sigma_S = b + \frac{1}{2\lambda}\ln\left(1+\lambda\Delta e^{\lambda(t-b)}\right), \\ e^{-2\rho_S(\sigma)} &= \frac{d\sigma^+}{dx^+}\frac{d\sigma^-}{dx^-}e^{-2\rho_S(x)} = e^{-2\lambda\sigma_S}\left[-\lambda^2 x_S^+(x_S^- + \Delta) - \frac{\varepsilon\pi G}{4}\ln\left(-\lambda^2 x_S^+ x_S^-\right) + \frac{\pi G M}{\lambda} + C^*\right] \\ &= \frac{1 - \left[\frac{\varepsilon\pi G}{4}\ln\left(1+\lambda\Delta e^{\lambda(t-b)}\right) + \frac{\varepsilon\pi G}{2}\lambda b - \frac{\pi G M}{\lambda} - C^*\right]e^{-2\lambda b}}{1+\lambda\Delta e^{\lambda(t-b)}}. \end{aligned} \tag{9.34}$$

By inserting (9.33) and (9.34) into the expression for the fine-grained entropy (9.31), we obtain:

$$S_{FG} = \frac{N}{12}\ln\frac{\left[2\lambda b + \ln\left(1+\lambda\Delta e^{\lambda(t-b)}\right) - \ln\frac{\varepsilon\pi G}{4}\right]^2\left(1+\lambda\Delta e^{\lambda(t-b)}\right)}{(\lambda\delta)^2\left[1-\left(\frac{\varepsilon\pi G}{4}\ln\left(1+\lambda\Delta e^{\lambda(t-b)}\right) + \frac{\varepsilon\pi G}{2}\lambda b - \frac{\pi G M}{\lambda} - C^*\right)e^{-2\lambda b}\right]}. \tag{9.35}$$

At the beginning of the evaporation process, this function is effectively linear, but with a highly nontrivial slope. We do not study this limiting behavior in detail. To regularize the UV divergence in (9.35), we impose that the fine-grained entropy vanishes at $t = 0$. This implies that $S_{FG}(t)$ is shifted to $S_{FG}(t) - S_{FG}(0)$. Denoting the expression in (9.35) by $S(t)$, the renormalized entropy becomes $S_{FG}(t) = S(t) - S(0)$. To determine whether information is lost, we must investigate the asymptotic behavior of (9.35) at late times, i.e., for $\lambda t \gg 1$. In this regime, we immediately obtain $\ln\left(1+\lambda\Delta e^{\lambda(t-b)}\right) \approx \ln(\lambda\Delta) + \lambda(t-b)$. Under this approximation, (9.35) takes the following form:

$$S_{FG} \approx \frac{N}{12}\ln\frac{\lambda\Delta e^{\lambda(t-b)}\left[\lambda(t+b) + \ln(\lambda\Delta) - \ln\frac{\varepsilon\pi G}{4}\right]^2}{(\lambda\delta)^2\left[1-\left(\frac{\varepsilon\pi G}{4}\ln(\lambda\Delta) + \frac{\varepsilon\pi G}{4}(t+b) - \frac{\pi G M}{\lambda} - C^*\right)e^{-2\lambda b}\right]} - S(0). \tag{9.36}$$

From this expression we identify a logarithmic term proportional to $\ln(\lambda t)$ as well as a term growing linearly with t. At late times, the linear contribution clearly dominates the entropy growth. Consequently, we obtain:

$$S_{FG} \approx \frac{N}{12}\lambda t. \tag{9.37}$$

Therefore, in the no-island configuration, the information is lost and the Page curve cannot be recovered. The behavior we find reproduces Hawking's original result [16], as anticipated. To achieve unitary evolution, one must include the island and evaluate the entropy using the island rule.

9.2.2 Island configuration

We now consider the situation in which an island region is present in the spacetime. In this case, both contributions in (1.6) are non-zero. As in the eternal black hole setup discussed in the previous subsection, reflective boundary conditions must be imposed at the spacetime boundary. Although the inaccessible region A is simply connected, these reflective boundary conditions imply that its projection onto the $\mathcal{J}^-$ hypersurface breaks up into two separate regions. Consequently, for this configuration we must employ a considerably more complicated formula for the semiclassical entropy in (1.6), namely the one given in (8.60):

$$S_{semi-cl} = \frac{N}{12} \ln \frac{(\sigma_I^+ - \sigma_S^+)^2 (\sigma_{\bar{I}}^+ - \sigma_{\bar{S}}^+)^2 (\sigma_I^+ - \sigma_{\bar{I}}^+)^2 (\sigma_S^+ - \sigma_{\bar{S}}^+)^2}{\delta^4 (\sigma_S^+ - \sigma_{\bar{I}}^+)^2 (\sigma_I^+ - \sigma_{\bar{S}}^+)^2 e^{-2\rho_S(\sigma)} e^{-2\rho_I(\sigma)}}. \tag{9.38}$$

Here, the labels S and $\bar{S}$ denote, respectively, the projection of the intersection between the constant-time slice and the cut-off hypersurface, and the projection of its reflection on the spacetime boundary onto past null infinity $\mathcal{J}^-$. Similarly, I and $\bar{I}$ represent the projections of the island boundary location and of its reflection on the spacetime boundary onto the hypersurface $\mathcal{J}^-$, respectively.

Figure 9.5 depicts how the configuration in Figure 9.4 is modified once an island region is included. The island, denoted by I, is indicated in blue, while the inaccessible region A is highlighted in red. All relevant projections, namely S, $\bar{S}$, I, and $\bar{I}$, are explicitly displayed. The $\sigma^\pm$ coordinates corresponding to these projections are determined using the definition of the spacetime boundary hypersurface (4.115), and take the form

$$\begin{aligned} \sigma_{\bar{S}}^+ &= \sigma_{\bar{S}}^- + 2\sigma_{cr} = \sigma_S^- + \frac{1}{\lambda} \ln \frac{\varepsilon \pi G}{4}, \\ \sigma_{\bar{I}}^+ &= \sigma_{\bar{I}}^- + 2\sigma_{cr} = \sigma_I^- + \frac{1}{\lambda} \ln \frac{\varepsilon \pi G}{4}. \end{aligned} \tag{9.39}$$

Because our goal is to analyze the time dependence of the fine-grained entropy, and the time coordinate is defined in terms of the new asymptotically flat coordinates of region II given in (4.59), we must rewrite (9.38) in this coordinate system.

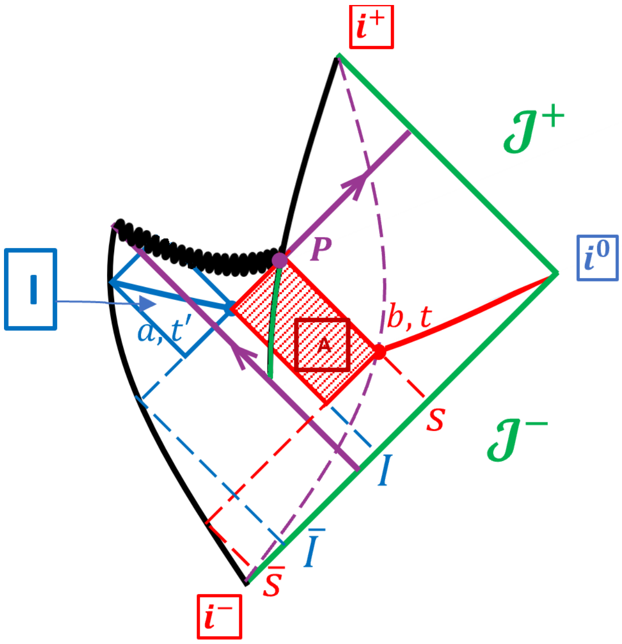

Figure 9.5: Penrose diagram illustrating the island setup for an evaporating black hole in the BPP model

We denote the island position by (t', a), whereas the coordinates on the cut–off surface are specified in the usual way as (t, b). In the large–mass limit, the horizon is located just below the hypersurface $x^- = -\Delta$ (see Section 4.3.4), implying that $x_I^- + \Delta$ is positive. Consequently, for the island coordinates, after using (4.59), we obtain:

$$\lambda x_I^+ = e^{\lambda(t'+a)} = e^{\lambda \sigma_I^+} \quad \wedge \quad \lambda(x_I^- + \Delta) = e^{-\lambda(t'-a)} = -e^{-\lambda \sigma_I^-} + \lambda \Delta. \tag{9.40}$$

Meanwhile, the coordinates on the cut-off surface are expressed as:

$$\lambda x_S^+ = e^{\lambda(t+b)} = e^{\lambda \sigma_S^+} \quad \wedge \quad \lambda(x_S^- + \Delta) = -e^{-\lambda(t-b)} = -e^{-\lambda \sigma_S^-} + \lambda \Delta. \tag{9.41}$$

By combining equations (9.40) and (9.41) and employing the relations given in (9.39), the coordinate differences that appear in the expression (9.38) for the semiclassical entropy take the following form:

$$
\begin{aligned}
&\sigma_I^+ - \sigma_S^+ = \hat{\sigma}_I^+ - \hat{\sigma}_S^+ = t' + a - (t+b),\\
&\sigma_{\bar{I}}^+ - \sigma_{\bar{S}}^+ = \sigma_I^- - \sigma_S^- = -\frac{1}{\lambda}\ln\left(\lambda\Delta - e^{-\lambda(t'-a)}\right) + \frac{1}{\lambda}\ln\left(\lambda\Delta + e^{-\lambda(t-b)}\right),\\
&\sigma_I^+ - \sigma_{\bar{I}}^+ = \sigma_I^+ - \sigma_I^- - \frac{1}{\lambda}\ln\frac{\varepsilon\pi G}{4} = t' + a + \frac{1}{\lambda}\ln\left(\lambda\Delta - e^{-\lambda(t'-a)}\right) - \frac{1}{\lambda}\ln\frac{\varepsilon\pi G}{4},\\
&\sigma_S^+ - \sigma_{\bar{S}}^+ = \sigma_S^+ - \sigma_S^- - \frac{1}{\lambda}\ln\frac{\varepsilon\pi G}{4} = t + b + \frac{1}{\lambda}\ln\left(\lambda\Delta + e^{-\lambda(t-b)}\right) - \frac{1}{\lambda}\ln\frac{\varepsilon\pi G}{4},\\
&\sigma_S^+ - \sigma_{\bar{I}}^+ = \sigma_S^+ - \sigma_I^- - \frac{1}{\lambda}\ln\frac{\varepsilon\pi G}{4} = t + b + \frac{1}{\lambda}\ln\left(\lambda\Delta - e^{-\lambda(t'-a)}\right) - \frac{1}{\lambda}\ln\frac{\varepsilon\pi G}{4},\\
&\sigma_I^+ - \sigma_{\bar{S}}^+ = \sigma_I^+ - \sigma_S^- - \frac{1}{\lambda}\ln\frac{\varepsilon\pi G}{4} = t' + a + \frac{1}{\lambda}\ln\left(\lambda\Delta + e^{-\lambda(t-b)}\right) - \frac{1}{\lambda}\ln\frac{\varepsilon\pi G}{4}.
\end{aligned}
\tag{9.42}
$$

In the early stages of the evaporation process, the configuration without an island yields the minimum of the fine-grained entropy. We now focus on the late-time regime, where the minimum is expected to switch to the spacetime configuration that includes an island. We start by analyzing the following quantity in the regime where $\lambda t \gg 1$ and $\lambda t' \gg 1$:

$$
\begin{aligned}
&\frac{(\sigma_I^+ - \sigma_{\bar{I}}^+)(\sigma_S^+ - \sigma_{\bar{S}}^+)}{(\sigma_I^+ - \sigma_{\bar{S}}^+)(\sigma_S^+ - \sigma_{\bar{I}}^+)} \qquad (9.43)\\
&= \frac{\left[t' + a + \frac{1}{\lambda}\ln\left(\lambda\Delta - e^{-\lambda(t'-a)}\right) - \frac{1}{\lambda}\ln\frac{\varepsilon\pi G}{4}\right]\left[t + b + \frac{1}{\lambda}\ln\left(\lambda\Delta + e^{-\lambda(t-b)}\right) - \frac{1}{\lambda}\ln\frac{\varepsilon\pi G}{4}\right]}{\left[t + b + \frac{1}{\lambda}\ln\left(\lambda\Delta - e^{-\lambda(t'-a)}\right) - \frac{1}{\lambda}\ln\frac{\varepsilon\pi G}{4}\right]\left[t' + a + \frac{1}{\lambda}\ln\left(\lambda\Delta + e^{-\lambda(t-b)}\right) - \frac{1}{\lambda}\ln\frac{\varepsilon\pi G}{4}\right]} \to 1.
\end{aligned}
$$

Thus, in analogy with the no-island configuration, the contribution (9.43) can be neglected in the late-time limit of (9.38), yielding:

$$
S_{semi-cl} = \frac{N}{6}\left(\rho_S(\sigma) + \rho_I(\sigma)\right) + \frac{N}{12}\ln\frac{(\sigma_I^+ - \sigma_S^+)^2(\sigma_{\bar{I}}^+ - \sigma_{\bar{S}}^+)^2}{\delta^4}. \tag{9.44}
$$

In this late-time regime, the difference of the reflected coordinates in (9.44) may be further approximated as:

$$
\sigma_{\bar{I}}^+ - \sigma_{\bar{S}}^+ = \frac{1}{\lambda}\left[\ln\left(1 + \frac{1}{\lambda\Delta}e^{-\lambda(t-b)}\right) - \ln\left(1 - \frac{1}{\lambda\Delta}e^{-\lambda(t'-a)}\right)\right] \approx \frac{1}{\lambda^2\Delta}\left(e^{-\lambda(t-b)} + e^{-\lambda(t'-a)}\right). \tag{9.45}
$$

We emphasize that the UV divergences must be regularized in exactly the same manner as in the configuration without an island (or in the eternal black hole case). This affects the result only by an additive constant. Consequently, the semiclassical entropy formula (9.44) becomes:

$$
S_{semi-cl} = \frac{N}{6}\left(\rho_S(\sigma) + \rho_I(\sigma)\right) + \frac{N}{6}\ln\frac{\left|\lambda(t + b - t' - a)\right|\left(e^{-\lambda(t-b)} + e^{-\lambda(t'-a)}\right)}{(\lambda\delta)^2(\lambda\Delta)} - S_0, \tag{9.46}
$$

where we have subtracted the additive constant S_0. We now consider the surface term appearing in (1.6). As in the eternal black hole scenario, it is again given by (8.82). Thus, we obtain:

$$\begin{aligned}\frac{A[I]}{4G} &= \frac{2}{G\hbar}e^{-2\phi_I} - \frac{N}{6}\phi_I + C \\ &= \frac{2}{G\hbar}\left[-\lambda^2 x_I^+(x_I^- + \Delta) - \frac{\varepsilon\pi G}{4}\ln\left(-\lambda^2 x_I^+ x_I^-\right) + \frac{\pi G M}{\lambda} + C^*\right] - \frac{N}{6}\phi_I + C \\ &= \frac{2}{G\hbar}\left[-e^{2\lambda a} - \frac{\varepsilon\pi G}{4}\ln\left(-e^{2\lambda a} + \lambda\Delta e^{\lambda(t'+a)}\right) + \frac{\pi G M}{\lambda} + C^*\right] - \frac{N}{6}\phi_I + C \\ &= \frac{2}{G\hbar}\left[-e^{2\lambda a} - \frac{\varepsilon\pi G}{4}\lambda(t'+a) - \frac{\varepsilon\pi G}{4}\ln(\lambda\Delta) + \frac{\pi G M}{\lambda} + C^*\right] - \frac{N}{6}\phi_I + C, \end{aligned} \tag{9.47}$$

where C is an arbitrary integration constant. For further details, see Section 8.3.2. In the second line we have inserted the metric (4.119). In the third line, we have used the island position (9.40). Finally, in the last line we have taken the large-t' limit. We now need to rewrite the dilaton field ϕ_I in terms of the metric function ρ_I. To do so, we use the fact that these two quantities coincide in Kruskal coordinates, and then transform them to the Eddington–Finkelstein coordinates of region II in Figure 4.6. Concretely, we have

$$e^{2\phi}\mathrm{d}x^+\mathrm{d}x^- = e^{2\rho(\sigma)}\mathrm{d}\sigma^+\mathrm{d}\sigma^- \quad\Longrightarrow\quad e^{2\phi_I} = \frac{\mathrm{d}\sigma^+}{\mathrm{d}x^+}\frac{\mathrm{d}\sigma^-}{\mathrm{d}x^-}e^{2\rho_I(\sigma)} = e^{-2\lambda\sigma_I}e^{2\rho_I(\sigma)}. \tag{9.48}$$

This leads to the following form for the dilaton field:

$$\phi_I = \rho_I(\sigma) - \lambda\sigma_I = \rho_I(\sigma) - \frac{1}{2}\ln\left(-e^{2\lambda a} + \lambda\Delta e^{\lambda(t'+a)}\right) = \rho_I(\sigma) - \frac{1}{2}\lambda(a+t') - \frac{1}{2}\ln(\lambda\Delta), \tag{9.49}$$

where, in the last step, we have again employed the large-t' limit. Substituting this expression into (9.47), we obtain

$$\frac{A[I]}{4G} = \frac{2}{G\hbar}\left[-e^{2\lambda a} + \frac{\varepsilon\pi G}{4}\lambda(a+t') + \frac{\varepsilon\pi G}{4}\ln(\lambda\Delta) + \frac{\pi G M}{\lambda} + C^*\right] - \frac{N}{6}\rho_I(\sigma) + C. \tag{9.50}$$

The generalized entropy is then defined as the sum of the semiclassical contribution (9.46) and the area term (9.50). It is given by the following expression:

$$\begin{aligned} S_{gen} =& \frac{2}{G\hbar}\left[-e^{2\lambda a} + \frac{\varepsilon\pi G}{4}\lambda(a+t') + \frac{\pi G M}{\lambda} + C^*\right] + \frac{N}{6}\rho_S(\sigma) \\ &+ \frac{N}{6}\ln\frac{\left|\lambda(t+b-t'-a)\right|\left(e^{-\lambda(t-b)} + e^{-\lambda(t'-a)}\right)}{(\lambda\delta)^2(\lambda\Delta)^{3/4}} + C - S_0. \end{aligned} \tag{9.51}$$

Next, we extremize this expression with respect to both the temporal coordinate t' and the spatial coordinate a:

$$\partial_{t'}S_{gen} = 0 \quad\Longleftrightarrow\quad \frac{N}{24}\lambda + \frac{N}{6}\lambda\left[\frac{1}{\lambda(t'+a-t-b)} - \frac{1}{1+e^{\lambda(t'-t+b-a)}}\right] = 0, \tag{9.52}$$

$$\partial_a S_{gen} = 0 \quad\Longleftrightarrow\quad -\frac{4\lambda}{G\hbar}e^{2\lambda a} + \frac{N}{24}\lambda + \frac{N}{6}\lambda\left[\frac{1}{\lambda(t'+a-t-b)} + \frac{1}{1+e^{\lambda(t'-t+b-a)}}\right] = 0. \tag{9.53}$$

After simplifying, this system of algebraic equations can be rewritten as:

$$\frac{1}{\lambda(t' + a - t - b)} + \frac{1}{1 + e^{\lambda(t' - t + b - a)}} = -\frac{1}{4} + \frac{2}{\varepsilon \pi G} e^{2\lambda a}, \tag{9.54}$$
$$\frac{1}{\lambda(t' + a - t - b)} - \frac{1}{1 + e^{\lambda(t' - t + b - a)}} = -\frac{1}{4}. \tag{9.55}$$

Subtracting these two equations yields a quadratic equation for $e^{\lambda a}$:

$$e^{2\lambda a} + e^{\lambda a} e^{\lambda(t' - t + b)} - \varepsilon \pi G = 0 \quad \Longrightarrow \quad e^{\lambda a} = \frac{1}{2} e^{\lambda(t' - t + b)} \left[\sqrt{1 + 4\varepsilon \pi G e^{-2\lambda(t' - t + b)}} - 1 \right]. \tag{9.56}$$

Only one root is physically acceptable, as we must have $e^{\lambda a} > 0$. This solution is very similar to the island location in the eternal black hole case, namely equation (9.24). However, here we still need to determine t' and a independently. To do so, we adopt the same approximation used for the eternal black hole, that is: $4\varepsilon \pi G e^{-2\lambda(t' - t + b)} \ll 1$. Under this approximation, the solution (9.56) simplifies to:

$$e^{\lambda a} = \varepsilon \pi G e^{-\lambda(t' - t + b)} \quad \Longrightarrow \quad e^{2\lambda a} = \varepsilon \pi G e^{-\lambda(t' - a + b - t)} = \varepsilon \pi G e^{-\mathrm{x}}, \tag{9.57}$$

where we introduced the auxiliary variable $\mathrm{x} = \lambda(t' - a + b - t)$. Adding equations (9.54) and (9.55) gives:

$$\mathrm{x} = \frac{1}{-\frac{1}{4} + e^{-\mathrm{x}}} + 2\lambda(b - a) = \frac{1}{-\frac{1}{4} + e^{-\mathrm{x}}} + 2\lambda b - \ln(\varepsilon \pi G) + \mathrm{x}, \tag{9.58}$$

where, in the second equality, we have used the approximate expression (9.57). Solving this equation for x leads to:

$$e^{-\mathrm{x}} = \frac{1}{4} + \frac{1}{\ln(\varepsilon \pi G e^{-2\lambda b})}. \tag{9.59}$$

Substituting this back into (9.57) yields:

$$e^{2\lambda a} = \frac{\varepsilon \pi G}{4} + \frac{\varepsilon \pi G}{\ln(\varepsilon \pi G e^{-2\lambda b})} \approx \frac{\varepsilon \pi G}{4}, \tag{9.60}$$

where the last approximation follows from the condition $\varepsilon \pi G e^{-2\lambda b} \ll 1$, which renders the second term negligible. Consequently, in the late stages of black hole evaporation, extremizing the generalized entropy gives an island located at:

$$e^{2\lambda a} = \frac{\varepsilon \pi G}{4} \quad \wedge \quad \lambda t' = \lambda(t - b) + \frac{1}{2} \ln(4\varepsilon \pi G). \tag{9.61}$$

Within this approximation, we observe that t' becomes very large. This validates our initial assumption that we can take $\lambda t' \gg 1$ whenever $\lambda t \gg 1$. The remaining step is to determine the contribution of this island to the fine–grained entropy of the radiation, and to verify whether it reproduces the Page curve. Substituting (9.61) directly into the expression for the generalized entropy (9.51) gives:

$$
\begin{aligned}
S_{gen} &= \frac{2}{G\hbar}\left[\frac{\varepsilon\pi G}{4}\lambda(t-b) + \frac{\pi G M}{\lambda} + 2C^{*} + \frac{\varepsilon\pi G}{4}\ln 2\right] + \frac{N}{6}\ln\frac{\frac{5}{4}\ln\left(\varepsilon\pi G e^{-2\lambda b}\right)}{(\lambda\delta)^{2}(\lambda\Delta)^{3/4}} + C - S_0 \\
&\quad - \frac{N}{6}\lambda(t-b) + \frac{N}{12}\ln\frac{1+\lambda\Delta e^{\lambda(t-b)}}{1-\left[\frac{\varepsilon\pi G}{4}\ln\left(1+\lambda\Delta e^{\lambda(t-b)}\right) + \frac{\varepsilon\pi G}{2}\lambda b - \frac{\pi G M}{\lambda} - C^{*}\right]e^{-2\lambda b}} \\
&= -\frac{N}{24}\lambda t + \frac{2}{G\hbar}\left[\frac{\pi G M}{\lambda} + \frac{\varepsilon\pi G}{4}\lambda b + 2C^{*} - \frac{\varepsilon\pi G}{4}\ln(\lambda\Delta) + \frac{\varepsilon\pi G}{4}\ln 2\right] \\
&\quad + \frac{N}{6}\ln\frac{\frac{5}{4}\left(\ln(\varepsilon\pi G) - 2\lambda b\right)}{(\lambda\delta)^{2}\sqrt{1-\left[\frac{\varepsilon\pi G}{4}\ln(\lambda\Delta) + \frac{\varepsilon\pi G}{4}\lambda(t+b) - \frac{\pi G M}{\lambda} - C^{*}\right]e^{-2\lambda b}}} + C - S_0. \qquad (9.62)
\end{aligned}
$$

Note that, within the large-mass approximation, the constant term in this expression approaches the Bekenstein–Hawking entropy (1.4), provided the constants C and S_0 are chosen appropriately. Consequently, at the saddle point determined by the island, the generalized entropy becomes:

$$
S_{gen} = S_{BH}^{(0)} - \frac{N}{24}\lambda t \quad \Longrightarrow \quad S_{FG} = \mathbf{min}\left\{\frac{N}{12}\lambda t,\, S_{BH}^{(0)} - \frac{N}{24}\lambda t\right\}. \qquad (9.63)
$$

The first observation is that the island lies precisely where anticipated: just beneath the black hole's horizon. We can specify its location using Kruskal coordinates as

$$
\lambda^{2} x_I^{+}(x_I^{-} + \Delta) = \frac{\varepsilon\pi G}{4}. \qquad (9.64)
$$

This shows that the island mirrors the apparent horizon across the hypersurface $x^{-} = -\Delta$, which almost exactly matches the horizon in large-mass limit.

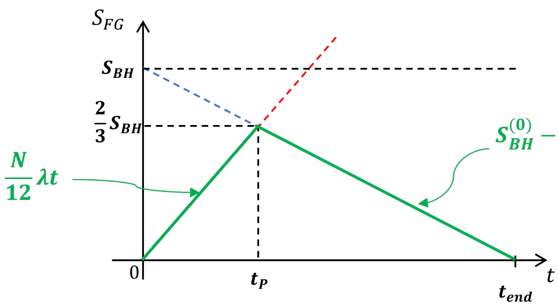

Figure 9.6: Page curve for an evaporating black hole in the BPP model

9.2.3 Page time and the validity of the Page curve

In this section, we examine the consistency of the solution obtained and determine several key parameters of the evaporation process, in particular the Page time. The Page time is defined as the moment when the phase transition in (9.63) takes place. Our first consistency check is to verify that the evaporation indeed terminates at the evaporation end-point (4.141). This follows immediately, since the fine-grained entropy (9.63) vanishes once we substitute (4.141). We now compute the Page time:

$$
\frac{N}{12}\lambda t_p = S_{BH}^{(0)} - \frac{N}{24}\lambda t_p \quad \Longrightarrow \quad t_p = \frac{16\pi M}{N\hbar\lambda^{2}}, \qquad (9.65)
$$

where we have used the classical expression for the Bekenstein–Hawking entropy of a black hole in the CGHS model (1.4). From this we infer that the phase transition occurs at one third of the total evaporation time, i.e. $t_p = \frac{t_{\text{end}}}{3}$. This is much earlier than the moment when quantum gravitational effects become significant, since the black hole remains macroscopically large at that time. Therefore, the semiclassical approximation is reliable at the Page time. It remains to evaluate the entropy at the Page time. We obtain:

$$
S_{FG,p} = \frac{N}{12}\lambda t_p = \frac{N}{12}\lambda\frac{8S_{BH}^{(0)}}{N\lambda} \quad \Longrightarrow \quad S_{FG,p} = \frac{2}{3}S_{BH}. \qquad (9.66)
$$

This is the maximum value attained by the fine-grained entropy of the radiation during black hole evaporation, and it is manifestly smaller than the Bekenstein–Hawking entropy of the black hole. We can thus conclude that unitarity is preserved. Consequently, the curve shown in Figure 9.6 is indeed the Page curve.

As we know, throughout the entire black hole evaporation process the island remains located behind the event horizon. At some point, the trajectory traced by the island over time (9.64) intersects the singularity. We must verify that this intersection happens only at the very end of evaporation, because the Page curve description is valid only as long as such an intersection does not occur. To this end, we need to solve the following system of equations:

$$\lambda^2 x^+_{col}(x^-_{col}+\Delta) = \frac{\varepsilon\pi G}{4}, \tag{9.67}$$

$$-\lambda^2 x^+_{col}(x^-_{col}+\Delta) - \frac{\varepsilon\pi G}{4}\ln\left(-\lambda^2 x^+_{col}x^-_{col}\right) + \frac{\pi G M}{\lambda} + C^* = 0, \tag{9.68}$$

where the second equation specifies the singularity hypersurface (4.120). We previously solved an analogous system when determining where the apparent horizon meets the singularity in Section 4.3.4. The solution to the present system is as follows:

$$\lambda x^+_{col} = \frac{\varepsilon\pi G}{4\lambda\Delta}\left[1+e^{-2+\frac{4M}{\varepsilon\lambda}}\right] \quad \wedge \quad \lambda(x^-_{col}+\Delta) = \frac{\lambda\Delta}{1+e^{-2+\frac{4M}{\varepsilon\lambda}}}. \tag{9.69}$$

Consequently, the collision time is given by:

$$e^{2\lambda t_{col}} = \frac{x^+_{col}}{x^-_{col}+\Delta} = \frac{\varepsilon\pi G}{4(\lambda\Delta)^2}\left(1+e^{-2+\frac{4M}{\varepsilon\lambda}}\right)^2. \tag{9.70}$$

We now determine when this intersection takes place relative to the total evaporation time. Using (4.124), the end-time can be written as:

$$e^{2\lambda t_{end}} = \frac{\varepsilon\pi G}{4(\lambda\Delta)^2}\left(e^{\frac{4M}{\varepsilon\lambda}}-1\right)^2. \tag{9.71}$$

Subtracting the time defined in (9.69) from that in (9.71) yields:

$$\begin{aligned}\lambda\Delta t = \lambda(t_{end}-t_{col}) &= \ln\left(e^{\frac{4M}{\varepsilon\lambda}}-1\right) - \ln\left(e^{-2+\frac{4M}{\varepsilon\lambda}}+1\right)\\ &= \frac{4M}{\varepsilon\lambda} + \ln\left(1-e^{-\frac{4M}{\varepsilon\lambda}}\right) - \left(-2+\frac{4M}{\varepsilon\lambda}\right) - \ln\left(1-e^{2-\frac{4M}{\varepsilon\lambda}}\right) \approx 2. \end{aligned} \tag{9.72}$$

We observe that this time gap is $\lambda\Delta t \approx 2$, which is of order $\mathcal{O}(1)$. For a large initial mass this contribution is negligible. Hence, the intersection effectively occurs just before the very end of the black hole's lifetime. At that stage, the black hole has shrunk to a size of order the Planck length, so quantum gravitational effects become important and the semiclassical approximation is no longer reliable. In a full theory of quantum gravity, one may therefore expect that the island and the singularity never actually collide.

As we can see, this does not pose a problem either, and we conclude that our semiclassical approximation remains valid until the very end of the black hole evaporation process. Completely identical results are obtained in the RST model [40].

9.2.4 Position of the island in terms of the Kruskal coordinates

In this subsection we repeat the computation of the island position using Kruskal coordinates. To do this, we express the generalized entropy in terms of the Kruskal coordinates and then extremize it, following the procedure in [41]. In these coordinates we no longer need to guess where the island should lie, since the Kruskal coordinates $x^{\pm}$ are analytic throughout the whole spacetime. We avoided this route at first because the asymptotic observer's time is defined via the $\hat{\sigma}^{\pm}$ coordinates, which directly encode the time dependence of the entropy. For that reason, the earlier method is more convenient for giving a physical interpretation of black hole evaporation process.

We now go directly to the late–time limit of the evaporation. In this limit the quantity (9.43) approaches unity. The remaining differences can then be easily evaluated:

$$\sigma_I^+ - \sigma_S^+ = \frac{1}{\lambda} \ln \frac{x_I^+}{x_S^+} \quad \wedge \quad \sigma_I^+ - \sigma_S^+ = \frac{1}{\lambda} \ln \frac{x_I^-}{x_S^-}. \tag{9.73}$$

Substituting (9.73) and the metric (4.119) into (9.38), the semi–classical entropy becomes

$$S_{semi-cl} = \frac{N}{12} \ln \frac{\ln^2 \frac{x_I^+}{x_S^+} \ln^2 \frac{x_I^-}{x_S^-} \left(-\lambda^2 x_I^+ x_I^-\right) e^{2\rho_S(\sigma)}}{(\lambda\delta)^4 \left[-\lambda^2 x_I^+ (x_I^- + \Delta) - \frac{\varepsilon\pi G}{4} \ln\left(-\lambda^2 x_I^+ x_I^-\right) + \frac{\pi G M}{\lambda} + C^*\right]} - S_0, \tag{9.74}$$

while the surface contribution (8.82) is

$$\begin{aligned}
\frac{A[I]}{4G} &= \frac{2}{G\hbar} e^{-2\phi_I} - \frac{N}{6}\phi_I + C \\
&= \frac{2}{G\hbar}\left[-\lambda^2 x_I^+ (x_I^- + \Delta) - \frac{\varepsilon\pi G}{4} \ln\left(-\lambda^2 x_I^+ x_I^-\right) + \frac{\pi G M}{\lambda} + C^*\right] \\
&\quad + \frac{N}{12} \ln\left\{-\lambda^2 x_I^+ (x_I^- + \Delta) - \frac{\varepsilon\pi G}{4} \ln\left(-\lambda^2 x_I^+ x_I^-\right) + \frac{\pi G M}{\lambda} + C^*\right\} + C.
\end{aligned} \tag{9.75}$$

Since we are interested only in the island position and not in the explicit closed form of the fine–grained entropy, we group all terms independent of $x_I^{\pm}$ into a single constant C_0. The generalized entropy can then be written as

$$S_{gen} = \frac{2}{G\hbar}\left[-\lambda^2 x_I^+ (x_I^- + \Delta) - \frac{\varepsilon\pi G}{4} \ln\left(-\lambda^2 x_I^+ x_I^-\right)\right] + \frac{N}{12} \ln\left(-\lambda^2 x_I^+ x_I^- \ln^2 \frac{x_I^+}{x_S^+} \ln^2 \frac{x_I^-}{x_S^-}\right) + C_0. \tag{9.76}$$

We now extremize this expression with respect to x_I^+ and x_I^-, obtaining

$$\partial_+ S_{gen} = 0 \quad \Longleftrightarrow \quad \frac{2}{G\hbar}\left[-\lambda^2 (x_I^- + \Delta) - \frac{\varepsilon\pi G}{4} \frac{1}{x_I^+}\right] + \frac{N}{12}\left[\frac{1}{x_I^+} + \frac{2}{\ln \frac{x_I^+}{x_S^+}} \frac{1}{x_I^+}\right] = 0, \tag{9.77}$$

$$\partial_- S_{gen} = 0 \quad \Longleftrightarrow \quad \frac{2}{G\hbar}\left[-\lambda^2 x_I^+ - \frac{\varepsilon\pi G}{4} \frac{1}{x_I^-}\right] + \frac{N}{12}\left[\frac{1}{x_I^-} + \frac{2}{\ln \frac{x_I^-}{x_S^-}} \frac{1}{x_I^-}\right] = 0. \tag{9.78}$$

Multiplying the first of these by x_I^+ and the second by x_I^- leads to

$$\lambda^2 x_I^+(x_I^- + \Delta) = \frac{\varepsilon\pi G}{4} + \frac{\varepsilon\pi G}{\ln\frac{x_I^+}{x_S^+}}, \tag{9.79}$$

$$\lambda^2 x_I^+ x_I^- = \frac{\varepsilon\pi G}{4} + \frac{\varepsilon\pi G}{\ln\frac{x_I^-}{x_S^-}}. \tag{9.80}$$

Consider now the second term in equation (9.79):

$$\frac{\varepsilon\pi G}{\ln\frac{x_I^+}{x_S^+}} = \frac{\varepsilon\pi G}{\ln x_I^+ - \ln x_S^+} = \frac{\varepsilon\pi G}{\ln x_I^+ - \lambda(t+b)} \to 0, \qquad \lambda(t+b) \gg 1. \tag{9.81}$$

In contrast, the second term in equation (9.80) does not vanish in this approximation. We now assume that we are located, if not exactly on $\mathcal{J}^+$, then at least very close to it. This implies $x_S^+ \to \infty$, while x_S^- remains finite. Under these conditions, the island position is determined by the same relation as in the preceding section (9.64):

$$\lambda^2 x_I^+(x_I^- + \Delta) = \frac{\varepsilon\pi G}{4}. \tag{9.82}$$

Chapter 10

Page curve in the DREH model

In this chapter, we demonstrate how the Page curve is recovered within the DREH model of two-dimensional dilaton gravity introduced in Chapter 5. The analysis parallels the derivation carried out for the BPP model in Chapter 9. In contrast to the BPP model, the DREH model contains the quantum-corrected Schwarzschild black hole solution, which has been experimentally tested. It is therefore not only qualitatively, but also quantitatively more relevant. For example, in Section 5.3, we show that the evaporation time obtained in this two-dimensional framework agrees with the four-dimensional thermodynamic expectations.

The key distinction between the BPP and DREH models is that, once quantum corrections are included, the DREH equations of motion are no longer analytically solvable and must be treated perturbatively, as in Section 5.2. Since the perturbative expansion fails near the end-point of evaporation, computing the Page curve there requires special care. Nevertheless, around this stage the effects of the full quantum gravity theory become significant [1], so the breakdown of perturbation theory is ultimately less concerning. In this chapter, we illustrate how equation (1.6) can be used to determine the Page curve for both eternal and evaporating black holes within the DREH model. The chapter is organized into three sections.

In the first section, we analyze the eternal black hole solution in the DREH model, introduced in Section 5.2.3. We demonstrate that if the area term in (1.6) is omitted, one recovers only Hawking's original conclusion of information loss [16]. In contrast, once the area term is included, the correct Page curve emerges. The resulting Page curve is the quantum-corrected counterpart of the one obtained in [59]. This section essentially reviews the findings of [42].

The second section studies the Page curve in the setting of a classical collapse, presented in Section 5.1.3. We show that the fine-grained entropy always remains below the thermodynamic upper limit given by the Bekenstein–Hawking formula (1.4). Nevertheless, the entropy does not decrease after the Page phase transition; instead, it asymptotically approaches and then remains fixed at the value S_{BH} as time tends to infinity. This behavior is anticipated, since the post-shockwave region of spacetime still admits a timelike Killing vector; only the global spacetime is truly non-stationary.

To explicitly break time-translation invariance, quantum corrections to the classical DREH action must be taken into account. The corresponding evaporating black hole solution was derived in [111] and is reviewed in Section 5.3. The Page curve associated with this solution is discussed in the final section of the chapter. We show that, once quantum corrections are included, there appears a decreasing contribution to the fine-grained entropy, thereby reproducing the full Page curve. The analysis in these last two sections is based on [43].

10.1 Page curve in the eternal black hole scenario

In this section, we examine how the fine-grained entropy of Hawking radiation evolves in time in the eternal black hole setup, using the QES formula (1.6). The eternal black hole in the DREH model is presented in Section 5.2.3. Our analysis parallels the procedure used for the BPP model in Section 9.1. Accordingly, we study two distinct configurations: the no-island case, which recovers the conventional Hawking information loss result [16], and the island case, which yields the Page curve. Our derivation largely follows that of [42].

10.1.1 No-island configuration

Let us first consider the situation in which no island is present. In this case, we expect to reproduce Hawking's original result [16]. For an eternal black hole, the relevant quantum state is the Hartle–Hawking state (3.97). Therefore, the semi-classical entanglement entropy in (1.6) must be expressed in the Kruskal coordinates. The corresponding expression is given in (8.51), namely:

$$S_{semi-cl} = \frac{1}{12} \ln \frac{(x_R^+ - x_L^+)^2 (x_R^- - x_L^-)^2}{\delta^4 e^{-2\rho_R} e^{-2\rho_L}}. \tag{10.1}$$

As usual, the subscripts R/L refer to the two wedges of the spacetime, depicted in Figure 10.1. To obtain the correct time dependence of the fine-grained entropy, we switch to (t, r_*) coordinates, or equivalently (t, r), since $r_* = r_*(r)$. The parameter δ serves as a UV cutoff.

Coordinates on the cutoff surface can therefore be written as either (t, b) or (t, b_*). The $t =$ const. slice is drawn in red. Because the time-like Killing vector reverses direction when one moves from right wedge to the left wedge, the constant-time slice in the left wedge corresponds to the coordinate $-t$. Consequently, the region that an asymptotic observer cannot access is indicated by the shaded red area in Figure 10.1. The black hole singularity is depicted by the wavy black curve, and the event horizon is shown as the green line.

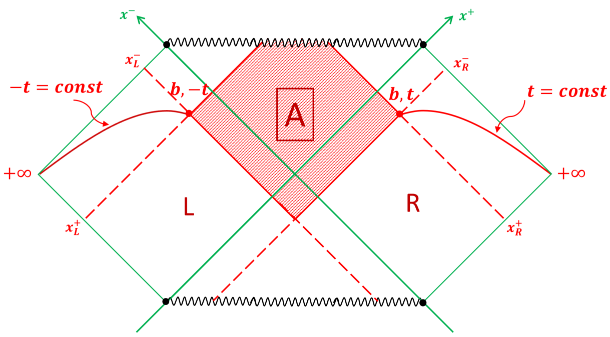

Figure 10.1: Penrose diagram depicting the no-island configuration for the eternal black hole in the DREH model.

To recover the time dependence of the fine-grained entropy S_{FG} along the cut-off surface, we switch to asymptotically flat Eddington–Finkelstein coordinates that incorporate the quantum-corrected surface gravity (5.89):

$$\kappa x_R^+ = e^{\kappa(t+b_*)}, \quad \kappa x_R^- = -e^{-\kappa(t-b_*)}, \quad \kappa x_L^+ = -e^{\kappa(-t+b_*)}, \quad \kappa x_L^- = e^{-\kappa(-t-b_*)}. \tag{10.2}$$

For more details see Appendix D.5. In the absence of an island, the fine-grained entropy (1.6) simply reduces to the semi-classical contribution (10.1). Employing the metric (5.93), for which $\rho = \frac{1}{2}\ln h + \epsilon\varphi - \kappa r_*$, and inserting (10.2) into (10.1), we obtain:

$$S_{FG} = S_{semi-cl} = \frac{1}{6} \ln \frac{4h(b)\cosh^2(\kappa t)}{(\kappa\delta)^2 e^{-2\epsilon\varphi(b)}}. \tag{10.3}$$

We regularize the UV divergence by imposing that the fine-grained entropy vanishes at the beginning of the evaporation, i.e. $S_{FG}(0) = 0$. Under this condition, (10.3) simplifies to:

$$S_{FG} = \frac{1}{3}\ln\left[\cosh(\kappa t)\right]. \tag{10.4}$$

We now distinguish two relevant regimes. At early times, near the beginning of evaporation, the entropy behaves as:

$$S_{FG} = \frac{1}{6}(\kappa t)^2. \tag{10.5}$$

In contrast, at late times $\kappa t \gg 1$, we find the anticipated linear growth:

$$S_{FG} \approx \frac{1}{3}\kappa t - \frac{1}{3}\ln 2, \tag{10.6}$$

which agrees with the behavior found in other dilaton gravity models [40, 41, 57, 58]. Therefore, the fine-grained entropy of the radiation increases monotonically, consistent with Hawking's original result. The crucial difference is that, unlike in the RST and BPP models, the DREH model predicts that the surface gravity receives a quantum correction.

10.1.2 Island configuration

In the presence of an island, the region that remains inaccessible to an asymptotic observer splits into two disconnected components, so we must employ formula (8.59):

$$S_{semi-cl} = \frac{1}{6}\ln\frac{d_{12}^2 d_{23}^2 d_{14}^2 d_{34}^2}{\delta^4 d_{24}^2 d_{13}^2 e^{-\rho_1}e^{-\rho_2}e^{-\rho_3}e^{-\rho_4}}, \tag{10.7}$$

where the Minkowski distances d_{ij} are defined as

$$d_{ij}^2 = (x_i^+ - x_j^+)(x_i^- - x_j^-). \tag{10.8}$$

As in the BPP model, we choose the labels i and j so that $(1,2,3,4) \longleftrightarrow (Ra, Rb, La, Lb)$ holds. Here, R denotes the right wedge and L the left wedge of the spacetime.

Meanwhile, a denotes the boundary of the island region, and b indicates the cut-off hypersurface. All these hypersurfaces are explicitly shown in Figure 10.2. The location of the island is specified by (t', a_*) in the asymptotically flat region on the right. In the left region, the corresponding point is obtained by reflection across the vertical axis. One can clearly see that the emergence of the island region I, highlighted in blue, inside the inaccessible region A of Figure 10.1 splits A into two smaller, disconnected subregions.

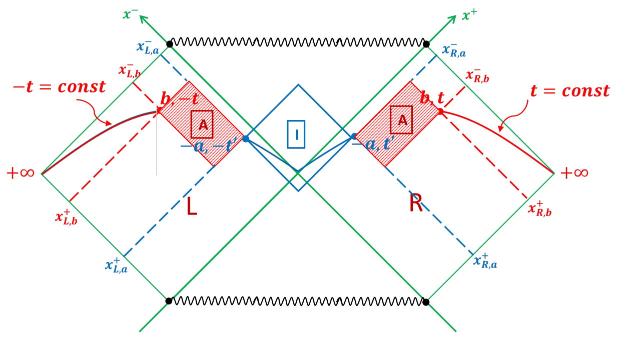

Figure 10.2: Penrose diagram depicting the no-island configuration for the eternal black hole in the DREH model.

In the asymptotically flat coordinates, the positions of the regions A and I in Figure 10.4 are as follows:

$$\begin{aligned}
&\kappa x_{Rb}^+ = e^{\kappa(t+b_*)}, \quad \kappa x_{Rb}^- = -e^{-\kappa(t-b_*)}, \quad \kappa x_{Lb}^+ = -e^{\kappa(-t+b_*)}, \quad \kappa x_{Lb}^- = e^{-\kappa(-t-b_*)},\\
&\kappa x_{Ra}^+ = e^{\kappa(t'+a_*)}, \quad \kappa x_{Ra}^- = -e^{-\kappa(t'-a_*)}, \quad \kappa x_{La}^+ = -e^{\kappa(-t'+a_*)}, \quad \kappa x_{La}^- = e^{-\kappa(-t'-a_*)}.
\end{aligned} \tag{10.9}$$

We now turn to the late-time regime of the evaporation process. In the limit of large times, one finds:

$$\frac{d_{23}^2 d_{14}^2}{d_{24}^2 d_{13}^2} = 16e^{2\kappa(b_*-a_*)}\frac{\cosh^2(\kappa t)\cosh^2(\kappa t')}{\left(e^{\kappa(t+b_*)}+e^{-\kappa(t'+a_*)}\right)^2\left(e^{\kappa(b_*-t)}+e^{\kappa(t'-a_*)}\right)^2} \approx 1;\;\; t,t' \to \infty. \tag{10.10}$$

Here we have used (10.9). In this regime it is straightforward to verify that $d_{12} = d_{34}$, $\rho_1 = \rho_4$, and $\rho_2 = \rho_3$. With these relations, equation (10.7) simplifies to:

$$S_{semi-cl} = \frac{1}{6}\ln\left(\frac{d_{12}^4}{\delta^4}e^{2\rho_1}e^{2\rho_2}\right). \tag{10.11}$$

Substituting the metric (5.93) and the Minkowski distances (10.8) into (10.11) yields:

$$S_{semi-cl} = \frac{1}{6}\ln\frac{h(a)h(b)\left(e^{\kappa(t+b_*)}-e^{\kappa(t'+a_*)}\right)^2\left(-e^{-\kappa(t-b_*)}+e^{-\kappa(t'-a_*)}\right)^2}{(\kappa\delta)^4 e^{2\kappa(b_*+a_*)}e^{-2\varepsilon(\varphi(a)+\varphi(b))}}. \tag{10.12}$$

Since the surface term is independent of t', we can immediately extremize with respect to t'. As in the BPP model (see Section 9.1), at late times one finds $t' = t$. Consequently, the semiclassical entropy (10.12) reduces to:

$$S_{semi-cl} = \frac{1}{3}(\rho_a+\rho_b) + \frac{2}{3}\ln\left(e^{\kappa b_*}-e^{\kappa a_*}\right) - \frac{2}{3}\ln(\kappa\delta). \tag{10.13}$$

We now proceed to analyze the surface term in the fine-grained entropy formula (1.6). It is given by:

$$\frac{A[I]}{4G_{\mathrm{N}}^{(4)}} = 2\frac{4\pi\lambda^2 a^2}{4G_{\mathrm{N}}\hbar}. \tag{10.14}$$

This expression coincides with the Bekenstein–Hawking entropy (1.4). The factor of two appears because the spacetime contains two asymptotically flat regions. Note that, unlike in the BPP model, we do not use the quantum-corrected area term (8.82). Instead, we employ the purely classical area obtained via dimensional reduction, as the model is derived from the four-dimensional Einstein–Hilbert action. Summing (10.13) and (10.14) then gives the generalized entropy in the form:

$$S_{gen} = \frac{2\pi\lambda^2 a^2}{G_{\mathrm{N}}\hbar} + \frac{1}{3}(\rho_a+\rho_b) + \frac{2}{3}\ln\left(e^{\kappa b_*}-e^{\kappa a_*}\right) - \frac{2}{3}\ln(\kappa\delta). \tag{10.15}$$

The last step in evaluating the fine-grained entropy is to extremize the generalized entropy (10.15) with respect to the island location a_*:

$$\partial_{a_*}S_{gen} = \left[\frac{4\pi\lambda^2 a}{G_{\mathrm{N}}\hbar} + \frac{1}{3}\frac{d\rho(a)}{dr}\right]\frac{da}{da_*} - \frac{2}{3}\frac{\kappa}{e^{\kappa(b_*-a_*)}-1} = 0, \tag{10.16}$$

which yields:

$$\left[a + \frac{4\varepsilon G_N}{\lambda^2}\frac{d\rho(a)}{dr}\right]h(a)e^{\epsilon\varphi(a)} = \frac{8\varepsilon G_N}{\lambda^2}\frac{\kappa}{e^{\kappa(b_*-a_*)}-1}. \tag{10.17}$$

We anticipate that the QES will lie close to, but outside, the horizon. Hence, we parametrize its position as $a = r_H + x$, where r_H denotes the quantum-corrected horizon position and $x \ll r_H$. Expanding the left-hand side of (10.17) in powers of small x up to first order, we obtain:

$$\text{LHS} \approx \left[r_H + \frac{4\epsilon G_N}{\lambda^2}\frac{d\rho}{dr}\bigg|_H\right]h(r_H)e^{\varepsilon\varphi(r_H)} + \left[r_H + \frac{4\varepsilon G_N}{\lambda^2}\frac{d\rho}{dr}\bigg|_H\right]\left(\frac{dh}{dr}e^{\varepsilon\varphi(r_H)}\right)\bigg|_H x. \tag{10.18}$$

The first term vanishes because $h(r_H) = 0$ by the definition of the horizon. For the second term, we use $\left(\frac{dh}{dr} e^{\varepsilon\varphi}\right)\Big|_H = 2\kappa$, which follows from the definition of the surface gravity.

Next, we examine the right-hand side of (10.17). We expand $e^{2\kappa a_*}$ around the horizon and find:

$$\begin{aligned} e^{2\kappa a_*} &\approx e^{2\kappa r_*(r_H)} + 2\kappa \left(e^{2\kappa r_*} \frac{dr_*}{dr} \right)\Big|_H x = 2\kappa x e^{1+\varepsilon(\alpha(r_H)-\varphi(r_H))} \lim_{r\to r_H} \left(\frac{\frac{r}{r_H} - 1}{h(r)} \right) \\ &= 2\kappa x e^{1+\varepsilon\alpha(r_H)} \frac{e^{-\varepsilon\varphi(r_H)}}{r_H h'(r_H)} = \frac{x}{r_H} e^{1+\varepsilon\alpha(r_H)}. \end{aligned} \tag{10.19}$$

The first term in the first line vanishes since $r_*(r_H) \to \infty$, and in the second line we used (5.91). Consequently, the right-hand side of (10.17) becomes:

$$\text{RHS} \approx \frac{8\varepsilon\kappa G_N}{\lambda^2} e^{-\kappa b_*} e^{\kappa a_*} \left(1 + e^{-\kappa b_*} e^{\kappa a_*}\right) = \frac{8\varepsilon\kappa G_N}{\lambda^2} \left[\sqrt{\frac{x}{r_H}} e^{\frac{1}{2}(1+\varepsilon\alpha(r_H))-\kappa b_*} + \frac{x}{r_H} e^{1+\varepsilon\alpha(r_H)-2\kappa b_*} \right]. \tag{10.20}$$

Combining (10.18) and (10.20), we arrive at the following solution for x:

$$x = \frac{1}{r_H} \frac{\left(\frac{4\varepsilon G_N}{\lambda^2 r_H}\right)^2 e^{1-2\kappa b_* + \varepsilon\alpha(r_H)}}{\left[1 + \frac{4\varepsilon G_N}{\lambda^2 r_H} \left(\frac{d\rho}{dr}\Big|_H - \frac{1}{r_H} e^{1-2\kappa b_* + \epsilon\alpha(r)} \right)\right]^2}. \tag{10.21}$$

Finally, using (4.110) and (5.91) and reinstating $\varepsilon = \frac{\hbar}{48\pi}$, we arrive at the position of the island:

$$a = r_H + \frac{1}{r_H} \left(\frac{\hbar G_N}{12\pi\lambda^2 r_H} \right)^2 e^{1-2\kappa b_*} \left[1 + \frac{\hbar G_N}{6\pi\lambda^2 r_H^2} \left(\frac{19}{16} + e^{1-2\kappa b_*} \right) \right]. \tag{10.22}$$

Note that the expression (10.22) for the island location coincides exactly with the result of [59] at leading order in the ε expansion. The key difference in our analysis is that we also incorporate the back-reaction of the radiation, so that the inclusion of quantum effects still preserves the appearance of an island in the vicinity of the quantum-corrected horizon.

Next, we substitute the island position (10.22) into (10.15) to compute the late-time fine-grained entropy. Since the island forms very close to the quantum-corrected horizon, we first expand around the horizon position:

$$S_{FG} = S_{gen}(r_H) - \frac{\hbar G_N}{36\pi\lambda^2 r_H^2} e^{1-2\kappa b_*} + \mathcal{O}(\hbar^2)\ . \tag{10.23}$$

The second term can be neglected, as it is of order $\mathcal{O}(\hbar)$, while the fine-grained entropy scales as $S_{FG} = (\mathcal{O}(1) + \hbar\mathcal{O}(1))/\hbar$. Consequently, we obtain:

$$S_{FG} = \frac{2\pi\lambda^2 r_H^2}{G_N \hbar} + \frac{1}{3}(\rho_H + \rho_b) + \frac{2}{3} \ln \frac{e^{\kappa b_*}}{\kappa\delta} = 2 \left[\frac{\pi\lambda^2 r_H^2}{G_N \hbar} + \frac{1}{12} \ln \frac{e^{4\kappa b_*}}{(\kappa\delta)^4 e^{-2\rho_H} e^{-2\rho_b}} \right]. \tag{10.24}$$

To leading order, the expression (10.24) matches precisely the classical Bekenstein-Hawking entropy (1.4), implying $S_{gen} = 2S_{BH}$, as anticipated. We return to the role of the quantum correction term in the next subsection. The fine-grained entropy of the Hawking radiation is therefore given by:

$$S_{FG} = \min\left\{ \frac{1}{3}\kappa t, 2S_{BH} \right\}. \tag{10.25}$$

To evaluate the Page time, we employ the classical value of the entropy, because the quantum correction becomes negligible in the large-mass regime. The Page time t_P is therefore determined by:

$$\frac{1}{3}\kappa c t_P = \frac{2\pi c^3 \lambda^2 r_0^2}{G_{\mathrm{N}}\hbar} \quad \Longrightarrow \quad t_P = \frac{96\pi M^3 G_{\mathrm{N}}^2}{\hbar \lambda^4 c^4}. \tag{10.26}$$

10.1.3 Relation to the Wald entropy

To analyze the second term in (10.24), we employ the quantum-corrected thermodynamic entropy, given by the Wald entropy formula. In this approach, the black hole entropy is interpreted as a conserved charge associated with the horizon and is expressed as

$$S_{Wald} = -2\pi \int_H dA \frac{\partial \mathcal{L}}{\partial \mathcal{R}_{\mu\nu\rho\sigma}} \varepsilon_{\mu\nu}\varepsilon_{\rho\sigma}, \tag{10.27}$$

where $\varepsilon_{\mu\nu}$ is the binormal satisfying $\varepsilon_{\mu\nu}\varepsilon^{\mu\nu} = -2$, dA is the infinitesimal area element on the event horizon, and $\mathcal{L}$ is the Lagrangian density specifying the theory. A straightforward evaluation for the DREH theory (2.19) coupled to the Polyakov–Liouville quantum correction term (3.72) gives

$$S_{Wald} = \frac{\pi\lambda^2 r_H^2}{G_{\mathrm{N}}\hbar} - \frac{1}{12}\psi(r_H). \tag{10.28}$$

We therefore need the exact solution for the auxiliary field. Substituting the solution for ψ (3.76) together with the Hartle–Hawking state condition (3.97), $t_\pm(x^\pm) = 0$, and the explicit expressions for the $t_\pm$ functions (3.78), we obtain the following differential equation for $f_\pm$:

$$\frac{1}{2}\partial_\pm^2 f_\pm - \frac{1}{4}(\partial_\pm f_\pm)^2 = 0. \tag{10.29}$$

Solving this equation yields:

$$f_\pm(x^\pm) = -2\ln\frac{x^\pm + c_\pm}{\delta} + d_\pm, \tag{10.30}$$

where $c_\pm$ and $d_\pm$ are integration constants. We interpret the constants $c_\pm$ as marking positions in spacetime. To ensure that ψ is invariant under local Lorentz transformations, we impose $d_+ + d_- = -2\rho_c$. Implementing this condition leads to

$$\psi(r) = -\ln\frac{(x^+ + c_+)^2(x^- + c_-)^2}{\delta^4 e^{-2\rho}e^{-2\rho_c}}, \tag{10.31}$$

where $c_\pm$ must be chosen on the cut-off hypersurface which defines a region belonging to the black hole (see Figures 10.3 and 10.4). This implies $\kappa^2 c_+ c_- = -e^{2\kappa b_*}$. To evaluate Wald's entropy, we insert (10.31) at the horizon, where $x_H^+ = x_H^- = 0$. Wald's entropy then takes the form of a quantum-corrected Bekenstein–Hawking formula:

$$S_{Wald} = \frac{\pi\lambda^2 r_H^2}{G_{\mathrm{N}}\hbar} + \frac{1}{12}\ln\frac{(e^{2\kappa b_*})^2}{(\kappa\delta)^4 e^{-2\rho_H}e^{-2\rho_b}}. \tag{10.32}$$

Comparing this with (10.24), we see that, to first order in perturbation theory, it coincides with precisely twice the Wald entropy (10.32). Hence, the Page curve is correctly reproduced in the eternal black hole solution of the DREH model. The fine-grained entropy of the radiation increases monotonically until it saturates at the coarse-grained Bekenstein–Hawking value, after which it stays fixed at $2S_{BH}$. Furthermore, Hawking's result for the generalized entropy in the no-island scenario can likewise be recovered from the Wald formula (10.28).

10.2 Page curve in the classical collapse scenario

In this section, we examine the Page curve for the classical gravitational collapse setup within the DREH model, as introduced in Section 5.1.3. Although we cannot determine the final stage of evaporation—since it lies at future time infinity in the classical limit—we can nonetheless extract some information about the qualitative behavior of the Page curve at zeroth order in ε. At this order, however, one does not expect a decreasing contribution to the entropy, as such behavior arises only once quantum corrections are taken into account. The time evolution of the fine-grained entropy of Hawking radiation is governed by the QES formula (1.6). As usual, we analyze two distinct configurations: the no-island configuration and the island configuration.

Figure 10.3 shows the spacetime of an evaporating black hole in the DREH model (5.150-5.153). This figure corresponds to Figure 3.3, where the general collapse scenario is illustrated. The event horizon is indicated by a dashed purple line, and the apparent horizon by a solid purple line. The shockwaves are drawn in blue, while the singularity and the spacetime boundary are both shown in black. Future and past null infinities are represented by green lines and denoted by $\mathcal{J}^+$ and $\mathcal{J}^-$, respectively. Likewise, future and past timelike infinities and spatial infinity are marked by $i^\pm$ and $i^)$, respectively. The δ and $\hat{\mathrm{x}}$ axes are explicitly displayed, corresponding to the coordinates defined in (3.107). The coordinates of the end-point of the evaporation $(\delta_E, \hat{\mathrm{x}}_E)$, are shown along the respective axes.

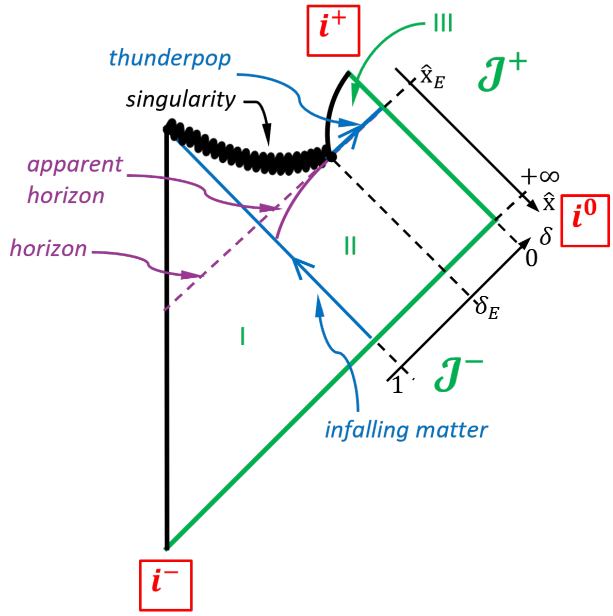

Figure 10.3: Penrose diagram of the quantum-corrected gravitational collapse scenario.

The spacetime is divided into three regions, separated by two shockwaves. Region I corresponds to the initial Minkowski spacetime. Upon crossing the $\delta = 1$ hypersurface, one enters region II, which contains the evaporating black hole. Finally, region III describes the end-state geometry, namely the quantum-corrected Minkowski spacetime given by (5.84). The purely classical collapse is recovered by pushing the $\delta = \delta_E$ hypersurface all the way to future null infinity $\mathcal{J}^+$, thereby eliminating the third region. The discussion here is largely based on [43].

10.2.1 No-island configuration

We begin by considering the setup without an island. In this case, the fine-grained entropy (1.6) simplifies to just the semiclassical entropy contribution. Because the vacuum is specified in the asymptotically flat coordinates of region I of the spacetime (see Figure 10.3), the entanglement entropy must likewise be written in these coordinates. The evaporating black hole possesses a spacetime boundary on which reflective boundary conditions are imposed. Consequently, the appropriate expression for the entropy of the quantum matter fields is given by (8.54), namely:

$$S_{semi-cl} = \frac{1}{12} \ln \frac{(\sigma_S^+ - \sigma_{\bar{S}}^+)^2}{4\epsilon^2 e^{-2\rho_S(\sigma)}}. \tag{10.33}$$

The label S denotes the boundary of the black hole region, while the label $\bar{S}$ refers to the mirror image of this point across the spacetime boundary, as illustrated in Figure 10.4. We employ the (t, r_*) coordinate system. On the cut-off surface, the coordinates are given by (t, b_*), or equivalently (t, b), where

$$\frac{b}{a} + \ln\left(\frac{b}{a} - 1\right) = \frac{b_*}{a}. \tag{10.34}$$

Note that the time coordinate t is defined with respect to the asymptotically flat coordinates of region II, given in (5.38) and (5.37), namely $t = \frac{\hat{\sigma}^+ - \hat{\sigma}^-}{2}$. The cut-off hypersurface is taken to lie close to asymptotic infinity, which requires b_* to be very large. Therefore, throughout the rest of this work we use the following approximation:

$$\frac{b_*}{a} \gg \frac{(\lambda a)^2}{\varepsilon}. \tag{10.35}$$

Note that we have relabeled the UV cut-off from the standard notation δ of Chapter 8, since δ is a coordinate within this setting.

The classical collapse configuration is depicted in Figure 10.4. The location of region A, which contains the degrees of freedom inaccessible to an asymptotic observer in the no-island classical scenario, is marked in red. The cut-off hypersurface is drawn in purple, and a time coordinate along this hypersurface, denoted by τ and introduced in (10.37), parameterizes it. The radiation degrees of freedom occupy a causal diamond based on a constant-time slice, indicated in blue. The coordinates of all relevant points—(δ_S, $\hat{\mathrm{x}}_S$) and their images under reflection from the the spacetime boundary, ($\delta_{\bar{S}}$)—are shown on both the δ- and $\hat{\mathrm{x}}$-axes.

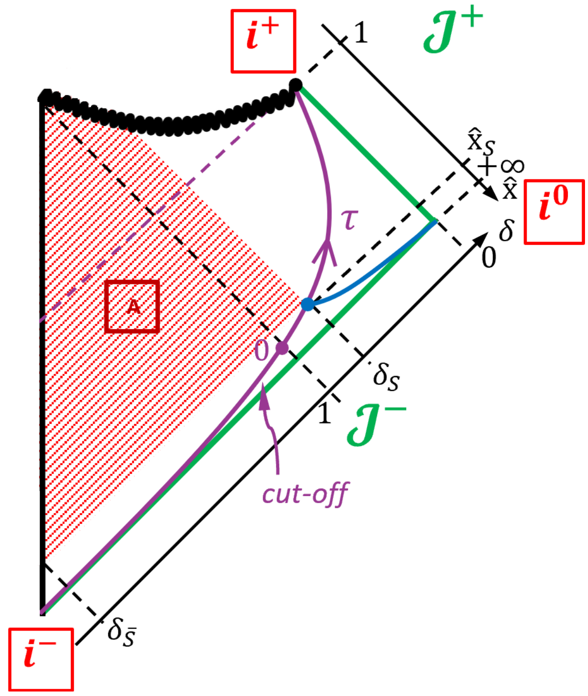

Figure 10.4: Penrose diagram illustrating the no-island case within the classical collapse scenario.

The reflective boundary condition at $\mathrm{x} = 0$ enforces $\sigma^+_{\bar{S}} = \sigma^-_S$. The onset of evaporation is determined by the intersection of the hypersurfaces $\sigma^+ = \sigma^+_0$ and $r_* = b_*$, yielding $t_0 = \sigma^+_0 - b_*$. The evaporation time is then defined as $\tau = t - t_0$. Employing equation (5.40), the cut-off hypersurface in region II of the the spacetime takes the form:

$$\frac{b_*}{a} = -\ln \delta_S + \hat{\mathrm{x}}_S + \ln(\hat{\mathrm{x}}_S - 1). \tag{10.36}$$

Note that the cut-off surface lies in the region exterior to the black hole event horizon, defined by equation (5.41), which entails $\hat{\mathrm{x}}_S > 1$. Using equations (5.37) and (5.38), one readily finds that the evaporation time τ is related to $\hat{\mathrm{x}}_S$ by the following transcendental relation:

$$\hat{\mathrm{x}}_S + \ln(\hat{\mathrm{x}}_S - 1) = \frac{b_*}{a} - \frac{\tau}{2a}. \tag{10.37}$$

Imposing the condition $S_{FG}(0) = 0$ removes the UV divergences in the expression for the entanglement entropy (10.33). Expressed in terms of $\hat{x}_S$, the fine-grained entropy evaluated on Hawking's saddle is

$$S_H(\hat{x}_S) = \frac{1}{12} \ln \frac{a^2(b-a)\hat{x}_S \left(\frac{b_*}{a} - \ln(\hat{x}_S - 1)\right)^2}{b^3(\hat{x}_S - 1)}. \tag{10.38}$$

An explicit analytic form of the fine-grained entropy (10.38) as a function of the evaporation time τ cannot be obtained because one would have to solve the transcendental equation (10.37), which links τ to the coordinate $\hat{x}_S$. Nevertheless, one can extract the behavior of the fine-grained entropy both at the beginning of evaporation and at late times. At the beginning of the evaporation ($\tau \to 0$), equation (10.37) can be solved perturbatively:

$$\hat{x}_S^{(0)} = \frac{b}{a} - \frac{b-a}{2ab}\tau. \tag{10.39}$$

Inserting the result (10.39) into equation (10.38) and expanding in powers of τ, one obtains the following early-time expression for the fine-grained entropy:

$$S_H^{(0)}(\tau) = \frac{a\tau}{8b^2}. \tag{10.40}$$

This behavior differs from the eternal black hole case, where the dependence is quadratic (10.5). At late times, the factor $\exp\left\{\left(\frac{b_*}{a} - \frac{\tau}{2a}\right)\right\}$ becomes very small, allowing us to expand $\hat{x}_S$ in powers of this quantity:

$$\hat{x}_S^{(\infty)} = 1 + e^{\frac{b_*}{a}-1} e^{-\frac{\tau}{2a}}. \tag{10.41}$$

Substituting (10.41) into (10.38) yields the anticipated Hawking result of a linearly increasing fine-grained entropy at late times [16]:

$$S_H^{(\infty)}(\tau) = \frac{\tau}{24a} + \frac{1}{12}\ln\frac{(b-a)\tau^2}{4b^3} - \frac{1}{12}\left(\frac{b_*}{a} - 1\right). \tag{10.42}$$

Observe that, in the late-time regime, the leading contribution in (10.42) is of the form $\frac{\kappa\tau}{12}$, where $\kappa = \frac{1}{2a}$ (see Appendix D.5) is the usual surface gravity of a Schwarzschild black hole. This is consistent with the fine-grained entropy obtained in various 2D dilaton gravity models [40, 41]. We explicitly confirm this within the BPP model in Section 9.2.

10.2.2 Island case

Analogously to the BPP model, the projection splits the inaccessible region A into two non-overlapping segments along past null infinity $\mathcal{J}^-$. Consequently, the appropriate expression for the semi-classical entropy in the presence of an island is given by (8.60), namely:

$$S_{semi-cl} = \frac{1}{12}\ln\frac{(\sigma_S^+ - \sigma_I^+)^2(\sigma_{\bar{S}}^+ - \sigma_{\bar{I}}^+)^2(\sigma_{\bar{S}}^+ - \sigma_S^+)^2(\sigma_{\bar{I}}^+ - \sigma_I^+)^2}{\epsilon^4(\sigma_{\bar{I}}^+ - \sigma_S^+)^2(\sigma_{\bar{S}}^+ - \sigma_I^+)^2 e^{-2\rho(\sigma_S)}e^{-2\rho(\sigma_I)}}. \tag{10.43}$$

Here the reflected points obey $\sigma_{\bar{I}}^+ = \sigma_I^-$ and $\sigma_{\bar{S}}^+ = \sigma_S^-$. To verify that (10.43) remains valid when the island vanishes, we consider the limit $\sigma_I^\pm \to \sigma_M^\pm$, where M denotes the point at which the island region meets the spacetime boundary. Since a UV cut-off is present, distances should not shrink to zero; instead, they should approach this UV cut-off. Implementing the limit $\sigma_I^\pm \to \sigma_M^\pm$, we obtain:

$$\epsilon^2 = \lim_{I\to M} g_{\mu\nu}(\sigma_I^\mu - \sigma_M^\mu)(\sigma_I^\nu - \sigma_M^\nu). \tag{10.44}$$

The island hypersurface is specified by the condition $\sigma^+ + \sigma^- = \text{const}$. Using the relation $\sigma_M^+ = \sigma_M^- = \frac{1}{2}(\sigma_I^+ + \sigma_I^-)$, one can straightforwardly verify that (10.43) reduces to (10.33) in the limit $I \to M$. The same regularization as in (10.38) must be applied. The expression (10.43) depends both on τ and on the location of the island. The τ-dependence enters through $\sigma_S^+ = \sigma_0^+ + \tau$ and $\sigma_S^- = \sigma_0^+ - 2a\hat{\mathrm{x}}_S(\tau)$.

Figure 10.5 illustrates this whole scenario. The location of the region A, which contains the inaccessible degrees of freedom when an island region I is present in the classical case, is indicated in red. The cut-off hypersurface, shown in purple, is parametrized by the time coordinate τ along it and originates at the incoming shockwave. The island-boundary hypersurface, also drawn in purple, passes through region A. The $\Delta\tau$-axis is aligned with this hypersurface, with its zero point defined at the ingoing shockwave. The radiation degrees of freedom occupy both a causal diamond built over a constant-time slice and the island region; these are depicted in blue. The coordinates of all relevant points (δ_S, δ_I, $\hat{\mathrm{x}}_S$, $\hat{\mathrm{x}}_I$), along with those obtained via reflection from the spacetime boundary ($\delta_{\bar{S}}$, $\delta_{\bar{I}}$), are displayed on both the δ-axis and the $\hat{\mathrm{x}}$-axis.

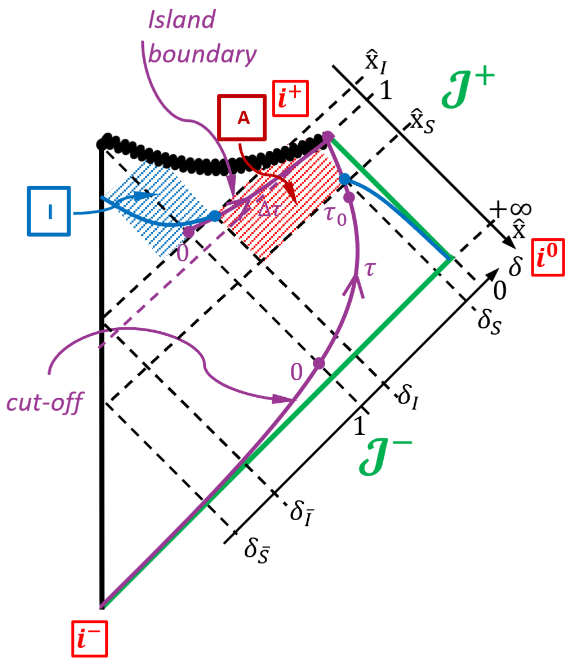

Figure 10.5: Penrose diagram illustrating the island case within the classical collapse scenario.

Next, we include the island's area contribution. Because the DREH model is obtained via dimensional reduction from the 4D Einstein–Hilbert action, this area term takes the usual Bekenstein–Hawking form (1.4), namely

$$\frac{A[\partial I]}{4G_{\mathrm{N}}^{(4)}} = \frac{4\pi\lambda^2 a^2}{4G\hbar}\mathrm{x}_I^2 = \frac{(\lambda a)^2}{12\varepsilon}\mathrm{x}_I^2. \tag{10.45}$$

The generalized entropy is then given by

$$\begin{aligned} S_{gen}(\tau, \sigma_I^+, \sigma_I^-) =& \frac{(\lambda a)^2}{12\varepsilon}\mathrm{x}_I^2 \\ &+ \frac{1}{12}\ln\left[\frac{4a^2(b-a)\hat{\mathrm{x}}_S\left(\frac{b_*}{a} - \ln(\hat{\mathrm{x}}_S - 1)\right)^2}{b^3(\hat{\mathrm{x}}_S - 1)}\frac{(\sigma_S^+ - \sigma_I^+)^2(\sigma_S^- - \sigma_I^-)^2(\sigma_I^+ - \sigma_I^-)^2}{\epsilon^2(\sigma_S^+ - \sigma_I^-)^2(\sigma_I^+ - \sigma_S^-)^2 e^{-2\rho(\sigma_I)}}\right]. \end{aligned} \tag{10.46}$$

The dependence $\mathrm{x}_I(\sigma_I^+, \sigma_I^-)$ is fixed by equation (5.152), while $\rho(\sigma_I^+, \sigma_I^-)$ is determined by (5.150). The parameter τ enters only through $\hat{\mathrm{x}}_S = \hat{\mathrm{x}}_S(\tau)$ via equation (10.36). According to the fine-grained entropy prescription (1.6), the expression (10.46) must be extremized with respect to the island location (σ_I^+, σ_I^-). Implementing this extremization with the help of (5.152) and

(5.150) leads to

$$1 - \mathrm{x}_I = \tilde{\varepsilon}\left[\frac{1}{2\mathrm{x}_I^2} + \frac{\hat{\mathrm{x}}_S - \ln\delta_S}{(\ln\delta_I - \ln\delta_S)(\ln\delta_I - \hat{\mathrm{x}}_S)} + \frac{1}{\hat{\mathrm{x}}_I - \ln\delta_I}\right], \tag{10.47}$$

$$1 - \mathrm{x}_I = \tilde{\varepsilon}\left[\frac{1}{2\mathrm{x}_I^2} - \frac{1}{2\hat{\mathrm{x}}_I^2} + \frac{\hat{\mathrm{x}}_I - 1}{\hat{\mathrm{x}}_I}\left(\frac{\hat{\mathrm{x}}_S - \ln\delta_S}{(\ln\delta_I - \ln\delta_S)(\ln\delta_I - \hat{\mathrm{x}}_S)} + \frac{1}{\hat{\mathrm{x}}_I - \ln\delta_I}\right)\right], \tag{10.48}$$

where we have introduced $\tilde{\varepsilon} = \frac{\varepsilon}{(\lambda a)^2}$. We first determine the island position along the initial shockwave, that is, on the hypersurface $\delta_I = 1$. Setting $\delta_I = 1$ and $\hat{\mathrm{x}}_I = \mathrm{x}_I$, equations (10.48–10.47) simplify to

$$1 - \mathrm{x}_I = \tilde{\varepsilon}\left[\frac{1}{2\mathrm{x}_I^2} + \frac{1}{\mathrm{x}_I} - \frac{\ln\delta_S - \hat{\mathrm{x}}_S}{\hat{\mathrm{x}}_S\ln\delta_S}\right], \tag{10.49}$$

$$\mathrm{x}_I^2 = \tilde{\varepsilon}\left[-1 + \frac{\ln\delta_S}{\mathrm{x}_I - \ln\delta_S} - \frac{\hat{\mathrm{x}}_S}{\mathrm{x}_I - \hat{\mathrm{x}}_S}\right]. \tag{10.50}$$

Equation (10.49) is a cubic in x_I and could be solved exactly, but it is sufficient to find a perturbative solution up to second order in $\tilde{\varepsilon}$. This yields

$$\mathrm{x}_I = 1 - \tilde{\varepsilon}\left(\frac{3}{2} - \zeta\right)(1 + 2\tilde{\varepsilon}), \tag{10.51}$$

where we have defined $\zeta = \frac{\ln\delta_S - \hat{\mathrm{x}}_S}{\hat{\mathrm{x}}_S\ln\delta_S}$. By writing $\delta_S = \delta_S(\hat{\mathrm{x}}_S, \zeta)$ and inserting the solution (10.51) into the second equation (10.50), we obtain an equation for $\hat{\mathrm{x}}_S$. Solving it gives

$$\hat{\mathrm{x}}_S = 1 + \tilde{\varepsilon}\left(\zeta - \frac{1}{2}\right) + \tilde{\varepsilon}^2\left(\zeta - \frac{3}{2} - \frac{1}{\zeta}\right). \tag{10.52}$$

Next, equation (10.36) becomes an equation for ζ:

$$\zeta = \frac{1}{\hat{\mathrm{x}}_S} + \frac{1}{\frac{b_*}{a} - \hat{\mathrm{x}}_S - \ln(\hat{\mathrm{x}}_S - 1)}. \tag{10.53}$$

Employing the approximation (10.35), the second term in (10.53) can be neglected, leaving

$$\zeta = 1 - \frac{\tilde{\varepsilon}}{2}. \tag{10.54}$$

Substituting (10.54) into (10.51) and (10.52), and using $\frac{\tau_0}{2a} = -\ln\delta_S$, we obtain the final expression for the island position along the $\delta_I = 1$ hypersurface, i.e. at the onset of evaporation.

$$\delta_I = 1, \tag{10.55}$$

$$\mathrm{x}_I = 1 - \frac{\tilde{\varepsilon}}{2}(1 + 3\tilde{\varepsilon}) = \hat{\mathrm{x}}_I, \tag{10.56}$$

$$\hat{\mathrm{x}}_S = 1 + \frac{\tilde{\varepsilon}}{2}(1 - 4\tilde{\varepsilon}), \tag{10.57}$$

$$\frac{\tau_0}{2a} = \frac{b_* - a}{a} - \ln\frac{\tilde{\varepsilon}}{2} + \frac{7}{2}\tilde{\varepsilon} = -\ln\delta_S^{(0)}. \tag{10.58}$$

We now turn to determining how the island hypersurface penetrates into region II of the spacetime (see Figure 10.5). From equation (10.58), we see that the island first appears (along the $\delta_I = 1$ hypersurface) only at late times, since $\tau_0/a \gg 1/\tilde{\varepsilon}$. Consequently, we are justified in taking the limit $|\ln\delta_S| \to \infty$ in equations (10.47) and (10.48). In this late-time regime, these equations reduce to:

$$1 - \mathrm{x}_I = \tilde{\varepsilon}\left[\frac{1}{2\mathrm{x}_I^2} - \frac{1}{\hat{\mathrm{x}}_S - \ln\delta_I} + \frac{1}{\hat{\mathrm{x}}_I - \ln\delta_I}\right], \tag{10.59}$$

$$1 - \mathrm{x}_I = \tilde{\varepsilon}\left[\frac{1}{2\mathrm{x}_I^2} - \frac{1}{2\hat{\mathrm{x}}_I^2} + \frac{\hat{\mathrm{x}}_I - 1}{\hat{\mathrm{x}}_I}\left(\frac{1}{\hat{\mathrm{x}}_I - \hat{\mathrm{x}}_S} + \frac{1}{\hat{\mathrm{x}}_I - \ln\delta_I}\right)\right]. \tag{10.60}$$

Motivated by the expressions for the island position along the $\delta_I = 1$ hypersurface in (10.55-10.58), we introduce the ansatz

$$\mathrm{x}_I = 1 - \xi, \quad \hat{\mathrm{x}}_I = 1 - \hat{\xi}, \quad \hat{\mathrm{x}}_S = 1 + \mu, \tag{10.61}$$

for the location of the island at arbitrary time $\tau \geqslant \tau_0$. Here, ξ, $\hat{\xi}$, and μ are small functions of δ_I, each expanded to second order in $\tilde{\varepsilon}$. With this substitution, equations (10.59-10.60) take the form

$$\xi = \tilde{\varepsilon}\left[\frac{1}{2} + \xi + \frac{\mu + \hat{\xi}}{(1 - \ln\delta_I)^2}\right], \tag{10.62}$$

$$\xi = \tilde{\varepsilon}\left[\xi - \hat{\xi} + \frac{\hat{\xi}}{\hat{\xi} + \mu}(1 + \hat{\xi}) - \frac{\hat{\xi}}{1 - \ln\delta_I}\right]. \tag{10.63}$$

Equating (10.62) and (10.63) yields

$$\frac{1}{2} + \hat{\xi} + \frac{\mu + \hat{\xi}}{(1 - \ln\delta_I)^2} = \frac{\hat{\xi}}{\hat{\xi} + \mu}(1 + \hat{\xi}) - \frac{\hat{\xi}}{1 - \ln\delta_I}. \tag{10.64}$$

On the right-hand side of (10.64), the only contribution of order $\mathcal{O}(1)$ is $\hat{\xi}/(\hat{\xi} + \mu)$. We therefore infer that this term must be of the form:

$$\frac{\hat{\xi}}{\hat{\xi} + \mu} = \frac{1}{2} + \eta, \tag{10.65}$$

where η is a new quantity of order $\tilde{\varepsilon}$. Substituting (10.65) into (10.64) then gives

$$\eta = \frac{1}{2}\hat{\xi} + \frac{\hat{\xi}}{1 - \ln\delta_I} + \frac{\mu + \hat{\xi}}{(1 - \ln\delta_I)^2}. \tag{10.66}$$

Using (10.65) and (10.66), we can straightforwardly solve for ξ and $\hat{\xi}$ in terms of μ and δ_I:

$$\xi = \frac{\tilde{\varepsilon}}{2}(1 + \tilde{\varepsilon})\left[1 + \frac{4\mu}{(1 - \ln\delta_I)^2}\right], \tag{10.67}$$

$$\hat{\xi} = \mu\left[1 + 4\mu\left(\frac{1}{2} + \frac{1}{1 - \ln\delta_I} + \frac{2}{(1 - \ln\delta_I)^2}\right)\right]. \tag{10.68}$$

The next step is to determine $\delta_I = \delta_I(\mu)$ using equation (5.152). Because this equation contains logarithmic terms, δ_I can only be fixed to first order in $\tilde{\varepsilon}$, even though the other quantities are known to second order. Carrying this out, we obtain

$$\delta_I = \frac{\hat{\xi}}{\xi}(1 + \xi - \hat{\xi}). \tag{10.69}$$

Inserting (10.67) and (10.68) into (10.69) then leads to the expression

$$\delta_I = \frac{\mu}{\tilde{\varepsilon}}\,(2-\tilde{\varepsilon})\left[1+4\mu\left(\frac{1}{4}+\frac{1}{1-\ln\delta_I}+\frac{1}{(1-\ln\delta_I)^2}\right)\right]. \tag{10.70}$$

Finally, we determine μ as a function of the evaporation time τ from equation (10.36), which yields

$$\mu = \frac{\tilde{\varepsilon}}{2}\frac{\delta_S(\tau)}{\delta_S(\tau_0)}\left(1-\frac{7}{2}\tilde{\varepsilon}\right)\left(1-\frac{\tilde{\varepsilon}}{2}\frac{\delta_S(\tau)}{\delta_S(\tau_0)}\right). \tag{10.71}$$

Combining equations (10.67-10.71), we obtain the position of the island as a function of the time elapsed since its formation, $\Delta\tau = \tau-\tau_0$. This provides an effective parametrization of the island hypersurface depicted in Figure 10.5.

$$\delta_I = e^{-\frac{\Delta\tau}{2a}}(1-4\tilde{\varepsilon})\left[1+2\tilde{\varepsilon}\frac{2+\frac{\Delta\tau}{2a}}{\left(1+\frac{\Delta\tau}{2a}\right)^2}e^{-\frac{\Delta\tau}{2a}}\right], \tag{10.72}$$

$$\hat{\mathrm{x}}_I = 1-\frac{\tilde{\varepsilon}}{2}e^{-\frac{\Delta\tau}{2a}}\left(1-\frac{7}{2}\tilde{\varepsilon}\right)\left[1+\frac{\tilde{\varepsilon}}{2}\left(1+4\frac{3+\frac{\Delta\tau}{2a}}{\left(1+\frac{\Delta\tau}{2a}\right)^2}\right)e^{-\frac{\Delta\tau}{2a}}\right], \tag{10.73}$$

$$\mathrm{x}_I = 1-\frac{\tilde{\varepsilon}}{2}(1+\tilde{\varepsilon})\left[1+\frac{2\tilde{\varepsilon}}{\left(1+\frac{\Delta\tau}{2a}\right)^2}e^{-\frac{\Delta\tau}{2a}}\right], \tag{10.74}$$

$$\hat{\mathrm{x}}_S = 1+\frac{\tilde{\varepsilon}}{2}e^{-\frac{\Delta\tau}{2a}}\left(1-\frac{7}{2}\tilde{\varepsilon}\right)\left[1-\frac{\tilde{\varepsilon}}{2}e^{-\frac{\Delta\tau}{2a}}\right]. \tag{10.75}$$

We infer that the island forms behind the horizon, as anticipated. The first consistency test is to check whether equations (10.72-10.75) reduce to the initial solution (10.55-10.57) in the limit $\Delta\tau\to 0$. A straightforward evaluation of this limit confirms that they do. Furthermore, in the opposite limit $\Delta\tau\to\infty$ we obtain $\delta_I\to 0$ and $\hat{\mathrm{x}}_I\to 1$, implying that the island extends to future time infinity. This is consistent with the absence of quantum corrections. In this limit we also find $\hat{\mathrm{x}}\to 1$. It is noteworthy that both the island and the cutoff surface almost reflect the position of the horizon at $\hat{\mathrm{x}}_H = 1$.

We now proceed to compute the fine-grained entropy of the radiation, given by (10.46), evaluated on the island hypersurface. A direct computation leads to:

$$S_{RW} = \frac{(\lambda a)^2}{12\varepsilon}-\frac{1}{12}-\frac{\varepsilon}{24(\lambda a)^2}+\frac{1}{12}\ln\left(\frac{\varepsilon}{2(\lambda a)^2}\frac{b-a}{b}\right)+\frac{1}{6}\ln\frac{-8a^2\ln\delta_S^{(0)}}{\epsilon^2}-\frac{\varepsilon}{6(\lambda a)^2}\frac{1-\frac{\Delta\tau}{2a}}{\left(1+\frac{\Delta\tau}{2a}\right)^2}e^{-\frac{\Delta\tau}{2a}}. \tag{10.76}$$

Expression (10.76) consists of a constant contribution and an exponentially decaying contribution. The constant piece must be regularized because it depends on the UV cutoff ϵ. Discarding the UV-sensitive part of this constant term, the leading contribution is precisely the Bekenstein–Hawking entropy (1.4), namely $S_{BH}^{(0)} = \frac{(\lambda a)^2}{12\varepsilon}$. Hence we can interpret the full constant part as the quantum-corrected Bekenstein–Hawking entropy S_{BH}^{corr}. Then, fine-grained entropy at late times is given by the following formula:

$$S_{FG} = \min\left\{\frac{\Delta\tau}{24a}+\frac{1}{6}\ln\frac{\tau}{2b}-\frac{1}{12}\ln\frac{\varepsilon}{2(\lambda a)^2},\, S_{BH}^{\mathrm{corr}}-\frac{\varepsilon}{6(\lambda a)^2}\frac{1-\frac{\Delta\tau}{2a}}{\left(1+\frac{\Delta\tau}{2a}\right)^2}e^{-\frac{\Delta\tau}{2a}}\right\}, \tag{10.77}$$

From (10.77) it follows that, at late times, the fine-grained entropy approaches a constant value close to the black hole's Bekenstein–Hawking entropy. Consequently, without including the back-reaction of quantum fields on the spacetime geometry, we do not obtain the correct Page curve and instead recover the same behavior as for an eternal black hole [42]. This outcome is natural, since the classical solution in region II is intrinsically static. Only by analyzing both regions simultaneously does one see that the entire spacetime is actually non-static, due to the discontinuity across the infalling shockwave hypersurface. Nevertheless, the extremization procedure at least guarantees that the coarse-grained entropy bound is not exceeded.

In Figure 10.6, the Page curve for the classical collapse setup, defined in equation (10.77), is shown. The blue curve denotes the fine-grained entropy evaluated on Hawking's saddle point, while the red curve indicates the entropy obtained from the replica-wormhole saddle point at late times. The purple curve illustrates the late-time asymptotic behavior of the fine-grained entropy on Hawking's saddle point. This figure clearly demonstrates how incorporating an island contrasts with the standard Hawking prediction.

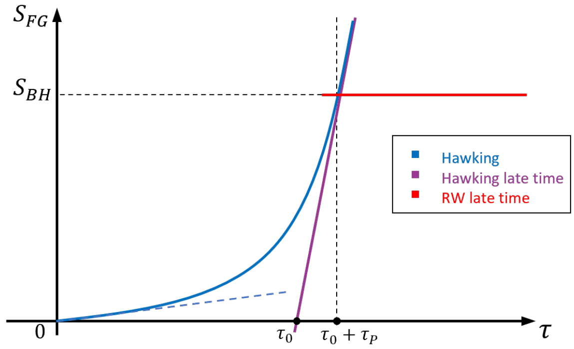

Figure 10.6: Page curve for the classical collapse scenario in the DREH model.

To determine the time at which the phase transition takes place, namely the Page time, we match the leading contributions in (10.77). This yields the Page time:

$$\tau_P = 24aS_{BH}^{\text{corr}}. \tag{10.78}$$

Expression (10.78) agrees with the result found for the eternal black hole (10.26). The relation between the time variable used in the eternal black hole case and (10.78) is $t_P = \frac{1}{2}\tau_P$. This factor-of-two difference arises because the eternal black hole possesses two asymptotically flat regions, which makes the coarse-grained entropy twice as large.

10.3 Page curve for the quantum-corrected collapse scenario

We now turn to the analysis of the Page curve for the quantum-corrected collapse setup introduced in Section 5.3. In the previous section, we saw that, for a purely classical evaporating black hole, the replica-wormhole saddle point fails to produce the decreasing part of the fine-grained entropy required to obtain the Page curve. By employing the fine-grained entropy formula (1.6), we demonstrate that this problem is resolved once quantum corrections are incorporated. In this way, we recover the expected decreasing contribution from the replica-wormhole saddle point. The structure of this section parallels that of the earlier ones: we begin by examining the no-island configuration and then move on to the island configuration. The derivation is based on [43].

10.3.1 No-island configuration

Here we examine how incorporating the back-reaction of quantum fields into the fine-grained entropy affects its evaluation along Hawking's saddle point. No significant deviations from the results of Section 10.2.1 are anticipated. We demonstrate that this procedure once more leads to Hawking's information loss paradox [16]. The fine-grained entropy (1.6) effectively reduces to its semi-classical contribution, given by the same expression (8.54) as in the purely classical analysis:

$$S_{semi-cl} = \frac{1}{12} \ln \frac{(\sigma^+_S - \sigma^+_{\bar{S}})^2}{4\epsilon^2 e^{-2\rho_S(\sigma)}}. \tag{10.79}$$

As in Section 10.2.1, the cut-off surface (10.36) is specified by the condition $r_* = b_*$. Substituting the expression (5.176) for the tortoise coordinate, we obtain the following relation defining the cut-off hypersurface:

$$\frac{b_*}{a} - \frac{\tau}{2a} = \mathcal{J}(\hat{\mathrm{x}}_S) - \frac{9}{2} - \frac{\tilde{\varepsilon}}{8}\left[(2\hat{\mathrm{x}}_S + 3)\ln \hat{\mathrm{x}}_S + 5\hat{\mathrm{x}}_S - 2\mathrm{L}_S\right], \tag{10.80}$$

where, as before, the evaporation time is introduced via $-\ln \delta_S = \frac{\tau}{2a}$ in complete analogy with (10.37).

The appropriate Penrose diagram for the no-island configuration in the quantum-corrected collapse scenario is presented in Figure 10.7. It contains the same key hypersurfaces, points (δ_S, $\hat{\mathrm{x}}_S$, $\delta_{\bar{S}}$), and associated coordinate axes δ and $\hat{\mathrm{x}}$ as in the classical collapse case shown in Figure 10.4. The essential distinction is the emergence of region III, which represents the remnant spacetime after the black hole has completely evaporated. The evaporation end-point $(\delta_E, \hat{\mathrm{x}}_E)$ is explicitly indicated. The newly formed region lies beyond this point and is characterized by $\delta < \delta_E$ and $\hat{\mathrm{x}} < \hat{\mathrm{x}}_E$. As before, the region A containing the inaccessible degrees of freedom is highlighted in red, while the cut-off hypersurface and the apparent horizon are drawn in purple. The constant-time slice associated with the radiation's degrees of freedom appears in blue. We continue to assume the validity of approximation (10.35), namely

$$b_* \tilde{\varepsilon} \gg a.$$

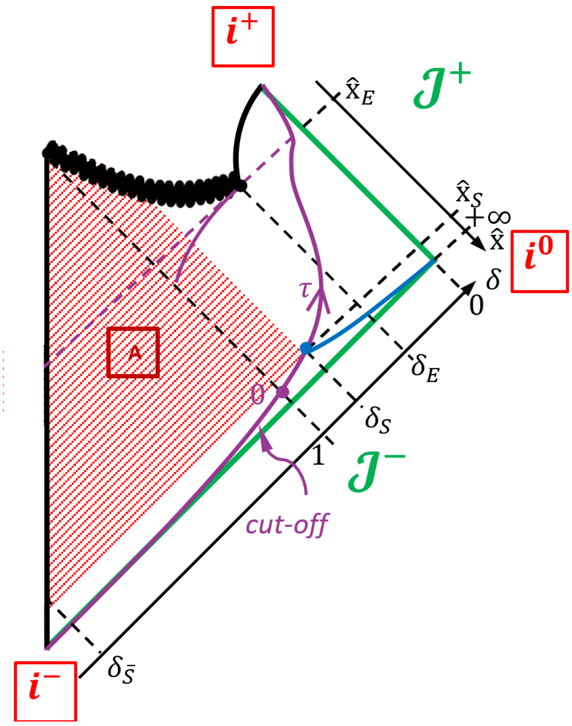

Figure 10.7: Penrose diagram illustrating the no-island case within the quantum-corrected collapse scenario.

We now evaluate the fine-grained entropy along Hawking's saddle point (10.79). Imposing the regularization condition $S_H(0) = 0$ gives

$$S_H(\tau) = \frac{1}{12} \ln \left(\frac{a^2}{b^2} \left(\frac{\tau}{2a} + \hat{\mathrm{x}}_S \right)^2 \frac{\mathrm{F}^+_S \mathrm{F}^-_S e^{2\rho_S}}{\mathrm{F}^-_S \mathrm{F}^+_S} \right). \tag{10.81}$$

Let us study the behavior of (10.81) at the beginning of the evaporation, i.e. for $\tau \to 0$, in direct analogy with the classical analysis of Section 10.2.1. The first step is to solve the transcendental equation (10.80) for $\hat{\mathrm{x}}_S$ as a function of τ. At $\tau = 0$ we obtain $\hat{\mathrm{x}}_S = \mathrm{x}_S = \frac{b}{a}$, implying that for small τ we can write $\hat{\mathrm{x}}_S = \frac{b}{a} + \eta$, with η a small parameter. Expanding equation (10.36) in this regime, we find

$$\hat{\mathrm{x}}_S^{(0)} = \frac{b}{a} - \frac{b-a}{2ab}\tau \left\{ 1 - \frac{\tilde{\varepsilon}}{8} \left[2 \ln \left(1 - \frac{a}{b} \right) + \frac{2a}{b-a} - \frac{a^2}{b^2} \right] \right\}. \tag{10.82}$$

Keeping only the leading term in the $\frac{a}{b} \to 0$ expansion, this simplifies to

$$\hat{\mathrm{x}}_S^{(0)} = \frac{b}{a} - \frac{b-a}{2ab}\tau \left(1 - \frac{\tilde{\varepsilon}}{6} \frac{a^3}{b^3} \right). \tag{10.83}$$

In comparison with equation (10.39), we observe a small shift induced by quantum corrections. A straightforward evaluation of the fine-grained entropy (10.81) then gives

$$S_H^{(0)}(\tau) = \frac{a\tau}{8b^2} \left(1 + \frac{\tilde{\varepsilon}}{4} \frac{b^2}{a^2} \right), \tag{10.84}$$

where, again, we have retained only the dominant contribution in the $\frac{a}{b} \to 0$ expansion. Comparing this with (10.40), we once more see that the effect of quantum corrections is a small modification.

Next, we turn to the late-time analysis of formula (10.81). Since at late times one has $\hat{\mathrm{x}}_S = 1 + \tilde{\varepsilon}\mu$, we expand equation (10.80) around the point $\hat{\mathrm{x}}_S = 1$:

$$\frac{b_* - a}{b_*} - \frac{\tau}{2a} = \left(1 + \frac{11}{8}\tilde{\varepsilon} \right) \frac{4}{\tilde{\varepsilon}} \left(e^{\frac{\tilde{\varepsilon}}{4} \ln \left(\tilde{\varepsilon} \left(\mu - \frac{1}{4} \right) \right)} - 1 \right) + \tilde{\varepsilon}\mu. \tag{10.85}$$

The solution of equation (10.85) can be written as

$$\hat{\mathrm{x}}_S^{(\infty)} = 1 + \frac{\tilde{\varepsilon}}{4} \left(1 + 3 e^{-\frac{\tau - \tau_0}{2\bar{a}}} \right), \tag{10.86}$$

where τ_0 will be introduced below via equation (10.103). For convenience, we define $\Delta\tau = \tau - \tau_0$. Since the metric becomes asymptotically flat at late times, we may approximate $\mathrm{F}_S^+ \mathrm{F}_S^- e^{2\rho_S} \approx -1$. In the regime $\hat{\mathrm{x}}_S \approx 1$, the coordinate transformations simplify to

$$\mathrm{F}_S^- \approx \hat{\mathrm{x}}_S^{(\infty)} - 1 - \frac{\tilde{\varepsilon}}{4} = \frac{3}{4}\tilde{\varepsilon} e^{-\frac{\Delta\tau}{2\bar{a}}}. \tag{10.87}$$

Substituting (10.86) and (10.87) into equation (10.81), we obtain

$$S_H^{(\infty)}(\tau) = \frac{\tau - \tau_0}{24\bar{a}} + \frac{1}{6} \ln \frac{\tau}{2b} - \frac{1}{12} \ln \left(-\frac{3\tilde{\varepsilon}}{4} \mathrm{F}_\infty^+ \right), \tag{10.88}$$

where F_∞^+ denotes the late-time value of the coordinate transformation, $\sigma^+ \to \infty$. Thus, for the Hawking saddle point, the fine-grained entropy exhibits linear growth both at early and at late times; only the slope of the linear dependence changes. Comparing with (10.42), we find that the entropy shows the same qualitative behavior as in the classical case, but with the surface gravity replaced by its quantum-corrected value, given later in equation (10.117).

10.3.2 Island configuration

We now analyze the replica-wormhole saddle point in the quantum-corrected setup. We demonstrate that, unlike in the classical island configuration discussed in Section 10.2.2, the contribution to the entropy here decreases, thereby yielding the Page curve. In the quantum-corrected geometry, the same expressions (10.45) and (10.43) still apply to the corresponding terms in the fine-grained entropy (1.6). Consequently, we can proceed directly with the extremization, which leads to the following equations determining the island position:

$$\mathrm{x}_I\partial_+\mathrm{x}_I + \tilde{\varepsilon}\partial_+\rho_I = -\frac{\tilde{\varepsilon}}{2a}\left[\frac{\hat{\mathrm{x}}_S - \ln\delta_S}{(\ln\delta_I - \ln\delta_S)(\ln\delta_I - \hat{\mathrm{x}}_S)} + \frac{1}{\hat{\mathrm{x}}_I - \ln\delta_I}\right], \tag{10.89}$$

$$\mathrm{x}_I\partial_-\mathrm{x}_I + \tilde{\varepsilon}\partial_-\rho_I = \frac{\tilde{\varepsilon}}{2a}\left[\frac{\hat{\mathrm{x}}_S - \ln\delta_S}{(\hat{\mathrm{x}}_I - \ln\delta_S)(\hat{\mathrm{x}}_I - \hat{\mathrm{x}}_S)} + \frac{1}{\hat{\mathrm{x}}_I - \ln\delta_I}\right]. \tag{10.90}$$

As in the classical analysis, we first determine the location of the island along the infalling shockwave and subsequently extend it into region II of the spacetime, where the evaporating black hole resides.

The Penrose diagram for the quantum-corrected island configuration is displayed in Figure 10.8. The region A, which contains the inaccessible degrees of freedom, is shown in red, while the island region I is indicated in blue. The cut-off hypersurface, together with the τ-axis that parametrizes it, is drawn in purple. Likewise, the island-boundary hypersurface and its parametrizing $\Delta\tau$-axis are also depicted in purple. The radiation degrees of freedom occupy a causal diamond built over a constant-time slice, indicated in blue as well. The coordinates of all relevant points (δ_S, δ_I, $\hat{\mathrm{x}}_S$, $\hat{\mathrm{x}}_I$, $\hat{\mathrm{x}}_E$, δ_E), along with those obtained by reflecting them across the spacetime boundary ($\delta_{\bar{S}}$, $\delta_{\bar{I}}$), are marked on both the δ-axis and the $\hat{\mathrm{x}}$-axis. The corresponding classical configuration is shown in Figure 10.5. The key difference between the two diagrams is that only the quantum-corrected one contains remnant spacetime in region III.

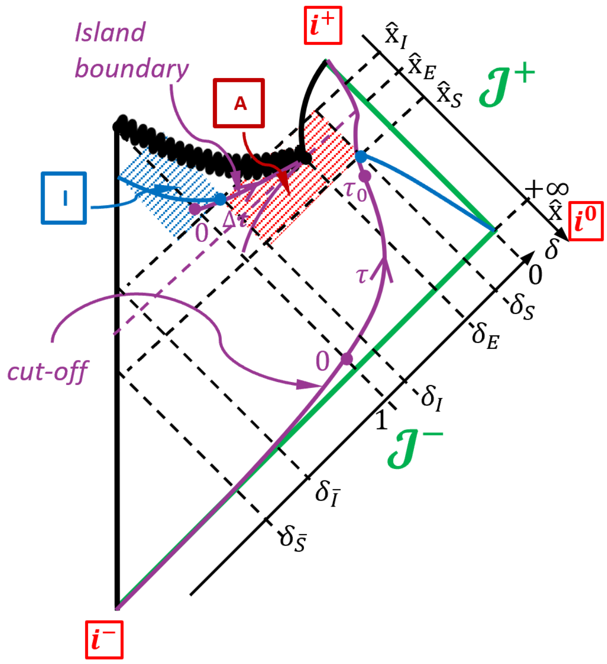

Figure 10.8: Penrose diagram illustrating the island case within the quantum-corrected collapse scenario.

We now analyze how the island appears along the $\delta_I = 1$ hypersurface, following the same procedure as in section 10.2.2. Along this hypersurface, we impose a continuity condition (see [111]), which leads to

$$\mathrm{x}_I\partial_+\mathrm{x}_I + \tilde{\varepsilon}\partial_+\rho_I = \frac{\mathrm{x}_I - 1}{2a}, \tag{10.91}$$

$$\mathrm{x}_I\partial_-\mathrm{x}_I + \tilde{\varepsilon}\partial_-\rho_I = -\frac{\mathrm{x}_I}{2a}. \tag{10.92}$$

Using these continuity relations, equations (10.89) and (10.90) take the form

$$1 - \mathrm{x}_I = \tilde{\varepsilon}\left[\frac{1}{\mathrm{x}_I} - \frac{\ln\delta_S - \hat{\mathrm{x}}_S}{\hat{\mathrm{x}}_S \ln\delta_S}\right], \tag{10.93}$$

$$\mathrm{x}_I^2 = \tilde{\varepsilon}\left[-1 + \frac{\ln\delta_S}{\mathrm{x}_I - \ln\delta_S} - \frac{\hat{\mathrm{x}}_S}{\mathrm{x}_I - \hat{\mathrm{x}}_S}\right]. \tag{10.94}$$

Observe that the second equation (10.94) coincides exactly with the classical equation (10.50), whereas the first one (10.93) is simpler than its classical analogue (10.49), reducing to a straightforward quadratic equation. As before, we introduce

$$\zeta = \frac{\ln\delta_S - \hat{\mathrm{x}}_S}{\hat{\mathrm{x}}_S \ln\delta_S}. \tag{10.95}$$

Both equations can then be solved exactly in terms of ζ, yielding

$$\mathrm{x}_I = \frac{1+\tilde{\varepsilon}\zeta}{2}\left[1 + \sqrt{1 - \frac{4\tilde{\varepsilon}}{(1+\tilde{\varepsilon}\zeta)^2}}\right], \tag{10.96}$$

$$\hat{\mathrm{x}}_S = \mathrm{x}_I \frac{1 + \frac{1}{2}\zeta \mathrm{x}_I\left(1 + \sqrt{1 + \frac{4\tilde{\varepsilon}}{\zeta \mathrm{x}_I^2(1+\tilde{\varepsilon}\zeta)}}\right)}{1 + \frac{\zeta \mathrm{x}_I^2}{1+\tilde{\varepsilon}\zeta}}. \tag{10.97}$$

Note that this solution is fully non-perturbative. To extract quantitative estimates, we expand (10.96) and (10.97) in powers of $\tilde{\varepsilon}$ up to second order:

$$\mathrm{x}_I = 1 + \tilde{\varepsilon}(1+\tilde{\varepsilon})(\zeta - 1), \tag{10.98}$$

$$\hat{\mathrm{x}}_S = 1 + \tilde{\varepsilon}\left(\zeta - \frac{\tilde{\varepsilon}}{\zeta}\right). \tag{10.99}$$

Next, we evaluate $\zeta = \frac{1}{\hat{\mathrm{x}}_S} - \frac{1}{\ln\delta_S}$. As in the classical analysis, we assume $\ln\delta_S \gg 1$, so the second term can be neglected. This gives $\zeta = 1 - \tilde{\varepsilon}(1+\tilde{\varepsilon})$. Finally, we determine τ_0 from equation (10.80). Plugging this expression for ζ into (10.98) and (10.99), the island's position along the $\delta_I = 1$ hypersurface becomes

$$\delta_I = 1, \tag{10.100}$$

$$\mathrm{x}_I = 1 - \tilde{\varepsilon}^2 = \hat{\mathrm{x}}_I, \tag{10.101}$$

$$\hat{\mathrm{x}}_S = 1 + \tilde{\varepsilon}(1 - 2\tilde{\varepsilon}), \tag{10.102}$$

$$\frac{\tau_0}{2a} = \frac{b_* - a}{a} - \left(1 + \frac{11}{8}\tilde{\varepsilon}\right)\frac{4}{\tilde{\varepsilon}}\left(e^{\frac{\tilde{\varepsilon}}{4}\ln\frac{3\tilde{\varepsilon}}{4}} - 1\right) - \tilde{\varepsilon}. \tag{10.103}$$

Comparing (10.100–10.103) with the classical expressions (10.55–10.58), we find that the leading correction to the island position x_I along the $\delta_I = 1$ hypersurface now appears at order $\mathcal{O}(\tilde{\varepsilon}^2)$, in contrast to the classical case, where it is of order $\mathcal{O}(\tilde{\varepsilon})$. Furthermore, the formation time of the island τ_0 agrees with the classical result up to terms of order $\mathcal{O}(1)$. Deviations at higher orders are expected, as they arise from incorporating quantum corrections to the metric.

We now generalize the solution for the island position to arbitrary times $\tau > \tau_0$. Since $b_*\tilde{\varepsilon} \gg a$, we can safely disregard terms of order $1/\ln\delta_S$, as in the purely classical analysis. With this approximation, equations (10.89) and (10.90) take the form

$$\mathrm{x}_I\partial_+\mathrm{x}_I + \tilde{\varepsilon}\partial_+\rho_I = \frac{\tilde{\varepsilon}}{2a}\left[\frac{1}{\hat{\mathrm{x}}_S - \ln\delta_I} - \frac{1}{\hat{\mathrm{x}}_I - \ln\delta_I}\right], \tag{10.104}$$

$$\mathrm{x}_I\partial_-\mathrm{x}_I + \tilde{\varepsilon}\partial_-\rho_I = \frac{\tilde{\varepsilon}}{2a}\left[\frac{1}{\hat{\mathrm{x}}_I - \hat{\mathrm{x}}_S} + \frac{1}{\hat{\mathrm{x}}_I - \ln\delta_I}\right]. \tag{10.105}$$

We adopt the following ansatz:

$$\mathrm{y}_I = 1 + \xi, \quad \hat{\mathrm{x}}_I = 1 + \hat{\xi}, \quad \hat{\mathrm{x}}_S = 1 + \mu, \tag{10.106}$$

where ξ, $\hat{\xi}$ and μ are quantities of order $\mathcal{O}(\tilde{\varepsilon})$. Inserting this ansatz into the expressions (5.157–5.158) for the derivatives of the dilaton field, together with (5.182–5.183) for the derivatives of the metric, we find

$$\partial_+ \mathrm{x}_I = \frac{1}{2a}\left(1 - \frac{1}{\sqrt{\mathrm{y}_I^2 - \tilde{\varepsilon}}}\right), \tag{10.107}$$

$$\partial_- \mathrm{x}_I = -\frac{1}{2a\mathrm{F}_I^-}\left(1 - \frac{1 - \frac{\tilde{\varepsilon}}{4}}{\sqrt{\mathrm{y}_I^2 - \tilde{\varepsilon}}}\right), \tag{10.108}$$

$$\partial_+ \rho = \frac{1}{4a\tilde{a}_I}\frac{\mathrm{y}_I}{(\mathrm{y}_I^2 - \tilde{\varepsilon})^{\frac{3}{2}}}, \tag{10.109}$$

$$\partial_- \rho = -\frac{1}{4a\mathrm{F}_I^-}\left(\frac{\hat{\mathrm{x}}_I^2 - 1}{\hat{\mathrm{x}}_I^2} - \frac{1}{\tilde{a}_I}\frac{\mathrm{y}_I^2 - 1}{\mathrm{y}_I^2}\right), \tag{10.110}$$

where y and $\tilde{a}$ are defined via equation (5.156). Using (10.107) and (5.182), equation (10.104) simplifies to $\mathrm{y}_I = 1$, i.e. $\xi = 0$. Note that we can determine the island position only up to $\mathcal{O}(\tilde{\varepsilon})$, since the solution itself is of that order. Consequently, the left-hand side of equation (10.104) vanishes. The quantity $\hat{\xi}$ then follows straightforwardly from (5.181), giving

$$\hat{\xi} = \frac{1}{4}(1 - \delta_I). \tag{10.111}$$

From equation (5.184) we infer that

$$\mathrm{F}^-(\hat{\mathrm{x}}_I) = \hat{\xi} - \frac{\tilde{\varepsilon}}{4}. \tag{10.112}$$

Substituting (10.112) into (10.105) yields

$$\frac{\tilde{\varepsilon}}{4} = \tilde{\varepsilon}\frac{\hat{\xi} - \frac{\tilde{\varepsilon}}{4}}{\hat{\xi} - \mu}. \tag{10.113}$$

Solving (10.113) and using (10.111), we obtain:

$$\mu = \frac{1}{4}\left(1 + 3\delta_I\right). \tag{10.114}$$

By inserting $\Delta\tau = \tau - \tau_0$ into (10.85), we derive the following relation for μ:

$$-\frac{\Delta\tau}{2a}\left(1 - \frac{11}{8}\tilde{\varepsilon}\right)e^{-\frac{\tilde{\varepsilon}}{4}\ln\frac{3\tilde{\varepsilon}}{4}} = \frac{4}{\tilde{\varepsilon}}\left(e^{\frac{\tilde{\varepsilon}}{4}\ln\frac{4\mu-1}{3}} - 1\right) + \tilde{\varepsilon}(\mu - 1). \tag{10.115}$$

Because the right-hand side of (10.115) contains logarithms, the equation is correct up to $\mathcal{O}(1)$. Taking the limit $\tilde{\varepsilon} \to 0$ and solving for μ gives

$$\mu = \frac{1}{4}\left(1 + 3e^{-\frac{\Delta\tau}{2\bar{a}}}\right), \tag{10.116}$$

where we have introduced a new constant $\bar{a}$, which can be interpreted as quantum-corrected surface gravity:

$$\kappa = \frac{1}{2\bar{a}} = \frac{1}{2a}\left(1 - \frac{11}{8}\tilde{\varepsilon}\right)e^{-\frac{\tilde{\varepsilon}}{4}\ln\frac{3\tilde{\varepsilon}}{4}}. \tag{10.117}$$

Combining (10.111), (10.114) and (10.116), we find the following expressions for the island position:

$$\delta_I = e^{-\frac{\Delta\tau}{2\bar{a}}}, \tag{10.118}$$

$$\hat{\mathrm{x}}_I = 1 + \frac{\tilde{\varepsilon}}{4}\left(1 - e^{-\frac{\Delta\tau}{2\bar{a}}}\right), \tag{10.119}$$

$$\mathrm{x}_I = 1 - \frac{\tilde{\varepsilon}}{4}\frac{\Delta\tau}{2\bar{a}}, \tag{10.120}$$

$$\hat{\mathrm{x}}_S = 1 + \frac{\tilde{\varepsilon}}{4}\left(1 + 3e^{-\frac{\Delta\tau}{2\bar{a}}}\right). \tag{10.121}$$

The island thus emerges behind the event horizon, as expected for an evaporating black hole. Comparing (5.189) with (10.119), we see that the island and the apparent horizon are symmetric with respect to the event horizon (5.208). Moreover, the island intersects the singularity slightly before the end-point of the evaporation, just as in the BPP model (see Section 9.2.3). In the limit $\Delta\tau \to 0$, the relations (10.118–10.121) reduce to equations (10.101–10.103). Unlike in the classical case, where x_I tends to a constant value at late times (10.74), here x_I decreases with time, which is precisely what is required to reproduce the Page curve, since the island must reach the singularity in a finite time.

We now evaluate the contribution of the replica–wormhole saddle to the fine-grained entropy. We begin with the semi-classical entropy term in (1.6). Substituting the island location (10.118–10.121) into equation (10.43), we obtain

$$S_{semi-cl-\mathrm{RW}} = \frac{1}{12}\ln\left(\frac{4\tilde{\varepsilon}\left(-\ln\delta_S^{(0)}\right)^2}{-3\mathrm{F}_\infty^+(\kappa\epsilon)^4}\right) - \frac{\tilde{\varepsilon}}{6}\frac{1}{1+\frac{\Delta\tau}{2\bar{a}}}e^{-\frac{\Delta\tau}{2\bar{a}}}, \tag{10.122}$$

where we used

$$\begin{aligned}
&\tilde{\mathrm{F}}^+\mathrm{F}^-e^{2\rho}\Big|_I = \frac{\tilde{\varepsilon}}{4} \;\wedge\; \mathrm{F}_I^- = -\frac{\tilde{\varepsilon}}{4}\delta_I \;\wedge\; \tilde{\mathrm{F}}_I^+ = -1,\\
&\mathrm{F}^+\mathrm{F}^-e^{2\rho}\Big|_S = -1 \;\wedge\; \mathrm{F}_S^- = \frac{3}{4}\tilde{\varepsilon}\delta_I \;\wedge\; \mathrm{F}_S^+ = \mathrm{F}_\infty^+,\\
&\text{Coord-part} = \left(-\ln\delta_S^{(0)}\tilde{\varepsilon}\delta_I\right)^2\left(1 - \frac{2\tilde{\varepsilon}\delta_I}{1-\ln\delta_I}\right).
\end{aligned} \tag{10.123}$$

In (10.123), $\tilde{\mathrm{F}}_I^+$ denotes a coordinate redefinition relative to the σ^+ coordinate, while F_S^+ is a coordinate transformation with respect to $\hat{\sigma}^+$. Moreover, "Coord-part" refers to the portion of (10.43) inside the logarithm that depends explicitly on the σ coordinates. Since the expression in (10.122) still involves the UV cut-off ϵ, we must perform a regularization. Next, we consider the area term appearing in (10.45). Plugging in (10.120) gives

$$\frac{A[\partial I]}{4G_\mathrm{N}^{(4)}} = \frac{1}{12\tilde{\varepsilon}}\left(1 - \frac{\tilde{\varepsilon}}{4}\frac{\Delta\tau}{2\bar{a}}\right)^2. \tag{10.124}$$

To fix the regularization, we impose that the island hits the singularity near the end of evaporation, ensuring that the fine-grained entropy vanishes at the evaporation end-point. Taking this requirement together with the minimization prescription (1.6), we arrive at the final expression for the late-time limit of the fine-grained entropy of Hawking radiation:

$$S_{FG} = \min\left\{\frac{\Delta\tau}{24\bar{a}} + \frac{1}{6}\ln\frac{\tau}{2b} - \frac{1}{12}\ln\left(\frac{-3\varepsilon F^{+}_{\infty}}{4(\lambda a)^2}\right),\right.$$
$$\left.\frac{(\lambda a)^2}{12\varepsilon}\left(1-\frac{\varepsilon}{4(\lambda a)^2}\frac{\Delta\tau}{2\bar{a}}\right)^2 - \frac{1}{12} - \frac{\varepsilon}{6(\lambda a)^2}\frac{1}{1+\frac{\Delta\tau}{2\bar{a}}}e^{-\frac{\Delta\tau}{2\bar{a}}}\right\}. \tag{10.125}$$

The Page time is then determined by equating the two branches inside (10.125). This yields

$$\kappa\tau_P = \frac{4(\lambda a)^2}{\varepsilon}\left(3-2\sqrt{2}\right). \tag{10.126}$$

At $\tau = \tau_P$, the fine-grained entropy reaches its peak value,

$$S_{FG}^{\max} = \frac{4}{3+2\sqrt{2}}S_{BH}^{(\mathrm{class})}. \tag{10.127}$$

Equation (10.127) shows that at all times the fine-grained entropy of the Hawking radiation remains below the coarse-grained (thermodynamic) bound set by the classical Bekenstein–Hawking entropy (1.4), as expected.

The resulting Page curve for the quantum-corrected collapse scenario is shown in Figure 10.10. The blue line denotes the fine-grained entropy evaluated on Hawking's saddle point, whereas the red line depicts the entropy along the replica-wormhole saddle point at late times. The purple line illustrates the late-time asymptotic behavior of the fine-grained entropy on Hawking's saddle point.

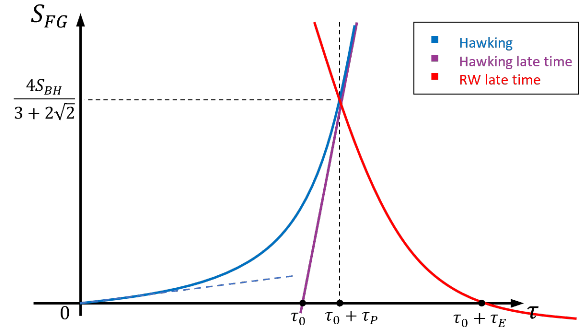

Figure 10.10: Page curve for the quantum-corrected collapse scenario in the DREH model.

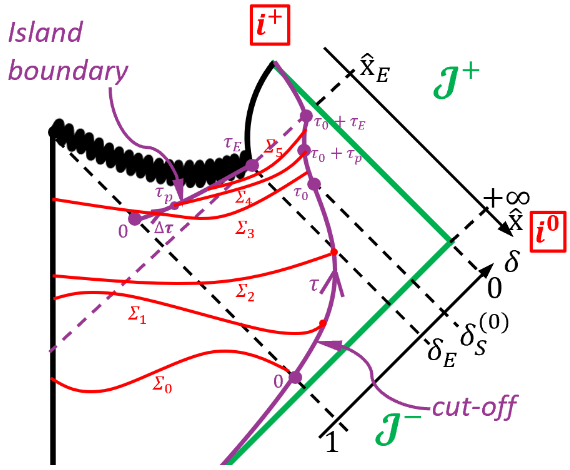

Figure 10.9: The complete process of black hole evaporation.

The evaporation process is depicted in Figure 10.9. The purple curve outside the horizon denotes the cut-off hypersurface, parameterized by the evaporation time τ. The second purple curve indicates the time-dependent location of the island, parameterized by $\Delta\tau$. Both τ and $\Delta\tau$ are initialized at zero along the $\delta = 1$ hypersurface. The red curves represent the region A, which contains the degrees of freedom that are inaccessible to the asymptotic observer.

Let us now summarize the overall mechanism of black hole evaporation. As τ increases, the black hole begins to evaporate. Initially, the minimum of the fine-grained entropy (10.125) is determined by Hawking's saddle point, so the red curves terminate at the spacetime boundary x = 0. When τ reaches $\tau = \tau_0$, an island first appears inside region II of the spacetime. This moment is characterized by $\Delta\tau = 0$ along the island-boundary curve. At this stage, the fine-grained entropy is still dominated by the Hawking contribution, and thus the red curves continue to end at the spacetime boundary. At $\tau = \tau_0 + \tau_P$, or equivalently $\Delta\tau = \tau_P$, a phase transition takes place. From that time on, the red curves terminate on the island boundary instead. The evaporation proceeds until $\tau_f = \tau_0 + \tau_E$, that is, until the island meets the singularity, meaning $\Delta\tau \approx \tau_E$. The instant $\tau = \tau_f$ coincides with the point at which the cut-off surface enters region III of the spacetime, thereby leaving the domain in which black hole radiation is present.

Note that we cannot precisely determine what occurs at the very end of the evaporation process, because at this stage the remaining distance to the end-point becomes so small that it is comparable to the Planck length. Consequently, quantum gravity effects become relevant, and the semi-classical approximation is no longer valid. Moreover, in this regime the perturbative treatment also breaks down (see Section 5.3). Nevertheless, we can still trust the reproduction of the Page curve up to its last few points.

Chapter 11

Conclusion

In this dissertation, we employ two-dimensional dilaton gravity as our main framework for probing quantum gravity effects within a semiclassical approximation. In this approach, the matter fields are quantized while the spacetime background is treated classically. The central question we aim to address is: Can a black hole be regarded as an ordinary quantum system? If so, its time evolution must be unitary. One strategy to investigate this is to compute the entanglement entropy of the Hawking radiation and examine whether it reproduces the Page curve. Although this can be attempted in the context of an eternal black hole, a more significant result is to obtain the Page curve for a genuinely evaporating black hole. To describe such an evaporating black hole, it is not sufficient to quantize only the matter fields; one must also incorporate the backreaction of the quantum fields on the classical geometry. Consequently, our first task is to formulate a consistent evaporating black hole scenario.

In Chapter 3, we developed a general formalism that accommodates both eternal and evaporating black hole configurations within two-dimensional dilaton gravity. The central element of this construction is a symmetric ansatz for arbitrary scalar, vector, tensor, or spinor fields in a 2D spacetime that admits a Killing vector. When the Killing vector is time-like we analyze black-hole-type solutions; when it is a space-like we instead study cosmological solutions. This ansatz exploits a distinctive feature of two-dimensional spacetimes: the Hodge dual of 1-form is still an 1-form, a property that holds only in two dimensions. Hence, given a Killing vector field, that vector and its Hodge dual together span the full space of 1-forms. This observation enables us to express any physical observable in terms of a single coordinate orthogonal to the Killing direction, rendering it independent of the coordinate associated with the Killing vector.

In this framework, the equations of motion simplify to a one-dimensional system, which is easier to solve. Yet this is not the only advantage of this construction. We demonstrated that the most general solution in any 2D theory—specified by the metric function Λ, the derivative of the dilaton field $\mathcal{D}$, and the torose coordinate $\frac{\sigma}{l}$—and even when coupled to matter, can be fully characterized by $(\mathrm{F}^{+}, \mathrm{F}^{-}, C, f)$. The functions $\mathrm{F}^{\pm}$ encode the coordinate transformations that map arbitrary coordinates to Eddington–Finkelstein-like coordinates adapted to the Killing vector; equivalently, they may be seen as the components of the Killing vector in the original coordinate system. The remaining two structures, C and f, represent respectively a set of constants corresponding to the conserved charges of the theory, and a set of arbitrary functions corresponding to residual gauge freedoms, typically originating from the dimensional reduction procedure by which the given 2D dilaton gravity theory is obtained.

We then showed that by employing static vacuum solutions written in this form, one can construct non-stationary spacetimes describing classical gravitational collapse. Concretely, the

Killing vector becomes discontinuous across the ingoing matter shockwave, so that each region of spacetime on either side of the shockwave is individually stationary, while the full spacetime lacks a single global Killing vector. This patchwise construction yields a genuine collapse geometry, and we demonstrated that, within this setup, one recovers the correct expression for the mass of the spacetime by starting from a massless background solution before introducing the ingoing shockwave.

It is then clear that if one includes quantum corrections and selects a quantum state such that the resulting geometry is stationary—for instance, the Hartle–Hawking or Boulware state—the same formalism still applies. In that case, the quantum expectation value of the EMT must satisfy the static ansatz, and the problem again reduces to one dimension. By contrast, for an evaporating black hole, one has to take into account the quantum back-reaction of the matter fields on the geometry. The corresponding solution is genuinely non-stationary, and at first sight this appears to invalidate our static ansatz. However, this is not the case if, from that point onward, one treats the problem perturbatively in the natural expansion parameter $\hbar$.

Because the quantum-corrected energy–momentum tensor is proportional to $\hbar$ at first order in perturbation theory, one evaluates it on the zeroth-order background solution. That zeroth-order solution coincides with the classical gravitational collapse obtained from the static ansatz. After obtaining the first-order correction, one could, at least in principle, continue to compute higher-order terms iteratively. Nevertheless, we demonstrate in explicit models that the first-order correction already suffices to construct a consistent quantum-corrected evaporating black hole geometry and, in turn, to determine its Page curve.

It is crucial to identify a well-defined pole in the tortoise coordinate in both eternal and evaporating black hole setups. All hypersurfaces of interest are located near the classical horizon, which corresponds to a clear pole of the classical tortoise coordinate. One therefore naturally adopts the dilaton as a radial coordinate, so that the tortoise coordinate relation becomes the only way to switch between the radial coordinate and Eddington–Finkelstein–type coordinates. In generic dilaton gravity theories there is a single pole in the tortoise coordinate, shifted slightly away from the pole in the classical solution. This is straightforward in the eternal black hole case, but for an evaporating black hole one must first introduce coordinates adapted to the evaporation process and then re-express the position of the pole in terms of these new coordinates.

In the following three chapters, we apply this framework in three models of 2D dilaton gravity. First, as a comparison sector, we reproduce a well known result for both the eternal and the evaporating black holes within the BPP model, and show that the symmetric ansatz together with the first-order perturbative expansion is enough to reproduce the correct evolution of the spacetime, from the initial spacetime, through the evaporating black hole region and finally to the black hole remanent spacetime which is what is left after the black hole fully evaporates. The most problematic step in this process is to find the end-point of evaporation, since it is well known that it is not analytical in $\hbar$, since it is proportional to $\sim \exp\left(-\frac{\alpha}{\hbar}\right)$. However, we showed that a good choice of coordinates mends this issue. We call these $(\delta, \hat{\mathrm{x}})$ coordinates the evaporation-adapted coordinates. Now that the end-point is found, continuously matching the solution across the $\hat{\mathrm{x}} = \hat{\mathrm{x}}_{\mathrm{E}}$ hypersurface is a straightforward process. Thus, we can also conclude the final state of black hole evolution as well as the end-state geometry.

We then applied the same framework to the DREH model and to the Riemannian sector of the DR5DCS model, successfully formulating both the eternal and evaporating black hole scenarios. Next, in Chapter 10, we take this analysis further and demonstrate that the framework accurately reproduces the Page curve in the DREH model. For the eternal black hole, the computation turns out to be straightforward once the appropriate pole of the tortoise coordinate is identified. In contrast, for the evaporating black hole solution, one must first determine the location of the island boundary across the ingoing shockwave and then extend that solution into the region where the evaporating black hole resides. Because the island also forms near the classical horizon, having a well-defined pole for the tortoise coordinate is crucial. We showed that the same qualitative behavior arises in the DREH model: the island hypersurface perfectly mirrors the apparent horizon across the quantum-corrected horizon, which is specified by the endpoint of evaporation, $\hat{\mathrm{x}} = \hat{\mathrm{x}}_{\mathrm{E}}$.

The second line of research in this dissertation focuses on how torsion affects the thermodynamic properties of gravitational systems. From the standpoint of coarse-grained entropy, numerous questions remain unresolved about the role of torsion in black hole thermodynamics. In certain models, torsion leads to a well-defined conserved quantity, often called torsion hair, whereas in others it effectively becomes a fundamental constant of spacetime. In the latter case, the first law of thermodynamics does not treat torsion as a thermodynamic variable, but rather as a fixed parameter. This already makes the study of torsion in classical gravity an important and active field of research.

Nonetheless, this is not the direction pursued in the present work. Here, torsion is of interest because its impact on the island formula (1.6), and hence on the Page curve, is presently unknown. The objective of this thesis is therefore to obtain well-defined solutions with torsion, so that in future studies one can analyze the fine-grained entropy in a gravitational system that includes torsion. A suitable framework featuring a well-known BTZ-like black hole solution with non-zero torsion is a five-dimensional Chern-Simons theory. However, for studying fine-grained entropy, it is crucial to have a well-defined torsional solution in two-dimensional spacetime. To this end, we preformed a dimensional reduction of the 5DCS theory over a three-sphere, yielding an effective 2D theory. The resulting model is a two-dimensional dilaton gravity theory that not only contains extra fields originating from the five-dimensional torsion, but also admits solutions with non-vanishing torsion in 2D.

To obtain these solutions, we examined various ways of coupling matter to gravity within the DR5DCS framework, choosing to treat matter as minimally coupled to the gravitational field. In this setup, we demonstrated that a real scalar field theory with a standard mass term yields a cosmological solution describing a spacetime that oscillates between big bang and big crunch events, with additional sudden curvature singularities appearing in between. Furthermore, we showed that when a local $U(1)$ symmetry is introduced—thereby generating an interaction between a massless complex scalar field and the electromagnetic field—the resulting geometry is again cosmological. Although the broader objective is to study the fine-grained entropy of cosmological spacetimes, this is not our present focus.

We found that pure electrodynamics alone does not support solutions with non-zero torsion. However, once the theory is restricted to its Riemannian sector, a charged black hole solution with a single horizon appears. This configuration is relevant for computing the Page curve and for analyzing how electric charge influences the fine-grained entropy in this model. Nevertheless, within this line of work our main interest lies in solutions featuring non-vanishing torsion. We also analyzed ideal fluid hydrodynamics and showed that, in this case, the metric function Λ remains undetermined, indicating a residual gauge symmetry. Yet, when an additional field—such as the electromagnetic field or a massless scalar field—is included, the metric is forced to be flat. Consequently, we arrive at a Minkowski vacuum solution endowed with non-zero torsion.

Finally, the most intriguing configurations appear when gravity is coupled to Dirac spinors. In this framework, a fermionic soliton-star solution arises. It exhibits a clearly defined phase transition. In the upper phase, the fermion density profile is distributed across the whole spacetime, the curvature remains finite, and no horizons are present. Thus, this describes a completely regular fermionic star. Moreover, one can impose appropriate junction conditions so that the star becomes a compact object smoothly matched to a generic BTZ-like vacuum solution, thereby behaving as a genuine star. Once the critical threshold is exceeded, however, the fermionic matter collapses and localizes at a specific point in spacetime. At that location, the fermion density diverges and in turn generates a curvature singularity, while at the same time a Killing horizon forms precisely there. This singular horizon is non-extremal, as it possesses a non-zero surface gravity, and is therefore unstable. Nonetheless, we anticipate that including quantum corrections will remove this singularity, while the fermions remain condensed in the lower phase.

Future work

In the first research program, a concrete method was developed for computing both eternal and evaporating black hole solutions, and this method was implemented in a physically relevant, dimensionally reduced model of Einstein–Hilbert gravity. Using this framework, the Page curve was obtained for both eternal and evaporating Schwarzschild black holes, which might suggest that this line of investigation is essentially complete. Nevertheless, there remain many important models for which the Page curve has not yet been derived, particularly in the context of evaporating black holes. Such models include, but are not limited to, Reissner–Nordström, Kerr–Newman, BTZ, and others.

A further direction is to use the new method to compute the Page curve via non-physical, ghost-like fields in a hybrid state—for example, a Hartle–Hawking state for physical fields combined with a Boulware state for non-physical ones. In this setup, the entanglement entropy shows Page-curve behavior without an island. These extra fields can render the effective central charge negative and remove the space-time singularity, which appears to drive the Page-curve-like evolution. It would be interesting to connect this approach to the standard Lewkowycz–Maldacena derivation of the island formula: Can these non-physical fields be interpreted within the gravitational path integral, and how do the resulting Page curves quantitatively compare? One may also further generalize the hybrid quantum state to entangled quantum states.

The second research program has a natural extension. Up to now, only the minimally-coupled matter theories have been analyzed, even though the general equations for non-minimally coupled fields are already available. It is therefore important to investigate the behavior of torsion in this broader framework as well. Existing results already suggest the presence of highly nontrivial phase transitions in the minimally coupled case, so one anticipates even richer dynamics when matter is coupled non-minimally.

Another possible line of inquiry is to incorporate quantum corrections and examine whether they can resolve the singular horizons that arise in fermionic star solutions. Finally, to construct more physically relevant models of 2D dilaton gravity with torsion, one should perform a dimensional reduction of the 4D Einstein–Cartan theory, employing the most general spherically symmetric ansatz for both the vielbein and the spin connection. Ultimately, the main goal of this research program is to determine how the island formula is modified in the presence of non-vanishing torsion.

References

[1] Ahmed Almheiri, Thomas Hartman, Juan Maldacena, Edgar Shaghoulian, and Amirhossein Tajdini. The entropy of hawking radiation. *Reviews of Modern Physics*, 93 (3), Jul 2021. ISSN 1539-0756. doi: 10.1103/revmodphys.93.035002. URL http://dx.doi.org/10.1103/RevModPhys.93.035002.

[2] A. Einstein. Die grundlage der allgemeinen relativitätstheorie. *Annalen der Physik*, 354(7):769–822, 1916. doi: https://doi.org/10.1002/andp.19163540702. URL https://onlinelibrary.wiley.com/doi/abs/10.1002/andp.19163540702.

[3] Karl Schwarzschild. On the gravitational field of a mass point according to Einstein's theory. *Sitzungsber. Preuss. Akad. Wiss. Berlin (Math. Phys.)*, 1916:189–196, 1916.

[4] Roy P. Kerr. Gravitational field of a spinning mass as an example of algebraically special metrics. *Phys. Rev. Lett.*, 11:237–238, Sep 1963. doi: 10.1103/PhysRevLett.11.237. URL https://link.aps.org/doi/10.1103/PhysRevLett.11.237.

[5] E T. Newman, R. Couch, K. Chinnapared, A. Exton, A. Prakash, and R. Torrence. Metric of a Rotating, Charged Mass. *J. Math. Phys.*, 6:918–919, 1965. doi: 10.1063/1.1704351.

[6] Larry Smarr. Mass formula for kerr black holes. *Phys. Rev. Lett.*, 30:71–73, Jan 1973. doi: 10.1103/PhysRevLett.30.71. URL https://link.aps.org/doi/10.1103/PhysRevLett.30.71.

[7] B. Carter. Black holes equilibrium states. In *Les Houches Summer School of Theoretical Physics: Black Holes*, pages 57–214, 1973.

[8] Herbert B Callen. *Thermodynamics and an introduction to thermostatistics; 2nd ed.* Wiley, New York, NY, 1985. URL https://cds.cern.ch/record/450289.

[9] S. W. Hawking. Black holes in general relativity. *Commun. Math. Phys.*, 25:152–166, 1972. doi: 10.1007/BF01877517.

[10] James M. Bardeen, B. Carter, and S. W. Hawking. The Four laws of black hole mechanics. *Commun. Math. Phys.*, 31:161–170, 1973. doi: 10.1007/BF01645742.

[11] S. W. Hawking. Black hole explosions. *Nature*, 248:30–31, 1974. doi: 10.1038/248030a0.

[12] S. W. Hawking. Particle Creation by Black Holes. *Commun. Math. Phys.*, 43:199–220, 1975. doi: 10.1007/BF02345020. [Erratum: Commun.Math.Phys. 46, 206 (1976)].

[13] S. W. Hawking. Black holes and thermodynamics. *Phys. Rev. D*, 13:191–197, Jan 1976. doi: 10.1103/PhysRevD.13.191. URL https://link.aps.org/doi/10.1103/PhysRevD.13.191.

[14] Jacob Bekenstein. Black holes and the second law. *Lettere al Nuovo Cimento (1971-1985)*, 4:737–740, 1972.

[15] Jacob D. Bekenstein. Black holes and entropy. *Phys. Rev. D*, 7:2333–2346, Apr 1973. doi: 10.1103/PhysRevD.7.2333. URL https://link.aps.org/doi/10.1103/PhysRevD.7.2333.

[16] S. W. Hawking. Breakdown of predictability in gravitational collapse. *Phys. Rev. D*, 14: 2460–2473, Nov 1976. doi: 10.1103/PhysRevD.14.2460. URL https://link.aps.org/doi/10.1103/PhysRevD.14.2460.

[17] Don N. Page. Information in black hole radiation. *Physical Review Letters*, 71(23): 3743–3746, Dec 1993. ISSN 0031-9007. doi: 10.1103/physrevlett.71.3743. URL http://dx.doi.org/10.1103/PhysRevLett.71.3743.

[18] Don N Page. Time dependence of hawking radiation entropy. *Journal of Cosmology and Astroparticle Physics*, 2013(09):028–028, Sep 2013. ISSN 1475-7516. doi: 10.1088/1475-7516/2013/09/028. URL http://dx.doi.org/10.1088/1475-7516/2013/09/028.

[19] Curtis G. Callan, Steven B. Giddings, Jeffrey A. Harvey, and Andrew Strominger. Evanescent black holes. *Physical Review D*, 45(4):R1005–R1009, Feb 1992. ISSN 0556-2821. doi: 10.1103/physrevd.45.r1005. URL http://dx.doi.org/10.1103/PhysRevD.45.R1005.

[20] R. Jackiw. Lower Dimensional Gravity. *Nucl. Phys. B*, 252:343–356, 1985. doi: 10.1016/0550-3213(85)90448-1.

[21] C. Teitelboim. Gravitation and Hamiltonian Structure in Two Space-Time Dimensions. *Phys. Lett. B*, 126:41–45, 1983. doi: 10.1016/0370-2693(83)90012-6.

[22] Alexander M. Polyakov. Quantum geometry of bosonic strings. *Physics Letters B*, 103: 207–210, 1981.

[23] Jorge G. Russo, Leonard Susskind, and Lárus Thorlacius. End point of hawking radiation. *Phys. Rev. D*, 46:3444–3449, Oct 1992. doi: 10.1103/PhysRevD.46.3444. URL https://link.aps.org/doi/10.1103/PhysRevD.46.3444.

[24] Jorge G. Russo, Leonard Susskind, and Larus Thorlacius. Cosmic censorship in two-dimensional gravity. *Phys. Rev. D*, 47:533–539, Jan 1993. doi: 10.1103/PhysRevD.47.533. URL https://link.aps.org/doi/10.1103/PhysRevD.47.533.

[25] Sukanta Bose, Leonard Parker, and Yoav Peleg. Semi-infinite throat as the end-state geometry of two-dimensional black hole evaporation. *Physical Review D*, 52(6):3512–3517, Sep 1995. ISSN 0556-2821. doi: 10.1103/physrevd.52.3512. URL http://dx.doi.org/10.1103/PhysRevD.52.3512.

[26] Thomas M. Fiola, John Preskill, Andrew Strominger, and Sandip P. Trivedi. Black hole thermodynamics and information loss in two dimensions. *Physical Review D*, 50 (6):3987–4014, Sep 1994. ISSN 0556-2821. doi: 10.1103/physrevd.50.3987. URL http://dx.doi.org/10.1103/PhysRevD.50.3987.

[27] Gerard 't Hooft. Dimensional reduction in quantum gravity. *Conf. Proc. C*, 930308: 284–296, 1993.

[28] Leonard Susskind. The world as a hologram. *Journal of Mathematical Physics*, 36(11): 6377–6396, Nov 1995. ISSN 1089-7658. doi: 10.1063/1.531249. URL http://dx.doi.org/10.1063/1.531249.

[29] Juan Martin Maldacena. The Large N limit of superconformal field theories and supergravity. *Adv. Theor. Math. Phys.*, 2:231–252, 1998. doi: 10.1023/A:1026654312961.

[30] Shinsei Ryu and Tadashi Takayanagi. Holographic derivation of entanglement entropy from the anti–de sitter space/conformal field theory correspondence. *Phys. Rev. Lett.*, 96:181602, May 2006. doi: 10.1103/PhysRevLett.96.181602. URL https://link.aps.org/doi/10.1103/PhysRevLett.96.181602.

[31] Veronika E. Hubeny, Mukund Rangamani, and Tadashi Takayanagi. A covariant holographic entanglement entropy proposal. *Journal of High Energy Physics*, 2007:062–062, 2007.

[32] G. W. Gibbons and S. W. Hawking. Cosmological event horizons, thermodynamics, and particle creation. *Phys. Rev. D*, 15:2738–2751, May 1977. doi: 10.1103/PhysRevD.15.2738. URL https://link.aps.org/doi/10.1103/PhysRevD.15.2738.

[33] Aitor Lewkowycz and Juan Martin Maldacena. Generalized gravitational entropy. *Journal of High Energy Physics*, 2013:1–29, 2013.

[34] Thomas Faulkner, Aitor Lewkowycz, and Juan Maldacena. Quantum corrections to holographic entanglement entropy. *Journal of High Energy Physics*, 2013(11), Nov 2013. ISSN 1029-8479. doi: 10.1007/jhep11(2013)074. URL http://dx.doi.org/10.1007/JHEP11(2013)074.

[35] Ahmed Almheiri, Raghu Mahajan, Juan Maldacena, and Ying Zhao. The page curve of hawking radiation from semiclassical geometry. *Journal of High Energy Physics*, 2020(3), Mar 2020. ISSN 1029-8479. doi: 10.1007/jhep03(2020)149. URL http://dx.doi.org/10.1007/JHEP03(2020)149.

[36] Ahmed Almheiri, Netta Engelhardt, Donald Marolf, and Henry Maxfield. The entropy of bulk quantum fields and the entanglement wedge of an evaporating black hole. *Journal of High Energy Physics*, 2019(12), Dec 2019. ISSN 1029-8479. doi: 10.1007/jhep12(2019)063. URL http://dx.doi.org/10.1007/JHEP12(2019)063.

[37] Geoffrey Penington. Entanglement wedge reconstruction and the information paradox, 2020.

[38] Ahmed Almheiri, Thomas Hartman, Juan Maldacena, Edgar Shaghoulian, and Amirhossein Tajdini. Replica wormholes and the entropy of hawking radiation. *Journal of High Energy Physics*, 2020(5), May 2020. ISSN 1029-8479. doi: 10.1007/jhep05(2020)013. URL http://dx.doi.org/10.1007/JHEP05(2020)013.

[39] Ahmed Almheiri, Raghu Mahajan, and Juan Maldacena. Islands outside the horizon, 2019.

[40] Thomas Hartman, Edgar Shaghoulian, and Andrew Strominger. Islands in asymptotically flat 2d gravity. *Journal of High Energy Physics*, 2020(7), Jul 2020. ISSN 1029-8479. doi: 10.1007/jhep07(2020)022. URL http://dx.doi.org/10.1007/JHEP07(2020)022.

[41] Xuanhua Wang, Ran Li, and Jin Wang. Page curves for a family of exactly solvable evaporating black holes. *Physical Review D*, 103(12), Jun 2021. ISSN 2470-0029. doi: 10.1103/physrevd.103.126026. URL http://dx.doi.org/10.1103/PhysRevD.103.126026.

[42] Stefan Đorđević, Aleksandra Gočanin, Dragoljub Gočanin, and Voja Radovanović. Page curve for an eternal schwarzschild black hole in a dimensionally reduced model of dilaton gravity. *Phys. Rev. D*, 106:105015, Nov 2022. doi: 10.1103/PhysRevD.106.105015. URL https://link.aps.org/doi/10.1103/PhysRevD.106.105015.

[43] Stefan Đorđević and Voja Radovanović. Page curve for an evaporating schwarzschild black hole in dimensionally reduced model of dilaton gravity. *Phys. Rev. D*, 113:105020, May 2026. doi: 10.1103/nc2z-hx6s. URL https://link.aps.org/doi/10.1103/nc2z-hx6s.

[44] Geoff Penington, Stephen H. Shenker, Douglas Stanford, and Zhenbin Yang. Replica wormholes and the black hole interior, 2020. URL https://arxiv.org/abs/1911.11977.

[45] Friðrik Freyr Gautason, Lukas Schneiderbauer, Watse Sybesma, and Lárus Thorlacius. Page Curve for an Evaporating Black Hole. *JHEP*, 05:091, 2020. doi: 10.1007/JHEP05(2020)091.

[46] Ahmed Almheiri, Raghu Mahajan, and Juan Maldacena. Islands outside the horizon, 2023. URL https://arxiv.org/abs/1910.11077.

[47] Ahmed Almheiri, Netta Engelhardt, Donald Marolf, and Henry Maxfield. The entropy of bulk quantum fields and the entanglement wedge of an evaporating black hole. *Journal of High Energy Physics*, 2019(12), December 2019. ISSN 1029-8479. doi: 10.1007/jhep12(2019)063. URL http://dx.doi.org/10.1007/JHEP12(2019)063.

[48] Hong Zhe Chen, Zachary Fisher, Juan Hernandez, Robert C. Myers, and Shan-Ming Ruan. Information flow in black hole evaporation. *Journal of High Energy Physics*, 2020(3), March 2020. ISSN 1029-8479. doi: 10.1007/jhep03(2020)152. URL http://dx.doi.org/10.1007/JHEP03(2020)152.

[49] Yiming Chen. Pulling Out the Island with Modular Flow. *JHEP*, 03:033, 2020. doi: 10.1007/JHEP03(2020)033.

[50] Chris Akers, Netta Engelhardt, Geoff Penington, and Mykhaylo Usatyuk. Quantum maximin surfaces, 2020. URL https://arxiv.org/abs/1912.02799.

[51] Hong Liu and Shreya Vardhan. A dynamical mechanism for the Page curve from quantum chaos. *JHEP*, 03:088, 2021. doi: 10.1007/JHEP03(2021)088.

[52] Donald Marolf and Henry Maxfield. Transcending the ensemble: baby universes, spacetime wormholes, and the order and disorder of black hole information. *Journal of High Energy Physics*, 2020(8), August 2020. ISSN 1029-8479. doi: 10.1007/jhep08(2020)044. URL http://dx.doi.org/10.1007/JHEP08(2020)044.

[53] Vijay Balasubramanian, Arjun Kar, Onkar Parrikar, Gábor Sárosi, and Tomonori Ugajin. Geometric secret sharing in a model of Hawking radiation. *JHEP*, 01:177, 2021. doi: 10.1007/JHEP01(2021)177.

[54] Aranya Bhattacharya. Multipartite purification, multiboundary wormholes, and islands in AdS_3/CFT_2. *Phys. Rev. D*, 102(4):046013, 2020. doi: 10.1103/PhysRevD.102.046013.

[55] Kanato Goto, Thomas Hartman, and Amirhossein Tajdini. Replica wormholes for an evaporating 2d black hole. *Journal of High Energy Physics*, 2021(4), April 2021. ISSN 1029-8479. doi: 10.1007/jhep04(2021)289. URL http://dx.doi.org/10.1007/JHEP04(2021)289.

[56] Herman Verlinde. Er = epr revisited: On the entropy of an einstein-rosen bridge, 2020. URL https://arxiv.org/abs/2003.13117.

[57] Takanori Anegawa and Norihiro Iizuka. Notes on islands in asymptotically flat 2d dilaton black holes. *Journal of High Energy Physics*, 2020(7), Jul 2020. ISSN 1029-8479. doi: 10.1007/jhep07(2020)036. URL http://dx.doi.org/10.1007/JHEP07(2020)036.

[58] Friðrik Freyr Gautason, Lukas Schneiderbauer, Watse Sybesma, and Lárus Thorlacius. Page curve for an evaporating black hole. *Journal of High Energy Physics*, 2020(5), May 2020. ISSN 1029-8479. doi: 10.1007/jhep05(2020)091. URL http://dx.doi.org/10.1007/JHEP05(2020)091.

[59] Koji Hashimoto, Norihiro Iizuka, and Yoshinori Matsuo. Islands in schwarzschild black holes. *Journal of High Energy Physics*, 2020(6), Jun 2020. ISSN 1029-8479. doi: 10.1007/jhep06(2020)085. URL http://dx.doi.org/10.1007/JHEP06(2020)085.

[60] Ming-Hui Yu and Xian-Hui Ge. Islands and Page curves in charged dilaton black holes. *Eur. Phys. J. C*, 82(1):14, 2022. doi: 10.1140/epjc/s10052-021-09932-w.

[61] Xuanhua Wang, Ran Li, and Jin Wang. Islands and Page curves of Reissner-Nordström black holes. *JHEP*, 04:103, 2021. doi: 10.1007/JHEP04(2021)103.

[62] Ahmed Almheiri, Raghu Mahajan, and Jorge E. Santos. Entanglement islands in higher dimensions. *SciPost Phys.*, 9(1):001, 2020. doi: 10.21468/SciPostPhys.9.1.001.

[63] Chen-Wei Tong, Dong-Hui Du, and Jia-Rui Sun. Island of Reissner-Nordström anti–de Sitter black holes in the large D limit. *Phys. Rev. D*, 109(10):104053, 2024. doi: 10.1103/PhysRevD.109.104053.

[64] Liqiang Wang and Ran Li. Entanglement islands and the Page curve of Hawking radiation for rotating Kerr black holes. *Phys. Rev. D*, 110(6):066012, 2024. doi: 10.1103/PhysRevD.110.066012.

[65] D. S. Ageev, I. Ya. Aref'eva, A. I. Belokon, A. V. Ermakov, V. V. Pushkarev, and T. A. Rusalev. Infrared regularization and finite size dynamics of entanglement entropy in Schwarzschild black hole. *Phys. Rev. D*, 108(4):046005, 2023. doi: 10.1103/PhysRevD.108.046005.

[66] Chih-Hung Wu and Jiuci Xu. Islands in non-minimal dilaton gravity: exploring effective theories for black hole evaporation. *JHEP*, 10:094, 2023. doi: 10.1007/JHEP10(2023)094.

[67] D. S. Ageev, I. Ya. Aref'eva, A. I. Belokon, V. V. Pushkarev, and T. A. Rusalev. Entanglement entropy in de Sitter: no pure states for conformal matter. *JHEP*, 05:308, 2024. doi: 10.1007/JHEP05(2024)308.

[68] Aleksandr I. Belokon. Finite entangling regions and information paradox in charged black holes. *Theor. Math. Phys.*, 222(1):154–169, 2025. doi: 10.1134/S004057792501012X.

[69] Gopal Yadav and Nitin Joshi. Cosmological and black hole islands in multi-event horizon spacetimes. *Phys. Rev. D*, 107(2):026009, 2023. doi: 10.1103/PhysRevD.107.026009.

[70] Aron C Wall. Maximin surfaces, and the strong subadditivity of the covariant holographic entanglement entropy. *Classical and Quantum Gravity*, 31(22):225007, Nov 2014. ISSN 1361-6382. doi: 10.1088/0264-9381/31/22/225007. URL http://dx.doi.org/10.1088/0264-9381/31/22/225007.

[71] Bartłomiej Czech, Joanna L Karczmarek, Fernando Nogueira, and Mark Van Raamsdonk. The gravity dual of a density matrix. *Classical and Quantum Gravity*, 29(15):155009, Jul 2012. ISSN 1361-6382. doi: 10.1088/0264-9381/29/15/155009. URL http://dx.doi.org/10.1088/0264-9381/29/15/155009.

[72] Matthew Headrick, Veronika E. Hubeny, Albion Lawrence, and Mukund Rangamani. Causality and holographic entanglement entropy. *Journal of High Energy Physics*, 2014 (12), Dec 2014. ISSN 1029-8479. doi: 10.1007/jhep12(2014)162. URL http://dx.doi.org/10.1007/JHEP12(2014)162.

[73] Shiin-Shen Chern and James Simons. Characteristic forms and geometric invariants. *Annals Math.*, 99:48–69, 1974. doi: 10.2307/1971013.

[74] S. Deser, R. Jackiw, and S. Templeton. Topologically massive gauge theories. *Annals of Physics*, 281:409–449, 04 2000. doi: 10.1006/aphy.2000.6013.

[75] Edward Witten. Quantum Field Theory and the Jones Polynomial. *Commun. Math. Phys.*, 121:351–399, 1989. doi: 10.1007/BF01217730.

[76] A. Achucarro and P. K. Townsend. A Chern-Simons Action for Three-Dimensional anti-De Sitter Supergravity Theories. *Phys. Lett. B*, 180:89, 1986. doi: 10.1016/0370-2693(86)90140-1.

[77] Edward Witten. (2+1)-Dimensional Gravity as an Exactly Soluble System. *Nucl. Phys. B*, 311:46, 1988. doi: 10.1016/0550-3213(88)90143-5.

[78] Máximo Bañados, Claudio Teitelboim, and Jorge Zanelli. Black hole in three-dimensional spacetime. *Physical Review Letters*, 69(13):1849–1851, September 1992. ISSN 0031-9007. doi: 10.1103/physrevlett.69.1849. URL http://dx.doi.org/10.1103/PhysRevLett.69.1849.

[79] Ali H. Chamseddine. Topological Gauge Theory of Gravity in Five-dimensions and All Odd Dimensions. *Phys. Lett. B*, 233:291–294, 1989. doi: 10.1016/0370-2693(89)91312-9.

[80] Andrew Strominger and Cumrun Vafa. Microscopic origin of the Bekenstein-Hawking entropy. *Phys. Lett. B*, 379:99–104, 1996. doi: 10.1016/0370-2693(96)00345-0.

[81] Milutin Blagojević. *Gravitation and Gauge Symmetries*. CRC Press, Boca Raton, 2002. ISBN 978-0-429-18716-2. doi: 10.1201/9781420034264.

[82] D. Lovelock. The Einstein tensor and its generalizations. *J. Math. Phys.*, 12:498–501, 1971. doi: 10.1063/1.1665613.

[83] Jorge Zanelli. Chern–simons forms in gravitation theories. *Classical and Quantum Gravity*, 29(13):133001, 2012. doi: 10.1088/0264-9381/29/13/133001.

[84] J. David Brown and Marc Henneaux. Central charges in the canonical realization of asymptotic symmetries: An example from three-dimensional gravity. *Communications in Mathematical Physics*, 104(2):207–226, 1986. doi: 10.1007/BF01211153.

[85] Olivera Mišković and Rodrigo Olea. On boundary conditions in three-dimensional AdS gravity. *Physics Letters B*, 640(2):101–107, 2006. doi: 10.1016/j.physletb.2006.07.045.

[86] Rodrigo Aros. Charges and the boundary in chern-simons gravity. *Physical Review D*, 73 (4), 2006. doi: 10.1103/physrevd.73.044023.

[87] Karim Ait Moussa, Gérard Clément, Hakim Guennoune, and Cédric Leygnac. Three-dimensional chern-simons black holes. *Physical Review D*, 78(6), 2008. doi: 10.1103/physrevd.78.064065.

[88] Luis Avilés, Patrick Concha, Javier Matulich, Evelyn Rodríguez, and David Tempo. Maxwell chern-simons gravity in 3d: Thermodynamics of cosmological solutions and black holes with torsion. *arXiv preprint*, 2025. doi: 10.48550/arxiv.2510.25559.

[89] Laura Andrianopoli, Gaston Giribet, Darío López Díaz, and Olivera Miskovic. Black holes with topological charges in Chern-Simons AdS_5 supergravity. *JHEP*, 11:123, 2021. doi: 10.1007/JHEP11(2021)123.

[90] Kazunori Akiyama et al. First M87 Event Horizon Telescope Results. I. The Shadow of the Supermassive Black Hole. *Astrophys. J. Lett.*, 875(1):L1, 2019. doi: 10.3847/2041-8213/ab0ec7.

[91] B. P. Abbott et al. Observation of gravitational waves from a binary black hole merger. *Phys. Rev. Lett.*, 116:061102, Feb 2016. doi: 10.1103/PhysRevLett.116.061102. URL https://link.aps.org/doi/10.1103/PhysRevLett.116.061102.

[92] John D. Barrow. Sudden future singularities. *Classical and Quantum Gravity*, 21(3): L79–L82, 2004. doi: 10.1088/0264-9381/21/3/L01.

[93] Jaume de Haro, Shin'ichi Nojiri, S. D. Odintsov, V. K. Oikonomou, and Supriya Pan. Finite-time cosmological singularities and the possible fate of the universe. *Physics Reports*, 1034:1–114, 2023. doi: 10.1016/j.physrep.2023.09.003.

[94] TH. KALUZA. On the unification problem in physics. *International Journal of Modern Physics D*, 27(14):1870001, October 2018. ISSN 1793-6594. doi: 10.1142/s0218271818700017. URL http://dx.doi.org/10.1142/S0218271818700017.

[95] Oskar Klein. Quantentheorie und fünfdimensionale relativitätstheorie. *Zeitschrift für Physik*, 37(12):895–906, 1926. doi: 10.1007/bf01397481. URL https://doi.org.

[96] David G. Boulware and S. Deser. String-generated gravity models. *Phys. Rev. Lett.*, 55: 2656–2660, Dec 1985. doi: 10.1103/PhysRevLett.55.2656. URL https://link.aps.org/doi/10.1103/PhysRevLett.55.2656.

[97] D. Lovelock. The Einstein tensor and its generalizations. *J. Math. Phys.*, 12:498–501, 1971. doi: 10.1063/1.1665613.

[98] Maja Buric, Voja Radovanovic, and Aleksandar R. Mikovic. One loop correction for Schwarzschild black hole via 2-D dilaton gravity. *Phys. Rev. D*, 59:084002, 1999. doi: 10.1103/PhysRevD.59.084002.

[99] Dušan Đorđević and Dragoljub Gočanin. Noncommutative $d = 5$ chern–simons gravity: Kaluza–klein reduction and chiral gravitational anomaly. *The European Physical Journal C*, 82(8), August 2022. ISSN 1434-6052. doi: 10.1140/epjc/s10052-022-10657-7. URL http://dx.doi.org/10.1140/epjc/s10052-022-10657-7.

[100] Maximo Banados, Claudio Teitelboim, and Jorge Zanelli. Dimensionally continued black holes. *Phys. Rev. D*, 49:975–986, 1994. doi: 10.1103/PhysRevD.49.975.

[101] Fabrizio Canfora, Alex Giacomini, and Ricardo Troncoso. Black holes, parallelizable horizons and half-BPS states for the Einstein-Gauss-Bonnet theory in five dimensions. *Phys. Rev. D*, 77:024002, 2008. doi: 10.1103/PhysRevD.77.024002.

[102] Branislav Cvetković and Dejan Simić. A black hole with torsion in 5D Lovelock gravity. *Class. Quant. Grav.*, 35(5):055005, 2018. doi: 10.1088/1361-6382/aaa3a7.

[103] Yvonne Kosmann. Dérivées de lie des spineurs. *Annali di Matematica Pura ed Applicata*, 91:317–395, 1972.

[104] Tomas Ortin. A Note on Lie-Lorentz derivatives. *Class. Quant. Grav.*, 19:L143–L150, 2002. doi: 10.1088/0264-9381/19/15/101.

[105] A. A. Belavin, A. M. Polyakov, and A. B. Zamolodchikov. Infinite conformal symmetry in two-dimensional quantum field theory. *Nuclear Physics B*, 241(2):333–380, 1984. doi: 10.1016/0550-3213(84)90052-X.

[106] Sean M. Carroll. *Spacetime and Geometry*. Cambridge University Press, 7 2019. ISBN 978-0-8053-8732-2, 978-1-108-48839-6, 978-1-108-77555-7.

[107] J. B. Hartle and S. W. Hawking. Path Integral Derivation of Black Hole Radiance. *Phys. Rev. D*, 13:2188–2203, 1976. doi: 10.1103/PhysRevD.13.2188.

[108] Yohan Potaux, Sergey N. Solodukhin, and Debajyoti Sarkar. Spacetime structure, asymptotic radiation, and information recovery for a quantum hybrid state. *Physical Review Letters*, 130(26), June 2023. ISSN 1079-7114. doi: 10.1103/physrevlett.130.261501. URL http://dx.doi.org/10.1103/PhysRevLett.130.261501.

[109] Yohan Potaux, Debajyoti Sarkar, and Sergey N. Solodukhin. Hybrid quantum states in 2d dilaton gravity. *Physical Review D*, 108(12), December 2023. ISSN 2470-0029. doi: 10.1103/physrevd.108.125012. URL http://dx.doi.org/10.1103/PhysRevD.108.125012.

[110] Yohan Potaux, Debajyoti Sarkar, and Sergey N. Solodukhin. Islands for black holes in a hybrid quantum state, 2024. URL https://arxiv.org/abs/2411.09574.

[111] Stefan Đorđević and Voja Radovanović. Collapse scenario and final state of evaporation for schwarzschild black hole in dimensionally reduced model of dilaton gravity. *Phys. Rev. D*, 113:105010, May 2026. doi: 10.1103/q2n7-qnc1. URL https://link.aps.org/doi/10.1103/q2n7-qnc1.

[112] A. Fabbri, S. Farese, J. Navarro-Salas, G. J. Olmo, and H. Sanchis-Alepuz. Semiclassical zero-temperature corrections to schwarzschild spacetime and holography. *Physical Review D*, 73(10), May 2006. ISSN 1550-2368. doi: 10.1103/physrevd.73.104023. URL http://dx.doi.org/10.1103/PhysRevD.73.104023.

[113] Pei-Ming Ho, Yoshinori Matsuo, and Yuki Yokokura. Analytic description of semiclassical black-hole geometry. *Physical Review D*, 102(2), July 2020. ISSN 2470-0029. doi: 10.1103/physrevd.102.024090. URL http://dx.doi.org/10.1103/PhysRevD.102.024090.

[114] Adrián del Río, F. Javier Marañón-González, and José Navarro-Salas. Singularity resolution in spherically reduced 2D semiclassical gravity with negative central charge. *Phys. Rev. D*, 111(4):045025, 2025. doi: 10.1103/PhysRevD.111.045025.

[115] Maja Burić and Voja Radovanović. Quantum corrections for an (anti)evaporating black hole. *Physical Review D*, 63(4), Jan 2001. ISSN 1089-4918. doi: 10.1103/physrevd.63.044020. URL http://dx.doi.org/10.1103/PhysRevD.63.044020.

[116] Jose P. S. Lemos. Thermodynamics of the two-dimensional black hole in the Teitelboim-Jackiw theory. *Phys. Rev. D*, 54:6206–6212, 1996. doi: 10.1103/PhysRevD.54.6206.

[117] Juan Crisostomo, Ricardo Troncoso, and Jorge Zanelli. Black hole scan. *Phys. Rev. D*, 62:084013, 2000. doi: 10.1103/PhysRevD.62.084013.

[118] Máximo Bañados, Marc Henneaux, Claudio Teitelboim, and Jorge Zanelli. Geometry of the 2+1 black hole. *Phys. Rev. D*, 48:1506–1525, Aug 1993. doi: 10.1103/PhysRevD.48.1506. URL https://link.aps.org/doi/10.1103/PhysRevD.48.1506.

[119] M. Banados, A. Schwimmer, and S. Theisen. Chern-Simons gravity and holographic anomalies. *JHEP*, 05:039, 2004. doi: 10.1088/1126-6708/2004/05/039.

[120] Stephen A. Fulling. Nonuniqueness of canonical field quantization in riemannian space-time. *Physical Review D*, 7:2850–2862, 1973.

[121] P Davies. Scalar production in schwarzschild and rindler metrics. *Journal of Physics A: Mathematical and General*, 8:609, 01 2001. doi: 10.1088/0305-4470/8/4/022.

[122] W. G. Unruh. Notes on black-hole evaporation. *Physical Review D*, 14:870–892, 1976.

[123] C. Holzhey. Ph.d. thesis. *unpublished*, 1993.

[124] Xi Dong, Aitor Lewkowycz, and Mukund Rangamani. Deriving covariant holographic entanglement. *Journal of High Energy Physics*, 2016(11), Nov 2016. ISSN 1029-8479. doi: 10.1007/jhep11(2016)028. URL http://dx.doi.org/10.1007/JHEP11(2016)028.

[125] Geoff Penington, Stephen H. Shenker, Douglas Stanford, and Zhenbin Yang. Replica wormholes and the black hole interior, 2020.

[126] Xi Dong and Aitor Lewkowycz. Entropy, extremality, euclidean variations, and the equations of motion. *Journal of High Energy Physics*, 2018(1), Jan 2018. ISSN 1029-8479. doi: 10.1007/jhep01(2018)081. URL http://dx.doi.org/10.1007/JHEP01(2018)081.

[127] J. Maldacena and L. Susskind. Cool horizons for entangled black holes. *Fortschritte der Physik*, 61(9):781–811, Aug 2013. ISSN 0015-8208. doi: 10.1002/prop.201300020. URL http://dx.doi.org/10.1002/prop.201300020.

[128] Ping Gao, Daniel Louis Jafferis, and Aron C. Wall. Traversable wormholes via a double trace deformation. *Journal of High Energy Physics*, 2017(12), Dec 2017. ISSN 1029-8479. doi: 10.1007/jhep12(2017)151. URL http://dx.doi.org/10.1007/JHEP12(2017)151.

[129] Daniel L. Jafferis, Aitor Lewkowycz, Juan Maldacena, and S. Josephine Suh. Relative entropy equals bulk relative entropy. *Journal of High Energy Physics*, 2016(6), Jun 2016. ISSN 1029-8479. doi: 10.1007/jhep06(2016)004. URL http://dx.doi.org/10.1007/JHEP06(2016)004.

[130] Xi Dong, Daniel Harlow, and Aron C. Wall. Reconstruction of bulk operators within the entanglement wedge in gauge-gravity duality. *Physical Review Letters*, 117(2), Jul 2016. ISSN 1079-7114. doi: 10.1103/physrevlett.117.021601. URL http://dx.doi.org/10.1103/PhysRevLett.117.021601.

[131] Ahmed Almheiri, Xi Dong, and Daniel Harlow. Bulk locality and quantum error correction in ads/cft. *Journal of High Energy Physics*, 2015(4), Apr 2015. ISSN 1029-8479. doi: 10.1007/jhep04(2015)163. URL http://dx.doi.org/10.1007/JHEP04(2015)163.

[132] Masanori Ohya and Dénes Petz. *Quantum Entropy and Its Use*. Springer-Verlag, Berlin, Heidelberg, 2nd edition, 2004. ISBN 978-3-540-20806-8. doi: 10.1007/1-4020-4876-9_6.

[133] Jordan Cotler, Patrick Hayden, Geoffrey Penington, Grant Salton, Brian Swingle, and Michael Walter. Entanglement wedge reconstruction via universal recovery channels. *Physical Review X*, 9(3), Jul 2019. ISSN 2160-3308. doi: 10.1103/physrevx.9.031011. URL http://dx.doi.org/10.1103/PhysRevX.9.031011.

[134] Adam R. Brown, Hrant Gharibyan, Geoff Penington, and Leonard Susskind. The python's lunch: geometric obstructions to decoding hawking radiation, 2019.

[135] Isaac Kim, Eugene Tang, and John Preskill. The ghost in the radiation: robust encodings of the black hole interior. *Journal of High Energy Physics*, 2020(6), Jun 2020. ISSN 1029-8479. doi: 10.1007/jhep06(2020)031. URL http://dx.doi.org/10.1007/JHEP06(2020)031.

[136] C. J. Wheeler, edited by DeWitt and B. DeWitt, editors. *Relativité, Groupes et Topologie: Proceedings, Ecole d'été de Physique Théorique, Session XIII, Les Houches, France, Jul 1 - Aug 24, 1963*, New York, 1964. Gordon and Breach.

APPENDICES

Appendix A

Riemann-Cartan geometry and spinors

The key distinction between Riemannian and Riemann-Cartan geometries lies in the presence of a non-vanishing torsion in the latter case. Then, the geometry is determined by two fundamental fields: vielbeins e^a and spin-connection ω^{ab}. Vielbeins $e^a = e^a{}_\mu \mathrm{d}x^\mu$ represent a specific basis in a 1-form space. They also satisfy the condition of orthogonality, so that the metric has a following form:

$$g = \eta_{ab} e^a \otimes e^b. \tag{A.1}$$

In this basis, the components of the metric are η_{ab}, that is, a flat Minkowski metric. For this reason, the frame defined by e^a is called local Lorentz frame, and the Latin indices $a, b, c, ...$ $(\hat{0}, \hat{1}, \hat{2}, ...)$ are called the local Lorentz indices. On the other hand, global space-time indices are denoted by Greek letters $\mu, \nu, \rho, ...$ $(0, 1, 2, ...)$. We adopt the $(-, +)$ signature, and adhere to the convention $\varepsilon^{\hat{0}\hat{1}} = +1$ for the Levi-Civita tensor. The vector field space is spanned by inverse vielbein $e_a = e_a{}^\mu \partial_\mu$, so that the relations of biorthogonality are satisfied:

$$e^a{}_\mu e_b{}^\mu = \delta^a{}_b, \qquad e^a{}_\mu e_a{}^\nu = \delta_\mu{}^\nu. \tag{A.2}$$

The construction of a Riemannian space equipped with the Levi-Civita connection does not allow for the non-vanishing torsion. Riemann-Cartan spaces are equipped with spin-connection which allows for non-zero torsion. For the purpose of defining parallel transport of different objects on a manifold, a Riemann-Cartan covariant derivative is defined by:

$$\mathrm{D} = \mathrm{d} + \frac{1}{2}\omega^{ab}\Sigma_{ab} \equiv \tilde{\nabla}_\mu \mathrm{d}x^\mu, \tag{A.3}$$

where d represents the exterior derivative, and Σ_{ab} denotes the local Lorentz generators within a specific representation of the Lorentz group, under which the corresponding object transforms. For example, in a case of a vector field, generators are given by:

$$(\Sigma_{ab})^c{}_d = \delta_a{}^c \eta_{bd} - \delta_b{}^c \eta_{ad}. \tag{A.4}$$

Using (A.4) the action of the Riemann-Cartan covariant derivative on a vector field $A = A^a e_a$is given by:

$$\mathrm{D}A^a \equiv \tilde{\nabla}_\mu A^a \mathrm{d}x^\mu = \left(\partial_\mu A^a + \omega^a{}_{b\mu} A^b\right) \mathrm{d}x^\mu. \tag{A.5}$$

On the other hand, the Riemann-Cartan connection coefficients $\tilde{\Gamma}^\rho_{\nu\mu}$ are defined as usual:

$$\tilde{\nabla}_\mu A^\nu = \partial_\mu A^\nu + \tilde{\Gamma}^\nu_{\rho\mu} A^\rho. \tag{A.6}$$

Demaning that these two equations (A.5) and (A.6) are consistent yields the metricity condition:

$$\tilde{\nabla}_\mu e^a{}_\nu \equiv \partial_\mu e^a{}_\nu + \omega^{ab}{}_\mu e_{b\nu} - \tilde{\Gamma}^\rho_{\nu\mu} e^a{}_\rho = 0. \tag{A.7}$$

After preforming antisymmetrization with respect to μ and ν indices and solving for $\omega^{ab}{}_\mu$ results into:

$$\omega^{ab}{}_\mu = \Delta^{ab}{}_\mu + \mathrm{K}^{ab}{}_\mu, \tag{A.8}$$

where $\mathrm{K}^{ab}{}_\mu$ is contorsion, while $\Delta^{ab}{}_\mu$ is called Ricci coefficient of rotation. They are given by:

$$\mathrm{K}_{\mu\rho\nu} = -\frac{1}{2}\left(T_{\mu\rho\nu} - T_{\nu\mu\rho} + T_{\rho\nu\mu}\right), \tag{A.9}$$

$$\Delta_{abc} = \frac{1}{2}\left(c_{abc} - c_{cab} + c_{bca}\right), \tag{A.10}$$

where $T^\mu_{\ \nu\rho} = \tilde{\Gamma}^\mu_{\rho\nu} - \tilde{\Gamma}^\mu_{\nu\rho}$ and $c^a{}_{\mu\nu} = \partial_\mu e^a{}_\nu - \partial_\nu e^a{}_\mu$. Since $T^\mu_{\ \nu\rho}$ is the antisymmetric part of the connection coefficients, $\tilde{\Gamma}^\rho_{\mu\nu}$ are expressed as:

$$\tilde{\Gamma}^\rho_{\mu\nu} = \Gamma^\rho_{\mu\nu} + \mathrm{K}^\rho{}_{\mu\nu}, \tag{A.11}$$

where $\Gamma^\rho_{\mu\nu}$ are the Christoffel symbols. Then the decomposition of the Riemann-Cartan covariant derivative into the Riemannian part and the remainder is as follows:

$$\tilde{\nabla}_\nu A_\mu = \nabla_\nu A_\mu - \mathrm{K}^\rho{}_{\mu\nu} A_\rho, \tag{A.12}$$

where ∇_μ is the covariant derivative with respect to the Christoffel symbols. The torsion and the curvature are defined as covariant derivatives of the spin-connection and the vielbein in the following manner:

$$\tilde{R}^{ab} = \mathrm{d}\omega^{ab} + \omega^a{}_c \wedge \omega^{cb}, \tag{A.13}$$

$$T^a = \mathrm{d}e^a + \omega^a{}_b \wedge e^b. \tag{A.14}$$

Then it is easy to show that the components of torsion $T^\mu_{\ \nu\rho}$ are indeed the antisymmetric part of the connection coefficients $\tilde{\Gamma}^\mu_{\nu\rho}$. The two-dimensional space-time has higher symmetry, which results in the simplified expressions for the spin-connection, contorsion, and curvature:

$$\begin{aligned}
&\omega^{ab}{}_\mu = \varepsilon^{ab}\omega_\mu, \quad \mathrm{K}^{ab}{}_\mu = \varepsilon^{ab}\mathrm{K}_\mu, \quad \Delta^{ab}{}_\mu = \varepsilon^{ab}\Delta_\mu, \\
&\tilde{R}^{ab}{}_{\mu\nu} = -\frac{1}{2}\varepsilon^{ab}\varepsilon_{\mu\nu}\tilde{R}, \quad \tilde{R} = 2\varepsilon^{\mu\nu}\partial_\mu\omega_\nu, \quad R = 2\varepsilon^{\mu\nu}\partial_\mu\Delta_\nu, \\
&T^a{}_{\mu\nu} = e^a{}_\alpha \mathrm{K}^\alpha \varepsilon_{\mu\nu},
\end{aligned} \tag{A.15}$$

where R is the Riemannian part of the scalar curvature. The following two identities involving the Levi-Civita tensor always hold in a two-dimensional spacetime:

$$\varepsilon_{\alpha\beta}\varepsilon_{\gamma\delta} = -g_{\alpha\gamma}g_{\beta\delta} + g_{\alpha\delta}g_{\beta\gamma}, \tag{A.16}$$

$$g_{\alpha\beta}\varepsilon_{\gamma\delta} + g_{\beta\gamma}\varepsilon_{\delta\alpha} + g_{\delta\beta}\varepsilon_{\alpha\gamma} = 0. \tag{A.17}$$

With this newly defined notation, we can now move on to rewriting the Dirac equation for a massive spinor field in curved space-time. The minimal coupling to the geometry gives the following:

$$\left(\gamma^\mu\tilde{\nabla}_\mu - m\right)\psi = 0, \tag{A.18}$$

where $\tilde{\nabla}_\mu$ represents the covariant derivative within the spinor representation and $\gamma^\mu = e_a{}^\mu \gamma^a$ are the coordinate-dependent γ-matrices due to their requirement to satisfy the Clifford algebra associated with the metric $g_{\mu\nu}$. Notice that the covariant derivative in (A.18) lacks an imaginary unit prefix. This is because the signature is $(-,+)$ instead of the usual $(+,-)$ typically used in the context of the Dirac equation. Additionally, we define local γ-matrices γ^a that adhere to the Clifford algebra corresponding to the metric η_{ab}, specifically:

$$\{\gamma^a, \gamma^b\} = 2\eta^{ab}. \tag{A.19}$$

Next, we make the following choice:

$$\gamma^{\hat{0}} = i\sigma_1 \quad \wedge \quad \gamma^{\hat{1}} = \sigma_2, \tag{A.20}$$

where $\sigma_{1,2}$ are Pauli matrices. Now the generators of the Lorentz group in two dimensions can be expressed as:

$$\Sigma_{ab} \equiv \frac{1}{4}\left[\gamma_a, \gamma_b\right] = -\frac{\sigma_3}{2}\varepsilon_{ab} \tag{A.21}$$

The Lorentz conjugate is given by the following:

$$\bar{\psi} = i\psi^\dagger \gamma^{\hat{0}}. \tag{A.22}$$

Lorentz covariant derivatives for the spinor field and its conjugate are:

$$\tilde{\nabla}_\mu \psi = \left(\partial_\mu + \omega_\mu \frac{\sigma_3}{2}\right)\psi, \quad \tilde{\nabla}_\mu \bar{\psi} = \partial_\mu \bar{\psi} - \bar{\psi}\frac{\sigma_3}{2}\omega_\mu. \tag{A.23}$$

Finally, the symmetrized action for the massive Dirac fermion is expressed as:

$$S_D = -\int \mathrm{d}^2x\sqrt{-g}\left[\frac{1}{2}\bar{\psi}\gamma^\mu\tilde{\nabla}_\mu\psi - \frac{1}{2}\tilde{\nabla}_\mu\bar{\psi}\gamma^\mu\psi - m\bar{\psi}\psi\right]. \tag{A.24}$$

For the metric written in a conformal gauge $\mathrm{d}s^2 = -e^{2\rho}\mathrm{d}x^+\mathrm{d}x^-$, the appropriate choice of vielbeins is given by:

$$e^{\hat{+}}{}_- = e^{\hat{-}}{}_+ = 0, \tag{A.25}$$
$$e^{\hat{+}}{}_+ = e^{\hat{-}}{}_- = e^\rho, \tag{A.26}$$

and the inverse vielbeins are:

$$e_{\hat{+}}{}^- = e_{\hat{-}}{}^+ = 0, \tag{A.27}$$
$$e_{\hat{+}}{}^+ = e_{\hat{-}}{}^- = e^{-\rho}, \tag{A.28}$$

The Ricci rotation coefficients can be represented using the metric as follows:

$$\Delta_\mu = \frac{1}{2}\varepsilon^{\alpha\beta}\left(\partial_\alpha g_{\mu\beta} - e^a{}_\beta \partial_\mu e_{a\alpha}\right) \tag{A.29}$$

Substituting metric in a conformal gauge results in:

$$\Delta_+ = \partial_+\rho \quad \wedge \quad \Delta_- = -\partial_-\rho. \tag{A.30}$$

Appendix B

Transcendental equation solution

Here we solve the transcendental equation (5.102), that is:

$$e^{\hat{\mathrm{x}}}(\hat{\mathrm{x}}-1)=\delta e^{\mathrm{x}}(\mathrm{x}-1), \tag{B.1}$$

when $\delta \leqslant 1$, $\hat{\mathrm{x}} \geqslant 0$ and $\mathrm{x} \geqslant 0$. Notice that when $\delta = 1$, we have a simple solution $\hat{\mathrm{x}} = \mathrm{x}$. This is the only solution, since both functions are monotonically increasing, which implies that they intersect at most once. This is true simply because when $\sigma^+ = \sigma_0^+$, the metric becomes that of the Minkowski space-time (see section 5.1.3). This fact will be extensively used as well as the fact that $\delta < 1$ when $\sigma^+ > \sigma_0^+$. Two cases will be studied, since the function on the right-hand side of Equation (B.1) behaves differently depending on whether $\mathrm{x} \geqslant 1$ or $\mathrm{x} \leqslant 1$.

It is important to further discuss the condition $\hat{\mathrm{x}} \geqslant 0$. Figure 3.2 shows space-time. In part I of space-time the boundary is defined by $\mathrm{x} = 0$. The formation of the singularity happens when the collapsing matter's world-line $\sigma^+ = \sigma_0^+$ hits the boundary of space-time. This corresponds to $\hat{\mathrm{x}} = 0$, which implies that $\hat{\mathrm{x}} \geqslant 0$.

Theorem 1. *The solution to equation (B.1)* $\hat{\mathrm{x}} = \hat{\mathrm{x}}(\mathrm{x}, \delta)$*, when* $\delta \leqslant 1$*,* $\hat{\mathrm{x}} \geqslant 0$ *and* $\mathrm{x} \geqslant 1$ *is given by the following functional series:*

$$\hat{\mathrm{x}}(\mathrm{x},\delta)=\mathrm{x}-\sum_{n=1}^{\infty}\frac{(1-\delta)^n}{n!}\left(1-\frac{1}{\mathrm{x}}\right)^n\mathrm{P}_{n-1}\left(\frac{1}{\mathrm{x}}\right), \tag{B.2}$$

where $\mathrm{P}_n(x)$ *are polynomials of the* n*-th degree, defined by the following recurrence relation,*

$$\mathrm{P}_n(x)=\left[n(x+1)+x^2\frac{\mathrm{d}}{\mathrm{d}x}\right]\mathrm{P}_{n-1}(x), \tag{B.3}$$

and the initial condition $\mathrm{P}_0(x) = 1$*.*

Proof. We expand the function $\hat{\mathrm{x}} = \hat{\mathrm{x}}(\mathrm{x}, \delta)$ in a Taylor series around $\delta = 1$:

$$\hat{\mathrm{x}}=\mathrm{x}+\sum_{n=1}^{\infty}\frac{1}{n!}\frac{\partial^n\hat{\mathrm{x}}}{\partial\delta^n}\bigg|_{\delta=1}(\delta-1)^n, \tag{B.4}$$

where we have used the fact that $\hat{\mathrm{x}}(\mathrm{x}, 1) = \mathrm{x}$. The differential of the function $\hat{\mathrm{x}} = \hat{\mathrm{x}}(x, \delta)$ is given by:

$$\mathrm{d}\hat{\mathrm{x}}=\frac{e^{\mathrm{x}}(\mathrm{x}-1)}{\hat{\mathrm{x}}e^{\hat{\mathrm{x}}}}\mathrm{d}\delta+\delta\frac{\mathrm{x}e^{\mathrm{x}}}{\hat{\mathrm{x}}e^{\hat{\mathrm{x}}}}\mathrm{dx}. \tag{B.5}$$

The n-th derivative can be written in the following form:

$$\frac{\partial^n \hat{\mathrm{x}}}{\partial \delta^n} = e^{n\mathrm{x}}(\mathrm{x}-1)^n \left(\frac{e^{-\hat{\mathrm{x}}}}{\hat{\mathrm{x}}}\frac{\mathrm{d}}{\mathrm{d}\hat{\mathrm{x}}}\right)^{n-1} \frac{e^{-\hat{\mathrm{x}}}}{\hat{\mathrm{x}}}. \tag{B.6}$$

Demanding that $\delta = 1$ is equivalent to replacing $\hat{\mathrm{x}} = \mathrm{x}$ on the right hand side of equation (B.6). We define the array of polynomials $\mathrm{P}_n\left(\frac{1}{\mathrm{x}}\right)$ by:

$$\mathrm{P}_{n-1}\left(\frac{1}{\mathrm{x}}\right) = (-1)^{n-1}\mathrm{x}^n e^{n\mathrm{x}} \left(\frac{e^{-\mathrm{x}}}{\mathrm{x}}\frac{\mathrm{d}}{\mathrm{dx}}\right)^{n-1} \frac{e^{-\mathrm{x}}}{\mathrm{x}}. \tag{B.7}$$

Using mathematical induction, it is easy to show that the Rodrigues formula (equation (B.7)) really defines polynomials of degree $n-1$. With the help of equation (B.7) it is straight forward to derive a recurrence relation for the $\mathrm{P}_n(1/\mathrm{x})$ polynomials, which is given by:

$$\mathrm{P}_n\left(\frac{1}{\mathrm{x}}\right) = \left[n\left(1+\frac{1}{\mathrm{x}}\right) - \frac{\mathrm{d}}{\mathrm{dx}}\right]\mathrm{P}_{n-1}\left(\frac{1}{\mathrm{x}}\right). \tag{B.8}$$

From this relation, the recurrence relation (B.3) is directly derived by the substitution $x = 1/\mathrm{x}$. Replacing $n = 1$ in equation (B.7), the initial condition reads $\mathrm{P}_0(x) = 1$. □

To properly use equation (B.2), it is important to show that this series is uniformly convergent. If so, then the solution of equation (B.1) when $\mathrm{x} \geqslant 1$ is given by equation (B.2).

Theorem 2. *The series $\sum_{n=1}^{\infty} \frac{(1-\delta)^n}{n!} f_n(\mathrm{x})$ is uniformly convergent when $\mathrm{x} \geqslant 1$. The functional array $f_n(x)$ is defined by the following equation:*

$$f_n(x) = \left(1-\frac{1}{x}\right)^n \mathrm{P}_{n-1}\left(\frac{1}{x}\right). \tag{B.9}$$

Proof. To prove this theorem, we need to prove the following lemma first.

Lemma 1. *The functions $f_n(x)$ are monotonically increasing functions of x when $x \geqslant 1$.*

Proof. We will calculate the derivative of the function $f_n(x)$, and show that it is positive when $x > 1$. Using equation (B.8) the derivative of the polynomial $\mathrm{P}_{\mathrm{n}-1}(x)$ can be eliminated, resulting in:

$$\frac{\mathrm{d}f_n(x)}{\mathrm{d}x} = \left(1-\frac{1}{x}\right)^{n-1}\left[n\mathrm{P}_{n-1}\left(\frac{1}{x}\right) - \left(1-\frac{1}{x}\right)\mathrm{P}_n\left(\frac{1}{x}\right)\right]. \tag{B.10}$$

Since $x > 1$, $f_n'(x) > 0$ is equivalent to proving that

$$n\mathrm{P}_{n-1}\left(\frac{1}{x}\right) > \left(1-\frac{1}{x}\right)\mathrm{P}_n\left(\frac{1}{x}\right), \ \forall n \geqslant 1. \tag{B.11}$$

We write the polynomials in terms of their coefficients as $\mathrm{P}_n(x) = \sum_{k=0}^{n} a_n^{(k)} x^k$. Equation (B.11) now takes the following form:

$$na_{n-1}^{(0)} - a_n^{(0)} + \sum_{k=1}^{n-1}\left[na_{n-1}^{(k)} + a_n^{(k-1)} - a_n^{(k)}\right]\frac{1}{x^k} + \left[a_n^{(n-1)} - a_n^{(n)}\right]\frac{1}{x^n} + a_n^{(n)}\frac{1}{x^{n+1}} > 0. \tag{B.12}$$

We will show that coefficient of every order in equation (B.12) is greater than 0. To do this we need the recurrence relation between the coefficients $a_n^{(k)}$, which is easily derived using recurrence relation (B.3). The result is given by:

$$k = 0: \; a_n^{(0)} = n a_{n-1}^{(0)}, \tag{B.13}$$

$$k = 1: \; a_n^{(1)} = n a_{n-1}^{(1)} + n a_{n-1}^{(0)}, \tag{B.14}$$

$$1 < k < n: \; a_n^{(k)} = n a_{n-1}^{(k)} + (n + k - 1) a_{n-1}^{(k-1)}, \tag{B.15}$$

$$k = n: \; a_n^{(n)} = (2n - 1) a_{n-1}^{(n-1)}. \tag{B.16}$$

Together with the initial condition $a_0^{(0)} = 1$, equations (B.13) through (B.16) give $a_n^{(0)} = n!$, $a_n^{(1)} = nn!$ and $a_n^{(n)} = (2n - 1)!!$ respectively. Now, we return to proving the inequality (B.12). From equation (B.13) it follows that the $k = 0$ term in the (B.12) vanishes. The first-order term vanishes because $a_n^{(1)} = nn!$. Now, the inequality (B.12) nay be recast as:

$$(\forall k \in \{2, 3, ..., n - 1\}) \; n a_{n-1}^{(k)} + a_n^{(k-1)} - a_n^{(k)} > 0. \tag{B.17}$$

With the help of the relation (B.15), the inequality (B.17) can be rewritten in the following form:

$$(n + k - 2) a_{n-1}^{(k-2)} > (k - 1) a_{n-1}^{(k-1)}. \tag{B.18}$$

Shifting $k - 1$ to k, and $n - 1$ to n, we arrive at the following expression:

$$(\forall k \in \{1, 2, ..., n - 1\}) \; (n + k) a_n^{(k-1)} > k a_n^{(k)}. \tag{B.19}$$

Now, we apply mathematical induction to prove this inequality. First, we prove the relation for $n = 3$ (the base case of the induction). The coefficients of the polynomial $\mathrm{P}_3(x) = 15x^3 + 25x^2 + 18x + 6$ clearly satisfy relations (B.19). We need to prove that the relation holds for $n + 1$ if relation (B.19) is satisfied for n (induction hypothesis):

$$(\forall k \in \{1, 2, ..., n\}) \; (n + k + 1) a_{n+1}^{(k-1)} > k a_{n+1}^{(k)}. \tag{B.20}$$

Using relation (B.15), the inequality (B.20) can be rewritten as:

$$\begin{aligned}(\forall k \in \{2, ..., n\}) \; (n + 1) &\left[(n + k) a_n^{(k-1)} - k a_n^{(k)}\right] \\ &+ (n + k + 1) \left[(n + k - 1) a_n^{(k-2)} - (k - 1) a_n^{(k-1)}\right] > 0.\end{aligned} \tag{B.21}$$

Following from the hypothesis, both terms are greater then 0. Only two cases remain to be proven: $k = 1$ and $k = n$. In the case of $k = 1$, the relation is given by $(n + 2) a_{n+1}^{(0)} > a_{n+1}^{(1)}$. Using the closed forms for these two coefficients, $(n + 2)(n + 1)! > (n + 1)(n + 1)!$, which is clearly satisfied. In the case of $k = n$, we are allowed to use formula (B.21), which takes the following form:

$$(n + 1) n \left[2 a_n^{(n-1)} - a_n^{(n)}\right] + (2n + 1) \left[(2n - 1) a_n^{(n-2)} - (n - 1) a_n^{(n-1)}\right] > 0. \tag{B.22}$$

The second term is greater then zero (from the hypothesis). Using relation (B.15) we get

$$2 a_n^{(n-1)} > 2n a_{n-1}^{(n-1)} = 2n(2n - 3)!! > (2n - 1)!! = a_n^{(n)}. \tag{B.23}$$

With this, the mathematical induction is finished and we have proven inequality (B.19), and subsequently the inequality (B.17).

The last remaining part of inequality (B.12) that needs to be proven is the relation $(\forall n \geqslant 1) a_n^{(n-1)} > a_n^{(n)}$. Using the relation (B.15) (and the result $a_n^{(n)} = (2n-1)!!$) repeatedly, it is easy to arrive at the following expression for the closed form of $a_n^{(n-1)}$:

$$a_n^{(n-1)} = \sum_{k=0}^{n-1} \frac{2^k (n-k)(n-1)!(2(n-k)-3)!!}{(n-k-1)!}. \tag{B.24}$$

The zeroth term in this sum is equal to $n(2n-3)!!$, and every other term is greater then $(2n-3)!!$, which means that: $a_n^{(n-1)} > (2n-1)(2n-3)!! = a_n^{(n)}$. This is what we needed to prove.

With this, we have proven inequality (B.12) and subsequently inequality (B.11), thus proving the lemma. □

To prove theorem 2, the Weierstrass criterion will be used. Lemma 1 implies that

$$(\forall x \geqslant 1) f_n(x) < \lim_{x\to\infty} f_n(x) = a_{n-1}^{(0)} = (n-1)!, \tag{B.25}$$

$\forall n \geqslant 1$. The inequality (B.25) implies the following inequality for the coefficients of the series $\sum_{n=1}^{\infty} \frac{(1-\delta)^n}{n!} f_n(x)$:

$$(\forall n \geqslant 1)(\forall x \geqslant 1) \left| \frac{(1-\delta)^n}{n!} f_n(x) \right| < \frac{(1-\delta)^n}{n}. \tag{B.26}$$

The next step is to prove that the series $\sum_{n=1}^{\infty} \frac{(1-\delta)^n}{n}$ converges. By the comparison test, this is true for $|1-\delta| < 1$, which is satisfied. Then, according to the Weierstrass criterion, the series $\sum_{n=1}^{\infty} \frac{(1-\delta)^n}{n!} f_n(x)$ converges uniformly. □

This result is important because the infinite sum may exchange places with integrals and limits with respect to x, which will be used in the main text. Now we move on to the case when $x < 1$.

Theorem 3. *The solution to equation (B.1)* $\hat{\mathrm{x}} = \hat{\mathrm{x}}(\mathrm{x}, \delta)$*, when* $\delta \leqslant 1$*,* $\hat{\mathrm{x}} \geqslant 0$ *and* $0 \leqslant \mathrm{x} \leqslant 1$ *is given by the following functional series:*

$$\hat{\mathrm{x}}(\mathrm{x}, \delta) = 1 - \sum_{n=1}^{\infty} \frac{\delta^n}{n!} \mathrm{P}_{n-1}(1) e^{n(\mathrm{x}-1)} (1-\mathrm{x})^n, \tag{B.27}$$

where $\mathrm{P}_n(x)$ *are the polynomials defined in theorem 1.*

Proof. If $0 \leqslant \mathrm{x} \leqslant 1$, then $0 \leqslant e^{\mathrm{x}}(1-\mathrm{x}) \leqslant 1$, which means that we can choose $\tilde{\delta} = \delta e^{\mathrm{x}}(1-\mathrm{x})$ as a small parameter, and expand the solution as a Taylor series with respect to $\tilde{\delta}$ around $\tilde{\delta} = 0$,

$$\hat{\mathrm{x}}(\tilde{\delta}) = \hat{\mathrm{x}}(0) + \sum_{n=1}^{\infty} \frac{\tilde{\delta}^n}{n!} \frac{\mathrm{d}^n \hat{\mathrm{x}}}{\mathrm{d}\tilde{\delta}^n}\bigg|_{\tilde{\delta}=0}. \tag{B.28}$$

The equation we are solving, in terms of $\hat{\mathrm{x}} = \hat{\mathrm{x}}(\tilde{\delta})$, is given by:

$$e^{\hat{\mathrm{x}}(\tilde{\delta})}(1 - \hat{\mathrm{x}}(\tilde{\delta})) = \tilde{\delta}. \tag{B.29}$$

With the help of the equation (B.29) the n-th derivative of the function $\hat{\mathrm{x}}(\tilde{\delta})$ is given by

$$\frac{\mathrm{d}^n\hat{\mathrm{x}}}{\mathrm{d}\tilde{\delta}^n} = (-1)^n \left(\frac{e^{-\hat{\mathrm{x}}}}{\hat{\mathrm{x}}}\frac{\mathrm{d}}{\mathrm{d}\hat{\mathrm{x}}}\right)^{n-1}\frac{e^{-\hat{\mathrm{x}}}}{\hat{\mathrm{x}}} = -\frac{e^{-n\hat{\mathrm{x}}}}{\hat{\mathrm{x}}^n}\mathrm{P}_{n-1}\left(\frac{1}{\hat{\mathrm{x}}}\right), \tag{B.30}$$

where equation (B.7) has been used. Using the fact that $\hat{\mathrm{x}} = 1$ when $\tilde{\delta} = 0$ we arrive at the following expression:

$$\frac{\mathrm{d}^n\hat{\mathrm{x}}}{\mathrm{d}\tilde{\delta}^n} = -e^{-n}\mathrm{P}_{n-1}(1). \tag{B.31}$$

Changing this result in formula (B.28) we find $\tilde{\delta} = \delta e^{\mathrm{x}}(1-\mathrm{x})$ and we have derived formula (B.27). □

To be able to use this result (B.27), once again we need to prove that the series appearing in equation (B.27) is uniformly convergent.

Theorem 4. *The series* $\sum_{n=1}^{\infty}\frac{\delta^n}{n!}\mathrm{P}_{n-1}(1)e^{n(x-1)}(1-x)^n$ *is uniformly convergent when* $0 \leqslant x \leqslant 1$.

Proof. Since $0 \leqslant x \leqslant 1$, we have $e^{nx}(1-x)^n < 1$, which means

$$\left|\frac{\delta^n}{n!}\mathrm{P}_{n-1}(1)e^{n(x-1)}(1-x)^n\right| < \frac{\delta^n}{n!}\mathrm{P}_{n-1}(1)e^{-n}, \tag{B.32}$$

$\forall 0 \leqslant x \leqslant 1$ and $\forall n \geqslant 1$. The next step is to prove that the series $\sum_{n=1}^{\infty}\frac{\delta^n}{n!}\mathrm{P}_{n-1}(1)e^{-n}$ is convergent. To be able to do this, we need a closed form for $\mathrm{P}_{n-1}(1)$, which will be derived in the following lemma, without proof.

Lemma 2. *The polynomials defined in theorem 1 have the following property:* $\mathrm{P}_n(1) = (n+1)^n$, $\forall n \geqslant 0$.

Now we can use the comparison test to check if the series $\sum_{n=1}^{\infty}\frac{\delta^n}{n!}\mathrm{P}_{n-1}(1)e^{-n}$ is convergent. Using lemma 2 we get

$$\frac{\frac{\delta^{n+1}}{(n+1)!}(n+1)^n e^{-(n+1)}}{\frac{\delta^n}{n!}n^{n-1}e^{-n}} = \frac{\delta}{e}\left(1+\frac{1}{n}\right)^{n-1} \underset{n\to\infty}{\longrightarrow} \delta, \tag{B.33}$$

which means that the series is convergent when $\delta < 1$. This requirement is satisfied by the theorem statement. Then, according to the Weierstrass criterion, the series $\sum_{n=1}^{\infty}\frac{\delta^n}{n!}\mathrm{P}_{n-1}(1)e^{n(x-1)}(1-x)^n$ converges uniformly. □

Sometimes functions of $\hat{\mathrm{x}}$ will appear in our calculations (for example, $\ln\hat{\mathrm{x}}$). Similar expressions to those of theorems 1 and 3 are needed for these functions.

Theorem 5. *The differentiable function* $\mathrm{F}(\hat{\mathrm{x}}(\mathrm{x},\delta))$, *where* $\hat{\mathrm{x}}$ *is a solution of the equation (B.1), when* $\delta \leqslant 1$, $\hat{\mathrm{x}} \geqslant 0$ *and* $\mathrm{x} \geqslant 1$, *is given by the following functional series:*

$$\mathrm{F}(\hat{\mathrm{x}}) = \mathrm{F}(\mathrm{x}) - \sum_{n=1}^{\infty}\frac{(1-\delta)^n}{n!}\left(1-\frac{1}{\mathrm{x}}\right)^n \mathrm{F}_{n-1}\left(\frac{1}{\mathrm{x}}\right), \tag{B.34}$$

where $\mathrm{F}_n(x)$ *is an array of functions, defined by the following recurrence relation,*

$$\mathrm{F}_n(x) = \left[n(x+1) + x^2\frac{\mathrm{d}}{\mathrm{dx}}\right]\mathrm{F}_{n-1}(x), \tag{B.35}$$

and the initial condition $\mathrm{F}_0(x) = -x^2\frac{\mathrm{dF}(1/x)}{\mathrm{d}x}$.

Proof. The proof is analogous to that of theorem 1. We start by writing the Taylor series of the function $\mathrm{F}(\mathrm{x}, \delta)$ around the point $\delta = 1$:

$$\mathrm{F}(\hat{\mathrm{x}}) = \mathrm{F}(\mathrm{x}) + \sum_{n=1}^{\infty} \frac{1}{n!} \frac{\partial^n \mathrm{F}(\hat{\mathrm{x}})}{\partial \delta^n}\bigg|_{\delta=1} (\delta - 1)^n. \tag{B.36}$$

The n-th derivative is now given by the following expression:

$$\frac{\partial^n \mathrm{F}(\hat{\mathrm{x}})}{\partial \delta^n} = e^{n\mathrm{x}}(\mathrm{x}-1)^n \left(\frac{e^{-\hat{\mathrm{x}}}}{\hat{\mathrm{x}}}\frac{\mathrm{d}}{\mathrm{d}\hat{\mathrm{x}}}\right)^{n-1} \frac{e^{-\hat{\mathrm{x}}}}{\hat{\mathrm{x}}}\frac{\mathrm{dF}(\hat{\mathrm{x}})}{\mathrm{d}\hat{\mathrm{x}}}. \tag{B.37}$$

The same way as in the theorem 1 we define an array of functions:

$$\mathrm{F}_{n-1}\left(\frac{1}{\mathrm{x}}\right) = (-1)^{n-1}\mathrm{x}^n e^{n\mathrm{x}} \left(\frac{e^{-\mathrm{x}}}{\mathrm{x}}\frac{\mathrm{d}}{\mathrm{dx}}\right)^{n-1} \frac{e^{-\mathrm{x}}}{\mathrm{x}}\frac{\mathrm{dF}(\mathrm{x})}{\mathrm{dx}}. \tag{B.38}$$

It is now obvious that the recurrence relation for the functions F_n would be the same as for the polynomials defined in the theorem 1. The only difference would be the initial condition, which is now given by $\mathrm{F}_0(1/\mathrm{x}) = \frac{\mathrm{dF}(\mathrm{x})}{\mathrm{dx}}$. Applying the substitution $\mathrm{x} \mapsto 1/\mathrm{x}$, we arrive at the expression given in the statement of the theorem. □

Once again, the question of uniform convergence must be asked. This time, it depends on the form of the function $\mathrm{F}(\hat{\mathrm{x}})$. The first requirement is that F does not diverge when $\hat{\mathrm{x}} \to \infty$, since the radius of convergence would depend on x, and the discussion of uniform convergence would become meaningless. From the proof of theorem 2 we can see that the necessary condition is:

$$(\forall \mathrm{x} \geqslant 1)(\exists n_0)(\forall n \geqslant n_0)\left|\left(1 - \frac{1}{\mathrm{x}}\right)^n \mathrm{F}_{n-1}\left(\frac{1}{\mathrm{x}}\right)\right| < n!. \tag{B.39}$$

The function $\ln \hat{\mathrm{x}}$ is the only one directly involved in the calculation. Since this is the case, we will take extra care of this function.

Corollary 1. *The function* $\ln \hat{\mathrm{x}}(\mathrm{x}, \delta)$ *when* $\delta \leqslant 1$, $\hat{\mathrm{x}} \geqslant 0$ *and* $\mathrm{x} \geqslant 1$, *is given by the following functional series:*

$$\ln \hat{\mathrm{x}} = \ln \mathrm{x} - \sum_{n=1}^{\infty} \frac{(1-\delta)^n}{n!} \left(1 - \frac{1}{\mathrm{x}}\right)^n \mathrm{Q}_{n-1}\left(\frac{1}{\mathrm{x}}\right), \tag{B.40}$$

where $\mathrm{Q}_n(x)$ *are polynomials of degree* $n+1$, *defined by the following recurrence relation:*

$$\mathrm{Q}_n(x) = \left[n(x+1) + x^2\frac{\mathrm{d}}{\mathrm{d}x}\right]\mathrm{Q}_{n-1}(x), \tag{B.41}$$

and the initial condition $\mathrm{Q}_0(x) = x$.

Proof. This corollary is a direct consequence of theorem 5. The initial condition is obvious since $-x^2(\ln(1/x))' = x$. We only need to prove that Q_n are polynomials of degree $n+1$, which follows directly from the recurrence relation (B.41) since it increases the degree of the polynomial by one, and the degree of the zeroth polynomial is 1. This concludes the proof. □

Theorem 6. *The series* $\sum_{n=1}^{\infty} \frac{(1-\delta)^n}{n!} f_n(x)$ *is uniformly convergent when* $\mathrm{x} \geqslant 1$. *The functional array* $f_n(x)$ *is defined by the following equation:*

$$f_n(x) = x\left(1 - \frac{1}{x}\right)^{n+1} \mathrm{Q}_{n-1}\left(\frac{1}{x}\right). \tag{B.42}$$

Proof. This proof will not be as detailed as the previous proofs since it is based on the same ideas. By mathematical induction, it is easy to prove that the functions $f_n(x)$ are monotonically increasing, the same way as in lemma 1. This fact implies that the functions $f_n(x)$ take their maximum value when $x \to \infty$. Then, the recurrence relations (B.41) tell us that the maximal value is $(n-1)!$. The rest of the proof is exactly the same as in theorem 2. □

Now we examine the $x < 1$ case.

Theorem 7. *The function* $\ln \hat{\mathrm{x}}(\mathrm{x}, \delta)$*, when* $\delta \leqslant 1$*,* $\hat{\mathrm{x}} \geqslant 0$ *and* $0 \leqslant \mathrm{x} \leqslant 1$ *is given by the following functional series:*

$$\ln \hat{\mathrm{x}} = -\sum_{n=1}^{\infty} \frac{\delta^n}{n!} \mathrm{Q}_{n-1}(1) e^{n(\mathrm{x}-1)} (1-\mathrm{x})^n, \tag{B.43}$$

where $\mathrm{Q}_n(x)$ *are the polynomials defined in corollary 1.*

Proof. The proof of this theorem is essentially the same as the proof of theorem 3. The only difference is the appearance of the polynomials Q_n instead of the polynomials P_n. □

Finally, we need to prove the uniform convergence of the series appearing in Equation (B.43).

Theorem 8. *When* $0 \leqslant x \leqslant 1$*, the functional series* $\sum_{n=1}^{\infty} \frac{\delta^n}{n!} \mathrm{Q}_{n-1}(1) e^{n(x-1)} (1-x)^n$ *is uniformly convergent.*

Proof. As in theorem 4, we can write:

$$\left| \frac{\delta^n}{n!} \mathrm{Q}_{n-1}(1) e^{n(x-1)} (1-x)^n \right| < \frac{\delta^n}{n!} \mathrm{Q}_{n-1}(1) e^{-n}. \tag{B.44}$$

Now we need the closed form of $\mathrm{Q}_{n-1}(1)$, which will be given by the following lemma without proof.

Lemma 3. *The polynomials defined in corollary 1 have the following property:* $(\forall n \geqslant 1)\ \mathrm{Q}_{n-1}(1) = (n-1)! \sum_{k=0}^{n-1} \frac{n^k}{k!}$.

Using lemma 3, the following inequality holds:

$$\mathrm{Q}_{n-1}(1) = (n-1)! \sum_{k=1}^{n-1} \frac{n^k}{k!} < (n-1)! e^n. \tag{B.45}$$

Using (B.45), the inequality (B.44) becomes:

$$\left| \frac{\delta^n}{n!} \mathrm{Q}_{n-1}(1) e^{n(x-1)} (1-x)^n \right| < \frac{\delta^n}{n}. \tag{B.46}$$

The next step would be to prove the convergence of the series $\sum_{n=1}^{\infty} \frac{\delta^n}{n}$. This series is convergent by the comparison test when $\delta < 1$, which is satisfied. □

Appendix C

Review of the Schwarzschild solution

The Schwarzschild solution represents the spherically symmetric, static solution of the vacuum Einstein equations, that is, to the system of equations:

$$\mathcal{R}_{\mu\nu} = 0. \tag{C.1}$$

Here, $\mathcal{R}_{\mu\nu}$ denotes the Ricci tensor. It can be shown that this metric constitutes the unique static, spherically symmetric solution of the vacuum Einstein equations. This result is encapsulated in Birkhoff's theorem. A static, spherically symmetric solution of the Einstein equations, or any appropriate subset thereof, represents the spacetime geometry in the vicinity of an arbitrary spherically symmetric gravitating source, and therefore also of static black holes. Within the class of stationary solutions, there also exist rotating black holes (provided the theory is not coupled to electrodynamics). These configurations, however, are not static. The metric components do not explicitly depend on time. This only implies invariance under time translations, but not under time reversal (which holds for static spacetimes). The most general stationary, asymptotically flat black hole solution is the Kerr–Newman solution. This solution simultaneously incorporates both electric charge and angular momentum (i.e., rotation) of the black hole. In this supplement, we shall largely follow the exposition presented in Chapter 4 of Carroll's book [106].

C.1 The Schwarzschild spacetime metric

In this section, we address the vacuum Einstein equations. The most general spherically symmetric metric can be expressed in the form:

$$\mathrm{d}s^2 = g_{aa}\mathrm{d}a^2 + 2g_{ar}\mathrm{d}a\mathrm{d}r + g_{rr}\mathrm{d}r^2 + r^2\left(\mathrm{d}\theta^2 + \sin^2\theta\mathrm{d}\phi^2\right). \tag{C.2}$$

Owing to the assumption of spherical symmetry, the metric components g_{ar}, g_{rr}, and g_{aa} do not depend on the angular coordinates θ and ϕ. It can be shown that this metric admits a diagonal representation upon introducing a new time coordinate whose differential is defined by:

$$\mathrm{d}t = I(a,r)\left(g_{aa}\mathrm{d}a + g_{ar}\mathrm{d}r\right). \tag{C.3}$$

Upon implementing this substitution, the metric may be expressed in the following form:

$$\mathrm{d}s^2 = \frac{\mathrm{d}t^2}{I^2 g_{aa}} + \left(g_{rr} - \frac{g_{ar}^2}{g_{aa}}\right)\mathrm{d}r^2 + r^2\left(\mathrm{d}\theta^2 + \sin^2\theta\mathrm{d}\phi^2\right). \tag{C.4}$$

Since we began with the most general expression for the metric, we can therefore conclude that restricting ourselves to a diagonal form of the metric does not entail any loss of generality in the resulting solution. Accordingly, for the ansatz we adopt:

$$\mathrm{d}s^2 = -e^{2\alpha(t,r)}\mathrm{d}t^2 + e^{2\beta(t,r)}\mathrm{d}r^2 + r^2\left(\mathrm{d}\theta^2 + \sin^2\theta \mathrm{d}\phi^2\right). \tag{C.5}$$

By inserting this ansatz into the equations and exploiting the diagonality of the metric, we obtain:

$$\Gamma^\rho_{\mu\nu} = \frac{1}{2}e^{\rho\lambda}\Big[\partial_\mu g_{\nu\lambda} + \partial_\nu g_{\mu\lambda} - \partial_\lambda g_{\mu\nu}\Big], \tag{C.6}$$

we can readily determine all components of the Christoffel symbols:

$$\begin{aligned}
&\Gamma^r_{tt} = e^{2(\alpha-\beta)}\partial_r\alpha, \quad \Gamma^t_{rr} = e^{-2(\alpha-\beta)}\partial_t\beta, \quad \Gamma^t_{rt} = \partial_r\alpha, \quad \Gamma^r_{tr} = \partial_t\beta,\\
&\Gamma^r_{\theta\theta} = -re^{-2\beta}, \quad \Gamma^r_{\phi\phi} = -r\sin^2\theta e^{-2\beta}, \quad \Gamma^\theta_{r\theta} = \frac{1}{r}, \quad \Gamma^\phi_{r\phi} = \frac{1}{r},\\
&\Gamma^\theta_{\phi\phi} = -\sin\theta\cos\theta, \quad \Gamma^\phi_{\theta\phi} = \cot\theta, \quad \Gamma^t_{tt} = \partial_t\alpha, \quad \Gamma^r_{rr} = \partial_r\beta.
\end{aligned} \tag{C.7}$$

To determine the solutions of the equations of motion, it is necessary to compute the components of the Ricci tensor. Specifically, we employ:

$$\mathcal{R}_{\mu\nu} = \mathcal{R}^\rho{}_{\mu\rho\nu} = \partial_\rho\Gamma^\rho_{\mu\nu} - \partial_\nu\Gamma^\rho_{\mu\rho} + \Gamma^\rho_{\alpha\rho}\Gamma^\alpha_{\mu\nu} - \Gamma^\rho_{\nu\alpha}\Gamma^\alpha_{\mu\rho}. \tag{C.8}$$

By inserting the Christoffel symbols (C.7) and the ansatz (C.5) into (C.8), we arrive at:

$$\mathcal{R}_{tt} = -\Big[\partial_t^2\beta + (\partial_t\beta)^2 - \partial_t\alpha\partial_t\beta\Big] + \Big[\partial_r^2\alpha + (\partial_r\alpha)^2 - \partial_r\alpha\partial_r\beta + \frac{2}{r}\partial_r\alpha\Big]e^{2(\alpha-\beta)}, \tag{C.9}$$

$$\mathcal{R}_{rr} = -\Big[\partial_r^2\alpha + (\partial_r\alpha)^2 - \partial_r\alpha\partial_r\beta - \frac{2}{r}\partial_r\beta\Big] + \Big[\partial_t^2\beta + (\partial_t\beta)^2 - \partial_t\alpha\partial_t\beta\Big]e^{2(\beta-\alpha)}, \tag{C.10}$$

$$\mathcal{R}_{\theta\theta} = 1 + \Big[r\partial_r(\beta-\alpha) - 1\Big]e^{-2\beta}, \tag{C.11}$$

$$\mathcal{R}_{\phi\phi} = \left\{1 + \Big[r\partial_r(\beta-\alpha) - 1\Big]e^{-2\beta}\right\}\sin^2\theta, \tag{C.12}$$

$$\mathcal{R}_{rt} = \frac{2}{r}\partial_t\beta. \tag{C.13}$$

These expressions constitute all non-vanishing components of the Ricci tensor. The equations of motion can therefore be obtained by imposing that each of these components vanishes. Immediately, from the rt-equation, we see that $\beta = \beta(r)$, so the rr and tt equations reduce to:

$$\left.\begin{aligned}
\partial_r^2\alpha + (\partial_r\alpha)^2 - \partial_r\alpha\partial_r\beta + \tfrac{2}{r}\partial_r\alpha = 0\\
\partial_r^2\alpha + (\partial_r\alpha)^2 - \partial_r\alpha\partial_r\beta - \tfrac{2}{r}\partial_r\beta = 0
\end{aligned}\right\} \implies \quad \partial_r\alpha = -\partial_r\beta. \tag{C.14}$$

By employing this result in the $\theta\theta$-equation, we obtain:

$$2r\frac{\mathrm{d}\beta}{\mathrm{d}r} - 1 = -e^{2\beta} \implies r\frac{\mathrm{d}e^{-2\beta}}{\mathrm{d}r} + e^{-2\beta} = 1 \implies \frac{\mathrm{d}}{\mathrm{d}r}\left(re^{-2\beta}\right) = 1 \implies e^{2\beta} = \frac{1}{1-\frac{C}{r}}, \tag{C.15}$$

where C is the integration constant. It remains to be verified whether this solution satisfies the rr-equation. A direct calculation shows that it is indeed satisfied for an arbitrary constant C. The only task left is to determine $\alpha(r,t)$. Since we have $\partial_r \alpha = -\partial_r \beta$, we conclude:

$$\alpha(t,r) = -\beta(r) + f(t) \quad \Longrightarrow \quad e^{2\alpha(t,r)}\mathrm{d}t^2 = e^{-2\beta(r)}\mathrm{d}t'^2, \quad \text{where} : \ \frac{\mathrm{d}t'}{\mathrm{d}t} = e^{f(t)}. \tag{C.16}$$

With this, we have completely eliminated the time dependence from the metric. This means that we have indeed obtained a static solution, as expected, i.e. a family of solutions depending on the constant C. It is clear that this constant must be related to the mass of the matter around which we sought the solution. In order to determine this relation, it is necessary to compute the non-relativistic limit of the Einstein equations. We do not perform that calculation here. It turns out that the non-relativistic gravitational potential can be identified with the quantity $\phi(r) = -\frac{1}{2}h_{00}$, where $g_{\mu\nu} = \eta_{\mu\nu} + h_{\mu\nu}$, representing the expansion around the flat spacetime metric $\eta_{\mu\nu}$. Since we know that in the non-relativistic case the following holds:

$$\phi(r) = -G\frac{M}{r} \quad \Longrightarrow \quad -\frac{1}{2}h_{00}(r) = -\frac{C}{2r} = -\frac{GM}{r} \quad \Longrightarrow \quad C = 2GM. \tag{C.17}$$

Therefore, the spacetime around a static, spherically symmetric mass distribution is given by the following metric:

$$\mathrm{d}s^2 = -\left(1 - \frac{2GM}{r}\right)\mathrm{d}t^2 + \frac{\mathrm{d}r^2}{1 - \frac{2GM}{r}} + r^2\left(\mathrm{d}\theta^2 + \sin^2\theta \mathrm{d}\phi^2\right). \tag{C.18}$$

C.2 Singularity

The most important concept related to black holes is the singularity. The first thing we notice when examining the metric from the previous section (Equation (C.18)) is that it diverges at $r = 0$ and at $r = 2GM$. We are interested in whether these are true singularities or merely coordinate singularities. To answer this question, it is necessary to determine invariants under diffeomorphisms (i.e., coordinate transformations). Two invariants are already known:

$$\mathcal{R} = g^{\mu\nu}\mathcal{R}_{\mu\nu} = 0 \quad \wedge \quad \mathcal{R}^{\mu\nu}\mathcal{R}_{\mu\nu} = 0. \tag{C.19}$$

Neither of these two invariants diverges at $r = 0$ or at $r = 2GM$. One invariant still remains to be determined, namely $\mathcal{R}^{\mu\nu\rho\sigma}\mathcal{R}_{\mu\nu\rho\sigma}$. In order to compute it, we first need to evaluate the components of the Riemann curvature tensor, which in turn requires the Christoffel symbols. Based on the formulas C.7 from the previous section, for the Christoffel symbols we obtain:

$$\begin{aligned}
&\Gamma^r_{tt} = \left(1 - \frac{2GM}{r}\right)\frac{GM}{r^2}, \quad \Gamma^r_{\theta\theta} = 2GM - r, \quad \Gamma^r_{\phi\phi} = (2GM - r)\sin^2\theta, \\
&\Gamma^r_{rr} = -\frac{1}{1 - \frac{2GM}{r}}\frac{GM}{r^2}, \quad \Gamma^t_{rt} = \frac{1}{1 - \frac{2GM}{r}}\frac{GM}{r^2}, \\
&\Gamma^\theta_{r\theta} = \frac{1}{r}, \quad \Gamma^\phi_{r\phi} = \frac{1}{r}, \quad \Gamma^\theta_{\phi\phi} = -\sin\theta\cos\theta, \quad \Gamma^\phi_{\theta\phi} = \cot\theta.
\end{aligned} \tag{C.20}$$

All other Christoffel symbols vanish. The next step is to compute the components of the Riemann tensor. Using:

$$\mathcal{R}^\rho{}_{\mu\sigma\nu} = \partial_\sigma\Gamma^\rho_{\mu\nu} - \partial_\nu\Gamma^\rho_{\mu\sigma} + \Gamma^\rho_{\alpha\sigma}\Gamma^\alpha_{\mu\nu} - \Gamma^\rho_{\nu\alpha}\Gamma^\alpha_{\mu\sigma}, \tag{C.21}$$

we obtain:

$$\begin{aligned}
\mathcal{R}^{\theta}{}_{t\theta t} &= \mathcal{R}^{\phi}{}_{t\phi t} = \left(1-\frac{2GM}{r}\right)\frac{GM}{r^3}, & \mathcal{R}^{r}{}_{trt} &= -\left(1-\frac{2GM}{r}\right)\frac{2GM}{r^3}, \\
\mathcal{R}^{\theta}{}_{r\theta r} &= \mathcal{R}^{\phi}{}_{r\phi r} = -\frac{1}{1-\frac{2GM}{r}}\frac{GM}{r^3}, & \mathcal{R}^{t}{}_{rtr} &= \frac{1}{1-\frac{2GM}{r}}\frac{2GM}{r^3}, \\
\mathcal{R}^{t}{}_{\theta t\theta} &= \mathcal{R}^{r}{}_{\theta r\theta} = -\frac{GM}{r}, & \mathcal{R}^{\phi}{}_{\theta\phi\theta} &= \frac{2GM}{r}, \\
\mathcal{R}^{t}{}_{\phi t\phi} &= \mathcal{R}^{r}{}_{\phi r\phi} = -\frac{GM}{r}\sin^2\theta, & \mathcal{R}^{\theta}{}_{\phi\theta\phi} &= \frac{2GM}{r}\sin^2\theta.
\end{aligned} \tag{C.22}$$

Since we know that $\mathcal{R}_{\mu\nu} = 0$, we see that the above components of the Riemann tensor are consistent. We can now determine the remaining invariant:

$$\mathcal{R}^{\mu\nu\rho\sigma}\mathcal{R}_{\mu\nu\rho\sigma} = \frac{48(GM)^2}{r^6}. \tag{C.23}$$

We observe that this quantity diverges at $r = 0$. Since this is an invariant under coordinate transformations, it must diverge in all coordinate systems, and we therefore conclude that $r = 0$ is a true singularity. Later we shall see what this implies. On the other hand, $r = 2GM$ is not a true singularity, but rather a coordinate singularity. This means that there exist coordinates in which this is not a singularity. Later we shall see that these are the Kruskal coordinates. Let us note that when we take the limit $r \to \infty$, the metric becomes the Minkowski spacetime metric. This implies that our spacetime is asymptotically flat. We conclude:

The Schwarzschild metric describes an asymptotically flat spacetime with a singularity at $r = 0$. The quantity $r_s = 2GM$ is called the Schwarzschild radius.

With the Christoffel symbols and the components of the Riemann curvature tensor, one can compute the geodesics as well as the geodesic deviation equation. However, we shall not pursue this here, since they are not of relevance for the thermodynamics of black holes.

C.3 The maximally extended Schwarzschild solution

In this section, we present a systematic procedure for constructing the maximally extended spacetime. Within this framework, the complete causal structure of the spacetime is rendered explicitly manifest. This requirement implies that our overarching objective is to identify a coordinate system in which null geodesics propagate at a constant angle of 45° at every point in spacetime. In other words, the light cones appear as they do in Minkowski space. However, the analysis becomes considerably more complicated once we impose the requirement that the metric remain regular over the entire spacetime, with the sole exception of the point $r = 0$.

First, we resolve the problem of the causal structure. Light rays propagate along hypersurfaces of null type. Let us consider radial light rays. This corresponds to fixing the angular coordinates θ and ϕ to prescribed constant values. Under these conditions, we obtain:

$$\mathrm{d}s^2 = 0 \iff -\left(1-\frac{2GM}{r}\right)\mathrm{d}t^2 + \frac{\mathrm{d}r^2}{1-\frac{2GM}{r}} = 0 \implies \frac{\mathrm{d}t}{\mathrm{d}r} = \pm\frac{1}{1-\frac{2GM}{r}}. \tag{C.24}$$

Here, $\pm$ denotes incoming and outgoing light rays. By solving this equation, we obtain:

$$t = \pm\left[r + 2GM\ln\left(\frac{r}{2GM}-1\right)\right] + \mathit{const}. \tag{C.25}$$

In Figure C.1, the graphs of the functions defined in Equation (C.25) are presented. The figure clearly illustrates that, as one approaches the hypersurface $r = 2GM$, the corresponding light cones become progressively narrower, and in the limit $r \to 2GM$, they degenerate and effectively close at $r = 2GM$. The cones illustrate the causal connection between the future and the past. As we approach $r = 2GM$, we obtain progressively less information, until ultimately at $r = 2GM$ we can no longer distinguish between future and past.

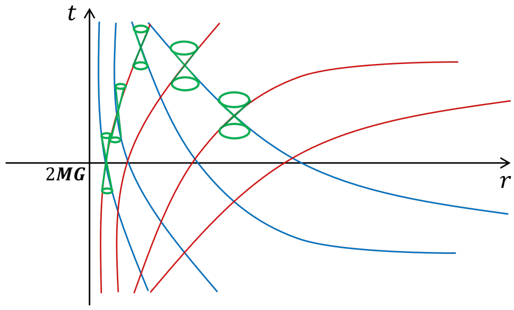

Figure C.1: Closing of light cones in (t, r) coordinates

Because the spacetime under consideration is static, it necessarily admits a timelike Killing vector. This Killing vector field is explicitly given by $\xi = \partial_t$. This implies that the time coordinate must remain fixed. Consequently, we infer that the spatial coordinate has to be redefined in order to obtain light cones that are inclined at an angle of 45° throughout the entire spacetime. To achieve this, we introduce the tortoise coordinate in the following way:

$$\mathrm{d}s^2 = \left(1 - \frac{2GM}{r}\right)\left(-\mathrm{d}t^2 + \frac{\mathrm{d}r^2}{\left(1-\frac{2GM}{r}\right)^2}\right) + r^2\mathrm{d}\Omega^2 \equiv \left(1 - \frac{2GM}{r}\right)\left(-\mathrm{d}t^2 + \mathrm{d}r_*^2\right) + r^2\mathrm{d}\Omega^2. \tag{C.26}$$

From this expression, we observe that the quantity r_* is defined by:

$$\frac{\mathrm{d}r_*}{\mathrm{d}r} = \frac{\mathrm{d}r}{1-\frac{2GM}{r}} \quad \Longrightarrow \quad r_* = r + 2GM \ln\left|\frac{r}{2GM} - 1\right|. \tag{C.27}$$

Observe that this coordinate (with the absolute value) is well-defined both for $r > 2GM$ and for $r < 2GM$. Consequently, the manifold decomposes into two coordinate patches: one covering the region $r > 2GM$ and the other covering the region $r < 2GM$. It therefore follows that:

$$\mathrm{d}s^2 = 0 \quad \Longrightarrow \quad \frac{\mathrm{d}t}{\mathrm{d}r_*} = 0 \quad \Longrightarrow \quad t = r_* + const, \tag{C.28}$$

that is, we have determined that the light cones exhibit precisely the same structure as in Minkowski spacetime. Nevertheless, the requirement of metric regularity over the entire spacetime, except at $r = 0$, has not been achieved. The problematic hypersurface at $r = 2GM$ persists; however, under the tortoise coordinate transformation it is mapped to $r_* \to -\infty$. To proceed, we introduce the Eddington–Finkelstein coordinates, which provide an adapted description of outgoing and ingoing null geodesics in the (t, r_*) coordinate system. These coordinates are defined by:

$$\sigma^{\pm} = t \pm r_* \quad \Longrightarrow \quad \mathrm{d}s^2 = -\left(1 - \frac{2GM}{r}\right)\mathrm{d}\sigma^+\mathrm{d}\sigma^- + r^2\left(\mathrm{d}\theta^2 + \sin^2\theta\mathrm{d}\phi^2\right). \tag{C.29}$$

Let us first move to the (σ^+, r) coordinates. In these coordinates, the metric is given by:

$$\mathrm{d}s^2 = -\left(1 - \frac{2GM}{r}\right)\mathrm{d}\sigma^{+2} + 2\mathrm{d}\sigma^+\mathrm{d}r + r^2(\mathrm{d}\theta^2 + \sin^2\theta\mathrm{d}\phi^2). \tag{C.30}$$

The light cones now satisfy the following equations:

$$\mathrm{d}s^2 = 0 \qquad \Longrightarrow \qquad \frac{\mathrm{d}\sigma^+}{\mathrm{d}r} = 0 \quad \wedge \quad \frac{\mathrm{d}\sigma^+}{\mathrm{d}r} = \frac{2}{1 - \frac{2GM}{r}}. \tag{C.31}$$

The left equation corresponds to incoming light rays (blue in Figure C.2), while the right equation corresponds to outgoing light rays (red in the figure). Let us immediately note that by introducing these coordinates we have resolved the problem of two charts that arose when using the coordinate r_*. From the figure it is clear that a freely falling observer can transmit information about their position as long as they have not yet reached $r = 2GM$. However, for $r < 2GM$, all timelike (and even null) trajectories are directed toward the singularity.

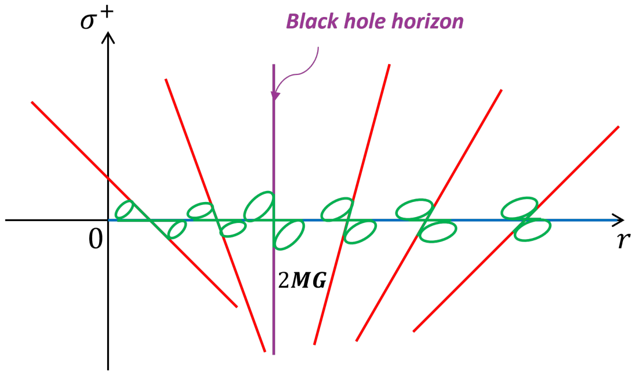

Figure C.2: Light cones in (σ^+, r) coordinates.

We conclude that once particles enter the region $r < 2GM$, they can no longer change their direction and return. Their future becomes uniquely determined. The spatial coordinate r behaves as a temporal coordinate. All particles inevitably end up at the singularity. Let us note that for $r < 2GM$ it is not even possible to remain at a fixed r. For this reason, the surface $r = 2GM$ is called the future event horizon. Since even light cannot escape the region bounded by this event horizon, we cannot know what occurs within this domain. It is precisely by this property that black holes received their name. The singularity at $r = 0$ is called the black hole singularity. Let us now move to the (σ^-, r) coordinates. In these coordinates, the metric is given by:

$$\mathrm{d}s^2 = -\left(1 - \frac{2GM}{r}\right)\mathrm{d}\sigma^{-2} - 2\mathrm{d}\sigma^-\mathrm{d}r + r^2(\mathrm{d}\theta^2 + \sin^2\theta\mathrm{d}\phi^2). \tag{C.32}$$

$$\mathrm{d}s^2 = 0 \quad \implies \quad \frac{\mathrm{d}\sigma^-}{\mathrm{d}r} = 0 \quad \wedge \quad \frac{\mathrm{d}\sigma^-}{\mathrm{d}r} = -\frac{2}{1 - \frac{2GM}{r}}. \tag{C.33}$$

In (σ^-, r) coordinates, the left equation represents outgoing rays, while the right equation represents incoming rays. We see that now a freely falling observer can transmit information about their position even when located in the region $r < 2GM$. On the other hand, they cannot send information toward the singularity! We conclude that the past of all particles that were located in the region $r < 2GM$ is the singularity. In the region $r > 2GM$, the observer can move in both directions along the r-axis, just as in the previous choice of coordinates.

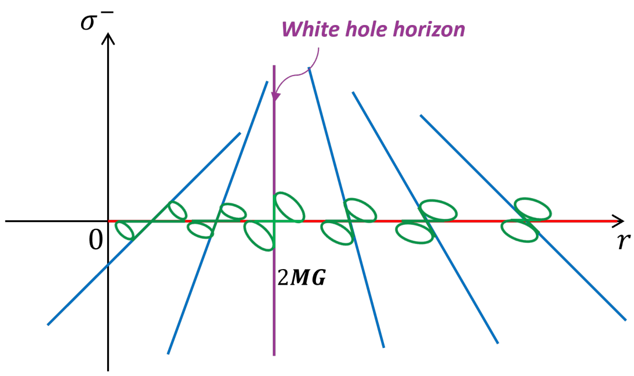

Figure C.3: Light cones in (σ^-, r) coordinates.

For the reasons stated above, the surface $r = 2GM$ is, in this case, called the past event horizon, while the singularity at $r = 0$ is referred to as the white hole singularity. This is not a phenomenon that occurs in nature. It merely represents another possible choice of coordinates.

Thus far, to the asymptotically flat region characterized by $r > 2GM$ we have appended both the white-hole and black-hole. However, this construction does not yet correspond to the maximally extended Schwarzschild solution. The maximally extended solution is realized when every geodesic can either be continued up to the maximal value of its affine parameter or else terminates at the singularity. In the coordinate chart defined by (t, r), this requirement is not satisfied. The coordinate t spans the entire real line, $-\infty < t < \infty$, whereas the radial coordinate r is restricted to the domain $2GM < r < \infty$. For the case of (σ^+, r) and (σ^-, r), this issue has been fully addressed. Nonetheless, it turns out that there exists an additional, distinct asymptotically flat region.

In the (σ^+, σ^-) coordinates we still encounter a problem. This is evident because the r_* coordinate behaves differently in the regions $r > 2GM$ and $r < 2GM$, so the coordinates σ^+ and σ^- span the entire range of values in both regions. What we seek are coordinates $x^\pm = x^\pm(\sigma^\pm)$ in which the metric is regular everywhere except at point $r = 0$, and which vary from $-\infty$ to ∞ across the entire spacetime. For this purpose, let us consider a transformation of the form:

$$\mathrm{d}x^+\mathrm{d}x^- = \begin{cases} e^{\frac{r_*}{2GM}}\mathrm{d}\sigma^+\mathrm{d}\sigma^-, & r > 2GM, \\ -e^{\frac{r_*}{2GM}}\mathrm{d}\sigma^+\mathrm{d}\sigma^-, & r < 2GM. \end{cases} \tag{C.34}$$

In Appendix B we shall explain why we choose a transformation of this type. After performing the calculation, in both cases we obtain the same metric, which is given by the following expression:

$$\mathrm{d}s^2 = -\frac{2GM}{r}e^{-\frac{r}{2GM}}\mathrm{d}x^+\mathrm{d}x^- + r^2\left(\mathrm{d}\theta^2 + \sin^2\theta\mathrm{d}\phi^2\right). \tag{C.35}$$

We observe that this metric is indeed regular everywhere except at $r = 0$. It has the same form for both $r < 2GM$ and $r > 2GM$, and the light cones are identical to those in Minkowski space! It remains to be verified whether the coordinates $x^\pm$ span precisely the interval $(-\infty, \infty)$. If this holds, we have obtained the maximally extended Schwarzschild solution.

1. First, we observe the case when $r > 2GM$. We can make two choices

$$\mathrm{d}x^+\mathrm{d}x^- = \left(e^{-\frac{\sigma^-}{4GM}}\mathrm{d}\sigma^-\right)\left(e^{\frac{\sigma^+}{4GM}}\mathrm{d}\sigma^+\right) \implies \frac{x^+}{4GM} = e^{\frac{\sigma^+}{4GM}} \quad \wedge \quad \frac{x^-}{4GM} = -e^{-\frac{\sigma^-}{4GM}}, \tag{C.36}$$

$$\mathrm{d}x^+\mathrm{d}x^- = \left(-e^{-\frac{\sigma^-}{4GM}}\mathrm{d}\sigma^-\right)\left(-e^{\frac{\sigma^+}{4GM}}\mathrm{d}\sigma^+\right) \implies \frac{x^+}{4GM} = -e^{\frac{\sigma^+}{4GM}} \quad \wedge \quad \frac{x^-}{4GM} = e^{-\frac{\sigma^-}{4GM}}. \tag{C.37}$$

First case matches: $x^+ \in (0, \infty)$ i $x^- \in (-\infty, 0)$ (I quadrant), while the second case matches: $x^+ \in (-\infty, 0)$ i $x^- \in (0, \infty)$ (II quadrant).

2. Now, we observe the first case: $r < 2GM$. Again, we can make two choices:

$$\mathrm{d}x^+\mathrm{d}x^- = \left(-e^{-\frac{\sigma^-}{4GM}}\mathrm{d}\sigma^-\right)\left(e^{\frac{\sigma^+}{4GM}}\mathrm{d}\sigma^+\right) \implies \frac{x^+}{4GM} = e^{\frac{\sigma^+}{4GM}} \quad \wedge \quad \frac{x^-}{4GM} = e^{-\frac{\sigma^-}{4GM}}, \tag{C.38}$$

$$\mathrm{d}x^+\mathrm{d}x^- = \left(e^{-\frac{\sigma^-}{4GM}}\mathrm{d}\sigma^-\right)\left(-e^{\frac{\sigma^+}{4GM}}\mathrm{d}\sigma^+\right) \implies \frac{x^+}{4GM} = -e^{\frac{\sigma^+}{4GM}} \quad \wedge \quad \frac{x^-}{4GM} = -e^{-\frac{\sigma^-}{4GM}}. \tag{C.39}$$

First case matches: $x^+ \in (0, \infty)$ i $x^- \in (0, \infty)$ (III quadrant), while the second case matches: $x^+ \in (-\infty, 0)$ i $x^- \in (-\infty, 0)$ (IV quadrant).

We see that with this transformation we have successfully achieved that the coordinates $x^{\pm}$ precisely cover the entire two-dimensional plane. The coordinates derived in this section are called the Kruskal coordinates. In them, the maximally extended Schwarzschild solution is given.

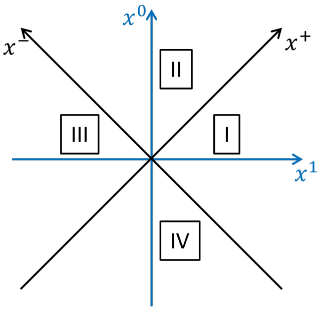

Figure C.4: Regions of spacetime diagrams.

Now we wish to draw the $t =$ const. and $r = \sigma =$ const. curves on the spacetime diagram:

$$\frac{x^0}{x^1} = \tanh\left(\frac{t}{4GM}\right) = \text{const.}$$

$$(x^1)^2 - (x^0)^2 = f(r) = \text{const.},$$

in regions I and III.

$$(x^0)^2 - (x^1)^2 = f'(r) = \text{const.},$$

in regions II and IV. The lines of constant r are hyperbolas, while the lines of constant t are straight lines passing through the coordinate origin.

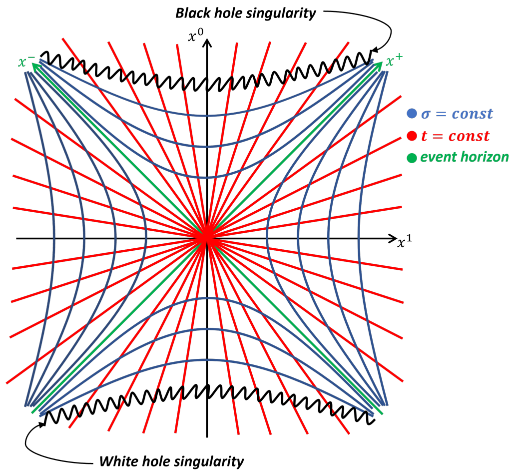

Figure C.5: Kruskal diagram.

We have two asymptotically flat regions: I and III, and two regions with singularities: II (the black hole singularity) and IV (the white hole singularity). The singularity lines $r = 0$ represent the outermost hyperbola in regions I and III, and are given by:

$$(x^0)^2 - (x^1)^2 = (4GM)^2 \quad \Longleftrightarrow \quad x^+x^- = (4GM)^2 \tag{C.40}$$

The event horizons are determined by $x^+ = 0$ and $x^- = 0$.

C.4 Conformal diagram

Conformal or Penrose diagrams represent spacetime diagrams constructed by means of a coordinate transformation that satisfies the following two conditions:

1. The causal structure of spacetime is visible in the diagram. This means that the light cones is oriented at an angle of 45°.

2. Spacetime is compactified, so that infinity becomes a finite boundary on the diagram. The complete structure of spacetime is thus represented.

In order to satisfy the second condition, coordinate transformations involving inverse trigonometric functions are usually employed. We shall now construct the conformal diagram for the static Schwarzschild black hole. We begin with the metric of the maximally extended Schwarzschild solution, expressed in the Kruskal coordinates $x^{\pm}$, which we derived in the previous section. We compactify the coordinates in the following manner:

$$\frac{X^+}{4GM} = \arctan\left(\frac{x^+}{4GM}\right) \quad \wedge \quad \frac{X^-}{4GM} = \arctan\left(\frac{x^-}{4GM}\right). \tag{C.41}$$

Since we know that the coordinates $x^{\pm}$ had the domain $(-\infty, \infty)$, the new coordinates $X^{\pm}$ have the domain $(-2\pi GM, 2\pi GM)$. In this way, the second condition is satisfied. We now express the metric in these coordinates and obtain:

$$\mathrm{d}s^2 = -\frac{2GM}{r} e^{-\frac{r}{2GM}} \frac{\mathrm{d}X^+ \mathrm{d}X^-}{\cos^2\left(\frac{X^+}{4GM}\right)\cos^2\left(\frac{X^-}{4GM}\right)} + r^2\left(\mathrm{d}\theta^2 + \sin^2\theta \mathrm{d}\phi^2\right). \tag{C.42}$$

From this metric we see that the causal structure has been preserved. In this way, both conditions are satisfied. Let us now determine where the singularity line lies on this diagram:

$$x^+x^- = (4GM)^2 \quad \Longleftrightarrow \quad \tan\left(\frac{X^+}{4GM}\right)\tan\left(\frac{X^-}{4GM}\right) = 1. \tag{C.43}$$

By using the trigonometric formula for the tangent of the sum of two angles, we obtain:

$$\tan\left(\frac{X^+ + X^-}{4GM}\right) = \frac{\tan\left(\frac{X^+}{4GM}\right) + \tan\left(\frac{X^-}{4GM}\right)}{1 - \tan\left(\frac{X^+}{4GM}\right)\tan\left(\frac{X^-}{4GM}\right)} \to \infty. \tag{C.44}$$

Since this quantity diverges, and the tangent function diverges when its argument equals $\pm\frac{\pi}{2}$, we conclude that the singularities of the black hole and the white hole are respectively given by:

$$X^+ + X^- = \pm 2\pi GM. \tag{C.45}$$

For the hypersurfaces $r =$ const. and $t =$ const. we have the following relations:

$$r = const. \quad \Longleftrightarrow \quad x^+x^- = const. \quad \Longrightarrow \quad \tan\left(\frac{X^+}{4GM}\right)\tan\left(\frac{X^-}{4GM}\right) = const., \tag{C.46}$$

$$t = const. \quad \Longleftrightarrow \quad \frac{x^+ - x^-}{x^+ + x^-} = const. \quad \Longrightarrow \quad \frac{\tan\left(\frac{X^+}{4GM}\right) - \tan\left(\frac{X^-}{4GM}\right)}{\tan\left(\frac{X^+}{4GM}\right) + \tan\left(\frac{X^-}{4GM}\right)} = const. \tag{C.47}$$

It is evident that the future null infinity, in the right asymptotically flat region $\mathcal{J}^+$, is obtained when $x^+ \to \infty$, which corresponds to $X^+ = 2\pi GM$. Analogously, the past null infinity $\mathcal{J}^-$ is obtained when $x^- \to -\infty$, i.e. $X^- = -2\pi GM$. At the intersection of these two hypersurfaces lies the point i^0, which represents spatial infinity. This is the point $(2\pi GM, -2\pi GM)$. The future timelike infinity i^+ is located at the intersection of the black hole singularity line and $\mathcal{J}^+$. This is the point $(2\pi GM, 0)$. Meanwhile, the past timelike infinity i^- lies at the intersection of the white hole singularity line and $\mathcal{J}^-$, i.e. at the point $(0, -2\pi GM)$. All of this follows from the above equations for $r =$ const. and $t =$ const.. So far, we have only considered the right asymptotically flat region. In the left asymptotically flat region, the entire structure is obtained by a mirror reflection with respect to the axis $X^+ + X^- =$ const.. The conformal diagram is shown in the figure below. The past and future event horizons correspond to $x^+ = 0$ and $x^- = 0$, which in the conformal diagram correspond to the hypersurfaces $X^+ = 0$ and $X^- = 0$.

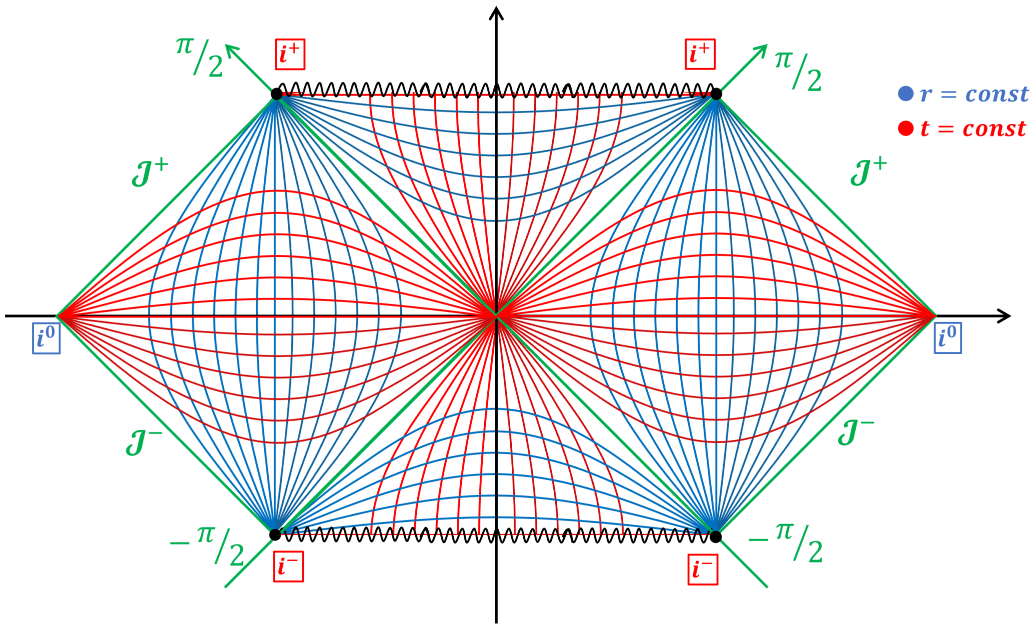

Figure C.6: Conformal diagram of the maximally extended Schwarzschild solution.

On this conformal diagram, as on the Kruskal diagram, it is evident that crossing the future event horizon necessarily leads to an inevitable end in the singularity!

By maximally extending the Schwarzschild solution we obtain a region corresponding to the black hole, a region corresponding to the white hole, our asymptotically flat universe, and another asymptotically flat universe connected to ours through a wormhole passing through the point $(0, 0)$ on the conformal diagram. What we know, however, is that this does not exist in nature. We are then led to ask: What does the conformal diagram of gravitational collapse look like?

If objects in the universe do not evolve, then nothing interesting happens, and spacetime appears as Minkowski space. However, this is not the case. Let us consider a star. Throughout its lifetime, it burns nuclear fuel and in this way generates nuclear pressure. This pressure is in equilibrium with the gravitational pressure for most of the star's life. However, toward the end of its lifetime, the star exhausts its nuclear fuel, and the gravitational pressure becomes increasingly stronger. As the gravitational attraction intensifies, gravitational collapse occurs. This event involves the reduction of the star's radius due to its own gravity. It is accompanied by an explosion in which the outer layers of the star's mass are expelled. If the mass exceeds a certain limit, gravitational contraction proceeds below the Schwarzschild radius. As a result, a singularity forms and the star becomes a black hole.

All that we have described can be represented on the portion of the conformal diagram of the maximally extended Schwarzschild solution corresponding to the right asymptotically flat region and the region where the black hole singularity exists. In the figure alongside, the diagram describing gravitational collapse is shown. The region shaded in green represents the domain in which matter undergoes collapse. The Schwarzschild solution is valid in the region outside the domain where matter exists. This diagram contains an additional part that we do not expect based on the Schwarzschild conformal diagram. It is the region that appears after the singularity disappears.

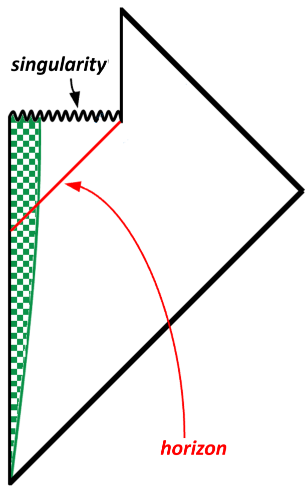

Figure C.7: Conformal diagram depicting a Schwarzschild black hole formed via the gravitational collapse of a star.

This is the diagram that describes the collapse of a star into a black hole, followed by the evaporation of the black hole. It turns out that, due to quantum corrections, black holes radiate, so that after a very long period of time the black hole will emit all of its mass. The singularity disappears, leaving behind flat Minkowski space.

Appendix D

Quantum fields in curved spacetime

To explain the phenomenon of Hawking radiation, it is necessary to know the basics of quantum field theory in curved spacetime. Since we are dealing with scalar fields, we will carry out everything using the example of scalar fields. In this appendix, for the most part (except in Section D.5), we will follow Chapter 9 of Carroll's book [106].

D.1 Canonical quantization in curved spacetime

First, it is necessary to introduce the Lagrangian–Hamiltonian formalism in curved spacetime. The Lagrangian of a scalar field, obtained by minimal coupling:

$$\partial_\mu \longrightarrow \nabla_\mu, \quad d^4x \longrightarrow d^4x\sqrt{-g}, \quad \eta_{\mu\nu} \longrightarrow g_{\mu\nu}, \tag{D.1}$$

is given by:

$$\mathcal{L} = \sqrt{-g}\left[-\frac{1}{2}g^{\mu\nu}\nabla_\mu\phi\nabla_\nu\phi - \frac{m^2}{2}\phi^2 - \frac{1}{2}\xi\mathcal{R}\phi^2\right]. \tag{D.2}$$

Here we have also added a term that couples the curvature to the scalar field. The interaction constant ξ can take several different values. The case of minimal coupling corresponds to the value: $\xi = 0$. In the case of conformal coupling we have: $\xi = \frac{n-2}{4(n-1)}$. This case represents the situation when the metric is invariant under conformal transformations. The number n denotes the number of dimensions of the space in which we are working. However, in nature neither of these two cases necessarily needs to be satisfied.
Now we continue with the generalization of the Hamiltonian formalism to curved spacetime. The generalized momentum and the Euler–Lagrange equations are generalized in the following way:

$$\pi = \frac{\partial\mathcal{L}}{\partial(\nabla_0\phi)}, \quad \nabla_\mu\frac{\partial\mathcal{L}}{\partial(\nabla_\mu\phi)} - \frac{\partial\mathcal{L}}{\partial\phi} = 0. \tag{D.3}$$

A straightforward computation based on Equations (D.2) and (D.3) yields the following equations of motion:

$$\left(\Box - m^2 - \xi\mathcal{R}\right)\phi = 0. \tag{D.4}$$

We could have arrived at the same result by the classical method of quantum field theory, i.e. by calculating the Euler–Lagrange equations without using the principle of minimal substitution. In order to proceed further, it is necessary first to define the scalar product on the functional space defined over the manifold we are working with. We choose an arbitrary spacelike hypersurface Σ, with the induced metric γ_{ij}, and the unit normal vector n^μ. Now we perform the generalization of the scalar product from flat spacetime:

$$(\phi_1, \phi_2) = -i \int_\Sigma d^{n-1}x \sqrt{\gamma} n^\mu \Big(\phi_1 \nabla_\mu \phi_2^* - \phi_2^* \nabla_\mu \phi_1 \Big). \tag{D.5}$$

This definition of the scalar product is independent of the choice of spacelike hypersurface Σ. That is a necessary condition in order to have a well-defined scalar product. The next step is solving the equation of motion. As in quantum mechanics, this involves finding a complete set of functions that will form the basis of the Hilbert space (defined over our manifold). By analogy with flat space, we would like to have positive-frequency and negative-frequency modes. However, we do not know if this is possible, because we do not know whether we can separate the variables, i.e. separate time from space. If we have a timelike Killing vector, then the system is stationary, and we have a conservation law for energy, so we can define the energies of the modes using it. However, this does not always have to be the case. What we can always find is a complete set of orthogonal solutions, such that the following holds:

$$(\forall i, j \in \mathbb{N}) \;\; (f_i, f_j) = \delta_{ij} \;\; \wedge \;\; (f_i^*, f_j^*) = -\delta_{ij}. \tag{D.6}$$

Notice that for now the index i is discrete. It is easily generalized to the continuous case. Now we can expand the field in terms of the basis functions:

$$\phi = \sum_i \Big[a_i f_i + a_i^\dagger f_i^* \Big]. \tag{D.7}$$

Here we have introduced, for now, the constants a_i and $a_i^\dagger$. The next step is the process of canonical quantization of the scalar field. The procedure is analogous to the case in flat spacetime, except for one small detail concerning the commutator of the field and the field momentum. We impose the equal-time commutation relations in the following way:

$$\Big[\phi(t,\vec{x}), \phi(t,\vec{x}^{\,\prime})\Big] = 0, \;\; \Big[\pi(t,\vec{x}), \pi(t,\vec{x}^{\,\prime})\Big] = 0, \;\; \Big[\phi(t,\vec{x}), \pi(t,\vec{x}^{\,\prime})\Big] = \frac{i\hbar}{\sqrt{-g}} \delta^{(n-1)} \Big(\vec{x} - \vec{x}^{\,\prime} \Big). \tag{D.8}$$

After quantization, the constants a_i and $a_i^\dagger$ become annihilation and creation operators, respectively. By enforcing the canonical commutation relations and utilizing the orthogonality of the basis functions, one recovers the standard commutation relations for the creation and annihilation operators, namely:

$$(\forall i, j \in \mathbb{N}) \;\; [a_i, a_j] = 0 \;\; \wedge \;\; \Big[a_i^\dagger, a_j^\dagger\Big] = 0 \;\; \wedge \;\; \Big[a_i, a_j^\dagger\Big] = 1. \tag{D.9}$$

Now we define the vacuum state associated with this choice of basis functions in the same way as in the case of flat space, and then construct the basis of the Fock space:

$$(\forall i \in \mathbb{N}) \;\; a_i \left|0_f\right\rangle = 0 \quad \Longrightarrow \quad \left|n_1, n_2, ...\right\rangle = \frac{\left(a_1^\dagger\right)^{n_1} \left(a_2^\dagger\right)^{n_2} ...}{\sqrt{n_1! n_2! ...}} \left|0_f\right\rangle. \tag{D.10}$$

Gravity is a theory that is invariant under diffeomorphisms, i.e. under the choice of coordinates. In order to define the basis $\{f_i \mid i \in \mathbb{N}\}$, it is necessary first to choose the coordinates in which we are working, and only then to solve the equation in those coordinates. Any complete set of functions obtained in the same coordinates will define annihilation operators that will annihilate the same vacuum. However, if we now choose new coordinates and solve the equations and define the basis $\{g_i \mid i \in \mathbb{N}\}$ in those coordinates, we obtain a new set of annihilation operators, which will now annihilate a new vacuum $|0_g\rangle$:

$$\phi = \sum_i \left[b_i g_i + b_i^\dagger g_i^*\right] \ \wedge \ (\forall i, j \in \mathbb{N}) \ \ [a_i, a_j] = 0 \ \wedge \ \left[a_i^\dagger, a_j^\dagger\right] = 0 \ \wedge \ \left[a_i, a_j^\dagger\right] = 1$$
$$\implies \ (\forall i \in \mathbb{N}) \ \ b_i |0_g\rangle = 0. \tag{D.11}$$

These two vacuum states are fundamentally different. In gravity, one choice of coordinates defines an observer who lives in those coordinates, while another choice defines another observer. In flat spacetime we only had Lorentz transformations (and not diffeomorphisms), which kept the vacuum invariant. That means that all inertial observers saw the same vacuum. However, now this is no longer the case. Different observers see different vacuum! This is the main feature of quantum field theory in curved spacetime. It means that if one observer sees the vacuum, another may see a particle spectrum. This is precisely the situation that occurs in the Unruh or Hawking effect!

D.2 Bogoliubov transformations

In Section D.1 we saw that for each choice of coordinates we have a different basis. Since all these bases are bases of the same Hilbert space (as we are dealing with a single manifold), there must exist some transformations that take us from one to another. These transformations are called Bogoliubov transformations. We often encounter them in condensed matter physics when considering many-particle systems, where the collective excitations are those observed in experiment. The basic example is the BCS theory of superconductivity. The specific form of the Bogoliubov transformation that connects the g_i modes with the f_i modes (Equation (D.11) and (D.7), respectively) is given by:

$$g_i = \sum_j \left[\alpha_{ij} f_j + \beta_{ij} f_j^*\right], \qquad f_i = \sum_j \left[\alpha_{ji}^* g_j - \beta_{ji} g_j^*\right], \tag{D.12}$$

where α_{ij} and β_{ij} are the Bogoliubov coefficients. It is clear that we can obtain them using the scalar product in the following way:

$$\alpha_{ij} = (g_i, f_j), \qquad \beta_{ij} = -\left(g_i, f_j^*\right). \tag{D.13}$$

From the condition that it is the same field expanded in different bases, the Bogoliubov relations on the modes give us the Bogoliubov relations on the annihilation and creation operators:

$$b_i = \sum_j \left[\alpha_{ij}^* a_j - \beta_{ij}^* a_j^\dagger\right], \qquad b_i^\dagger = \sum_j \left[-\beta_{ij} a_j + \alpha_{ij} a_j^\dagger\right], \tag{D.14}$$
$$a_i = \sum_j \left[\alpha_{ji} b_j + \beta_{ji}^* b_j^\dagger\right], \qquad a_i^\dagger = \sum_j \left[\beta_{ji} b_j + \alpha_{ji}^* b_j^\dagger\right]. \tag{D.15}$$

From the mutual orthogonality of the f-basis and the g-basis, one obtains a set of constraints that the Bogoliubov coefficients are required to satisfy. On the other hand, those same relations guarantee the preservation of the commutation relations between creation and annihilation operators when passing from one set of coordinates to another.

Now we observe how this formalism leads us to the conclusion that different observers see different vacuum. Let observer A live in the coordinates that give the f-basis, while observer B lives in the coordinates that give the g-basis. Let the quantum state be such that observer A sees no particles, i.e. $|\psi\rangle = |0_f\rangle$. We are interested in what observer B sees in this state. Let us determine the expectation values of the occupation numbers associated with the particle spectrum seen by observer B:

$$\begin{aligned}\langle 0_f|\, n_{ig}\, |0_f\rangle = \langle 0_f|\, b_i^\dagger b_i\, |0_f\rangle &= \langle 0_f| \sum_{j,k} \left(-\beta_{ij} a_j + \cancelto{0}{\alpha_{ij} a_j^\dagger}\right)\left(\cancelto{0}{\alpha_{ik}^* a_k} - \beta_{ik}^* a_k^\dagger\right)|0_f\rangle \\ &= \sum_{j,k} \beta_{ij}\beta_{ik}^* \langle 0_f|\, a_j a_k^\dagger\, |0_f\rangle = \sum_{j,k} \beta_{ij}\beta_{ik}^* \delta_{jk} = \sum_j |\beta_{ij}|^2. \end{aligned} \tag{D.16}$$

We arrive at the following result:

$$(\forall i \in \mathbb{N}) \;\; \langle 0_f|\, n_{if}\, |0_f\rangle = 0 \;\; \wedge \;\; \langle 0_f|\, n_{ig}\, |0_f\rangle = \sum_j |\beta_{ij}|^2. \tag{D.17}$$

This relation says: Although observer A does not see any particle spectrum, observer B does see a particle spectrum as long as at least one Bogoliubov coefficient is different from zero! The main question is how we detect these particles. If we have some detector in curved spacetime, we ask how to define positive- and negative-frequency modes associated with it. The simplest answer is to consider:

$$\frac{D}{\mathrm{d}\tau} f_i = -i\omega_i f_i. \tag{D.18}$$

If we can find modes that satisfy this equation, we have solved the problem. However, this may not always be possible! We know that it is certainly possible if the metric is static. Then it can be chosen so that the following conditions are satisfied:

$$\partial_0 g_{\mu\nu} = 0 \qquad \wedge \qquad g_{0i} = 0. \tag{D.19}$$

We write what the $\Box$ operator represents:

$$\Box = g^{00}\partial_0^2 + g^{ij}\partial_i\partial_j - g^{00}\Gamma^i_{00}\partial_i - g^{ij}\Gamma^k_{ij}\partial_k. \tag{D.20}$$

Now we can separate the variables in the Klein–Gordon equation into a temporal part and a spatial part:

$$\partial_0^2\phi = \frac{1}{g^{00}}\left[-g^{ij}\partial_i\partial_j + g^{00}\Gamma^i_{00}\partial_i + g^{ij}\Gamma^k_{ij}\partial_k + m^2 + \xi\mathcal{R}\right]\phi. \tag{D.21}$$

It is now clear that we can introduce the substitution of the type $f_\omega(t,\vec{x}) = e^{-i\omega t}F_\omega(\vec{x})$. In this manner we define the positive-frequency modes. By conjugating this equation we also obtain the negative-frequency modes. Obviously, these modes satisfy the following equation:

$$\partial_0 f_\omega = -i\omega f_\omega \qquad \Longrightarrow \qquad \mathcal{L}_\xi f_\omega = -i\omega f_\omega, \tag{D.22}$$

where the second equation is the coordinate-free expression in which the Killing vector ξ appears. It is clear that, in such a choice of coordinates, it coincides with $\xi = \partial_0$.

D.3 Unruh effect

The Unruh effect represents the phenomenon that a uniformly accelerated observer in the Minkowski vacuum state perceives a particle spectrum at a temperature proportional to the observer's own acceleration. Such an observer is called a Rindler observer. Let us first determine the coordinates in which the Rindler observer lives. Acceleration can only be defined in the observer's own reference frame. Let a denote this acceleration. Since we are in Minkowski space, the relevant question is: How does this acceleration transform under Lorentz transformations? Let us consider a reference frame $S^{'}$ moving along the positive x-axis of the laboratory frame S with velocity u, and let us consider a body moving with velocity $v^{'}$ in the frame $S^{'}$. We know that velocity transforms according to the relativistic velocity addition law:

$$v = \frac{\mathrm{d}x}{\mathrm{d}t} = \frac{\mathrm{d}x^{'} + u\mathrm{d}t^{'}}{\mathrm{d}t' + \frac{u}{c^2}\mathrm{d}x'} = \frac{v^{'} + u}{1 + \frac{uv'}{c^2}}. \tag{D.23}$$

We now determine the law of acceleration transformation (a_l is the acceleration in the laboratory system S):

$$a_l = \frac{\mathrm{d}v}{\mathrm{d}t} = \frac{\mathrm{d}v}{\mathrm{d}v'}\frac{\mathrm{d}v'}{\mathrm{d}t'}\frac{\mathrm{d}t'}{\mathrm{d}t} = a\left(\frac{\sqrt{1-\frac{u^2}{c^2}}}{1+\frac{uv'}{c^2}}\right)^3. \tag{D.24}$$

This is the general law of acceleration transformation under Lorentz transformations. Our problem restricts us to the case when the body does not move in the $S^{'}$ system, since this is the proper system attached to the body. This means that from now on $S^{'}$ is the system moving together with the observer. We then conclude that $u = v$ (the instantaneous velocity of the observer) and $v^{'} = 0$. Therefore:

$$a_l = \frac{a}{\gamma^3} \quad \Longrightarrow \quad \frac{dv}{dt} = a\left(1-\frac{v^2}{c^2}\right)^{\frac{3}{2}} \quad \Longrightarrow \quad v(t) = \frac{at}{\sqrt{1+\left(\frac{at}{c}\right)^2}}. \tag{D.25}$$

This holds under the initial condition $v(0) = 0$. We now determine how the position of the observer changes with time:

$$\frac{\mathrm{d}x}{\mathrm{d}t} = v \quad \Longrightarrow \quad x(t) = \frac{c^2}{a}\left(\sqrt{1+\left(\frac{at}{c}\right)^2} - 1\right) + x_0. \tag{D.26}$$

We now seek the dependence $t(\tau)$, since we want to express everything in terms of the proper time:

$$\frac{\mathrm{d}t}{\mathrm{d}\tau} = \gamma = \frac{1}{\sqrt{1-\frac{v^2}{c^2}}} \quad \Longrightarrow \quad t(\tau) = \frac{c}{a}\sinh\left(\frac{a\tau}{c}\right). \tag{D.27}$$

The initial condition is chosen such that $t(0) = 0$. We can now also express x as a function of the proper time:

$$x(\tau) = \frac{c^2}{a}\sqrt{1+\sinh^2\left(\frac{a\tau}{c}\right)} + x_0 - \frac{c^2}{a} \quad \Longrightarrow \quad x(\tau) = \frac{c^2}{a}\cosh\left(\frac{at}{c}\right) + x_0 - \frac{c^2}{a}. \tag{D.28}$$

The initial condition (or coordinate origin) can be chosen such that $x_0 = \frac{c^2}{a}$. With this choice, in units where $c = 1$, we obtain the following coordinate transformations:

$$t(\tau) = \frac{1}{a}\sinh(a\tau) \quad \wedge \quad x(\tau) = \frac{1}{a}\cosh(a\tau). \tag{D.29}$$

We see that this trajectory is a hyperbola in Minkowski space, parametrized by the proper time:

$$(ax)^2 - (at)^2 = 1. \tag{D.30}$$

An observer moving along a geodesic necessarily ends up in the future timelike infinity. A uniformly accelerated observer does not end up in timelike infinity; instead, their trajectory is tangent to the light cone. Our goal is to switch to coordinates that describe the uniformly accelerated observer. The time coordinate must be tied to the proper time, while in the spatial coordinate the observer should remain at zero, since they do not move in these coordinates. Let us consider the following coordinate transformation:

$$t = \frac{1}{a}e^{a\xi}\sinh(a\eta) \quad \wedge \quad x = \frac{1}{a}e^{a\xi}\cosh(a\eta). \tag{D.31}$$

These coordinates are called Rindler coordinates (η, ξ). We see that the uniformly accelerated observer lies along the trajectory $\xi = 0$, which is exactly what we wanted. The time coordinate $\eta = \tau$ is equal to the proper time of the uniformly accelerated observer.

The domain of these coordinates is $\mathbb{R}$. This means that they are maximally extended. It is evident that this observer has access only to the first quadrant. The light cone determines the boundaries of this region. This observer has two Rindler horizons. The hypersurface $x^+ = 0$ is called the future Rindler horizon, while the hypersurface $x^- = 0$ is called the past Rindler horizon. We see that spacetime in these coordinates strongly resembles the Schwarzschild geometry in region I.

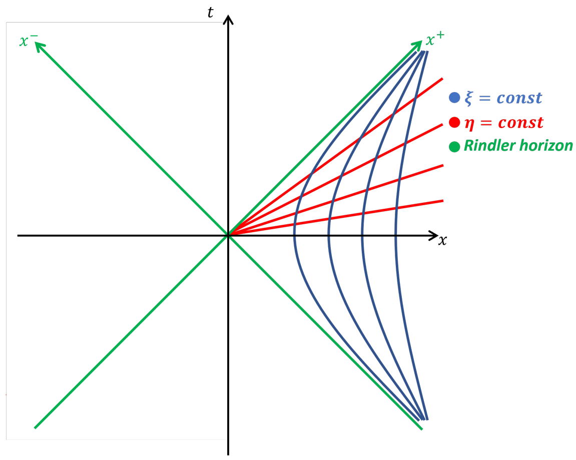

Figure D.1: Constant coordinate hypersurfaces in Rindler coordinates.

From now on we consider the situation as if we are in two dimensions. Let us express the metric in Rindler coordinates:

$$\mathrm{d}s^2 = e^{2a\xi}\left(-\mathrm{d}\eta^2 + \mathrm{d}\xi^2\right). \tag{D.32}$$

We see that the metric does not depend on η. This means that, in these coordinates, we have a Killing vector $K = \partial_\eta$. Let us compute it in the (x, t) coordinates in order to see what it actually represents. After the calculation, we obtain:

$$K = a\left(x\partial_t + t\partial_x\right), \quad K^\mu K_\mu = -e^{2a\xi} = a(t - x). \tag{D.33}$$

We see that this Killing vector is timelike in region I. This is expected, since η is the time coordinate. However, we notice that it becomes spacelike when crossing the Rindler horizons. This means that it represents a Killing horizon. Let us move to the light-cone coordinates $\sigma^{\pm} = \eta \pm \xi$:

$$x^+ = t + x = \frac{1}{a} e^{a\xi} \left[\sinh(a\eta) + \cosh(a\eta)\right] = \frac{1}{a} e^{a(\xi+\eta)} \quad \Longrightarrow \quad ax^+ = e^{a\sigma^+}, \tag{D.34}$$

$$x^- = t - x = \frac{1}{a} e^{a\xi} \left[\sinh(a\eta) - \cosh(a\eta)\right] = -\frac{1}{a} e^{a(\xi-\eta)} \quad \Longrightarrow \quad ax^- = -e^{-a\sigma^-}. \tag{D.35}$$

In Section 8.2.1 we deal specifically with the Rindler observer. In this section we also determined the Bogoliubov coefficients when the quantum state is the Minkowski vacuum, and proved that the Rindler observer sees a particle spectrum in this state. Moreover, it turns out that this is exactly a thermal spectrum at the temperature:

$$T = \frac{\hbar a}{2\pi k_B c}. \tag{D.36}$$

Here we have restored the constants. Indeed, the temperature is proportional to the proper acceleration of the observer. This temperature is detected by the observer located at $x = 0$. We may then ask: what temperature of particles is detected by an observer at an arbitrary ξ? The entire calculation is exactly the same as for the observer located at $\xi = 0$. The only difference lies in his proper acceleration α. Namely, his trajectory should be:

$$t = \frac{1}{\alpha} \sinh\left(\alpha \tau'\right) = \frac{1}{a} e^{a\xi} \sinh(a\eta) \quad \wedge \quad x = \frac{1}{\alpha} \cosh\left(\alpha \tau'\right) = \frac{1}{a} e^{a\xi} \cosh(a\eta), \tag{D.37}$$

where τ' is the proper time of this observer. From here we see his trajectory in the (η, ξ) coordinates:

$$\eta = \frac{\alpha}{a} \tau' \quad \wedge \quad \xi = \frac{1}{a} \ln \frac{a}{\alpha}. \tag{D.38}$$

We conclude that the temperature measured by this observer will be:

$$T' = \frac{\hbar \alpha}{2\pi k_B c} = \frac{\hbar a}{2\pi k_B c} e^{-a\xi} \quad \Longrightarrow \quad T' = T e^{-a\xi}. \tag{D.39}$$

We see that the temperature becomes zero when $\xi \to \infty$. This is expected, since as we approach infinity the hyperbolae become flatter, and we recover Minkowski space. It is necessary to clarify how this is possible. A Minkowski observer does not detect any particles, while a Rindler observer does see a thermal particle spectrum. For the Rindler observer to detect these particles, he must carry a detector with him. In order for the detector to accelerate, it must continuously perform work. From the perspective of the inertial observer, the detector simultaneously absorbs and emits particles, while from the perspective of the Rindler observer it detects particles and undergoes acceleration.

D.4 Event horizon and Kiling horizons

We ask ourselves how to determine the event horizon of a black hole. In Appendix A we did this by observing what happens at $r = 2GM$. However, what should we do if we are given a metric? We ask: does a horizon exist at all? When we have a static, asymptotically flat spacetime with spherical topology, there exist coordinates in which the position of the event horizon can be easily determined. In this case we have a timelike Killing vector ∂_t. Then we can choose the metric such that $\partial_t g_{\mu\nu} = 0$. On each $t =$ const. hypersurface we can choose coordinates (r, θ, ϕ) in which the metric is asymptotically flat. If we have chosen the coordinates wisely, we can imagine a process in which we start from infinity (where the metric is flat) and descend toward the singularity, using the coordinate r. We consider hypersurfaces $r =$ const.. These will be spacelike until some hypersurface $r = r_H$. Beyond it they become timelike hypersurfaces. That hypersurface $r = r_H$ must then everywhere be null (or a $NULL$ hypersurface). If we choose coordinates poorly, it may happen that it is null only in some regions. Beyond it, light cannot escape to infinity. This means that event horizons are $NULL$ hypersurfaces! It is now clear how we can determine the event horizon. We can use the one-form $\partial_\mu r$. It is normal to the hypersurfaces $r =$ const.. At the moment when these hypersurfaces become $NULL$, this vector must itself become $NULL$ (lightlike), i.e.:

$$0 = g^{\mu\nu}\partial_\mu r \partial_\nu r = g^{rr} \quad \Longrightarrow \quad g^{rr}(r_H) = 0. \tag{D.40}$$

In Section D.3 we encountered the notion of Killing horizons. This is a hypersurface along which a certain Killing vector becomes $NULL$. It turns out that every event horizon in a stationary asymptotically flat spacetime is a Killing horizon for some Killing field ξ. If the spacetime is also static (which in two dimensions is always the case), then it is $\xi = \partial_t$. The converse does not hold. Not every Killing horizon must also be an event horizon. As we saw in the previous section, the Rindler horizons are indeed Killing horizons, but they are not event horizons. A Killing horizon is defined by the condition $\xi^\mu \xi_\mu = 0$ on the horizon itself. This means that $\nabla_\nu(\xi^\mu \xi_\mu)$ is a one-form normal to the Killing horizon. On the other hand, we also know that ξ^μ is the normal vector to that horizon. This implies that the following must hold:

$$\nabla_\nu \left(\xi^\mu \xi_\mu\right) = 2\kappa \xi_\nu \quad \Longrightarrow \quad \xi^\mu \nabla_\mu \xi^\nu = -\kappa \xi^\nu, \tag{D.41}$$

where κ is a constant on the Killing horizon. It is called the surface gravity. We shall later see what it represents. By using Frobenius' theorem: $\xi \wedge d\xi = 0$, κ can be easily calculated. One obtains:

$$\kappa^2 = -\frac{1}{2}\nabla^\mu \xi^\nu \nabla_\mu \xi_\nu. \tag{D.42}$$

We assume that this expression is evaluated on the horizon. At first sight, it seems that κ could be arbitrary, since a Killing vector remains a Killing vector even after being multiplied by an arbitrary constant. However, in a static asymptotically flat spacetime the timelike Killing vector can be fixed by the following choice:

$$\xi^\mu \xi_\mu \to -1, \quad \text{when } r \to \infty. \tag{D.43}$$

For a static observer holds that his four-velocity is proportional to the timelike Killing vector. The proportionality coefficient between the Killing vector and the four-velocity of the stationary observer is called the redshift factor, i.e.

$$\xi^\mu = V(x)U^\mu \;\wedge\; U^\mu U_\mu = -1 \quad \Longrightarrow \quad V(x) = \sqrt{-\xi^\mu \xi_\mu}. \tag{D.44}$$

This quantity is called the redshift factor because it relates the photon frequencies measured by a stationary observer at two different positions in space, due to the redshift. Let us consider a photon with four-momentum p^μ. The conserved energy of this photon is defined using the timelike Killing vector, i.e. $E = -\xi^\mu p_\mu$. If we have a stationary observer with four-velocity U^μ, we know that the energy of the photon measured by him is given by: $\omega = -U^\mu p_\mu$. Let us determine the relation between the two photon frequencies measured by stationary observers at different positions in space:

$$\frac{\omega_1}{\omega_2} = \frac{-U_1^\mu p_\mu}{-U_2^\nu p_\nu} = \frac{V(x_2)\xi^\mu p_\mu}{V(x_1)\xi^\nu p_\nu} = \frac{V(x_2)E}{V(x_1)E} = \frac{V(x_2)}{V(x_1)}. \tag{D.45}$$

Let us now determine the expression for the four-acceleration of a stationary observer:

$$\begin{aligned} a^\mu &= \frac{DU^\mu}{d\tau} = \frac{dx^\nu}{d\tau}\nabla_\nu U^\mu = U^\nu \nabla_\nu U^\mu = \frac{\xi^\nu}{V}\nabla_\nu\left(\frac{\xi^\mu}{V}\right) = \xi^\mu\xi^\nu\nabla_\nu\left(\frac{1}{V}\right) + \frac{1}{V^2}\xi^\nu\nabla_\nu\xi^\mu \\ &= \xi^\mu \cancelto{0}{\partial_t\left(\frac{1}{V}\right)} - \frac{1}{V^2}\xi^\nu\nabla^\mu\xi_\nu = -\frac{1}{2V^2}\nabla^\mu\left(\xi^\nu\xi_\nu\right) = \frac{1}{2V^2}\nabla^\mu\left(V^2\right) = \nabla^\mu \ln V. \end{aligned} \tag{D.46}$$

The first equality in the second line holds for two reasons. Since $V(x)$ does not depend on time, the first term is equal to zero. For the second term we applied the Killing equation: $\nabla_\nu \xi^\mu = -\nabla^\mu \xi_\nu$. In the second equation we can apply the defining equation for the surface gravity (D.41):

$$a^\mu = -\frac{1}{2V^2}\nabla^\mu\left(\xi^\nu\xi_\nu\right) = -\frac{\kappa}{V^2}\xi^\mu \quad \Longrightarrow \quad a^2 = -a^\mu a_\mu = \frac{\kappa^2}{V^4}\xi^\mu\xi_\mu = \frac{\kappa^2}{V^2}. \tag{D.47}$$

From this relation we obtain an additional, and conceptually simpler, method for determining the surface gravity:

$$\kappa = aV \quad \wedge \quad \kappa = \sqrt{\nabla^\mu V \nabla_\mu V}. \tag{D.48}$$

We again assume that this expression is evaluated on the horizon. We can now proceed to interpret this result. Let us consider what the expression would represent:

$$a^{'} = \frac{V_1}{V_2}a. \tag{D.49}$$

This expression represents the acceleration measured by the observer at position 2, if the observer at position 1 measures an acceleration a. In our case we have $V_1 = V$, the value of the redshift factor on the horizon, while $V_2 = 1$. According to Equation (D.43), this holds at infinity. We can therefore conclude what the surface gravity physically represents:

In a static, asymptotically flat spacetime, the surface gravity represents the acceleration of a static observer in the vicinity of the event horizon, as measured by an observer at infinity.

For this statement to be valid, the spacetime must be static. Otherwise, the surface gravity defined on the horizon does not admit this interpretation. In the stationary case we still have a timelike Killing vector, but the difficulty arises from the fact that it is not $NULL$ on the event horizon, but rather on a hypersurface outside of it. This hypersurface is called the ergosurface. The event horizon remains a Killing horizon, but now with respect to a linear combination of the two Killing vectors present in this case: $\partial_t + \Omega_H \partial_\phi$. The quantity Ω_H is referred to as the angular velocity of the horizon. We shall not pursue stationary non-static solutions further, since in two dimensions all stationary solutions are also static.

D.5 Regularity of the metric at the horizon

Since we know that the singularity at $r = 2GM$, in the case of the Schwarzschild black hole, is merely a coordinate singularity, there must exist coordinates that are regular on this hypersurface (see Appendix C.3). We shall now demonstrate that, at the moment of crossing below the event horizon, a radially freely falling observer does not perceive anything special. We will show that this holds in the case of a static spacetime with spherically symmetric topology (since such spacetimes are almost always considered in $2D$). Let the metric be the most general:

$$ds^2 = g_{tt}dt^2 + g_{rr}dr^2 + r^2\left(d\theta^2 + \sin^2\theta d\phi^2\right). \tag{D.50}$$

We assume that the following holds: $g_{tt} = g_{tt}(r)$ and $g_{rr} = g_{rr}(r)$. Let us now demonstrate that any such metric can be written so that the relation $g_{tt} = -g^{rr}$ is satisfied:

$$ds^2 = g_{tt}\left(dt^2 + \frac{g_{rr}}{g_{tt}}dr^2\right) + r^2 d\Omega^2 = g_{tt}\left(dt^2 + \frac{dr^{'2}}{g_{tt}^2}\right) + r^2 d\Omega^2. \tag{D.51}$$

In this way we have defined the transformation of the radial coordinate: $r^{'} = r^{'}(r)$:

$$\frac{g_{rr}}{g_{tt}}dr^2 = \frac{dr^{'2}}{g_{tt}^2} \quad \Longrightarrow \quad \frac{dr^{'}}{dr} = \sqrt{g_{rr}g_{tt}}. \tag{D.52}$$

Since we have reduced the problem to an integral, we may assume that the metric satisfies $g_{tt} = -g^{rr}$. From the previous section we know that the horizon is determined by the equation $g^{rr}(r_H) = 0$. Let us expand the metric around this coordinate value, i.e. $r = r_H + \varepsilon$:

$$\begin{aligned}
\mathrm{d}s^2 &= \left(\cancelto{0}{g_{tt}(r_H)} + \partial_r g_{tt}(r_H)\varepsilon\right)\mathrm{d}t^2 + \frac{\mathrm{d}\varepsilon^2}{\cancelto{0}{g^{rr}(r_H)} + \partial_r g^{rr}(r_H)\varepsilon} + f(\varepsilon)\mathrm{d}\Omega^2 \\
&= \partial_r g_{tt}(r_H)\varepsilon\mathrm{d}t^2 + \frac{\mathrm{d}\varepsilon^2}{\partial_r g^{rr}(r_H)\varepsilon} + f(\varepsilon)\mathrm{d}\Omega^2.
\end{aligned} \tag{D.53}$$

We now introduce a new coordinate ρ, defined such that the following relation holds:

$$\mathrm{d}\rho^2 = \frac{\mathrm{d}\varepsilon^2}{\partial_r g^{rr}(r_H)}\varepsilon \quad \Longrightarrow \quad \frac{\mathrm{d}\rho}{\mathrm{d}\varepsilon} = \frac{1}{\sqrt{\partial_r g^{rr}(r_H)\varepsilon}} \quad \Longrightarrow \quad \varepsilon = \frac{1}{4}\rho^2\partial_r g^{rr}(r_H). \tag{D.54}$$

Accordingly, the metric takes the form:

$$\mathrm{d}s^2 = -\left(\frac{1}{2}\partial_r g^{rr}(r_H)\right)^2 \mathrm{d}t^2 + \mathrm{d}\rho^2 + f(\rho)\mathrm{d}\Omega^2. \tag{D.55}$$

Let us now determine the surface gravity in this metric:

$$V = \sqrt{-\xi^\mu \xi_\mu} = \sqrt{-g_{\mu\nu}\xi^\mu \xi^\nu} = \sqrt{-g_{tt}} \implies \kappa = \sqrt{\nabla^\mu V \nabla_\mu V} = \sqrt{g^{rr}\left(\partial_r V\right)^2}. \tag{D.56}$$

$$\implies \kappa = -\frac{1}{2}\sqrt{\frac{g^{rr}}{-g_{tt}}}\partial_r g_{tt} = \frac{1}{2}\partial_r g^{rr}(r_H). \tag{D.57}$$

We observe that this is precisely the quantity appearing in the metric alongside dt^2. Let us now rewrite the metric:

$$\mathrm{d}s^2 = -\kappa^2\rho^2\mathrm{d}t^2 + \mathrm{d}\rho^2 = -\rho^2\mathrm{d}\theta^2 + \mathrm{d}\rho^2, \tag{D.58}$$

where we introduced a new coordinate $\theta = \kappa t$. If we now define the coordinates (t, x) in the following manner, we obtain:

$$X = \rho\cosh\theta \quad \wedge \quad T = \rho\sinh\theta \quad \implies \quad \mathrm{d}s^2 = -\mathrm{d}T^2 + \mathrm{d}X^2. \tag{D.59}$$

We thus conclude that a freely falling observer indeed perceives nothing special when crossing below the horizon, since we have obtained the Minkowski spacetime metric. Let us now determine what the tortoise coordinate (C.27) represents in the vicinity of the horizon:

$$\mathrm{d}s^2 = g_{tt}\mathrm{d}t^2 + g_{rr}\mathrm{d}r^2 + f(r)\mathrm{d}\Omega^2 = g_{tt}\left(\mathrm{d}t^2 + \frac{g_{rr}}{g_{tt}}\mathrm{d}r^2\right) + f(r)\mathrm{d}\Omega^2 \implies \frac{\mathrm{d}r_*}{\mathrm{d}r} = g_{rr}. \tag{D.60}$$

We now expand this relation and obtain the following:

$$\frac{\mathrm{d}r_*}{\mathrm{d}\varepsilon} = \frac{1}{\cancelto{0}{g^{rr}(r_H)} + \partial_r g^{rr}(r_H)\varepsilon} \quad \implies \quad 2\kappa r_* = \ln\varepsilon + C', \tag{D.61}$$

where c' is a constant that must be chosen appropriately. As expected, this quantity tends to negative infinity as we approach the horizon! Let us now determine the relation between r_* and ρ:

$$2\kappa r_* = \ln\left(C^2\rho^2\right) \quad \implies \quad C\rho = e^{\kappa r_*}. \tag{D.62}$$

By substituting this expression into the defining relations for the (X, T) coordinates, we obtain:

$$X = Ce^{\kappa r_*}\cosh(\kappa t) \quad \wedge \quad T = Ce^{\kappa r_*}\sinh(\kappa t). \tag{D.63}$$

We observe that we have now fully recovered the Rindler coordinates. The only remaining undetermined constant is C, but by noting how the Rindler coordinates are defined, it is clear that it must be $C = 1/\kappa$. Therefore, we can now write the transformation law for the light-cone coordinates: $\sigma^{\pm} = t \pm x \;\rightarrow\; x^{\pm} = T \pm X$:

$$\kappa x^{+} = e^{\kappa\sigma^{+}} \qquad \wedge \qquad \kappa x^{-} = -e^{-\kappa\sigma^{-}}. \tag{D.64}$$

This relation provides the coordinates in which the metric is regular at the event horizon. We see that, in a systematic manner, we have obtained the Kruskal coordinates. In the Schwarzschild case one has $\kappa = 1/4GM$. Naturally, we now analytically continue this transformation so that it holds throughout the entire spacetime, and not only in the vicinity of the horizon. In this way we immediately obtain the maximally extended solution! This transformation is highly general. Moreover, it applies not only to static solutions, but also to stationary ones!

D.6 Hawking effect

The Hawking effect is a phenomenon stating that black holes emit a thermal spectrum of particles at the Hawking temperature. This means that a stationary observer, located very far from the black hole, detects a thermal spectrum of particles. Considering the derivations presented thus far, we conclude that there must exist an observer who perceives the vacuum. Depending on this, we may speak about the particles observed by another observer. What the previous section has shown is that a freely falling observer perceives nothing special while crossing the event horizon. Moreover, the metric becomes the Minkowski spacetime metric. This means that such an observer perceives the Minkowski vacuum. This is indeed one of the quantum states that can be chosen for the system under consideration. It is called the Hartle–Hawking state. Since the metric is regular throughout the entire spacetime, this state describes a black hole in thermal equilibrium with its surroundings.

Our goal is to determine the temperature of the particles that reach the asymptotically flat region at $\mathscr{J}^{+}$. Let us first compute the redshift factor in the Schwarzschild geometry:

$$V = \sqrt{-\xi^{\mu}\xi_{\mu}} = \sqrt{-g_{\mu\nu}\xi^{\mu}\xi^{\nu}} = \sqrt{-g_{tt}} \qquad \Longrightarrow \qquad V = \sqrt{1 - \frac{2GM}{r}}. \tag{D.65}$$

The next step is to determine the acceleration experienced by a freely falling observer at the horizon:

$$a = \sqrt{\nabla_{\mu} \ln V \nabla^{\mu} \ln V} = \frac{\sqrt{g^{rr}}}{V}\partial_r V = \frac{1}{2\sqrt{g^{rr}}}\partial_r g_{rr} \qquad \Longrightarrow \qquad a = \frac{GM}{r^2\sqrt{1 - \frac{2GM}{r}}}. \tag{D.66}$$

We note that this value of acceleration diverges precisely at the horizon. Since a freely falling observer at the horizon perceives Minkowski spacetime, yet is strongly attracted inward by the large acceleration toward the black hole, a static observer just outside the horizon then behaves as a Rindler observer, opposing this acceleration in order to remain at a constant distance from the event horizon. This means that such an observer detects a thermal spectrum of particles (just as a Rindler observer does), at the temperature $\frac{a}{2\pi}$. Our interest is in what an asymptotic observer, located far away from the black hole, detects. This observer also detects these particles, but with a temperature that has undergone gravitational redshift. Therefore, we can write that the temperature detected by this observer is given by:

$$T = \lim_{r_1 \to 2GM} \lim_{r_2 \to \infty} \frac{V(r_1)}{V(r_2)} \frac{a}{2\pi} = \frac{1}{2\pi} \lim_{r \to 2GM} \frac{\sqrt{1 - \frac{2GM}{r}}}{r^2 \sqrt{1 - \frac{2GM}{r}}} = \frac{1}{8\pi GM}. \tag{D.67}$$

When we restore all constants, we obtain the following expression for the Hawking temperature:

$$T = \frac{\hbar c^3}{8\pi G k_B M}. \tag{D.68}$$

We see that the temperature is inversely proportional to the mass. At first glance, this is peculiar, since it implies that black holes possess a negative heat capacity. It should be emphasized that this is the temperature of the radiation; however, this radiation is in thermal equilibrium with the black hole (since the quantum state is everywhere regular, namely the Hartle–Hawking state), and therefore it is also the temperature of the black hole itself. We can now employ the standard thermodynamic relations to calculate the entropy of the black hole. We begin with Einstein's relation connecting mass and energy: $E = Mc^2$. The thermodynamic relation of relevance here is: $dE = TdS$. After integrating with respect to the mass, we obtain the following result for the entropy:

$$S = k_B \frac{4\pi G M^2}{\hbar c}. \tag{D.69}$$

We note that the Schwarzschild radius is proportional to the mass, so the square of the mass is proportional to the area. Taking this into account, we obtain that the entropy is proportional to the area of the event horizon. The final relations for the mass, temperature, and entropy of black holes are given by:

$$E = Mc^2 \quad \wedge \quad T = \frac{\kappa}{2\pi} \quad \wedge \quad S = \frac{A}{4l_p^2}. \tag{D.70}$$

It turns out that these relations are general and can be applied to almost all black hole solutions, whether static or stationary. Let us further note that the acceleration of the Rindler observer is in fact the surface gravity, i.e. $\kappa = a$. This is yet another fact that confirms the equivalence principle!

Biografija

Stefan Đorđević rođen je 1997. godine u Beogradu. Osnovnu školu „Ćirilo i Metodije" završio je 2012. godine u Beogradu, dok je „Matematičku gimnaziju" u Beogradu završio 2016. godine. Osnovne studije fizike završava 2020. godine na Fizičkom fakultetu Univerziteta u Beogradu, na smeru teorijska i eksperimentalna fizika, sa prosečnom ocenom 10.00. Iste godine završva i osnovne studije elektrotehnike i računarstva na Elektrotehničkom fakultetu, Univerziteta u Beogradu sa prosečnom ocenom 10.00 kao student generacije. Naredne, 2021. godine završava master studije iz teorijske i eksperimentalne fizike na Fizičkom fakultetu Univerziteta u Beogradu, sa prosečnom ocenom 10.00, odbranivši master rad na temu *"Entropija Hokingovog zračenja u 2D dilatonskoj gravitaciji"*. Naredne godine osvaja nagradu „Prof dr Ljubomir Ćirković" za najbolji master rad odbranjen na Fizičkom fakultetu tokom školske 2020/2021. Oktobra 2021. godine upisao je doktorske studije na Fizičkom fakultetu Univerziteta u Beogradu. Od maja 2022. godine je zaposlen na ovom fakultetu, a u zvanje istraživač-saradnik izabran je krajem novembra 2024. godine.

Stefan je držao računske vežbe iz predmeta Relativistička kvantna mehanika na Fizičkom fakultetu. Učestvovao je na većem broju međunarodnih konferencija. Do sada je objavio 4 rada u međunarodnim časopisima. Član je, ili je bio član dva projekta koja su finansirana od strane Fonda za nauku Republike Srbije. Oblasti njegovog interesovanja iz fizike visokih energija su: (kvantna) gravitacija, termodinamika crnih rupa, kvantna teorija polja; kao i oblasti fizike čvrstog stanja: topološka kvantna mehanika, topološki izolatori, kvantni holov efekat, ne-hermitski disipativni sistemi.

Ime i prezime autora: Stefan Đorđević

Broj indeksa: 8008/2021

Izjavljujem

da je doktorska disertacija pod naslovom

Page curve in 2D dilaton gravity (Pejdžova kriva u 2D dilatonskoj gravitaciji)

- rezultat sopstvenog istraživačkog rada;
- da disertacija u celini ni u delovima nije bila predložena za sticanje druge diplome prema studijskim programima drugih visokoškolskih ustanova;
- da su rezultati korektno navedeni i
- da nisam kršio autorska prava i koristio intelektualnu svojinu drugih lica.

Potpis autora

U Beogradu, ____________________ ___________________________________

Izjava o istovetnosti štampane i elektronske verzije doktorskog rada

Ime i prezime autora: Stefan Đorđević

Broj indeksa: 8008/2021

Studijski program: kvantna polja, čestice i gravitacija

Naslov rada: Page curve in 2D dilaton gravity

Mentor: prof. dr Voja Radovanović

Izjavljujem da je štampana verzija mog doktorskog rada istovetna elektronskoj verziji koju sam predao/la radi pohranjivanja u Digitalnom repozitorijumu Univerziteta u Beogradu.

Dozvoljavam da se objave moji lični podaci vezani za dobijanje akademskog naziva doktora nauka, kao što su ime i prezime, godina i mesto rođenja i datum odbrane rada.

Ovi lični podaci mogu se objaviti na mrežnim stranicama digitalne biblioteke, u elektronskom katalogu i u publikacijama Univerziteta u Beogradu.

Potpis autora

U Beogradu, ____________________ ____________________________________

Izjava o korišćenju

Ovlašćujem Univerzitetsku biblioteku „Svetozar Marković“ da u Digitalni repozitorijum Univerziteta u Beogradu unese moju doktorsku disertaciju pod naslovom:

Page curve in 2D dilaton gravity (Pejdžova kriva u 2D dilatonskoj gravitaciji)

koja je moje autorsko delo.

Disertaciju sa svim prilozima predao/la sam u elektronskom formatu pogodnom za trajno arhiviranje.

Moju doktorsku disertaciju pohranjenu u Digitalnom repozitorijumu Univerziteta u Beogradu i dostupnu u otvorenom pristupu mogu da koriste svi koji poštuju odredbe sadržane u odabranom tipu licence Kreativne zajednice (Creative Commons) za koju sam se odlučio/la.

1. Autorstvo (CC BY)
2. Autorstvo – nekomercijalno (CC BY-NC)
3. Autorstvo – nekomercijalno – bez prerada (CC BY-NC-ND)
4. Autorstvo – nekomercijalno – deliti pod istim uslovima (CC BY-NC-SA)
5. Autorstvo – bez prerada (CC BY-ND)
6. Autorstvo – deliti pod istim uslovima (CC BY-SA)

(Molimo zaokružiti samo jednu od šest ponuđenih licenci. Kratak opis licence je sastavni deo ove izjave.)

Potpis autora

U Beogradu, ____________________ ________________________

1. **Autorstvo (CC BY)** Dozvoljavate umnožavanje, distribuciju i javno saopštavanje dela, i prerade, ako se navede ime autora na način određen od strane autora ili davaoca licence, čak i u komercijalne svrhe. Ovo je najslobodnija od svih licenci.

2. **Autorstvo – nekomercijalno (CC BY-NC)** Dozvoljavate umnožavanje, distribuciju i javno saopštavanje dela, i prerade, ako se navede ime autora na način određen od strane autora ili davaoca licence. Ova licenca ne dozvoljava komercijalnu upotrebu dela.

3. **Autorstvo – nekomercijalno – bez prerada (CC BY-NC-ND)** Dozvoljavate umnožavanje, distribuciju i javno saopštavanje dela, bez promena, preoblikovanja ili upotrebe dela u svom delu, ako se navede ime autora na način određen od strane autora ili davaoca licence. Ova licenca ne dozvoljava komercijalnu upotrebu dela. U odnosu na ostale licence, ovom licencom se ograničava najveći obim prava korišćenja dela.

4. **Autorstvo – nekomercijalno – deliti pod istim uslovima (CC BY-NC-SA)** Dozvoljavate umnožavanje, distribuciju i javno saopštavanje dela, i prerade, ako se navede ime autora na način određen od strane autora ili davaoca licence i ako se prerada distribuira pod istom ili sličnom licencom. Ova licenca ne dozvoljava komercijalnu upotrebu dela i prerada.

5. **Autorstvo – bez prerada (CC BY-ND)** Dozvoljavate umnožavanje, distribuciju i javno saopštavanje dela, bez promena, preoblikovanja ili upotrebe dela u svom delu, ako se navede ime autora na način određen od strane autora ili davaoca licence. Ova licenca dozvoljava komercijalnu upotrebu dela.

6. **Autorstvo – deliti pod istim uslovima (CC BY-SA)** Dozvoljavate umnožavanje, distribuciju i javno saopštavanje dela, i prerade, ako se navede ime autora na način određen od strane autora ili davaoca licence i ako se prerada distribuira pod istom ili sličnom licencom. Ova licenca dozvoljava komercijalnu upotrebu dela i prerada. Slična je softverskim licencama, odnosno licencama otvorenog koda.